

Aircraft Landing Gear Design: Principles and Practices

Norman S. Currey

Lockheed Aeronautical Systems Company
Marietta, Georgia



AIAA EDUCATION SERIES

J. S. Przemieniecki

Series Editor-in-Chief

Air Force Institute of Technology

Wright-Patterson Air Force Base, Ohio

Published by

American Institute of Aeronautics and Astronautics, Inc.
370 L'Enfant Promenade, S.W., Washington, D.C. 20024

Text Published in the AIAA Education Series

Re-Entry Vehicle Dynamics

Frank J. Regan, 1984

Aerothermodynamics of Gas Turbine and Rocket Propulsion

Gordon C. Oates, 1984

Aerothermodynamics of Aircraft Engine Components

Gordon C. Oates, Editor, 1985

Fundamentals of Aircraft Combat Survivability Analysis and Design

Robert E. Ball, 1985

Intake Aerodynamics

J. Seddon and E. L. Goldsmith, 1985

Composite Materials for Aircraft Structures

Brian C. Hoskin and Alan A. Baker, Editors, 1986

Gasdynamics: Theory and Applications

George Emanuel, 1986

Aircraft Engine Design

Jack D. Mattingly, William Heiser, and Daniel H. Daley, 1987

An Introduction to The Mathematics and Methods of Astrodynamics

Richard H. Battin, 1987

Radar Electronic Warfare

August Golden Jr., 1988

Advanced Classical Thermodynamics

George Emanuel, 1988

Aerothermodynamics of Gas Turbine and Rocket Propulsion, Revised and Enlarged

Gordon C. Oates, 1988

Re-Entry Aerodynamics

Wilbur L. Hankey, 1988

Mechanical Reliability: Theory, Models and Applications

B. S. Dhillon, 1988

American Institute of Aeronautics and Astronautics, Inc., Washington, DC

Library of Congress Cataloging in Publication Data

Currey, Norman S.

Aircraft landing gear design: principles and practices.

p. cm—(AIAA education series)

Bibliography: p.

Includes index

1. Airplanes—landing gear—Design and construction.

I. Title. II. Series.

TL682.C87 1988 629.134'381—dc19 88-21116 CIP

ISBN 0930403-41-X

Fourth Printing

Copyright © 1988 by the American Institute of Aeronautics and Astronautics, Inc. All rights reserved. Printed in the United States of America. No part of this publication may be reproduced, distributed, or transmitted, in any form or by any means, or stored in a data base or retrieval system, without prior written permission of the publisher.

FOREWORD

It has been thirty years since the publication of the last text on landing gear design. In 1958, *Landing Gear Design*, by the well-known British aeronautical engineer H. G. Conway, presented essentially the period's state-of-the-art. Not since then has there appeared a comparable publication except, in the early eighties, the Lockheed-Georgia Company report "Landing Gear Design Handbook" written by the author of this new AIAA Education Series text. Recognizing the need in this area, AIAA encouraged the preparation of a comprehensive text book based on the compendious Lockheed Company handbook.

Norman S. Currey's *Aircraft Landing Gear Design: Principles and Practices* captures the professional experience of the author as a designer and engineer and provides detailed documentation of current design practices and trends. The historical background given in the text allows the reader to follow the engineering development in landing gear design from very simple concepts to modern designs for contemporary civil and military aircraft.

This text provides much technical information for aircraft designers. Other AIAA Education Series textbooks in progress will likewise serve the student and designer.

J. S. PRZEMIENIECKI
Editor-in-Chief
AIAA Education Series

PREFACE

“I have but one lamp by which my feet are guided,
and that is the lamp of experience,” said Patrick Henry.

Engineers who have experienced the birth and subsequent development of aircraft landing gears are rapidly fading from the scene in the world's aircraft industry. This book is then an endeavor to provide the light by which the feet of a new generation of designers may be guided.

The American Institute of Aeronautics and Astronautics recognizes the need for such a document and has promoted the writing of it. H. G. Conway provided the first book on this subject (“Landing Gear Design,” Chapman & Hall Ltd., 1958). It is now out of print, difficult to obtain, and needs to be either updated or expanded in some areas. “Landing Gear Design Handbook” (written by myself and published by the Lockheed-Georgia Company in 1982) also needs to be updated and modified for general usage.

It has been said that landing gear design encompasses more engineering disciplines than any other aspect of aircraft design. It includes heavy forgings, machined parts, mechanisms, sheet metal parts, electrical systems, hydraulic systems, and a wide variety of materials such as aluminum alloys, steels, titanium, beryllium, carbon and composites—and today's gear designer must also have a working knowledge of airfield strength calculations.

With so many sciences involved, it is inevitable that some materials usage and systems will become outdated within a short time. Radial tires, integrated brake controls, and digital fiberoptic controls, for instance, are likely to replace many of the older tires and systems.

Particular thanks are due to the many companies that provided data and drawings, and every attempt has been made to recognize these sources in the text. Some of the data also were obtained from government documents and from the data published by the SAE A-5 “Aerospace Landing Gear Systems Committee.” Special thanks are also due to M. B. Crenshaw, W. Sharples and W. C. Cook of Lockheed for their help in writing this book.

The opinions and methods quoted herein are those of the author and do not necessarily represent those of his employer (Lockheed Aeronautical Systems Company). Although great care has been exercised to ensure the accuracy and validity of the material presented in this book, the author and publisher are not liable for any damages incurred as a result of usage of the said book, for misinterpretations, or for typographical errors. Landing gear design is a rapidly evolving branch of engineering; consequently, the

requirements, techniques, and materials are constantly changing. It is left to the good sense and judgment of the reader to ensure that the latest requirements, procedures, and design principles are used.

NORMAN S. CURREY

Lockheed Aeronautical Systems Company

Marietta, Georgia

TABLE OF CONTENTS

- ix **Preface**
- 1 Chapter 1. Introduction**
 - 1.1 Purpose of This Book
 - 1.2 Background and History
 - 1.3 Landing Gear Types
 - 1.4 Data Sources
- 13 Chapter 2. The Design Process**
 - 2.1 Components of Landing Gear Design
 - 2.2 Development of First Concepts
 - 2.3 Preliminary Design
 - 2.4 Postcontractual Design
 - 2.5 Air Vehicle Test
- 25 Chapter 3. Initial Layout**
 - 3.1 Conceptual Design Phase
 - 3.2 Project Definition Phase
- 43 Chapter 4. Requirements**
 - 4.1 Abbreviations
 - 4.2 Terminology
 - 4.3 Operating Conditions
 - 4.4 Layout
 - 4.5 Gas/Oil Shock Absorbers
 - 4.6 Tires
 - 4.7 Wheels
 - 4.8 Brakes
 - 4.9 Skid Control
 - 4.10 Steering Systems
 - 4.11 Locks
 - 4.12 Retraction/Extension Mechanisms
 - 4.13 Cockpit Requirements
 - 4.14 Protection
 - 4.15 Doors and Fairings
 - 4.16 Maintenance
 - 4.17 Strength
 - 4.18 Tail Bumpers
 - 4.19 Arresting Hooks

- 69 Chapter 5. Shock Absorber Design**
- 5.1 Shock Absorber Types
 - 5.2 Some Basic Considerations and Tradeoffs
 - 5.3 Stroke Calculation
 - 5.4 Rubber Shock Absorber Design
 - 5.5 Leaf Spring Shock Absorber Design
 - 5.6 Liquid Spring Design
 - 5.7 Oleo-Pneumatic Shock Absorber Design
 - 5.8 Detail Design of a Single-Acting Oleo-Pneumatic Strut
 - 5.9 Piston Valves Used for Load/Stroke Modification
 - 5.10 Contracting Shock Struts
 - 5.11 Orifice Design
- 123 Chapter 6. Tires**
- 6.1 Tire Construction
 - 6.2 Design Considerations and Requirements
 - 6.3 Rolling Radius
 - 6.4 Radius of Gyration
 - 6.5 Crush Load
 - 6.6 Temperature Effects
 - 6.7 Tire Rolling Resistance
 - 6.8 Tire Friction
 - 6.9 Side Forces and Slip Angles
 - 6.10 Hydroplaning
- 137 Chapter 7. Brakes, Wheels, and Skid Control**
- 7.1 Requirements
 - 7.2 Brake Sizing
 - 7.3 Brake Material
 - 7.4 Brake Design
 - 7.5 Wheel Design
 - 7.6 Brake Heat
 - 7.7 Skid Control
 - 7.8 Autobrakes
 - 7.9 Hydraulic Brake Systems
 - 7.10 Emergency Brake Systems
 - 7.11 Brake Control Pedal
 - 7.12 Advanced Brake Control System (ABCS)
- 175 Chapter 8. Kinematics**
- 8.1 General Guidelines
 - 8.2 Kinematic Concepts
 - 8.3 Kinematic Detail
 - 8.4 Mathematical Kinematic Analysis

- 197 Chapter 9. Steering Systems**
 - 9.1 Design Considerations and Requirements
 - 9.2 Actuation
 - 9.3 Hand-Wheel Installations
 - 9.4 Shimmy Damping
 - 9.5 Castering Nose Wheels

- 225 Chapter 10. Detail Design**
 - 10.1 Materials
 - 10.2 Lugs and Pins
 - 10.3 Bushings
 - 10.4 Lubrication
 - 10.5 Finishes
 - 10.6 Seals
 - 10.7 Jack Pads and Tow Fittings
 - 10.8 Locks

- 259 Chapter 11. Weight**
 - 11.1 Weight Estimation: Method 1
 - 11.2 Weight Estimation: Method 2
 - 11.3 Method Comparison
 - 11.4 Preliminary Component Weight Estimate
 - 11.5 Analytical Weight Estimate

- 267 Chapter 12. Airfield Considerations**
 - 12.1 Background
 - 12.2 Definitions and Parameters
 - 12.3 Airfield Surface Types
 - 12.4 Flotation
 - 12.5 Flotation on Paved Airfields
 - 12.6 Flotation on Unpaved Airfields
 - 12.7 Limited Operation
 - 12.8 Aircraft Classification Number—Pavement Classification Number (ACN—PCN)
 - 12.9 Roughness

- 305 Chapter 13. Unorthodox Landing Gears**
 - 13.1 Overall Review
 - 13.2 Skids
 - 13.3 Skis
 - 13.4 Tracks
 - 13.5 Air-Cushion Landing System (ACLS)

- 323 Chapter 14. Design Data**
- 365 Chapter 15. Specifications**
- 369 Subject Index**

INTRODUCTION

1.1 PURPOSE OF THIS BOOK

This book is part of the AIAA Education Series of textbooks and monographs, the intent of which is to meet the growing need for guidance in the highly specialized disciplines of aeronautics and astronautics. Some of today's landing gear designers started their careers when nearly all aircraft had tail wheels or skids and when the shock absorber was, at best, an ultrasimple oleo-pneumatic strut. Since that time, not only has much been learned about all aspects of landing gear design, but new materials have become available to help the designer provide the most efficient shock absorption, in the smallest space, with the lowest weight and cost. Over the past 20 years, another factor has increased in importance—flotation; thus, the landing gear designer must now become familiar with the characteristics of the surface upon which the aircraft is operating.

The purpose of this book is to help those engineers who must design tomorrow's landing gears. It describes the step-by-step design process and some of the lessons learned. Section 1.4 provides information about the many sources from which more detailed data may be obtained.

1.2 BACKGROUND AND HISTORY

The first wheeled landing gears appeared shortly after the Wright Brothers' maiden flight in December 1903. Santos-Dumont's "No. 14 bis" had a wheeled landing gear; this airplane made the first flight in Europe in October 1906. This was followed quickly by wheeled aircraft designed or flown by Voisin (1907), Delagrange (1907), Farman (1908), Bleriot (1908), Curtiss (1908), Cody (1908), Ellehammer (1908), McCurdy (1909), Roe (1909), and Short (1909). Several of these were "first" flights: Bleriot across the Channel, McCurdy in the British Empire, and Roe in the United Kingdom.

Then came World War I, by which time the configurations had more or less settled down to tail wheel types, employing fairly rugged struts attached to the fuselage and landing gears that had some degree of shock absorption through the use of bungee cords wrapped around the axles, as illustrated in Fig. 1.1.

The Sopwith Camel, SPAD VII and SE5 were typical World War I fighter/scout aircraft. Both the Camel and SPAD had axles that pivoted from the spreader bars, the main difference being in the location of the bungee that restrained the axle from moving. The Camel's bungees were at the extreme ends of the spreaders and permitted 4 in. of wheel travel. The SPAD's shock

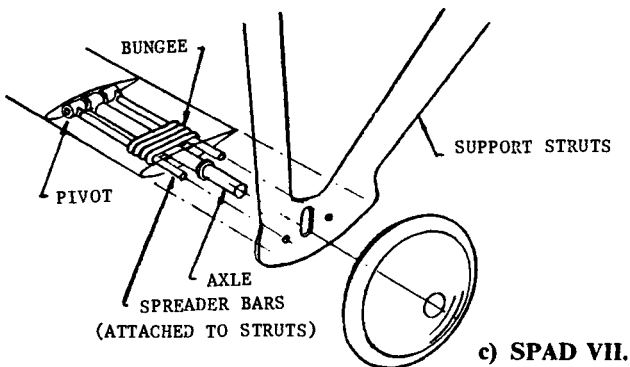
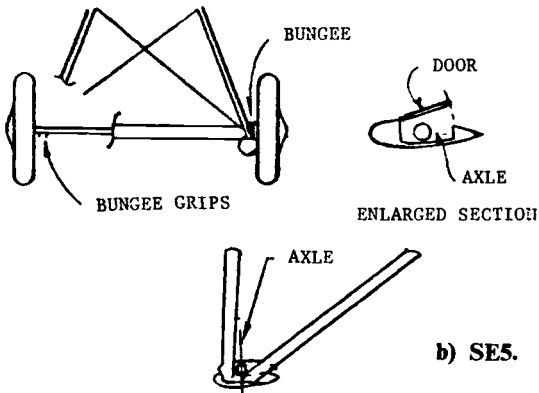
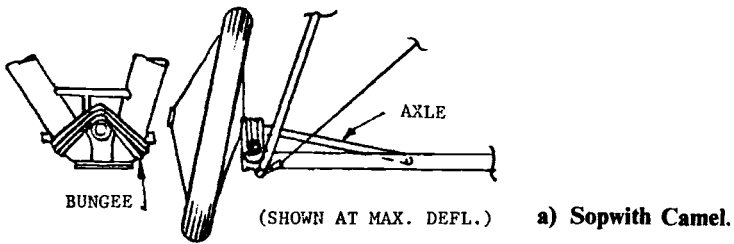


Fig. 1.1 Bungee cords on World War I aircraft.

cords permitted 3–4 in. of travel (depending on the model), but were located inboard of the gear support struts.

The SE5 gear utilized a continuous axle with a wheel at each end. This was dropped into a cavity in the upper surface of a fixed crossbeam; bungee was then wrapped around the ends to restrain the axle from moving upward out of the cavity.

In the 21 years between World Wars I and II, landing gear design developed

as fast as airframe design. The latter changed from braced wood and fabric biplanes to aluminum alloy monoplanes and the landing gears became retractable, employing a variety of shock-absorbing systems. Increased shock absorption became necessary in order to accommodate the constantly increasing aircraft weights and sink speeds. Although the shock absorber stroke is not a function of aircraft weight, it was important to increase that stroke in order to lower the landing load factors and thereby minimize the structure weight influenced by the landing loads.

Larger-section tires provided some of the desired shock absorption, but size limitations and relatively low (47%) efficiency prevented a major contribution from this source. Therefore, shock-absorbing support struts were devised. As will be seen in the later chapters, these ranged from rubber blocks and compression springs to leaf springs, oleo-pneumatic struts, and liquid springs.

The Ford Trimotor (1932) is typical of the early usage of rubber-block shock absorbers (see Fig. 1.2).

The earliest retractable landing gear that the author has been able to find is that used on the Bristol (England) Jupiter racing aircraft of the late 1920's.

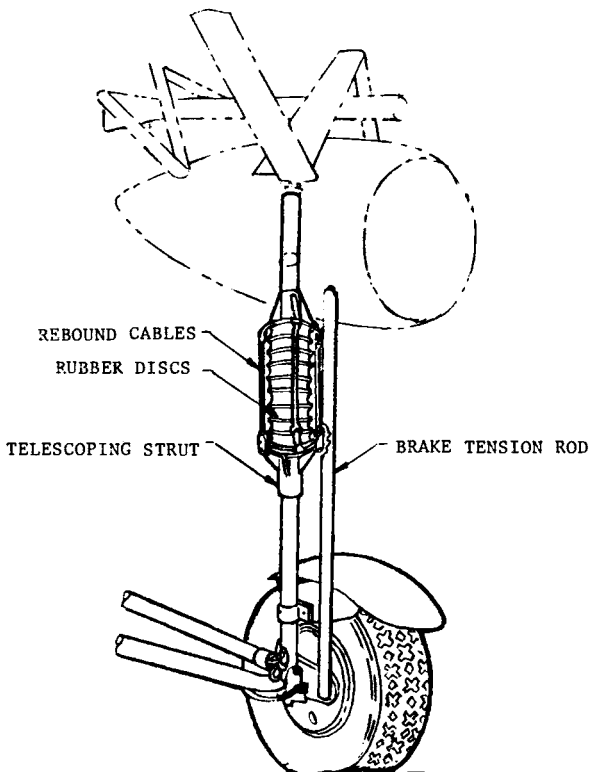


Fig. 1.2 Ford Trimotor landing gear.

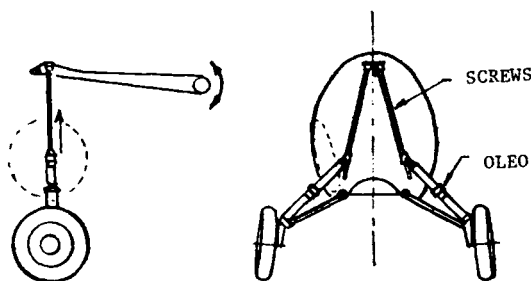


Fig. 1.3 Retraction system on Curtiss Export Hawk III C.

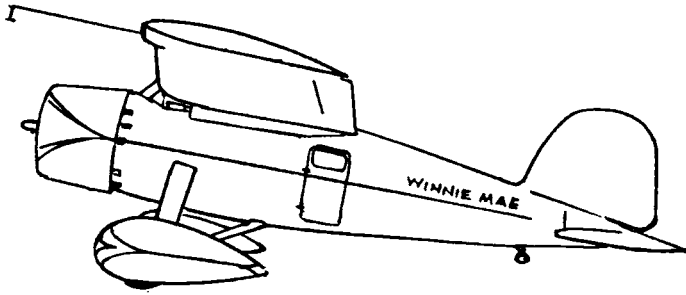
In the United States, Lockheed's Model 8D Altair, which first flew in 1930, had a fully retractable landing gear and Boeing was certainly in the vanguard with their partially retracted gear on the Y1B-9 bomber (1931). The Grumman FF-1 fighter of 1932 had the wheels pulled up into the fuselage side and the Douglas DC-1 had a retracted gear in 1933. However, only one of those aircraft was ever built. Then, in 1934 retractable gears were used on two types of production commercial transport aircraft—the Douglas DC-2 and the Boeing 247-D.

Figure 1.3 shows the method used to retract the gear on one of those early types—the Curtiss Export Hawk III C. It is a relatively simple system employing hand-cranked screwjacks to pull the top of the oleo strut upward into its stored position.

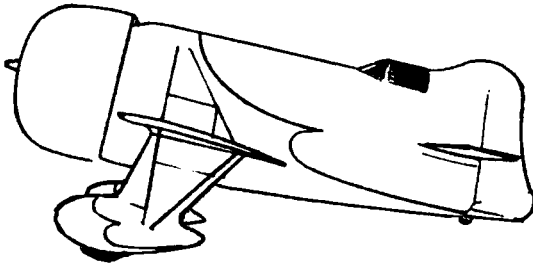
It should be noted, however, that until World War II most aircraft had fixed landing gears, often with exotic-looking spats to reduce drag. The Gee Bee Super-Sportster of 1932 and Wiley Post's Lockheed Winnie Mae are typical examples and are illustrated in Fig. 1.4. One of the methods of providing shock absorption on a "spatted" landing gear is illustrated in Fig. 1.5: the leg is pivoted near the fuselage skin and the load is reacted through a lever into an oleo strut with a surrounding coil spring to provide rebound forces.

By the time World War II began, almost all of the operational fighters and bombers had retractable landing gears. There were a few notable exceptions, such as the Fairey Swordfish torpedo bomber that did so much damage to the battleship *Bismarck*, and the Gloster Gladiator biplane fighter—three of which (named Faith, Hope, and Charity) fought off daily bomber formations over Malta. The Junkers-87 Stuka had a fixed gear, as did the basic trainers used by the U.S. Air Force (Army Air Force in those days) and Royal Air Force. Some U.S. Navy aircraft such as the Vought-Sikorsky Kingfisher also had fixed landing gears.

Since World War II, landing gear design has progressed in all areas: tire design has moved through many stages and radials are now on the threshold of general acceptance; brake materials such as beryllium and carbon have been developed; skid control systems are now being digitized with fiberoptic controls; super-high-strength steels and stress-corrosion-resistant aluminum alloys have become available; the intricacies of highly efficient shock absorption are better understood; and detail design has made major strides.



a) Lockheed Winnie Mae.



b) Gee Bee Super-Sportster.

Fig. 1.4 Spatted landing gears.

Aircraft design has become a very sophisticated form of engineering in the last 30 years or so and the landing gear designer has had to keep pace. He is constantly faced with achieving a satisfactory compromise between the sometimes conflicting demands of structures engineers, aerodynamicists, runway designers, and operational personnel. Transport aircraft are considerably heavier than they used to be—the Boeing 747 is more than twice as heavy as the 707-320C and nearly 28 times as heavy as the DC-3. So, larger landing gears are required and, to meet the requirements of the airframe designers and aerodynamicists, they must somehow be stowed in areas that have a minimum effect on the basic airframe structure and aircraft drag. Runway designers insist that high-density operations of these heavy aircraft not break up their runways. Military customers even want them to land on bare soil!

The Lockheed C-5A main landing gear is a typical example of design sophistication in meeting all of the various requirements imposed upon it.

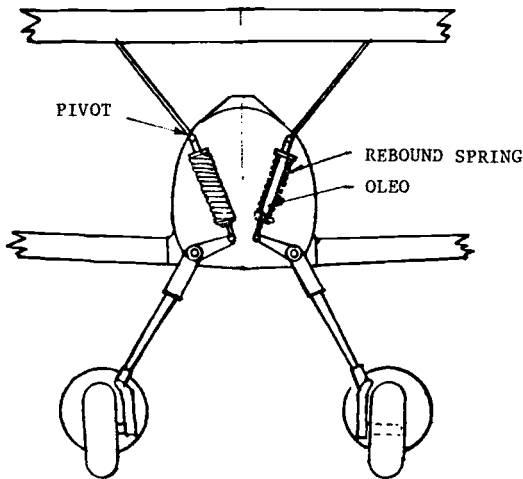


Fig. 1.5 Curtiss P-6E shock absorption.

Illustrated in Fig. 1.6, the most noticeable feature is its unique six-wheel bogie—an arrangement devised to maximize its flotation on bare soil by spreading the load over a wide area and avoiding, as much as possible, tires following in the same ruts. Many other unusual features were incorporated, however, to meet the severe requirements. It has a double-acting shock absorber to improve capabilities on a rough field; it has a kneeling system to lower the fuselage so that the cargo floor is a 5 ft (approximately) above the

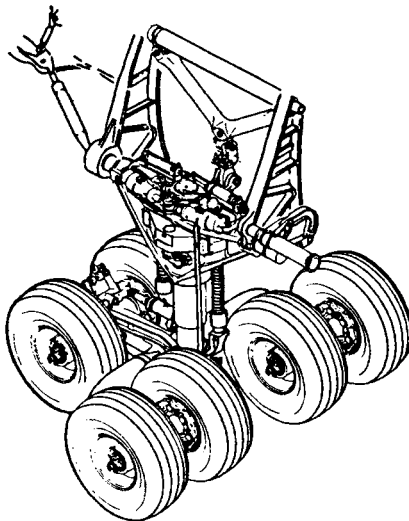


Fig. 1.6 Lockheed C-5A main landing gear.

ground; and it has a crosswind positioning system that rotates the bogies 20 deg left or right to enable the aircraft to land in a severe crosswind without a last-minute correction of the fuselage heading. Finally, it has an in-flight tire-deflation system to lower tire pressures to a preset level to maximize flotation before landing on a bare soil field.

As landing gear design proceeds toward the 21st century, carbon brakes are becoming fashionable, radial tires are being used on several aircraft to provide many benefits that will be described in later chapters, composite materials are being tested for landing gear applications, shock absorbers are reaching high efficiencies and can tolerate increased levels of airfield roughness, and worldwide standards are gaining recognition for the determination and reporting of airfield strengths.

1.3 LANDING GEAR TYPES

Landing gears are generally categorized by the number of wheels and their pattern. Figure 1.7 illustrates the basic types. This terminology is rapidly gaining worldwide acceptance. For instance, the USAF/USN Enroute Supplements define the strength of a given field as T-50/TT-100, indicating that the airfield is cleared to accept aircraft weighing 50,000 lb with a twin-wheel gear or 100,000 lb with a twin-tandem gear.

There are also hybrid arrangements such as the 12-wheel arrangement

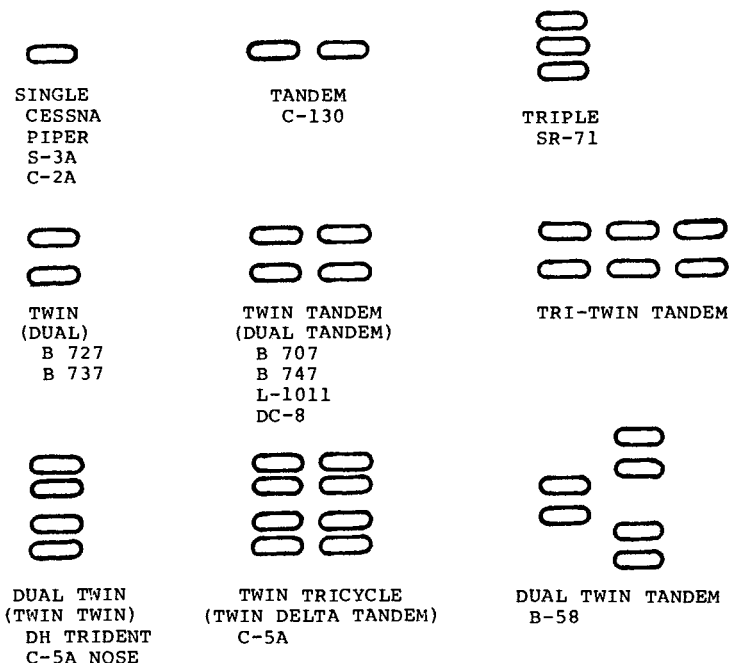


Fig. 1.7 Standard landing gear types.

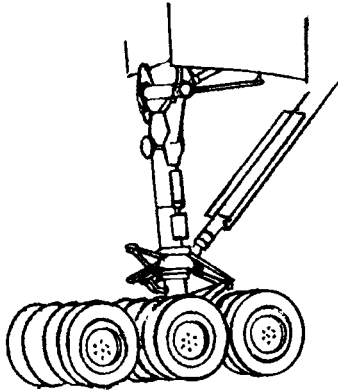


Fig. 1.8 TU-144 main landing gear.

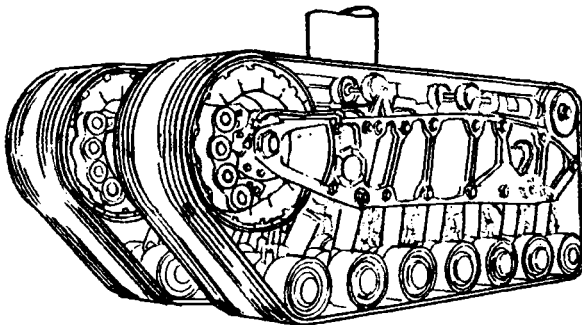


Fig. 1.9 Track-type gear.

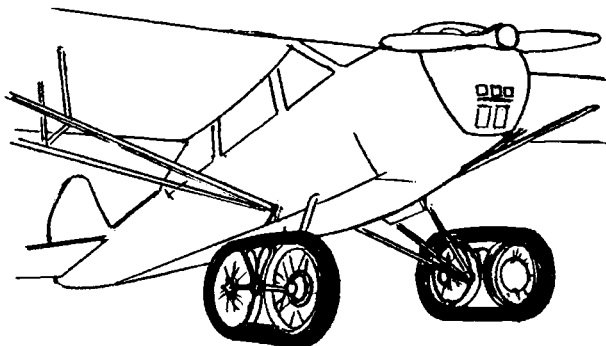
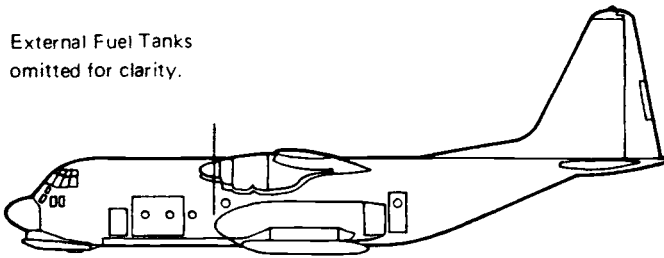
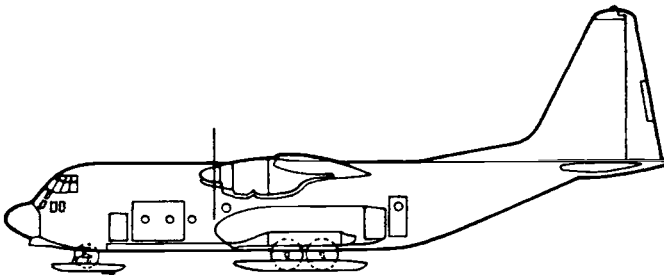


Fig. 1.10 Bonmartini gear.

External Fuel Tanks
omitted for clarity.

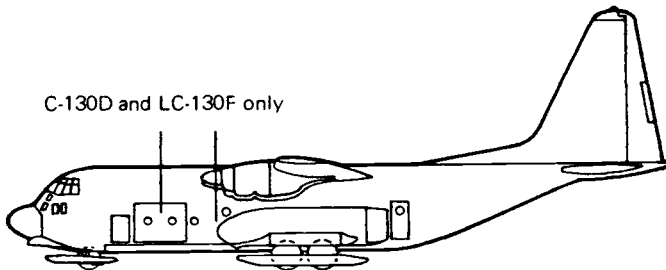


Landing Gear Retracted



Ski Landing

C-130D and LC-130F only



Wheel Landing

Fig. 1.11 Ski-C-130 gear.

used on the Soviet TU-144 supersonic transport depicted in Fig. 1.8 and the track gears that were tested on the Fairchild Packet, Boeing B-50, and Convair B-36—the latter is illustrated in Fig. 1.9. The objectives of the track gear were to reduce the weight and size attributable to the tires and to improve flotation by having a larger contact area.

Track gears did have higher flotation by keeping the contact pressures as low as 30 psi, but there was no weight reduction. In fact, aircraft weight was increased by about 1.8% (1.78% on the Packet and 1.87% on the B-36). Maintainability and reliability were also degraded substantially because of the complicated mechanism (multiple shock absorbers in the track bogie), low bearing life, low belt life, and high spin-up loads.

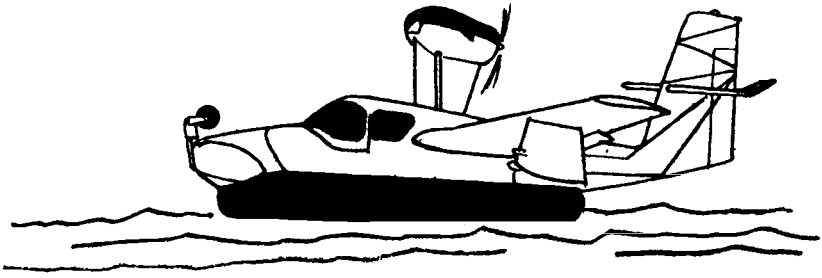


Fig. 1.12 LA-4 air cushion gear.

The Italian Bonmartini track gear was also tested successfully, but it too was heavier than a conventional gear. It used a pneumatic belt to encompass the two wheels; see Fig. 1.10.

Various types of skids and skis have been devised to replace conventional gears. The purpose of the skis is, obviously, to enable operation on snow; the Lockheed C-130R is an example of a large contemporary aircraft so equipped. As Fig. 1.11 shows, it has two configurations: one in which the wheels protrude below the skis for takeoff from conventional runways and one in which the skis are lowered below the wheels for a snow landing.

Usage of skids during and after World War II has been an endeavor to reduce the landing gear weight below the normal 3–6% of gross weight and, to a great extent, this has been accomplished. However, in most cases, the aircraft must use a trolley beneath the skids for takeoff, with the trolley being retrieved after the aircraft has left it.

Although this book is not intended to discuss the intricacies of skids and skis, for the sake of completeness some design details are included in later chapters.

Air cushion systems are another type of unconventional gear, which have been pioneered by Bell-Textron in the United States. The LA-4 was their first venture; it was a small aircraft (Fig. 1.12) that operated successfully on plowed ground, over tree stumps up to 6 in. high, over 3 ft wide ditches, on soft muddy ground, and over both sand and water. Further details of this and other systems, including the ACLS Buffalo, are also provided in later chapters.

1.4 DATA SOURCES

Although this book defines the principles and practices of landing gear design, the reader should be aware of many sources of information that provide detailed recommendations, requirements, and/or lessons learned.

The Society of Automotive Engineers (SAE), through its A-5 Aerospace Landing Gear Systems Committee, has developed many Aerospace Information Reports, Recommended Practices, and Standards (AIR, ARP, AS) in this field. A list of those cited in this volume is included in Chapter 15.

Military specifications are issued by the U.S. Department of Defense and civilian specifications by the Federal Aviation Agency. The British Civil Airworthiness Requirements (BCAR) are issued by the British Civil Aviation Authority. Those cited here are also included in Chapter 15.

Details of other references are given at the end of each chapter, as appropriate.

THE DESIGN PROCESS

2.1 COMPONENTS OF LANDING GEAR DESIGN

The landing gear has been described as “the essential intermediary between the aeroplane and catastrophe” (Ref. 1, p. 323). In support of this definition, landing gear design is considered to include the following items:

- 1) Forward and aft landing gears.
- 2) Tail bumpers.
- 3) Wing tip (or outer wing) gears.
- 4) Arresting hooks.
- 5) Jacking, mooring, and towing attachments.
- 6) Landing gear doors and their operating equipment.
- 7) Holdback installations.
- 8) Electrical and hydraulic equipment up to the interface point with airframe-mounted equipment.
- 9) Layouts to show ground clearances at various aircraft attitudes and with varying degrees of strut/tire inflation.
- 10) Layouts to show catapulting and arresting attitudes.
- 11) Calculations to show compatibility with airfield surfaces (sometimes accomplished by special groups).

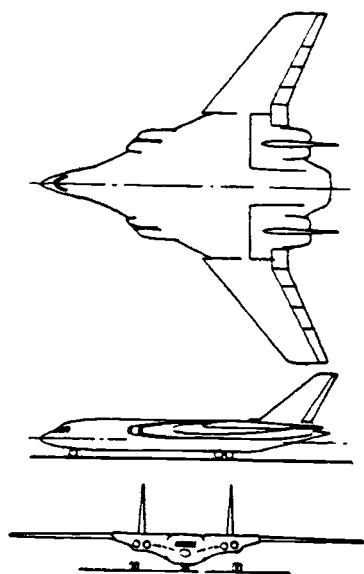
2.2 DEVELOPMENT OF FIRST CONCEPTS

Like the aircraft itself, the first concepts of a landing gear are usually prepared long before the establishment of a formal contract. Marketing organizations determine that there is a need for a new or modified aircraft. This may be the result of market surveys, discussions with potential customers, or close attention to deliberations being made by various airlines or military organizations. The marketing and preliminary design departments then cross-pollinate their thoughts, establish what they consider to be the basic requirements, and begin to prepare basic concepts.

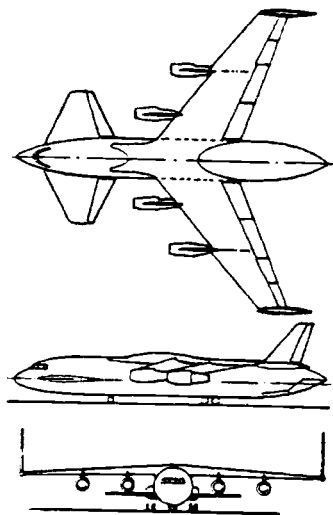
From this point onward, it may be weeks, months, or even several years before a Request for Proposal (RFP), or its commercial equivalent, is issued by the customer; the time allotted to proposal preparation may be anywhere from 30 days to several months. Since the proposal preparation time may be extremely short, the advantages of extensive preproposal activity are obvious.

As an example, the following is a very brief summary of Lockheed C-5A activities up to first flight:

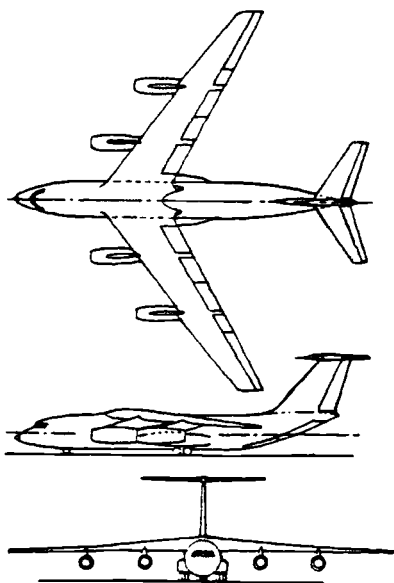
- 1) October 1961: U.S. Air Force issued a Qualitative Operational Requirement for a C-133 replacement.



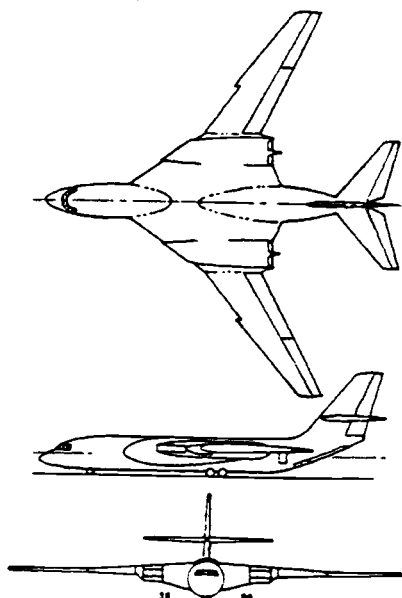
a) Lambda wing.



c) Canard.



b) High wing.



d) Burried engine.

Fig. 2.1 Some early C-5A configurations.

2) October 1961 to April 1964: preconcept formulation phase. During this time, the USAF issued the Specific Operational Requirement (SOR) defining payloads, performance, powerplant desires, reliability, maintainability, availability, and details of preferred loading methods and cargo compartment size.

3) April 1964: Lockheed "froze" their initial design.

4) May 1964 to December 1964: concept formulation phase.

5) December 1964: RFP issued for project definition phase.

6) December 1964 to October 1965: project definition phase.

7) April 1965: proposal submitted (36 volumes, 7766 pages).

8) December 1965: Lockheed awarded C-5A contract.

9) June 1966: Preliminary Design Review conducted.

10) August 1967: Critical Design Review conducted.

11) June 1968: first flight.

Similar time spans are encountered on current fighter and bomber aircraft; even commercial aircraft are not entirely immune to lengthy concept formulation periods. For example, serious design work on the Boeing 757/767 series started in 1973.² Even without the cumbersome governmental decision-making systems, it took eight years from concept definition to first flight and another two years to initial deliveries of this commercial aircraft.

In the conceptual phase, the landing gear designer is often faced with a very wide variety of configurations. On the C-5A, low, high, variable-sweep, canard, and modified-delta wing configurations were considered, all with their own particular landing gear problems. Some of these configurations are depicted in Fig. 2.1. At the same time, the aircraft gross weight fluctuated between 550,000–750,000 lb, so the main landing gears ranged from a 4-wheel bogie on each side to configurations having up to 16 wheels per side. Needless to say, there is no point at this stage in trying to define any details, but flotation and tire/wheel/brake sizing are given serious consideration. This procedure is described in the next chapter.

2.3 PRELIMINARY DESIGN

Throughout the entire design process, from the development of first concepts through to production configurations, it is extremely important that complete documentation be maintained. For each aircraft configuration, there should be, at the very minimum, a listing of its assumed weights and geometric data in the landing gear files—and the designer should have a summary attached to it to show the basic essentials of the gear. The depth to which that summary is given depends upon the seriousness of that particular configuration and/or the complexity or uniqueness of the landing gear involved.

The objectives in the preliminary design phase can be summarized as follows:

1) In the concept formulation phase, the landing gear location and the number and size of the wheels is determined. The former is, at this time, a function of center-of-gravity location and general structural arrangement. The number and size of wheels is dependent upon the weight of the aircraft, braking requirements, and, if specified, the flotation requirement.

2) In the project definition phase, the general configuration of the aircraft has been decided and the preliminary design activity becomes more analytical and more detailed. Proposal preparation usually occurs at the end of this phase and a concerted effort must be made to provide as much detail and credibility as possible. The objective of the proposal is to sell the product; to do that, the customer must be convinced that every facet of the proposed aircraft is what he wants and that it is better than any competitor's product—hence, the need for detail and analysis to dispel any argument concerning its capability.

Figure 2.2 illustrates the preliminary design activity and the factors to be recognized. Note that, in the early phases, the landing gear designer may be called upon to influence the requirements in the RFP. For instance, in one project, the flotation requirement was established after an analysis had been

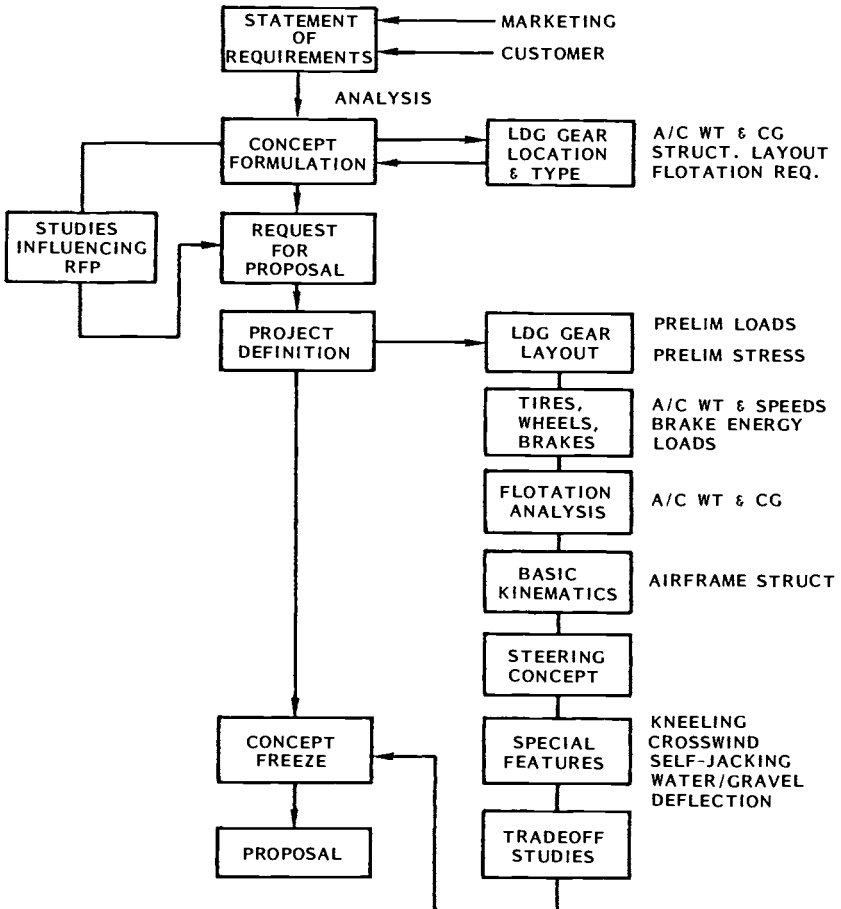


Fig. 2.2 Preliminary design activity.

made of many landing gear configurations and flotation was then related to cost. The partial results of this analysis are shown in Fig. 2.3.

In another project, it was determined that an already-available landing gear (with minor modifications) was ideally suited to the new aircraft and, because of cost considerations, this became a driver in the design, precluding substantial deviation from that concept.

Referring to Fig. 2.2, landing gear activity in the concept formulation phase must recognize that there will probably be a number of widely varying aircraft concepts and that only a brief analysis is required for each one. As

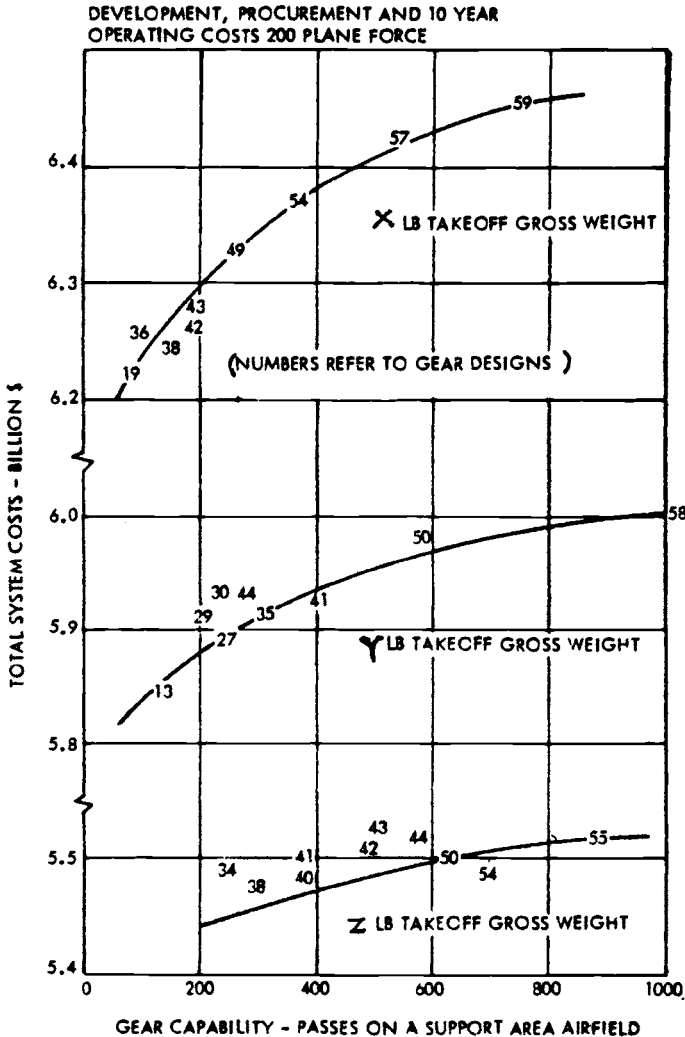


Fig. 2.3 Flotation vs cost (development, procurement, and 10 year operating costs of 200 plane force).

a minimum, the gear designer must know the aircraft weight and its range of center-of-gravity (c.g.) position. From this, the options for wheel numbers and sizes can be determined, e.g., two large tires or four smaller tires at the end of a shock strut.

These options will be reviewed to see how they match the airframe structure and the flotation requirements (if any). Cost, weight, availability, and overall complexity are other factors to consider in the evaluation of options.

Landing gear location and length are determined by the c.g. location, tail-down angle requirements to suit takeoff and landing attitudes, tipover, and general airframe configuration. Flotation is checked for the various wheel sizes, using rigid, flexible, and bare soil rules as applicable. As noted above, this inevitably results in a small tradeoff study to determine the most cost-effective arrangement.

During this phase, there is very often considerable discussion with the prospective customer who is trying to formulate the RFP and the results of various tradeoff studies may be used to modify the original requirements. Once the RFP has been issued to the competitors, informal discussions with the customer come to an end. Questions and the resulting discussion are allowed at the Bidders Conference that takes place shortly after issuance of the RFP, but all competitors are present and questions must, therefore, be carefully worded (usually in writing) to avoid revealing one's ideas or concerns to the competition.

In the subsequent project definition phase, there is an urgency to freeze the design concept quickly. The best overall aircraft concept is selected and the landing gear design becomes more detailed. The continuing aircraft weight and c.g. analysis (and subsequent loads derivation) allows the designer to refine the gear location and gear loads. Based upon the defined sink rates, the approximate strokes are determined at the main gear and nose gear and, from a rough layout, the landing gear dimensions and sizes are established. A layout is then prepared to evaluate, and in particular to document, the tail-down angles, turnover angle, and clearances to deflected surfaces, engine nacelles, and propellers (if used) with various conditions of strut and tire inflation/deflation.

Tire, wheel, and brake vendors are brought in at this point. It is possible that a new tire should be developed for the aircraft or plies added to an existing tire, both of which may be a subject of vendor negotiation. If the aircraft is carrier-based, the cable-crossing and catapult requirements would also be discussed. The matching of tire and wheel size to brake size is another important activity. To address this subject adequately, the takeoff load/speed/time data, plus dynamic taxi loads and landing loads, should be available, as well as the takeoff speed profile used for any brake kinetic energy calculations. The relative size, cost, and weight of steel, beryllium, and carbon brakes would be evaluated at this time—although beryllium now seems to be fading out of the picture in favor of carbon.

With tire sizes, wheel arrangements, loads, and c.g. range being determined, the flotation calculations are recycled. The methods used are described in later chapters. Airfield roughness requirements (if any) are also evaluated at this time.

The basic kinematics of the landing gear demand a great deal of ingenuity on the part of the designer. It involves the retraction, extension, and locking systems with due consideration to emergency conditions, including free-fall. As will be seen later, this involves a wide variety of possible systems, ranging from simple up-and-down motion to systems that rotate the entire strut about its axis while, at the same time, properly positioning the bogie. In all cases, the objective is to retract the gear into a cavity that has the least effect on basic airframe structure and also to minimize any external contour changes that might increase aircraft drag.

The steering concept is a fundamental part of the nose gear design and it must be determined before proposal preparation. Figure 2.4 illustrates the four most common types and notes the limitations of push-pull actuators. However, the latter are still the most common type of steering mechanism.

The peculiar requirements imposed on the C-5A were discussed previously; Fig. 2.2 lists four such requirements: kneeling, crosswind positioning, self-jacking, and deflection of water or gravel. The first two are good candidates for any large transport, although crosswind positioning is very debatable. Self-jacking refers to the ability to change tires without having to use jacks—a definite attribute for a military aircraft that has flat tires after landing at a remote austere base. Water and/or gravel deflection is sometimes required to prevent water or gravel sprayed from the nose wheel being ingested in the engines—this is usually accomplished by chine treads on the

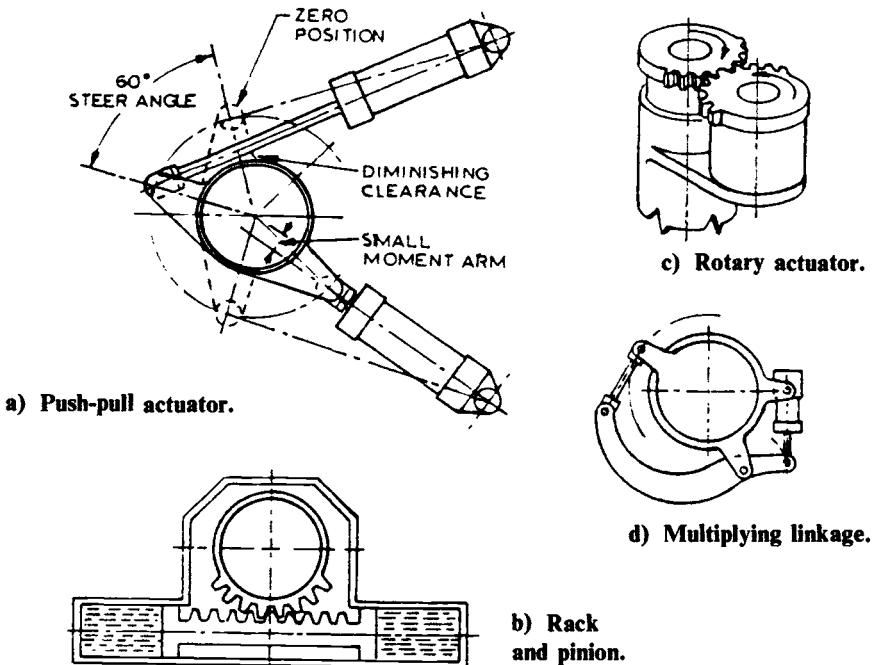


Fig. 2.4 Common types of steering systems.

tires or by deflector plates attached to the nose gear. Other special features could include in-flight tire deflation, ability to land on extremely soft surfaces, or ability to land on extremely rough surfaces—possibly with tree stumps or bomb craters.

Tradeoff studies have been mentioned previously in this chapter and a number of these are appropriate in the project definition phase. They should be fully documented and kept on file. Some examples are

- 1) Number and size of tires vs cost, weight, and flotation.
- 2) Location of main gear (wing, nacelle, or fuselage) vs cost, weight, and performance.
- 3) Brake material selection.
- 4) Use of auxiliary braking systems.
- 5) Electric vs hydraulic systems for retraction, extension, and brakes.

When all of the above tasks have been completed in the project definition phase, the concept is frozen, the proposal is written, and the next milestone is contract award. The customer may have been influenced by certain aspects of a competitor's proposal and, as a result, may ask for certain design changes at this point—with appropriate impact on cost, weight, and performance.

2.4 POSTCONTRACTUAL DESIGN

By definition, the preliminary design phase continues until the Preliminary Design Review (PDR) has been completed, although by this time the personnel involved may well have changed to those who are more oriented toward project design activity. These are the engineers who are better acquainted with design details such as tolerances, surface finishes, current fastener types, and anticorrosive measures.

For military aircraft, the PDR must be scheduled prior to starting the manufacture of parts. During a PDR, the engineers describe the design to the customer, using sketches, block diagrams, concept drawings, and informal documentation. The customer determines that the design meets the specification requirements.

From this point until the Critical Design Review (CDR), the design is refined in every detail so that it can be finalized and the parts manufactured. A diagram for the work involved is provided in Fig. 2.5.

Prior to the CDR, the following tasks are performed:

- 1) Tire and wheel selection or design is concluded, load/speed/time data revised, and vendors established. If there are any peculiar requirements that the tire has not met, compliance is accomplished at this point. This could include, for instance, passage over deck arresting cables or step bumps.
- 2) Brake energy requirements are updated, vendors selected, and the design is finalized. If other deceleration devices, such as drag chutes, are used on the aircraft, then calculations are made to determine the decelerations attributable to each device.
- 3) Shock absorber details and support structure are sized to be compatible with the revised loads.
- 4) Electrical and hydraulic power requirements are defined for retraction,

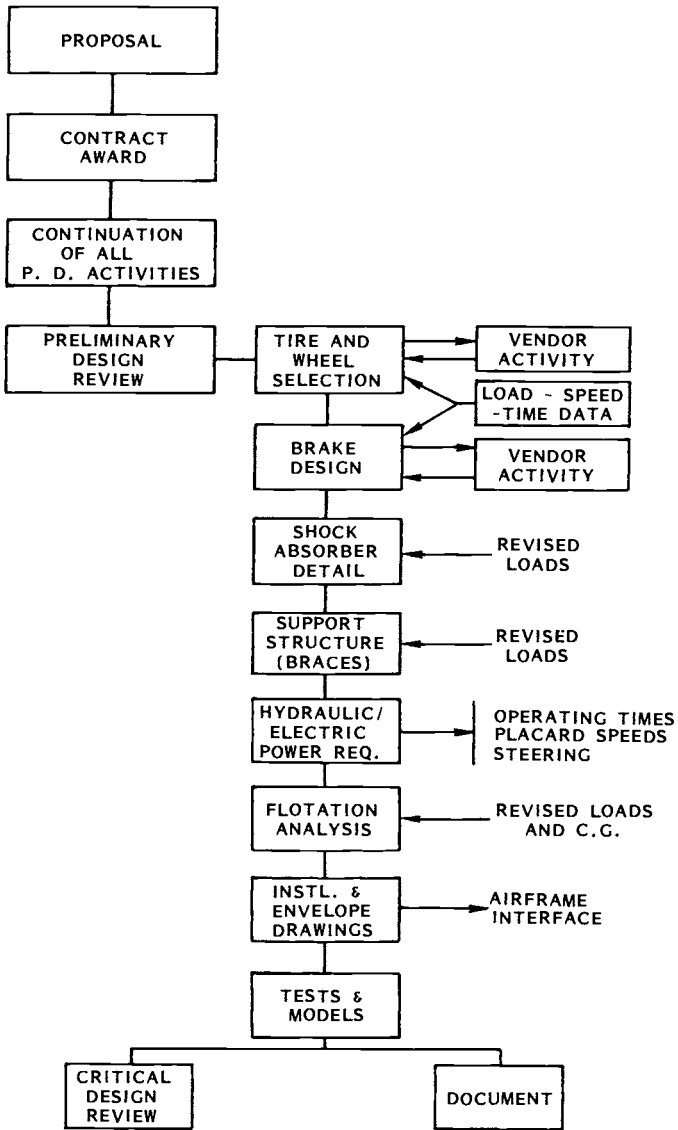


Fig. 2.5 Postcontractual design activity through CDR.

extension, and steering. Operating times, placard speeds, steering angle, and steering rate are determined and turning diagrams prepared.

5) Flotation analyses are updated again to reflect changes in loading on the landing gear.

6) Installation and space envelope drawings are prepared to facilitate determination of stowed landing gear clearances and to provide appropriate information to the airframe designers. This is a primary item for inclusion in the aircraft "Basic Data Book" that should be in the course of preparation at this time.

7) Tests and models may be used in this phase to acquire confidence in the proposed design, to gain a better understanding of problem areas, to display complex kinematics, and to evaluate the locking mechanisms.

8) The entire design is then documented for presentation at the CDR.

The detail design and manufacture of the landing gear (or parts thereof) may be subcontracted to one of several companies that specialize in those parts. This practice varies considerably—some aircraft companies design and build their own gears, some design the gears and have the shock struts built by a specialist company, some ask these companies to undertake all of the detail design and manufacture, and some bring in the specialists during the project definition phase. Typical examples of these specialist companies are Cleveland Pneumatic Co. and Menasco in the United States, Dowty Rotol in England and Canada, and Messier-Hispano-Bugatti in France.

The work involved in this phase includes detail design of the parts for production, system schematics, system installations, assembly drawings, installation drawings, loads analysis, power analysis (hydraulic and electrical), tests, and procurement activity. Forging and casting drawings are usually completed first because of the long lead times needed. Working mockups (full scale) are sometimes employed to prove the kinematics and structural clearances and to facilitate hydraulic routing. Analyses are conducted to evaluate shimmy, dynamic response to airfield roughness, and fatigue and damage tolerances.

Various tests are conducted before first flight. During the design phase, photoelastic tests are often used to show areas of high stress concentration and to modify the design accordingly. Static structural tests measure the deflections and spring rate of the gear under load and also confirm its structural integrity. Drop tests are employed to verify shock absorber efficiency and to modify metering pin/orifice sizes to improve that efficiency if necessary. Shock strut proof pressure and leak tests are conducted and overall fit, function, and endurance tests are performed.

Procurement activity involves such items as wheels, tires, brakes, skid control, actuators, miscellaneous valves and fittings, position switches, as well as the basic landing gears themselves if they are being designed and/or built by a subcontractor. The normal procedure here is to prepare specifications and vendor drawings to which competing vendors can respond. These responses are then analyzed and rated to select vendors, who, in many cases, must then provide Qualification Test Procedures for approval by the airframe manufacturer. When the parts have been built, they are tested by the vendor, who then submits a Qualification Test Report for approval. This

ensures that all of the contractor-specified requirements have been met and full documentation is available to prove it.

Other reports that should be completed before first flight are the failure modes and effects analysis (FMEA) and reliability and maintainability analyses. The FMEA is particularly important in that it evaluates the effects of the failure of any part in the overall landing gear system to determine its effect on the aircraft. Since this analysis may uncover some deficiencies that had been overlooked, its timing should be such that design changes can be made without affecting the first flight schedule.

Reliability and maintainability analyses have been required in the last 20 years or so in recognition of a growing demand for increased mission readiness and improved economics. Life cycle costs and durability are becoming more and more important. Evidence must be produced to show how measures have been taken to minimize maintenance man-hours per flight hour.

2.5 AIR VEHICLE TEST

Despite all of the analyses, tests, and mock-ups conducted in the design phase, there are still tests to be conducted after the landing gears and systems have been installed on the aircraft. It is surprising how many problems still occur—although they are usually easily correctable.

Prior to flight test, tests are made to retract and extend the gear a number of times, with the aircraft on jacks. Initially, the retraction rate is lowered so that clearances can be checked in every area while the gear slowly proceeds to its up and locked position. The doors are often disconnected in the first tests so that there is adequate room to examine the clearances. After the low-rate retraction tests have been completed with doors operable, the tests are repeated at full power to verify that dynamic effects do not impair the correct functioning of the gears.

Proof loading tests are often conducted before first flight, with simulated air loads applied to the gears and doors; with these loads applied, the gear is again cycled. Apart from checking the ability to operate properly under load, the gapping of doors is examined. Aerodynamic suction forces tend to pull the doors outward and, if this is severe enough, the air forces penetrate the inside surfaces of the doors and blow them off the aircraft—hence, the need to check gapping.

Vibration tests on the aircraft determine the landing gear spring rate and natural frequency. The test results are then compared with earlier analyses to verify system stability under the complete spectrum of anticipated operational conditions.

During taxi tests, the normal and emergency brake systems are evaluated along with the skid control and steering system. Stop distances are compared with predictions and the aircraft is maneuvered to examine steering and damping with normal and emergency systems. Shimmy tests are also conducted.

Demonstrations are conducted to show how towing, jacking, and mooring requirements have been met and, then, with the aircraft on jacks, a thorough

inspection is made again of the landing gear and its proper functioning before first flight.

Initial flight tests check the landing gear operation under normal conditions. As confidence grows, the envelope is expanded to include gear functioning up to its placard speed, rejected takeoffs, and operation at maximum gross weight.

Some defects that the author has observed in this final stage of development are:

- 1) Dragging brakes that overheat the tires and result in tire failure.
- 2) Inadequate attention to tire heat buildup during extended taxiing at high weight, causing premature tire failure.
- 3) Excessive wear on bearings due to improper sizing or material selection.
- 4) Failure of position switches due to the support brackets being too flimsy.
- 5) Doors being ripped off the aircraft due to improper rigging and/or inadequate stiffness. In this case, a plea must be made for simple rigging instructions to reduce the chances of it being done incorrectly.

References

¹Conway, H. G., *Landing Gear Design*, Chapman & Hall, London, 1958.

²Swihart, J. M., "The Boeing New Airplane Family," AIAA Paper 79-0526, 1979.

Bibliography

Ohly, B. "Landing Gear Design—Contemporary Views and Future Trends," *International Journal of Aviation Safety*, March 1985, pp. 6–10.

Young, D. W., "Aircraft Landing Gears—The Past, Present and Future," *Proceedings of the Institution of Mechanical Engineers*, Vol. 200, No. D2, 1986, pp. 75–92.

3 INITIAL LAYOUT

3.1 CONCEPTUAL DESIGN PHASE

Transformation of Requirements to Pictorial Configuration

As noted in the previous chapter, market intelligence and discussions with potential customers provide the aircraft industry with advance information that new requirements are being considered. Initial concepts are prepared based upon some degree of guesswork. Supposed requirements are listed and, using the company's data bank together with rough calculations by the aerodynamics, structures, and weights departments, an iterative approach is taken to develop a series of possible configurations.

The customer eventually releases the Specific Operational Requirement (SOR) or its equivalent. This is not necessarily intended to lead up to a contract, but is intended to stimulate interest and to start serious design investigations (using company funds). A typical case recently was the advocacy of a 150-passenger transport by some U.S. airlines. The SOR defines the customer's overall needs, including such items as payload/range, takeoff and landing distances, cruise performance, accommodation, cargo to be carried (weight and size), availability date, and special characteristics that depend upon the type of aircraft. Items such as gross weight are not defined—these are a fallout, determined by the airframe manufacturer.

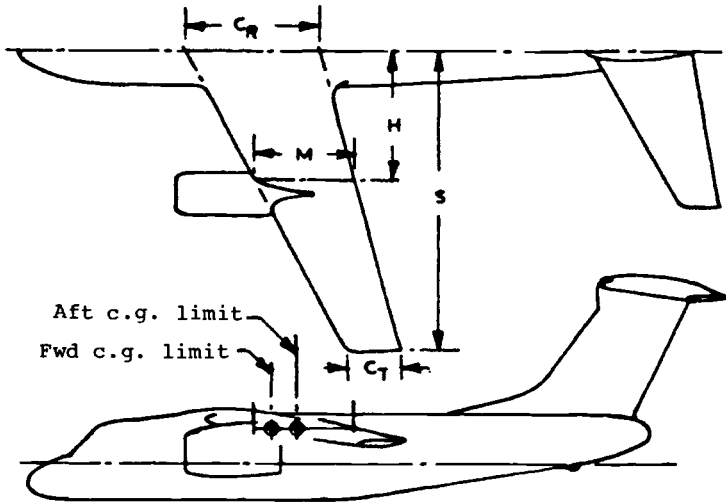
The major aerospace companies now have computer programs to perform the iterative analysis mentioned above. The program uses the requirements as input data, adds the data bank stored in its memory, and prints out the aircraft's vital characteristics from which layouts can be made. Among these characteristics are the maximum gross weight and the mean aerodynamic chord (MAC) location.

At this point, no thought is given to kinematics, structural sizing, or brake requirements. Instead, the landing gear is represented by a "stick diagram." The following paragraphs represent a typical step-by-step approach that would be taken by the landing gear designer.

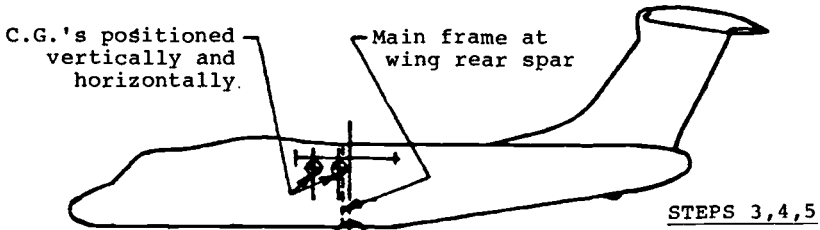
Landing Gear Location

Referring to Fig. 3.1, step 1 involves superimposing the MAC on an aircraft side and plan view. (Note: the MAC length shown in the figure is for a straight tapered wing and its determination is not usually the responsibility of the landing gear designer.) Step 2 is to locate the forward and aft center-of-gravity (c.g.) limits on the MAC. These limits are obtained from the

$$\text{MAC LENGTH (M)} = \frac{2}{3} \left[C_R + C_T - \frac{C_R C_T}{C_R + C_T} \right] \quad H = \frac{S(C_R - M)}{C_R - C_T}$$



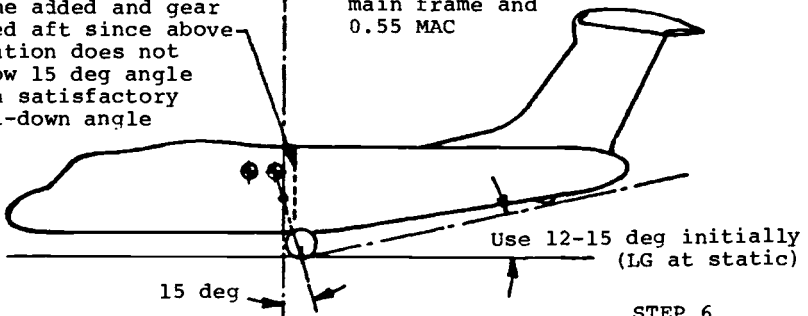
STEPS 1,2



STEPS 3,4,5

Frame added and gear moved aft since above location does not allow 15 deg angle with satisfactory tail-down angle

Gear located by main frame and 0.55 MAC



STEP 6

Fig. 3.1 First steps in longitudinal location.

department specializing in aircraft weight and balance and are based on negotiations with the Stability and Control Department.

In step 3, lines are drawn vertically from these forward and aft c.g. limits to locate the vertical position of the c.g. along these lines. Since the vertical c.g. position is generally of little importance in the determination of aircraft configurations, its position will probably not have been calculated at this stage and a "guesstimate" must be made. The gear designer is interested only in the upper limit of this vertical c.g., so if the aircraft is, for instance, a high-wing cargo aircraft, an approximate calculation will be made assuming full wing fuel and no cargo. A low-wing passenger aircraft would be critical with no wing fuel and a full load of passengers.

In step 4, from observations of wing spar locations and other structure, the main gear is placed in a position that appears to be the most conducive to the efficient transmission of loads. In wing-mounted and nacelle-mounted gears, except for light aircraft with little or no wing sweep, it is common to mount the main trunnion of the aft side of the wing rear spar. If the gear is retractable, it will swing forward into a pod or nacelle or it will swing inboard into a cavity behind the spar. Apart from light aircraft, it is unusual to retract the gear into an area between the spars, because it compromises structural integrity where bending loads are reacted in the wing skins. The British Aerospace Nimrod and its forerunner the Comet are exceptions to this rule.

In fuselage-mounted gears, it is usual to have a main frame in the fuselage attached to the wing rear spar. This is an ideal structure for mounting the landing gear, although on swept-wing aircraft the MAC moves aft with the sweepback; thus, the c.g., having also moved aft, is often too close to the rear spar bulkhead to suit mounting of the gear at that point. In that event, a secondary frame must be added aft of the rear spar frame, with the landing gear loads transmitted forward to the rear space—probably by shear in the fuselage skin.

Step 5 involves a recheck of the ensuing location of the main landing gear. It should be between about 50–55% of the MAC.

In step 6, a line is drawn from the aft c.g. at 15 deg to the vertical, as depicted in Fig. 3.1, until it meets the vertical line drawn through the wheel center. The intersection of these lines is the first approximation of the static ground line. The 15 deg figure has been used for many years and is based on two parameters: aft towing and tail tipping. For aft towing, it ensures that the aircraft will not tip if the brakes are applied to cause a deceleration of 8 ft/s/s. Tail tipping is prevented because the aft fuselage and/or tail bumper design will not permit the tail to be lowered by as much as 15 deg in most aircraft and the c.g. will not, therefore, rotate over and aft of the main gear.

At this point, the main gear has been located for a contemporary tricycle-gear aircraft. Procedures for other aircraft types are given later, but the process is similar in all cases. The next step is to select tire sizes, but this cannot be done until the static loads have been determined. However, for rough approximations, a designer may assume, say, 92% of the gross weight on the main gear at aft c.g. conditions.

It is usual, however, to locate the nose landing gear at this stage. It should

be placed as far forward as possible to minimize its load, maximize flotation, and maximize stability. Conversely, the load should not be too light; in that event, steering would be difficult and the righting moment in a drift landing would be marginal. Nose gear loads in the static condition generally vary about 6–20%, but these should be considered as extremes. A preferable range would be 8% with the c.g. aft, increasing to 15% with the c.g. forward.

From a review of the structure, a suitable support frame must be determined, preferably so that the gear will retract forward, as illustrated in Fig. 3.2 and thereby have free-fall capability. The latter feature is most desirable

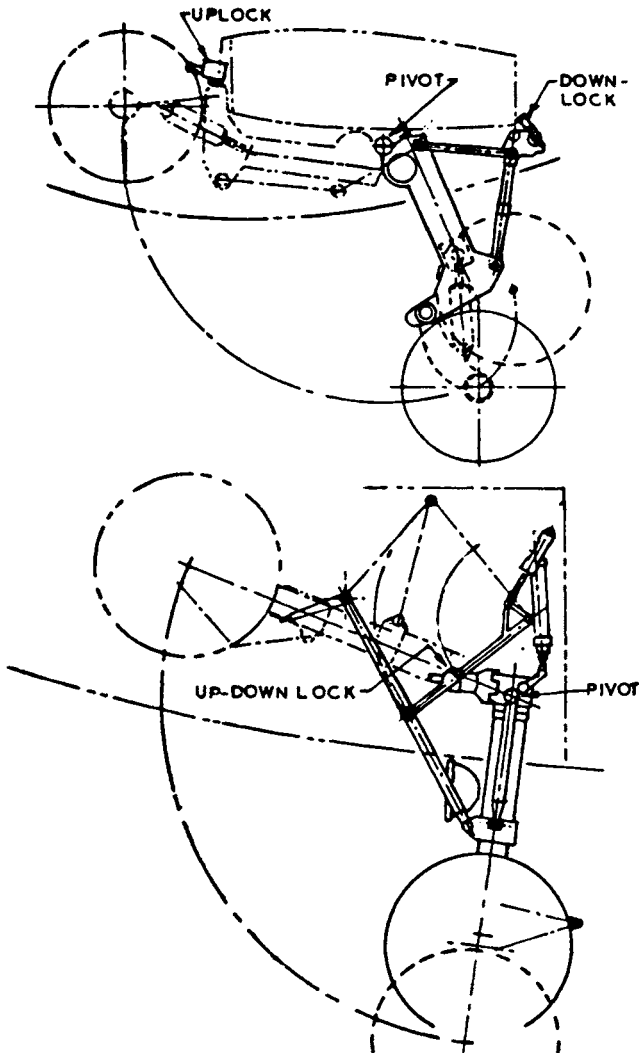


Fig. 3.2 Forward retracting landing gears.

since a complete failure in the extension system does not necessarily lead to a wheels-up landing. The pilot merely pulls an emergency release lever that releases the uplocks and the trapped actuator fluid (if used), after which gravity and air drag pull the gear into a down-and-locked position. This capability should also be used on the main gear if possible.

Having selected the appropriate support frame, the next step is to suspend the gear from it and to assume initially that the wheel center will be about 3 in. aft of the strut centerline to provide adequate shimmy prevention. Then, the nose gear load must be calculated.

The calculation of nose gear load uses the diagram shown in Fig. 3.3 and the following appropriate formulas:

$$\text{Max static main gear load (per strut)} = W(F - M)/2F$$

$$\text{Max static nose gear load} = W(F - L)/F$$

$$\text{Min static nose gear load} = W(F - N)/F$$

where W is the maximum gross weight and the other quantities are defined in Fig. 3.3.

When the tires are selected, at a later step, it is necessary to know the nose gear dynamic load. For convenience, this load is usually calculated at the same time as

$$\text{Max braking nose gear load} = \text{max static load} + \frac{10J \cdot W}{32.2F}$$

where the braking supplied 10 ft/s/s deceleration and the other quantities are defined in Fig. 3.3.

If the minimum static nose gear load is too small, i.e., less than 6% of the aircraft weight, either the nose gear or the main gear must be moved aft. Note that very small main gear movements usually have a pronounced effect on nose gear loads. If the maximum static nose gear load is too high, the

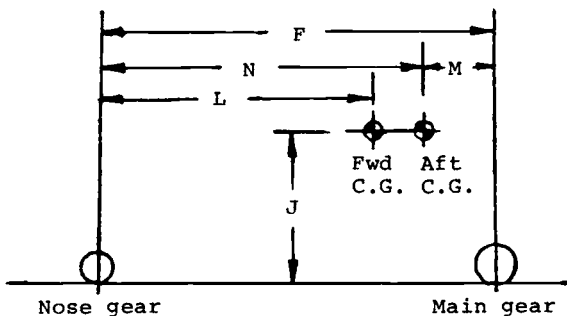


Fig. 3.3 Diagram for nose landing gear load calculation.

Table 3.1 Tires Used on Typical Aircraft

| Aircraft | Gross weight × 1000 lb | Wheels per strut | Tire size | Tire press, psi | Gear type ^a |
|-------------|---------------------------|---------------------|--------------|-----------------------|---------------------------|
| C-45G | 9.6 | 1 | 11.0 × 12 | 35 | S |
| C-10A | 14.5 | 1 | | | S |
| DC-3 | 28.0 | 1 | 17.0 × 16 | 50 | S |
| C-7A | 28.5 | 2 | 11.0 × 12 | 40 | T |
| C-8A | 38.0 | 2 | 15.0 × 12 | | T |
| C-47D | 33.0 | 1 | 17.0 – 16 | 56 | S |
| C-140A | 42.0 | 2 | 26 × 6.6 | 205 | T |
| F-27-40 | 43.5 | 2 | 33.4 × 9.7 | 80 | T |
| NORATLAS | 45.4 | 1 | 18.5 × 20 | | S |
| Convair 440 | 50.0 | 2 | 34 × 9.9 | 75 | T |
| C-2A | 54.8 | 1 | 36 × 11 | 185 | S |
| C-46F | 55.0 | 1 | 19.0 × 23 | 70 | S |
| C-123K | 60.0 | 2 | 17.0 – 20 | 81 | T |
| C-131E | 60.5 | 2 | 12.5 – 16 | 70 | T |
| C-119G | 72.7 | 2 | 15.5 – 20 | 80 | T |
| C-54G | 82.5 | 2 | 15.5 – 20 | 82 | T |
| DC-4 | 82.5 | 2 | 15.5 – 20 | 82 | T |
| DC-6B | 107.0 | 2 | 15.5 – 20 | 107 | T |
| C-9A | 108.0 | 2 | 40 × 14 | 155 | T |
| B-737-200 | 111.0 | 2 | 40 × 14 | 145 | T |
| C-118A | 112.0 | 2 | 15.5 – 20 | 120 | T |
| DC-9-41 | 115.0 | 2 | 41 × 15 | 165 | T |
| L-188 | 116.0 | 2 | 13.5 × 16 | 135 | T |
| C-130A | 124.2 | 2 | 20.0 – 20 | 65 | ST |
| C-130B | 135.0 | 2 | 20.0 – 20 | 75 | ST |
| L-1049 | 140.0 | 2 | 17.0 × 20 | 130 | T |
| DC-7C | 143.0 | 2 | 15.5 – 20 | 127 | T |
| C-121G | 145.0 | 2 | 17.2 – 20 | 145 | T |
| L-100-30 | 155.0 | 2 | 56 × 20 | 105 | ST |
| B-727-200 | 173.0 | 2 | 49 × 17 | 168 | T |
| C-130E | 175.0 | 2 | 20.0 – 20 | 95 | ST |
| C-130H | 175.0 | 2 | 56 × 20 | 105 | ST |
| Convair 880 | 185.0 | 4 | 12.5 × 16 | 150 | TT |
| C-97G | 187.0 | 2 | 55.0 – 16 | 175 | T |
| C-124C | 216.4 | 2 | 25.0 – 28 | 65 | T |
| B-720B | 235.0 | 4 | 40 × 14 | 145 | TT |
| Convair 990 | 253.0 | 4 | 41 × 15 | 170 | TT |
| C-133B | 300.0 | 4 | 20.0 – 20 | 95 | TT |
| C-141A | 316.1 | 4 | 44 × 16 | 180 | TT |
| B-707-320C | 336.0 | 4 | 46 × 16 | 180 | TT |
| DC-8-63F | 358.0 | 4 | 44 × 16 | 200 | TT |
| L-1011-1 | 409.0 | 4 | 50 × 20 | 175 | TT |
| DC-10 | 533.0 | 4 ^b | 50 × 20 – 20 | 185 | TT + T |
| C-5A | 769.0 | 6 ^c | 49 × 17 | 155 | TTDT |
| B-747B | 775.0 | 4 ^c | 46 × 16 | 210 | DTT |

^aS = single wheel, ST = single tandem, TTDT = two twin delta in tandem, T = twin wheel, TT = twin tandem, DTT = double twin tandem.

^bThree struts. (Two struts are normal)

^cFour struts.

reverse procedure must be used (i.e., move the nose gear forward or move the main gear forward). In many cases, it is necessary to move both the nose and main gears somewhat to obtain a satisfactory overall compromise in the loading. It may also be necessary to deviate slightly from the 12–15 deg angles used in step 6. If the aircraft is designed for commercial requirements, a 7% safety factor must be added to the above loads prior to tire selection.

The nose and main gears have now been located in the side view and the static loads are known. A preliminary tire selection can now be made. It is first necessary to decide how many tires will be used on each strut. In many cases, the answer is obvious. Table 3.1 indicates that all aircraft weighing 60,000–175,000 lb seem to have two main struts and two tires per strut. All aircraft weighing 235,000–400,000 lb have two main gear struts and four tires per strut. Below 60,000 lb, it is possible to use either one or two tires per strut. If it is practical, two tires per strut should be used—it is safer! Between 175,000 and 235,000 lb, a decision must be made as to whether there will be two or four tires per strut. The answer is controlled to some extent by the anticipated stowage concept. For instance, the C-130 uses two very large tires on each side of the aircraft; they are placed in tandem and the fuselage pod can be relatively slim. If a four-wheel bogie had been used, the pod would have been fatter—even though the tire sizes might have been smaller.

As aircraft approach 500,000 lb, runway loading becomes more important, a factor that cannot always be sufficiently alleviated by merely increasing the tire size or number of tires per strut. In that event, the only solution is to increase the number of struts. The Boeing 747 and Lockheed C-5 are typical examples.

Tire Selection

From the maximum main gear static load previously calculated, it is necessary to divide that load by the number of tires per strut to obtain the static single wheel load. Two problems have to be considered for the nose gear: the static and braking loads. These loads (previously calculated) are divided by the number of nose gear wheels to obtain the single-wheel static and braking loads. With these data, it is then possible to use the tire manufacturers' catalogs to select the tires. Typical data for tires are given in Table 3.2.

As an example, consider an aircraft with the following characteristics:

| | |
|-------------------------------------|------------------|
| Maximum gross weight | = 45,000 lb |
| Maximum main gear load (static) | = 21,400 lb/gear |
| Maximum nose gear load (static) | = 6,300 lb |
| Maximum nose gear braking load | = 11,300 lb |
| Maximum speed of aircraft on ground | = 180 mph |

Table 3.2 Typical Tire Selection Data

| Type | Size | Ply rating | Load rating, lb | Infl. press., psi | Speed rating, mph | Max diam, in. | Max width, in. | Weight, lb |
|-----------|--------------|------------|--------------------|-------------------|-------------------|---------------|----------------|------------|
| Main gear | | | | | | | | |
| VII | 30 × 6.6 | 14 | 12,950 | 320 | 225 | 30.12 | 6.50 | 38.0 |
| VII | 25 × 6.75 | 18 | 13,000 | 300 | 275 | 25.50 | 6.85 | 35.5 |
| VII | 29 × 7.7 | 16 | 13,800 | 230 | 200 | 28.40 | 7.85 | 41.5 |
| VIII | 26 × 8.0-14 | 16 | 12,700 | 235 | 275 | 26.00 | 8.00 | 38.0 |
| ND | 34 × 9.25-16 | 16 | 15,500 | 155 | 200 | 34.00 | 9.25 | 55.5 |
| Nose gear | | | | | | | | |
| VII | 20 × 4.4 | 12 | 7,725 ^a | 275 | 200 | 20.00 | 4.45 | 14.5 |
| VII | 18 × 5.5 | 14 | 9,300 ^a | 215 | 275 | 17.90 | 5.70 | 14.6 |
| VII | 18 × 5.7 | 14 | 9,300 ^a | 215 | 230 | 17.80 | 5.60 | 13.7 |
| VII | 26 × 6.6 | 8 | 7,950 ^a | 120 | 200 | 25.75 | 6.65 | 27.2 |

^aThe load rating quoted for nose gear application is the "maximum nose load," i.e., the maximum load applied during the braking (10 ft/s² deceleration) condition. That rating is chosen because it is more severe than the static rating, a feature that is discussed further in Chapter 6.

The specifications require two tires on each main gear and two tires on the nose gear. Thus, the tire loads are as follows:

$$\begin{aligned} \text{Main gear tire load} &= 10,700 \text{ lb} \\ \text{Nose gear tire load (static)} &= 3,170 \text{ lb} \\ \text{Nose gear braking load} &= 5,750 \text{ lb} \end{aligned}$$

To avoid costly redesign as the aircraft weight fluctuates during the design phase and to accommodate future weight increases due to anticipated aircraft growth, the above loads are factored upward before selecting the tires. A 25% growth factor is often used. With this factor, the loads are as follows:

$$\begin{aligned} \text{Main gear tire load} &= 13,373 \text{ lb} \\ \text{Nose gear tire load} &= 3,938 \text{ lb} \\ \text{Nose gear braking load} &= 7,188 \text{ lb} \end{aligned}$$

The rated loads of the selected tires should be as close as possible to the above values if the minimum weight is to be realized.

The tires listed in Table 3.2 are appropriate to this example. It is clear that several tires are capable of meeting the required load conditions. The selection, then, must be based upon factors other than load. If the aircraft is a

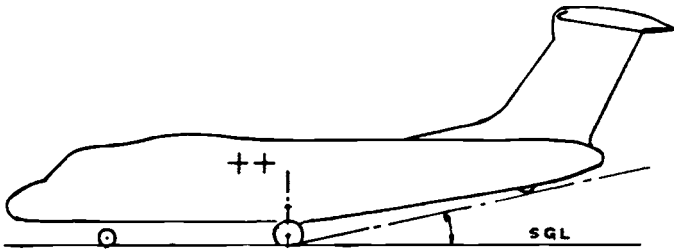


Fig. 3.4 Final step of concept.

fighter, minimum weight and size will be particularly important, irrespective of tire pressure. In this case, a 25×6.75 tire would be selected for the main gear. If the aircraft is a corporate jet, a 29×7.7 tire would be chosen for the main gear. Load and pressure vary almost linearly at normally considered tire deflections; thus, if 230 psi is required for 13,800 lb, only 180 psi will be required for an actual load of 10,700 lb. Commercial operators prefer the lower pressures in order to maximize tire life and minimize runway stresses. The nose gear tire selected for the corporate jet would be the 26×6.6 ; ~ 90 psi inflation pressure would be required for the actual load.

Some of the tradeoffs involved in tire selection are discussed in later chapters. For instance, the nose gear tire weighs 27.2 lb, while the smaller high-pressure 18×5.7 tire weighs 13.7 lb. With two tires per aircraft, a weight penalty of 27 lb is thus paid to obtain the lower tire pressure.

To place the tires in the deflected vertical position, note their loaded radii on the tire selection charts. For the 29×7.7 main gear tire, the radius is 12.2 in. This is the distance from the ground to the axle center with the aircraft static and the tire at optimum deflection. The nose gear tire is a bit more complicated: by definition, its tire deflection will be 48% under dynamic loads appropriate for 10 ft/s/s braking. Using the load/deflection curve for the particular tire and the nose tire pressures obtained above (90 psi for the 26×6.6 tire), it is possible to determine the deflection with the static nose gear load. This allows the nose gear axle center to be determined and, as with the main gear, it becomes the starting point for determining compressed and extended shock strut positions.

At this point, no further work is usually done on the landing gear in the conceptual design phase. The tires are shown on the three-view drawing with no visible means of connection to the airframe. The static ground lines and tail-down lines are also shown, as depicted in Fig. 3.4.

3.2 PROJECT DEFINITION PHASE

Approximate Strokes and Kinematics Concepts

Based upon the required sink speeds and load factors, the vertical wheel travel must be determined. Except for levered-suspension gears, this is the same as the shock strut stroke, so a decision must be made as to whether a

levered suspension will be used—and if so, how much leverage will be applied. Assume that the gear is a normal design in which the wheel and strut travel are the same. The first step is to determine the maximum load acceptable in the shock strut. This load comprises the static load plus the dynamic reaction load. When that load is divided by the static load, the reaction factor N is obtained. This is sometimes called the landing gear load factor or merely the landing load factor. Its value ranges from 0.75–1.5 for large aircraft to 3.0 for small “utility” aircraft and to 5.0 for some fighters. Its permissible magnitude is determined by the airframe designers and structures specialists. They must design the airframe to accommodate those factors during landing.

Initially, the aircraft is assumed to be a rigid body, with no relative acceleration between the c.g. and the gear attachment point. Thus, the load factor at the c.g. is the same as the attachment.

To understand fully the relationship between the load factor at the center of gravity $N_{c.g.}$ and the landing gear load factor N , consider a free body being acted upon by shock strut forces and lift, as

$$N_{c.g.} = \frac{\text{sum of all external forces}}{\text{mass}} = \frac{F_S + L}{\text{mass}}$$

where F_S is the shock strut force and L the lift. Thus,

$$N_{c.g.} = \frac{F_S}{\text{mass}} + \frac{L}{W/g}$$

When lift = weight W (as specified in FAR Part 25 for transport-type aircraft*),

$$N_{c.g.} = \frac{F_S}{\text{mass}} + g = 1 + \frac{F_S}{\text{mass}}$$

If, for convenience, the landing gear load factor N is defined as being equal to F_S/mass , then

$$\underline{N_{c.g.} = 1 + N \text{ for FAR Part 25 aircraft}}$$

On utility and aerobatic aircraft, the rules of FAR Part 23* apply and lift = $0.67W$; i.e., $W = L/0.67$, as

$$\begin{aligned} N_{c.g.} &= \frac{F_S}{\text{mass}} + \left(L \times \frac{0.67g}{L} \right) \\ &= \frac{F_S}{\text{mass}} + 0.67 \end{aligned}$$

*See Chapter 15.

Therefore,

$$\underline{N_{c.g.} = 0.67 + N \text{ for FAR Part 23 aircraft}}$$

Thus, for a given aircraft load factor, N will be higher for FAR Part 23 aircraft than for FAR Part 25 aircraft. When the aircraft comes to rest on the ground, the lift is zero and the shock strut force is equal to the aircraft weight; i.e., $F_S = W$. Therefore,

$$N_{c.g.} = \frac{F_S}{W/g} = \frac{W}{W/g} = g$$

So,

$$\underline{N_{c.g.} = 1.0 \text{ when the aircraft is at rest}}$$

Later in the design process, it is often desirable to recognize the inertial reaction of the gear unsprung weight (wheel, tire, brake, axle, piston, and oil—if the gear uses an oleo-pneumatic shock absorber). The methodology is as follows.

Referring to Fig. 3.5, if M_u is the mass of tires, wheels, brakes, axle, piston, and oil, then $F_S = F_t - M_u \dot{S}$. During landing, the shock absorber and tire must also absorb the sum of the kinetic energy and potential energy of the aircraft; thus,

$$(S_t \times n_t \times NW) + (S \times n_s \times NW) = \frac{WV^2}{2g} + (W - L)(S + S_t)$$

tire energy strut energy kinetic energy potential energy

where

S_t = tire deflection under N times static load, ft

S = vertical wheel travel, ft (unknown)

n_t = tire efficiency, generally assumed to be 0.47

n_s = shock strut efficiency (assumed initially as 0.80 on an oleo-pneumatic strut)

N = reaction factor

W = aircraft weight, lb

L = lift, lb

V = sink speed, ft/sec

Dividing both sides of the above equation by W , we have

$$S_t n_t N + S n_s N = \frac{V^2}{2g} + \frac{(W - L)(S + S_t)}{W}$$

Let $K = L/W$, the lift ratio. Then,

$$\underline{N(S_t n_t + S n_s) = \frac{V^2}{2g} + (1 - K)(S + S_t)}$$

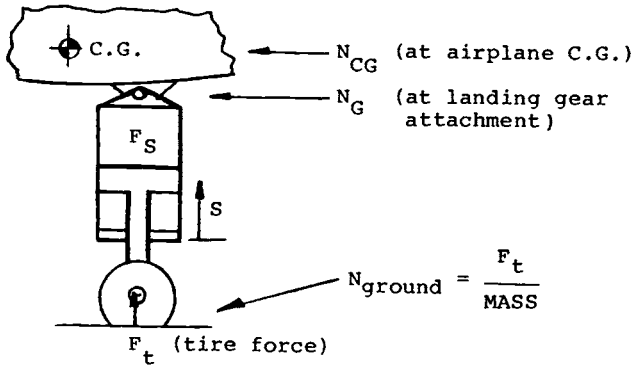


Fig. 3.5 Shock strut basic dynamics.

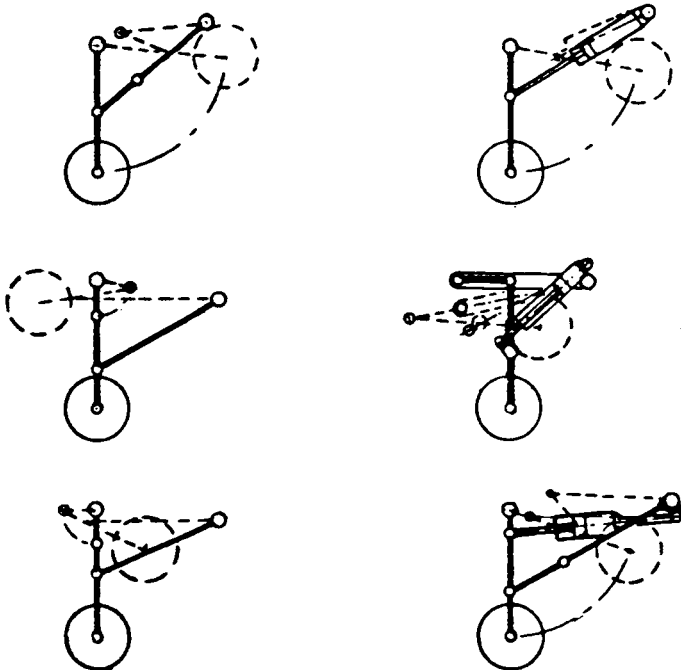


Fig. 3.6 Typical stick diagrams.

Inserting the assumed values into this equation, for an oleo-pneumatic strut, it becomes

$$\underline{N(0.47S_t + 0.8S) = V^2/2g + (1 - K)(S + S_t)}$$

For instance, let $N = 2.0$, $S = 0.33$ ft, and $V = 10$ ft/s and assume 1 g wing lift such that $L/W = 1.0$. Then,

$$2[(0.47 \times 0.33) + (0.8S)] = 10^2/64.4 + (1 - 1)(S + 0.33)$$

$$0.3102 + 1.6S = 1.55$$

Therefore, $S = 0.77$ ft = 9.3 in.

By adding 1 in. to this approximate stroke, the resultant shock strut will usually be satisfactory.

For an initial layout, assume that a quarter to a third of the total stroke is used in moving from static to compressed. Thus, for a 9.3 in. stroke, 3.1 in. is the distance from static to compressed and 6.2 in. that from static to extended. The ground lines with gears compressed and the tail-down line and angle can now be added to the side view.

The next step is to develop the basic kinematics concepts from which the "stick diagrams" are prepared. Some typical examples are shown in Fig. 3.6. The possibilities are limitless, depending on the ingenuity, imagination, and know-how of the designer.

Lateral Location of Main Landing Gear

The lateral location of the main landing gear affects the turnover angle and the ground clearances with movable surfaces such as ailerons and flaps, wing tips, engine nacelles, and, if used, propellers.

Figure 3.7 shows the method for calculating the turnover angle. The diagram shows a twin-wheel nose gear (which is different from that shown in various requirements documents where a single wheel is shown). With the latter, X and C are obviously zero. When there are more than one wheel at either the nose gear or main gear, assume that the aircraft will tip along a line drawn through the outboard wheels.

The angle θ must not be more than 63 deg for land-based aircraft or 54 deg for carrier-based aircraft. Although some aircraft do, in fact, approach these values, it is desirable to make it as small as possible. Table 3.3 lists the turnover angles of a number of aircraft. Note that it is sometimes extremely difficult to have low angles on high-wing aircraft because their landing gears are often mounted on the fuselage side and thereby have narrow tracks. Since short takeoff and landing (STOL) aircraft are usually high-wing configurations, a high turnover angle is one of the problems the designer must solve. Lockheed, Boeing, and McDonnell-Douglas cargo transports, STOL and otherwise (C-130, C-141, C-5, AMST, and C-17), are all high-wing aircraft with

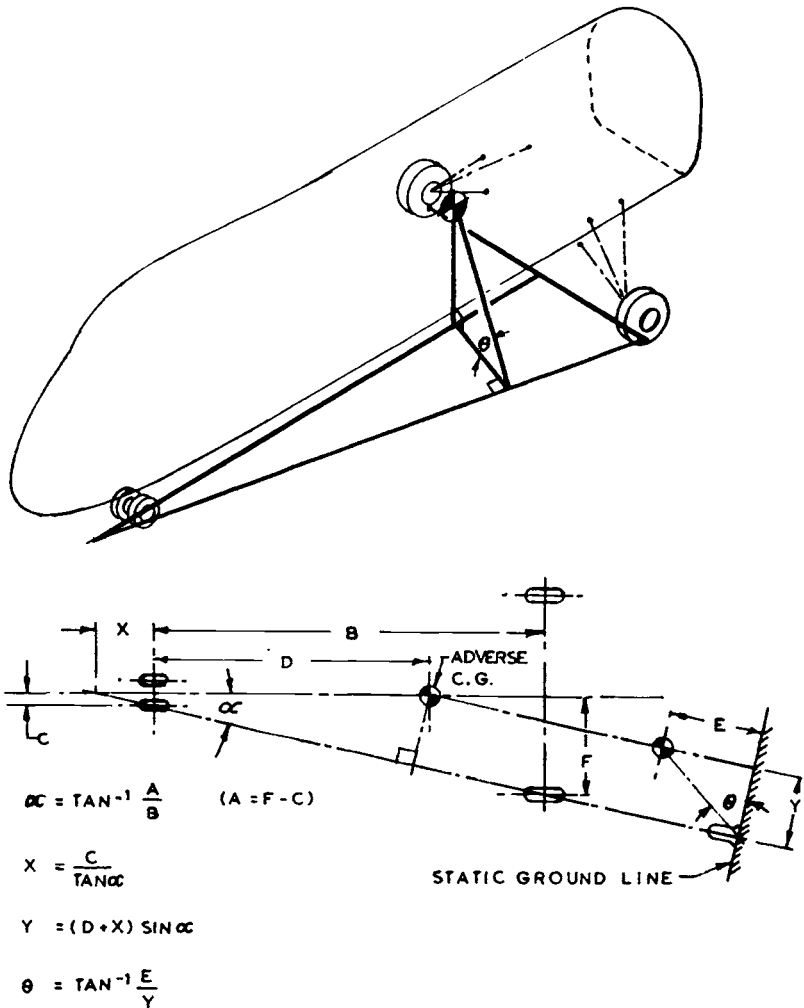


Fig. 3.7 Turnover angle calculation.

relatively narrow-track gears mounted on the fuselage. De Havilland Canada aircraft such as the DHC-5, Dash-7, and Dash-8 have nacelle-mounted gears with a consequent reduction in the turnover angle. Figure 3.8 shows the DHC-5 nacelle-mounted arrangement. Another approach is to use a bicycle-type gear, as on the B-47, with outrigger wheels between the siamese engine nacelles to restrict turnover. This is illustrated in Fig. 3.9.

Figure 3.10 depicts a method that was used by the author some years ago on a design that did not proceed beyond the study stage. The gear is suspended from the rear spar of a high wing and retracts forward into a streamlined pod.

Table 3.3 Turnover Angles

| Aircraft | Turnover angle, deg | Aircraft | Turnover angle, deg |
|---------------------|---------------------|-----------------------|---------------------|
| Low-wing transports | | High-wing transports | |
| Lockheed Electra | 34 | DHC Buffalo | 37 |
| Boeing 747 | 39 | Lockheed C-141A | 53 |
| A-300B | 41 | Breguet 941 | 61 |
| Lockheed L1011 | 43 | Lockheed L100-20 | 61 |
| Mercure | 44 | Fregat | 63 |
| Boeing 737-200 | 46 | Other | |
| Concorde | 47 | Aero Commander | 38 |
| DC-9-10 | 48 | Piper Turbo Navajo | 43 |
| Boeing 707-320B | 49 | Beech B9 ⁰ | 44 |
| Boeing 727-200 | 49 | Piper Comanche | 45 |
| Fighters | | Beech U-21A | 47 |
| F-4E | 39 | Bonanza | 51 |
| F-104G | 36 | Piper Super Cub | 59 |

Note: The above values were calculated by the author and may vary somewhat from manufacturers' calculations due to differences in assumed critical center-of-gravity positions.

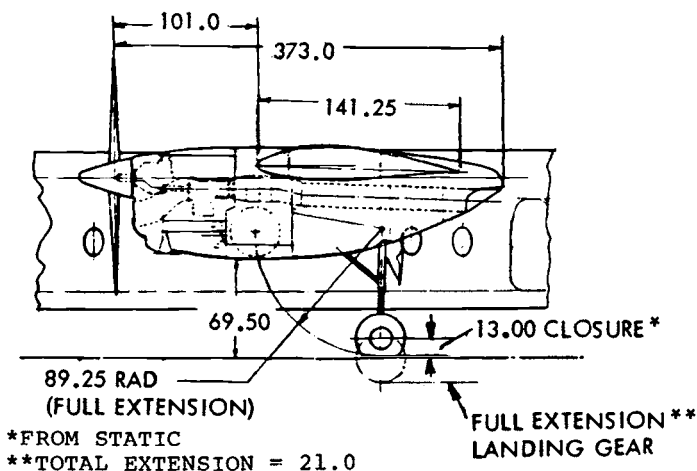


Fig. 3.8 DHC-5 nacelle-mounted gear (source: de Havilland Aircraft of Canada, Ltd.).

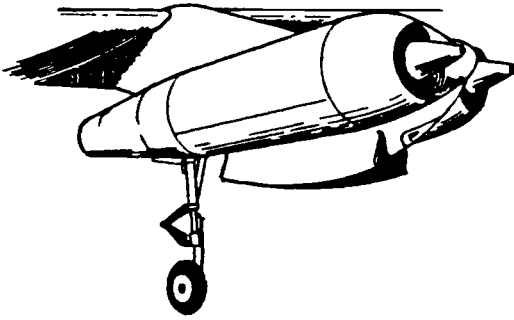


Fig. 3.9 Siamese podded engines (B-47).

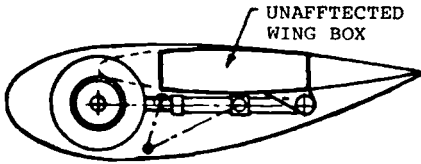


Fig. 3.10 Gear housed in wing pod.

Clearance Checks

There is now sufficient information to enable clearance checks to be made. This is where present-day computer graphics are particularly valuable. In a nutshell, these checks involve placing the aircraft in all the worst attitudes possible, with several landing gear failure conditions, and then checking to see if there are still adequate clearances with all moving and fixed parts of the aircraft. The results of these analyses often require changes to be made in the airframe and/or landing gear geometry. These changes can include refairing the aft fuselage, moving or shortening belly antennas, moving the engines inboard or upward, restricting control surface deflection, and lengthening the landing gear or moving it outboard.

In addition to drawings, a pitch/roll limitation diagram is often prepared, an example of which is shown in Fig. 3.11.

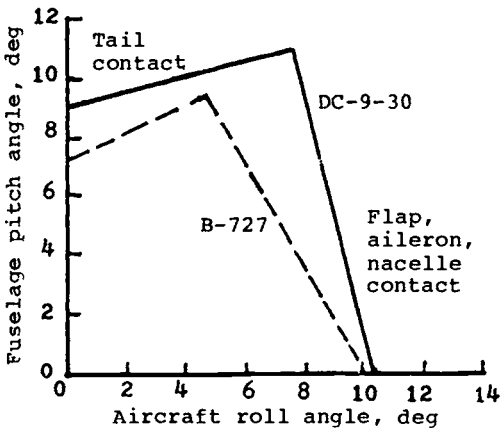
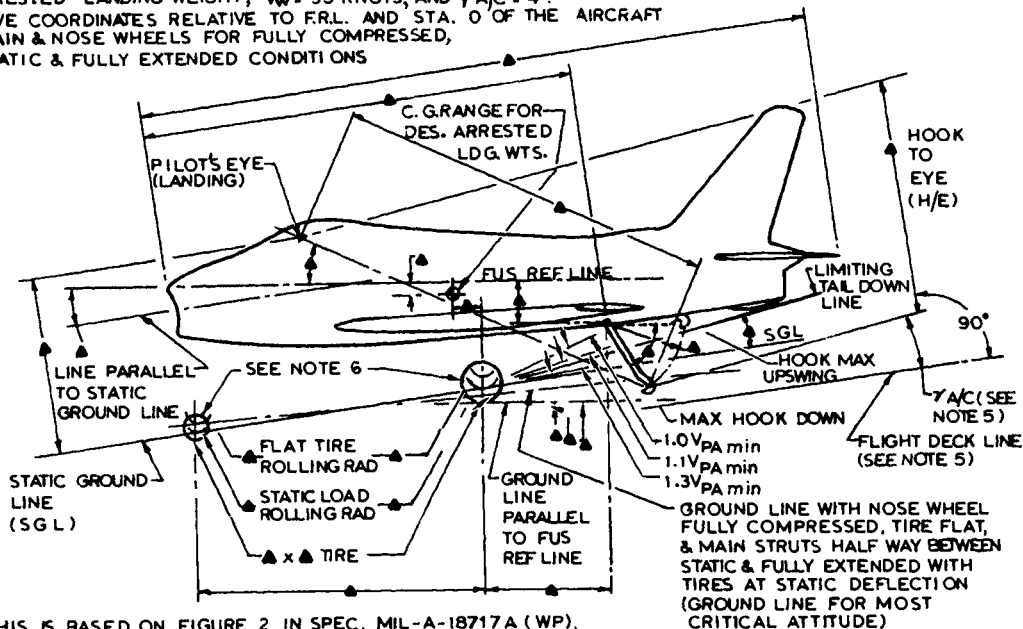


Fig. 3.11 Pitch and roll limitation diagram.

- NOTES:
1. REFERENCE SOURCE OF AERODYNAMIC DATA
 2. DIMENSIONS MARKED \blacktriangle TO BE INDICATED ON DRAWING
 3. DRAWING TO BE MADE ACCURATELY TO A SCALE NOT LESS THAN 1/16
 4. IF HOOK IS DISPLACED Laterally FROM THE ζ AIRCRAFT, DIMENSION THE DISPLACEMENT AT HOOK PIVOT & HOOK HEAD.
 5. USE FLIGHT DECK LINE OF FIG. A-4, IN SPEC MIL-1-1877A, DEFINED BY $V = V_{PA \text{ min}}$ AT CARRIER DESIGN ARRESTED LANDING WEIGHT, $V_w = 35$ KNOTS, AND $\gamma/A/C = 4^\circ$.
 6. GIVE COORDINATES RELATIVE TO F.R.L. AND STA. 0 OF THE AIRCRAFT MAIN & NOSE WHEELS FOR FULLY COMPRESSED, STATIC & FULLY EXTENDED CONDITIONS



THIS IS BASED ON FIGURE 2 IN SPEC. MIL-A-18717A (WP),
ARRESTING HOOK INSTALLATIONS, AIRCRAFT.

Fig. 3.12 Arresting landing arrangement.

The following checks are suggested:

1) Are the nose and main gear shock struts operating properly and the tires at normal inflation?

2) Is the nose gear shock strut fully compressed and the tire flat? Is the main gear shock strut fully compressed and the tire flat on one side, with static deflection and normal tire inflation on the other side?

3) Are all nose and main gear shock struts fully compressed and the tires flat?

4) Is the tail bumper touching the ground, with the main gear shock strut on one side halfway between static and fully extended and its tire at static deflection? Is the main gear shock strut on the other side fully compressed and the tire flat?

5) For Navy aircraft, there are also specific deck angles that have to be checked at this time because of catapulting, arresting, and landing attitude considerations. They are summarized in Fig. 3.12 and detailed in U.S. Navy Specification SD-24, "General Specification for Design and Construction of Aircraft Weapon Systems," Department of the Navy, Bureau of Naval Weapons.

REQUIREMENTS

This chapter provides the designer with requirements relating to landing gear design. No attempt is made to define detail requirements on parts that are normally provided by vendors, e.g., size and placement of part numbers on wheels, their surface finish, or types of bearings. Also, the source of a requirement is not given whenever it is considered to be acceptable internationally and by both military and civil authorities. In a few cases, U.S. Navy requirements are peculiar and these are noted; also British requirements are slightly different in some areas and these too are highlighted.

Although it is sometimes necessary for cost, weight, and schedule reasons to meet only the requirements of the first customer, it is often beneficial to design the aircraft to meet other customers' requirements and/or international requirements. This allows follow-on sales of a commercial vehicle, for instance, or a derivative of it to military customers or to foreign countries. The penalties paid are often minor if these requirements are considered initially.

As an example, some agencies require the main landing gears to be interchangeable left and right. This is obviously a benefit, so the feature should be incorporated whenever possible, whether it is required or not.

The specifications cited in this chapter are listed in Chapter 15.

4.1 ABBREVIATIONS

- BCAR = British Civil Airworthiness Requirements, Civil Aviation Authority
- EAS = equivalent airspeed, the indicated airspeed (IAS) corrected for position error and compressibility effects
- FAR = Federal Aviation Regulations, Airworthiness Standards (listed in Chapter 15)
- KE = kinetic energy, $\text{ft}\cdot\text{lb} = \frac{1}{2}mv^2$, where v is in feet/second
- USAF = U.S. Air Force, which originated the Air Force Systems Command Design Handbook (DH2-1)
- USN = U.S. Navy, originator of Specification SD-24 (see Chapter 15)
- V_1 = multiengine minimum takeoff controllability speed when the critical engine is suddenly made inoperative; used for brake design and rejected takeoff (RTO)
- V_C = design cruise speed

- V_{S1} = calibrated stalling or minimum speed, in knots, at which the aircraft is controllable, with 1) engines idling, throttles closed (or at not more than the power necessary for zero thrust at a speed not more than 110% of the stalling speed); 2) propeller pitch in the takeoff position; and 3) aircraft in other respects (such as flaps and landing gear) in the condition existing in the test in which V_{S1} is being used
- V_{S0} = calibrated stalling or minimum speed, in knots, at which the aircraft is controllable, with 1) engines idling, throttles closed (or at not more than the power necessary for zero thrust at a speed not more than 110% of the stalling speed); 2) propeller pitch in the takeoff position; 3) landing gear down; 4) wing flaps in the landing position; 5) cowl flaps closed; and 6) center of gravity in the most unfavorable position within the allowable range
- V_{LO} = landing gear operating speed, chosen so as to be not less than $1.6 V_{S1}$ with wing flaps retracted and at maximum landing weight
- W_L = landing weight
- W_{TO} = takeoff weight

4.2 TERMINOLOGY

Official landing gear terminology is illustrated in Fig. 4.1, taken from Specification MIL-L-8552. AIR 1489 provides a complete 47-page dictionary-like listing of 645 terms that are used in landing gear design—tending to reinforce those critics who proclaim that landing gear designers have their own language! It is, however, an extremely useful compendium of terminology that should be studied by anyone who is seriously involved with this subject.

4.3 OPERATING CONDITIONS

Retraction mechanisms, doors, and support structure must be designed for the combination of friction, inertia, brake torque, and air loads occurring during retraction and extension up to airspeeds of $1.6V_{S1}$, with flaps in the approach position at the design landing weight (according to FAR and BCAR requirements).

Unless there are other means to decelerate the aircraft in flight at speeds up to $1.6V_{S0}$, the landing gear, retracting mechanism, and aircraft structure (including doors) must be designed to withstand the loads with the landing gear extended at speeds up to $0.67V_C$ (FAR).

It should be possible to retract and extend the landing gear satisfactorily under the most adverse flight conditions occurring throughout the range of airspeeds from V_{S0} to V_{LO} and accelerations of 0.8–1.2 g, where V_{S0} is at maximum landing weight (BCAR).

A list of typical airspeed limits is provided in Table 4.1.

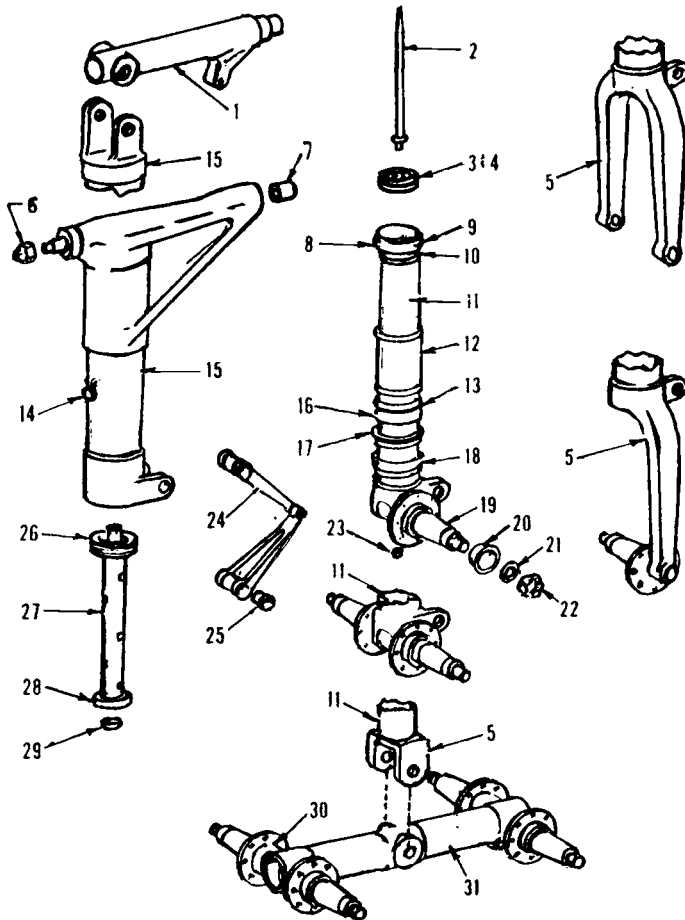
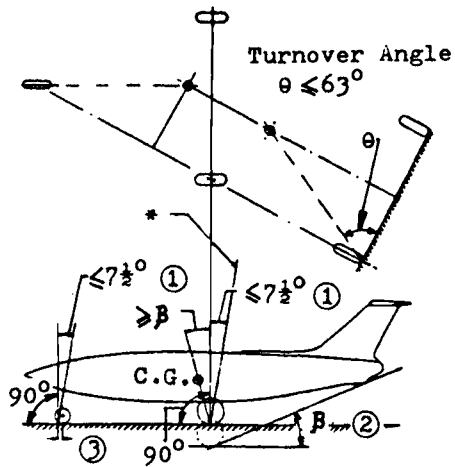
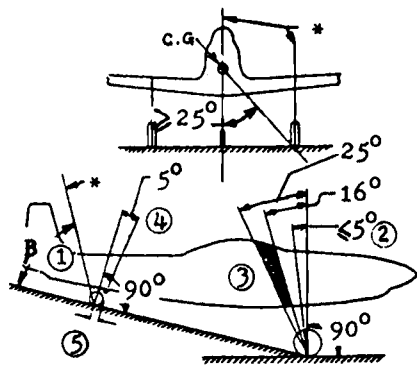


Fig. 4.1 Landing gear terminology.

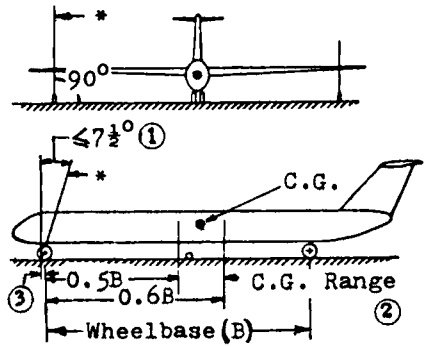
- | | |
|--------------------------------------|-------------------------------------|
| 1) Beam, trunnion | 17) Retainer, packing |
| 2) Rod, metering | 18) Packing nut |
| 3) Diaphragm, piston | 19) Axle, landing gear |
| 4) Base, metering rod | 20) Spacer, wheel bearing |
| 5) Fork, landing gear | 21) Washer, key |
| 6) Nut, castellated, hexagon | 22) Nut, slotted, hexagon |
| 7) Bearing sleeve | 23) Adapter, aircraft jacking point |
| 8) Bearing sleeve | 24) Torque arm, landing gear |
| 9) Set screw | 25) Bearing, sleeve or bushing |
| 10) Valve, snubber | 26) Base, restrictor support tube |
| 11) Piston, landing gear | 27) Tube, support restrictor |
| 12) Stop, piston extension | 28) Adapter, restrictor |
| 13) Packing, preformed | 29) Restrictor |
| 14) Adapter, aircraft mooring/towing | 30) Adapter, axle |
| 15) Cylinder, landing gear | 31) Beam, axle |
| 16) Bearing, sleeve | |



- Notes:
- 1) Preferred value is 7.5 deg. This requirement does not apply if a levered suspension type of gear is used.
 - 2) Provide a tail skid or buffer to protect the control surfaces and rear portion of the structure from damage.
 - 3) The projection of the swivel axis on the ground line must be ahead of the center of the tire contact area by at least 8% of the wheel diameter under any shock absorber deflection.



- Notes:
- 1) Angle β can be 45–90 deg; however, the optimum value is 60 deg.
 - 2) The line of motion of the main wheels resulting from shock absorber deflection must be at an angle of 5 deg or less from the vertical.
 - 3) The design gross weight c.g. must fall within the 16–25 deg limits in the side view.
 - 4) Incline the tail wheel knuckle spindle axis forward at an angle of 5 deg from the normal to the ground line in the taxiing position. It should vary from this angle as little as possible with shock absorber deflection.
 - 5) With any shock absorber inflation, the intersection of the spindle axis with the ground line must fall ahead of the center of the tire contact area by at least 10% of the tail wheel diameter.



- Notes:
- 1) Preferred value is 7.5 deg for main and outrigger wheels.
 - 2) In some aircraft configurations, the c.g. may be placed aft of the 0.6B limit, but never forward of the 0.5B limit.
 - 3) The projection of the swivel axis on the ground line must be ahead of the center of the tire contact area by at least 8% of the wheel diameter under any shock absorber deflection.

*Line of wheel motion resulting from shock absorber deflection.

Fig. 4.2 USAF landing gear layout requirements.

Table 4.1 Typical Airspeed Limits, knots

| Air vehicle type | Airspeed limits | | | |
|------------------|-----------------|---------|--------|------------------|
| | Gear down | Retract | Extend | Emergency extend |
| A-7 | 244 | 220 | 220 | 180 |
| A-10 | 200 | 200 | 200 | 200 |
| B-52 | 305 | 220 | 305 | 305 |
| B-57 | 200 | 200 | 200 | 200 |
| B-66 | 250 | 250 | 250 | 250 |
| F-4 | 250 | 250 | 250 | 250 |
| F-5A/B | 240 | 240 | 240 | 240 |
| F-5E | 260 | 260 | 260 | 260 |
| F-15 | 300 | 300 | 300 | 250 |
| F-16 | 300 | 300 | 300 | 300 |
| F-100 | 230 | 230 | 230 | 230 |
| F-105 | 275 | 240 | 275 | 275 |
| F-106 | 280 | 280 | 280 | 250 |
| F-111 | 295 | 295 | 295 | 295 |
| T-37 | 150 | 150 | 150 | 150 |
| T-38 | 240 | 240 | 240 | 240 |
| T-39 | 180 | 180 | 180 | 180 |

Source: MIL-L-87139.

4.4 LAYOUT

The landing gear designer must comply with the general requirements of Fig. 4.2 when developing an aircraft for the U.S. Air Force and with Fig. 4.3 for the U.S. Navy. In both cases, at the design gross weight, the designer must ensure that the plane of each wheel is vertical.

4.5 GAS/OIL SHOCK ABSORBERS

Since shock absorbers are usually the most complex part of the landing gear, substantial detail is included in this section. Much of this information is based on specifications developed cooperatively by industry, government, and various engineering societies (see Chapters 1 and 15). The word "shall" is used in such specifications to denote a definite requirement and is thus repeated here.

Shock absorbers shall be designed to meet the requirements of MIL-L-8552 and shall be drop tested in accordance with MIL-T-6053 (USAF and USN).

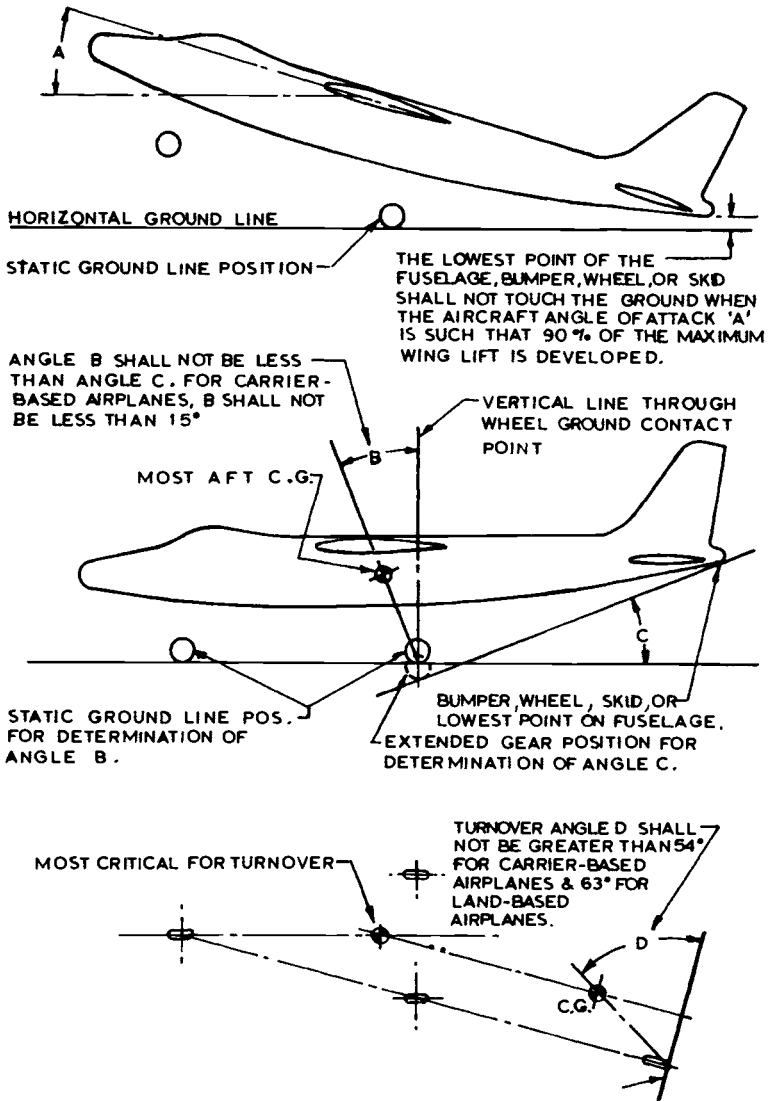


Fig. 4.3 U.S. Navy landing gear layout requirements (source: U.S. Navy Specification SD-24J).

Preliminary drawings sent to the customer shall include the following: construction and operating features; materials; weight; compression ratios; fluid levels at static, extended, and compressed positions; surface treatments; material strengths; and applicable specifications. Schematics shall include static, extended, and compressed positions of the nose and main wheels; angular relation of the shock absorber to the ground line (tail down and tail up); center-of-gravity positions and associated gross weights; and static wheel reactions at the landing gross weight (USAF/USN).

The report that accompanies these drawings shall indicate tire sizes, tire inflation pressures, design sink speeds, total air volume, and isothermal pressure in the extended, static, and compressed shock absorber positions at maximum takeoff gross weight, as well as the preliminary loads imposed upon the landing gear (USN).

The shock strut efficiency obtained during the drop test shall not be less than 75% using the following formula:

$$\text{Efficiency, \%} = \frac{A}{L \times S}$$

where A is the energy absorbed by the strut during its stroke (obtained by integrating the area beneath the strut loadstroke curve), L the maximum load (in pounds) obtained during the stroke, and S the maximum stroke obtained during the test (USAF/USN).

The strut shall be designed to use MIL-H-5606 hydraulic fluid. The air connections shall conform to AND 10071 and the air valve shall be in accordance with MS 28889. Packing to prevent air/oil leakage shall conform to MIL-P-5514 and MIL-P-5516 and the O-ring sizes to MIL-P-5514. All struts shall incorporate MS 28776 scraper rings installed per MS 33675. The packing gland nuts at the end of the shock absorber shall have wrench slots as defined in MIL-S-8552.

The portion of the piston that slides through the lower bearing shall be ground, hard chrome-plated, and have a surface finish of 5–16 $\mu\text{in.}$ per MIL-STD-10 and specification QQ-C-320. Minimum chrome plating thickness shall be 0.001 in. on land-based aircraft and 0.0035 in. on carrier-based aircraft.

Means shall be provided to permit drainage of most of the fluid prior to major disassembly or removal of the piston from the aircraft, using either the extended or retracted position (USAF/USN).

To demonstrate that there is sufficient oil above the orifice to avoid foaming, two successive drops shall be made within 5 min and then repeated after removing oil corresponding to 0.5 in. of the stroke. This test is not required if the oil above the orifice equals 125% of the piston diameter or 5 in., whichever is less (USAF/USN).

To avoid having to provide a binding analysis, the distance between the outer ends of the bearings (piston/cylinder, upper and lower) shall be at least 2.75 times the piston diameter, with the strut fully extended, and bearing stresses shall not exceed 6000 psi based on the limit load and uniform distribution. On a fully extended pin-ended strut, the distance

between the outer ends of the bearings shall be at least 1.25 times the piston diameter (USAF/USN).

At the threads for the wheel bearing retainer nut, there shall be two cotter pin holes at 90 deg spacing. Use steel retaining nuts (USAF/USN).

Provide adequate rebound snubbing as indicated in MIL-T-6053 and MIL-A-8629 (USAF/USN).

Static inflation pressure shall not exceed 2500 psi and the gear shall be capable of satisfactory operation at all temperatures between -65 and $+160^{\circ}\text{F}$ and under all applicable load conditions (USAF/USN).

Concerning drop tests FAA and BCAR have some particular requirements that are summarized below.

For normal, utility, and aerobatic category aircraft being certificated by FAR Part 23, the sink speeds and wing lift are determined by formulas given in Part 23. The wing lift, for instance, cannot be more than two-thirds of the aircraft weight at touchdown, the inertia load factor cannot be less than 2.67, and the ground reaction factor cannot be less than 2.0 unless it can be proved otherwise for the terrain used by that aircraft.

For all other types, refer to FAR Part 25, paragraphs 25.723–25.727 and BCAR Chapter D3-5, paragraph 4. Some of the requirements are summarized below:

- 1) Show by tests that selected takeoff and landing limit load factors are not exceeded and demonstrate the reserve energy at a 12 ft/s sink speed at the design landing weight with wing lift no greater than 1 g. If these measurements are made by drop tests, the free drop heights must not be less than 18.7 in. at the design landing weight and 6.7 in. at the design takeoff weight. Refer to FAR 25.725 for determination of the effective weight and load factor and FAR 25.727 for reserve energy data.

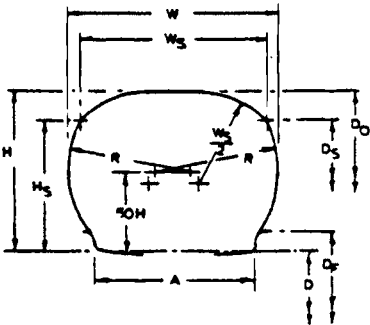
- 2) Proof velocity of descent. At the design landing weight, the sink rate shall be $5.0 + 0.06V_{50}$ ft/s, but not less than 7 ft/s and not more than 10 ft/s. Sink rates can be reduced by 20% for tail wheel units. At the design takeoff weight, the sink rate shall not be less than 6 ft/s.

- 3) Ultimate velocity of descent. Demonstrate that there is sufficient capacity to withstand landing at 1.2 times the sink rates used for proof velocity of descent and determine the reaction factors obtained. Details of cases, attitudes, forces, and sink rates are given in BCAR D3-5.

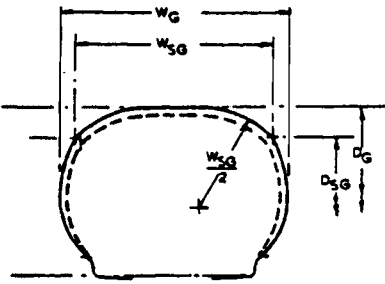
4.6 TIRES

Tires are designed in accordance with MIL-T-5041 and clearances with surrounding structure/equipment should be in accordance with Fig. 4.4. The tire and wheel flange dimensions are taken from the manufacturers' catalogs.

Usually, the tires are inflated to pressures less than the maximum rated values listed in the catalogs and MIL-T-5041; in that event, the pressures are reduced linearly with load. Where twin tires are used, inflate to equal pressures. Calculated loads must be increased by a 7% safety factor on commercial aircraft. The tire load rating must not be exceeded under 1) equal loads on each main gear tire at the critical combination of



NEW TIRE



USED TIRE

- D = bead seat diameter
- D_F = flange diameter
- D_O = outside diameter
- D_S = shoulder diameter
- W = section width
- W_S = shoulder width
- H = section height
- $H = (D_O - D) / 2$
- $H_S = (D_S - D) / 2$

Deflection

- d = deflection (difference between loaded and unloaded section height)
- B = deflection, %
- FH = free height (unloaded section height above wheel flange)
- $FH = (D_O - D_F) / 2$
- $B = d / FH \times 100\%$
- $d = B / 100 \times FH$

Growth

- $W_G = G_W W$
- $D_G = D \cdot G_H H$
- $W_{SG} = G_W W_S$
- $D_{SG} = D \cdot G_H H_S$

Where growth factors are:

| Tire type | G_W | G_H |
|------------|-------|-------|
| III | 1.04 | 2.08 |
| VII | 1.04 | 2.10 |
| VIII | 1.04 | 2.14 |
| New design | 1.04 | 2.14 |

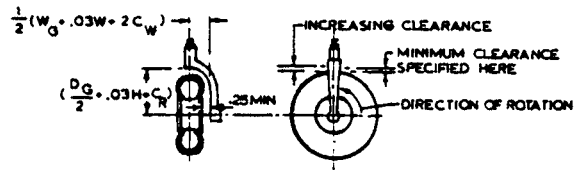
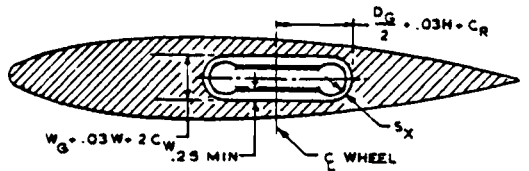
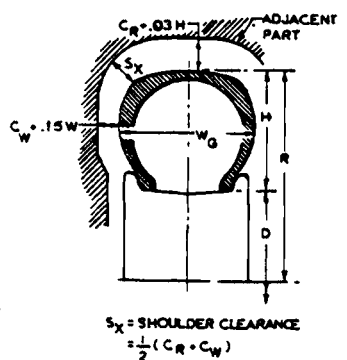
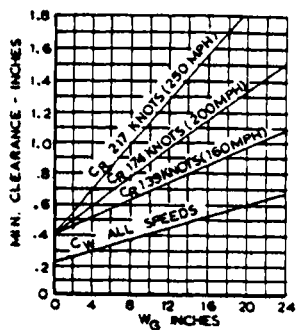


Fig. 4.4 Tire/wheel clearance requirements.

maximum takeoff weight and c.g. position and 2) equal loads on each nose gear tire based upon the following conditions:

a) The static ground reaction for the tire with the most critical combination of takeoff weight and c.g. position. This load factored by 1.07 must not exceed the tire's static load rating.

b) The dynamic ground reaction for the tire at maximum landing weight, with the most critical c.g. position, exerting forces 1.0 g downward and 0.31 g forward (reacted by brakes). This load, with 1.07 factor, must not exceed the tire's dynamic rating.

c) The tire's dynamic ground reaction at design takeoff weight, with the most critical c.g. position, exerting forces 1.0 g downward and 0.20 g forward (reacted by brakes). This load, with 1.07 factor, must not exceed the tire's dynamic rating.

Nose wheel tire inflation pressures are based on maximum allowable dynamic loads. These loads for low-pressure (type III) and high-pressure (type VII and others) tires are, respectively, 1.40 and 1.35 times the allowable static loads. The dynamic load used for nose wheel tire selection is that caused by braking and is assumed to be equal to the static load plus the increment caused by braking at a deceleration of 10 ft/s at the aircraft's maximum gross weight.

In selecting main gear tires, make an allowance for at least 25% growth (USAF) in aircraft gross weight, without changing the external tire or wheel dimensions, to reduce the necessity for major changes during the life of the aircraft. This may be accomplished, for instance, by adding plies to the tires.

On a multiwheel main gear, design it so that if one tire or wheel fails during taxi or takeoff at the maximum gross weight, the remaining tires and wheels on that gear can withstand the most severe overload conditions imposed. Determination of this overload must be based on an elastic analysis of the aircraft and all parts of the landing gear.

On U.S. Navy aircraft, the ply rating shall be at least two plies less than the maximum rating recommended by the Tire and Rim Association. On land-based aircraft, the operating pressure shall be that appropriate to 32% tire deflection at static load. On carrier-based aircraft, the operating pressure shall not exceed 1.3 times the static pressure at the rated load and 32% deflection. A minimum tire section width of 6 in. shall be provided on carrier aircraft. Clearances between the tire and adjacent parts of the aircraft shall be based upon a 3% growth in tire section width and height from the MIL-T-5041 dimensions. In addition, unless the tire is prevented from spinning during retraction, an extra 2.5% increase in section height should be allowed for centrifugal growth.

4.7 WHEELS

Interface requirements to be supplied by the airframe manufacturer to the wheel manufacturer are provided in paragraph 3.4.4 of ARP 1493.

Wheels are designed in accordance with MIL-W-5013. The aircraft manufacturer is responsible for calculating the maximum static and dynamic loads on the wheels, which must be less than their rated loads.

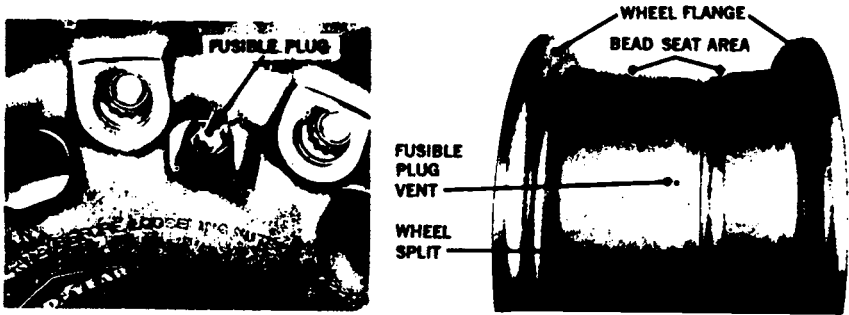


Fig. 4.5 Wheel details.

MIL-W-5013 also calls for the installation of thermal-sensitive pressure-release devices (fuse plugs), such as depicted in Fig. 4.5, with the requirement that they function whenever the bead ledge temperature reaches 400°F. They are placed in the wheel 120 deg apart to prevent tire or wheel explosion due to tire and/or brake overheating. To prevent tire damage or failure, insure that the wheel bead seat temperature from brake heat does not exceed 350°F for normal energy and overload energy.

A means must be provided to prevent water from entering the wheel bearings. Static test the combined wheel and tire to a pressure equal to 3.5 times the rated pressure and ensure that there is no excessive deformation or leakage. Consider the use of nonfrangible wheels to prevent airframe damage due to wheel disintegration after tire failure. This wheel type is capable of rolling for a specified distance without shedding any pieces capable of piercing the airframe.

Clearances were shown in Fig. 4.4. On U.S. Navy carrier-based aircraft, the centers of the main wheel axles must clear the deck by at least 6.5 in. when the tires are flat.

USAF requirements stipulate, and BCAR recommends, that wheels shall be stopped from rotating during retraction or prevented from rotating in the retracted position. This prevents parts inside the wheel well from being damaged by the flailing of a damaged tire and prevents undesirable wheel-rotation noise from being transmitted to the crew and passengers. It may be accomplished by braking the wheels or by friction pads. FAR Part 25 does not require this, but it does require that a loose tire tread must not cause any damage—which may amount to the same thing!

4.8 BRAKES

Interface requirements to be supplied by the airframe manufacturer to the brake manufacturer are listed in paragraph 3.4.4 of ARP 1493.

The main wheel units of the landing gear must be fitted with brakes (BCAR) designed in accordance with MIL-W-5013, TSO-C26b, or BCAR Chapter D4-5, paragraph 3, as applicable. Brake control systems are designed in accordance with MIL-B-8584.

Energy capacity determination shall use either of the following two methods, as approved by the customer. The U.S. Navy requires the use of method II (SD-24, paragraph 3.8.2.2.1).

Method I

$$\text{Kinetic energy} = CWV^2 \text{ ft} \cdot \text{lb}$$

where

$C = 0.0423$ for nose or bicycle gear aircraft*

$= 0.0344$ for tail wheel aircraft†

$W =$ weight of aircraft, lb

$V =$ power-off stall speed at the weight W being considered, knots
($= \text{mph} \times 0.87$)

Method II. Calculate the required brake capacity, recognizing (and noting) the effects of the following parameters at various aircraft weights:

- 1) Aircraft energy at touchdown.
- 2) Integration of the kinetic energy added to the aircraft by the thrust of the aircraft's propulsion system during the stop.
- 3) Integration of the kinetic energy absorbed by the aircraft's aerodynamic drag, including propeller drag (if applicable) during stopping.
- 4) Integration of the kinetic energy absorbed by any auxiliary deceleration devices (such as reverse thrust or drag chute) during the stop.
- 5) Integration of the kinetic energy to be absorbed by the wheel brakes during the stop.
- 6) Effect of wing lift in reducing wheel load, thereby reducing brake torque capability.
- 7) Distribution of load and brake capacity among the various wheels.
- 8) Total stopping distance.
- 9) Static force available for holding the aircraft stationary while running up the engines.
- 10) Appropriate ground winds, airport altitudes, and ambient atmospheric conditions.
- 11) Landing speed and weight for the aircraft shall not be less than those defined in MIL-A-8860 or MIL-S-8698, as applicable.
- 12) Brake retarding force vs time curves and brake retarding force vs speed curves for each design condition.

The BCAR method referred to under method I is defined as the certified normal brake energy capacity. That document also has a requirement for

*This value is from MIL-W-5013; FAR uses 0.0444; BCAR uses $KE = \frac{1}{2}MV^2$, where V (ft/s) is the greatest of 1.0 times the normal touchdown speed, 1.1 times the stalling speed in a landing configuration, or 1.15 times the recommended brake application speed associated with a normal landing.

†This value is from MIL-W-5013; BCAR uses 0.7 times the value obtained from nose wheel aircraft.

certified emergency brake energy capacity. This is the greater of 1.67 times the normal capacity or the capacity to stop the aircraft in an accelerate-stop maneuver with allowances for the residual brake temperatures caused by taxiing. Usage of these two capacities is reflected in the tests conducted—95 stops at normal capacity and 1 stop under the emergency condition. (Note: unlike U.S. requirements, the BCAR also stipulates a brake that is nearing the end of its recommended life when conducting the emergency brake tests.)

Wheel brake capacity requirements for U.S. military aircraft are defined in Table 4.2 and for U.S. commercial aircraft in Table 4.3. For military aircraft, there are two published tables of wheel brake capacity requirements: MIL-W-5013 and ARP 1493. The former, shown in Table 4.2, is used on all U.S. Navy aircraft and has been used on USAF aircraft, although the current MIL-PRIME specification (MIL-L-87139) does not legislate any particular requirement for new aircraft brake capacities. In that event, the requirements of AIR 1493 may be more appropriate since they were determined by SAE experts representing both industry and government and reflect current thinking. (See Table 4.4.) The wheel brake field service life spectrum illustrated in Table 4.5 is the same as in MIL-W-5013 and ARP 1493.

The BCAR tests are too comprehensive to be properly summarized here, so reference should be made to BCAR Chapter D4-5, Appendix 3. There are many details to be recognized, but to provide the reader with a suitable example, the following is an abbreviation of the two methods for evaluating general performance and wear:

BCAR Method 1. At least 25 stops should be made with kinetic energy equal to the certified normal brake energy capacity, with constant brake pressure at the normal value. The brake may be cold at the beginning of each run and may be cooled between runs except that one run is used to obtain the natural cooling/time curve. Measure the stopping time for each run.

BCAR Method 2. At least 5 stops should be made as shown in method 1, plus 95 similar stops which may be made at reduced speed to allow maximum brake usage in stopping the aircraft from the greater of the following: 1) the recommended brake application speed associated with a normal landing at the normal touchdown speed or 2) the stalling speed in the landing configuration.

In addition to the above, the BCAR includes tests for static force, reduced speed stopping, overload, and certified emergency brake energy.

Flexible lines should be routed so that brake heat cannot cause them to rupture. Locate all brake lines on the aft side of the shock strut so that they are protected from foreign object damage. Provide an emergency system capable of stopping the aircraft in the same distance as the normal system. Note: The emergency system shall be completely independent of the normal system upstream of the brake shuttle valve (or its equivalent). If drag chutes are used to augment deceleration, they should be in accordance with MIL-D-9056.

In addition to the above, the FAR has the following requirements.

Table 4.2 Military Brake Capacity Requirements

| Type of aircraft | No. of dynamometer stops | Average rate of deceleration of aircraft, ^a ft/s/s | Aircraft weight condition | Energy credit ^b | |
|-------------------------------------|--|---|----------------------------------|--------------------------------------|------------------|
| | | | | Reversed propellers or engine thrust | Drag parachute |
| Land and carrier based | | | | | |
| Bomber | 45 | 10 | Land plane landing design, gross | Yes ^c | Yes ^c |
| Fighter or interceptor | | | | | |
| Attack | 5 | 10 | Maximum landing, gross | No | Yes ^c |
| Reconnaissance | | | | | |
| Tankers (refueling) | | 10 | Maximum landing, gross | No | No |
| | 2 ^e | | | | |
| | 2 ^d | 10 | Maximum design, gross | No | Yes ^c |
| Land based | | | | | |
| Patrol or antisubmarine | | | | | |
| Minelayer | 100 | 10 | Land plane landing design, gross | Yes ^c | Yes ^c |
| Cargo or transport | | | | | |
| Ground support | 2 ^d | 10 | Maximum design, gross | No | No |
| Trainer | | | | | |
| Liason | | | | | |
| Helicopter | 20 | 6 | Land plane landing design, gross | NA | NA |
| Research and other types not listed | As specified by the procuring activity | | — | — | — |

Source: MIL-W-5013.

^aTo be used in connection with method I. If method II is used, aircraft deceleration and dynamometer deceleration shall be consistent with computations submitted and be a minimum of those listed.

^bThe amount of energy credit shall be approved by the procuring activity in each instance.

^cIf used in standard landing procedure.

^dThe friction materials used for the 45 and 5 stops, or the 100 stop conditions (whichever is applicable) will be used for the worn brake rejected takeoff (RTO) stop. New friction materials and other parts damaged beyond use by the worn brake RTO may be replaced before the new brake RTO stop. The worn brake RTO stop is for information only; however, it will be included as part of the test report.

^eTest to whichever condition is the more critical.

Table 4.3 Commercial Brake Capacity Requirements

| Type of aircraft | Dynamic torque tests | |
|------------------|---|--|
| | Method I calculation | Method II calculation |
| Transport | A) 65 stops at average of 10 ft/s ² ^{a,b,h} | A) 65 stops at average ⁱ of 10 ft/s ² ^{b,c,h} |
| | B) 1 stop at average of 6 ft/s ² ^{b,c,h} | B) 1 stop at average ⁱ of 6 ft/s ² ^{b,f,h} |
| Nontransport | A) 35 stops at average of 10 ft/s ² ^{a,g,h} | A) 35 stops at average ⁱ of 10 ft/s ² ^{e,g,h} |
| Rotorcraft | A) 20 stops at average of 6 ft/s ² ^{d,g,h} | |

Source: AS 227.

^aSea level power-off stalling speed at design landing weight and configuration.

^bOne change of friction materials is permissible in meeting the 66 stops. For other than friction materials, the assembly shall withstand the 65 stops without failure or impairment of operation.

^cAt the most critical combination of takeoff weight and anticipated optimum V_1 speed.

^dAt anticipated takeoff weight. Rotorcraft speed at brake application shall be determined by analysis.

^eAt airplane speed at brake application as determined by method II and dynamometer inertia equivalent to give the brake energy as determined by method II, at design landing weight.

^fAt anticipated optimum speed V_1 as determined by method II and dynamometer inertia equivalent to give the anticipated brake energy as determined by method II, at design takeoff weight.

^gNo change of friction materials is permissible in this test. The assembly shall withstand the test without failure and without impairment of operation, for other than friction materials.

^hProgrammed deceleration may be used when airplane speed-torque requirement is determined by analysis. The average deceleration shall not be less than the average noted in Table 4.3, unless otherwise specified.

ⁱUnless otherwise determined in method II analysis.

Design the brake system so that, if any connecting or transmitting element fails or if any source of operating energy is lost, it will still be possible to stop the aircraft under the specified conditions, with a mean deceleration of at least 50% of that obtained in determining the normal landing distance. The aircraft must have a parking brake that, when set by the pilot, will prevent the aircraft from rolling on a paved, level runway with takeoff power on the critical engine.

The BCAR has the same requirement as FAR concerning the achievement of 50% deceleration after the loss of any single source of brake power. It also requires a parking brake with the above capability. In addition, BCAR requires that brake forces must increase or decrease progressively as the force or movement is increased or decreased at the brake control.

Requirements for automatic braking systems are given in ARP 1907 and

Table 4.4 Wheel Brake Capacity Requirements

| Aircraft type | No. of dynamometer stops | Average rate of deceleration, ^a ft/s/s | Aircraft weight | Energy credit ^b |
|-----------------------------------|---|---|---|---|
| Rotary wing | 20 1 | 6 8.8 | Basic design, gross Max landing, gross | Not applic. None |
| Research and types not listed | As specified by the procuring activity | | | |
| Fixed wing land and carrier based | 30 ^c 3 ^c 1 ^c | 10 10 10 | Land plane landing design, gross Max landing, gross Max landing, gross, or max design, gross (RTO) ^f | Reverse prop or engine thrust; also drag chute ^d Drag chute ^d None Drag chute ^d |

Source: ARP 1493.

^aAircraft deceleration and dynamometer deceleration shall be consistent with the approved brake energy analysis.

^bAmount of energy credit shall be approved by the procuring activity in each instance.

^cThe 30-3 dynamic torque sequence shall be conducted with 3 sequences of 10 land plane landing design gross weight stops followed by 1 maximum landing gross weight stop.

^dIf used in standard landing procedure.

^eA new brake shall be used for the rejected takeoff (RTO) stop. This brake may be conditioned prior to the RTO demonstration.

General Notes:

1) The calculations for capacity requirements shall represent the worst situation that affects overall sizing of the brake.

2) Maximum operating pressure will be applied to the brake assembly and released prior to each of the 30-3-1 stop demonstrations.

3) Success criteria:

30-3 sequence

KE absorption
Torque pressure relationship
No failed parts permitted
No malfunctions
No lining fusing
Fuse plugs must not activate
Thermal limits applicable
Stop distance

RTO Test

KE absorption
Stop distance
Brake torque pressure
No malfunctions
Fuse plug activation
Thermal limits as applicable

^fTest to whichever condition is more critical.

Table 4.5 Wheel Brake Field Service Life Spectrum

| Brake stop description | Typical field service landing | Short field landing | Overweight landing ^a | Aborted mission |
|---|---|------------------------------|---------------------------------|---|
| Taxi distance at 30 knots, ft | 7500 (before and after stop) | 3000 (before and after stop) | 7500 (before and after stop) | 3000 (before stop) |
| No. of 30 knot stops during taxi (one of which is to be at max effort) | 2 (before and after stop) | 2 (before and after stop) | 2 (before and after stop) | 2 (before stop) |
| No. of stops and sequence of stops at each condition (read left to right and top to bottom) | 5 5 20 60 5 ^b 5 | — 1 1 — — — | 1 — — 3 1 — | — — — — — 1 ^c |
| Totals | 100 | 2 | 5 | 1 |

Source: MIL-W-5013 and ARP 1493.

^aMaximum energy landing.

^bUsing wear data obtained, calculate the safe removal point in aircraft service. At this point, rework the stack of heat sink members and/or linings such that the minimum thickness remains for the final 12 stop demonstration.

^cThe worn brake RTO stop is conducted to determine the aborted mission KE capacity of a worn brake and to demonstrate the ability of the brake to complete an aborted mission stop to reasonable conditions. See general note 1.

General Notes

- 1) The analysis is to be based on realistic average conditions expected to be experienced in service usage of the aircraft.
- 2) The brake assembly and the wheel assembly used for the 30-3 sequence of Table 4.4 shall be used for the testing per Table 4.5. The brake will be refurbished with a new complement of disks or other heat sink members, linings, and seals.
- 3) The brake drag and energy absorbed during taxi shall be consistent with the operational environment defined for the specific aircraft. Cooling air of 30 knots may be used during all taxis. Taxi snubs during rolling may be specified if applicable to the aircraft system.
- 4) Extrapolate wear data achieved as testing proceeds to judge the conformity of performance to the design goal.

considerations relative to carbon heat sink brakes are included in AIR 1934. If arresting hooks are used for deceleration, requirements pertaining to their installation are shown in MIL-A-18717.

4.9 SKID CONTROL

Guidance on skid control design is provided in AIR 804, ARP 1070A, AIR 1739, AS 483A, ARP 862, and AIR 764B; requirements are given in MIL-B-8075 for all U.S. military aircraft.

FAR Part 25 and the USAF requires that the system must be designed so that no single failure will result in a hazardous loss of braking capability or directional control of the aircraft. FAR considers the airworthiness portions of MIL-B-8075 to be acceptable.

The USAF requires adequate ground control when landing on wet or icy runways or with strong crosswinds. Also, all aircraft that touch down above 100 knots must be equipped with antiskid brake control systems, although deviations will be granted if the contractor can prove that they are unnecessary.

The BCAR requires that antiskid devices be no less reliable than the rest of the braking system, that a warning be provided to the crew to show failure of the electrical power supply to the system, and that, if any part of the system malfunctions, the affected brake units will automatically revert to a control ensuring no hazardous loss of braking or directional control.

4.10 STEERING SYSTEMS

Steering systems on military aircraft are designed in accordance with MIL-S-8812; for guidance, reference should be made to ARP 1595 and AIR 1752. U.S. Navy aircraft have an additional requirement (SD-24) that the nose wheel shall swivel through 360 deg without manually disconnecting the steering linkage.

The BCAR stipulates that, after extension of the gear and prior to touchdown, the nose wheel shall be automatically positioned in a fore-and-aft attitude; or, if it is otherwise positioned, it will neither be overstressed nor cause any hazardous maneuver. No exceptional skill must be required to steer the aircraft, including the conditions in crosswind or sudden power unit failure. Design the nose gear towing attachments so that no damage will be caused on the nose wheel assembly or steering assembly. In a powered steering system, the normal power supply for steering shall continue without interruption if any one power unit fails. At ground idling, the remaining power unit(s) shall be capable of completing an accelerate-stop and a landing rollout. In addition, no single fault shall result in a hazardous maneuver.

U.S. requirements note that the steering system should be protected from damage from flailing tires, water, rocks, dust, dirt, and moisture. The system must have sufficient torque to turn the steered wheels through their full steering angle without requiring forward motion of the aircraft or asymmetric engine thrust. This capability must be available throughout the design temperature range, at critical weight and c.g. conditions, and with a 0.8 runway coefficient of friction.

There are no specific requirements for steering rate, other than a qualitative statement that it must provide smooth handling at all ground speeds and permit satisfactory maneuverability for turns, parking, and catapult spotting.

Aircraft designed to MIL-S-8812 must have free-swivel ranges as depicted in Fig. 4.6. These ranges shall not require any manual disconnects unless authorized by the customer; automatic disconnects are allowed, provided that they re-engage automatically when the wheel re-enters the power steering range.

The system shall provide dynamic and damping stability for all ground speeds up to $1.3V_{S1}$. The shimmy requirements shall be determined by a nonlinear dynamic analysis that recognized deadband, friction, wheel unbalance, and damping characteristics. The system shall provide sufficient damping to reduce shimmy oscillation amplitude to one-fourth or less of the original disturbance after three cycles.

The BCAR requires that the nose wheel should be capable of free casting while on the ground. Also, the engagement of any locking devices should not restrict that capability. This document also specifies that, unless the nose wheel is automatically centered when lowered, tests must be made to prove its satisfactory functioning when the aircraft is landing with the nose wheel offset at its maximum possible angle.

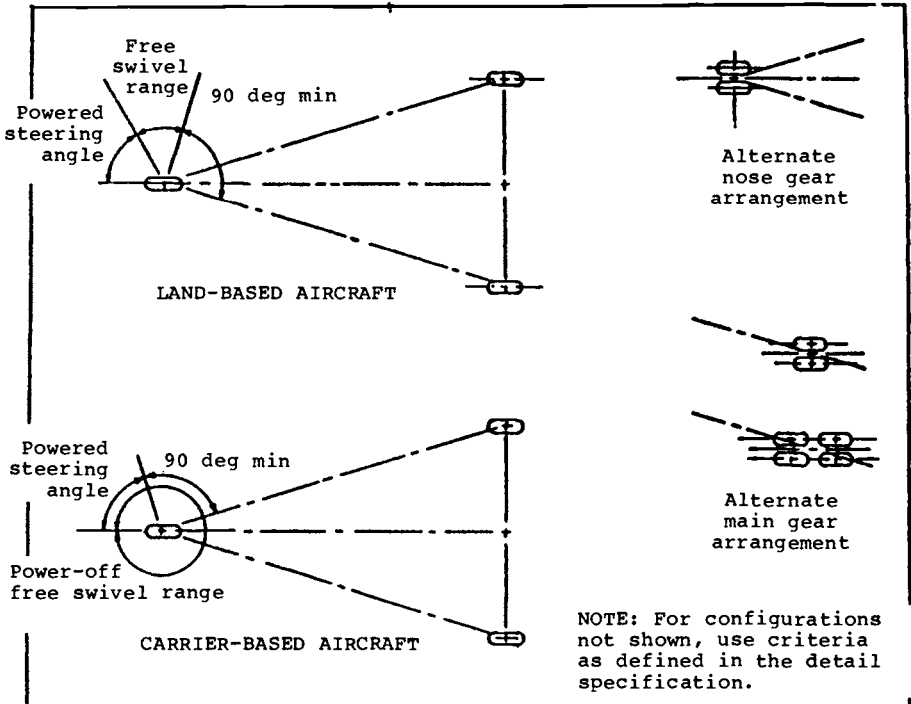


Fig. 4.6 Powered steering angle: free swivel range (source: MIL-S-8812).

Note that steering systems are categorized into two types as follows:

Class A: the system normally used and required for all ground maneuvers.

Class B: used for taxiing, parking, and catapult spotting, but is not required or used for landing and takeoff operations.

4.11 LOCKS

The USAF requires that landing gears lock automatically in the up and down positions, using positive mechanical locks, and that there must be a mechanical means for emergency release of uplocks. They must be capable of preventing retraction or extension under all loads applied to the gear. It is not permissible to hold the gear in the up position by using door locks; the gear must not rest against the doors at any time. An uplock must not be dependent upon proper servicing of the shock absorber. Hydraulically operated locks must not be capable of unlocking due to pressure variations and electrically operated locks must not unlock due to any faults in the electrical system. Downlocks are generally not allowed to be stressed by ground loads, but when this is unavoidable they must have adequate strength, be nonadjustable, and be easily inspectable. A ground safety lock is required on each retractable gear, which should be lightweight, quickly releasable, installed manually, easily removable, and incapable of being installed incorrectly.

On U.S. Navy aircraft, it is further required that whenever overcenter links are used, a positive integral mechanical lock shall be provided at the knee. Down-and-locked position switches shall be actuated directly by the lock. Rigging of locks shall be simple and devoid of close-tolerance adjustments.

Commercial aircraft requirements state that there must be a positive means to keep the gear extended, in flight and on the ground. However, it is normal practice to apply most of the military requirements to commercial aircraft.

4.12 RETRACTION/EXTENSION MECHANISMS

On aircraft with retractable landing gears, the mechanisms shall be designed to accommodate the loads occurring in the flight conditions as defined in Sec. 4.3.

On military aircraft, AFSC DH2-1 provides a performance requirement relating to operating times, shown here in Table 4.6. Table 4.7 lists typical operating times for various aircraft. The landing gear should be operable for at least 5000 cycles using the normal system and 1000 cycles using the emergency system. Hydraulic components should be in accordance with MIL-H-5440 and any pneumatic parts in accordance with MIL-P-5518. Do not use cables or pulleys except in emergency systems.

Provide an emergency extension/locking system that is entirely independent of the primary system. A gravity system is preferable, assisted if necessary by a spring. Do not use a system that requires hand-pumping by the pilot. Actuators should be installed per MIL-C-5503 and MIL-H-8775.

Table 4.6 AFSC Landing Gear Performance Requirements

| If landing gear system is | And temperature is | Then maximum allowable time to extend and lock gear is ^a | And maximum allowable time to retract and lock gear is ^b | And |
|---------------------------|---|---|---|--|
| Power operated | Above -20°F -65°F to -20°F | 15 s 30 s ^c | 10 s 10 s ^c | Gear must be retracted and locked before aircraft reaches 75% of gear placard speed at maximum rate of acceleration |
| Manually operated | Above -20°F -65°F to -20°F | 15 s 30 s ^c | 30 s 60 s ^c | Power required to operate the system must not exceed 3000 ft-lb/min and maximum force required on the operating handle must not exceed 50 lb |

Source: AFSC D2-1.

^aIf the landing gear is used as a speed reducing device, the time to extend and lock the gear must be determined by the desired performance.

^bFor zero-launch aircraft, the landing gear retraction sequence must be completed 1 s prior to reaching the gear placard speed.

^cThe system must meet these requirements when stabilized at the temperature extremes without allowing warmup time.

^dFor multiengine aircraft, the system must meet these requirements during an engine-out condition.

Note: These requirements may be superseded by the requirements of MIL-L-87139, which demands that the time to retract or extend and lock the gear and doors be compatible with air vehicle performance. This would overcome the situation where an aircraft accelerates so rapidly that the landing gear limit speed is reached prior to complete gear retraction.

Table 4.7 Typical Landing Gear Operating Times, s

| Air vehicle type | Retract | Extend | Air vehicle type | Retract | Extend |
|------------------|---------|--------|------------------|---------|--------|
| A-7 | | | F-4 | | |
| A-10 | 6-9 | 6-9 | F-5 | 6 | 6 |
| B-52 | 8-10 | 10-12 | F-16 | | |
| B-66 | 10 | 8 | F-100 | 6-8 | 6-8 |
| | | | F-105 | 4-8 | 5-9 |
| C-5 | 20 | 20 | F-111 | 18 | 26 |
| C-123 | 9 | 6 | | | |
| C-130 | 19 | 19 | T-37 | 10 | 8 |
| C-135 | 10 | 10 | T-38 | 6 | 6 |

Sequencing systems should be used as little as possible; if used, connect mechanically operated valves with nonadjustable linkages. Do not use telescoping rods or slotted links. If these systems are electrically operated, use rugged switches that will not ice-up and mount them on rigid supports to prevent malfunctions due to bracket deflections or the presence of foreign matter. Also, ensure that the gear can be extended if an electrical circuit fails.

On U.S. Navy aircraft, the gear shall be retractable in not more than 10 s. A safety lock is required to prevent retraction when the aircraft is on the ground and an over-ride must be provided to enable the pilot to bypass this lock if conditions warrant it. If a touchdown switch is used to provide this safety lock, then it must operate when the main gear has compressed not more than 1 in. from the fully extended position.

U.S. Navy aircraft are required to be able to extend the gear in 15 s or less and an emergency system must be provided to extend the gear if any part of the normal system, or its power supply, fails. A gravity system is preferred for this purpose, with direct mechanical release of the locks.

4.13 COCKPIT REQUIREMENTS

The landing gear designer is not usually responsible for cockpit layout, but he should be aware of the basic requirements pertaining to the gear.

Generally accepted military/commercial requirements demand cockpit indication that the gear is up-and-locked or down-and-locked when a retractable gear is used; that there be an aural warning device to indicate when a landing gear is not fully extended and locked; and that there be specific requirements for steering and braking. FAR Part 25 has detailed requirements on aural warning devices and on switches to actuate position indicators. A typical detail requirement for an aural warning system, complying with MIL-S-9320, is provided in MIL-L-87139, paragraph 3.2.6.2.

The BCAR requires a green lamp to illuminate when the gear is down and locked and when the gear selector is in the landing position. A red light is illuminated whenever the gear is not down and locked and when the gear, its doors, and its selector are in the retracted position.

Cockpit controls for steering systems are provided in MIL-S-8812. The brake control system specification MIL-B-8075 requires a warning light to show any brake system malfunction; the parking brakes were discussed previously in Sec. 4.8. Controls are also required to engage or disengage the antiskid system (if used) and also to set the degree of braking if an automatic brake system is employed.

U.S. Navy requirements (SD-24) note that emergency landing gear control shall be separate from, but as close as practical to, the normal control unless approved otherwise. The design must preclude interaction between normal and emergency operation; the failure of the normal control must not impair actuation of the emergency system.

4.14 PROTECTION

Some requirements have been noted previously; for instance, the need to stop tires from rotating prior to retraction in order to avoid hazards associated with flailing tires, the need to place brake lines on the aft side of the shock strut, and the need to protect the steering systems.

MIL-L-87139 includes the following suggested requirements that are associated with protection:

- 1) The lowest part of the land gear, door fairing, airframe, or external stores should clear the ground by at least 6 in. under the most adverse combination of tire or shock strut failure.

- 2) In the event of a landing gear structural failure, no landing gear component shall pierce a crew station or passenger seating area or result in fuel spillage in sufficient quantity to constitute a fire hazard (this is also part of U.S. Navy requirements).

- 3) As noted previously, protection must be provided against overheating of the brakes—including the use of brake heat shields and wheel fuse plugs.

- 4) The landing gear shall be capable of operating under specified conditions of temperature, humidity, fungus, vibration, dust, salt fog, acceleration, shock, and electromagnetic environments.

ASFC DH2-1 requires shock struts, forks, and axles to be designed so that mud will be prevented from entering internal cavities. Special care should be taken to plug the axles so that mud cannot contaminate the bearings. The U.S. Navy also requires that the fairings design shall preclude the accumulation of mud, dirt, or cinders. Exposed mechanisms, equipment, electrical wires, and fluid lines should be positioned so that they will not be damaged by foreign objects thrown from the tires. It is suggested that one partial solution is to close the landing gear doors after gear extension and to provide easily removable covers to exposed parts. The U.S. Navy requires that any wheels and tires that are retracted into a position close to a heat source must be protected from that heat.

FAR Part 25 requires that equipment in the wheel well be protected from

a burst tire unless it can be shown that a tire cannot burst from overheat, as well as from a loose tire tread unless such a tread cannot cause damage.

BCAR requires that brakes be protected from the ingress of any foreign matter that may impair their proper functioning. It has a similar requirement to those stated above concerning the effects of burst tires and wheels. In Appendix 1 to BCAR Chapter D4-5, there are detailed protection requirements that, in addition to the above, require equipment, supply lines, and controls to be located either outside the wheel well, away from the tires, and/or protected by structure or shields.

4.15 DOORS AND FAIRINGS

On U.S. military aircraft, the fairings and doors should be easily cleanable without removal and, as noted above, they should be designed so that mud does not accumulate. On U.S. Navy aircraft, doors that close after gear extension should be designed so that they can be opened from the ground. Also, any doors and fairings in the vicinity of the wheels must be infrangible and any strut doors/fairings must be so located/designed that they can withstand the effects of tire blowout.

4.16 MAINTENANCE

Refer to MIL-L-87139, paragraph 3.4, for guidance on USAF aircraft. Further guidance is provided in AFSC DH2-1, which advocates that all hydraulic mechanisms have their filler plugs, bleeder plugs, and air valves placed for easy servicing. Design shock struts so that it is possible to determine the extent of its inflation by using only a scale. Prepare the interior of the wheel wells with a MIL-P-8585 primer coating. Jacking facilities should be in accordance with MIL-STD-809 and each gear should be designed to be jacked. It should be possible to remove a wheel without removing any other part of the gear and the jack pads should be so located that the jacks will not affect operation of the gear.

4.17 STRENGTH

Prior to the recent issue of MIL-PRIME specifications, U.S. military aircraft have used MIL-A-8860 (and component detail specifications) as the basis for landing gear strength—it defines all of the loading conditions and it is still expected that most of these conditions will be used to satisfy the general MIL-PRIME requirements. Details of these conditions are too voluminous to be included here and reference should be made to the specification.

AFSC DH2-1 notes that the design of a multiple-wheel gear should be such that, if one tire or wheel fails during a maximum weight takeoff, the remaining tires and wheels on that gear can absorb the severest overload conditions imposed. This overload is determined by an elastic analysis of the aircraft and its landing gear.

Commerical requirements are given in FAR Part 25, Subpart C-Structure, and in BCAR Chapter D4-5, paragraph 2.7 and Subsection D3-Structures.

4.18 TAIL BUMPERS

The only requirements that the author has been able to find on tail bumpers are 1) that they should be provided and 2) that the tail bumper should not touch the ground when the main wheel is at the static position and the aircraft angle of attack is appropriate to 90% maximum wing lift (USN SD-24). However, some guidance is provided in MIL-L-87139 and in ARP 1107 and AIR 1800.

4.19 ARRESTING HOOKS

The design and installation of arresting hooks is governed by specification MIL-A-18717. This specification defines the location of the hook, the obstacles to be overcome on the carrier deck, the design of the hook itself, its installation details, the applied loads, the controls associated with the hook, and the requirements pertaining to its shock absorber. The Appendix to this specification shows how to determine the aircraft pitch attitude.

5

SHOCK ABSORBER DESIGN

The shock absorber is the one item that is common to all current landing gears. Some do not have tires, wheels, brakes, antiskid devices, retraction systems, or steering systems, but all of them have some form of shock absorber. While the carrier landing has sometimes been called a "controlled crash," it would be a complete catastrophe without the shock absorber. Since this part is undoubtedly the most important component in the landing gear, this chapter will discuss it in considerable detail.

The basic function of the shock absorber, or shock strut as it is often called, is to absorb the kinetic energy during landing and taxiing to the extent that accelerations imposed upon the airframe are reduced to a tolerable level.

5.1 SHOCK ABSORBER TYPES

There are two basic types of shock absorbers: those using a solid spring made of steel or rubber and those using a fluid spring with gas or oil, or a mixture of those two that is generally referred to as oleo-pneumatic. The gas is usually dry air or nitrogen. Figure 5.1 compares the efficiencies and relative weights of the various shock absorber types.

In selecting the type, due recognition must be given to the simplicity, reliability, maintainability, and relatively low cost of the solid-spring shock absorbers. On smaller utility aircraft, the weight penalty is usually negligible and the noted advantages far outweigh the penalties in such cases. The de Havilland of Canada (DHC) Twin Otter aircraft uses rubber compression blocks, as shown in Fig. 5.2, and can be considered a classic example of low cost, high reliability, and low maintenance in this area.

Steel Coil Springs and Ring Springs

These were used by the German Luftwaffe during World War II; the Junkers JU 88, for instance, had a ring spring gear. They are rarely considered in present-day aircraft because they weigh about seven times as much as an oleo-pneumatic gear and are only about 60% as efficient.

Steel Leaf Spring

These are used on some light aircraft equipped with nonretractable landing gears and are ideal from the standpoints of simplicity, reliability,

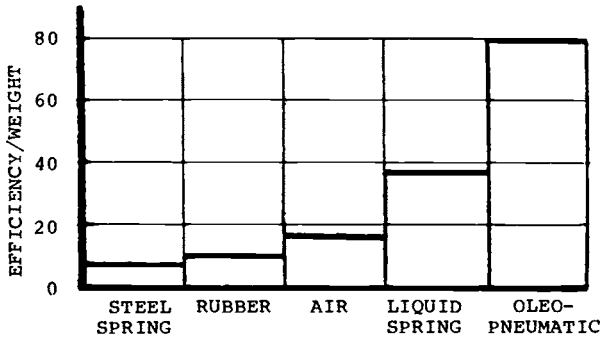
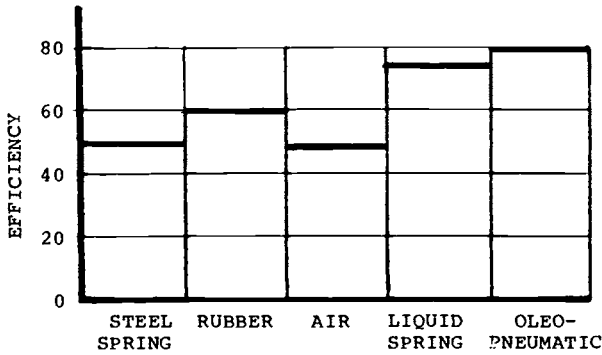


Fig. 5.1 Shock absorber efficiency.

and maintainability. A simplified procedure is included later in this chapter to calculate the characteristics of this type of gear.

Rubber Springs

Shock absorber efficiency is dependent upon the degree to which the shock-absorbing medium is uniformly stressed. To obtain about 60% efficiency, rubber is therefore usually used in the form of disks. These are vulcanized to plates and are stacked as shown in Fig. 5.3. In order to permit satisfactory vulcanizing, each disk is generally no more than 1.5 in thick. They have been widely used—the Twin Otter design shown previously is an example. During World War II, de Havilland used them on the Mosquito (Figs. 5.4 and 5.5) in accordance with the general philosophy of that aircraft—to eliminate, as far as possible, the necessity to use strategic materials, to minimize cost, and to minimize precision machining. Further details of designing with rubber blocks are given later in this chapter.

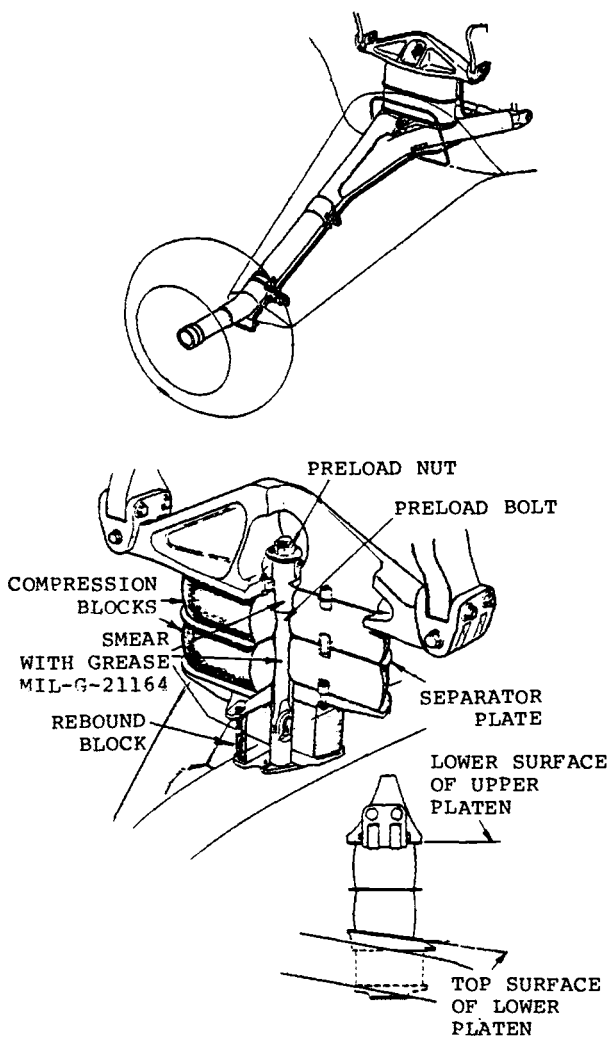


Fig. 5.2 DHC Twin Otter landing gear.

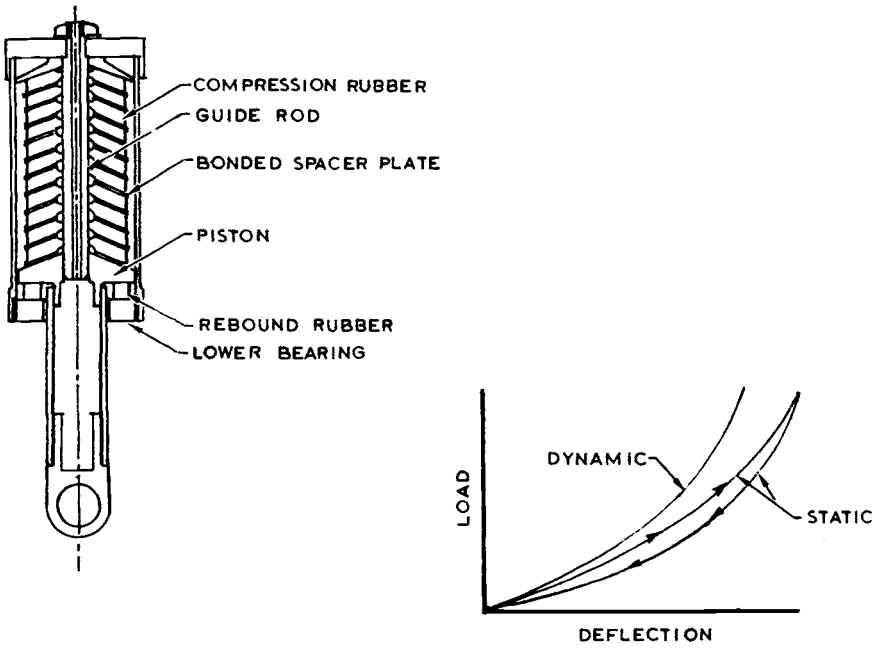


Fig. 5.3 Typical rubber shock strut.

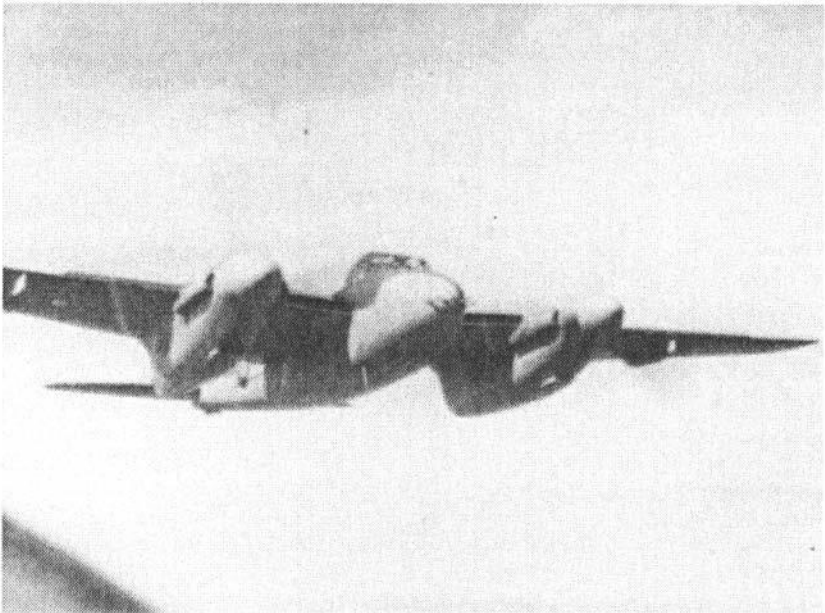


Fig. 5.4 de Havilland Mosquito (source: British Aerospace).

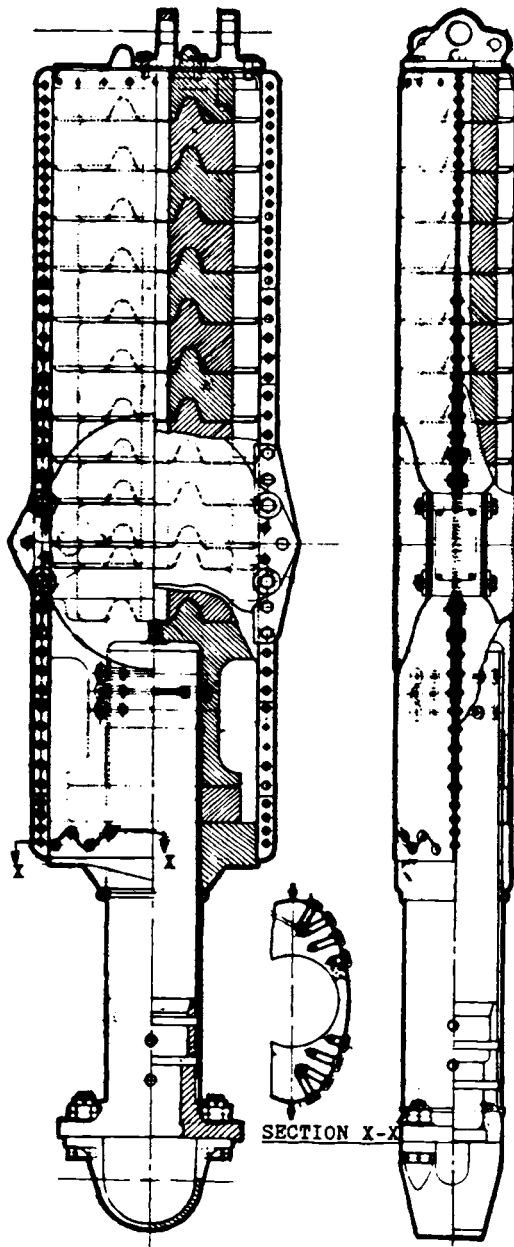


Fig. 5.5 DH Mosquito landing gear strut (source: British Aerospace).

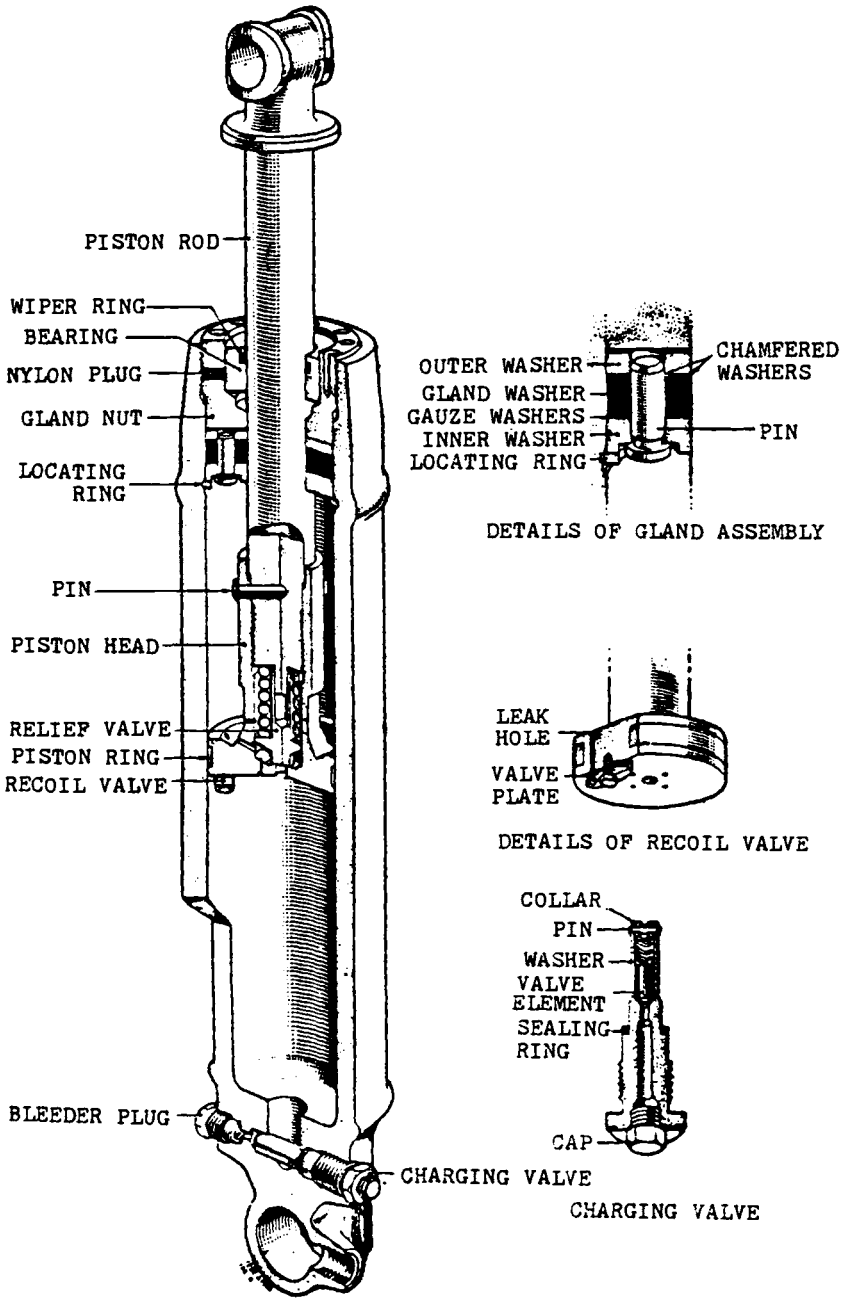


Fig. 5.6 Liquid spring (source: Dowty Rotol Ltd.).

Air

Pneumatic shock absorbers have been used (e.g., the Turner design), but not in recent years. They are similar in design to the oleo-pneumatic shock absorber, but are heavier, less efficient, and less reliable and have no inherent means of lubricating the bearings. Since they are not used today, no further details are given here.

Oil

The so-called “liquid spring” (Fig. 5.6) is an example of an oil-type shock absorber. It was developed by Dowty and first used in World War II. They are still used today, mostly in levered-suspension designs. They have 75–90% efficiency and are as reliable as an oleo-pneumatic unit, although their weight is higher due to the robust design needed to accommodate the high fluid pressures. Its advantages are low fatigue due to the robust construction and relatively small size. Its disadvantages are the fact that fluid volume changes at low temperatures affect shock absorber performance, the shock absorber can be pressurized only while the aircraft is on jacks (i.e., when the gear is extended) due to the high pressures required, the high pressures must be sealed, and the unit has high mechanical friction. Typical calculations are provided later in this chapter.

Internally Sprung Wheels

Although these are no longer in use, the concept is interesting enough to warrant documentation in this section. The internally sprung wheel was developed by Dowty in the 1930's and was used on the Gloster Gladiator. It is shown in Fig. 5.7. Its advantages were that it enabled a rigid leg to be used, but its disadvantages were that a large tire was needed to match the large wheel required for reasonable shock absorber travel; also, the difficulty in accommodating a brake is obvious. In addition, the available stroke is really too small for contemporary aircraft.

Gas/Oil (Oleo-Pneumatic)

Most of today's aircraft use oleo-pneumatic shock absorbers, a typical design of which is shown in Fig. 5.8. They have the highest efficiencies of all shock absorber types and also have the best energy dissipation; i.e., unlike a coil spring that stores energy and then suddenly releases it, the oil is returned to its uncompressed state at a controlled rate, as shown in Fig. 5.9.

In the design shown in Fig. 5.8, MIL-H-5606* oil was poured in, with the strut compressed, until the prescribed level was reached. This was controlled by a standpipe protruding from the filler valve to the oil level—when oil came out of the filler valve, the correct level had been reached. The space above the oil was then pressurized with dry air or nitrogen (an inert

*See Chapter 15 for list of specifications.

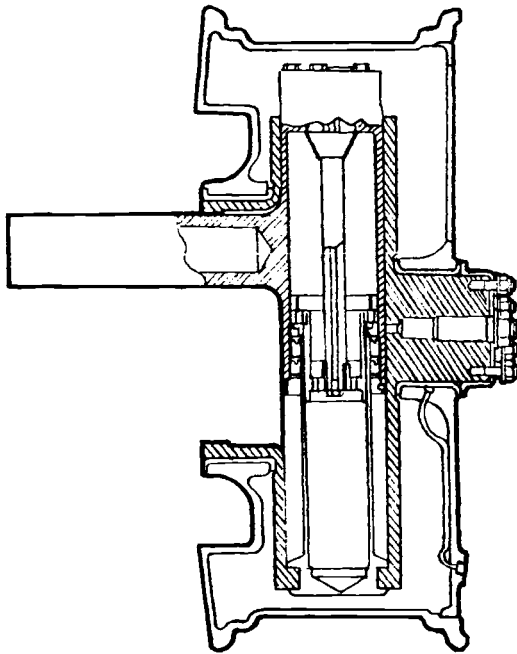


Fig. 5.7 Dowty sprung wheel.

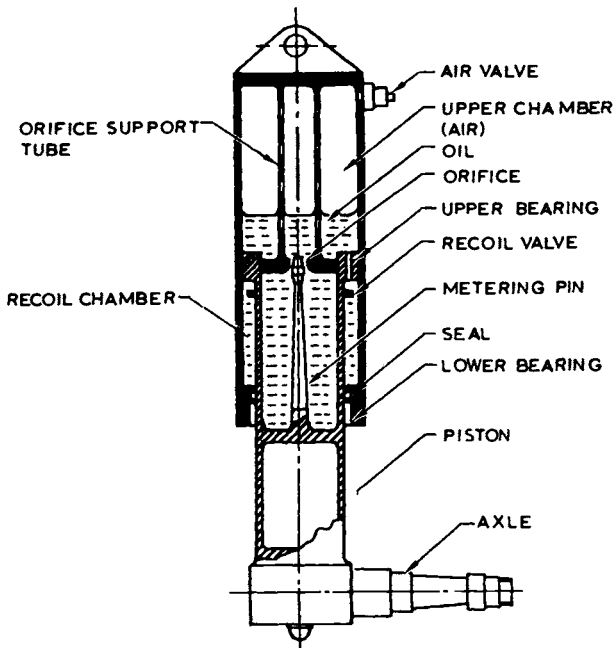


Fig. 5.8 Oleo-pneumatic shock absorber.

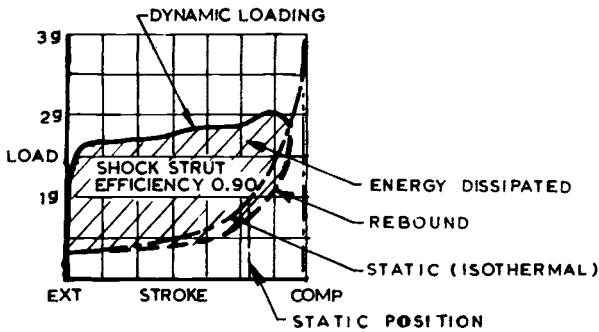


Fig. 5.9 Strut load variation.

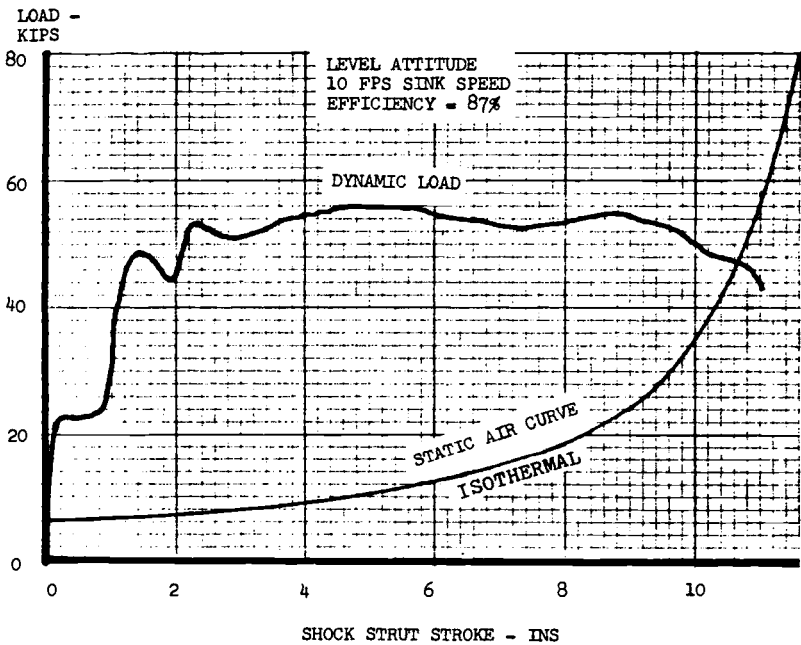


Fig. 5.10 Shock absorber load-deflection curve.

gas). When the aircraft lands, oil is forced from the lower chamber to the upper chamber through the orifice. Although this need only be a hole in the orifice plate, the hole area is often controlled by a varying-diameter metering pin, as depicted in Fig. 5.8, to maximize efficiency by obtaining a fairly constant strut load during dynamic loading—similar to that shown in the drop test curve of Fig. 5.10. A 100% efficient strut would have a rectangular-shaped drop test curve, but in practice the obtained efficiency is usually between 80 and 90%.

Typical calculations for an oleo-pneumatic strut are provided later in this chapter.

5.2 SOME BASIC CONSIDERATIONS AND TRADEOFFS

In the initial design stages, the basic considerations that affect the shock absorber are sink speed, load factor, stroke, and shock absorber type. Some finer points will emerge as the design progresses—such as whether the design will specifically prevent mixing of the gas and oil.

Sink Speed

This is usually legislated by the procuring authority and/or the accepted regulations pertaining to that category of aircraft. For instance, a transport aircraft in the United States would normally be required to withstand the shock of landing at 10 ft/s at design landing weight and 6 ft/s at maximum gross weight. In practice, sink speeds of this magnitude are very rarely achieved.

These types of aircraft normally approach at a 2–3 deg glide slope. At a typical 113 knots approach speed, the sink speed would be 10 ft/s, but ground effects and flare prevent this from continuing through to touchdown. Navy aircraft are designed to higher sink speeds in recognition of the effect of heaving decks (equivalent to an 8 ft/s sink rate), the minimum-or-no-flare landings, and the slightly higher approach path.

Short takeoff and landing (STOL) aircraft are designed to approach at a higher angle (5–8 deg) and to minimize flare. A typical aircraft would have high-lift flaps and a drooped or slatted wing leading edge to maximize lift, spoilers to help the leading-edge device to raise the nose so that a flat attitude is obtained at touchdown, a glide slope of 6 deg, and a sink rate of about 10 ft/s at landing. To meet the requirements that stipulate that the aircraft touchdown sink rate shall be no more than two-thirds of the design sink rate, a 15 ft/s gear would be required for that aircraft.

Load Factor

Load factors applied to the landing gear should not be confused with aircraft load factors. The latter result from maneuvers or atmospheric disturbance. The landing gear load factor is, to some extent, a matter of choice, the details of which are given in Chapter 3.

As a very rough approximation during the conceptual stage, the available strut length can be estimated and, knowing that the strut length is about $2\frac{1}{2}$ times the stroke, the stroke can be determined. From this, the approximate available load factor can be obtained and used in the overall structural analysis. From this and subsequent iterations, the landing gear load factors are prescribed by the structures department.

In many cases, the airframe design will not be controlled by the landing load factor, except for localized areas adjacent to the gear. The author was involved in such a design (a STOL aircraft) where the aft fuselage loads were controlled by the high empennage loads and most of the wing was controlled by gust, flap, and aileron loads. Only the wing engine mounts were affected by the landing gear loads.

As a general guide, the following are typical landing load factors:

| | |
|-------------------------------|---------|
| Fighter aircraft (land-based) | 3–5 |
| Small utility aircraft | 2–3 |
| Transport aircraft | 0.7–1.5 |

Note that the above values refer to the (reaction) factor N used in stroke calculation (see Chapter 3). To convert these to aircraft load factors (at the c.g.), the appropriate amount of wing lift must be used. Thus, on a C-130, the landing gear load factor (sometimes called the reaction factor) is 1.5 and the factor at the c.g. is 2.5.

Stroke

Stroke has been discussed above and in Chapter 3. Quite simply, stroke is roughly a linear function of the load factor and is the vertical distance moved by the wheels. This distance may, or may not, be the stroke of the shock absorber. For instance, Navy aircraft land at high sink speeds; so, to keep the ensuing load factor within reasonable limits, the stroke is often large. To obtain a compact, space-saving landing gear, a levered suspension design is often used. In a design such as shown in Fig. 5.11, the shock absorber stroke is less than the wheel stroke.

No general recommendations can be made as to whether a levered suspension system should be used—it is often the subject of a tradeoff study, comparing it to a conventional design. The levered suspension design (sometimes called a trailing-arm gear) is somewhat more complex and probably slightly heavier, but these characteristics may be offset by the

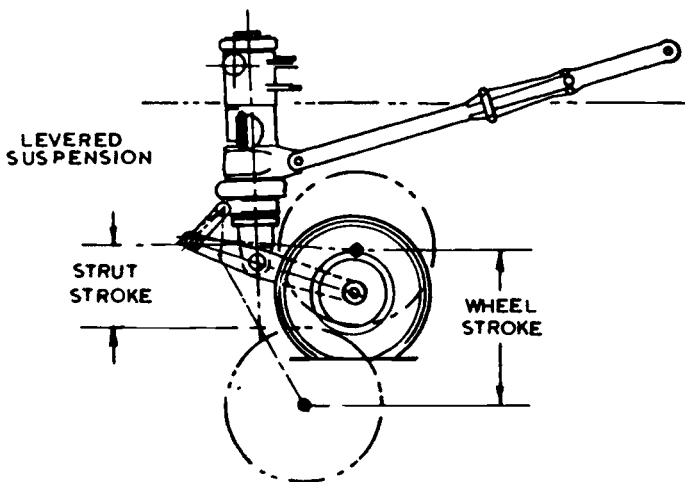


Fig. 5.11 Levered suspension design.

smaller stowage space needed (for long strokes), which causes less disruption of the airframe structure, and where airfield roughness is a consideration, by its superior ability to accommodate that roughness.

Landing Gear Type

For a modern transport aircraft, there is no question as to which type of shock absorber to use—it will be oleo-pneumatic (for reasons stated earlier). But for some aircraft, such as light bush planes or utility aircraft, a tradeoff study could be used to determine, first, whether the gear should be retractable or not. If it is not retractable (e.g., DHC Twin Otter, Piper Cherokee and Cub, Cessna 172, etc.), then a leaf spring or a levered system compressing a rubber (or other type) spring could be considered.

If the gear is retractable and simplicity/low cost is important, stacked rubber blocks could be considered—particularly for a light aircraft. If a levered-suspension system is used, a liquid spring could be traded off against an oleo-pneumatic strut.

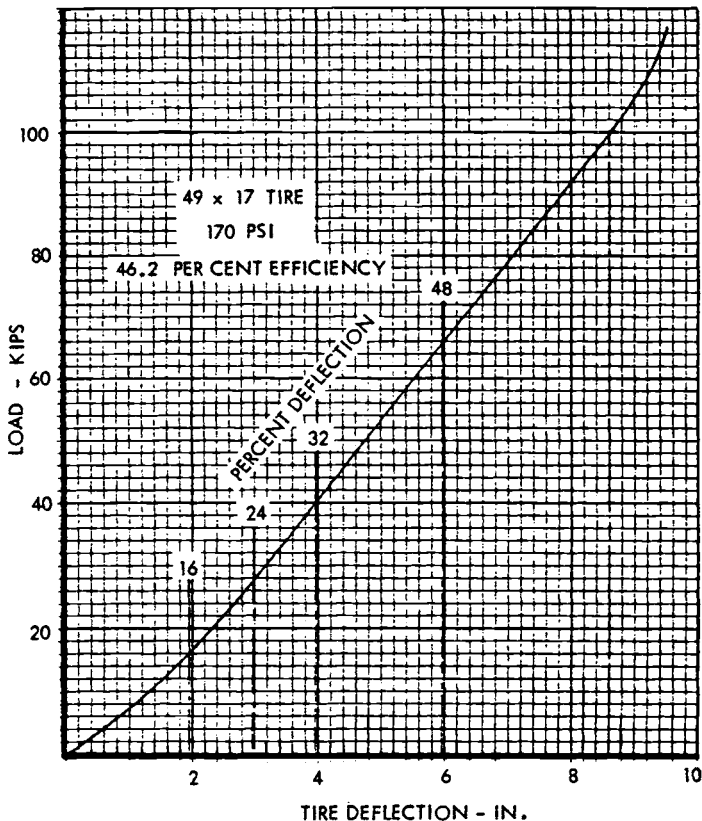


Fig. 5.12 Tire load-deflection curve.

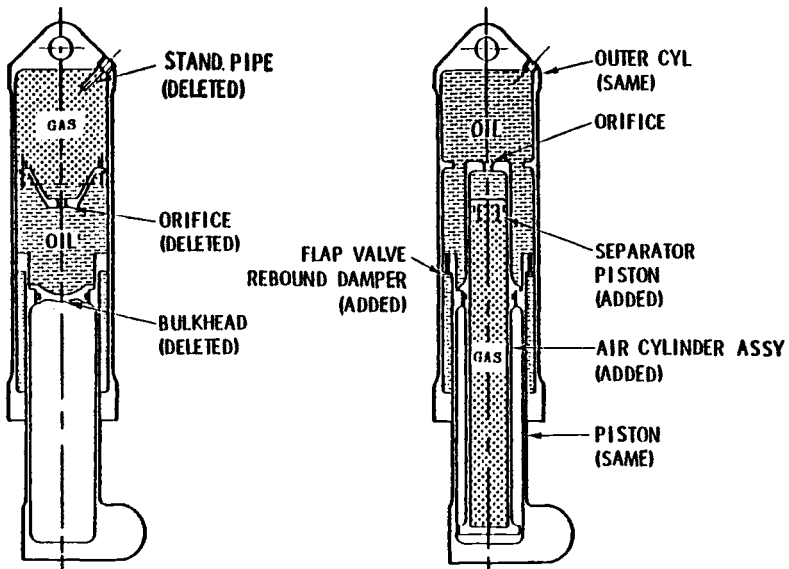
Tire

A full discussion of tires is provided in Chapter 6, but it is pertinent at this point to note their effect on the shock absorption calculations. The calculations in Chapter 3 used a tire efficiency of 0.47 and the total energy absorption recognized tire deflection multiplied by this efficiency as a contributing factor. When a high-efficiency oleo-pneumatic shock strut is used and the stroke requirements are substantial, the relatively low-efficiency tire plays only a small part in the total equation, but it should be recognized. In some cases, where large tires are used, the effect can be appreciable.

Figure 5.12 shows a load-deflection curve for the popular 49×17 tire at 170 psi. The first observation is that this curve indicates a 46.2% efficiency, close to the 47% assumed for stroke calculation. The second observation is that this tire deflects about 4 in. during landing, equivalent to about 2.4 in. of shock absorber travel—an appreciable contribution.

Air/Oil Mixing

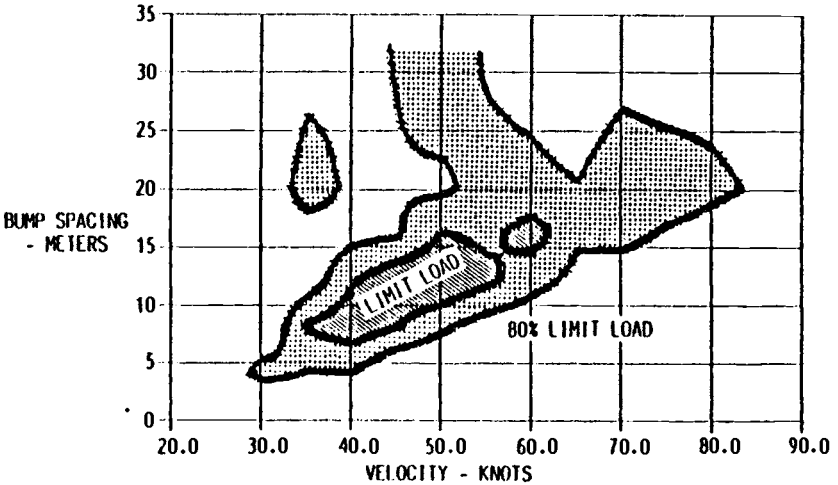
It has been said many times that air (or nitrogen) and oil should not be mixed in an oleo-pneumatic shock absorber. Conway says, "Oil issuing from an orifice should be deflected or turned sideways. It should not impinge on the air, where it will cause froth, and indeed serious loss of adiabatic compression by cooling the air" (Ref. 1, p. 187).



a) Basic strut without gas/oil separation. b) Improved strut with gas/oil separation.

Fig. 5.13 Lockheed C-130 landing gear with and without gas/oil mixing.

a) Conditions where 100 and 80% limit loads are reached with no separation of gas and oil.



b) With gas and oil separated, 100% limit load is never obtained, and 80% load contour is much smaller; i.e., its ability to operate on rough fields is greatly increased.

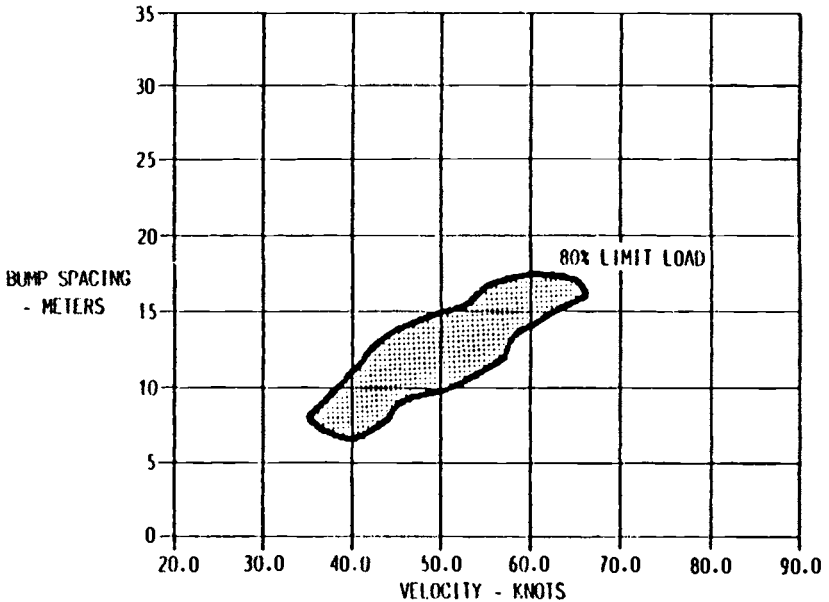


Fig. 5.14 Effect of C-130 gas/oil separation when traversing 70 mm bumps.

Wahi of Boeing² says: "...for a content of only 0.17 per cent (by volume) of compressible entrained air at 3000 psi, the theoretical bulk modulus is cut in half." He notes that as a result of that, "...small amounts of air may alter the shape of the load-stroke curve considerably, reducing the gear load in the initial part of the stroke, and increasing it towards the compressed position."

Lockheed-Georgia has done considerable research in this area and has been able to provide quantitative results by modifying a C-130 landing gear (both nose and main). The baseline gear is typical of most U.S. gears in that the air and oil are allowed to mix. This gear was redesigned to include a separator piston between the air and oil and drop tests were conducted. Existing gears may be modified to this new configuration using a kit. The "before and after" designs are illustrated in Fig. 5.13 and the test results in Fig. 5.14.

5.3 STROKE CALCULATION

Although there are some minor factors that should be included in the stroke formula given in Chapter 3, these factors are not precise and the complications involved in their inclusion are not usually warranted.

Summarizing the discussion of Chapter 3, the method is based on the fundamental work/energy relationship,

$$\text{Change in kinetic energy} = \text{work done}$$

Applying that to a landing gear,

$$\begin{aligned} \text{Change in KE} &= \text{reduction of vertical velocity to zero} \\ &= (-W \cdot V^2)/2g \end{aligned}$$

$$\text{Work done by the strut} = -S \cdot n_s \cdot NW$$

$$\text{Work done by the tire} = -T \cdot n_t \cdot NW$$

$$\text{Work done by gravity} = +W(S + T)$$

$$\text{Work done by wing lift} = -L(S + T)$$

where

W = aircraft weight, lb

V = sink speed, ft/s

S = vertical wheel travel, ft

n_s = shock absorber efficiency

N = landing gear load factor

S_t = tire deflection, ft, when subjected to factor N

n_t = tire efficiency

Hence,

$$0 - \frac{W \cdot V^2}{2g} = -S \cdot n_s \cdot NW - S_t \cdot n_t \cdot NW + (W - L)(S + S_t)$$

If the wing lift is assumed equal to aircraft weight (e.g., transport aircraft), this equation is reduced to

$$\underline{V^2/2g = S \cdot n_s \cdot N + S_t \cdot n_t \cdot W = N(S \cdot n_s + S_t \cdot n_t)}$$

As noted in Chapter 3, 0.75–1.0 in. is usually added to the calculated value of S to allow for inaccuracies.

5.4 RUBBER SHOCK ABSORBER DESIGN

Chapter 1 showed the earliest aircraft landing gear shock absorbers, using bungee cord wrapped round the axles of World War I fighters. These cords may be stretched to 200% of their free length, although 175% is the maximum recommended, and they should be pretensioned to 70% of their static load.

Rubber disks have been used for many years. The thickness of each disk is limited by the thickness that can be vulcanized to the plates or washers used to separate the disks in the stack. This thickness should not be more than 1.50 in. Disks are stacked in sufficient numbers to provide the required stroke; although a rule-of-thumb statement limits disk deflections to 50%, the actual values should be obtained from the disk manufacturers.

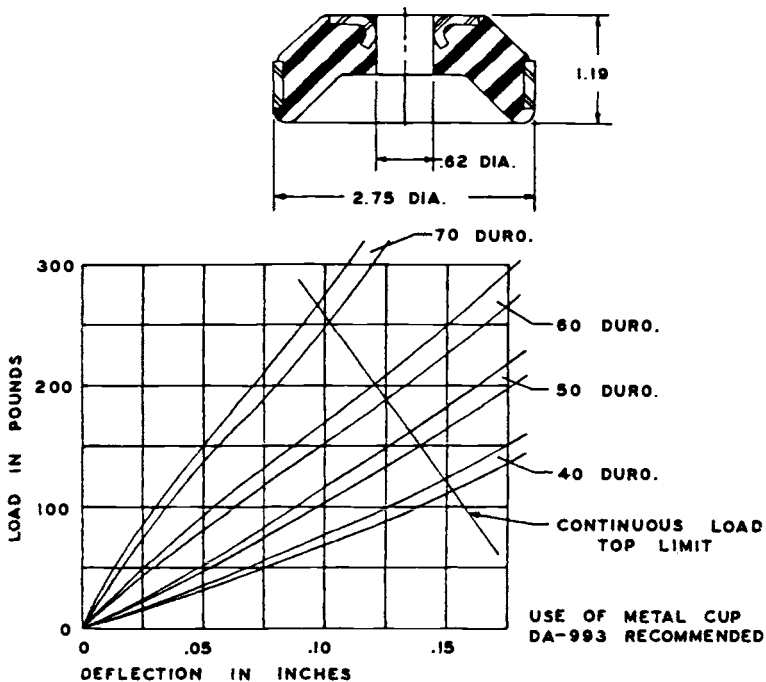


Fig. 5.15 Rubber shock-absorbing disk.

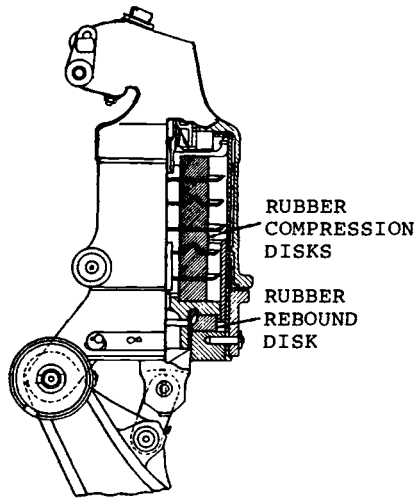


Fig. 5.16 DH Mosquito tail wheel.

One such manufacturer is the Firestone Tire and Rubber Company; Fig. 5.15 shows the characteristics of a typical disk. Figure 5.16 is included to illustrate the design of a typical unit (DH Mosquito tail wheel) using stacked rubber disks.

The de Havilland Dove, weighing 8950 lb, has rubber disk main gear shock absorbers, comprising 14 disks. It uses a central tube to keep all the disks in line; the hole in the center of each disk is lined with fabric. During compression, these holes become smaller and the fabric contacts the tube—thereby absorbing some of the energy by way of friction.

5.5 LEAF SPRING SHOCK ABSORBER DESIGN

As noted earlier, this is a useful type of shock absorber for light aircraft, since it is relatively inexpensive and essentially trouble-free. A thorough analysis of leaf spring landing gear design involves an iterative process; although the principle is elementary, the process is tedious. For instance, having first obtained a spring that is strong enough, it is likely that its deflection is either too small or too large to match the desired load factor; so the dimensions are adjusted until deflection and strength are satisfactory.

It is suggested that an approximate method be used first and then the obtained dimensions be checked by a thorough analysis. The latter would resolve the vertical applied load into loads perpendicular to and normal to the spring and the deflections would be obtained normal to the ground. In this analysis, the basic energy equation still applies, although the tire effect can probably be ignored for simplicity. The relationship is then,

$$S \times n_s \times NW = \frac{W \cdot V^2}{2g} + (W - L)(S)$$

wing lift effect

where

- S = vertical wheel travel, ft
 n_s = spring efficiency = 0.5
 N = reaction factor
 W = aircraft weight, lb

Let $K = L/W$, the lift ratio. Then

$$0.5NS = \frac{V^2}{2g} + S(1 - K)$$

Referring to Fig. 5.17,

$$\text{Deflection} = \frac{P_1 l^3}{3EI} = \frac{12P_1 l^3}{3Ebt^3} = \frac{4 \cdot P_1 \cdot l^3}{e \cdot b \cdot t^3}$$

when t and b are constants. When t and/or b vary along the length, a conventional graphical analysis is required.

From the strength standpoint,

$$F_b = \frac{6P_1 l}{W_R \cdot t^2}$$

The approximate method assumes that t is constant and that sink speed is defined as

$$V = 4.4(W/A)^{0.25}$$

where A is the wing area in square feet.

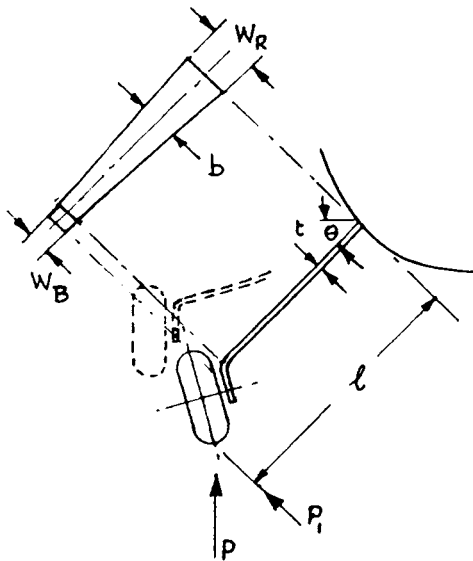


Fig. 5.17 Leaf spring gear.

It will be seen in the following equations that any differences from this definition can be readily incorporated.

K. S. Coward provided the methodology in a very old issue (date unknown) of *Aero Digest*. It is summarized as follows:

Assuming $W = 860$ lb, wing loading (W/A) = 9 psf, $l = 33$ in., and $\theta = 45$ deg, find W_R , W_B , t , stiffness, and load factor as follows:

1) Determine b (the beam width parameter), as

$$\begin{aligned} b &= (0.0067)W(W/A)^{0.5} && \text{for steel} \\ & && (F_b = 220,000 \text{ psi}) \\ &= (0.01373)W(W/A)^{0.5} && \text{for aluminum alloy} \\ & && (F_b = 90,000 \text{ psi}) \\ &= \frac{(0.0067)(860)(3)}{33} && = 0.523 \end{aligned}$$

Let

$$a = \frac{W_R - W_B}{1} = \text{slope of spring taper}$$

Then

$$W = W_B + ax$$

2) Using Fig. 5.18 for the b value obtained, find that $W_R = 3.3$ and $W_B = 1.65$.

3) Let $t = W_R/8 = 0.413$ (assume 7/16 in.) and let $W_R = 3.5$.

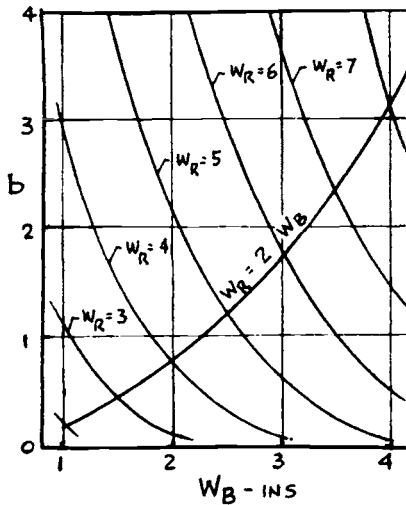


Fig. 5.18 Leaf spring sizing.

$$4) \text{ Load factor} = \frac{(0.388)(W/A)^{0.25} E^{0.5} W_R^{1.5}}{W^{0.5} \cos\theta b^{0.5} (1/t)^{1.5}}$$

For steel, $E^{0.5} = 5480$ and $N = 2.45$.

$$5) \text{ Stiffness} = \frac{96b \cos^2\theta (1/t)^3}{E \cdot W_R^3} \text{ in./lb}$$

$$= 0.00834 \text{ in./lb}$$

5.6 LIQUID SPRING DESIGN

As noted earlier, liquid springs have lower efficiencies than oleo-pneumatic units and, when the strut length is considered, they probably weigh about the same as an oleo-pneumatic unit. They can be serviced only with the aircraft weight removed from the gear and they are sensitive to temperature change—although the latest Dowty designs using nitrogen gas are less sensitive. However, they are reliable, compact, and rugged.

Design is based on the fact that all liquids are compressible to some degree. Figure 5.19 depicts the compressibility of two fluids used.

Operation of System

Figure 5.6 illustrates the general features of a liquid spring and Fig. 5.20 shows the operation of this system. Its essential components are a cylinder filled with fluid, a piston, and a valve or special metering head. Fluid is compressed by the piston occupying progressively more volume as it moves from the no-load position. The piston head houses a valve that opens during compression and closes during recoil to dampen the movement. The gland in the cylinder, which surrounds the piston rod, must prevent leakage

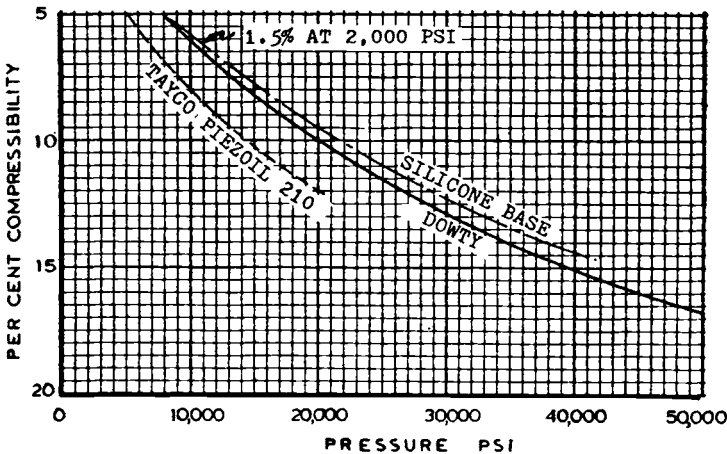


Fig. 5.19 Compressibility of liquid-spring fluid.

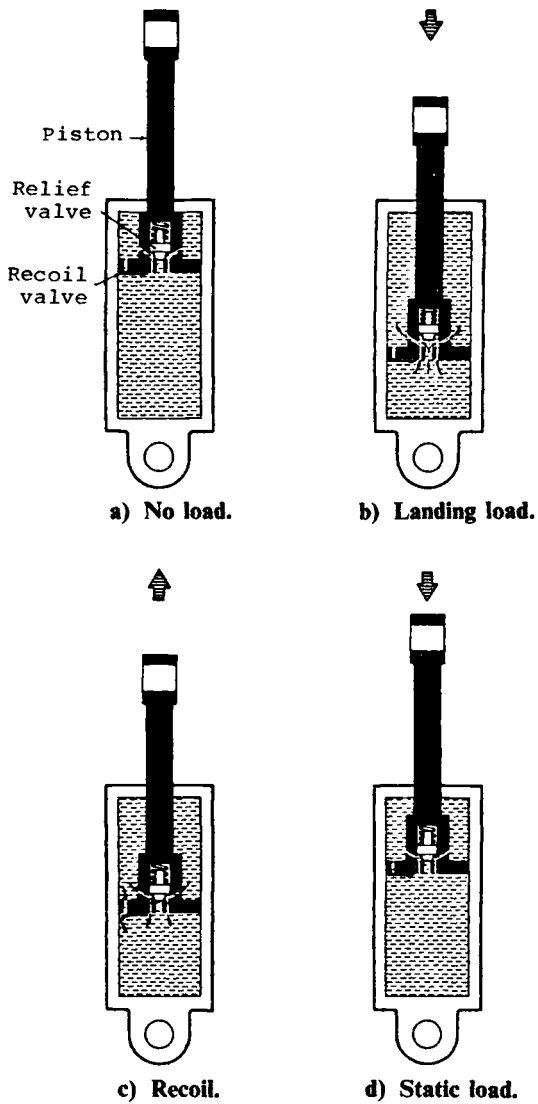


Fig. 5.20 Liquid-spring operation (source: Dowty Rotol Ltd.).

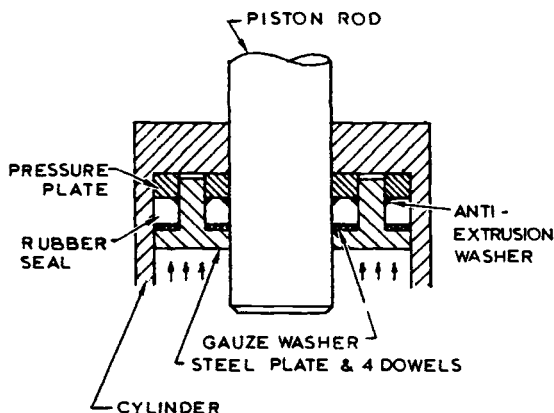


Fig. 5.21 Dowty's seal principle.

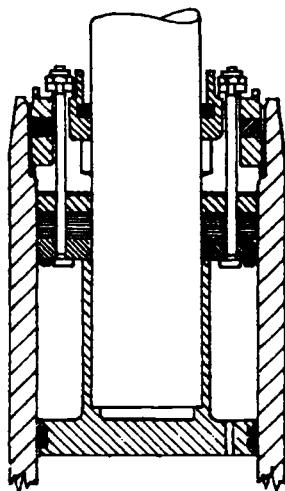


Fig. 5.22 Typical liquid spring seal.

at pressures up to 50,000 psi, while still permitting smooth movement of the rod. The Dowty gland comprises a steel backing plate held in place by the gland retaining nut, a resilient gland to prevent leakage, a gauze washer to act as a pressure lock, and a pressure plate with four dowels projecting down through the gauze, resilient material, and pressure plate. Its principle is shown in Fig. 5.21 and a practical application of it in Fig. 5.22.

Liquid Spring Calculation

A maximum pressure of 40,000–50,000 psi should be used for minimum weight and a minimum pressure of 2000 psi should be used for elimination

of free play at low temperatures. Knowing these two values and the stroke, the piston rod volume can be determined. It is the piston rod that lowers the volume by, say, 17% at maximum pressure.

The piston rod area must then be modified to allow for volume changes due to cylinder stretch and compression of the rubber packing gland (if such a gland is used). Cylinder volume increases about 1% per 30,000 psi and a rubber gland compresses about 5% per 30,000 psi.³ To illustrate a typical case and using the method given in Ref. 4,† assume that the shock absorber moves at a maximum velocity of 10 ft/s, with a 60,000 lb load (20,000 lb with a 3.0 load factor, for instance). Then,

$$\begin{aligned}\text{Kinetic energy} &= \frac{1}{2} \cdot \frac{60,000}{32.2} \cdot (10)^2 \cdot 12 \\ &= 1,117,000 \text{ in.-lb}\end{aligned}$$

Assuming 90% efficiency and letting $N = 3.0$,

$$\begin{aligned}\text{Stroke} &= \frac{V^2}{0.9(2g)N} = \frac{10^2}{0.9(64.4)3} \\ &= 0.574 \text{ ft} = 6.9 \text{ in.}\end{aligned}$$

$$\begin{aligned}\text{Shock force } F_{ps} &= \frac{KE}{\text{stroke}(\text{efficiency})} \\ &= \frac{1,117,000}{6.9(0.90)} = 180,000 \text{ lb}\end{aligned}$$

Let the peak shock pressure be 40,000 psi. Then,

$$\begin{aligned}\text{Bore area} &= \frac{F_{ps}}{\text{peak shock press}} \\ &= \frac{180,000}{40,000} = 4.50 \text{ in.}^2 (2.39 \text{ diam})\end{aligned}$$

To determine the piston rod diameter, use the Johnson column formula,

$$F_c = S_y A \left[1 - \frac{S_y (L_e)^2}{4\pi^2 E K^2} \right] + S_y A \left[1 - \frac{S_y L_e^2 A}{4\pi^2 E I} \right]$$

where

- S_y = yield strength of rod material
- L_e = effective column length = $0.7L$ (assumed)
- A = column area
- $I = 0.049(\text{column diameter})^4$

†Copyright © 1971 Society of Automotive Engineers, Inc. Reprinted with permission.

Assume that the rod material has a 200,000 psi yield and the rod diameter is 1.50 in. Then,

$$\begin{aligned} F_c &= 200,000(\pi) \frac{(1.5)^2}{2} \left\{ 1 - \frac{200,000(1.5/2)^2 \pi [(0.7)(6.9)]^2}{4\pi^2(30)(10^6)(0.049)(1.5)^4} \right\} \\ &= 352,500 \left[1 - \frac{112,400 \times 73.1}{39.55(1.47)(10^6)(5.06)} \right] \\ &= 342,000 \text{ psi} \end{aligned}$$

With this value, the column safety factor will be too high; i.e., it is heavier than it needs to be. The next step is to try a 1.25 in. rod diameter.

At a 1.25 in. diameter, $F_c = 238,000$ psi and the column safety factor is $238,000/180,000 = 1.32$. To find the spring forces, assume a 2000 psi minimum spring pressure. Then,

$$\text{Area} = (1.25)^2 \pi / 4 = 0.393 \text{ in.}^2$$

$$\text{Preload} = \text{pressure} \times \text{area (PA)} = 2000(0.393) = 786 \text{ lb}$$

Assuming a 40,000 psi maximum pressure, then

$$\text{End load spring force (EL)} = 40,000 \times 0.393 = 15,720 \text{ lb}$$

Referring to Fig. 5.19, a silicone fluid compressibility curve shows that

$$\left. \frac{\Delta V}{V} \right|_{2000 \text{ psi}} = 0.015 \quad \left. \frac{\Delta V}{V} \right|_{40,000 \text{ psi}} = 0.14$$

Defining δ as $\Delta V/V$ leads to

$$\Delta\delta = 0.14 - 0.015 = 0.125$$

But,

$$\begin{aligned} V_i &= \text{total fluid volume} = \frac{(\text{rod area})(\text{stroke})}{\Delta\delta} \\ &= \frac{(0.393)(6.9)}{0.125} = 21.7 \text{ in.}^3 \end{aligned}$$

Since the unit has some initial precompression, $\Delta V/V = 0.015$. Then,

$$V_{\text{geometric}} = \frac{V_i}{1 + \delta_p} = \frac{21.7}{1.015} = 21.4 \text{ in.}^3$$

This would yield a fluid chamber length (with a bore diameter of 2.39 in.)

$$L = \frac{21.4}{\pi(2.39/2)^2} = \frac{21.4}{4.5} = 4.76 \text{ in.}$$

This length should be slightly reduced due to compressibility of the seal, fluid pockets in the seal, and cylinder wall expansion under pressure.

Experimental data show that the equation $S = P + PR/T$ holds for computing cylinder wall parameters if P is the end load spring pressure and S the cylinder stress.

Using a safety factor of 1.25 on P (i.e., $P = 50,000$ psi approximately and R equals $2.39/2 = 1.195$ in.), let S be 200,000 psi yield and solve for T , as

$$\text{Wall thickness } T = \frac{R}{(S/P) - 1} = \frac{1.195}{4 - 1} = 0.40 \text{ in.}$$

To compute the initial orifice area, a rough approximation can be made by the Bernoulli equation,

$$P = \rho V^2/2g + C$$

where V is the fluid velocity through orifice and ρ the fluid density.

But, by the mass continuity equation,

$$V = A_B/A_O \quad \text{and} \quad C = 2V^2\rho/g$$

where

A_B = bore area

A_O = orifice area

V = piston velocity

p = 40,000 psi = 5,760,000 psf (peak shock pressure)

$\rho_{\text{silicone}} = 0.97(\rho_{\text{water}}) = 0.97(62.4) = 60.5 \text{ lb/ft}^3$

Solving for V ,

$$V^2 = \frac{2gp}{3\rho} = \frac{2(32.2)(5,760,000)}{3(60.5)} = 2,045,000$$

$$V = 1430 \text{ ft/s}$$

$$V_p = 10 \text{ ft/s at impact}$$

$$A_O = A_B \cdot \frac{V_p}{V} = 4.5 \left(\frac{10}{1430} \right) = 0.0315 \text{ in.}^2$$

$$\text{Area of piston o.d.} = 4.5 - 0.0315 = 4.4685 \text{ in.}^2$$

$$\text{Diameter of piston} = \sqrt{4(4.4685)/\pi} = 2.38 \text{ in.}$$

With a cylinder bore of 2.39 in., the peripheral clearance is 0.005 in.

Figure 5.23 depicts a liquid spring that is somewhat different in detail from the Dowty design—it is one of a series of such designs from Taylor Devices Inc.

LOAD AT SUPPORT 3129 LB
 STROKE AT SUPPORT 0.90 INS
 MAX STROKE 2.75 INS
 PEAK SHOCK FORCE 13,600 LB
 ULTIMATE ENERGY ABSORPTION 29800 IN.-LB

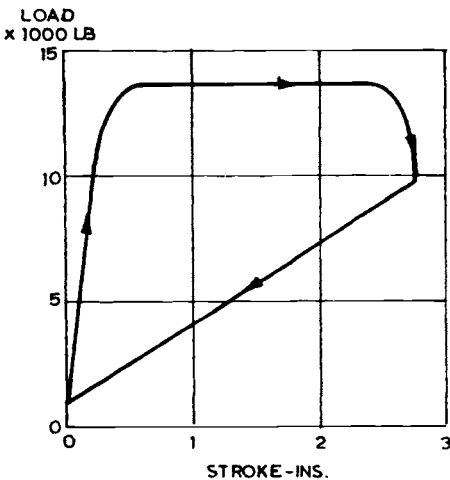
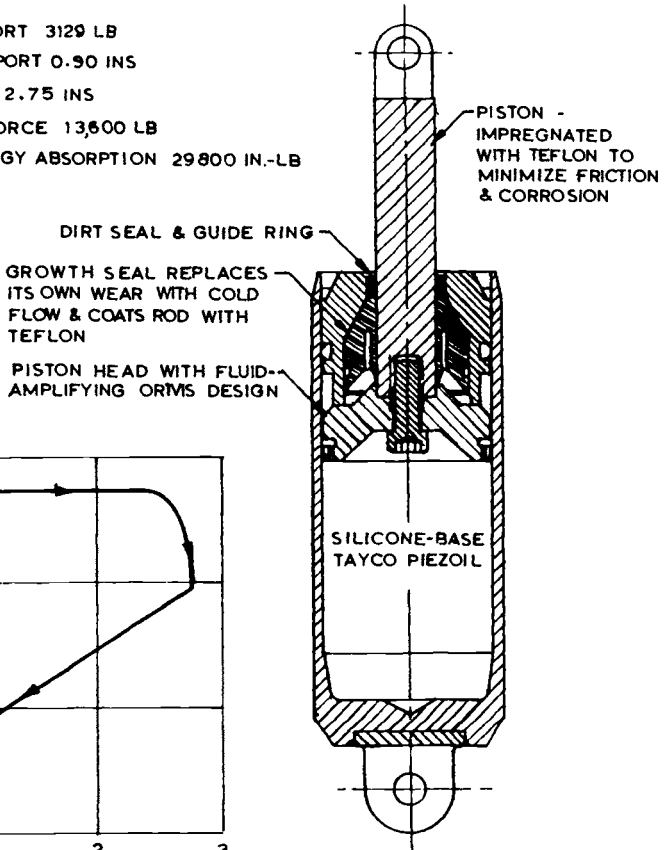


Fig. 5.23 Taylor "Fluidic Shok" liquid spring.



5.7 OLEO-PNEUMATIC SHOCK ABSORBER DESIGN

Oleo-pneumatic shock struts (diagramed in Fig. 5.24) absorb energy by "pushing" a chamber of oil against a chamber of dry air or nitrogen and then compressing the gas and oil. Energy is dissipated by the oil being forced through one or more orifices and, after the initial impact, the rebound is controlled by the air pressure forcing the oil to flow back into its chamber through one or more recoil orifices. If oil flows back too quickly, the aircraft will bounce upward; if it flows back too slowly, the short wavelength bumps (found during taxiing) will not be adequately damped because the strut has not restored itself quickly enough to the static position.

The distance (stroke) from static to fully compressed positions is largely a matter of choice. Conway¹ suggest an inflation pressure that provides one-third extension at maximum weight and not more than one-half

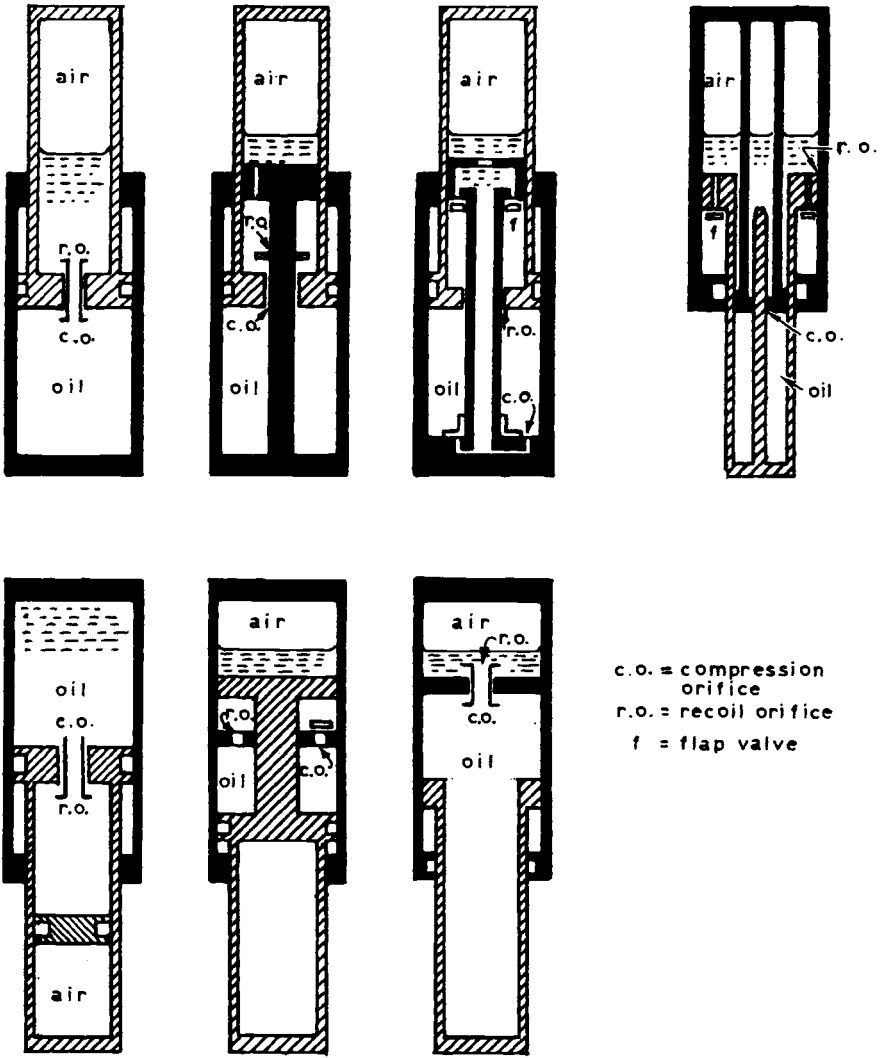


Fig. 5.24 Oleo-pneumatic shock absorber types.

Table 5.1 Shock Strut Static Extensions

| Aircraft (main gear) | Distance (static to compressed) | | Total stroke |
|-------------------------|------------------------------------|-------|-----------------|
| DC-9 | 0.875 | (6%) | 16.0 |
| DC-10 | 2.5 | (10%) | 26.0 |
| F-4 | 1.52 | (10%) | 15.88 |
| C-141 | 3.0 | (11%) | 28.0 |
| Electra | 2.2 | (11%) | 20.0 |
| L-1011 | 3.5 | (13%) | 26.0 |
| Boeing 707-320 | 3.0 | (14%) | 22.0 |
| Boeing 720B | 3.0 | (15%) | 20.0 |
| Boeing 737-200 | 2.1 | (15%) | 14.0 |
| Boeing 727-200 | 2.5 | (18%) | 14.0 |
| JetStar | 3.5 | (23%) | 15.5 |
| C-130 | 3.0 | (29%) | 10.5 |
| Beech U-21A | 3.3 | (31%) | 10.79 |
| Piper Turbo Navajo | 2.8 | (35%) | 8.0 |
| Piper Aztec | 3.1 | (39%) | 8.0 |
| Beech 99 | 4.77 | (40%) | 11.95 |
| Aero Commander | 3.5 | (40%) | 8.75 |
| F-104G | 5.6 | (41%) | 13.8 |
| Piper Comanche | 2.75 | (45%) | 6.06 |

extension at light load. Table 5.1 indicates the wide variation in these extensions; note that transport aircraft have extensions of about 16%. This tends to give a hard ride while taxiing, but restricts lateral "wallowing"; also, with the static position being so far up the load-deflection curve, weight changes do not result in substantial gear deflections. In summary, the designer selects an initial static position, based on similar aircraft and/or experience, and then modifies this position as the design progresses.

Where the aircraft's maximum and minimum weights vary considerably, the shock strut characteristics should be checked for both conditions and inflation pressures should be calculated for all applicable aircraft weights. These pressures are shown on a plate attached to the cylinder for use by ground personnel.

Oleo-Pneumatic Shock Strut Sizing

Rough approximation. It is unlikely that an ideal shock strut will be obtained initially. By trial and error and by modifying initial assumptions, a satisfactory design will be obtained. The process therefore starts with a rough approximation as follows:

1) Decide what compression ratios will be used. These are the ratios of the pressure at one point (e.g., fully compressed) divided by the pressure at

another point (e.g., fully extended). Two compression ratios are normally considered: fully extended to static and static to fully compressed. For a small aircraft or one in which the variation in floor height with aircraft weight is important, the following ratios would be satisfactory:

Static to extended 2.1/1

Compressed to static 1.9/1

For larger aircraft, particularly cargo aircraft (where floor height variation is important), the following ratios can be used:

Static to extended 4/1

Compressed to static 3/1

2) Calculate loads at fully extended, static, and extended positions. The static load is known, i.e., strut load at maximum gross weight, adverse c.g. position, aircraft stationary. Using the above 4/1 and 3/1 figures and a static load of, say, 50,000 lb, the loads are

$$\text{Load extended} = \frac{1}{4} \times 50,000 = 12,500 \text{ lb}$$

$$\text{Load static} = 50,000 \text{ lb}$$

$$\text{Load compressed} = 3 \times 50,000 = 150,000 \text{ lb}$$

3) From the previously calculated stroke, select an appropriate static position, using a similar aircraft as a guide.

4) Draw a preliminary load-stroke curve through the three points and note the static position. If, for example, the total stroke was 20 in. and the static position was 16% from fully compressed, the previously calculated loads and strokes would be:

| Load, lb | Stroke, in. |
|----------|-------------|
| 12,500 | 0 |
| 50,000 | 16.8 |
| 150,000 | 20.0 |

Parameters to consider in final sizing. The data required are

- 1) Total stroke: from previous calculations.
- 2) Static position: from a study of similar aircraft or from item 5 below.
- 3) Static load: at 1 g, maximum gross weight, using a forward c.g. for the nose gear and an aft c.g. for the main gear.
- 4) Compression ratio: use the values quoted above and adjust as necessary during the design process.
- 5) Air volume with strut compressed (V_3): in some cases, the designer

will not select an arbitrary static position. Instead, it will be assumed that V_3 is 10% of the displacement. The calculation proceeds as follows:

Assume 1500 psi static pressure in the strut,

$$\text{Piston area } A = \frac{\text{max static load}}{1500}$$

The total stroke is known and displacement D is equal to the stroke times A . Since V_3 is 10% of displacement,

$$V_3 = 0.10(\text{stroke} \times A)$$

Using a 3/1 compression ratio from compressed to static,

$$\text{Max strut pressure} = 3 \times 1500 = 4500 \text{ psi} = P_3$$

$$\text{Fully extended volume} = V_3 + D = V_1$$

$$P_1 V_1 = P_3 V_3$$

$$P_1 = \text{extended pressure}$$

Note: P_1 should not be less than 60 psig to avoid sticking and it should not be more than 300 psig to avoid bouncing. Thus,

$$P_1 = \frac{P_3 V_3}{V_1} = \frac{4500 \times V_3}{V_3 + D}$$

$$\text{Static volume} = \frac{P_1 V_1}{P_2} = V_2$$

From this, V_2 is calculated and the stroke from extended to static is given by

$$S_s = \text{total stroke} - (V_2 - V_3)/A$$

If the value so obtained is satisfactory (similar to other aircraft of the same type), then the calculations may proceed to determine the load-stroke curve.

Values and Abbreviations Used in Final Sizing

P_1 = air pressure at full extension. This should be sufficient to overcome the friction forces that tend to prevent the piston from reaching full extension. Provided that a good surface finish is applied to the piston (rms 16 or better), there should be no problem. However, in some cases, at P_1 , pistons have extended properly with zero pressure due to g forces on the unsprung mass. To verify that the pistons extend

properly when taxiing at light loads, apply the appropriate loads to the axle, determine the resulting load on the upper and lower cylinder bearings, and multiply these by a 0.10 (pessimistic) friction coefficient. The resulting force must be overcome by strut pressure. If the strut pressure is insufficient, the piston will not extend smoothly.

P_2 = air pressure at the static position. Assume about 1500 psi for this pressure—it enables standard compressors to be used for servicing, with enough margin to allow for aircraft growth. Some gears are serviced with the gear clear of the ground and a simple procedure of pouring in the oil and then replacing the filler cap. In this case, the extended pressure P_1 is known to be 0 psig (14 psia) and P_2 is calculated.

P_3 = air pressure in the compressed position. The strut is not fully bottomed, since there is a small space left for reserve energy, but it is the position that was used in the compression ratio calculation. P_3 equals P_2 multiplied by the compression ratio from static to compressed.

V_1 = air volume at full extension

V_2 = air volume at static extension

V_3 = air volume at compressed position

D = displacement (= total stroke \times piston area)

Single-Acting Shock Absorber Calculation

Most shock absorbers are of the single-acting type. The difference between this type and the double-acting type is discussed in the next section. Assume:

Total stroke = 20.0 in.

Static load = 50,000 lb

Compression ratio = 4/1 static to extended
3/1 compressed to static

Static pressure = 1500 psi

Then,

$$P_1 = \frac{1}{4} \times 1500 = 375 \text{ psi}$$

$$P_2 = \text{basic assumption} = 1500 \text{ psi}$$

$$P_3 = 3 \times 1500 = 4500 \text{ psi}$$

$$\text{Piston area } A = 50,000/1500 = 33.33 \text{ in.}^2$$

$$\text{Displacement} = 20 \times 33.33 = 666.7 \text{ in.}^3$$

$$P_1 V_1 = P_3 V_3 = \text{const}$$

So $V_1 = P_3 V_3 / P_1$. Therefore,

$$V_1 = \frac{4500(V_1 - 666.7)}{375} = 12V_1 - 8000 = 728 \text{ in.}^3$$

$$V_2 = \frac{P_1 V_1}{P_2} = \frac{375 \times 728}{1500} = 182 \text{ in.}^3$$

Knowing that displacement = $V_1 - V_3 = 666.7$,

$$V_3 = V_1 - 666.7 = 728 - 666.7 = 61.3 \text{ in.}^3$$

Summarizing:

$$P_1 = 375 \text{ psi} \quad V_1 = 728 \text{ in.}^3 \quad \text{Load} = 12,500 \text{ lb}$$

$$P_2 = 1500 \text{ psi} \quad V_2 = 182 \text{ in.}^3 \quad \text{Load} = 50,000 \text{ lb}$$

$$P_3 = 4500 \text{ psi} \quad V_3 = 61.3 \text{ in.}^3 \quad \text{Load} = 150,000 \text{ lb}$$

The load-stroke curve may now be drawn. At any stroke X ,

$$P_x = \frac{P_1 V_1}{V_x} = \frac{375 \times 728}{V_x} = \frac{273,000}{V_x}$$

These points are plotted in Fig. 5.25 from the calculations shown in Table 5.2 and are defined by the isothermal compression curve. This is representative of normal ground handling activity. An additional curve is shown—the polytropic compression. This is representative of dynamic (fast) compression cases such as landing impact, bump traversal, etc. The

Table 5.2 Calculation of Isothermal Compression

| Stroke, in. | V , in. ³ | P , psi | Load (=33.33 P) |
|-------------|------------------------|-----------|-----------------------|
| 0 | 728 | 375 | 12,500 |
| 2 | 661.3 | 413 | 13,750 |
| 4 | 594.7 | 459 | 15,300 |
| 6 | 528 | 518 | 17,270 |
| 8 | 461.3 | 592 | 19,730 |
| 10 | 394.7 | 691 | 23,050 |
| 12 | 328 | 831 | 27,730 |
| 14 | 261.3 | 1045 | 34,850 |
| 16 | 194.6 | 1402 | 46,700 |
| 18 | 128 | 2135 | 71,150 |
| 20 | 61.3 | 4500 | 150,000 |

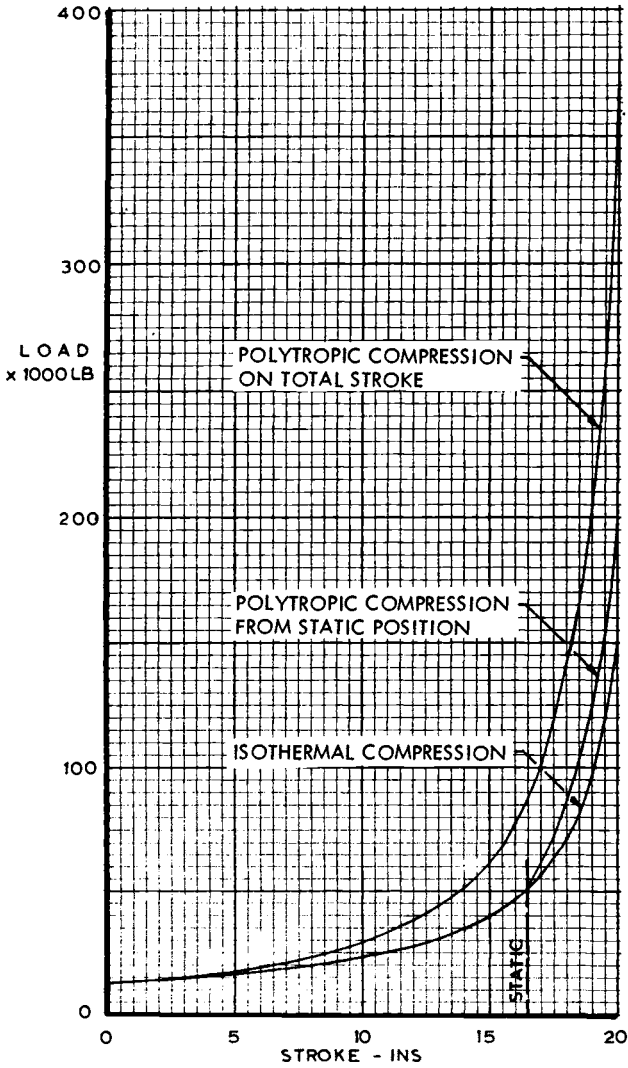


Fig. 5.25 Load-stroke curve, single-acting shock strut.

Table 5.3 Calculations of Polytropic Compression

| Stroke, in. | Isothermal vol V_{th} , in. ³ | Polytropic vol $V_{th}^{1.35}$, in. ³ | P_{abs} , ^a psi | P_{gage} , psi | Load = $33.33P_g$, lb |
|----------------|---|--|---------------------------------|---------------------|---------------------------|
| 0 | 728.0 | 7309 | 390 | 375 | 12,500 |
| 2 | 661.3 | 6400 | 445 | 430 | 14,330 |
| 4 | 594.7 | 5055 | 564 | 539 | 17,970 |
| 6 | 528.0 | 4750 | 600 | 585 | 19,500 |
| 8 | 461.3 | 3950 | 721 | 706 | 23,550 |
| 10 | 394.7 | 3200 | 890 | 875 | 29,200 |
| 12 | 328.0 | 2500 | 1,140 | 1,125 | 37,500 |
| 14 | 261.3 | 1830 | 1,557 | 1,542 | 51,400 |
| 16 | 194.6 | 1220 | 2,335 | 2,320 | 77,300 |
| 18 | 128.0 | 665 | 4,350 | 4,335 | 145,200 |
| 20 | 61.3 | 258 | 11,050 | 11,035 | 368,500 |

^a P_{abs} = gas constant polytropic volume. (Gas constant = $PV_{th}^{1.35} = 390 \times 7309 = 2,850,510$.)

polytropic curve is based upon either $PV^{1.35}$ or $PV^{1.1}$ being constant. The former is used when the gas and oil are separated and the latter when they are mixed during compression. Calculations of polytropic compression are given in Table 5.3.

Examination of these values indicates that a 20 in. stroke would probably never be used since $368,500/50,000 = 7.37 g$ would be required. In this case, it would be more appropriate to plot the polytropic compression such that isothermal values are used up to the 50,000 lb (1 g) deflection; dynamic compression would be considered only from that point to fully compressed. Thus, at 16.4 in. compression, the polytropic air volume is $181.4^{1.35}$ or 1012 in.³, the absolute pressure 1515 psi, and the gas constant 1,534,000. At 20 in. compression, the polytropic volume is 258 in.³, the absolute pressure 5950 psi, the gage pressure 5935 psi, and the load 197,700 lb or 4 g approximately. The latter values are satisfactory in that the pressure is below 6000 psi (a desirable goal because of seal leakage) and the g forces are about right.

Double-Acting Shock Absorber Calculation

Double-acting shock struts improve shock absorption characteristics during taxi conditions over rough or unpaved fields. If such conditions are an important aspect of the aircraft's requirements, then this type of strut should be considered since its secondary chamber (shown in Fig. 5.26) substantially reduces loads beyond the static position. They generally have lower overall efficiencies than single-acting struts; they are also more expensive and somewhat heavier.

V-22 MAIN LANDING GEAR SHOCK STRUT

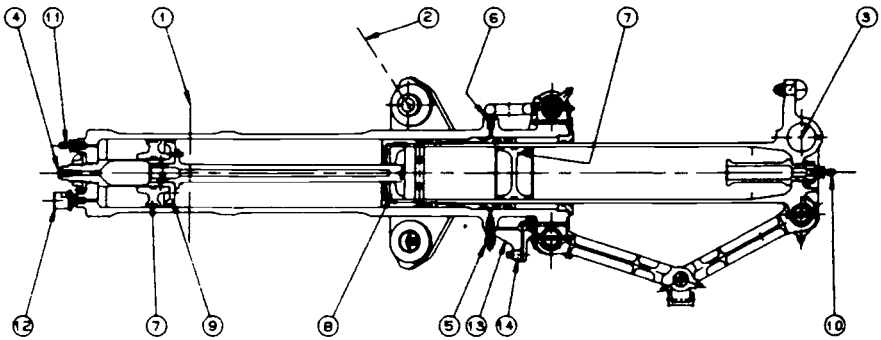


Fig. 5.26 Double-acting shock absorber (source: Ref. 7).

- | | |
|--|---|
| 1) Landing gear attachment to airframe for cantilever strut arrangement centerline | 7) Oil/air separator pistons |
| 2) Drag strut retraction actuator centerline | 8) First-stage damping |
| 3) Axle centerline for twin-wheel tires and brakes | 9) Second-stage damping |
| 4) Oil charge and bleed plug | 10) Charge valve, first-stage nitrogen |
| 5) Oil charging valve | 11) Charge valve, second-stage nitrogen |
| 6) Oil drain plug | 12) Pressure gage |
| | 13) Brake hydraulic manifold |
| | 14) Weight-on wheel switch subassembly |

V-22 main landing gear shock strut designed by Dowty Canada Ltd. Includes floating pistons to separate nitrogen and oil; metering pin provides damping in the first stage and orifice damps in the second stage. Design sink speed is 24 ft/s.

In addition to the abbreviations noted previously, the following must be used when calculating the size of this type of shock strut:

- P_e = pressure in primary chamber at full extension (this is the same as P_1 used for a single-acting strut)
- P_s = pressure in primary chamber at static position—usually 1500 psi (same as P_2)
- P_c = pressure in primary chamber at full compression—determined by the desired compression ratio
- P_{1s} = pressure in primary chamber required to actuate the secondary chamber—should be roughly 1.2 times P_s to prevent on-and-off secondary chamber actuation during normal airport maneuvering
- P_{2s} = pressure in secondary chamber (the precharge pressure) at full extension—equal to P_{2e}
- P_{2c} = pressure in secondary chamber at full extension
- P_{2e} = pressure in secondary chamber prior to its actuation—equal to P_{2s}
- V_e = air volume in primary chamber at full extension

V_s = air volume in primary chamber at static extension

V_c = air volume in primary chamber at full compression

V_{1s} = air volume in primary chamber when secondary is actuated

V_{2s} = air volume in secondary chamber at full extension

V_{2c} = air volume in secondary chamber at full compression

V_{2e} = air volume in secondary chamber prior to its actuation—equal to V_{2s}

In making a preliminary estimate of load factor, assume that strut efficiency is 0.70. Thus,

$$\frac{V^2}{2g} = N(0.7S_p + nS_s + 0.47T)$$

where S_p is the stroke of primary chamber, n the efficiency of secondary (about 60%), S_s the stroke of secondary chamber, and T the tire stroke (deflection). For preliminary estimates,

$$V^2/2g = N(0.7S + 0.47T)$$

where S is the total stroke.

Before starting the calculation, it is necessary to know or assume the following: fully compressed strut load, static strut load, fully extended strut load, stroke-to-static position, total stroke, breakover point, and static pressure.

The fully compressed main gear strut load can be about twice the static load, rather than three times as in the single-acting strut. On a nose gear strut, due to steady breaking loads, the fully compressed load can be about three times the static load, rather than the four or five times in the single-acting strut. These differences are caused by the spring rate being so much lower in the double-acting strut; thus, overcompression will not "spike up" the load as much as in a single-acting strut. However, to afford a true comparison with the previously calculated single-acting strut, the fully compressed load will be assumed to be three times static.

The fully extended strut load can be about one-third of the static load rather than one-quarter as in the single-acting strut. For comparison, the previously used value will still be used, but it should be emphasized that the selection is somewhat arbitrary.

These compression ratios and the static position are selected primarily by experience. Quick calculations are made for several values, the results compared, and a final selection made.

The total stroke is determined by the load factor requirements, using the method shown above. For comparison with the single-acting strut, the same 20 in. stroke is assumed.

As noted, the static position is arbitrarily selected. A position representing 50–60% of total stroke (measured from the fully extended position) is a good value to use, but any position will result in lower spring rates at peak loads.

The breakover point is an arbitrary position at which the secondary

chamber becomes active and causes the sudden change in the load-stroke curve. For rough fields, select a breakover point at about 1.2 *g*. If fatigue reduction, or a soft taxi ride, is paramount, then select a breakover point at about 0.8 *g*, in which case the spring rate is low in the region of 1 *g*.

The static pressure should still be about 1500 psi.

An additional illustration of a double-acting strut is provided in Fig. 5.27.

The calculation proceeds as follows. It is known (or assumed):

| | | |
|---|--|--------------------------|
| Fully compressed strut load | = 3 × static | = 15,000 lb |
| Static strut load | = 50,000 lb | |
| Fully extended strut load | = ¼ × static | = 12,500 lb |
| Breakover point | = 1.2 <i>g</i> | = 60,000 lb |
| Total stroke | = 20.0 in. | |
| Stroke to static | = 11.0 in. | |
| Static pressure | = 1500 psi | |
| Piston area <i>A</i> | = 50,000/1500 | = 33.33 in. ² |
| <i>P_e</i> (extended pressure) | = 12,500/33.33 | = 375 psi |
| <i>V_s</i> (static primary vol) | = <i>V_e</i> - (stroke to static × <i>A</i>) | |
| | = <i>V_e</i> - 366.6 | |
| <i>V_e</i> (extended primary vol) | = <i>P_s</i> <i>V_s</i> / <i>P_e</i> | |
| <i>P_s</i> | = 1500 psi | |

$$\text{So } V_e = \frac{1500[V_s - (366.6)]}{375} = 489 \text{ in.}^3$$

It was shown previously that $V_s = V_e - 366.6$. Thus,

$$V_s = 122.4 \text{ in.}^3$$

$$P_{1s} = \frac{1.2 \times \text{static}}{A} = \frac{1.2 \times 50,000}{33.33} = 1800 \text{ psi}$$

$$V_{1s} = \frac{P_e V_e}{P_{1s}} = \frac{375 \times 489}{1800} = 102 \text{ in.}^3$$

$$\text{Stroke to } V_{1s} = \frac{V_e - V_{1s}}{A} = \frac{489 - 102}{33.33} = 11.6 \text{ in.}$$

$$P_c = \frac{\text{compressed load}}{A} = \frac{150,000}{33.33} = 4500 \text{ psi}$$

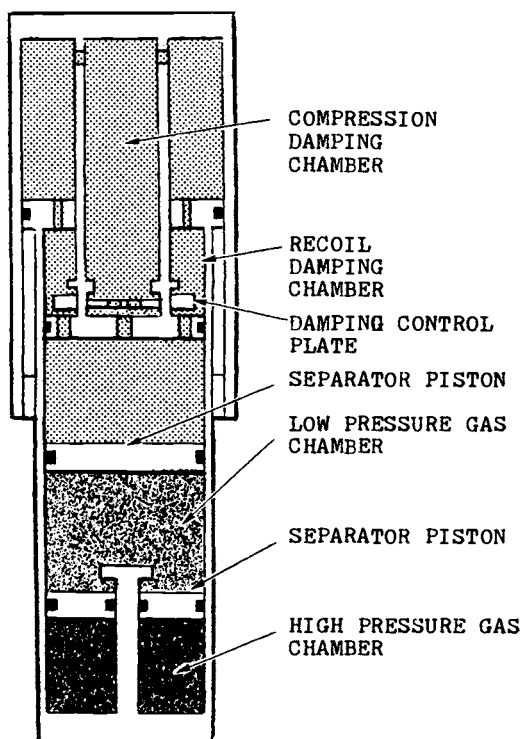


Fig. 5.27 Nose gear double-acting shock absorber.

$$P_c = P_{2c}$$

$$V_c = \frac{P_e V_e}{P_c} = \frac{375 \times 489}{4500} = 30.7 \text{ in.}^3$$

δV_c is the total volume change from actuation of secondary chamber to fully compressed, or

$$\delta V_c = (20 - \text{stroke}) \cdot A = 33.33(20 - 11.6) = 280 \text{ in.}^3$$

$$\delta V_c - V_c = V_{2s} - V_{2c}$$

where $V_{2s} - V_{2c}$ is the secondary chamber displacement. Thus

$$280 - 30.7 = V_{2s} - V_{2c}, \quad V_{2c} = V_{2s} - 239.3$$

$$P_{2s} \times V_{2s} = P_{2c} \times V_{2c}, \quad P_{2s} = P_{1s} = 1800 \text{ psi}$$

So, $1800 V_{2s} = 4500(V_{2s} - 239.3)$. Therefore,

$$V_{2s} = 398 \text{ in.}^3, \quad V_{2c} = V_{2s} - 239.9 = 158.7 \text{ in.}^3$$

Summarizing

$$\begin{aligned}
 P_e &= 375 \text{ psig (390 psia)} & V_e &= 489 \text{ in.}^3 \\
 P_s &= 1500 \text{ psig (1515 psia)} & V_s &= 122 \text{ in.}^3 \\
 P_c &= 4500 \text{ psig (4515 psia)} & V_c &= 41 \text{ in.}^3 \\
 P_{1s} &= 1800 \text{ psig (1815 psia)} & V_{1s} &= 102 \text{ in.}^3 \\
 P_{2s} &= 1800 \text{ psig (1815 psia)} & V_{2s} &= 389 \text{ in.}^3 \\
 P_{2c} &= 4500 \text{ psig (4515 psia)} & V_{2c} &= 159 \text{ in.}^3 \\
 P_{2e} &= 1800 \text{ psig (1815 psia)} & V_{2e} &= 389 \text{ in.}^3
 \end{aligned}$$

Load-stroke curve for isothermal compression is given by $P_1V_1 = P_2V_2$.
Up to the breakover point

$$V_2 = V_1 - (\text{stroke} \times A) = 489 - (\text{stroke} \times 33.33)$$

$$P_2 = \frac{P_e V_e}{V_2} = \frac{375(489)}{V_2} = \frac{183,375}{V_2}$$

$$\text{Load} = P_2 \times 33.33$$

Beyond the breakover point.

$$\begin{aligned}
 V_2 &= (V_{2e} + V_{1s}) - (\text{stroke} \times A) \\
 &= 491 - (\text{stroke from break} \times 33.33)
 \end{aligned}$$

$$P_2 = \frac{P_{1s} \cdot V_{\text{total}}}{V_2} = \frac{1800 \times 491}{V_2} = \frac{883,800}{V_2}$$

The data can now be calculated as shown in Table 5.4.

Table 5.4 Calculation for Compression of Double-Acting Shock Absorbers

| Stroke, in. | V_2 , in. ³ | P_2 , psi | Load, lb |
|-------------|--------------------------|-------------|----------|
| 0 | 489.00 | 375 | 12,500 |
| 2 | 422.34 | 434 | 14,480 |
| 4 | 355.68 | 516 | 17,200 |
| 6 | 289.02 | 635 | 21,150 |
| 8 | 222.36 | 823 | 27,400 |
| 10 | 155.70 | 1179 | 39,300 |
| 11.6 | 102.37 | 1792 | 59,700 |
| 14 | 412.01 | 2143 | 71,500 |
| 16 | 345.35 | 2560 | 85,300 |
| 18 | 278.69 | 3170 | 105,700 |
| 20 | 212.03 | 4170 | 139,000 |

A polytropic compression curve is also calculated, using the same method as described for the single-acting strut, originating at the 1 g point.

Comparison: Single-Acting vs Double-Acting Shock Struts

Figure 5.28 shows the isothermal load-stroke curve for this strut and compares it with that calculated for the single-acting strut of identical length. Curve AA' shows what would happen if the secondary piston were clamped.

Curve AB is the load-stroke curve for the double-acting strut with the secondary piston acting normally. If slowly loaded, the secondary piston begins to move along the curve B at 58% stroke of the primary piston. From this point on, with slow loading pressures in the primary and secondary air chambers, as well as in the oil reservoir below the orifice plate, remain equal as the load increases.

Curve C represents the load-stroke curve of the conventional single-acting shock absorber calculated previously.

Line JJ demonstrates that the load-stroke curve of the double-acting shock absorber closely approximates that of a linear spring. With the maximum static load occurring at 50–60% of the stroke, the optimum increments of stroke are available for traversing either bumps or hollows, with approximately equal increments of load for equal increments of stroke in each direction. Compared to this distribution, the conventional shock absorber at static load has very little of the total stroke available for the higher compressive loads resulting from traversing bumps.

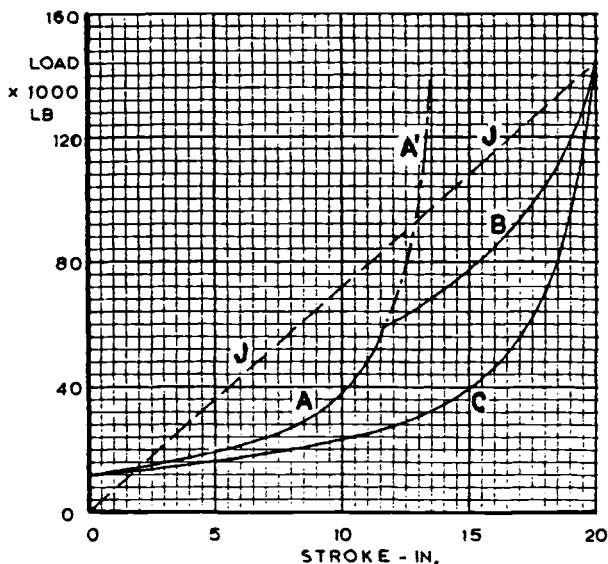
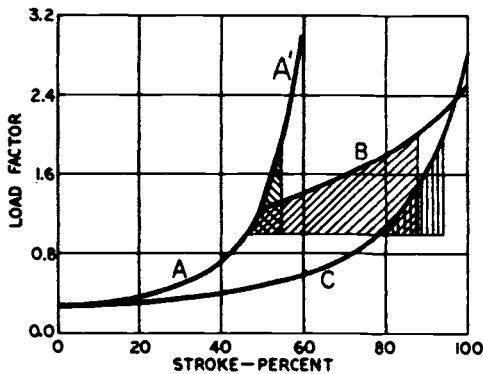


Fig. 5.28 Comparison of double- and single-acting struts.

Figure 5.29, and the discussion of it, are taken from Ref. 5. It illustrates the relative stroke and energy absorption capabilities of the conventional double-acting and elongated conventional shock struts, based on a unit increment in load factor of $+1.0$ – 2.0 . The cross-hatched areas represent the energy increments of the three configurations between these limits. The figure also shows a tabulated summary of those values and their relative magnitudes ratioed to the conventional shock absorber represented by AA'. The gains in stroke and energy increments are 5 and 6.2, respectively, for the double-acting strut, compared to 1.9 for the elongated conventional shock absorber. Based on the incremental energy ratio of 6.2, the double-acting shock absorber is capable of surmounting a step or short wavelength bump with an amplitude equal to the square root of 6.2, or approximately 2.5 times the amplitude capability of the conventional shock absorber with the same unit load factor increment.

Double-acting shock struts may also be used to some advantage on nose landing gears, where the effective vertical velocities can vary a great deal. They are a maximum when brakes are applied and the aircraft pitches onto the nose gear, but that gear must also be fully effective in damping the small velocities that occur during taxiing. Conventional nose gears do not perform too well in effectively damping both types of pitching oscillations. The nose gear braking reaction on a conventional strut causes the maximum



| Shock absorber type: | Conventional | Double acting | Elongated conventional |
|-------------------------------------|--------------|---------------|------------------------|
| Curve | AA' | AB | C |
| Stroke increment, ^a % | 8.4 | 41.6 | 16.0 |
| Stroke increment ratio ^a | 1.0 | 5.0 | 1.9 |
| Energy increment ^a | 3.8 | 23.7 | 7.2 |
| Energy increment ratio | 1.0 | 6.2 | 1.9 |

^aIncrements are percent of stroke for unit load factor increment from $+1.0$ to $+2.0$.

Fig. 5.29 Shock absorber stroke and energy comparison (source: SAE Paper 650844, reprinted with permission). © 1965 Society of Automotive Engineers, Inc.

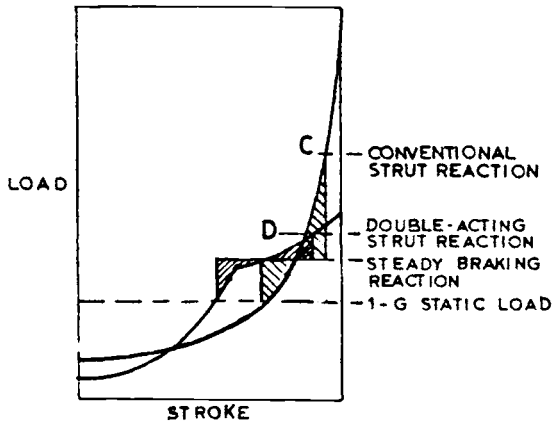


Fig. 5.30 Double-acting strut used to lower nose gear braking reaction (source: SAE Paper 650844, reprinted with permission). © 1965 Society of Automotive Engineers, Inc.

load to be at point C on Fig. 5.30, whereas it reaches only point D if a double-acting unit is used.

5.8 DETAIL DESIGN OF A SINGLE-ACTING OLEO-PNEUMATIC STRUT

This section describes how to calculate the major internal dimensions of a conventional oleo-pneumatic shock strut. For convenience, the author has selected a single-acting strut for which detailed calculations are available. The sizes and characteristics are different from the ones calculated previously in this chapter. Its load-stroke curve is depicted in Fig. 5.31.

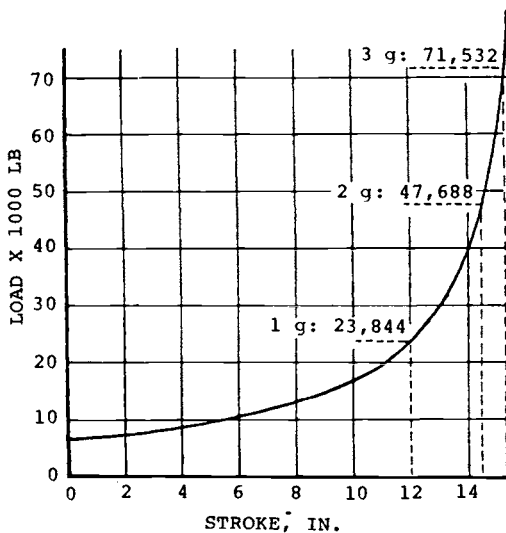


Fig. 5.31 Load-stroke curve: example gear.

Basic Data

Piston outside diameter = 4.50 in.
(assuming 1500 psi desired static pressure)

Pressure ratios = 3.48 compressed to static
3.44 static to extended

Stroke
Total = 15.50

Extended to static = 12.00

Static to compression = 3.50

Air pressure
Fully extended = 436 psig

Extended 3.1 in. = 525 psig (80% stroke)

Static = 1500 psig

Fully compressed = 5196 psig

Internal Cylinder Length

The MIL-L-8552 requirement is that the distance between the outer ends of the bearings shall be not less than 2.75 times the piston outside diameter,

$$\text{Min permissible overlap} = 2.75 \times 4.50 = 12.375$$

Referring to Fig. 5.32, the minimum shock strut length is given by

$$\text{Length} = \text{stroke} + \text{overlap} = 15.5 + 12.375 = 27.975$$

Assume that the cylinder is made 29 in. long from the bottom of the lower bearing to the top of the bore. This means that the overlap is 13.5 in. (3.0 times piston diameter) and the stroke is still 15.5 in.

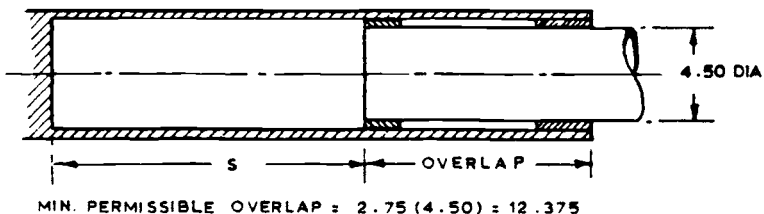


Fig. 5.32 Shock strut overlap.

Volumes

First, the strut-compressed case is considered. Using the fully compressed air volume calculated in determining the load-stroke curve, the depth of air is established. This defines the oil level in that condition and the consequent location of the filler valve. The calculations assume the diameters for the orifice support tube, the inside of the piston, and the inside of the cylinder. These dimensions should be checked early in the design by stress calculations and the volumes modified accordingly if necessary.

In the design shown in Fig. 5.33, the hole in the orifice support tube and oil filler location are such that the air space is restricted to the inside of the orifice support tube diameter.

The area of the inside of the orifice support tube is

$$A = \frac{\pi(2.55)^2}{4} = 5.107 \text{ in.}^2$$

It is known from the shock strut calculations that the fully compressed air volume, $V = 22.588 \text{ in.}^3$. Therefore,

$$L = 22.588/5.107 = 4.423 \text{ in.}$$

The fully extended case is then considered. The calculated fully extended air volume is used and, allowing for the volume of internal parts, the oil level for that condition is determined.

Referring to Fig. 5.34,

$$\begin{aligned} \text{Volume } V &= 8.37\pi/4(5.003^2 - 4.375^2 + 4.035^2 - 2.75^2 + 2.55^2) \\ &= 138.777 \text{ in.}^3 \end{aligned}$$

$$\text{Vol below point } X = 0.7854(20.001) = 15.709 \text{ in.}^3$$

$$\text{Vol above point } X = 138.777 + 22.588 = 161.365 \text{ in.}^3$$

$$\text{Air vol required} = 269.1 \text{ (extended)} = 107.7 \text{ in.}^3 \text{ below point } X$$

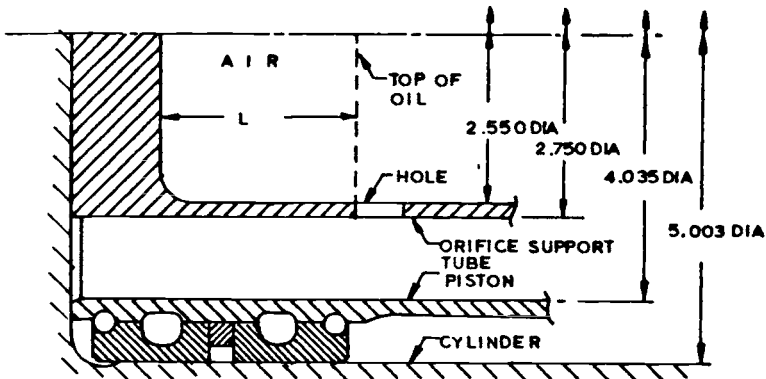


Fig. 5.33 Air volume: strut compressed.

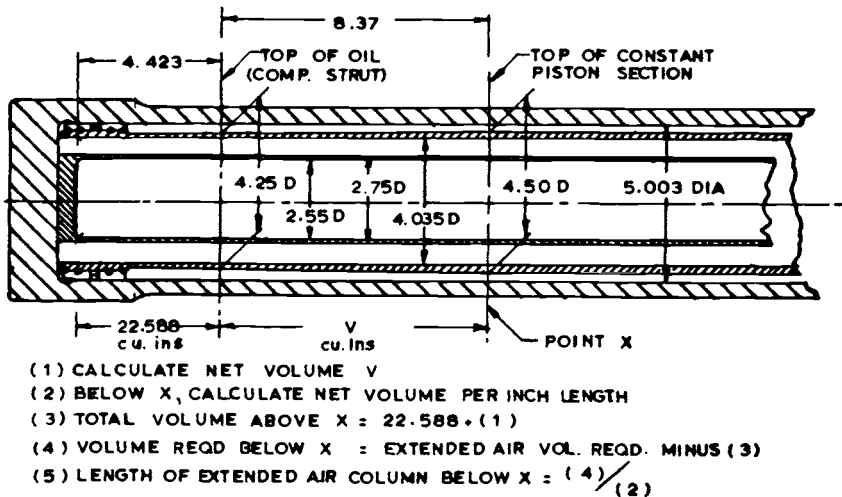


Fig. 5.34 Air volume: strut extended.

Therefore, the length of the air column is given by

$$\text{Below point } X = 107.7/15.709 = 6.856$$

MIL-L-8552 requires that the fully extended oil level must cover the orifice by at least 5 in. or proof must be provided that oil foaming is of no consequence. Using this value, the orifice can be located and the metering pin (if used) designed to suit. Note: the author is of the opinion that, in many cases, 5 in. of oil above the orifice will not necessarily prevent foaming and that air/oil separation should be provided, as noted previously.

Details

Figures 5.35–5.37 are provided to show typical details.

Oil Compression/Cylinder Growth Effects

After the basic dimensions and volumes have been established, the effects of oil compression and cylinder growth should be recognized. These modify the previously calculated load-stroke curves.

First, determine the change in oil volume in compression. At any given pressure the compressed volume is given by

$$V_{\text{comp}} = k \times \text{normal fluid volume}$$

where k is the compressibility factor.

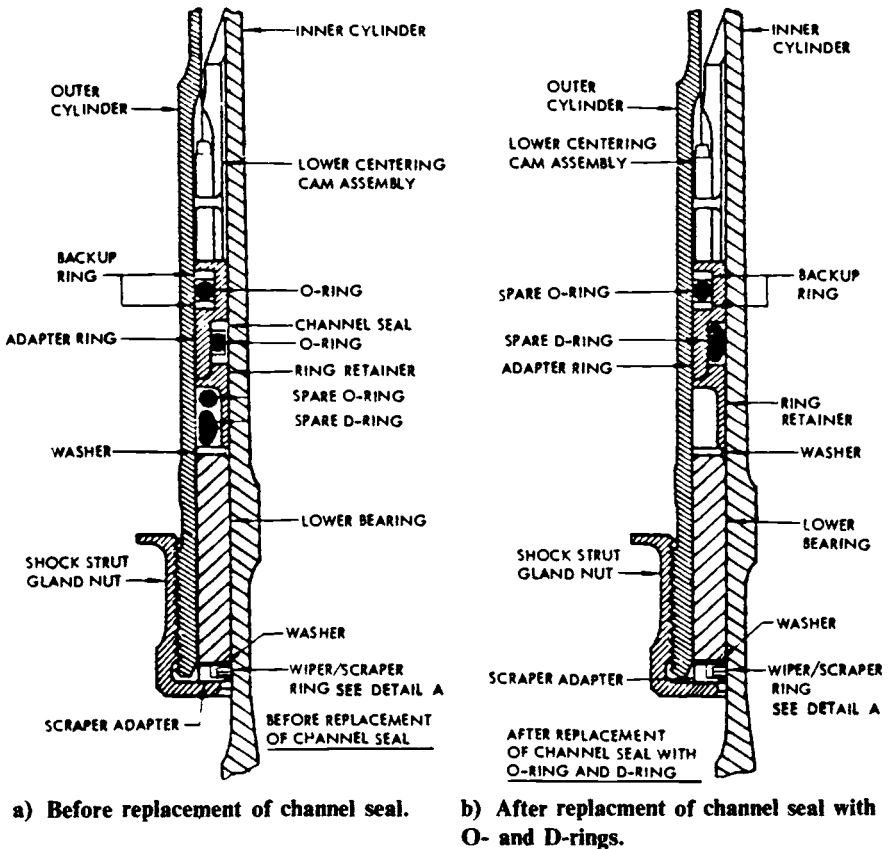


Fig. 5.35 Lower bearing detail.

Typical values for k are as follows:

| Pressure | k | Pressure | k |
|----------|--------|----------|--------|
| 0 | 1.0000 | 3000 | 0.9882 |
| 1000 | 0.9955 | 4000 | 0.9850 |
| 2000 | 0.9917 | 5000 | 0.9820 |

Thus, the compressed volume at 3000 psi is 0.9882 times the normal volume; i.e., the volume change is 0.0118 times the normal volume.

Second, determine the volume change due to diametric cylinder growth. This is given by

$$\text{Volume change} = 2\pi p R_m^3 / Et$$

where p is the pressure, R_m the mean radius, E Young's modulus, and t the wall thickness.

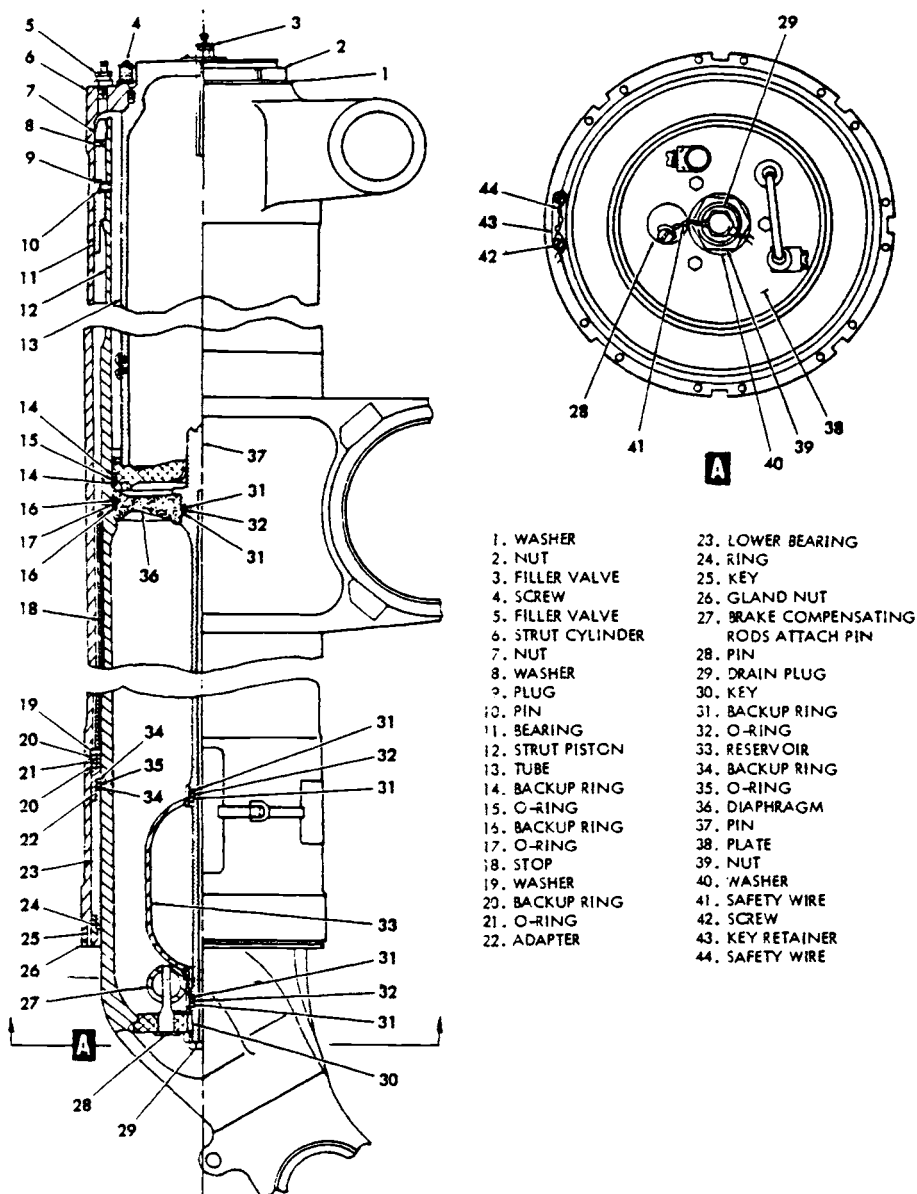


Fig. 5.36 C-141 main gear shock strut (source: Lockheed).

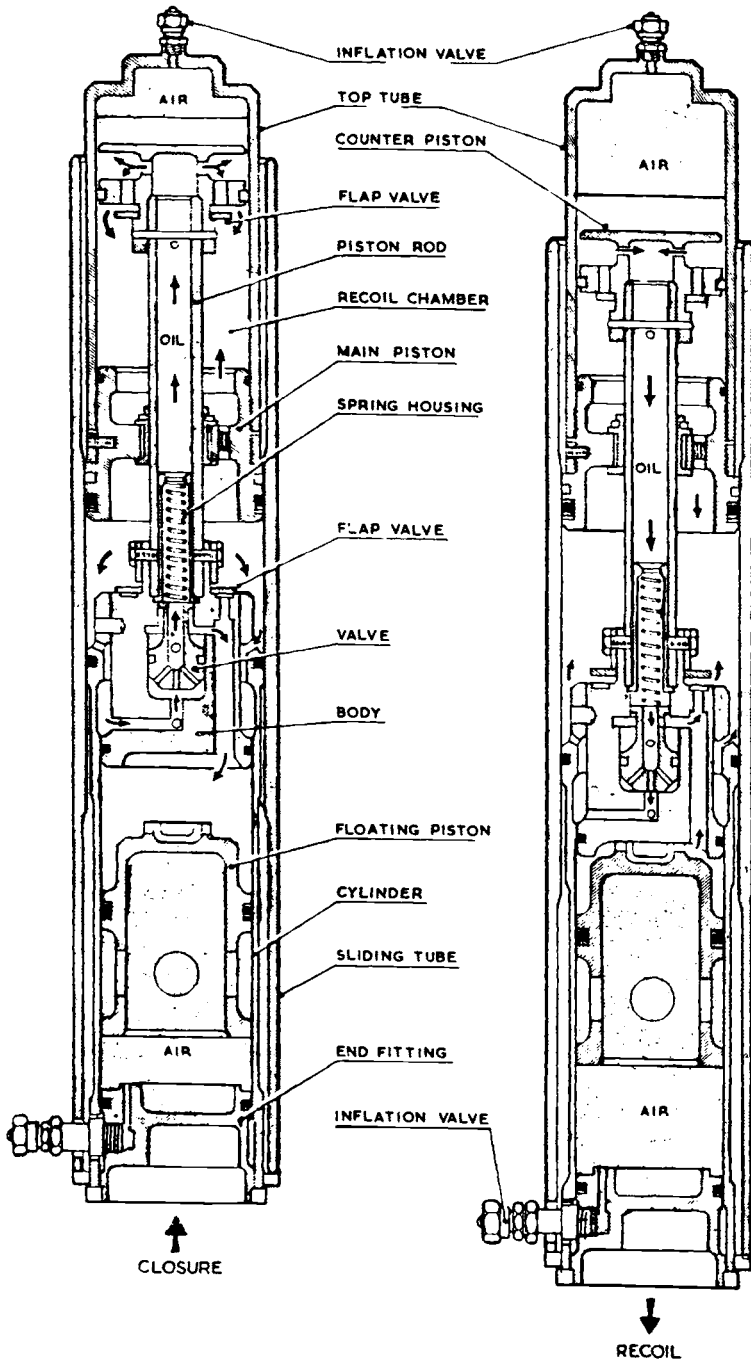


Fig. 5.37 B.Ae. 748 nose gear shock strut (source: British Aerospace Corp.)

Note: where the cross section varies considerably along the cylinder length, the volume change may have to be calculated in segments and then totaled.

Third, the effect of longitudinal cylinder stretch is included and the average stress in the cylinder is calculated by the conventional formula: maximum load divided by the cross-sectional area of the cylinder wall. Divide this stress by Young's modulus to obtain the strain per inch and multiply this figure by the cylinder length to obtain the strain in inches. The volume change is this strain times the internal cross-sectional area.

To obtain the total volume change, add all of the above three effects. In one typical case, these effects were considerable. The strut contained about 5 gal of oil and had a 72,000 lb maximum load. Its internal diameter was 6 in., so the maximum isothermal pressure was 2550 psi. The oil volume change was 13.7 in.³, the volume change due to radial strain 3.5 in.³, and the volume change due to longitudinal stretch 0.7 in.³. Thus, the total volume change was 17.9 in.³.

5.9 PISTON VALVES USED FOR LOAD/STROKE MODIFICATION

A piston-mounted valve may be used to modify the load-stroke curve for operation on rough fields. This valve is spring loaded so that it opens at a given load, thereby modifying the shock strut spring rate. The Rockwell OV-10A employs this type of valve in both the nose gear and main gear. Figure 5.38 is a schematic of that arrangement.⁶ The conventional orifice/metering pin adequately controls the shock absorption throughout the

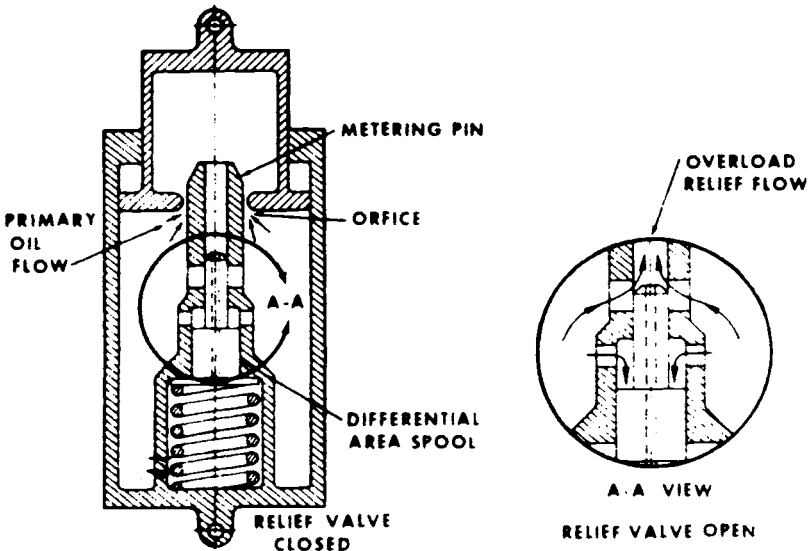


Fig. 5.38 Piston-mounted valve (source: SAE Paper 670562, reprinted with permission). © 1967 Society of Automotive Engineers, Inc.

normal design envelope. When loads are suddenly changed by encountering a bump or hollow, the spring-loaded valve is moved by the subsequent pressure change and allows extra fluid to pass through the orifice. It prevents greatly increased closure velocities and attenuates peak loads when the gear rides over step bumps.

5.10 CONTRACTING SHOCK STRUTS

In some cases, shock absorber contraction is considered as a means of minimizing the free length, thus minimizing stowage requirements. There are essentially two basic types: those contracted by cable and those contracted by hydraulic means.

The cable extends from the airframe to the axle. By layout, a point on the airframe is selected that causes the cable to pull the gear shorter while it retracts. Although simple, this method results in a gear that is highly loaded during flight, possibly causing failures in structure, pressure, seals, or bearings. Hydraulic contraction may be accomplished by cable actuation, pump pressure, or a linear actuator placed in series with the shock absorber. The cable method shortens the gear as described above, but high loads are avoided by employing retraction pressure to open a valve that enables pressurized fluid to pass into an accumulator. When retraction is completed, the retraction pressure is shut off, the valve closes, and the precharge pressure in the accumulator is sufficient to extend the gear when required.

Figure 5.39 shows a contraction method using pump pressure to open a valve and force the piston into a contracted position. Figure 5.40 illustrates an actuator-in-series arrangement.

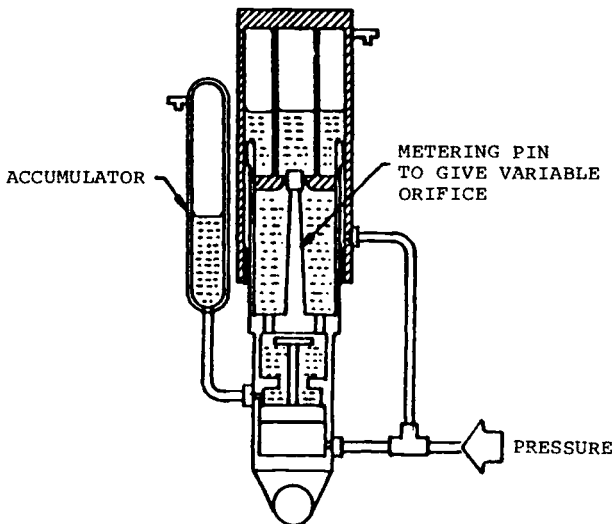


Fig. 5.39 Contraction by pump pressure.

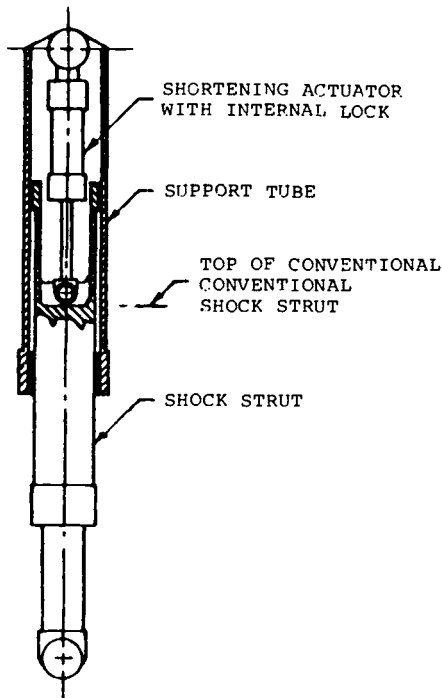


Fig. 5.40 Contraction by actuator in series.

5.11 ORIFICE DESIGN

On small aircraft, it is often possible to use a simple hole at the orifice. Efficiencies up to 85% are obtainable with this design. As aircraft size increases, it is often necessary to have a variable orifice. As the shock strut begins to compress, closure velocity is low and, therefore, the orifice needs to be small to maximize efficiency. As the static position is approached, closure velocity increases and the orifice should be reduced again since closure speed approaches zero.

Orifices can be varied by a hydraulic valve or a metering pin. The valve senses pressure change and opens or closes to increase or decrease flow through the orifice. The metering pin approach is simpler, more reliable, maintenance-free, and—unlike the hydraulic valve—an optimum variable orifice can be obtained by slightly modifying the pin diameter during drop tests. It often requires several drop tests to develop a pin that provides satisfactory performance.

Orifice size may be calculated by the equation (Ref. 1, p. 187),

$$\text{Total orifice area, in.}^2 = \frac{0.30A}{r} \sqrt{\left(\frac{As}{W}\right)}$$

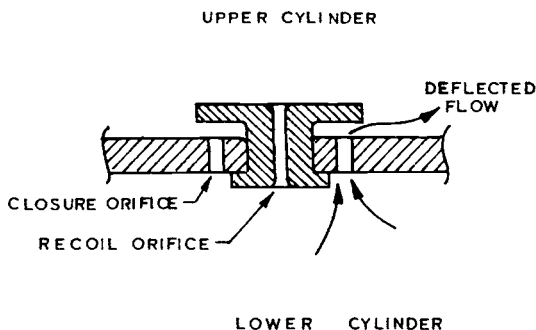


Fig. 5.41 Simple orifice design.

where

A = piston area, in.²

r = applicable load/static load

s = total stroke, in.

W = shock absorber static load, lb

If a plain hole design is used, a good design practice is shown in Fig. 5.41. Note that the oil is deflected laterally as it passes through the orifice. This is to minimize frothing.

References

- ¹Conway, H. G., *Landing Gear Design*, Chapman & Hall, London, 1958.
- ²Wahi, M. K., "Oil Compressibility and Polytropic Air Compression Analysis for Oleopneumatic Shock Struts," *Journal of the Royal Aeronautical Society*, Vol. 13, Oct. 1976, p. 527.
- ³Bingham, A. E., *Aircraft Hydraulics*, Chapman & Hall, London, 1956.
- ⁴Taylor, D. P., "Applications of the Hydraulic Shock Absorber to a Vehicle Crash Protection System," SAE Paper 710537, June 1971.
- ⁵Williams, W. W., Williams, G. K., and Garrard, W. C. J., "Soft and Rough Field Landing Gears," SAE Paper 650844, Oct. 1965.
- ⁶Smith, E. W. and Woodward, R. S., "OV-10A Landing Gears," SAE Paper 670562, June 1967.
- ⁷Darlington, R. F., "Landing Gear—A Complete Systems Approach," *Vertiflite* Vol. 33, March/April 1987, p. 32 (published by American Helicopter Society).

Bibliography

Fewtrell, H. E., "Consideration of Mechanical, Physical, and Chemical Properties in Bearing Selection for Landing Gear of Transport Aircraft," *Lubrication Engineering*, Vol. 39, March 1983, pp. 153-157.

Young, D. W., "Aircraft Landing Gears—the Past, Present and Future," *Proceedings of the Institute of Mechanical Engineers*, Vol. 200, No. D2, 1986, pp. 75-92.

6 TIRES

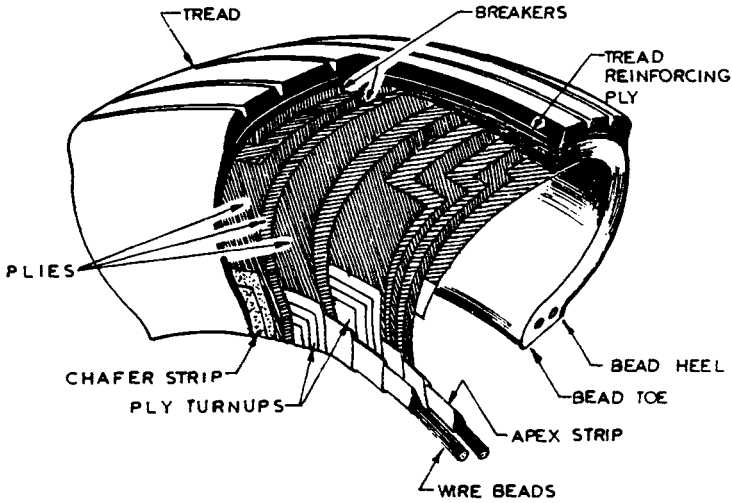
This chapter discusses tires from the landing gear designer's standpoint and does not, therefore, attempt to become involved with the science of tire design. The gear designer is interested in the following characteristics: 1) load-deflection, 2) size and weight, 3) loaded radius, 4) flat tire radius, 5) rolling radius, 6) tire life (sometimes), and 7) crush load capability (sometimes). Other features, such as radius of gyration, effects of temperature, effects of centrifugal forces, friction, side forces, and hydroplaning are all evaluated where appropriate.

Aircraft tires are subjected to a wide variety of high dynamic and thermal loads and their failure can have disastrous consequences. Even with all of today's safety factors and recent advances in tire design, there are still instances such as the Pan Am DC-10-30 accident on Sept. 30, 1980. While taking off from London, a tire on the right-hand gear burst. The pilot rejected his takeoff and passengers were evacuated. One passenger suffered a broken leg while using the escape slide, there were two localized fires on the center and right-hand gears, and there was considerable aircraft damage. All of the tires on the right-hand gear were destroyed and the braking system damaged. Pieces of the tires made holes in the wing, engine nacelle, and horizontal tail—all of this from the failure of one main gear tire! Touchdown speeds are creeping upward in some cases and the associated spin-up loads can have very severe effects on the tires. The Space Shuttle, touching down at 220 knots, on a very abrasive surface such as the Kennedy Space Center, can wear through 11 plies if a crosswind is present. Therefore, it is extremely important to insure that the tires are adequate for the missions to be performed.

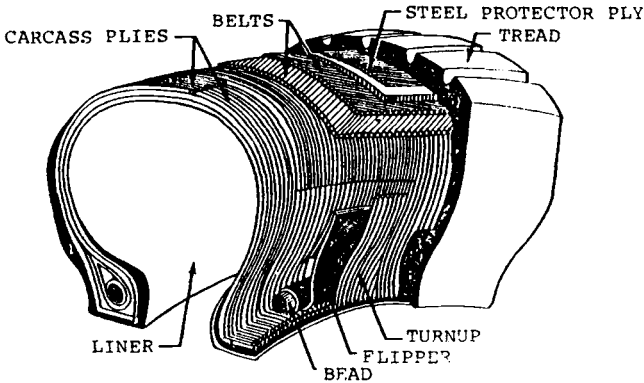
6.1 TIRE CONSTRUCTION

The designer should be aware of the general construction of a tire in order to have a proper understanding of its characteristics; the two basic types are illustrated in Fig. 6.1—bias ply and radial ply. The latter are being installed for test and operation on some aircraft such as the A300 and various USAF fighters. The ATR-42 transport is the first aircraft to use radials as original equipment.

The overall relationship between tire deflection, aircraft speed, carcass design, and tire life was summarized very well in Ref. 1: "The design deflection of an aircraft tire is about double that of a car tire. This high deflection promotes high stresses in both the sidewalls and the contact area. Stresses in the contact area are particularly complex and are aggravated by high



a) Bias ply.



b) Radial ply.

Fig. 6.1 Basic types of tires.

deflection, high speed, thick carcass and tread sections, and the curvature of the tread section. These stresses induce high temperatures in the carcass”

It is this consideration that led to the change from type III high-aspect-ratio (tire section height/width $\times 100$) tires to the types VII and above lower-aspect-ratio tires used for high-speed operation. Tread depth was also decreased to alleviate the tendency for high-speed centrifugal forces to result in tread separation. The shallower treads also provide better cooling of tire hot spots.

Bias-Ply Tire

The inner casing consists of a number of layers of rubberized fabric (a longitudinal-weave nylon), wrapped on a bias, with each layer biased opposite to the preceding layer. At the bead heel, the plies are turned up to envelope the steel wire beads. Outside these plies at the bead heel, chafer strips and breakers are added for additional protection and a synthetic rubber sidewall and tread are added outside the ply periphery. On reinforced-tread tires, an extra ply is added directly beneath the tread. The sidewall and tread are a mixture of natural rubber and cis-polybutadiene.

The tread must have high abrasion resistance, should be as thin as possible to enhance cooling properties, and yet be thick enough to provide adequate life. The tire must be capable of absorbing the shock loads imposed upon it, including deck cables and step bumps, and the bead wires must withstand the circumferential stresses.

Radial-Ply Tire

Michelin's H. C. Schwerdtfeger was quoted in 1984² as follows: "We think by the end of the decade all commercial aircraft manufacturers will have radial tires as standard equipment on their new aircraft An aircraft tire must handle three times the speed, four times the load, two times the tire pressure and three times the deflection in comparison to one of our radial truck tires."* The Michelin Air X radial tire has a much thinner sidewall and a lower aspect ratio (section height/width) and, as shown in Fig. 6.1, the carcass plies are wrapped radially. Biased-wrapped belts are wrapped outside of the carcass plies and a steel protector ply is used directly beneath the tread. Compared to current bias-ply tires, the radials have about 88% stiffness vertically, 60% laterally, and 84% longitudinally; their cornering force is lower and their footprint is about 10% higher (higher flotation and less hydroplaning). Their durability is higher (40–60% tread wear improvement), they run cooler, and they weigh between 72 and 88% as much as an equivalent bias-ply tire. (Michelin calculated a total weight saving of 1710 lb if they were used on a Boeing 727-200, which translates to over $\$1 \times 10^6$ /aircraft/year in increased revenue.) Wheel stresses are lower; there is less rolling resistance and the cut resistance is higher.

6.2 DESIGN CONSIDERATIONS AND REQUIREMENTS

In most cases, tire selection is based on the simple requirement that its load rating must be compatible with the applied loads. On the nose gear, the applied loads include both the static and braking loads. On the main gear, the static load is usually the driving parameter, although on Navy aircraft the landing load and/or cable-crossing loads may predominate. The nose gear braking load is that due to 10 ft/s/s deceleration referred to in Chapter 3. Formulas for calculating the static and braking loads are also given in that chapter.

*Copyright © 1984 McGraw-Hill, Inc. Reprinted with permission.

The rated loads must not be exceeded in the static and braking conditions; a 7% safety factor should be used.

In selecting the tire, allow for 25% growth in aircraft weight. This growth should not require a change in tire or wheel size—it can be accommodated by increasing the number of plies. The tire ply rating (PR) should be at least 2 PR less than the maximum allowed by the Tire and Rim Association.

When the gear has more than one tire per strut, a tire failure will increase the load on the remaining tire(s). Calculations of airframe and gear loads/deflections must show that these tires can withstand the overloads on those remaining tires.

The tire selection process involves listing all candidate tires from the manufacturer's catalogs and identifying those that meet the loads and space requirements, meet the ground speed requirements, have wheel size large enough to accommodate the brakes, and are the lightest. If flotation is important, it may over-ride the weight requirement in order to obtain a satisfactory ground contact area. If airfield roughness must be accommodated, then a large section height may be the predominant factor. Figure 6.2 illustrates a typical tire selection chart.

Basic requirements are quoted in Sec. 4.6 and Fig. 4.5 shows how to draw the tire section based on catalog data. Growth factors are also shown and grown dimensions should be used in all drawings used to illustrate clearances.

| NO. | SIZE | PR | LOAD RATING | | INFL PRESS PSI | SPEED RATING MPH (KTS) | TIRE O.D. INS | BEAD LEDGE DIA. INS | WIDTH INS | BUMP CAPAB INS | QUALIFIC ^N STATUS |
|---|---------------|----|---------------|--------------|-------------------|------------------------------|------------------|------------------------|--------------|-------------------|---------------------------------|
| | | | STATIC LB. | DYNAM LB. | | | | | | | |
| 1 | 24 x 5.5 | 16 | 11,500 | N.A. | 355 | 200 | 24.15 | 14.0 | 5.70 | 1.6 | MIL |
| 2 | 25 x 6.0 | 16 | 12,000 | N.A. | 330 | 160 | SPEED RATING | | | | INADEQUATE. |
| 3 | 22 x 6.6-10 | 20 | 12,000 | N.A. | 290 | 225 | 22.20 | 10.0 | 6.80 | 2.2 | MIL |
| 4 | 26 x 6.6 | 16 | 12,000 | N.A. | 270 | 200 | 25.75 | 14.0 | 6.65 | 1.9 | MIL |
| 5 | 30 x 6.6 | 14 | 12,950 | N.A. | 320 | 225 | 30.12 | 20.0 | 6.50 | 1.1 | MIL |
| 6 | 25 x 6.75 | 18 | 13,000 | N.A. | 300 | 275 | 25.50 | 14.00 | 6.85 | 1.6 | MIL |
| 7 | 29 x 7.7 | 16 | 13,800 | N.A. | 230 | 200 | 28.40 | 15.00 | 7.85 | 2.1 | COMM.L. |
| 8 | 26 x 8.0-14 | 16 | 12,700 | N.A. | 235 | 275 | 26.00 | 14.00 | 8.00 | 1.6 | MIL. |
| 9 | 32 x 11.50-15 | 12 | 11,200 | N.A. | 120 | 200 | 32.00 | 15.00 | 11.50 | 3.2 | COMM.L. |
| | | | | | | | | | | | |
| | | | | | | | | | | | |
| SELECTION FACTORS INFLATION PRESSURE ELIMINATES: <u>1, 2, 3, 4, 5, 6</u> WHEEL DIAMETER ELIMINATES: <u>2</u> DIMENSIONS ELIMINATES: <u>5, 9</u> OTHER: (MINOR FACTOR: NOT QUAL. FOR MIL. USE) <u>7</u> | | | | | | | | | | | |
| SELECTED TIRES MAIN <u>No. 8 26 x 8.0-14 16 PR, OPER. AT 170 PSI</u> NOSE _____ | | | | | | | | | | | |

Fig. 6.2 Example of tire selection chart.

In establishing the static ground line, it is necessary to know the recommended operating deflections. Type III tires use 35%, +1%, -4%. All other types use 32%, +3%, -4%. Recent studies by the USAF have evaluated the effects of using large deflections in order to obtain higher contact areas and, hence, to improve flotation—operation on low-strength bare soil was the objective. The results showed that a 49% tire deflection was satisfactory, provided the associated reduced tire life was acceptable—and in a wartime emergency it probably would be.

6.3 ROLLING RADIUS

Reference 1 quotes formulas that may be used to calculate rolling radius. When the tire is rolling freely and the only effect on the tire is vertical deflection, the approximate rolling radius is given by

$$R_v = R - d/3$$

where R_v is the rolling radius for unyawed and unbraked rolling, R the outside free radius of tire, and d the vertical deflection for purely vertical loading conditions.

If brakes are applied, the rolling radius increases and is given by

$$R_{VB} = R - \frac{d}{3} + \frac{F_x}{K_x}$$

where F_x is the instantaneous drag or fore-and-aft force and K_x the fore-and-aft spring constant.

Finally, if the tire is at a yaw angle ψ , the rolling radius increases and the formula for its calculation is

$$R_{VY} = \frac{R - (d/3)}{\cos\psi}$$

where ψ is the tire yaw angle.

6.4 RADIUS OF GYRATION

The following formula may be used to calculate radius of gyration of tires (it applies to new tires and is accurate to within 5%):

$$\text{Radius of gyration} = \frac{\text{Max outside diam} + \text{min outside diam}}{4K}$$

where

- $K = 1.26$ for type III tires up to 11.00-12
- $= 1.30$ for type III tires larger than 11.00-12
- $= 1.26$ for type VII tires (except tail wheel)
- $= 1.30$ for type VII tail wheel tires
- $= 1.31$ for type VIII tires

For wheel assemblies, including rotating brake parts, the radius of gyration is calculated† as follows:

$$\text{Radius of gyration} = 0.40 \times \text{bead ledge diam } D$$

6.5 CRUSH LOAD

On carrier-based aircraft, it is necessary to recognize the extra tire loads imposed by crossing a cable on the deck—a condition called the crush load. Pessimistically, this load can occur at the instant of touchdown, in which case the tire is already close to bottoming when the cable-crossing load is superimposed. If this happens, the shock loads are absorbed by deflection of the tire material and, perhaps, even the wheel rim. There is no specific definition of tire crush load capability; one company uses three times the bottoming load, while another has a formula based on tire plies as

$$\text{Crush load} = \text{bottoming load} + 11 \text{ lb/ply rating} \\ \text{up to 12 PR}$$

or

$$= \text{bottoming load} + 700 \text{ lb/ply rating} \\ \text{from 20 PR upward with linear variation} \\ \text{between 12 and 20 PR}$$

The bottoming load for the above formula is assumed to be equal to 2.5 times rated static load.

Ultimately, the only way to verify tire capability in this scenario is by testing.

6.6 TEMPERATURE EFFECTS

Tires may be subjected to abnormally high temperatures from proximity to VTOL engine exhaust, proximity to engines when the gear is retracted, aerodynamic heating of the aircraft skin, or braking conditions. Studies have been made to develop tires that have increased resistance to some of these effects. Figure 6.3 depicts the effect of high-temperature engine exhaust on tire life; in this case, the tire material was specially developed for usage in this environment.

Most tire applications, however, do not involve proximity to engine exhaust, whereas nearly all aircraft have tires heated by brake action. Such situations are causing increasingly severe problems due to the trend toward shorter landing distances, shorter turnaround times, and increased taxiing time caused by traffic congestion.

Normally, the aircraft manufacturer supplies the tire, wheel, and brake vendors with load/speed/time data similar to those shown in Fig. 6.4.

†From B. F. Goodrich.

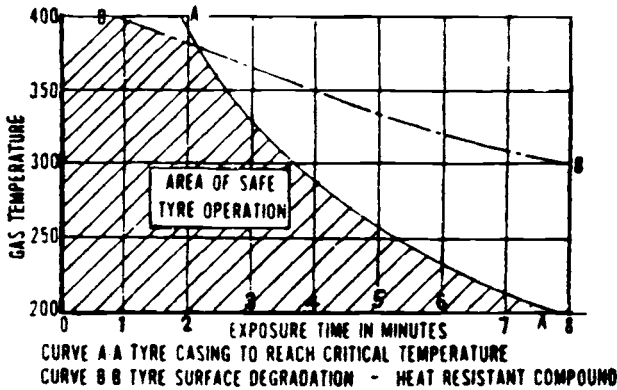
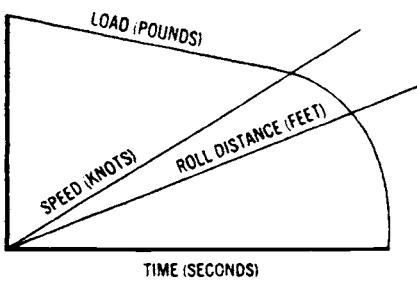
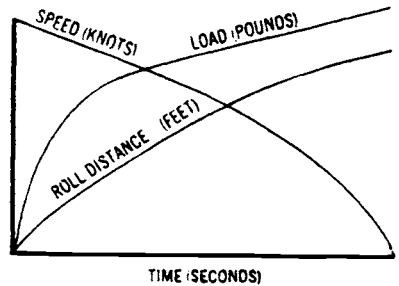


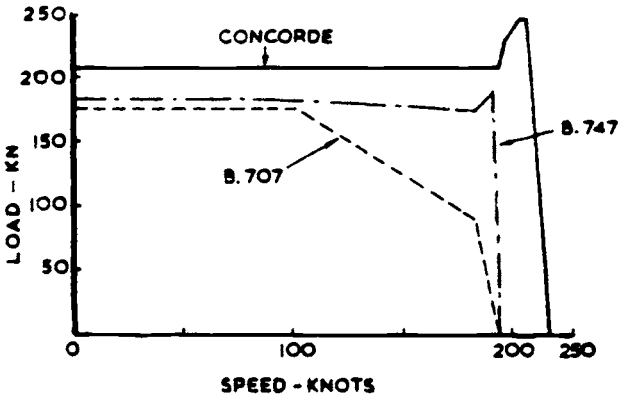
Fig. 6.3 Effect of high-temperature jet blast on tire degradation (source: Ref. 3, reprinted with permission).



a) Typical takeoff curve.



b) Typical landing curve.



c) Takeoff curves.

Fig. 6.4 Load/speed/time curves.

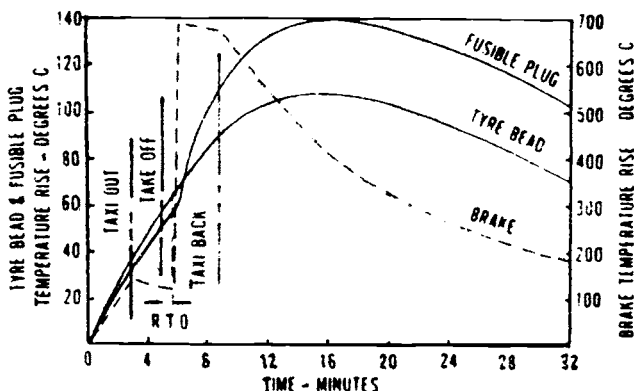


Fig. 6.5 Bead heat buildup in rejected takeoff (source: Ref. 3, reprinted with permission).

However, when a succession of takeoffs and landings are made within a relatively short time, these data must be supplemented by information that allows the vendor to recognize the effects of short cooling times between successive landings.

The peak tire temperature usually occurs during a rejected takeoff (RTO) at maximum weight. After such an event, the tire, wheel, and brake are usually removed and thoroughly inspected. Reference 3 gives the following sequence of events:

1) During taxi, the tire bead temperature will rise 10–15°C (50–59°F) per mile. This will be increased somewhat by intermittent brake applications.

2) During the takeoff run, the bead temperature will increase by a further 30–35°C (86–95°F).

3) If takeoff is rejected, the tire beads will generate 25–35°C (77–95°F) and the brake heat sink temperature will rise to 600–1000°C (1112–1832°F).

4) Peak tire temperature occurs after the aircraft has taxied back to its starting point and has stopped, with brake heat soaking through the tire.

Figure 6.5 illustrates this temperature rise. Fuse plugs are installed in the wheels (as shown in Fig. 4.6) to prevent tire/wheel explosion at high temperatures. Melting of these plugs, at about 400°F, may cause some minor damage, but far less than might be caused by a blowout.

6.7 TIRE ROLLING RESISTANCE

The rolling friction of a tire depends upon the runway surface and tire type. The coefficients of rolling friction are 0.008–0.02 on a normal runway surface, 0.05 on dry, firm grass fields, and 0.10 on wet, soft grass fields.

Typical B. F. Goodrich data from tests on a 15.50–20 tire with 18,000 lb of vertical load shows a 0.0156 coefficient at 0–85 mph and 0.0245 at 93–120 mph. An 18 × 5.5 tire, with a 5050 lb vertical load, had 0.0115 coefficient at 0–84 mph and 0.0153 at 90–116 mph.

These tests verified that rolling resistance increases with aircraft speed. It

is necessary to do work on the tire to keep it rolling and this work is converted to heat inside the tire. Thus, increasing the rolling resistance causes increased heat until a critical speed is reached, at which point the tire temperature rises rapidly and standing waves are formed.

6.8 TIRE FRICTION

Figure 6.6 illustrates coefficient of friction vs aircraft speed for various runway conditions. Tire loads are based on a 0.8 coefficient (i.e., slow speed on dry concrete). Turning friction has to be considered when calculating the torque required to steer the wheel with the aircraft stationary. The following formula may be used for this:

$$\text{Torque} = 0.80(0.02L - 0.15)W \text{ lb-ft}$$

where

L = length of tire contact area, in. = $1.457\sqrt{A}$

W = tire load, lb

A = tire contact area, in.²

Additional data are shown in Table 6.1.

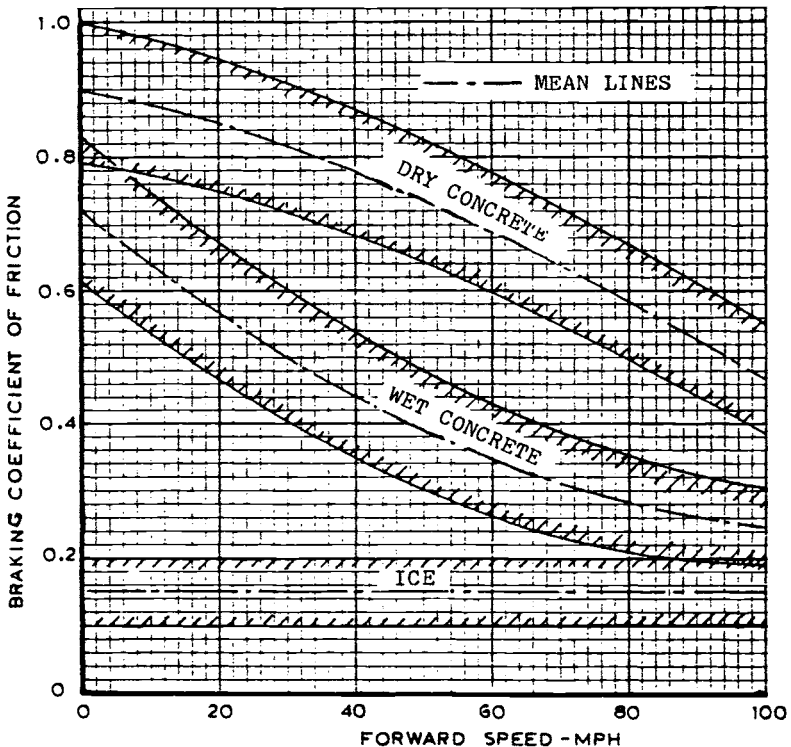


Fig. 6.6 Tire friction vs forward speed (source: Ref. 4, reprinted with permission).

Table 6.1 Some Measured Friction Coefficients during Braking

| Surface | Dry | | Wet | |
|-----------------------|-------|--------|-------|--------|
| | 5 mph | 40 mph | 5 mph | 40 mph |
| Asphalt | 0.95 | 0.75 | 0.95 | 0.65 |
| Concrete, rough | 0.92 | 0.73 | 0.70 | 0.40 |
| Concrete, smooth | — | — | 0.58 | 0.45 |
| Gravel | 0.65 | 0.72 | 0.70 | 0.71 |
| Snow, dry, packed | | | 0.45 | 0.45 |
| Snow, moist, packed | | | 0.50 | 0.52 |
| 0.5 in. Snow over ice | | | | 0.30 |
| Grass | | 0.40 | | 0.20 |

6.9 SIDE FORCES AND SLIP ANGLES

When a tire centerline is at an angle to the direction of motion, the tire tread must be displaced to some extent as it contacts the ground. Most of this displacement occurs behind the center of the contact area and, since the ensuing load is offset from the contact area center, a moment is caused about that center.

Referring to Fig. 6.7, the angle between the tire and direction of motion is called the slip angle, the displacement load the cornering force, the moment arm between the center of the displacement area and the contact area the pneumatic trail, and the moment that tries to straighten the tire toward the direction of motion the self-aligning torque. Thus,

$$\text{Self-aligning torque} = \text{cornering force} \times \text{pneumatic trail}$$

The cornering coefficient is defined as the cornering force per degree of slip angle per unit of vertical load. Typical values for this coefficient, with tires at normal deflection, are 0.06 at 100 psi tire inflation pressure, varying to about 0.045 at 200 psi. A tire at 200 psi, with a 10,000 lb vertical load would, therefore, have $10,000 \times 0.045$ lb cornering force per degree of slip angle.

The side force coefficient is the side load per unit of vertical load. Figure 6.8 shows typical values as a function of yaw (slip) angle.

If a gear has two or more wheels per strut, some degree of slip may be unavoidable. Figure 6.9 shows such an arrangement, with two wheels corotating, that is, one tire must slip relative to the other. The distance that each tire travels on a given circular arc can be calculated for the condition when that tire is free to rotate by itself. This is then compared with the distance obtained when it is coupled to the adjacent tire. This shows the slip, which results in extra tire wear.

If the gear is arranged as shown in Fig. 6.10, unavoidable tire slip will be caused when the aircraft is turned. This figure notes the side force coefficient obtained as a function of turn radius and wheel spacing.

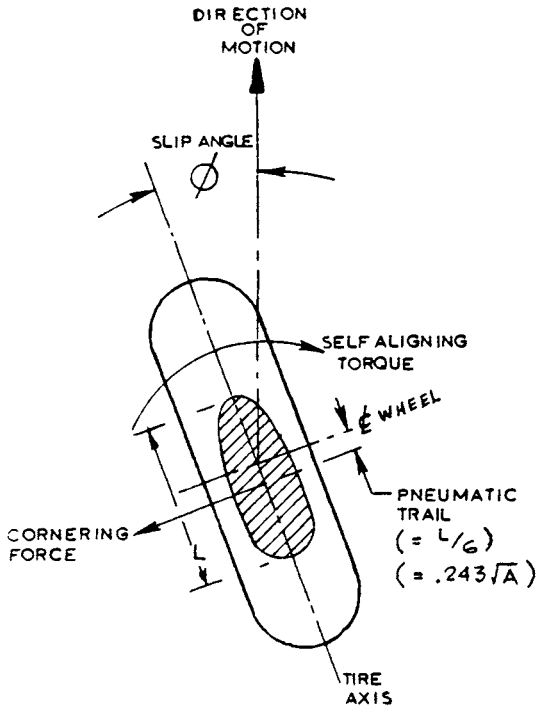


Fig. 6.7 Tire slip.

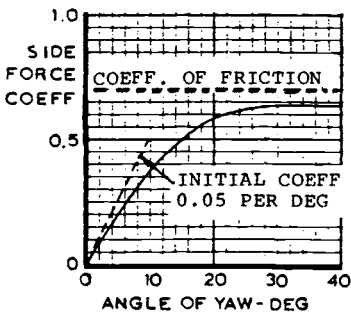


Fig. 6.8 Side force coefficient variation with yaw angle (source: Ref. 5, reprinted with permission).

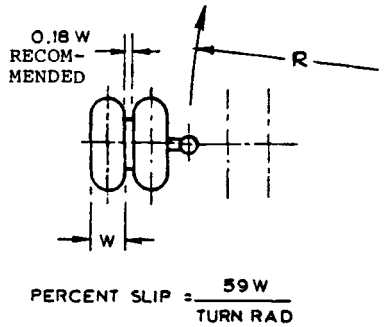


Fig. 6.9 Corotating wheels.

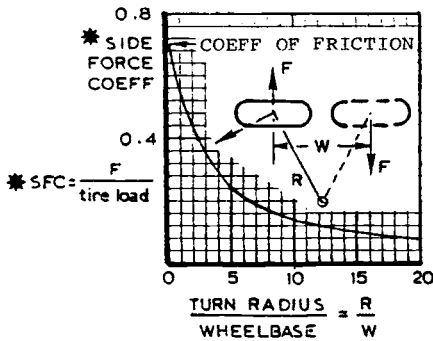


Fig. 6.10 Side force coefficient variation with turn radius (source: Ref. 6, reprinted with permission).

6.10 HYDROPLANING

When a tire is traversing a wet runway, there is a relationship between the forward speed and the inflation pressure at which the tire is essentially lifted above the water film. When this occurs, the tire is said to be hydroplaning. Prior to reaching hydroplaning speed, there is a severe loss of traction due to a portion of the contact area being lifted from the surface.

As the leading edge of the tire encounters the water film, a hydrodynamic wedge is formed, lifting the leading edge and producing an inclined surface at the contact area. The upthrust of the tire is equal to the change in momentum of the water squeezed out beneath the tire. The momentum change is dependent upon water depth, tread configuration, and tire forward speed. A very approximate formula that has been used for many years to determine minimum hydroplaning speed is

$$V_p = 9.0\sqrt{P}$$

where V_p is the minimum hydroplaning speed in knots and P the tire inflation pressure in psi.

Of all the variants involved, tread configuration is the only one that a designer can do anything about—although, in some cases, it must be admitted that water depth is being reduced by runway grooving. It should be noted that some tests have indicated hydroplaning speeds 1.5 times greater than those predicted by the above formula.

To reduce hydroplaning, tire treads have been modified to remove water from under the contact area. The approach taken on automobile tires has been described well in several papers, such as Refs. 7–10, but the tread fragmentation used on those tires is not suitable for aircraft tires. The latter have far higher inflation pressures and, under such conditions, the tread would distort badly and have more wear. Also, high aircraft braking loads would tend to tear the automobile tread patterns.

The above discussion refers to dynamic hydroplaning, where the water depth is more than the tire tread depth, i.e., more than about 0.40 in. There is, however, viscous hydroplaning and reverted rubber skidding, both of which are discussed in Ref. 11.

Viscous hydroplaning (due to a thin film of water acting as a lubricant) can occur even when the pavement is covered with a heavy dew. It is generally a problem only on very smooth runways. Tests have shown that a textured runway surface satisfactorily alleviates this condition. Reference 11 includes data to show the effects of surface moisture for both smooth and textured runways. There is very little that can be done to the tire to alleviate viscous hydroplaning. The best solutions are to groove the runway surfaces and to use a modern skid control system that constantly monitors the available friction coefficient and thereby minimizes the possibility of a skid.

The latter device is also the best protection against reverted rubber skidding. During a prolonged skid, the heat generated by the braking tire turns surface water into steam. Indications are that this steam may be hot enough to melt the surface rubber. In any event, the tire effectively planes across the surface on a cushion of steam, leaving distinctive white streaks on the runway. The melted rubber fills the pores in the runway surface, making it extremely slick—therefore, further compounding the problem.

References

¹Smiley, R. F. and Horne, W. B., "Mechanical Properties of Pneumatic Tires with Special Reference to Modern Aircraft Tires," NASA TR R-64, 1960.

²Mordoff, K. F., "Michelin Testing Radial Tires on Aircraft," *Aviation Week*, March 26, 1984, p. 57.

³Clifton, R. G. and Leonard, J. L., "Aircraft Tyres—An Analysis of Performance and Development Criteria for the 70's," *Aeronautical Journal of the Royal Aeronautical Society*, April 1972, pp 195–216.

⁴Pike, E. C., "Coefficients of Friction," *Journal of the Royal Aeronautical Society*, 1949, pp. 1085–1094.

⁵Hancock, K. G. and Person, P., "Power Steering for Aircraft," *Journal of the Royal Aeronautical Society*, July 1952.

⁶Blinkhom, J. W., "Loads on Multi-Wheel Undercarriages during Ground Maneuvering and Take-off," *Journal of the Royal Aeronautical Society*, July 1952.

⁷Kelley, J. D. and Allbert, B. J., "Tread Design of Tire Affects Wet Traction Most," *SAE Journal*, Vol. 76, Sept. 1968, pp. 58–66.

⁸Allbert, B. J., "Tires and Hydroplaning," SAE Paper 680140.

⁹De Vinney, W., "Factors Affecting Tire Traction," SAE Paper 670461.

¹⁰Horne, W. and Joyner, U., "Pneumatic Tire Hydroplaning and some Effects on Vehicle Performance," SAE Paper 650145.

¹¹Horne, W. B., "Skidding Accidents on Runways and Highways can be Reduced," *Astronautics and Aeronautics*, Vol. 5, Aug. 1967, pp. 48–55.

Bibliography

Daugherty, R. H. and Stubbs, S. M., "The Generation of Tire Cornering Forces in Aircraft with a Free-Swiveling Nose Gear," SAE Paper 851939, Oct. 1985.

Holden, D., "Tire Selection for Modern Aircraft," *Aeroplane and Commercial Aviation News*, March 25, 1965.

"Rolling Resistance and Carcass Life of Tires Operating at High Deflections," U.S. Air Force Flight Dynamics Laboratory, Rept. AFFDL-TR-70-138, Sept. 1970.

BRAKES, WHEELS, AND SKID CONTROL

Brakes, in conjunction with a skid control system (if provided), are used to stop, or help stop, an aircraft. They are also used to steer the aircraft by differential action, to hold the aircraft stationary when parked and while it is running up its engines, and to control speed while taxiing. Most aircraft use disk brakes. The primary variables to consider are disk material and diameter and the number of disks.

Skid control systems are used to minimize stopping distance and to reduce the possibility of excessive tire wear and blowout caused by excessive skidding. The systems do this by constantly sensing the available degree of friction coefficient and by monitoring brake pressure to provide a fairly constant brake force almost up to the skidding point.

In order to illustrate the terminology and configuration of wheels and brakes, Figs. 7.1 and 7.2 are included to show sections through typical assemblies; Figs. 7.3 and 7.4 show further details of a matching wheel and brake.

7.1 REQUIREMENTS

Chapter 4 provides a comprehensive review of the requirements that are of interest to the landing gear designer. Applicable requirements for brakes are ARP 1493, BCAR Chapter D4-5, MIL-W-5013, TSO-C26b, U.S. Navy SD-24, and MIL-PRIME specification MIL-L-87139. For wheels, the requirements refer to ARP 1493 and 1907, AIR 1934, MIL-W-5013, and FAR Part 25. Guidance for skid control design is provided in AIR 804 and 1739, ARP 107A, 764B, and 862, and AS 483A. Requirements for skid control systems are provided in MIL-B-8075, FAR Part 25, and BCAR.*

Chapter 4 also quotes the methods for calculating brake capacity in terms of kinetic energy, as well as a listing of brake capacity requirements.

In general, the brake must stop the aircraft within a specified distance, must do it smoothly and repeatedly over the brake's life, and must be able to stop the aircraft in a rejected takeoff condition.

7.2 BRAKE SIZING

Although detail sizing will be calculated by the brake manufacturers, the preliminary design organization at the aircraft company should be able

*See Chapter 15 for list of specifications.

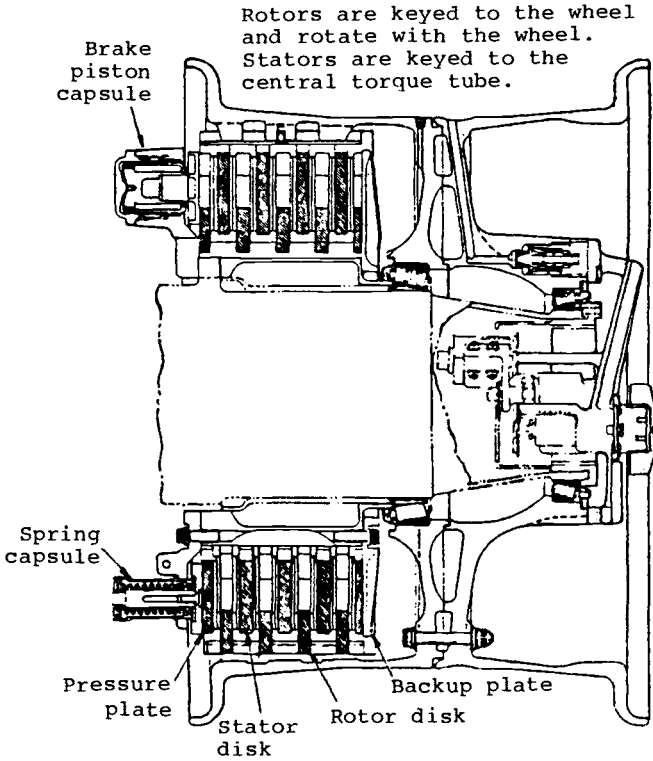


Fig. 7.1 Beryllium brake.

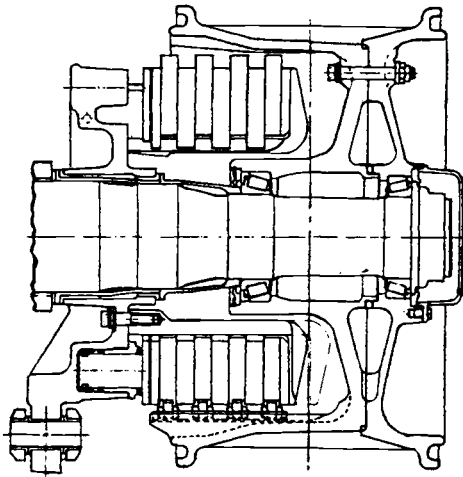


Fig. 7.2 Carbon brake.

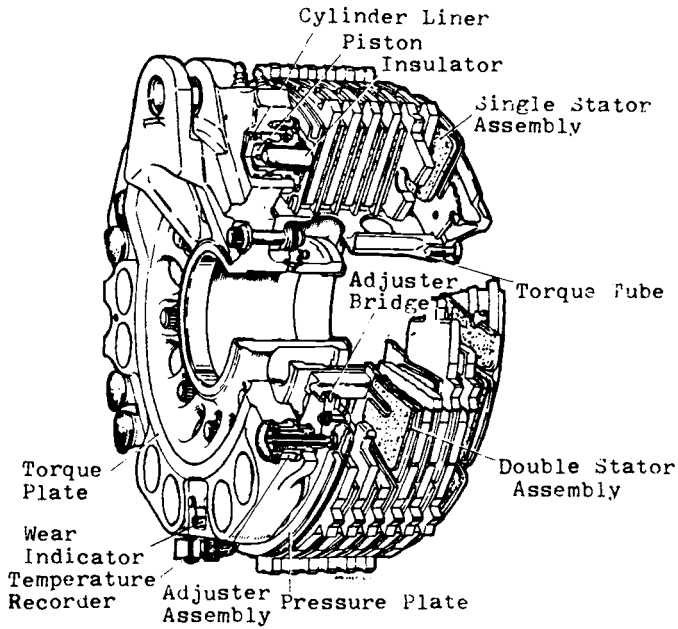


Fig. 7.3 Brake detail (source: Dunlop).

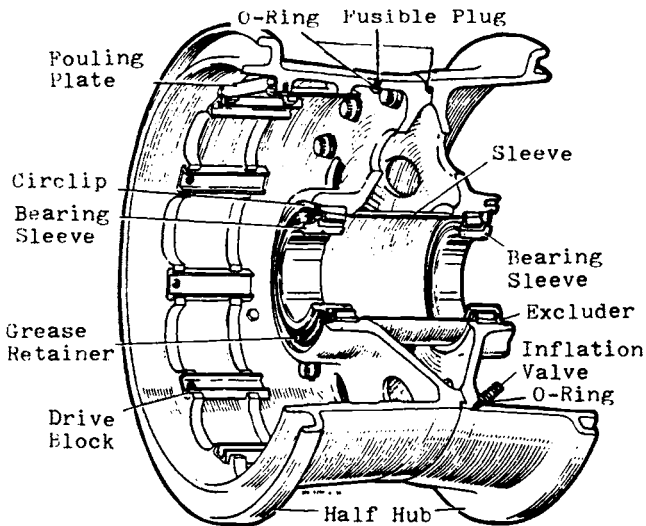


Fig. 7.4 Wheel detail (source: Dunlop).

to estimate the approximate sizes to facilitate conceptual designs of the landing gear. Reference 1 provides some guidelines for this approximation, in which the following criteria are used:

1) Lining loading: a measure of the total amount of energy being absorbed by each square inch of lining and its mating surface over a short time period or a single stop, that is,

$$\text{Lining loading (LL)} = \frac{\text{kinetic energy (KE), ft-lb}}{\text{disk swept area (DSA) in.}^2}$$

2) Lining power: a measure of the average amount of energy entering a square inch of lining and its mating surface during each second, i.e.,

$$\text{Lining power (LP)} = \frac{\text{LL, ft-lb/in.}^2}{\text{stop time, s}}$$

3) Heat sink loading: a measure of the total amount of energy per pound absorbed by the heat sink in a single stop, i.e.,

$$\text{Heat sink loading (HSL)} = \frac{\text{kinetic energy, ft-lb}}{\text{disk and lining carrier segment weight, lb}}$$

4) Friction unit force: a measure of the shearing force on the friction material. This parameter is used in combination with lining power to predict wear rate,

$$\text{Friction unit force} = \frac{\text{brake torque, lb-in.}}{\text{brake radius, in.} \times \text{DSA in.}^2}$$

5) Actuation pressure: the pressure required to develop the required calculated torque, i.e.,

$$\text{Actuation pressure} = \frac{\text{brake torque, lb-in.}}{\text{lining friction coeff.} \times \text{brake radius, in.} \times \text{no. of surfaces} \times \text{piston area, in.}^2} + \text{pressure required to overcome retractor springs}$$

6) Calculated wheel torque: the torque required to stop the aircraft,

$$\text{Wheel torque} = \text{IE, lb} \times \text{rolling radius, in.} \times \frac{\text{deceleration, ft/s/s}}{32.2}$$

Design Example

Assume the following conditions:

- 1) Wheel: 34 × 9.9 with a 11,200 lb static rating.
- 2) Normal brake energy: 100 stops at 9.0 × 10⁶ ft-lb.
- 3) Maximum landing condition: 5 stops at 15.0 × 10⁶ ft-lb.
- 4) Rejected takeoff (RTO) brake energy: 1 stop at 21.0 × 10⁶ ft-lb.

Determine the following:

- 1) Which energy condition designs the brake?
- 2) What is the estimated brake assembly weight?
- 3) What are the heat sink volume and dimensions?
- 4) Can the heat sink fit within the wheel envelope of the selected rim size?
- 5) What is the estimated wheel weight?

Procedure (assuming a steel brake): from Fig. 7.5, find point A for the RTO and point B for normal energy. It is noted that the brake energy designed only for RTO will weigh 107 lb. The brake designed for five stops will weigh 117 lb and the brake designed for normal energy will weigh 118 lb. Figure 7.6 is used to determine the assembly weight for lower kinetic energy levels.

A compromise brake, obtained by interpolation as noted by A' and B' would weigh 114 lb. The heat sink loadings for this compromise would be interpolated as follows:

$$\text{HSL (B')} = 150,000 - \frac{10}{12} (35,000) = 121,000 \text{ ft-lb/lb}$$

$$\text{HSL (A')} = 300,000 - \frac{3}{23} (100,000) = 287,000 \text{ ft-lb/lb}$$

Using Fig. 7.7, the volume of the heat sink for this brake would be 305 in.³. If a 16 in. diameter rim is considered, Fig. 7.8 would define a heat sink

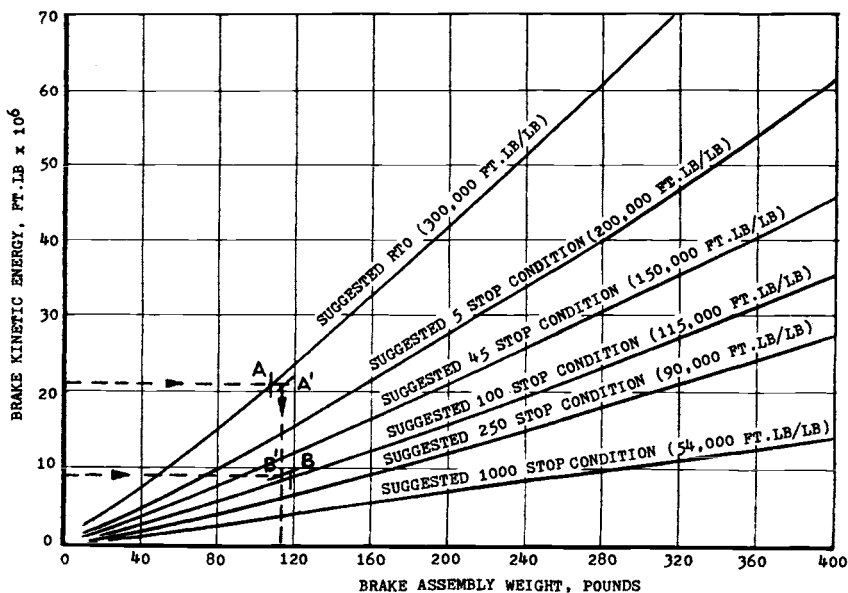


Fig. 7.5 Estimated brake assembly weight vs brake energy.

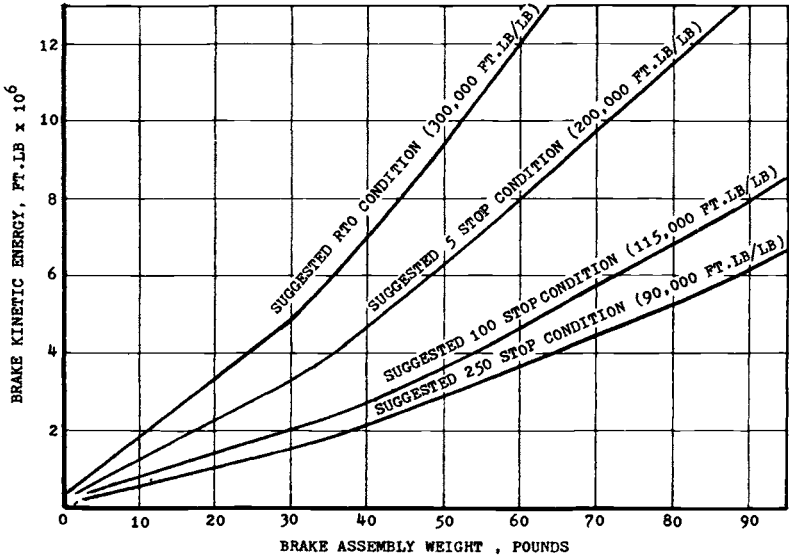


Fig. 7.6 Estimated brake assembly weight vs brake energy.

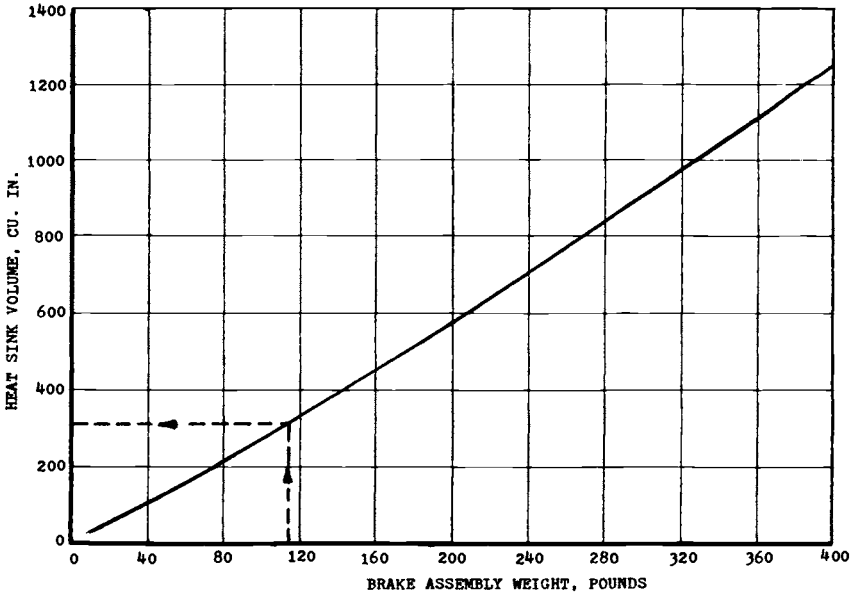


Fig. 7.7 Estimated heat sink volume vs brake assembly weight.

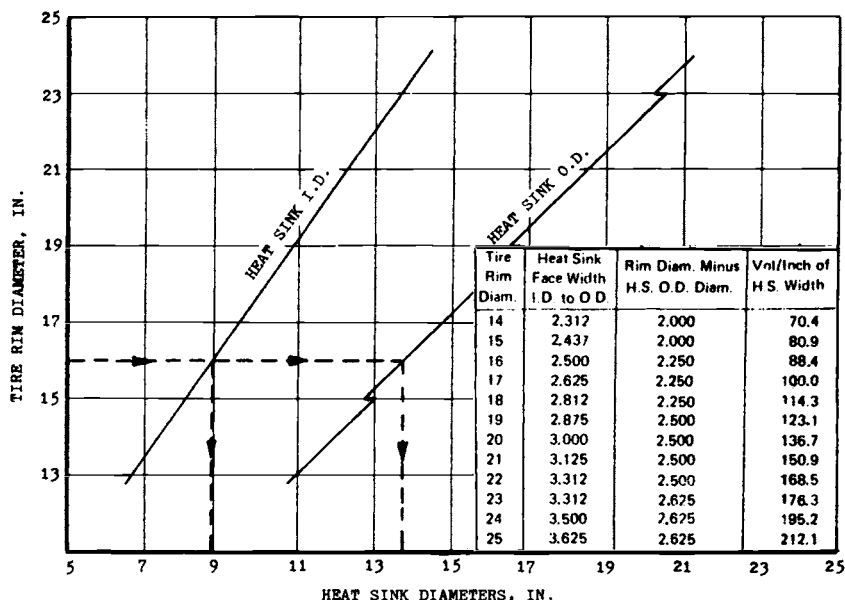


Fig. 7.8 Heat sink dimensions vs tire wheel diameter.

dimension of 8.75 in. inside diameter, 13.75 in. outside diameter, and a volume per inch width from the chart on this figure of 88.4 in.³. (Figure 7.9 enables heat sink volume to be determined for smaller brakes and Fig. 7.10 shows the heat sink dimensions for those brakes.)

The necessary heat sink width would be $305/88.4 = 3.46$ (say $3\frac{1}{2}$ in.).

Adding 0.75 in. on the heat sink inside diameter and end facing the wheel centerline establishes the envelope for the heat sink and torque plate carrier. The piston housing envelope can be approximated by adding 2 in. on the actuation side of the heat sink for the piston housing.

The piston housing dimension can only be approximated, since this dimension can be defined during the detail design only by considering the required piston travel, which is a function of the number of rubbing surfaces and the amount of usable lining per surface.

The estimate wheel weight for a forged aluminium wheel with the assumed static rating of 11,200 lb is estimated at 34.5 lb by using Fig. 7.11.

For a 34×9.9 tire, the average outside diameter is 33 in., so the weight factor is

$$F_w = \frac{11,200 \times 33}{1000} = 370$$

The answers to the questions asked at the beginning of this example are therefore as follows:

- 1) The energy condition designing the brake is: normal energy.
- 2) The estimated brake assembly weight is: a) 107 lb if designed only for

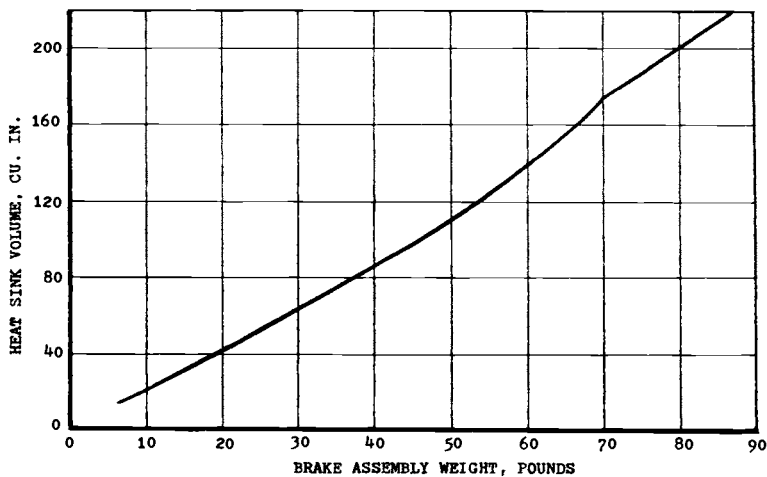


Fig. 7.9 Estimated heat sink volume vs brake assembly weight.

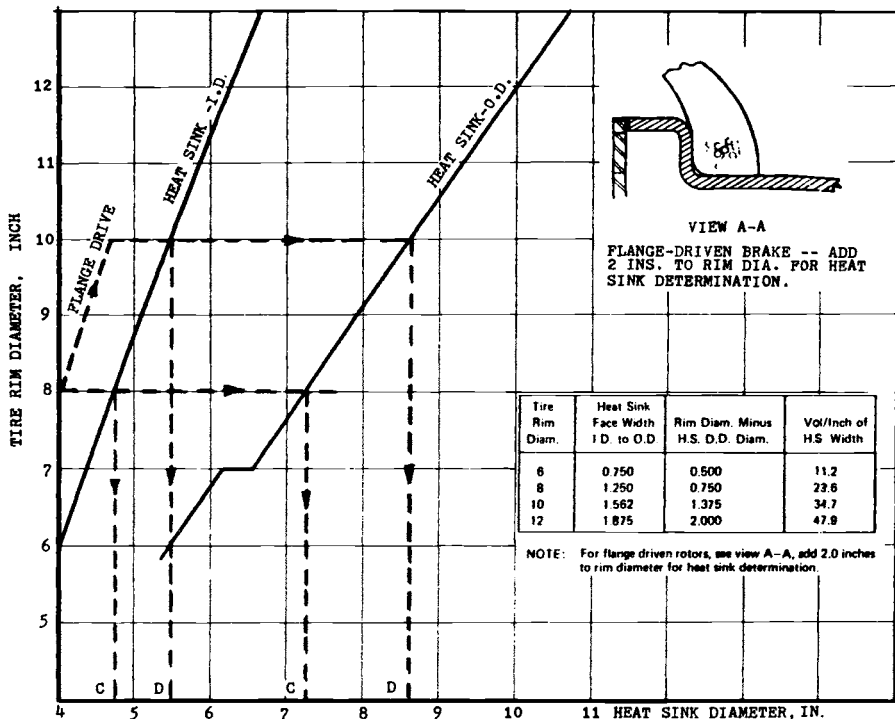


Fig. 7.10 Heat sink dimensions vs tire wheel rim diameter.

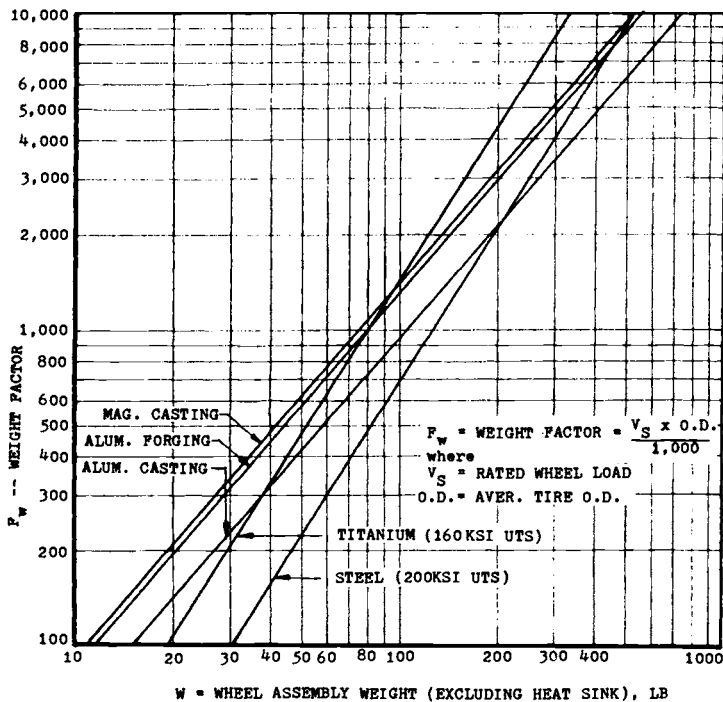


Fig. 7.11 Aircraft wheel assembly weight.

RTO, b) 118 lb if designed only for normal energy, or c) 114 lb if a compromise brake is used.

3) The heat sink volume and dimensions are: 305 in.³ volume; in a 16 in. rim, it would have the following dimensions: 13.75 in. outside diameter, 8.75 in. inside diameter, and 3.5 in. width.

4) The heat sink will fit within the wheel envelope.

5) Estimated wheel weight is 34.5 lb.

Brake Materials Other than Steel

As noted at the beginning of this section, these sizing data are very approximate and are intended only for preliminary design purposes. Final sizing depends on many variables and detailed analyses that involve both static and dynamic conditions. All of this work is conducted by the wheel and brake manufacturer.

The foregoing method showed how to approximate the sizes of a steel brake. Similar curves for other materials are not available, but Table 7.1 shows how to relate the steel volumes and weights to obtain those values for other materials. The data shown in Table 7.1 are supplemented by information from other manufacturers shown in Fig. 7.12.

Table 7.1 Brake Materials Data

| Brake configuration | | Heat sink volume | Brake assembly weight |
|----------------------|----------------------|------------------|-----------------------|
| Rotor | Stator | | |
| Segmented steel | Steel + lining | 1.00 | 1.00 |
| Segmented carbon | Steel + lining | 1.60 | 0.86 |
| Structural carbon | Structural carbon | 1.80 | 0.65 |
| Structural beryllium | Structural beryllium | 1.40 | 0.65 |
| Segmented beryllium | Segmented beryllium | 1.50 | 0.69 |

Source: B. F. Goodrich Co.

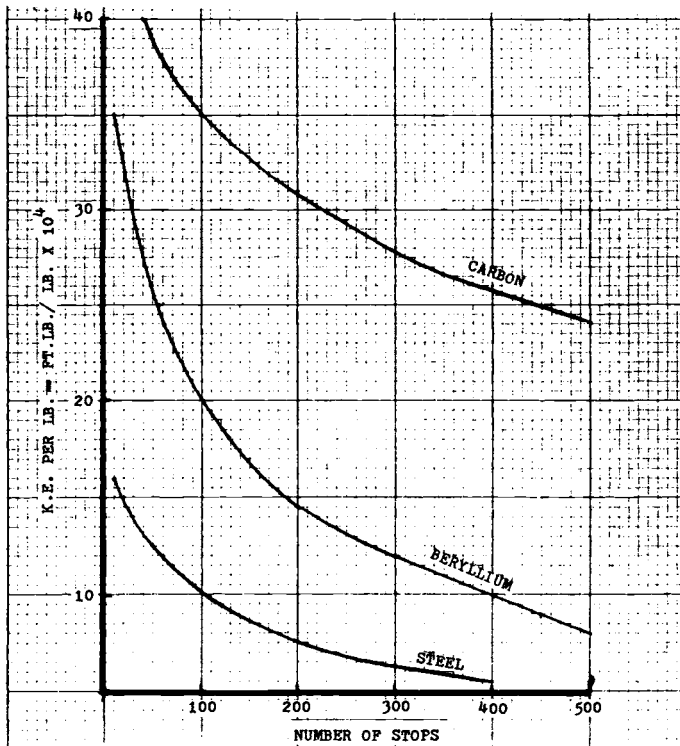


Fig. 7.12 Estimated number of stops vs kinetic energy per pound.

Some Useful Formulas Relating to Brake Sizing

Formulas for calculating the kinetic energy (KE) to be absorbed are given in Chapter 4. Conway² quotes the following equation to show the relationship between KE and brake weight:

$$KE = M \times \theta^{\circ}\text{C} \times \text{specific heat} \times 1400$$

where

- M = mass of brake, lb
 θ = temperature rise, $^{\circ}\text{C}$
 Spec. heat = 0.12 for steel (average)

The temperature rise quoted by Conway is 500°C , corresponding to 12 lb of brake weight per 10^6 ft-lb absorbed. He goes on to note that this temperature is normally classified as a dull red, visible in daylight, but that 800°C may be reached in a "double stop" of the "overuse" test.

An equation that shows the number of brake disks per wheel is (see Fig. 7.13)

$$\mu PR_R = \int_{R_1}^{R_2} 2\pi r^2 S(2N) dr = (4/3)N\pi S(R_2^3 - R_1^3)$$

where

- P = load on wheel, lb
 μ = tire-to-ground friction coefficient
 R_1 = inner radius of brake disk, in.
 R_2 = outer radius of brake disk, in.
 R_R = rolling radius of tire, in.
 S = shear strength of brake lining, psi
 N = number of brake disks per wheel

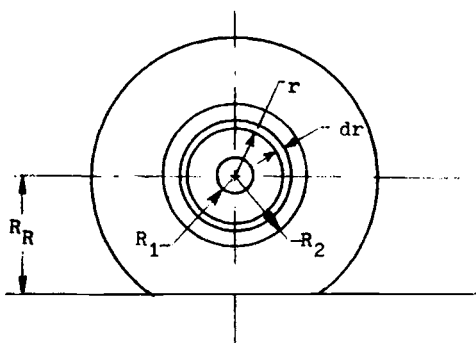


Fig. 7.13 Data for brake disk equation.

It is common practice to assume that about 94% of the gross weight is supported by the main landing gear; thus,

$$mP = 0.94W$$

where m is the number of braked wheels and W the aircraft weight in pounds.

For a deceleration of 10 ft/s/s,

$$\mu mP = (W/g) \cdot a = 10W/g$$

then,

$$\mu = 10/0.94g = 0.321$$

and,

$$10WR_R/mg = (4/3)\pi NS(R_2^3 - R_1^3)$$

Therefore,

$$N = \frac{30WR_R}{4\pi(R_2^3 - R_1^3)mgS}$$

7.3 BRAKE MATERIAL

Until about 1963, most brake heat sinks were made from steel. Beryllium was selected for the Lockheed C-5A to save about 1600 lb on the aircraft's 24 brakes. It is also used on other aircraft such as the Lockheed S-3A and the Grumman F-14. More recently, carbon has been introduced (e.g., C-5B, Boeing 757, Concorde). Figure 7.12 compares the weight and volume of different heat sink materials.

It was reported in 1986 that the substitution of carbon for beryllium brakes on the C-5B saved 400 lb per aircraft and that they gave equal or better performance.³ In addition, overhaul time for the carbon brakes was 37% less than the beryllium brakes.

Characteristics of current heat sink materials are provided in Table 7.2. As shown, carbon has properties that make it highly desirable as a heat absorber. Its high specific heat reduces brake weight. High thermal conductivity ensures that heat transfer, throughout the disk stack, is more uniform and occurs at a faster rate.

It is obvious, therefore, that there are several factors other than weight to consider; in the case of beryllium, one of its problems is the toxicity of beryllium oxide. This requires special precautions when handling the material. In particular, the rubbing of beryllium against any other material must be avoided to prevent formation of a toxic dust.

Another aspect in the carbon vs beryllium comparison is their relative strengths at high temperatures. Figure 7.14 compares the specific strengths

Table 7.2 Comparison of Heat Sink Materials

| Property | Carbon | Beryllium | Steel | Desired |
|---|--------|-----------|-------|---------|
| Density, lb/in. ³ | 0.061 | 0.066 | 0.283 | High |
| Specific heat at 500°F, Btu/lb · °F | 0.310 | 0.560 | 0.130 | High |
| Thermal conductivity at 500°F, Btu/h · ft ² · °F | 100 | 75 | 24 | High |
| Thermal expansion at 500°F, 10 ⁻⁶ × in./in./°F | 1.500 | 6.400 | 8.400 | Low |
| Thermal shock resistance index, × 105 | 141 | 2.700 | 5.500 | High |
| Temperature limit, °F | 4000 | 1700 | 2100 | High |

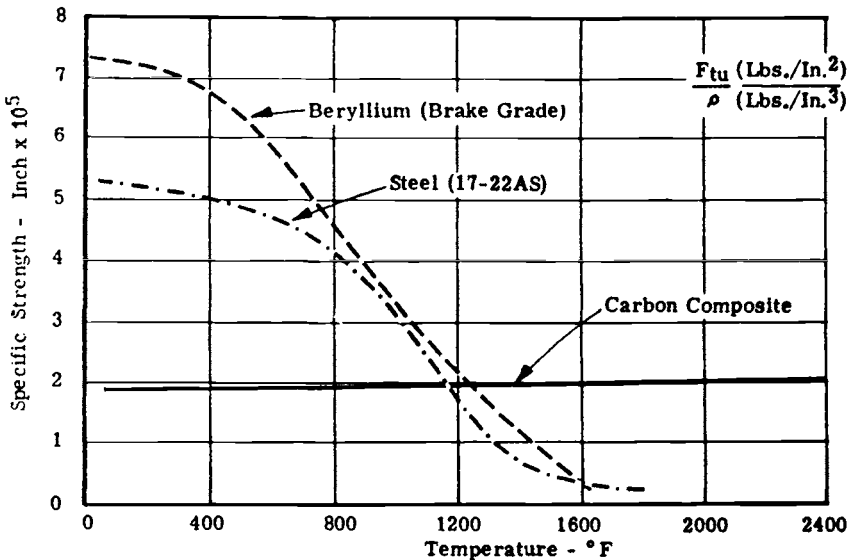


Fig. 7.14 Brake materials: specific strength vs temperature.

of candidate brake materials as a function of temperature, where specific strength equals ultimate tensile strength (psi) divided by density (lb/in.³). It shows how carbon retains its strength at high temperature. Relative to a steel heat sink, the beryllium and carbon heat sinks require a larger volume of brake, which sometimes causes design problems.

To illustrate some of the economics, it was estimated in 1971 that on the Concorde carbon would probably allow 3000 landings vs 500–600 landings for steel before brake refurbishment and would save 1200 lb weight, equivalent to 5% of the estimated transatlantic payload.⁴

7.4 BRAKE DESIGN

The aircraft designer defines the brake in its broadest terms. Detail brake design is conducted by the wheel and brake company. The following summarizes some of the considerations involved in that design phase.

In stopping the aircraft, kinetic energy is transferred to heat energy by the heat sink. It comprises rotors, stators, and (sometimes) wear pads. Rotors are keyed to the wheel and rotate with it. The stators are keyed to the torque tube attached to the axle and are therefore stationary. The pads (if used) are attached to both sides of the rotors and stators and have high thermal conductivity to help ensure that the entire heat sink functions as one unit. Typical brakes, in normal use, operate in the range of 400–500°C (750–930°F) but may provide adequate braking up to 1100°C (2000°F)—a condition appropriate to rejected takeoff. During the analysis, the thermal gradient is determined throughout the heat sink.

Where friction pads are used, they are commonly made from a sintered iron-base compound, because it has little friction variation over either a wide thermal range or a wide dynamic range.

The torque plate transmits the pressure to actuate the brake, transmits brake torque to the landing gear structure, houses the brake pistons, and

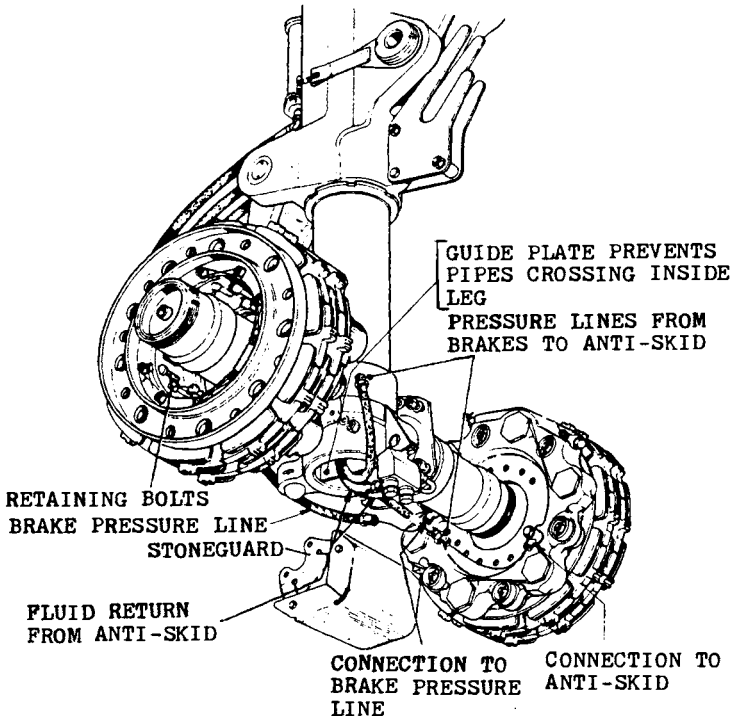


Fig. 7.15 Brake removal/installation of the B.Ae. 748 (source: British Aerospace Corp.).

houses automatic brake adjusters and return springs. Torque plates are often made from aluminum alloy forgings such as 2014-T6.

Brake pistons are housed in aluminum alloy cylinders that are screwed into the torque plate. Mating surfaces are hard anodized for long wear and the entire cylinder is sealed with an O-ring where it joins the torque plate. The whole assembly must withstand temperatures from -60°F (-50°C) up to the maximum temperature conducted by the heat sink.

Brake wear indicators are installed to provide visual indication of the amount of wear. A protruding pin indicates the stack thickness—the thinner the stack, the more the wear!

Figure 7.15 is provided to show more details of a typical brake and its relationship to the landing gear.

To quote MIL-L-87139: "Brake squeal is the induced vibration of the stationary parts of the brake assembly and its mounting. It generally has a natural frequency of several hundred cps as compared to chatter frequency of 6–25 cps. Brake chatter has been so severe that gear walk was induced on the F101 and F105 aircraft." These problems are caused by lining/rubbing surface interactions and lack of structural stiffness. Further details can be obtained in Ref. 5.

Other considerations, such as heat sink material and overall layout, were discussed in the earlier part of this chapter.

7.5 WHEEL DESIGN

The aircraft wheel design is influenced primarily by its requirement to accommodate the required tire, to be large enough to house the brake, and to accomplish these tasks with minimum weight and maximum life. The ability to quickly and easily remove the tire is also important.

In the 1940's, the automobile-type well-base construction was used (i.e., a one-piece wheel). When tires became larger and stiffer, the removable-flange wheel was used. These were replaced by the present-day split-wheel designs in which the wheel is made in two halves and bolted together, as depicted in Fig. 7.16.

Wheels are usually made from forged aluminum alloy, such as 2014-T6. Magnesium alloy is looked upon with disfavor today because of its propensity to burn and because of corrosion problems. It is important to design the forging such that optimum grain flow is obtained, with particular attention to the tire bead seat areas. Photostress and stress lacquer techniques are used to show the general stress distribution and to ensure that the item is free from harmful stress concentrations.

Figure 7.17 illustrates the critical areas of stress concentration. The rim contour is in accordance with international standards. Static and fatigue loads design the flange bead ledge and wheel well area, with the flange acting as a torsion ring to hold the tire bead in position. The flange must also distribute the shear loads from ground reaction into the rest of the wheel.

The two wheel halves are joined together by a number of tiebolts. This area of the wheel is designed for high stiffness. They are lubricated prior to

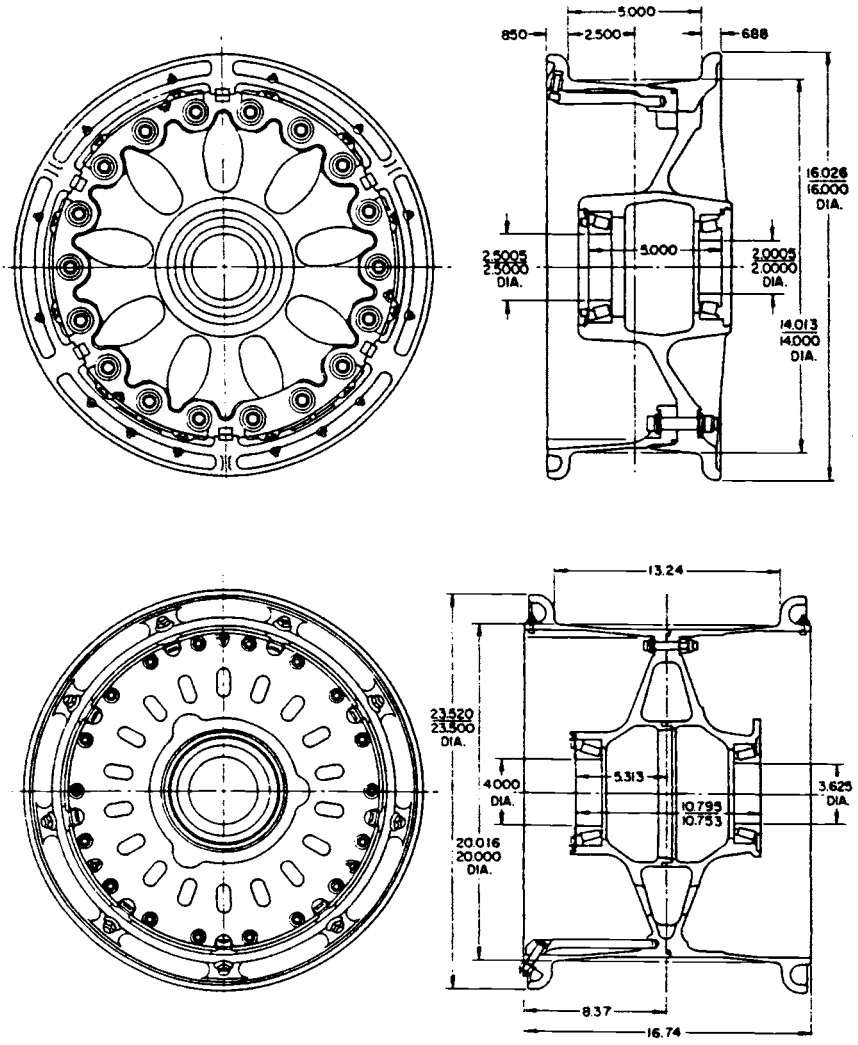


Fig. 7.16 Wheel dimensions (source: Ref. 6).

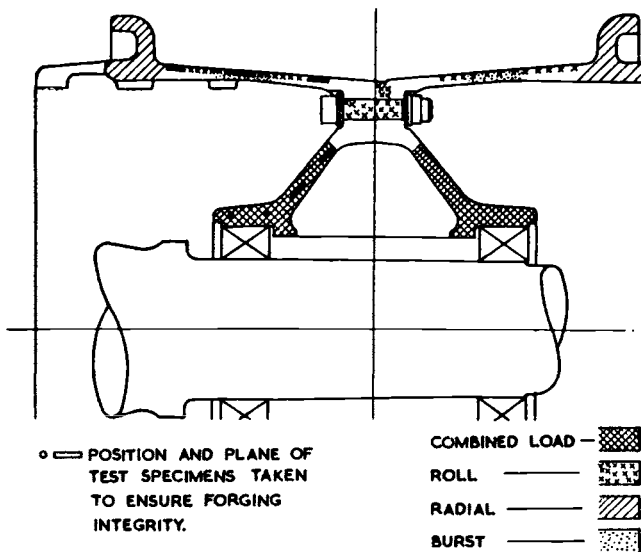


Fig. 7.17 Critical stress areas in wheel (source: Dunlop).

assembly to minimize torque/tension variation and are then torqued to very precise values in order to optimize fatigue life.

At the center of the wheel, the hub is designed to house the wheel bearings. In many cases, sufficient material is left so that oversize bearings can be installed if required. The bearings are of the taper-roller type and are sealed to ensure that their grease is not ejected at high speed, as well as to protect the bearings from contamination.

A standard tire inflation valve is installed in the outboard wheel, usually near the tiebolt flange. Fusible thermosensitive pressure release plugs are also installed in the wheel in this area. As noted in Chapter 6, these plugs release the tire pressure if the local temperature reaches a predetermined level. Each plug is sealed by an O-ring and consists of a hollow casing housing, a eutectic insert, a solid piston, and a rubber seal.

Other items that have to be considered include the rotor drive keys or blocks, a heat shield if required, and possibly a tire change counter. The drive blocks are high-strength steel and are dovetailed into the wheel half surrounding the brake. Heat shields are sometimes provided to minimize heat transfer from the brake. The tire change counter is sometimes specified to record tire changes.

Figure 7.18 illustrates the dimensional data required on a wheel drawing. Figures 7.19 and 7.20 are included to enhance overall understanding of wheel removal.

7.6 BRAKE HEAT

In recent years, trends in aircraft operation have caused brake heat to be more of a problem. Military and commercial aircraft are being designed for

1. SPECIFY TAPER ANGLE FOR DEFINING WHEEL BEARING GREASE SEAL INTERFACE.

2. DEFINITION OF TERMS USED - SEE ILLUSTRATION:

2a. TIRE RIM DIAMETER

2b. HEAT SINK FACE WIDTH

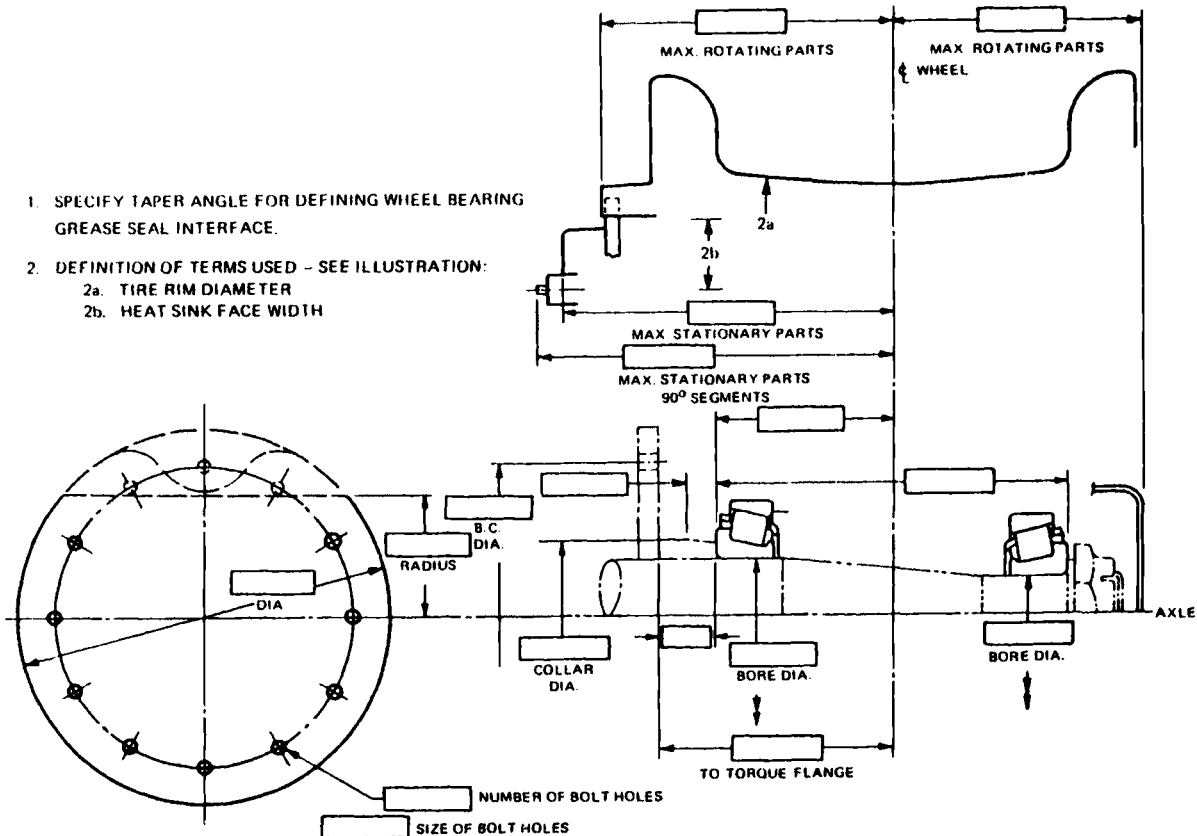


Fig. 7.18 Specification wheel dimensions.

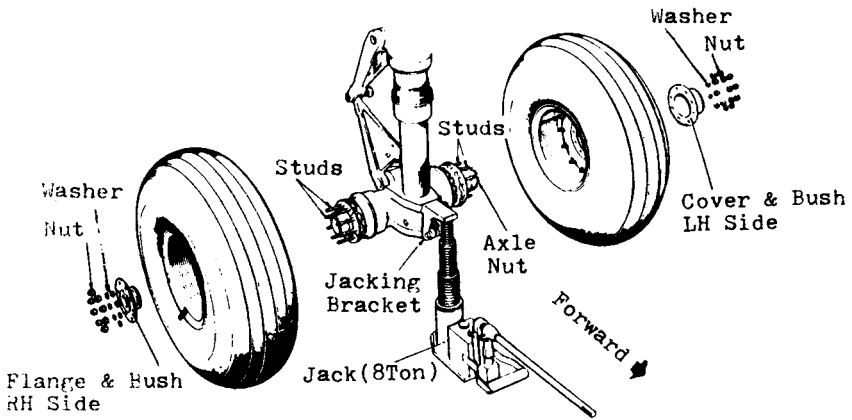


Fig. 7.19 Nose wheel removal on B.Ae. 748 (source: British Aerospace Corp.).

short turnaround times, short landing distances, and, in many cases, short stage lengths. The short turnaround times and short flight times reduce brake cooling times between usage and short landing distances often result in brake applications being increased. Therefore, brakes are sometimes applied while they are still hot—and the available kinetic energy in the brakes is correspondingly reduced.

There are two ways of attacking the problem: make a thorough analysis of expected operations and design the brake accordingly or provide the brake with a cooling device.

Analysis is conducted by the brake manufacturer based upon mission profile data from the “airframer.” Figure 7.21 shows typical data provided to the brake manufacturer who filled in the blank spaces and prepared the brake temperature spectrum illustrated in Fig. 7.22. A particular brake was used in this analysis. In the case described, the initial brake selection was marginally acceptable and had to be changed to accommodate the temperature rise.

It is noteworthy that the only really effective cooling is in the air—after takeoff. While on the ground, the cooling during taxi is essentially cancelled by frequent brake applications.

Brake Cooling

In the 1960’s Eastern Airlines tried to install cooling fans on its aircraft scheduled to operate on short stage lengths.¹ A B. F. Goodrich forced-air cooling system was used, comprising an axle-mounted electric fan with cast aluminum blades. The impeller “pulled” air in from the outboard side of the wheel and passed it through cutouts in the wheel web, over the hot brake, and out the inboard side of the wheel. Figure 7.23 shows the results of this study.

The cooling unit was capable of delivering 260 ft³/min of air against a

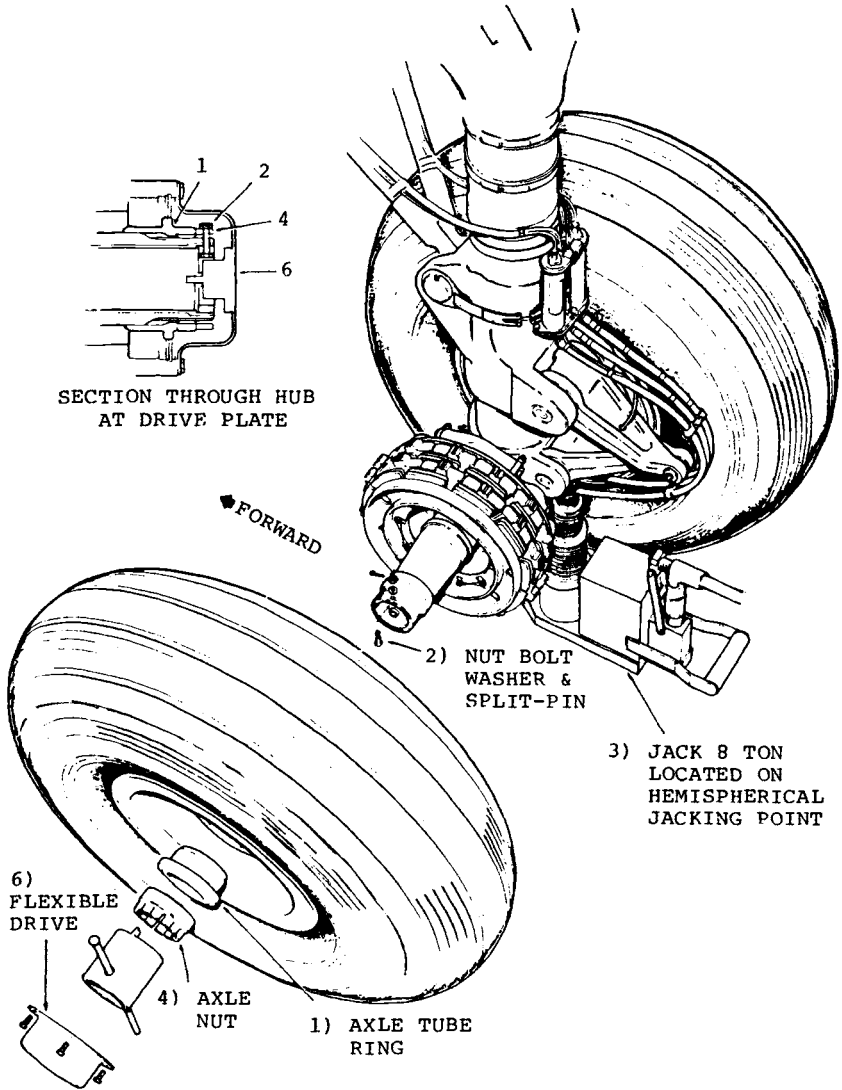


Fig. 7.20 Main wheel removal/installation on B.Ae. 748 (source: British Aerospace Corp.).

| CYCLE NO. | OPERATION | INITIAL TEMP | | GROSS WEIGHT | SPEED | | NORMAL TEMPERATURE | | RTO | | RTO TEMP | | TIME | |
|-----------|-----------|--------------|----|--------------|-------|------|--------------------|----|------|------|----------|----|------|------|
| | | °F | °F | | LB | KTS | MPH | °F | °F | KTS | MPH | °F | °F | MIN |
| 1 | T.O. | 80 | 80 | 42,000 | | | | | 66.0 | 4.81 | | | | 7.3 |
| | LANDING | 80 | | 42,070 | 66.3 | 4.62 | | | | | | | | 7.0 |
| 2 | T.O. | | | 48,890 | | | | | 64.0 | 4.42 | | | | 7.16 |
| | LANDING | | | 47,990 | 64.0 | 4.34 | | | | | | | | 7.0 |
| 3 | T.O. | | | 47,810 | | | | | 61.9 | 4.08 | | | | 7.0 |
| | LANDING | | | 46,935 | 64.5 | 4.32 | | | | | | | | 7.0 |
| 4 | T.O. | | | 46,785 | | | | | 60.0 | 3.72 | | | | 6.9 |
| | LANDING | | | 46,910 | 66.0 | 4.42 | | | 60.0 | 3.64 | | | | 7.0 |
| | | | | 46,730 | | | | | | | | | | 6.7 |

Fig. 7.21 Brake temperature—mission profile.

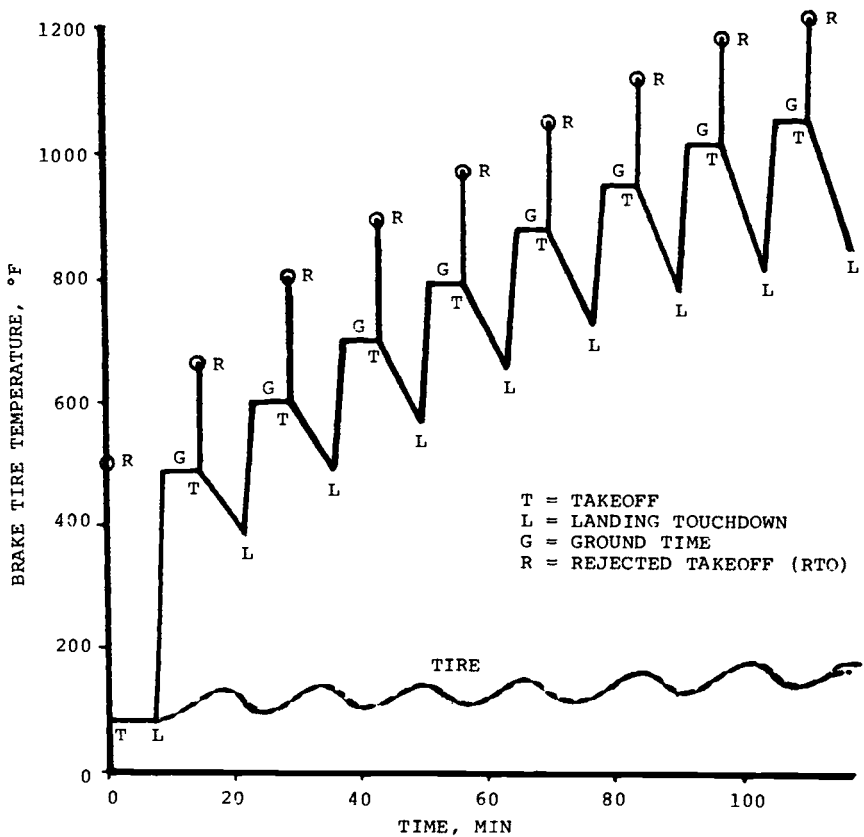
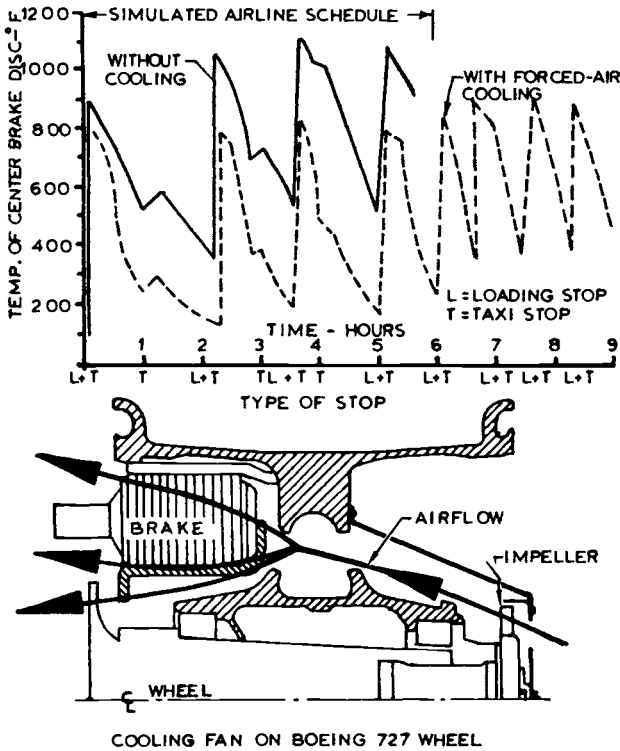


Fig. 7.22 Brake temperature spectrum.

TEST CONDUCTED ON EASTERN AIRLINES' BOEING 720 TO EVALUATE B.F. GOODRICH FORCED AIR BRAKE COOLING SYSTEM



JANUARY 1965

Fig. 7.23 Example of brake cooling (source: Ref. 7, reprinted with permission).

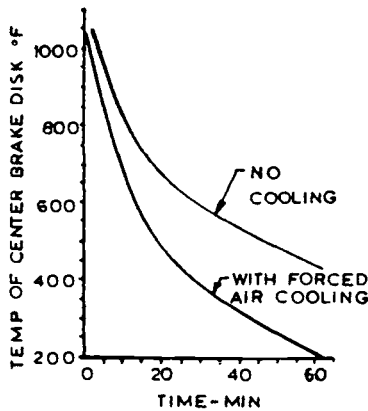
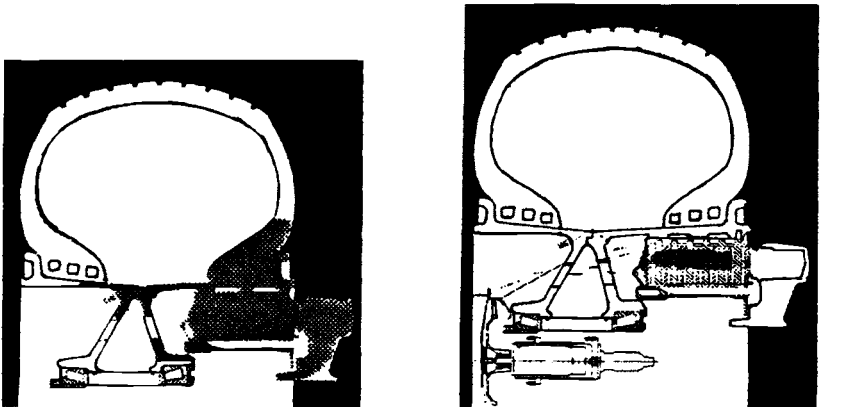


Fig. 7.24 Forced-air cooling test (source: Ref. 7, reprinted with permission).

static pressure of 0.16 in. of water. It weighed 2.5 lb and was driven by a 0.04 hp, 400 cycle, 3-phase electric motor. Figure 7.24 shows how the temperature of the center brake disk varied with and without cooling.

Dunlop uses a similar system in their fan cooling system, depicted in Figure 7.25. They refer to it as "forced convection"; and the fan is used to blow air directly on the heat sink. It has been installed on the VC-10, Trident, BAe 111, and Comet. Figure 7.26 illustrates some of the test results obtained from it. Figure 7.27 shows the brake cooling design for the Concorde.



a) No brake cooling system: heat soaks into the wheel rim and tire beads.

b) Dunlop air-cooling system in use: heat dissipated by fan installation.

Fig. 7.25 Dunlop fan cooling system.

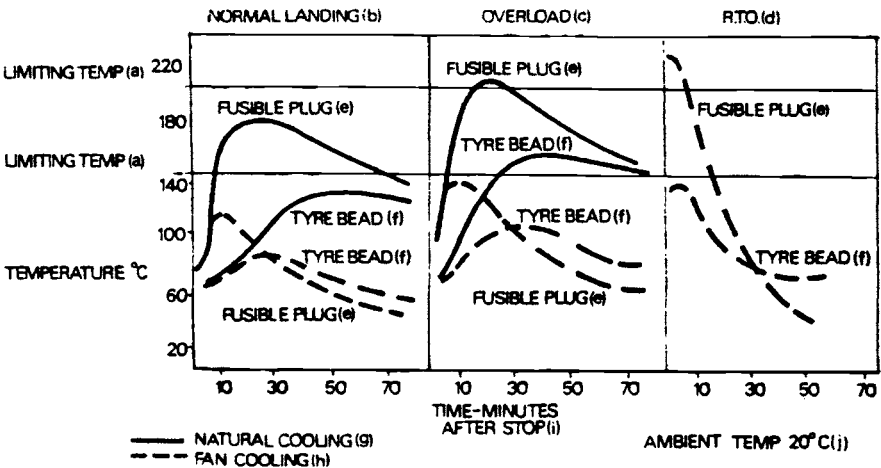
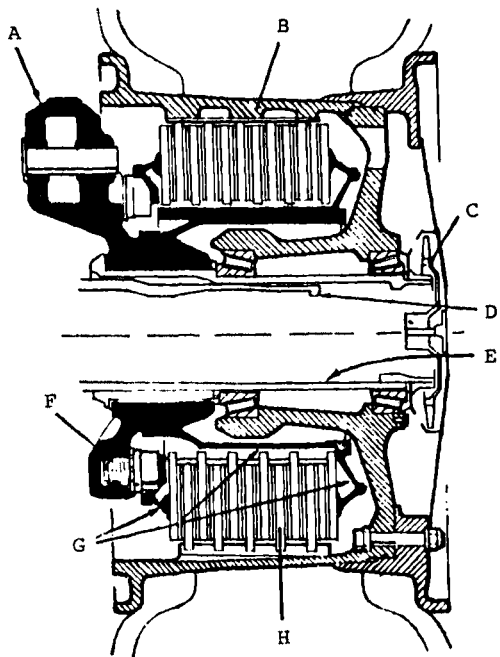


Fig. 7.26 Dunlop fan cooling effectiveness.



General arrangement of the Concorde wheel and brake: A) torque plate common to all types of brakes; B) wheel suitable for all types of brakes or axles; C) fan, optional; D) telescopic axle or E) fixed axle; F) integral piston/cylinder adjuster assembly with facility to change piston head length to accommodate different heat packs; G) torque tube, pressure plate, and thrust plate common to all types of brakes; H) heat pack alternatives: steel, beryllium, carbon.

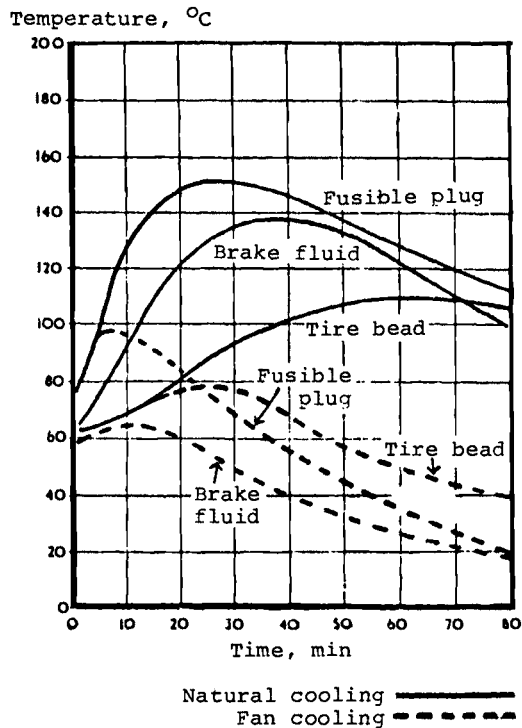


Fig. 7.27 Dunlop brake cooling for Concorde (source: Ref. 13, reprinted with permission).

Temperature Sensing

Recognizing that brake temperature is becoming an ever-increasing problem, some commercial and military operators are now requesting that a temperature sensing capability be installed into the brake units. After a rapid turnaround, the pilot then has an indication of the brake temperatures and, from this, can determine whether there is sufficient RTO capability for takeoff.

The sensor will also indicate a malfunctioning brake (a dragging brake, for example), enabling appropriate maintenance action to be taken. Complete brake temperature monitoring systems are now available.

In one typical installation, the sensor is located on the first double stator. In this position, the installation is relatively simple: there is no danger of fouling the wheel and it does not have to be removed each time the heat sink is serviced. Also, it can be removed easily without removing the wheel or brake.

Dunlop uses a chrome-alumel type of temperature transducer. The thermocouple comprises a twin-insulated wire, with the wires fully insulated against each other and housed in a $\frac{5}{16}$ in. diameter wire braided sheath. The dc voltage generated at the thermocouple junction is transmitted to the control unit on the flight deck. The sensor has an operating range of 95–1090°C (200–1400°F) and a survival temperature of 962°C (1800°F).

Another type of sensor uses platinum resistance wire wrapped round a ceramic rod. The entire assembly is glass-coated and is encapsulated in a stainless steel body. It is attached to the stator plate at the threaded end and operates in a temperature range of 70–1090°C (–94 to 1994°F).

7.7 SKID CONTROL

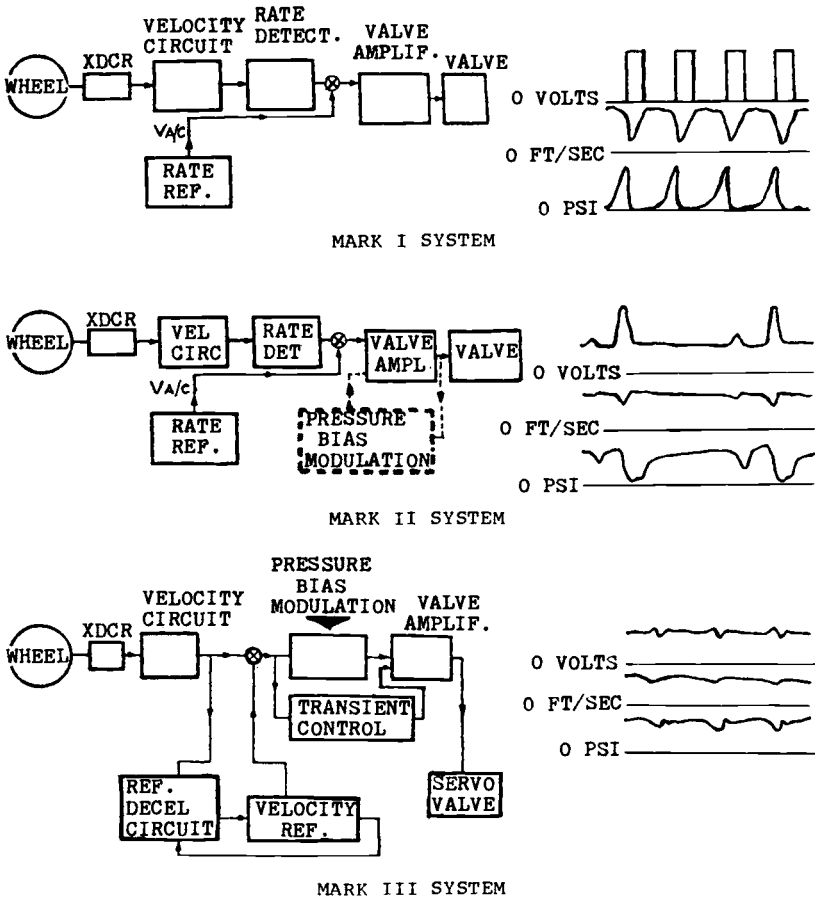
With faster speeds and heavier payloads, the braking requirements of today's aircraft must provide consistently shorter stopping distances under all types of runway conditions. Because of the desire for greater comfort in passenger air travel, aircraft should also have smoother and more gentle power through solid ground stabilization.

From the safety standpoint, a scrubbing tire in an undetected skid can, in seconds, burn through its many plies and blow out. In an even shorter time, the tire can "flat spot" and be doomed to be removed and perhaps scrapped. These problems are eliminated by using a modern skid control system that combines mechanical, electrical, and hydraulic technology. It incorporates a high-response, closed-loop servo with a broad bandwidth so as to maintain control over resonance problems with the landing gear, gear bogie bounce, or shimmy.

In the United States, skid control systems are available from several companies, all of which produce high-efficiency, full-time control units. The Grumman F-14 has a Bendix system, the DC-10 and L-1011 have Goodyear systems, and the F-15 and Boeing 747 have Hydro-Aire systems.

Mark I-IV Systems

A convenient way of tracing the development of these systems is to use the Mark I, II, III, and IV definitions used by Hydro-Aire. The first three are described in Ref. 8; Fig. 7.28 is reproduced from that paper to illustrate in block diagrams the differences between the systems. Figure 7.29 compares the stopping distances possible with the three systems. As an expansion of the stopping distance data, consider also that, on a wet pavement, the optimum distance for a ground coefficient of 0.6 was 2860 ft and a Hydro-Aire Mark III system stopped the aircraft in 2970 ft, while a Mark II system required 3230 ft. Thus, even on a wet pavement, the Mark III system stopped the aircraft in 96% of the optimum distance.



a) Block diagrams.

b) Performance curves: typical brake pressure and servo valve signals under normal antiskid operations.

Fig. 7.28 Skid control systems (source: Ref. 8, reprinted with permission).

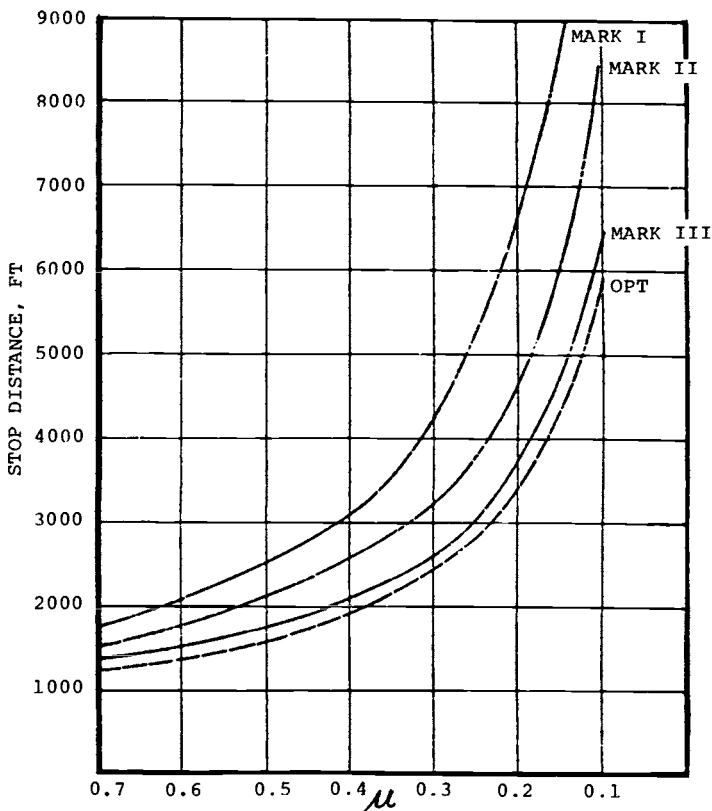


Fig. 7.29 Stop distance vs μ for different skid control systems (source: Ref. 8, reprinted with permission).

Mark I systems were first used in 1948 and the Mark II was introduced in 1958 on the Convair 990. The Mark III appeared in 1967 on the DC9-30, Boeing 747, A7D and other aircraft; Mark IV is used on the Boeing 757 and 767.

Early skid control systems, such as the Hydro-Aire Mark I, were on-off types. They were either mechanical (overdriven clutch) devices or relay-operated solenoid valves controlled by a wheel-driven tachometer. The brake pressure was released once a tire entered a deep skid and was reapplied upon spin-up.

In the next skid control development (for example, the Hydro-Aire Mark II), the wheel velocity is sensed by either a dc generator or a pulse-count alternator driven by the wheel. This signal is then differentiated to obtain wheel deceleration, which is then compared to a fixed reference. When it exceeds the reference level, the skid control valve is commanded to reduce brake pressure to a level just below that which caused the wheel to skid. Brake pressure is then allowed to increase slowly until the wheel again

decelerates above the reference level; the whole cycle is then repeated. This is called a "modulated" system, since the brake pressure is applied and released in a modulated flow as opposed to the direct on-off flow used on the earlier system.

The systems of the 1960's, however, did not do much for improving stopping distance on wet pavements and thus a new system was born. Hydro-Aire called it the Hytrol Mark III and Goodyear the adaptive brake control system. It operates on a different concept from the earlier systems in that it attemptst to optimize tire runway slip to achieve a maximum friction coefficient. Previous systems were based upon a "rate error," whereas the new system is a "slip error" device that computes the actual tire slip. It modulates the brake pressure around the optimum slip point. The system constantly computes tire slip and makes small brake pressure adjustments to compensate for it. As shown in Fig. 7.28, the brake pressure fluctuations are moderate. The cyclic on-off braking is avoided and the time during which some degree of braking is being applied is consequently increased, thus decreasing the stopping distance.

The Mark IV system operates on the same theory as the Mark III, but it is a digital system, whereas the Mark III is analog. Its precision and the flexibility of its microprocessor-based system permit system control over a much broader range of aircraft performance. To quote Hirzel,⁹ "Refinements and performance limits are achievable with the digital memory-based Mark IV that would be impractical with the operational amplifier-based Mark III." From that same reference, Table 7.3 is reproduced to summarize the two systems.

Table 7.3 Comparison of Mark IV and Mark III Antiskid Systems

| Features | Digital (Mark IV) | Analog (Mark III) |
|--|---|--|
| Component technology | Microprocessor | Operational amplifiers |
| Accuracy and consistency | Very precise; does not change | Dependent on stability and accuracy of individual components used |
| Control functions | Contained in program memory chip | Contained in physical circuit configuration and component values |
| Tuning adjustments | Requires only software changes to program in memory chip | Requires value changes and circuit configuration changes |
| Flexibility for complex changes to control functions | Easily accomplished with software program changes only; no additional circuitry | Requires additional circuitry; difficult to achieve and limited by card area |

Source: Hydro-Aire Div., Crane Co.

Description of a Hydro-Aire Mark IV System Installation

The system described here is that used on the Boeing 757 and 767 aircraft. In addition to providing skid control, it also includes an autobrake.

The system comprises a control unit, a wheel speed transducer on each of the eight main gear wheels, two valve modules for the normal braking system, and two for the alternate system. Each normal system valve module contains four antiskid control valves, while each alternate system module contains two. In addition to these components provided by Hydro-Aire, Boeing provides the autobrake control panel, autobrake hydraulic module, annunciators, status displays, and associated hardware. The overall system is diagrammed in Fig. 7.30.

The control unit contains four identical and interchangeable main wheel cards, in addition to an autobrake card, BITE (built-in test equipment) card, BITE interface card, interconnect harness, front panel display, and various switches. Braking of each wheel is controlled by an independent skid control channel. Each card controls two channels, i.e., wheels 1 and 5 are controlled by a single card, wheels 2 and 6 by another, and so on. Each card channel accepts a wheel velocity input from its associated wheel transducer. After calculating wheel slip, the channel supplies brake pressure correction signals to its respective skid control servo valve.

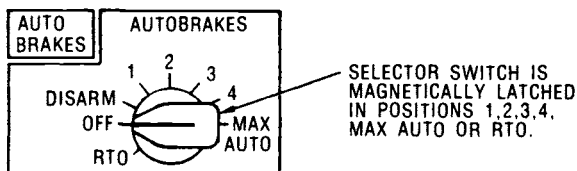
Transducers are mounted in each of the eight main wheel axles and are driven by wheel hubcap rotation. Transducer output signals are routed through shielded wiring to the control unit, where the wheel speed data are converted from analog to digital form. The information is processed and analyzed so that correction signals can be produced.

These brake pressure corrections are converted back to analog form and smoothly varying correction currents are sent from the control unit to each control valve, where brake pressure is varied to maintain optimum braking efficiency.

Skid control calculations are performed in the following manner. The instantaneous speed of each wheel is periodically updated and compared to a calculated aircraft velocity. The difference between wheel speed and aircraft velocity represents wheel slip. When the slip exceeds a given magnitude, braking effectiveness begins to decrease. The control unit detects this excessive wheel slip and produces a brake release signal proportional to the skid severity. The release signal commands a brake pressure reduction until the wheel slip returns to the optimum level. When slip is below the amount required to produce maximum braking, no release signal is generated. The pilot's brake pedal input controls the braking level.

Locked wheel protection is provided to each of the eight wheels and is active above 25 knots. Wheels are paired in tandem for this protection. If a wheel slows to 30% or less of the speed of its mate, a full brake release signal is sent to the slow wheel's skid control valve.

If the normal system hydraulic source fails, the alternate system is automatically activated. This system uses a separate set of antiskid valves. Wheels are paired laterally in the alternate mode, with a single valve



(Note: ARP 4102/2 recommends the following switch selections: RTO/OFF/MIN/MED/MAX, where MIN = $\sim 0.1-0.2 g$, MED = $0.2-0.3 g$.)

Fig. 7.31 Autobrake system flight deck selector panel.

controlling the pressure to each pair of wheels. Conventional pedal-actuated power brake valves, operating in parallel, control the left and right brake pressures in the normal and alternate systems.

The autobrake system, when selected, applies brake pressure independent of the pilot's metering valves. The control unit is equipped with an autobrake card where brake pressure application signals are computed and the deceleration level is determined by the autobrake control panel switch setting. (See Fig. 7.31.)

The pilot may choose from five levels of autobraking and an optional RTO mode. The antiskid has overriding control over the brake pressure. To arm the autobrake, the following conditions must exist: air/ground and throttle position logic must be correct, no metered brake pressure may be applied, and no antiskid or autobrake failures may be indicated. When these arming conditions are met, the autobrake rotary selector switch magnetically latches in its selected position.

7.8 AUTOBRAKES

Some details of a typical autobrake system were provided in preceding section. Automatic brakes are applied typically by the wheel spin-up signal and the subsequent deceleration is controlled by a pilot-operated switch such as that described above. The primary objective, when used in the landing mode, is to reduce ground run. In some cases that the writer has been involved with, this reduction amounted to 200 ft. Side benefits are increased passenger comfort due to controlled deceleration and smooth braking, as well as reduced pilot workload. System diagrams and discussions are found in ARP 1907 and Ref. 10. Figure 7.32 illustrates a system that incorporates an autobrake.

7.9 HYDRAULIC BRAKE SYSTEMS

Reference 11 provides a comprehensive review of hydraulic brake systems applicable to modern commercial and military aircraft. In addition to describing the overall systems, it describes and diagrams the various components such as antiskid valves and autobrake valves. Figures 7.33-7.35

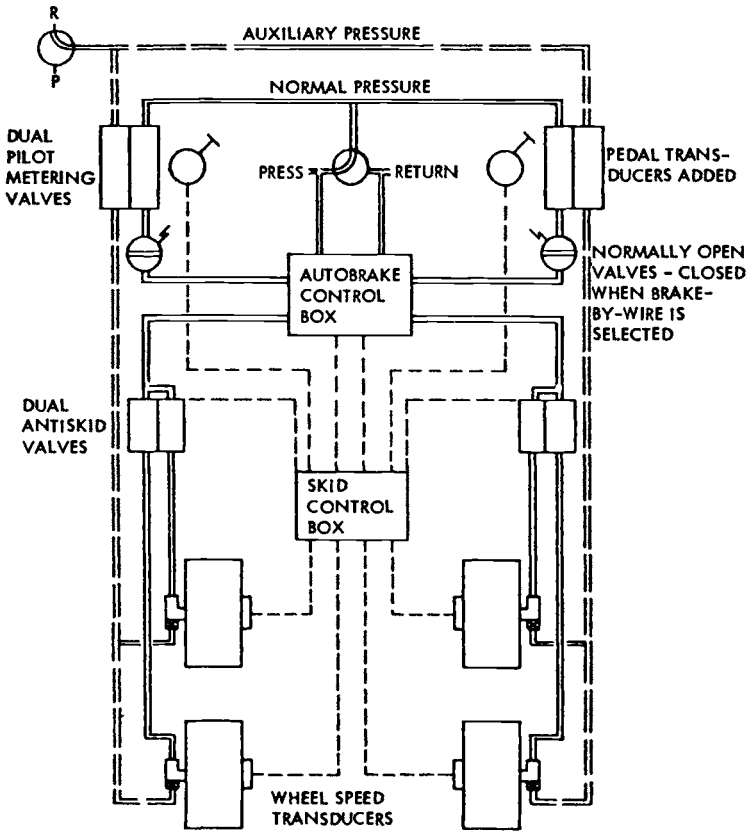


Fig. 7.32 Autobrake and brake-by-wire system.

are taken from that report to show systems of gradually increasing complexity. Figure 7.30 should also be reviewed since it is a complete and modern system used in the Boeing 757/767. Figure 7.36 is included to show the system used in the Lockheed L-100.

7.10 EMERGENCY BRAKING SYSTEM

An emergency braking system is often required. Auxiliary air bottles have been used frequently for this purpose. They replace hydraulic fluid as the means of generating pressure and separate lines are used down to the brake shuttle valve, bypassing the antiskid system. However, this system has several problems: limited number of brake applications due to limited bottle capacity, no antiskid protection, and higher maintenance cost due to having to bleed the lines. An alternate approach, used on the F-111, B-1, and F-16, uses brake lines from two separate hydraulic systems.

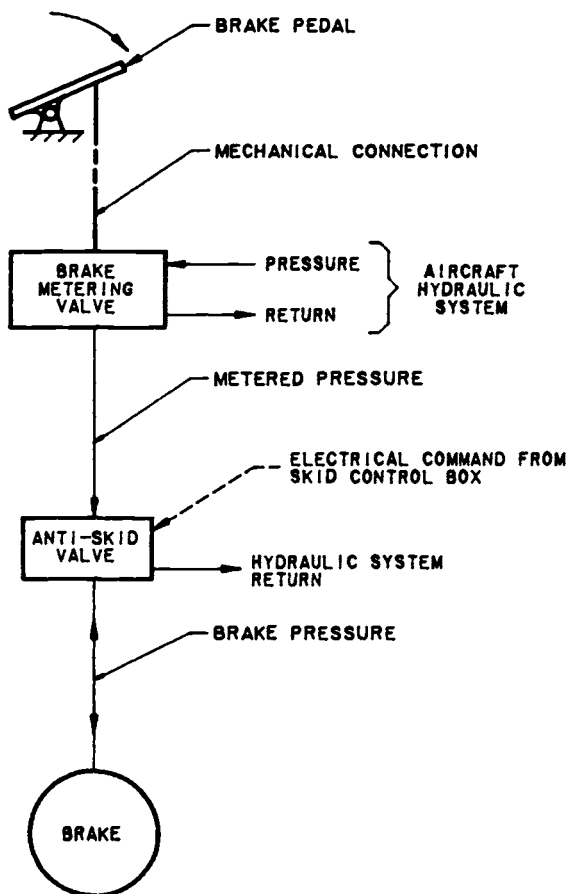


Fig. 7.33 Simplified brake system, separate metering valve (source: Ref. 11).

7.11 BRAKE CONTROL PEDAL

Until recently, brake pressure was applied by the pilot depressing the brake pedal, which mechanically actuated the brake metering valve. The degree of braking was a function of pedal movement, which in turn was a function of the pressure applied by the pilot to overcome the valve break-out force. This force is very sensitive in that, if it is too much, the pilot tends to press too hard to overcome it and, as a result, the braking may be too severe. Conversely, if it is too low, the brakes may be applied inadvertently during the ground operations. An alternate approach now being used is an electrical system in which pedal travel is recognized electrically and a feel spring is used to control pilot application. A later system, currently in the experimental stage, involves the use of fiber optics rather than electrical wires.

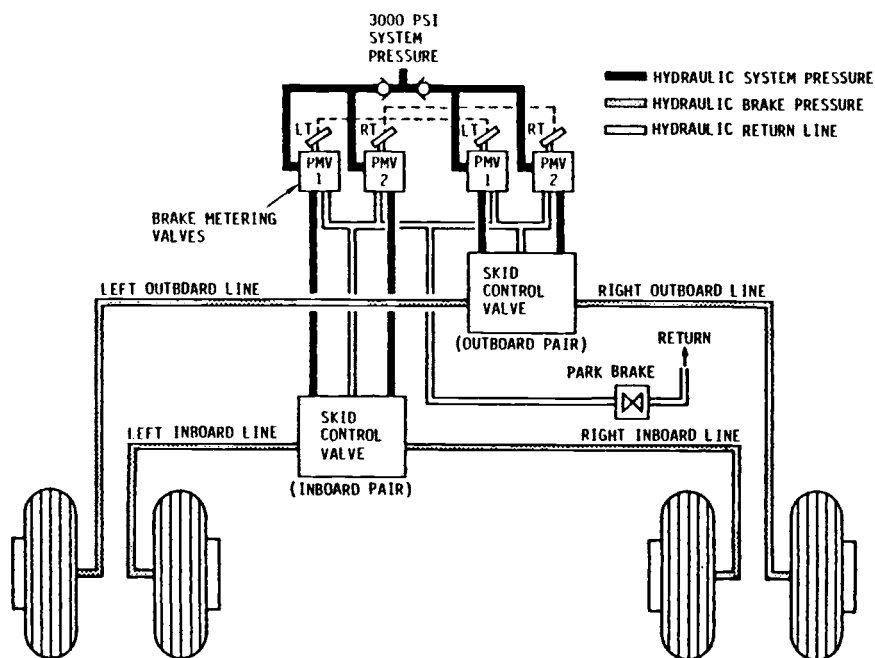


Fig. 7.34 Paired wheel system hydraulic schematic (source: Ref. 11).

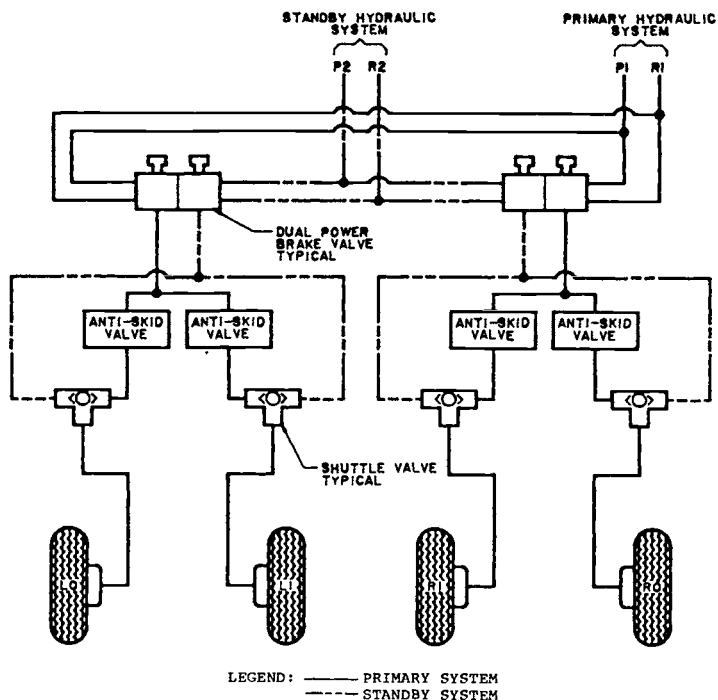


Fig. 7.35 Individual wheel control brake system (source: Ref. 11).

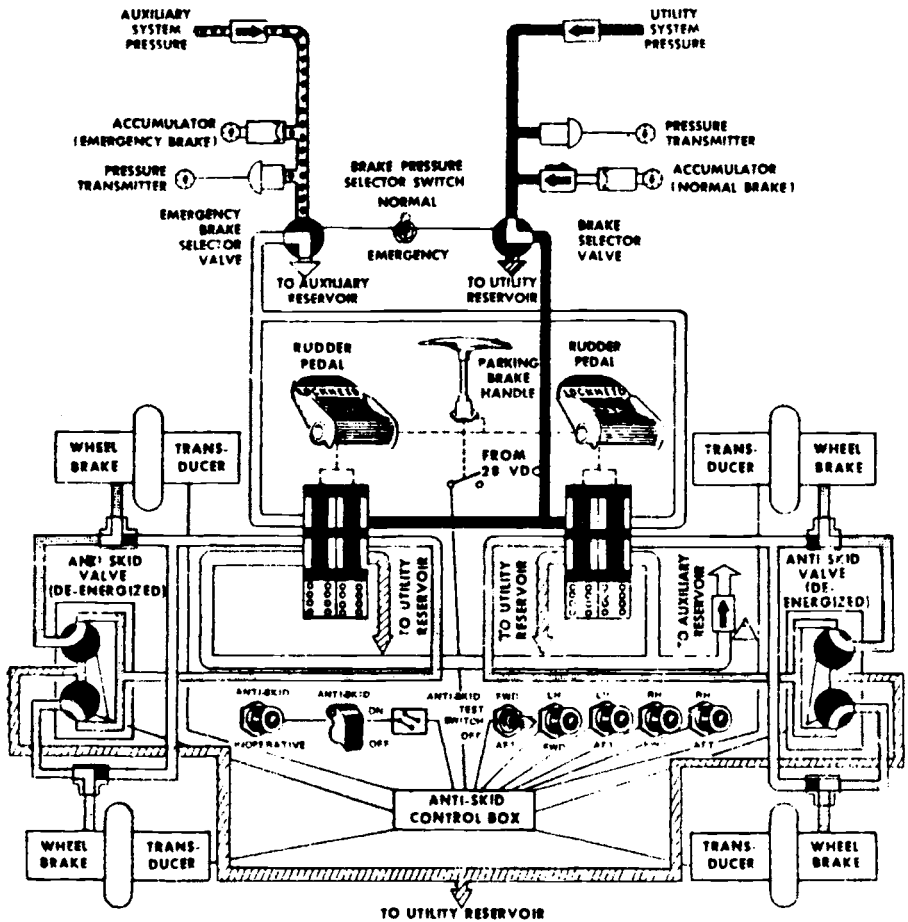


Fig. 7.36 Main gear brake control system of the L-100 (source: Lockheed).

7.12 ADVANCED BRAKE CONTROL SYSTEM (ABCS)

At the time of writing, the ABCS is currently under development. It integrates the nose gear steering, rudder, and braking controls to provide improved automatic ground handling, particularly during high crosswinds and slippery runway operation. Configurations have already been developed for the F-4, F-16, and F-111 aircraft.

When landing on a slippery surface under crosswind conditions, the pilot must apply sufficient control to prevent the aircraft from sliding off the runway. The ABCS helps the pilot by coordinating all of the systems related to directional control and by applying corrective action far more quickly than it could have been applied manually. Tendencies to overcorrect are also avoided.

Problems may occur at any time during the landing ground roll. For instance, immediately after touchdown, the aircraft is at high speed and fast action is required to correct any deviations from the desired heading. In this case, the rudder is the most effective control. At low speed, rudder control is poor, so steering control becomes the predominant control.

The control panel in the flight station comprises the following items: a switch to select fully automatic (hands-off), semiautomatic, or manual control, a runway heading indicator, and a runway friction indicator. After selecting, say, automatic control, the pilot inputs the runway heading and the expected runway friction coefficient. A heading trim control is also provided to make minor corrections.

Further details of this system are provided in Ref. 12.

References

¹“Wheel and Brake Design Guide for Airframe Engineers,” B. F. Goodrich Company, Troy, OH.

²Conway, H. G., *Landing Gear Design*, Chapman & Hall, London, 1958, p. 73.

³*Aviation Week*, Aug. 4, 1986, p. 128.

⁴*Flight International*, Dec. 30, 1971.

⁵Biehl, F. A., “Aircraft Landing Squeal and Strut Chatter Investigation,” *Shock and Vibration Bulletin*, Jan. 1969.

⁶Fecher, D. J. and Cervelli, R. V., “Advanced Undercarriage Systems,” U.S. Air Force Flight Dynamics Laboratory, Rept. FDL-TDR-64-143, March 1965.

⁷*American Aviation*, Jan. 1965.

⁸Hirzel, E. A., “Antiskid and Modern Aircraft,” SAE Paper 720868, Oct. 1972.

⁹Hirzel, E. A., “Brake Control Technology and Innovations,” Crane Hydro-Aire Div., Burbank, CA, May 1985.

¹⁰Hirzel, E. A., “Real Time Microprocessor Technology Applied to Automatic Braking Systems,” SAE Paper 801194, Oct. 1980.

¹¹Bluhm, S. R., “Hydraulic Brake Systems,” Crane Hydro-Aire Division, Burbank, CA, May 1985.

¹²Warren, S. M. and Kilner, J. R., “Advanced Brake Control System,” Air Force Wright Aeronautical Laboratories, Rept. AFWAL-TR-80-3082, Vol. 1, Aug. 1980.

¹³Stimson, I. L., “First Lightweight Disc Brakes for a Civil Aircraft,” *Aircraft Engineering*, June 1971.

Bibliography

Bax, R. A., "Boeing 737-300 Anti-Skid Control System," Hydro-Aire, May 1985.

Browning, William A., "Automatic Braking Systems from an Airline Engineer's Perspective," American Airlines, May 1985.

Hirzel, E. A., "Brake Control Theory and Concepts," Crane Hydro-Aire Div., May 1985.

Slaughter, G., "Service Experience with the Boeing 767 Antiskid/Autobrake System," TWA, May 1985.

8.1 GENERAL GUIDELINES

Kinematics is the term applied to the design and analysis of those parts used to retract and extend the gear, with particular attention to the determination of the geometry in the retracted and extended positions. Basic guidelines are as follows:

- 1) Start with a geometric layout, but replace this with a mathematical analysis as soon as possible.
- 2) Ensure that satisfactory moment arms are provided throughout the travel.
- 3) Use the simplest possible kinematics.
- 4) Approximate the actuator "dead length" (see Fig. 8.1) in the preliminary design layout. The following are suggested:

No internal lock, dead length = 6–7 in.

One internal lock, dead length = 8–11 in.

Two internal locks, dead length = 12–15 in.

The lower and higher values generally apply to smaller/larger diameter actuators, respectively. For instance, the Lockheed JetStar side brace actuator, with one internal lock, has a dead length of 10.5 in.

The above values include an estimated 1 in. of length for the actuator end fitting. This can be deducted if a trunnion mount is used (such as shown in Fig. 8.2), but on a hydraulic or pneumatic actuator, this type of mount is relatively expensive. It is, however, the optimum type for ball screw actuators, in which the trunnion is at the ball nut. Offset mounts (Fig. 8.3) should be avoided, since they cause undesirable stresses and deflections in the actuator. It should also be recognized that these dead lengths are ultimately dependent upon the detail design of the actuator to meet specific conditions and may vary somewhat from the above suggestions. Other factors to keep in mind are:

- 1) Internal locking actuators or braces should be used with caution. Some customers demand a visual means of determining that the gear is down *and locked*, which may be difficult to accomplish with an internal lock. Figure 8.4 shows the basic essentials of an internal lock. This typical example is satisfactory for downlocking. However, it would require more complexity if it were used as an uplock, since a manual emergency system would then need to be incorporated in addition to the normal release.

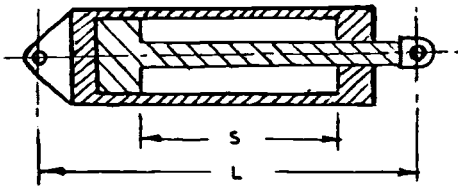


Fig. 8.1 Actuator dead length.
DEAD LENGTH
 $= L - S$

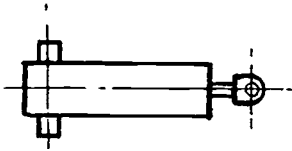


Fig. 8.2 Trunnion-mounted actuator.

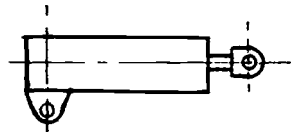


Fig. 8.3 Offset-mounted actuator.

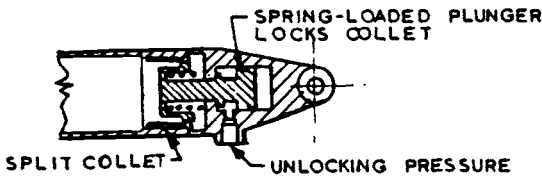


Fig. 8.4 Internal lock.

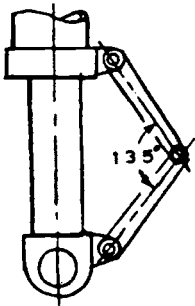


Fig. 8.5 Torque links geometry.

2) Whenever possible, the landing gear doors should be moved by the gear actuator, such that the gear and doors move together. Figure 8.4 shows an example of such an arrangement. This eliminates sequencing, improves reliability, and saves weight.

3) Torque links (Fig. 8.5) should be designed such that their included angle is no more than 135 deg when the gear is extended.

8.2 KINEMATIC CONCEPTS

The simplest kinematics are shown in Fig. 8.6. It is employed on the Lockheed JetStar and has only two basic parts—the shock absorber and the actuator/side brace with a internal downlock. Thus, not only is a

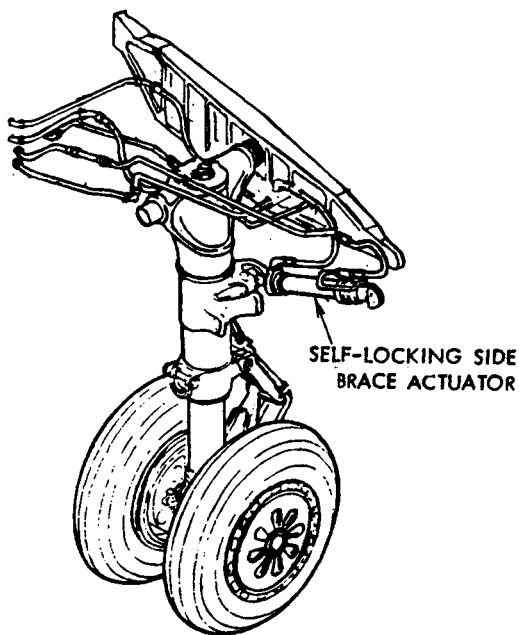


Fig. 8.6 Lockheed JetStar main landing gear.

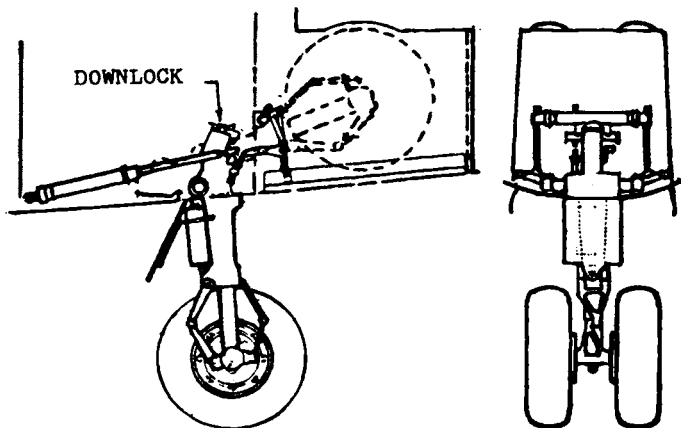


Fig. 8.7 B.Ae. Harrier main landing gear.

separate side brace eliminated, but also a separate downlock. The split-collet type of internal lock has proved to be reliable, with no failures having occurred in many years of operation.

The B.Ae. Harrier also has a simple system. Its main gear dispenses with a separate side brace, but has a separate downlock; see Fig. 8.7. It has two basic parts—the shock strut and the actuator. At the top of the strut, a downlock plunger is installed to mate with an appropriate part on the airframe.

Figure 8.8 shows an assortment of kinematic concepts, adapted from some of those given in Ref. 1. Type a is used in many aircraft because of

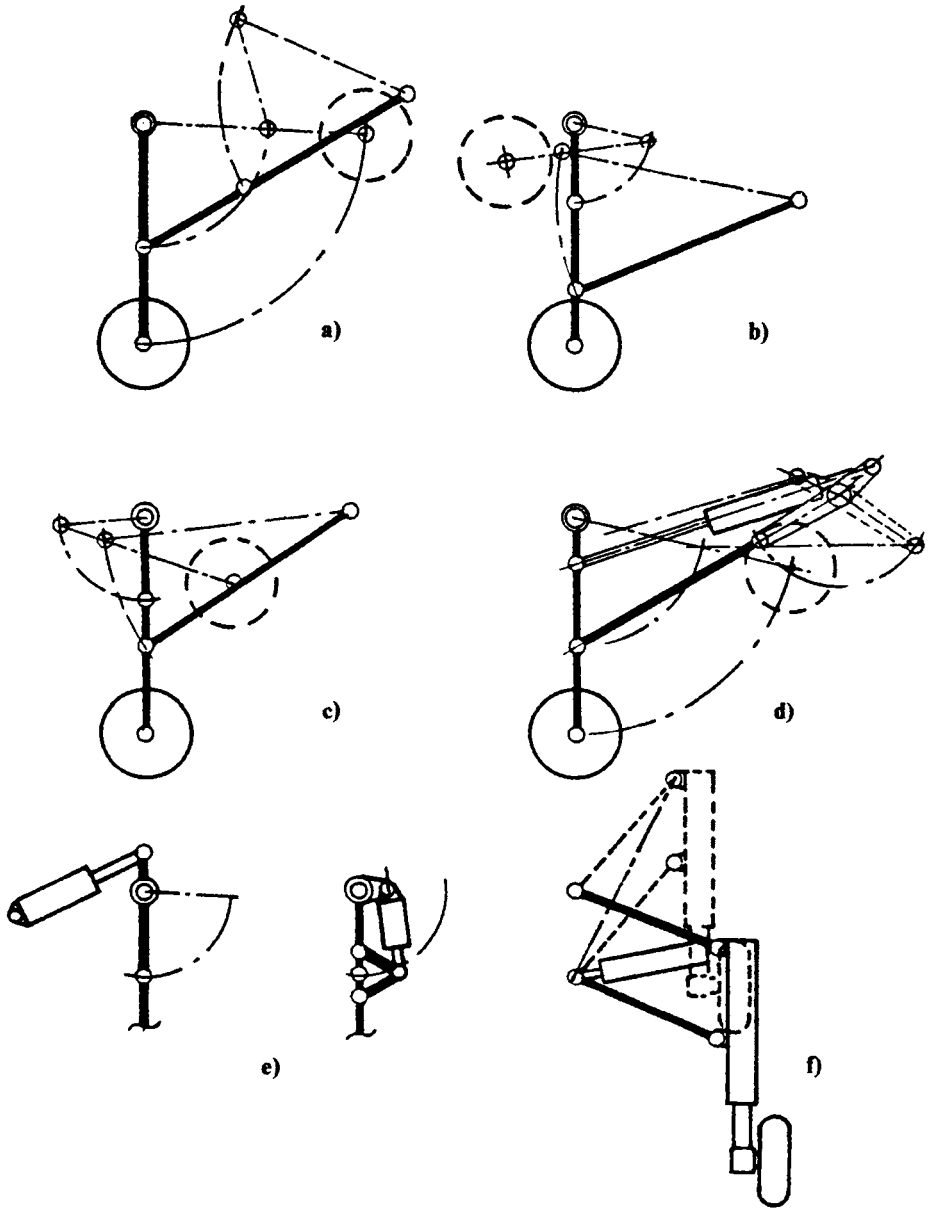


Fig. 8.8 Kinematic concepts.

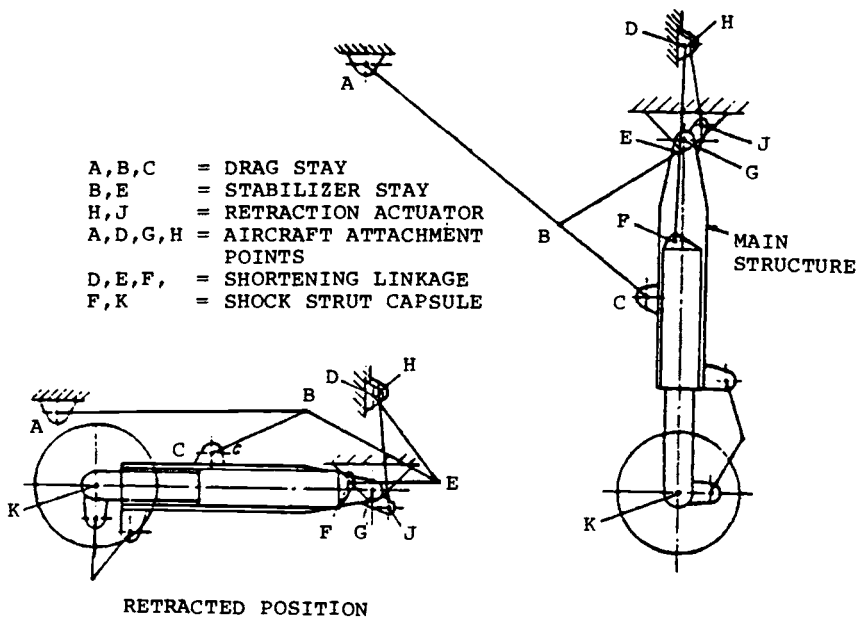


Fig. 8.9 Main gear geometry of DHC Caribou (source: Canadian Aviation).

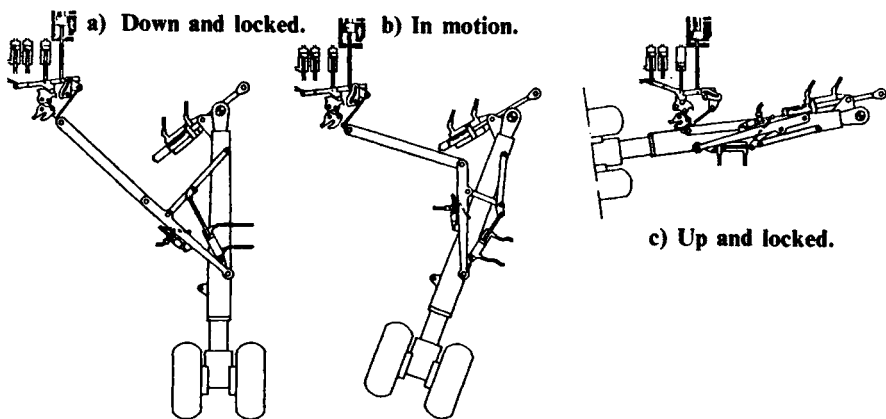


Fig. 8.10 A-300B main gear operation (source: Aerospatiale).

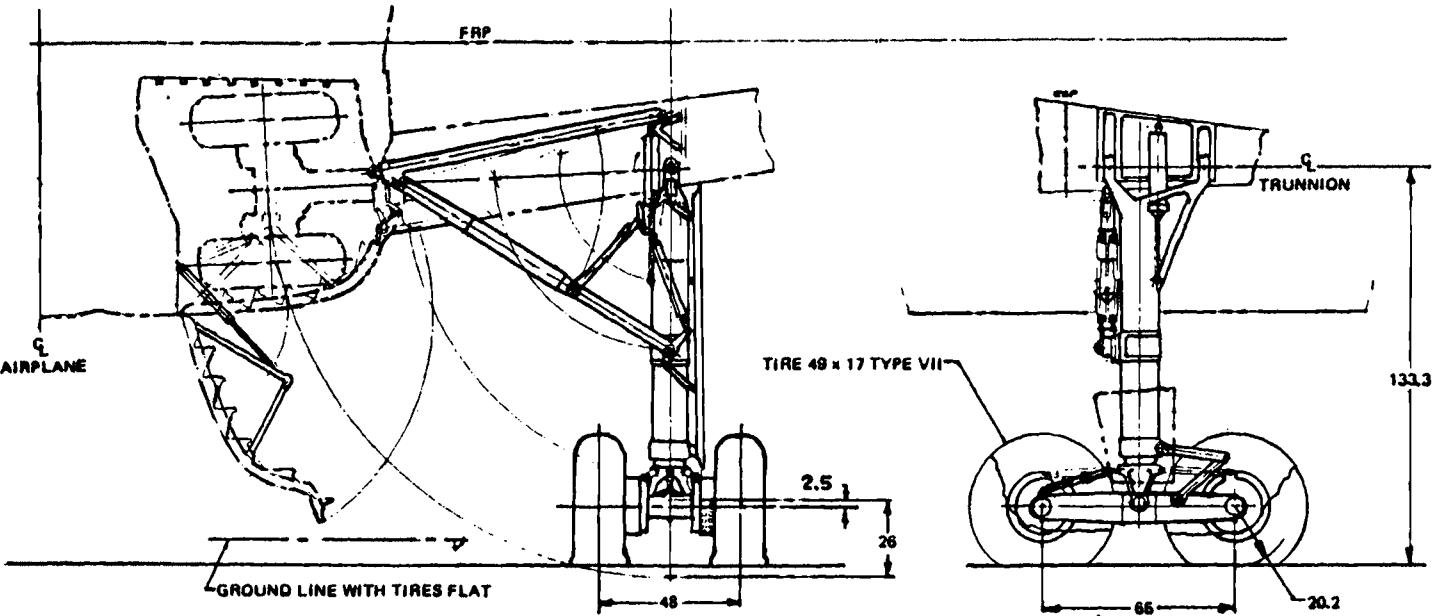


Fig. 8.11 DC-10 main gear.

its simplicity. There are many variants of this type—a more unusual one involves the use of an extra bracing link extending from the top of the shock strut to the drag or side brace elbow. This provides extra support for the brace and thereby minimizes the structure weight. Figures 8.9–8.11 show how these extra braces were installed on the DHC-4 Caribou, A-300B, and DC-10.

Types b and c in Fig. 8.8 are similar and can be used whenever it is required to retract the wheel into a cavity almost vertically above the down position. Concept d is an example of how the retraction actuator can be incorporated into the kinematics such that the loads are balanced within the gear structure, as opposed to concept a where the actuator must be mounted on the airframe.

Concept e shows two methods of rotating the top of a type b leg. There are many variants of these—the Lockheed C-141 main gear (Fig. 8.12) and the C-5A nose gear (Fig. 8.13) are two examples.

Concept f in Fig. 8.8 was used on several Navy aircraft in the 1930's. It is a simple and reliable method of raising the gear into the side of the fuselage or flying boat hull.

Figures 8.14–8.17 show the interesting retraction systems employed by the main gears on the BAC 111, Fokker 50, B.Ae. 146, and Comet. In

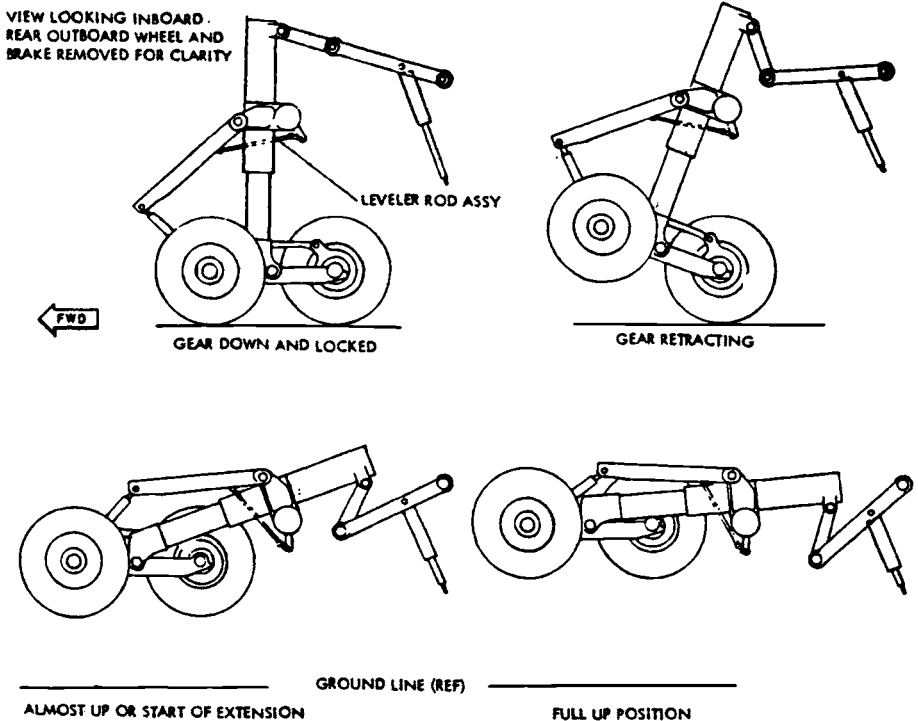


Fig. 8.12 Lockheed C-141 main gear.

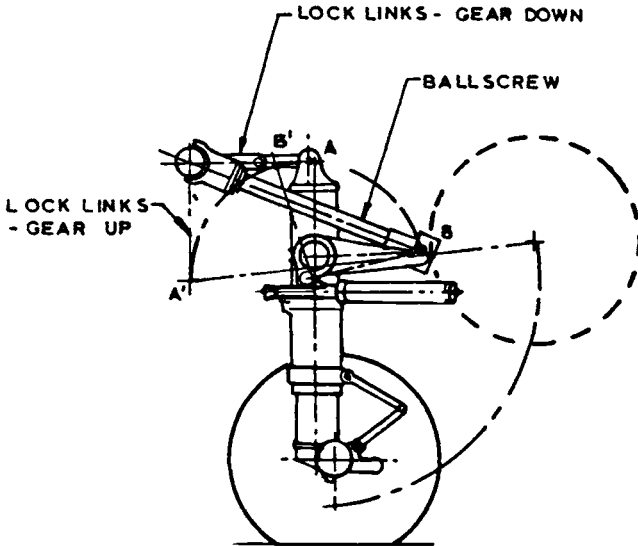


Fig. 8.13 C-5A nose gear.

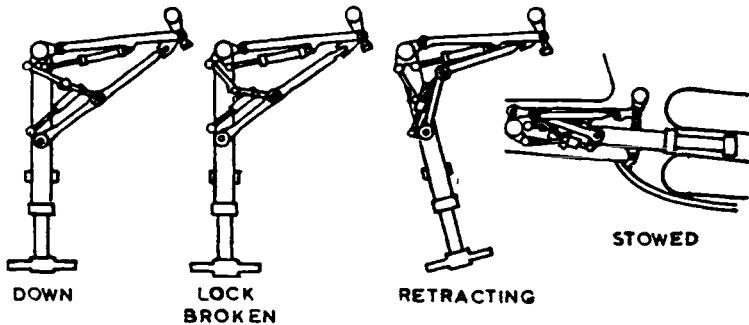


Fig. 8.14 BAC 111 main gear retraction (source: Ref. 3).

many cases, the bogie or wheels must be rotated to fit inside the available space; as with linkages, there are many ways to do this. If the wheel must be rotated during retraction, a radius link can be used, as depicted in Fig. 8.18, or bevel gears can be used at the top of the gear to rotate the piston. Some degree of wheel rotation can be accomplished by appropriate choice of a skewed axis, as in the A-7, for example.

Figure 8.19 shows the basic essentials of folding a bogie so that it occupies minimum space when retracted. The B.Ae. Vulcan uses such a system and has a complex, but very efficient, kinematic arrangement. See Fig. 8.20.

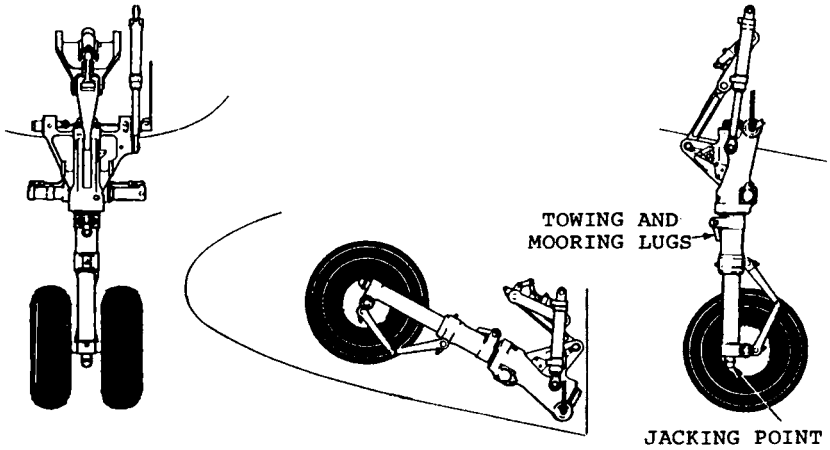


Fig. 8.15 Fokker 50 nose landing gear (source: Dowty Rotol Ltd.).

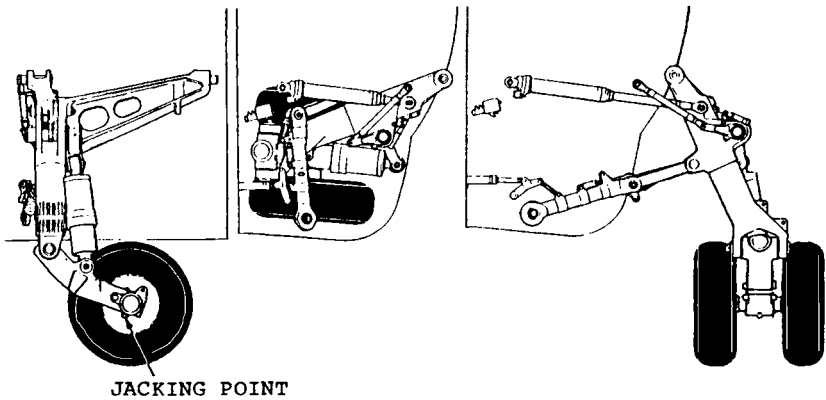


Fig. 8.16 Retraction system of B.Ae.146 main gear (source: Dowty Rotol Ltd.).

Ramps are sometimes used to rotate the bogies. Figure 8.21 illustrates the basic concept involved. In type a, as the gear retracts, the forward tire encounters the ramp and cams the bogie over into the retracted position. The type b bogie is rotated in the opposite direction to type a and, instead of the tire riding over the ramp, a roller is used. When the Lockheed C-5A gear was in the conceptual stage, a type b ramp was considered with the tire riding on it. However, tire sizes vary considerably, which would create a variation in the gear-up position. Also, with a large gear being retracted quickly, tire bounce would be severe; for these reasons, a roller is used. To eliminate bounce and to accurately position the retracted gear, the roller enters a track with a contour similar to type b.

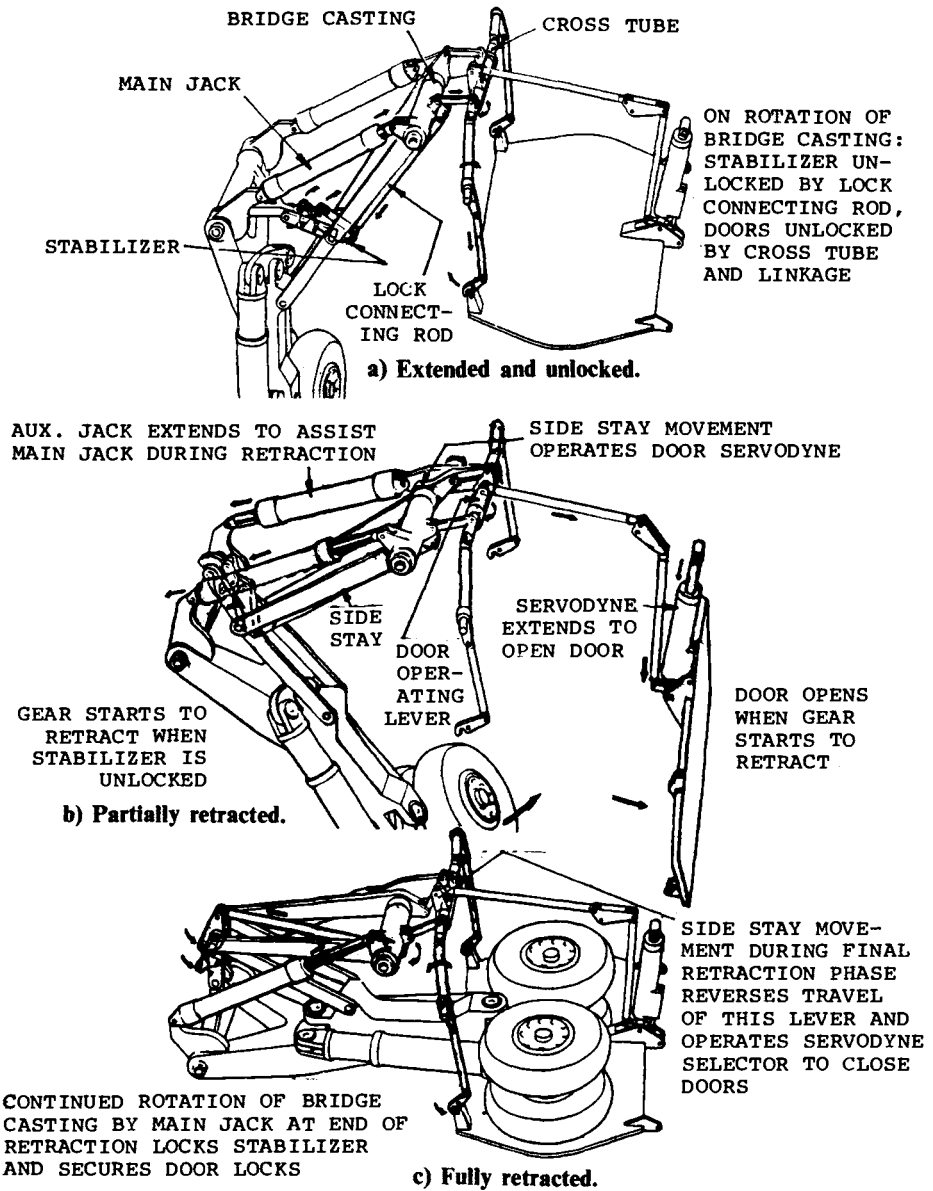


Fig. 8.17 Retraction system of B.Ae.Comet (source: British Aerospace Corp.).

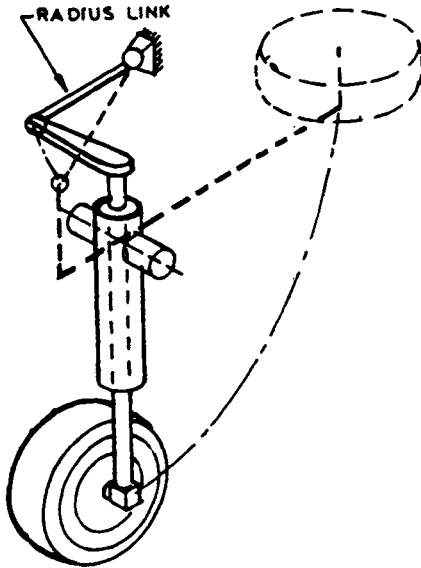


Fig. 8.18 Radius link to rotate wheel 90 deg.

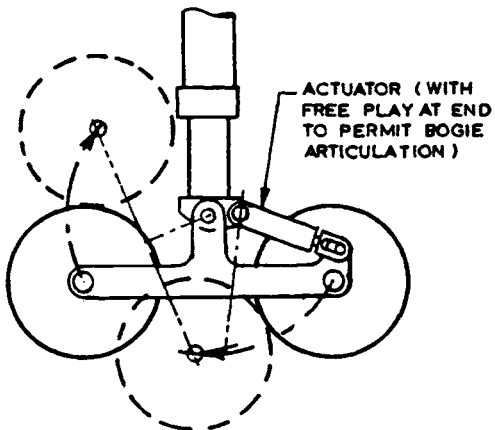


Fig. 8.19 Folding bogie prior to retraction.

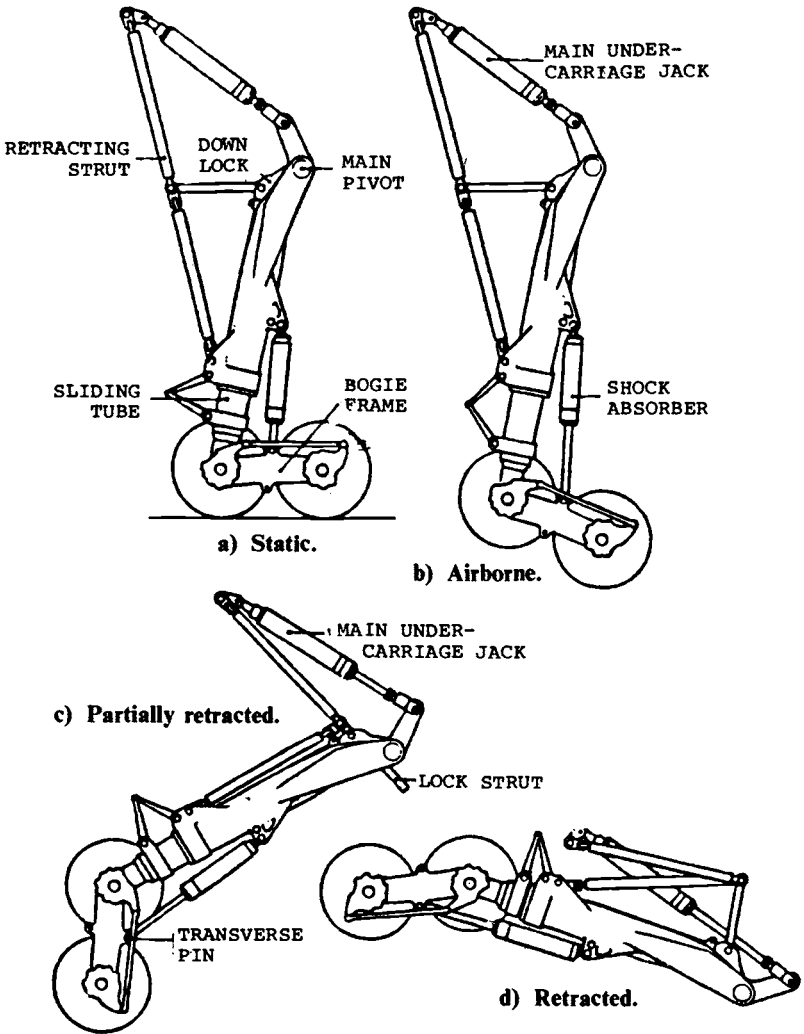


Fig. 8.20 B.Ae.Vulcan main landing gear retraction system (source: Dowty Rotol Ltd.).

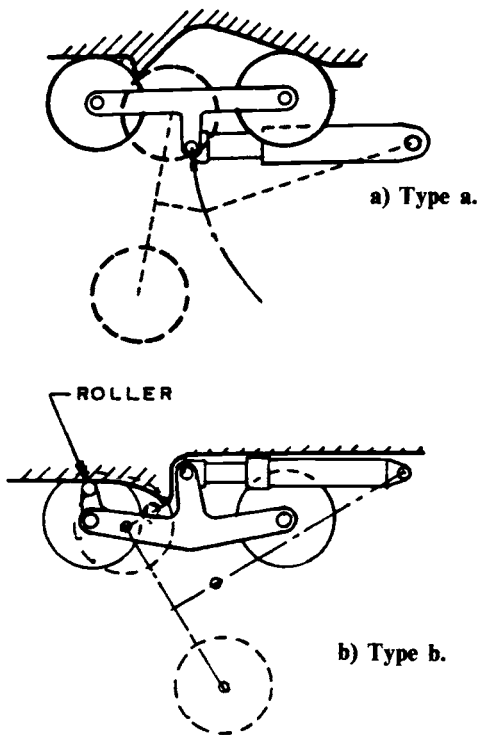


Fig. 8.21 Ramps used for bogie rotation.

8.3 KINEMATICS DETAIL

After checking clearances during the retraction cycle and ensuring that moment the arms are satisfactory, a curve may be drawn to show the efficiency of the system. To do this, apply a unit load (vertically) to the wheels and calculate the actuator load at, say, 10 different positions of the retraction sequence. Then plot a curve similar to that of Fig. 8.22. The curve of 1.25 times gear weight is used to determine maximum actuator load. Retraction efficiency is obtained by relating the area under the curve to the area of the enclosing rectangle. Efficiency of 70% would represent a high value. It becomes apparent that the efficiency is sensitive to small changes in kinematics, the system should be reviewed and perhaps modified, because, in production, small errors and design changes, as well as friction, may result in an inadequate system.

Many aircraft have low-efficiency landing gears in order to obtain simplicity or to stow the gear in some particular envelope. There is nothing wrong with this approach, provided it is realized that the ensuing efficiency loss is paid for by either a longer retraction time or extra weight.

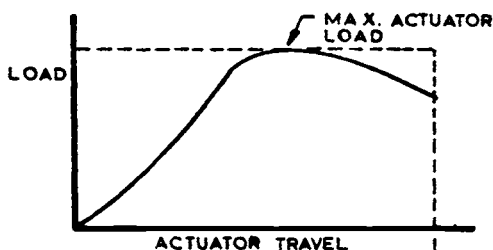


Fig. 8.22 Retraction efficiency curve.

8.4 MATHEMATICAL KINEMATIC ANALYSIS

A mathematical kinematics analysis should be used as soon as possible in the design—it is quicker than a geometric analysis and it is far more accurate. The example shown here can probably be adapted to almost any type of gear configuration. Figure 8.23 shows the dimensions that are known, or can be assumed, in the initial computation. The method is attributed to K. W. Hetzel.²

Let $AB = a = 7.88$ in. ($a^2 = 62.094$)

$$X_A - X_B = 0, \quad Y_A - Y_B = +7.88, \quad Z_A - Z_B = 0$$

From the given dimensions,

$$X_B = -13.35, \quad Y_B = -5.00, \quad Z_B = 70.21$$

and if r is the distance from point P to any point,

$$r^2 = X^2 + Y^2 + Z^2$$

$$r_B^2 = (-13.35)^2 + (-5.00)^2 + 70.21^2 = 5132.667$$

Similarly,

$$X_A = -13.35, \quad Y_A = 2.88, \quad Z_A = 70.21$$

$$r_A^2 = (-13.35)^2 + 2.88^2 + 70.21^2 = 5115.961$$

From this side view,

$$X_B = -15.10 \quad \text{and} \quad Z_B = -0.10$$

$$r_B^2 = X_B^2 + Y_B^2 + Z_B^2$$

Therefore,

$$\begin{aligned} Y_B^2 &= r_B^2 - (X_B^2 + Z_B^2) \\ &= 5132.667 - (15.10^2 + 0.10^2) = 4904.647 \end{aligned}$$

$$\underline{Y_B = 70.033}$$

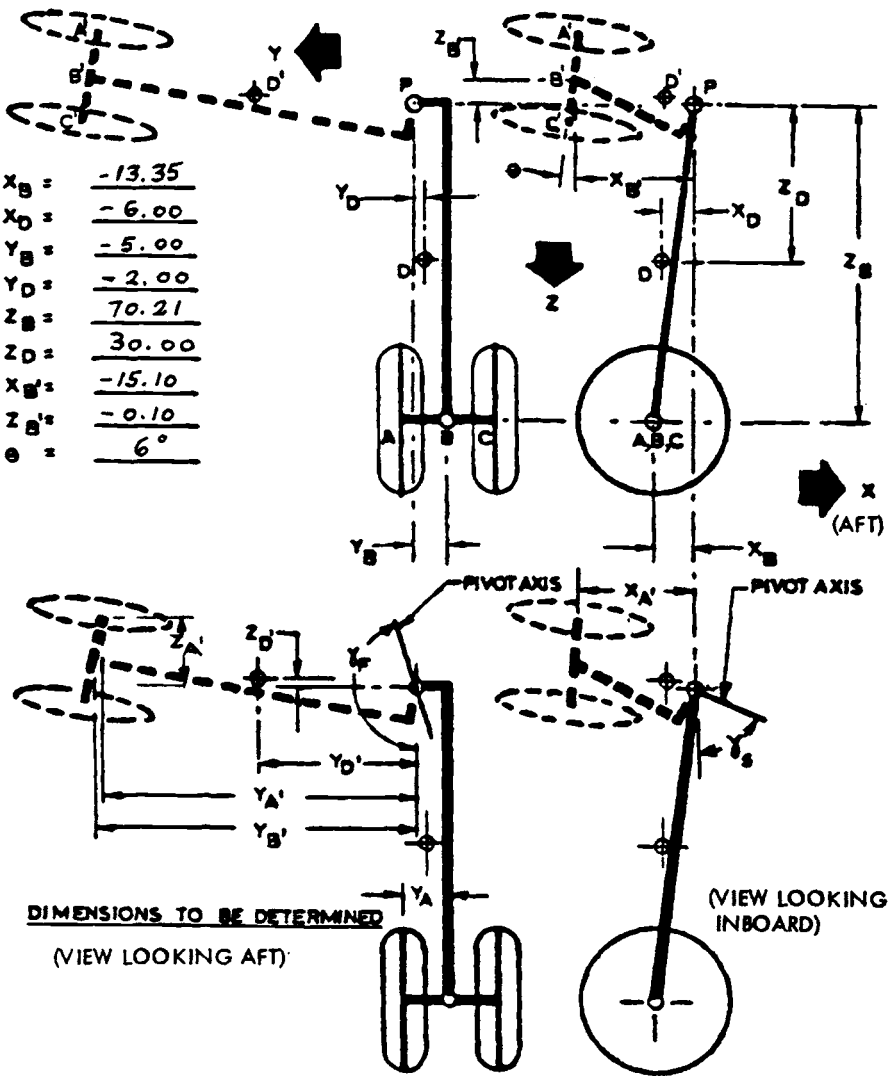


Fig. 8.23 Kinematics example: known dimensions.

It is known that $\theta = -6$ deg (negative when angle is as shown in Fig. 8.23).

$$\cos\theta = 0.99452, \quad \sin\theta = -0.10453$$

The retracted position of axle is

$$\begin{aligned} r_A^2 - r_B^2 - a^2 &= 5115.961 - 5132 &&= -78.800 \\ (r_A^2 - r_B^2 - a^2)^2 &= (-78.800)^2 &&= 6209.44 \\ X_B \sin\theta &= (-15.10)(-0.10453) &&= 1.5784 \\ Z_B \cos\theta &= (-0.10)(0.99452) &&= -0.09945 \\ X_B \sin\theta + Z_B \cos\theta &&&= 1.4789 \\ (X_B \sin\theta + Z_B \cos\theta)^2 &&&= 2.1871 \end{aligned}$$

It was previously shown that $Y_B^2 = 4904.647$. Therefore,

$$\begin{aligned} (X_B \sin\theta + Z_B \cos\theta)^2 + Y_B^2 &= 2.1871 + 4904.647 \\ &= 4906.8341 \\ 2[(X_B \sin\theta + Z_B \cos\theta) + Y_B^2] &= 9813.6683 \\ &= G, \text{ say} \end{aligned}$$

Since $a^2 = 62.094$, $4a^2 = 248.376$,

$$\begin{aligned} 4a^2[(X_B \sin\theta + Z_B \cos\theta)^2 + Y_B^2] &= 248.376(4906.8341) \\ &= 1,218,739.826 \end{aligned}$$

Also, as shown previously,

$$(r_A^2 - r_B^2 - a^2)^2 = 6209.440$$

Therefore,

$$\begin{aligned} 4a^2[(X_B \sin\theta + Z_B \cos\theta)^2 + Y_B^2] &= -(r_A^2 - r_B^2 - a^2)^2 = R, \text{ say} \\ &= 1,212,530.386 \\ \sqrt{R} &= 1101.1496 \\ \pm Y_B \sqrt{R} &= \pm (70.033)(1101.1496) \\ &= \pm 77,116.808 \quad (\text{item 1}) \\ (r_C^2 - r_B^2 - a^2)(X_B \sin\theta + Z_B \cos\theta) &= (-78.800)(1.4789) \\ &= -116.537 \quad (\text{item 2}) \end{aligned}$$

$$\text{Items 1 + 2} = G \cdot k = -77,253.987$$

$$\text{or } +77,000.271$$

The axle is to be directed upward in the retracted position, so from observation on the side view $X_{A'}$ must be greater than X_A .

Using the equation, $X_{A'} = X_{B'} + k \sin\theta$, $k \sin\theta$ must be positive, but $\sin\theta$ is negative; it is accordingly the *negative* value of k that must be used.

Since $G \cdot k = -77,253.987$; $G = 9813.668$ and $k = -7.872$,

$$k \sin\theta = (-7.872)(-0.10453) = 0.82286$$

$$X_{B'} = \underline{-15.10000}$$

$$\text{Sum} = X_{A'} = -14.277$$

$$X_{A'}^2 = 203.837$$

$$k \cos\theta = (-7.872)(0.99452) = -7.829$$

$$Z_{B'} = -0.100$$

$$\text{Sum} = Z_{A'} = -7.929$$

$$Z_{A'}^2 = 62.869$$

Therefore,

$$Y_{A'}^2 = r_A^2 - X_{A'}^2 - Z_{A'}^2 = 5115.961 - 203.837 - 62.869$$

$$= 4949.255$$

$$Y_{A'} = \underline{69.637}$$

The front view shows that this value is positive.

Checking,

$$Y_{A'} - Y_{B'} = \pm\sqrt{a^2 - k^2}$$

$Y_{A'}$ is less than $Y_{B'}$, so use positive value of square root,

$$a - k = 7.880 + 7.872 = 15.752$$

$$a + k = 7.880 - 7.872 = \underline{0.008}$$

Therefore,

$$\sqrt{a^2 - k^2} = \sqrt{0.1256} = 0.3546 = Y_{A'} - Y_{B'}$$

$$Y_{B'} = Y_{A'} - 0.3546 = 69.637 - 0.355 = 69.282$$

$$Y_{B'} + \sqrt{(a^2 - k^2)} = Y_{A'}$$

$$Y_{A'} = 69.282 + 0.355 = \underline{69.637}$$

This is precisely the same as previously calculated above.

The coordinates are summarized in Table 8.1.

Table 8.1 Summary of Coordinates from Initial Kinematic Analysis

| | | | |
|----------------|----------------|--------------------|--------------------|
| $X_A = -13.35$ | $X_B = -13.35$ | $X_{A'} = -14.277$ | $X_{B'} = -15.100$ |
| $Y_A = 2.88$ | $Y_B = -5.00$ | $Y_{A'} = 69.637$ | $Y_{B'} = 69.282$ |
| $Z_A = 70.21$ | $Z_B = 70.21$ | $Z_{A'} = -7.929$ | $Z_{B'} = -0.100$ |

Direction Cosines of the Pivot Axis

$$X_{B'} - X_B = -1.75 \quad X_{A'} - X_Z = -0.927$$

$$Y_{B'} - Y_B = 74.282 \quad Y_{A'} - Y_A = 66.757$$

$$Z_{B'} - Z_B = -70.31 \quad Z_{A'} - Z_A = -78.139$$

$$\begin{aligned} (Y_{B'} - Y_B)(Z_{A'} - Z_A) &= -5804.321 \\ -(Z_{B'} - Z_B)(Y_{A'} - Y_A) &= +4693.685 \\ \text{Sum} &= -1110.636 \end{aligned}$$

$$\begin{aligned} (Z_{B'} - Z_B)(X_{A'} - X_A) &= +65.177 \\ -(X_{B'} - X_B)(Z_{A'} - Z_A) &= -136.743 \\ \text{Sum} &= -71.566 \end{aligned}$$

$$\begin{aligned} (X_{B'} - X_B)(Y_{A'} - Y_A) &= -116.825 \\ -(Y_{B'} - Y_B)(X_{A'} - X_A) &= +68.859 \\ \text{Sum} &= +47.966 \end{aligned}$$

Therefore, the direction cosines of the pivot axis are

$$l : m : n = -111.064 : -7.157 : -4.797$$

$$\begin{aligned} \text{Sum of the squares of these values} &= 12,335.212 + 51.223 + 23.011 \\ &= 12,409.446 \end{aligned}$$

$$\sqrt{12,409.446} = 111.398$$

Therefore,

$$l = \frac{-111.064}{111.398} = -0.9970$$

$$m = \frac{-7.157}{111.398} = -0.0642$$

$$n = \frac{-4.797}{111.398} = -0.0431$$

$$l/n = 23.1323$$

$$\tan^{-1} l/n = \underline{87.525 \text{ deg side view}}$$

$$m/n = 1.4896$$

$$\tan^{-1} m/n = \underline{56.125 \text{ deg front view}}$$

Angle of Retraction

$$(X_B - X_B)^2 = 3.063$$

$$(Y_B - Y_B)^2 = 5517.816$$

$$(Z_B - Z_B)^2 = 4943.496$$

$$\text{Sum} = 10,464.373$$

$$\sqrt{\text{Sum}} = 102.296$$

$$lX_B = 13.310$$

$$mY_B = 0.321$$

$$nZ_B = -3.026$$

$$lX_B + mY_B + nZ_B = +10.605$$

$$(lX_B + mY_B + nZ_B)^2 = 112.466$$

$$r_B^2 = 5132.667 \quad (\text{from previous calculation})$$

$$r_B^2 - (lX_B + mY_B + nZ_B)^2 = 5020.201$$

$$\sqrt{5020.201} = 70.853$$

If ϕ is the retraction angle, then

$$\sin \frac{\phi}{2} = \frac{1}{2} \cdot \frac{102.296}{70.853} = 0.7219$$

$$\frac{\phi}{2} = 46.211 \text{ deg}$$

$$\phi = \underline{92.421 \text{ deg}}$$

Retracted Position of Point D

Point D could represent, for instance, the side brace attachment. The following calculations are based on the data shown in Table 8.2.

$$lX_D + mY_D + nZ_D = 4.8174$$

$$l(lX_D + mY_D + nZ_D) = -4.8029$$

$$l(lX_D + mY_D + nZ_D) - X_D = +1.1971$$

$$m(lX_D + mY_D + nZ_D) = -0.3093$$

$$m(lX_D + mY_D + nZ_D) - Y_D = +1.6907$$

Table 8.2 Data for Calculation of Retracted Point D

| | | | |
|---------------|-------------------|----------------------------|------------------|
| $l = -0.9972$ | $X_D = -6.00$ | $\phi = 92.42 \text{ deg}$ | |
| $m = -0.0642$ | $Y_D = -2.00$ | $1 - \cos\phi = 1.0422^a$ | |
| $n = -0.0431$ | $Z_D = +30.00$ | $\sin\phi = 0.9991$ | |
| l | m | n | |
| X_D | $lX_D = + 5.9820$ | $mX_D = +0.3852$ | $nX_D = +0.2586$ |
| Y_D | $lY_D = + 1.9940$ | $mY_D = +0.1284$ | $nY_D = +0.0862$ |
| Z_D | $lZ_D = -29.9100$ | $mZ_D = -1.9260$ | $nZ_D = -1.293$ |

^aNote that $\cos 92.42 \text{ deg} = -\cos(180 - 92.42)$.

$$n(lX_D + mY_D + nZ_D) = -0.2076$$

$$n(lX_D + mY_D + nZ_D) - Z_D = -30.2076$$

$$mZ_D - nY_D = -2.0122$$

$$nX_D - lZ_D = +30.1686$$

$$lY_D - mX_D = +1.6088$$

$$[(lX_D + mY_D + nZ_D) - X_D](1 - \cos\phi) = +1.2476$$

$$(mZ_D - nY_D) \sin\phi = -2.0104$$

$$X_D = -6.0000$$

$$\text{Sum} = X_{D'} = -6.7628$$

$$[m(lX_D + mY_D + nZ_D) - Y_D](1 - \cos\phi) = +1.7620$$

$$(nX_D - lZ_D) \sin\phi = +30.1414$$

$$Y_D = -2.0000$$

$$\text{Sum} = Y_{D'} = +29.9034$$

$$[n(lX_D + mY_D + nZ_D) - Z_D](1 - \cos\phi) = -31.4824$$

$$(lY_D - mX_D) \sin\phi = +1.6074$$

$$Z_D = +30.0000$$

$$\text{Sum} = Z_{D'} = +0.1250$$

To check the accuracy of the above, $X_D^2 + Y_D^2 + Z_D^2$ should be equal to $X_{D'}^2 + Y_{D'}^2 + Z_{D'}^2$.

Summary of the side brace attachment coordinates is

$$X_D = -6.00 \quad X_{D'} = -6.763$$

$$Y_D = -2.00 \quad Y_{D'} = +29.903$$

$$Z_D = +30.00 \quad Z_{D'} = +0.125$$

Figure 8.24 shows the complete dimensions.

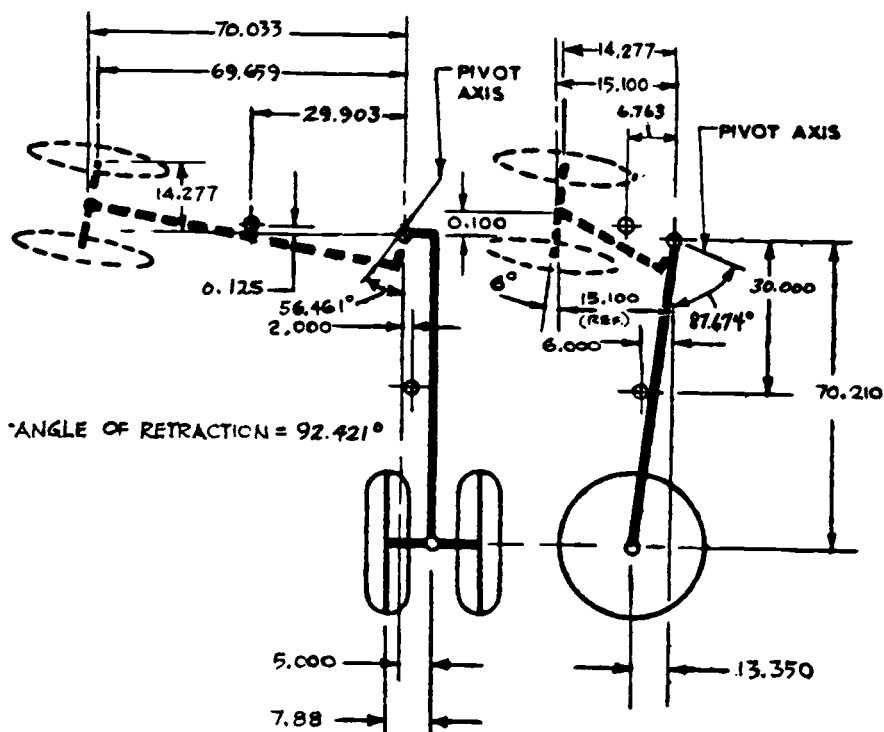


Fig. 8.24 Kinematics example: complete dimensions.

It should be emphasized that the great value of this method is that it not only calculates the overall gear geometry, pivot axis, and retraction angle, but having calculated the direction cosines as part of the procedure, subsequent determination of any other retracted point location is simple. A side brace attachment point was calculated above, but the same method could be used for any point where precise location is required.

References

¹Conway, H. G., *Landing Gear Design*, Chapman and Hall, London, 1958, pp. 223-231.

²Hetzel, K. W., *Journal of the Royal Aeronautical Society*.

³*Aircraft Engineering*, May 1963, p. 145.

STEERING SYSTEMS

9.1 DESIGN CONSIDERATIONS AND REQUIREMENTS

Aircraft are steered by either differential braking or turning the nose gear. The former is satisfactory for tail wheel and light aircraft, although it is now common practice to equip even the light planes with a form of nose gear steering. Differential braking, as the name implies, involves applying the brakes to the left or right wheels as required to turn the aircraft, but it is unusual to use this as the primary system on transport aircraft.

Nose wheels may be turned by the rudder pedal or by a wheel or bar in the cockpit, or by a combination of both. On light aircraft, the rudder pedals may be connected to the nose wheel, but current practice usually involves a power-assist system. Fighter-type aircraft control the nose gear angle by rudder pedal action, with this action in turn controlling an electrical or hydraulic actuator to steer the gear. On larger aircraft, a wheel is usually provided in the cockpit for ground maneuver; cargo aircraft designed in accordance with MIL-STD-203* are required to have hand-wheel steering. The latest techniques involve the use of both rudder pedal and hand-wheel steering for such aircraft. Rudder pedal steering is used to correct the heading during takeoff and the initial part of the landing. High-authority hand-wheel steering is used for smoother operation on taxiways and in the terminal area, resulting in a better ride for the passengers.

The general requirements will usually specify the runway width for a 180 deg turn, how the aircraft's directional control on the ground will be accomplished, the crosswind conditions to be accommodated, and the control required after normal system failure. In addition, the probability of failure will often be specified. The manufacturer's analysis will be used to predict the system capabilities, which will later be verified by flight tests, including evaluation of the emergency system. Failure analyses must be prepared, using historical data to predict the failure rates. All of the requirements will usually be based upon the use of dry concrete surfaces; maneuverability requirements on other types of surfaces are usually avoided because of the extreme difficulty in proving compliance in situations having many variables. However, characteristics on wet and icy runways will often be determined for handbook purposes.

Concerning the emergency system, a logical requirement could stipulate

*See Chapter 15 for a list of specifications.

that, after normal system failure, the aircraft must be able to make a landing ground roll, keeping within, say, 10 ft of the centerline, and must be able to turn 180 deg on a 150 ft wide runway. If this is obtainable using differential braking, then such a system may be acceptable as the emergency system, although differential braking is not suitable in some cases—it causes severe ground erosion on unpaved fields and its constant use can result in landing gear failure.

The following are some of the elements to consider in designing a steering system:

1) Nose wheel steering angles greater than ± 60 deg impose restrictions on the methods available to provide the steering action. Large angles eliminate the use of simple push-pull actuators, as shown in Fig. 9.1. Alternate methods are rack and pinion, rotary actuators, and multiplying linkage, all of which are illustrated in Fig. 9.2.

2) On larger aircraft, the turn radius should be checked early in the design. The accepted method (involving minor inaccuracies) is shown in Fig. 9.3. On these type of aircraft, it is sometimes specified that the aircraft must be able to make a 180 deg turn on a 150 ft wide runway. If this is required, then the nose wheel steering angle may be critical. Another factor on large aircraft is their ability to maneuver satisfactorily on a 75 ft taxiway.

3) Appropriate disconnect systems must be considered between the various elements involved, i.e., the rudder, rudder pedals, hand-wheel, and nose gear. The most important of these is that all steering functions *must* be disconnected prior to retracting the gear. A centering cam, such as shown in Fig. 9.4, or a centering spring may be used to ensure that the gear is centered prior to retraction. A method sometimes used to eliminate any subsequent steering commands being transmitted to the gear is to allow the steering cables to slacken while the gear is being retracted. This can be accomplished easily by a suitable geometry of the pulleys and links. Other methods of disconnect involve the use of a microswitch or hydraulic valve,

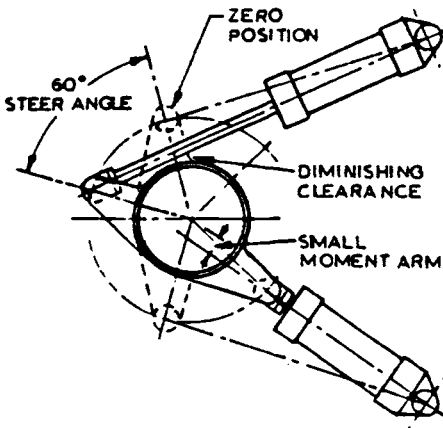
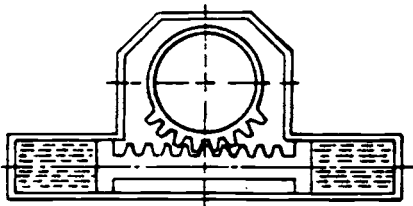
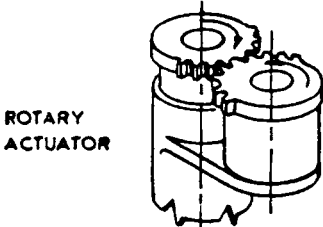


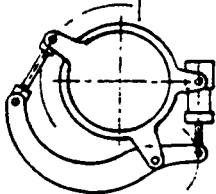
Fig. 9.1 Steer angle limitation.



RACK & PINION



ROTARY ACTUATOR



MULTIPLYING LINKAGE

Fig. 9.2 Steering mechanisms.

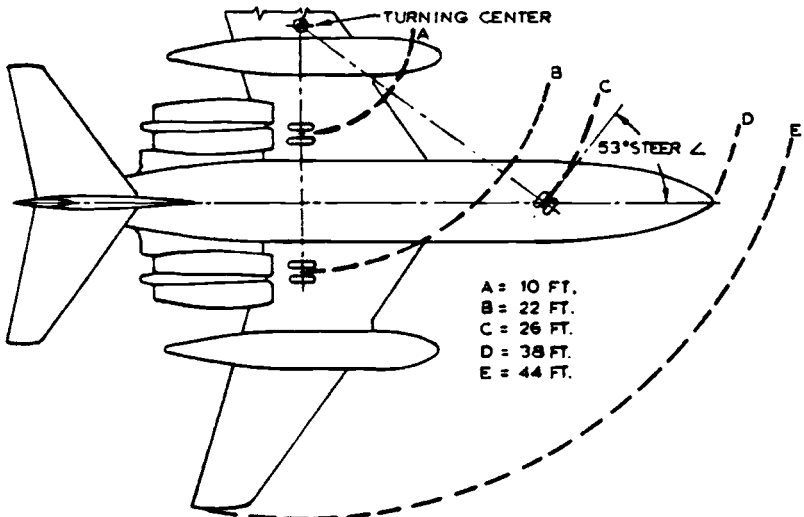


Fig. 9.3 Turning radius.

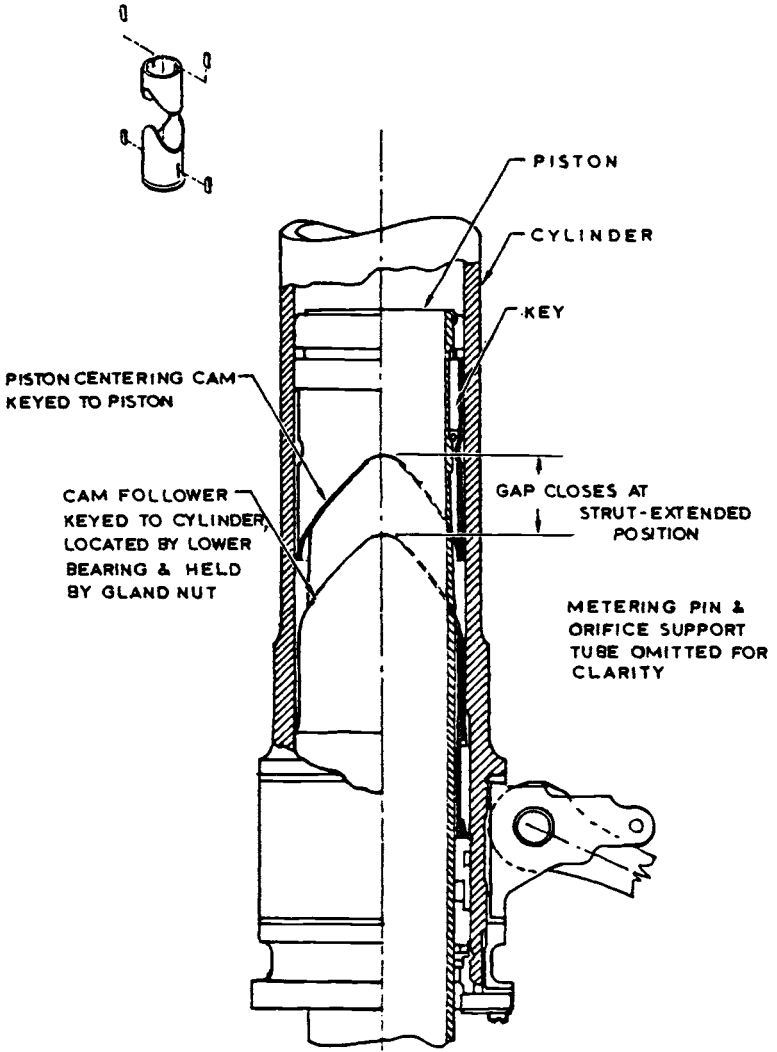


Fig. 9.4 Centering cam.

both of which sense when the aircraft has touched the ground and enable steering commands to be transmitted only after that signal has been given.

4) Shimmy damping must be provided. The steering system is often used as part of this damping system. Other elements of a shimmy damping system may be corotating wheels on the nose gear, an appropriate amount of trail (the distance that the wheel centers are behind the shock strut centerline), and friction. The steering system can contribute to shimmy damping by restricting motion in the steering actuator or motor. For instance, using a hydraulic steering actuator, oil leaving the actuator passes through a restrictor valve; an accumulator is used to insure that the actuators are kept full. Figure 9.5 shows a typical hydraulic system in which shimmy damping is provided. Shimmy damping may also be obtained by canting the nose gear. Table 9.1 depicts the characteristics of some nose landing gears and their respective shimmy characteristics.

5) In many cases, a means must be provided for allowing the nose gear to be turned by a tow vehicle to angles greater than the angle required for steering. In fact, some gears allow the wheels to be turned through 360 deg while the tow vehicle maneuvers the aircraft inside hangers or on aircraft carriers. Disconnects will usually be required to permit such operations, an exception being the case in which rotary actuators are used to drive the top of the piston.

6) The steering torque requirements must be based on a method similar to that shown in Fig. 9.6. This assumes a coefficient of friction between the tire and the ground of 0.8 and, in compliance with requirements, provides enough torque to steer the wheels without forward motion of the aircraft.

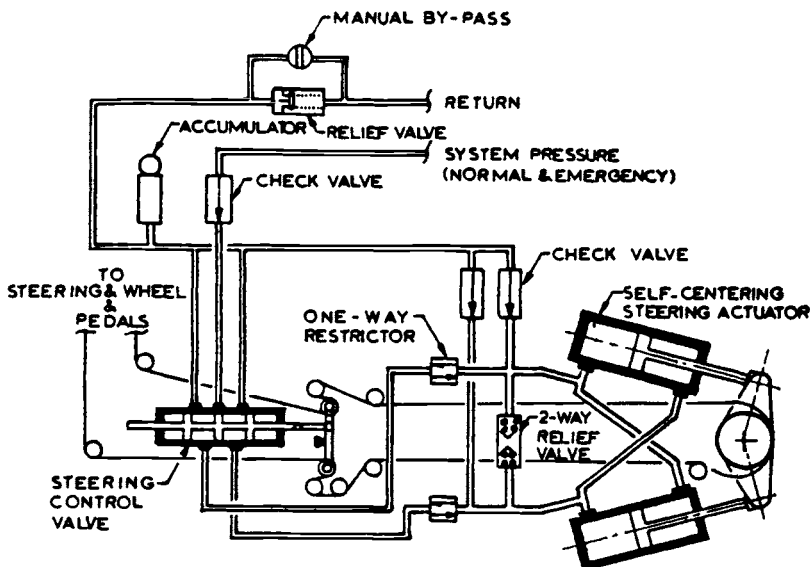


Fig. 9.5 Steering system.

Table 9.1 Typical Shimmy Characteristics

| Aircraft | Nose gear cant angle, deg | Nose gear mechanical trail | Shimmy characteristics |
|----------|---------------------------|----------------------------|------------------------|
| CF-5 | 13 | 0.8 | Exceptionally stable |
| F-16 | 9 | -0.6 | Very stable |
| F-5E | 7 | 0.8 | Stable |
| T-38 | 0 | 1.6 | Marginal |
| F-5A | 0 | 1.6 | Marginal |

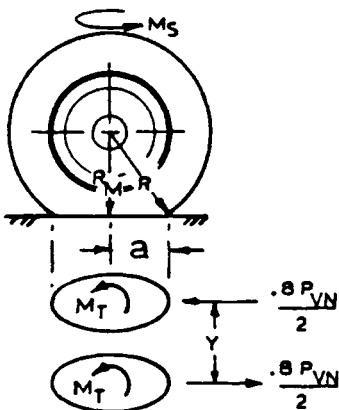
Typical Problems and Solutions

T-38/F-5 shimmy caused by wheel rpm matching strut/structure bending natural frequency. Solution: add weight to apex of torque links.

JetStar shimmy corrected by using corotating twin-nose wheels (live axle).

C-130 shimmy corrected by reducing mechanical trail from 6 to 3 in.

Source: AIR 1752.



FOR COROTATING WHEELS

$$M_T = \frac{.8 P_{VN}}{2} \left[\frac{4a}{3\pi} \right]$$

$$\begin{aligned} \therefore M_S &= \frac{.8 P_{VN}}{2} \cdot Y + 2 \times \frac{.8 P_{VN}}{2} \left[\frac{4a}{3\pi} \right] \\ &= .4 P_{VN} \left[Y + \frac{8a}{3\pi} \right] \text{ (TWIN WHEEL GEAR)} \end{aligned}$$

WHERE

M_S = STEERING TORQUE

P_{VN} = MAX STATIC VERTICAL LOAD (C.G.FWD)

$$a = \sqrt{R^2 - R_M^2}$$

THERE MUST BE NO FAILURES WITH ULTIMATE PRESSURE IN STEERING ACTUATOR.

CHECK TORQUE ALSO DUE TO SPIN-UP CONDITION WITH ONE FLAT TIRE .

Fig. 9.6 Steering torque calculation for corotating wheels.

7) The available steering angle during the actual takeoff and landing phases should probably be restricted. Experience has shown that on wet and icy runways, for instance, the pilot may overcontrol, thus causing the turning force to be less than the applied force—which has caused several accidents.

8) A follow-up linkage will be required, such as that described in Sec. 9.2.

9) In the cockpit, it is a good idea to have a switch to “arm” the steering system. This ensures that steering commands will be transmitted to the nose gear only when the pilot considers it safe and desirable to do so. If a hand wheel is used to steer the gear during taxi and terminal operations, it should be designed so that full steering travel can be selected with one hand, without the pilot having to change his or her grip. For instance, on the Lockheed JetStar, 106 deg of hand-wheel movement causes the wheels to be steered through 53 deg; on the Boeing 727, 95 deg of hand-wheel movement steers the wheels 78 deg.

In summary, a power steering system will consist of one or two steering actuators (linear, rotary, hydraulic, or electric), a power supply, a control valve, a follow-up device between the gear steering collar, control valve, and pilot's control, and usually a pilot-operated steering wheel, lever, or rudder pedal linkage. Use the smallest possible steering angle; provide means of decommissioning the steering system prior to or during retraction; provide a centering device to align the gear prior to retraction; consider shimmy damping; and consider complete disconnection of the nose gear steering system for towing, if required—but try to avoid it. Consider the provision of a separate arming device and provide the maximum steering rate that is safe for the aircraft; this may vary 5–60 deg/s (loaded), depending on the anticipated use of the aircraft.

Reference 1 provides a particularly good description of modern steering systems and the considerations involved.

9.2 ACTUATION

Figure 9.7 is a schematic drawing of the Lockheed C-141 steering system. The control valve is operated by rocking a horseshoe link that is, in turn, moved by differential tension in the cables. Movement of the control valve ports hydraulic fluid to the right or left sides of the rack-and-pinion actuator; the subsequent movement of the rack rotates the nose wheel piston through a pinion mounted on the piston. Referring to Fig. 9.7, a tension load in cable X causes cable Y to relax. The input pulley (10) rotates the input link (6) to the left around pin (9).

The control valve (5) ports pressure to the cylinder cavity, moving piston (3) to the right. The piston rack (4) moves the sector gear (2) counterclockwise. Control valve feedback is through cables X and Y and takes up any relaxation in cable Y, thus applying a force to input pulley (10) to rotate input link (6) to the right around pivot pin (9). This returns the control valve (5) to neutral when the output piston (3) achieves the position originally commanded by the input signal of cable Y.

The device includes a centering mechanism (8) to hold the input link (6)

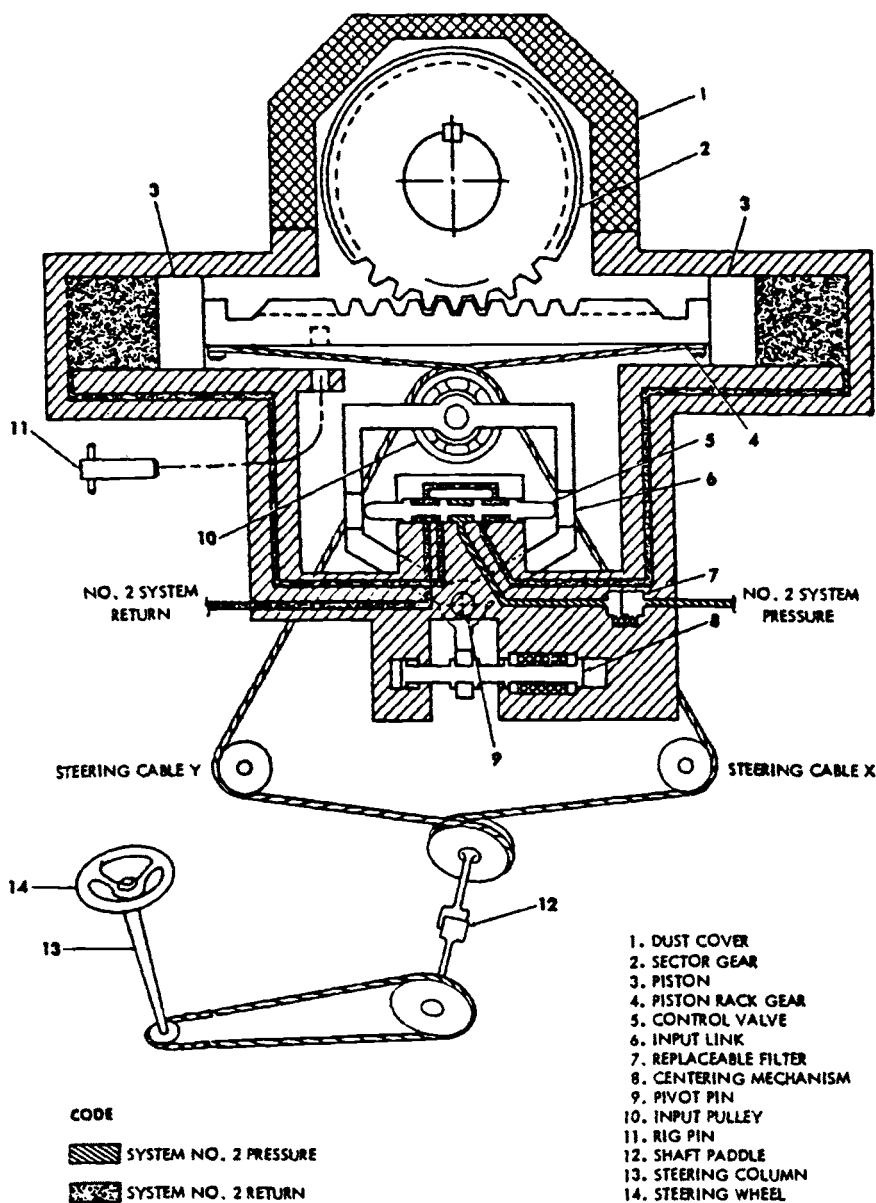


Fig. 9.7 C-141 steering system detail.

and control valve (5) in neutral when no loads are being applied by cables X and Y. This allows the unit to caster freely in the neutral position. The control valve (5) allows interflow between cylinder cavities through the return passage, thus allowing sector gear (2) to rotate in response to castering load torques.

The C-141 steering device can be considered typical of rack-and-pinion systems. It is an excellent—and compact—method for achieving high steering angles, but this type of system is deficient in one respect: the entire steering torque must be reacted on a small number of teeth and in some cases, the tooth size required is too large for practical application. The A-300B uses two rack-and-pinion actuators in parallel to overcome the tooth load problem.

Figure 9.8 illustrates a gear that is steered by an epicyclic gear train

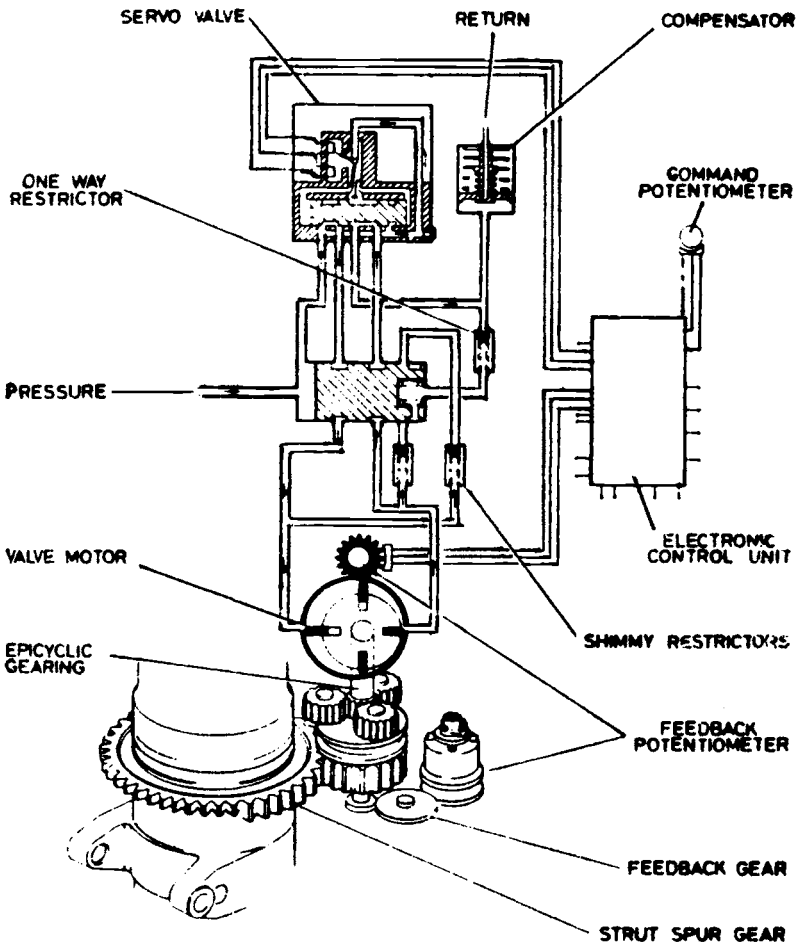


Fig. 9.8 Tornado steering schematic (source: Dowty Rotol Ltd., From Ref. 1, reprinted with permission). © Society of Automotive Engineers, 1985.

which is controlled by a steer-by-wire system. This Tornado system was based on that used by the F-4 Phantom and is powered by 4000 psi hydraulic pressure. A complete discussion of it is provided in Ref. 1.

To illustrate a particular application of a rotary actuator to a Navy aircraft, the actuator was required to rotate the gear at 100 deg/s at no load, using 3000 psi hydraulic pressure. Maximum stall torque was 40,000 in.-lb. The unit provides damping in the "power-off" mode and will center the gear automatically upon application of "gear-up" or "gear-down" pressure. The time required to center the gear from 60 to 0 deg is 2 s. Up to 20 min of free play is allowed at the wheels. Figure 9.9 is a block diagram of the system.

The most widely used actuation system uses one or two push-pull linear actuators. These are supported from the nonrotating part of the gear and they push and pull on an arm attached to the steering collar.

A system using a single actuator is illustrated in Fig. 9.10. It steers the wheels ± 45 deg. Hydraulic power for steering is taken from the "gear-down" line to insure that the system is inoperative when the gear is retracted. The circuit is armed by depressing a switch in the cockpit and is allowed to operate by actuation of the touchdown switch. These actions cause an electrohydraulic steering selector valve to direct hydraulic fluid to

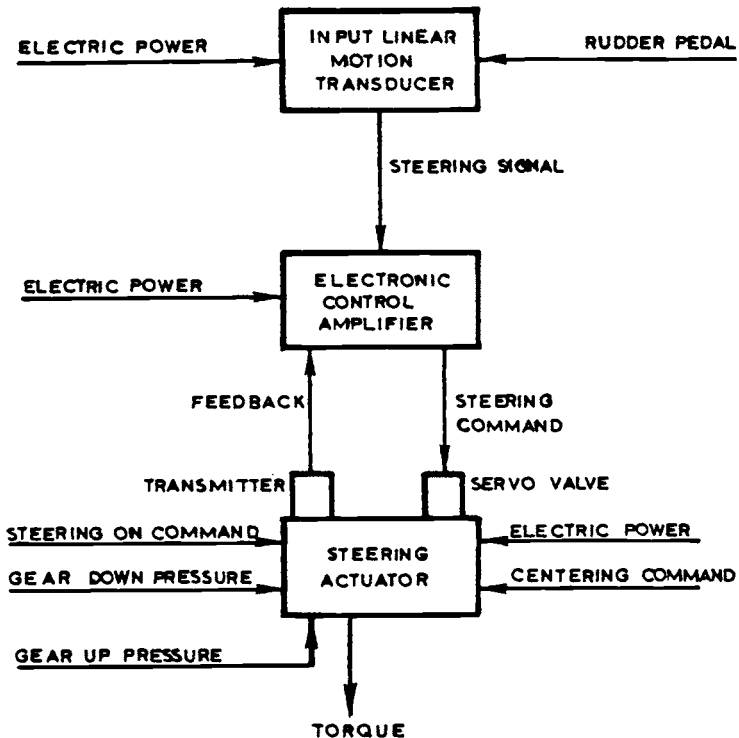


Fig. 9.9 Rotary steering system block diagram.

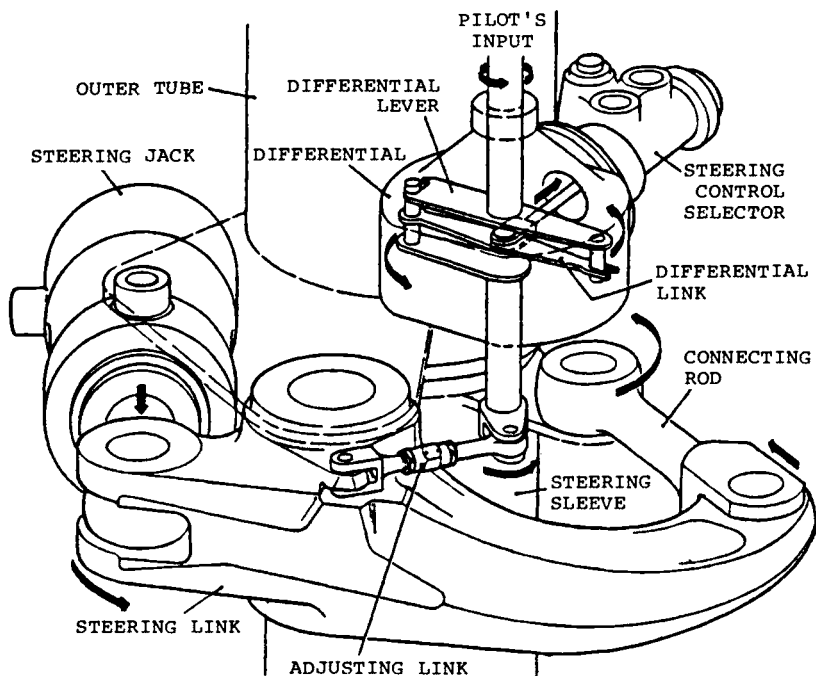


Fig. 9.10 B.Ae. 748 steering mechanism (source: British Aerospace Corp.).

the steering control valve. Movement of the cockpit-located steering tiller results in hydraulic pressure moving the steering actuator. Note that the differential follow-up mechanism is similar in principle to that shown earlier in Fig. 9.7.

The Lockheed JetStar also uses a single hydraulic linear actuator; Figure 9.11 is a schematic of the overall system. When the aircraft is on the ground, the steering selector valve is energized by a nose gear torque link switch to admit hydraulic power to the steering control valve. This valve is positioned by mechanical linkage to the steering wheel to admit hydraulic power to the proper sides of the actuation cylinder that turns the steering collar. The collar applies a load to the torque arms (scissors) to turn the nose wheels in accordance with steering input commands.

The foregoing sequence can be accomplished only if the landing gear selector valve is in the *gear-down* position. After takeoff, the scissors switch de-energizes this valve and thereby blocks hydraulic power from the steering control valve.

The control valve is mounted near the top of the gear and routes normal or auxiliary hydraulic power to the actuator according to input signals from the steering wheel. When this wheel is turned, a spool is moved in the control valve to route fluid to the left or right side of the steering actuator. The spool is centered by springs when the input signal stops; this action is

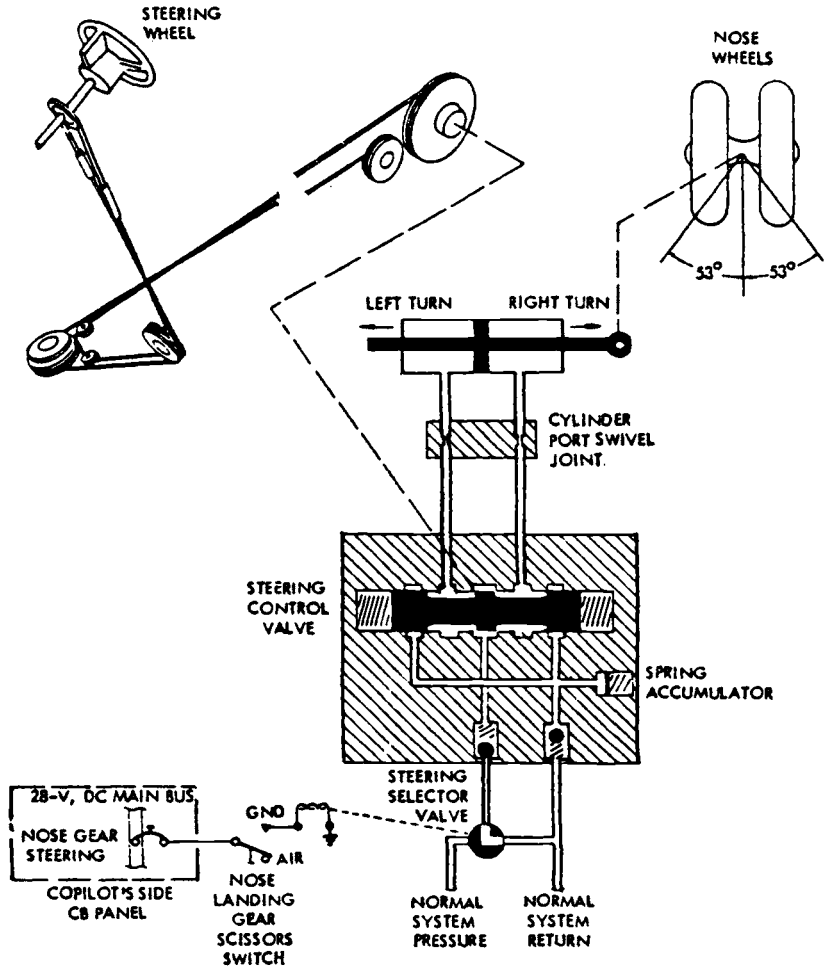


Fig. 9.11 JetStar steering system (source: Lockheed-Georgia).

used to center the wheels as well as to route fluid to both sides of the actuator for shimmy damping.

Figure 9.12 illustrates the Gulfstream I steering system in which two actuators are used. The steering solenoid valve is energized by the nose gear and main gear touchdown switches, the downlock switch, and the nose wheel steering switch, which must be turned on by the pilot before steering can be initiated. When all of these conditions are met, normal-circuit hydraulic pressure passes through the filter, selector valve, and steer swivel to the steer damper. When the pilot moves the steering control tiller, the slide valve in the damper is moved mechanically. When this valve moves to the left, hydraulic pressure enters the head end of the left cylinder and the

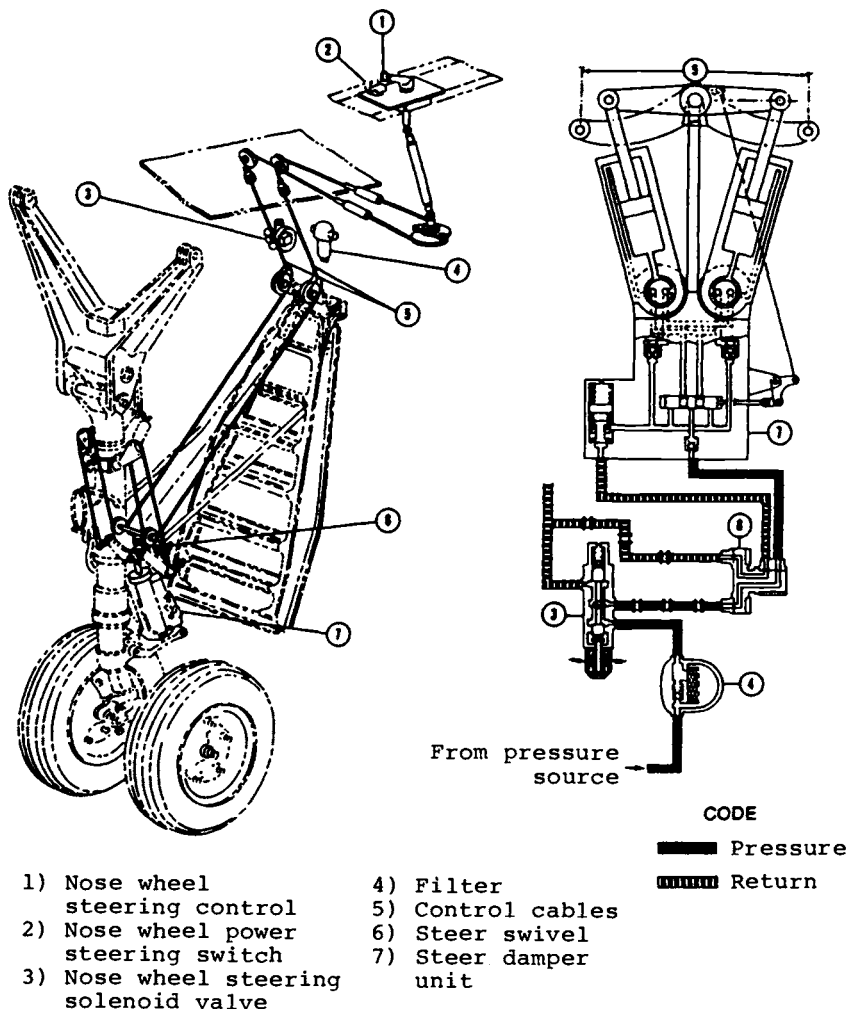


Fig. 9.12 Gulfstream steering system (source: Gulfstream Aerospace Corp.).

rod end of the right cylinder, causing the left piston to extend and the right piston to contract, steering the aircraft to the right. When the cockpit switch is turned off, the steer damper acts as a shimmy damper.

The Boeing 727 system (Fig. 9.13) is typical of those found on current transport aircraft. It is hydraulically powered, uses two linear actuators, and is controllable by either a cockpit hand wheel or rudder pedals. For towing operations, the steerable part of the gear can be disconnected to permit nose gear angles up to 90 deg. Centering cams are used to align the gear when it is extended.

To steer the aircraft, the pilot turns the hand wheel at his left forward

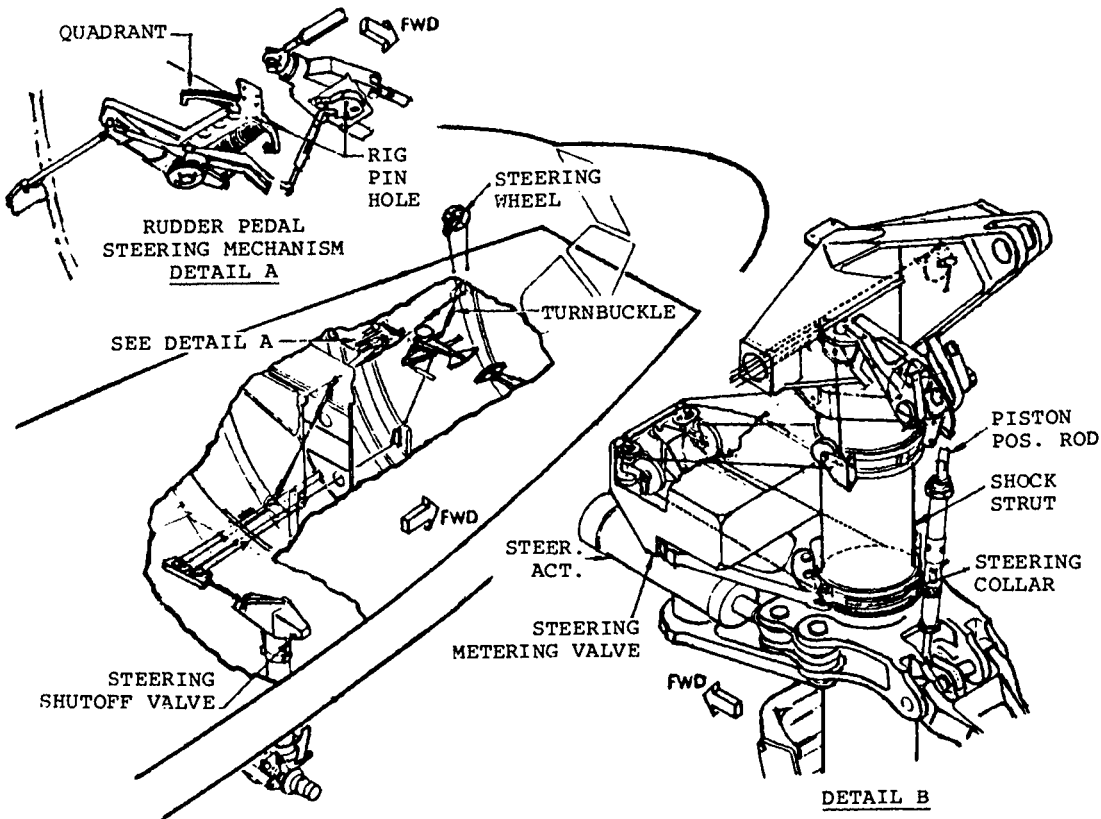


Fig. 9.13 Boeing 727 steering system.

side. This pulls one of two cables that move the steering metering valve, thereby allowing 3000 psi of pressure to be directed to the steering actuators. Up to 78 deg of nose wheel motion can be obtained.

When the aircraft is landing or taking off and only small directional changes are required, rudder pedal steering is used and only $5\frac{1}{2}$ deg of steering can be obtained.

System operation is as follows. The steering cables from the cockpit pass around pulleys at each end of the rocker arm on the metering valve. This differential rocking moves the metering valve piston, allowing hydraulic pressure to be applied to opposite ends of the two actuators, providing a push-pull movement on the left and right sides of the steering collar, as depicted in Fig. 9.14. When the selected angle has been obtained, the valve piston is moved back to neutral by follow-up action of the cables, thereby shutting off any further pressure to the actuators.

For shimmy damping, about 100 psi pressure is maintained against the actuator pistons. In addition, two pressure relief valves are incorporated into the system to relieve pressure if nose gear torque should be applied by a tow vehicle (for instance) without disconnecting the torque links. A steering shutoff valve is located upstream from the metering valve and, by cam action, it shuts off hydraulic pressure to the metering valve whenever the gear is out of the fully down position.

Figures 9.15 and 9.16 show the rudder pedal steering mechanism for the Boeing 727. That system is active only when the gear is subjected to ground loads. Cables from the torque links rotate an eccentric beneath the pedals, moving the clutch crank so that its stops do not contact the clutch arm and moving the clutch arm so that it contacts the steering crank stops. This allows the rudder pedal movement to be transmitted to the quadrant, which is, in turn, connected to the steering cables. It moves whenever the gear is steered and drives the cables in the rudder pedal mode.

The DC-8 also has two linear steering actuators, swivel glands, control valve, steering wheel, and rudder pedal steering mode. However, rudder

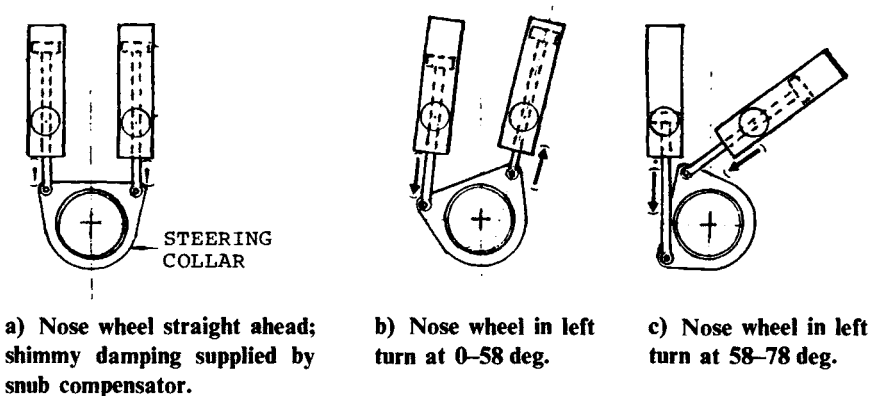


Fig. 9.14 Steering system detail of Boeing 727.

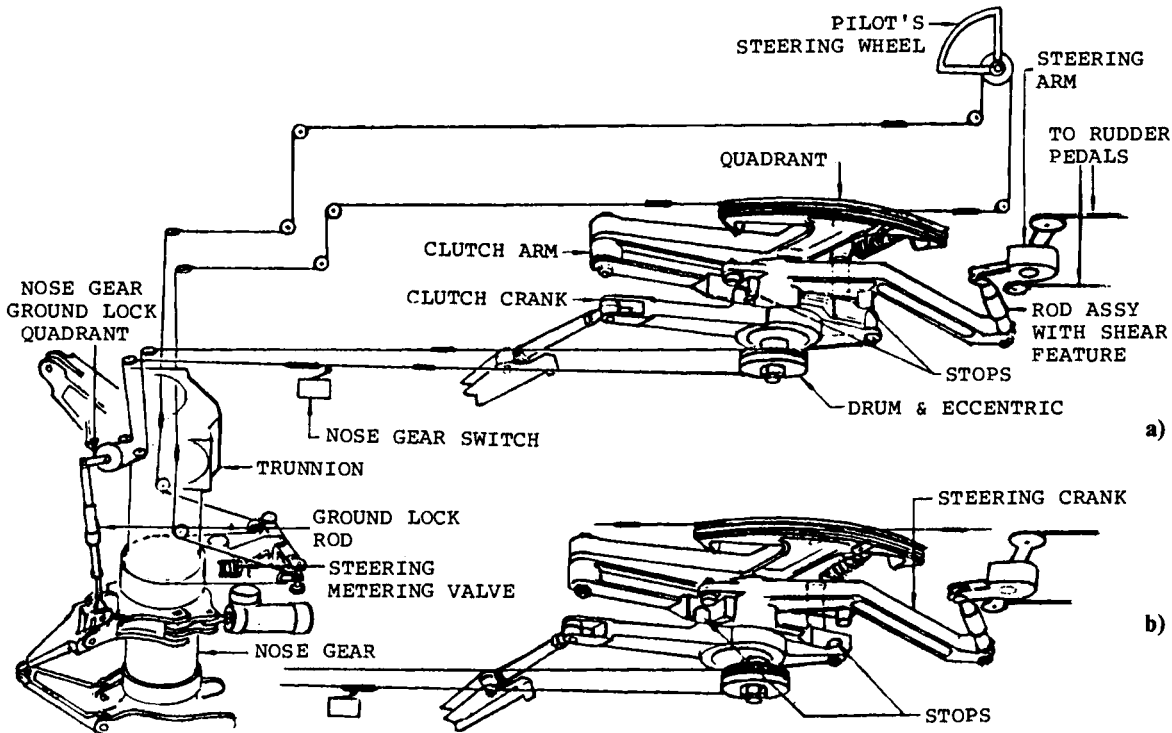
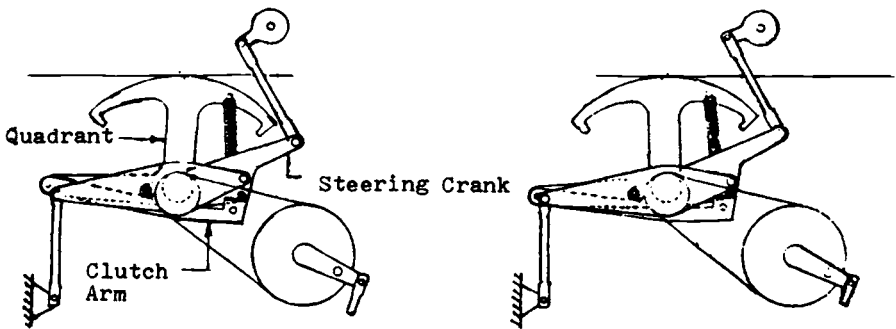
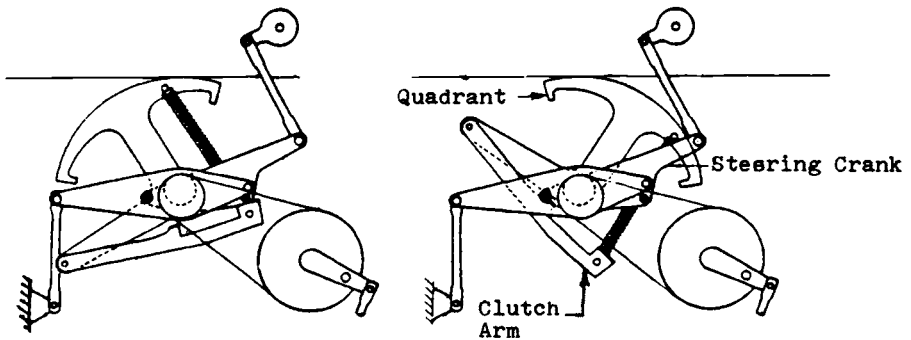


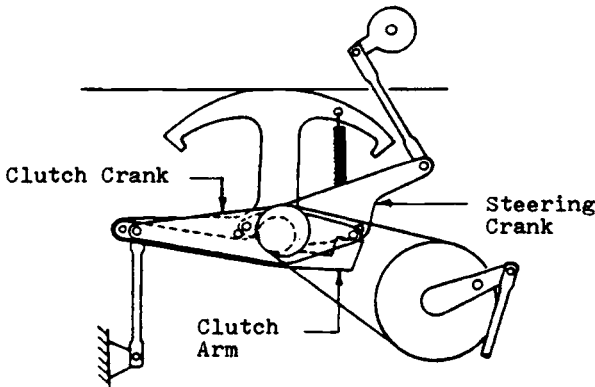
Fig. 9.15 Rudder pedal steering of Boeing 727. a) Nose gear compressed. b) Nose gear extended.



a) Condition 1: action of rudder pedal steering mechanism when used for steering. Clutch arm rides on stops on steering crank. Quadrant and clutch arm work together and are driven by action of steering crank.



b) Condition 2: action of rudder pedal steering mechanism when normal steering is used. Clutch arm rides on stops on steering arm. Quadrant, etc., are driven by cable action.



c) Condition 3: action of rudder pedal steering with nose gear extended and clutch arm riding on stops on clutch crank. Steering crank is free to move with rudder movement and does not contact clutch arm. Clutch crank with stops moved into contact by action of drum and eccentric.

Fig. 9.16 Pedal steering mechanism of Boeing 727.

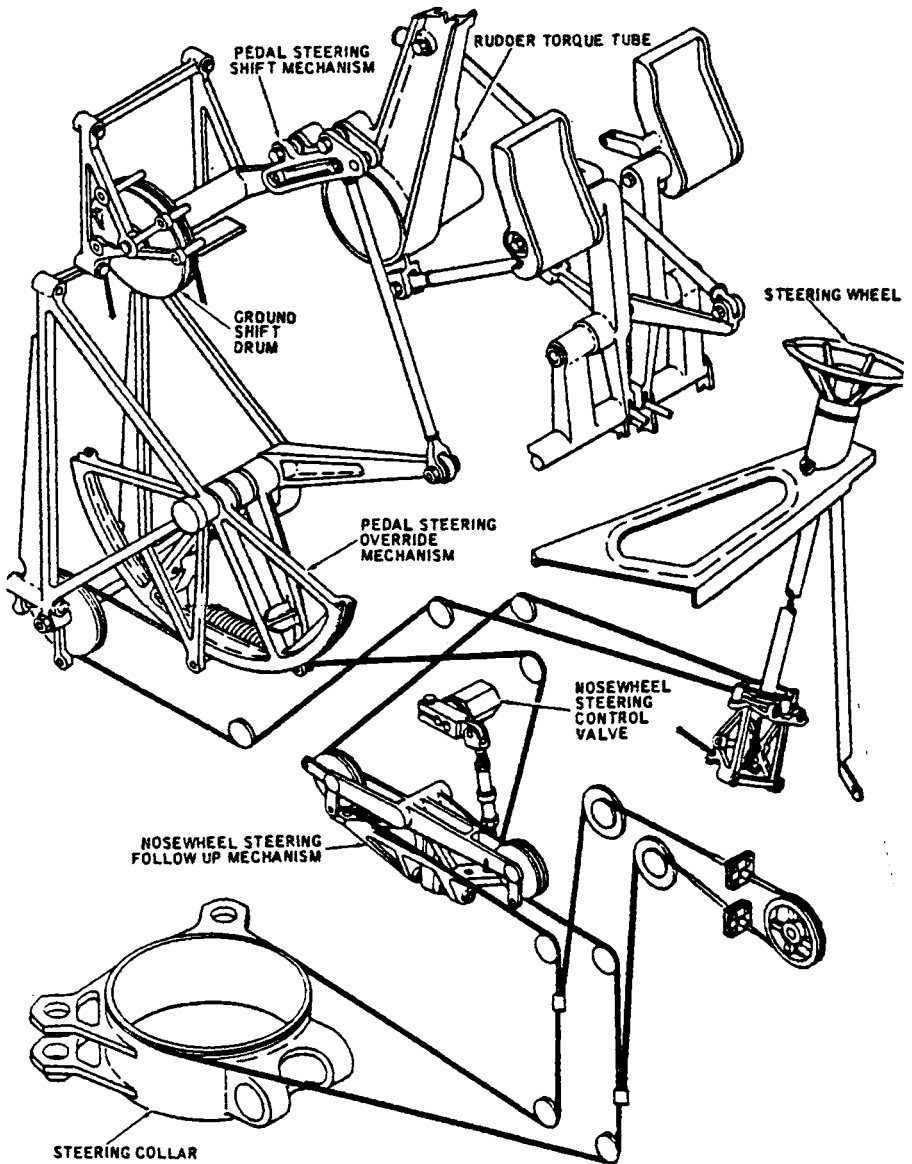


Fig. 9.17 Mechanical steering system of DC-8.

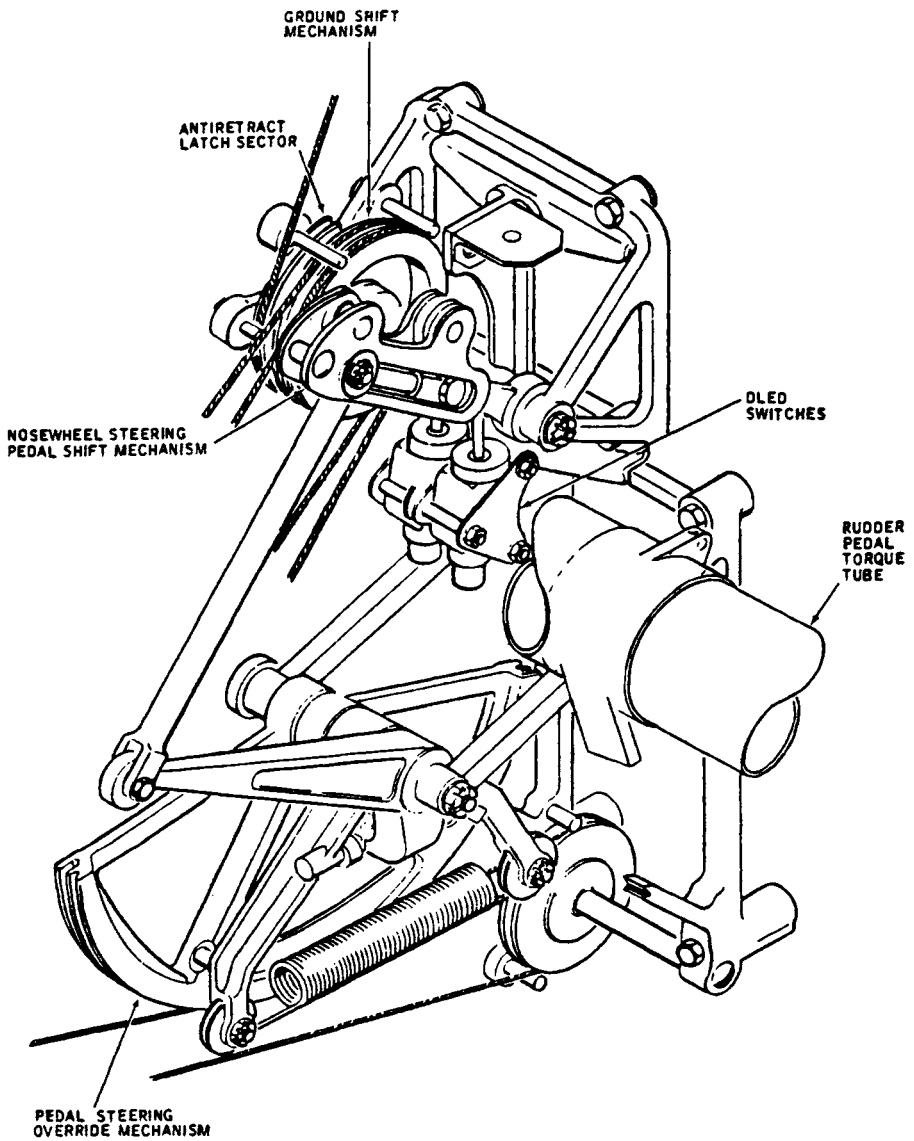


Fig. 9.18 Pedal steering override mechanism of DC-8.

pedals on this aircraft can steer the aircraft up to ± 15 deg. Figure 9.17 illustrates the mechanical portion of this steering system. Shock strut compression results in the ground shift mechanism being moved, which allows the rudder pedal depression to move the over-ride mechanism. This displaces the nose wheel and the steering wheel. In detail, rudder pedal depression moves the pushrod connected to the shift mechanism drive arm on the over-ride mechanism (Fig. 9.18). The pushrod moves the over-ride drive sector through the spring-loaded actuator arms, thus loading the turning cable that moves the follow-up differential. The differential opens the steering control valve, porting pressure to the steering cylinders.

If the steering wheel is used instead of the rudder pedals, it over-rides the pedal steering, due to the spring-loaded mechanism in the over-ride. When the steering wheel moves the cable to a position in excess of the maximum pedal steering movement, the over-ride sector continues to move. This stretches the spring and permits the over-ride sector to move the applicable spring-loaded actuator arm away from the drive arm.

The follow-up differential transmits cable motion through a linkage to operate the steering control valve. It also returns that valve to neutral when the desired nose wheel angle has been reached. The differential is free to rotate under the influence of cable loads from the pedals or hand wheel. A load in the left or right steering cable rotates the differential beam to operate the steering valve and pressurizes the left or right steering actuators. When these actuators have rotated the wheels to the desired angle, the cable load is relieved, thus allowing the differential to neutralize the control valve. This valve is shown in Fig. 9.19; it is a slide type with springs for self-centering. By having the inlet closed and all other connections open,

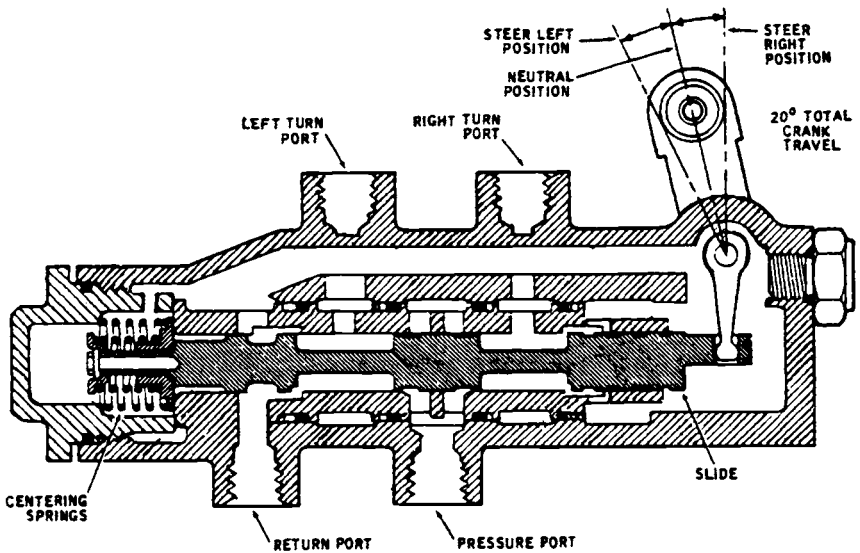


Fig. 9.19 Nose wheel steering hydraulic control of DC-8.

the wheels can caster freely. Free castering should always be provided since an aircraft is usually landed with steering power off and the nose wheels must be allowed to move to their neutral angle. In crosswind landings, this neutral angle may not be zero.

9.3 HAND-WHEEL INSTALLATIONS

Figures 9.20–9.23 are included to illustrate some typical hand-wheel installations. The drawings are self-explanatory and no further description is needed. Ideally, hand-wheel motion should be such that about ± 75 deg of rotation will move the nose wheels through their normal steering angle.

9.4 SHIMMY DAMPING

A wheel is said to shimmy when it oscillates about its caster axis. It can be caused by a lack of torsional stiffness (structural or fluidic) in the gear, excessive torsional freeplay, inadequate trail (too much or too little), and improper wheel balancing or worn parts. Steerable nose wheels are particularly susceptible to shimmy and various methods are used to dampen it. As a general rule, the amplitude should be reduced to one-third of the original amplitude within 3 s.

Obviously, it is first desirable to provide high torsional stiffness in the gear, to provide a stiff backup structure, and to provide appropriate trail. Table 9.2 lists some typical trail values. In addition, the following measures can be considered: corotating wheels, friction damping, hydraulic damping, and inclining the gear.

Corotating wheels add some degree of complication and increase the steering torque somewhat. It is a very effective method of preventing shimmy: even with one of the two tires burst, the shimmy that occurs with the remaining tire is usually tolerable.

Friction can be used to minimize or eliminate shimmy, but is seldom used because excessive friction is not conducive to good maneuverability and adds to the rudder pedal forces required in a manual steering system. It has been determined that the rotational friction between the steerable and nonsteerable portions should be about $0.12CP$, where C is the sum of the mechanical and caster trails and P the wheel load. Pneumatic trail is equal to $L/6$, where L is the footprint length; footprint length is $1.457\sqrt{A}$, where A is the contact area. The caster trail is determined by extending the shock strut axis to the ground and measuring the distance from that intersect to the point at which a vertical line from the wheel center touches the ground. Mechanical trail is the distance of the axle aft of the strut centerline measured perpendicular to the shock strut axis.

Hydraulic damping is the usual method for suppressing shimmy. A linear (or rotary) damper may be used, with both sides loaded at all times. Several methods of achieving this have been shown in the preceding figures of this chapter.

It was noted previously in this chapter that canting the shock strut at an angle to the vertical (in the side view) has a stabilizing effect. Table 9.2 shows some typical cant angles.

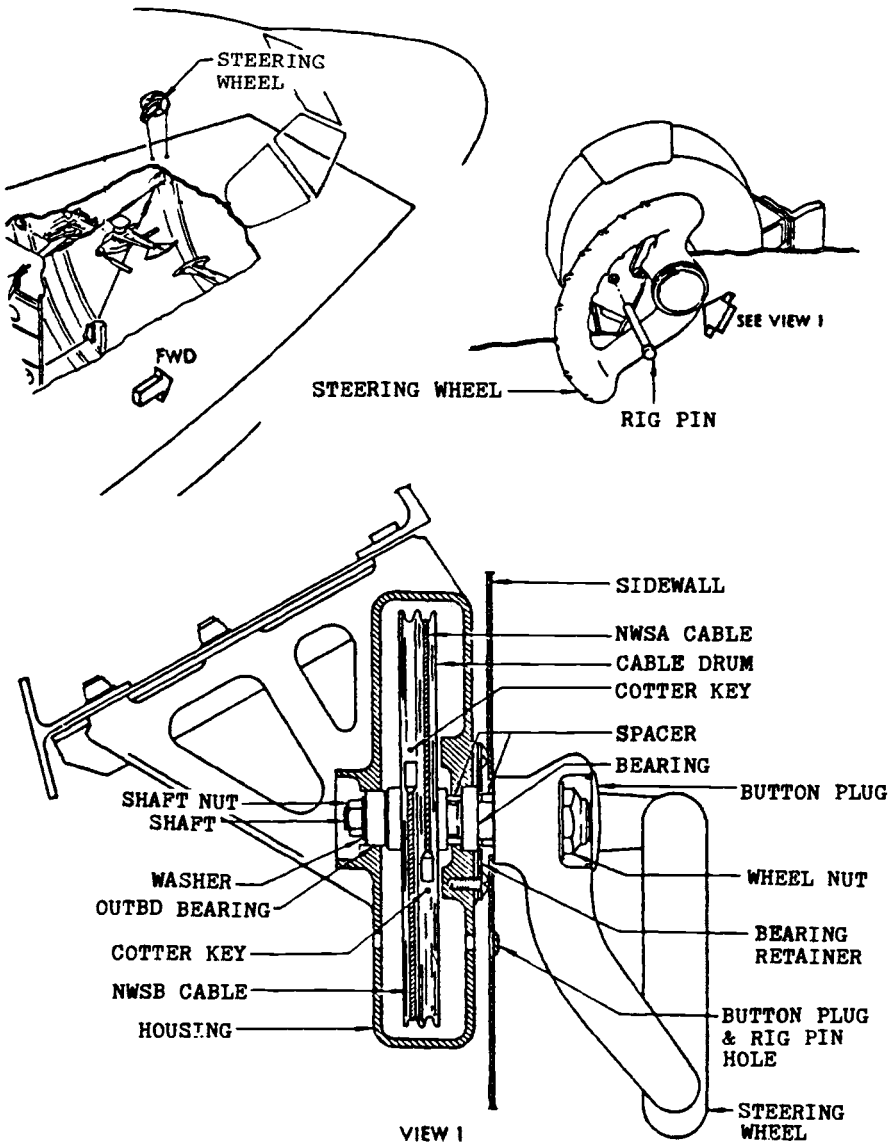


Fig. 9.20 Steering wheel and cable drum installation on Boeing 727.

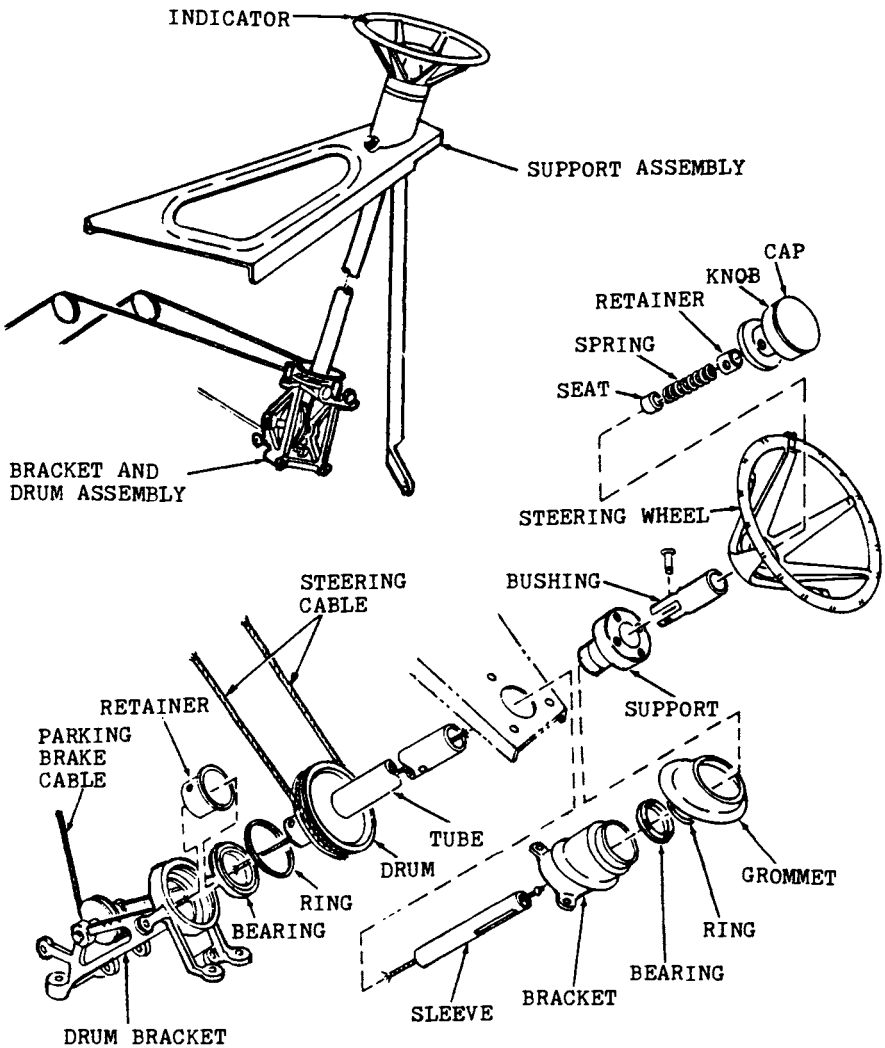


Fig. 9.21 Steering wheel and drum of DC-8.

Shimmy characteristics should be predicted by analysis while the design is under way. Component and system tests should be conducted and their characteristics used to modify the original predictions. The next step is to conduct a test using a full-scale gear to stimulate landing and takeoff by lowering the gear onto a fly wheel. When satisfactory results have been obtained from these tests, the gear can then be subjected to flight tests.

The calculations involved are too lengthy to be included here. References 2-4 contain the details.

It should be noted that although most shimmy analyses seem to be

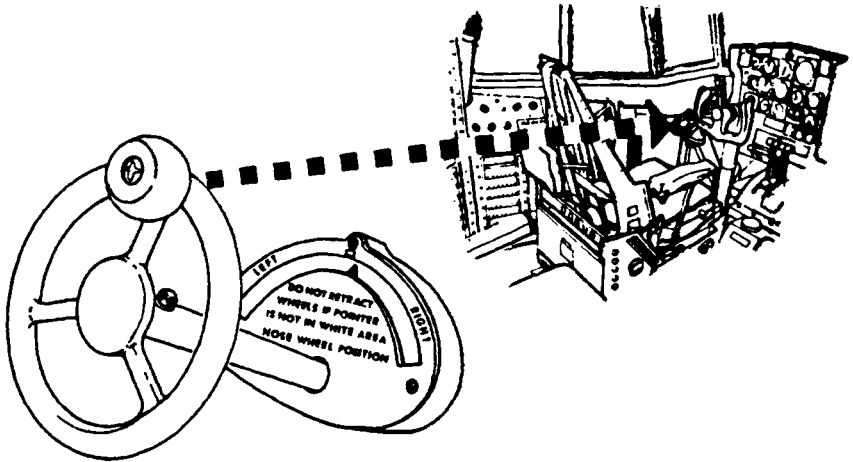


Fig. 9.22 Steering wheel of C-130 (source: Lockheed).

Table 9.2 Nose Gear Mechanical Trail and Gear Inclination Values

| Aircraft | Strut inclination, deg | Mechanical trail, in. |
|------------|------------------------|-----------------------|
| A-6B | 1.0 ^a | 2.5 |
| A-7E | 0 | 14.7 ^b |
| AV-8B | 4.5 ^a | 14.1 ^b |
| B-1 | 0 | 5.0 |
| Boeing 707 | 0 | 3.0 |
| Boeing 727 | 0 | 3.0 |
| Boeing 737 | 5 | 2.0 |
| Boeing 747 | 0 | 5.0 |
| Boeing 757 | 0 | 3.0 |
| Boeing 767 | 0 | 3.0 |
| C-5 | 0 | 4.5 |
| C-130 | 0 | 3.0 |
| DHC Dash 7 | 3.0 | 0.5 |
| DC-9 | 8.0 | 0 |
| F-4J | 0 | 3.5 |
| F-5E | 7.0 | 1.5 |
| F-14A | 0 | 3.0 |
| F-15C | 0 | 3.0 |
| F-18 | 0 | 3.0 |
| L-1011 | 0 | 3.0 |

^aTrail aft.

^bLevered suspension.

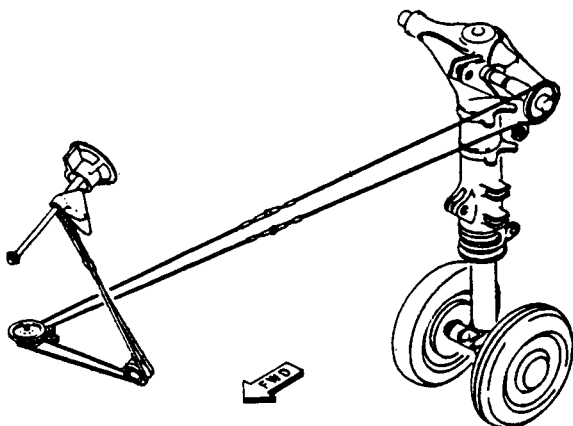


Fig. 9.23 Hand wheel steering of JetStar (source: Lockheed).

directed toward nose landing gears, shimmy can also occur in main landing gears. Thus, these should also be evaluated where appropriate.

From the practical standpoint, as opposed to the above predictions and analyses, McRay⁸ has reviewed the methods of isolating the possible causes of shimmy in a C-130 aircraft. He suggests that the aircraft be taxied at a speed high enough to allow the nose wheels to be lifted from the ground, at which point the following questions and their answers should be addressed:

1) Did the shimmy stop while the nose wheels were off the ground or did it continue?

2) During taxi with all wheels on the ground, did the steering pointer move back and forth rapidly during shimmy or was it relatively steady?

If the shimmy continued with the wheels off the ground, wheel or tire imbalance is indicated. Check for worn spots on the tires or any other cause for imbalance. Another possibility is that there may be water in the tires. Such a condition may occur if the tires had been inflated with compressed air rather than dry nitrogen; also, the water could have frozen (by a flight at high altitude, for instance).

If the shimmy ceased at nose wheel lift-off, then the observations of question 2 must be considered: if the shimmy produced no noticeable movement of the steering wheel pointer with the wheels on the ground, looseness due to excessive wear in mechanical components is indicated. Check the torque arms where the attach bolts and apex bolts/bushings may have worn. Check the steering actuator rod-end bearings and check for worn wheel bearings and axle nut torque.

If the steering wheel pointer did move back and forth, a steering control valve problem is indicated. This valve will accept steering commands from either the steering wheel or nose gear, permitting vibration to be transmitted back through the valve to the pointer. Since the pointer is connected to the steering control valve shaft, it will be displaced whenever the shaft is displaced.

Check the tires—uneven tire pressure and dissimilar or faulty treads tend to promote instability. Finally, check the steering control valve to ensure that it is functioning satisfactorily; in particular, make sure that it is not sticking or leaking at the relief valve.

Another excellent example of shimmy investigation is provided in Ref. 9. The analysis describes the results of tests made on the F-15 to evaluate the effects of out-of-tolerance torsional free-play. The shimmy, detected by lateral acceleration at the pilot seat and by rod-end strain on the steering actuator, was very pronounced at certain speeds. Analytical results are also presented to show the sensitivity of shimmy to tire parameters and strut frictional coefficients as well as to the above-mentioned torsional free-play. In describing the test procedures, Grossman⁹ notes that the most effective way found to induce shimmy was to vary the nose gear load by application of main gear brakes and stabilator position.

9.5 CASTERING NOSE WHEELS

Many light aircraft allow the nose wheel to caster, a subject discussed in Ref. 10.

Figure 9.24 depicts the various possibilities. The swivel axis should be ahead of the nose wheel; the trail is designated as t . This is the distance,

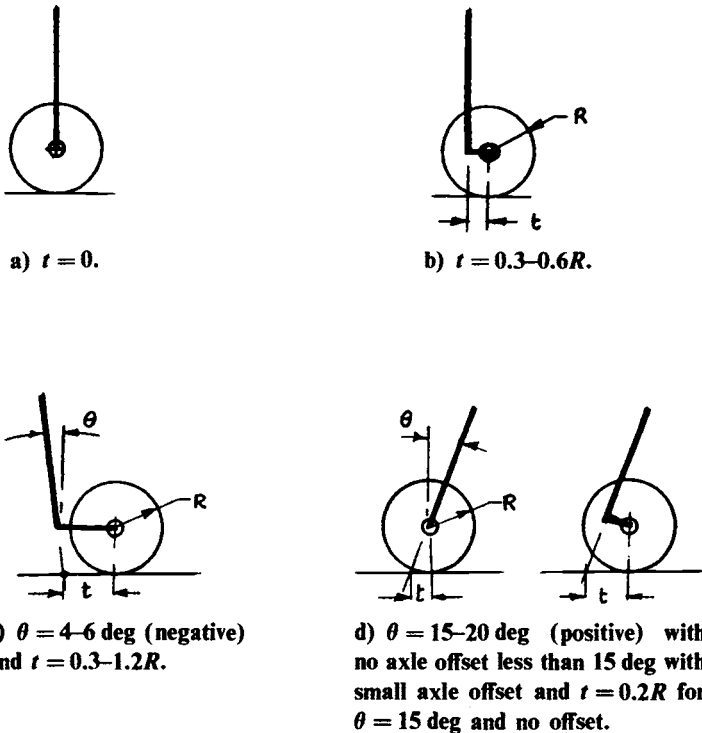


Fig. 9.24 Castering nose wheel configurations.

measured along the ground from the strut centerline intersection with the ground to the center of the contact area. Statically, the center of the contact area is directly beneath the axle center. When the wheel is moving, the center of the contact area moves aft slightly; this is then designated as the "dynamic trail."

Configurations a and b in Fig. 9.24 are statically neutral and dynamically stable in both forward and aft movement. In the latter configuration, the wheel swivels 180 deg for aft movement. A shimmy damper is required for both configurations unless corotating wheels are used.

Configuration c is statically and dynamically stable in both forward and reverse and also requires shimmy damping except, possibly, when $t = R - 1.2R$.

Configuration d is statically unstable and dynamically stable. It is unstable in reverse and the gear must be locked or steered for this operation. Shimmy damping is required. This configuration is often used for tail wheels, using friction to provide shimmy damping.

References

¹Young, D. W. S. and Ohly, B., "European Aircraft Steering Systems," SAE Paper 851940, Oct. 1985.

²Black, R. J., "Realistic Evaluation of Landing Gear Shimmy Stabilization by Test and Analysis," SAE Paper 760496, April 1976.

³Collins, R. L., "Theories on the Mechanics of Tires and Their Applications to Shimmy Analysis," *Journal of Aircraft*, Vol. 8, April 1971, pp. 271-277.

⁴Rogers, L. C., and Brewer, H. K., "Synthesis of Tire Equations for Use in Shimmy and Other Dynamic Studies," *Journal of Aircraft*, Vol. 8, Sept. 1971, pp. 689-697.

⁵Williams, D., "The Theory and Prevention of Aeroplane Nose-Wheel Shimmy," Royal Aircraft Establishment, Structures Rept. 125, Aug. 1952.

⁶Moreland, W. J., "The Story of Shimmy," *Journal of the Aeronautical Sciences*, Dec. 1954.

⁷Berry, R. W. and Tsien, V. C., "Mathematical Analysis of Corotating Nose Gear Shimmy Phenomena," *Journal of the Aeronautical Sciences*, Dec. 1962.

⁸McRay, B., "Nose Landing Gear Shimmy," *Lockheed Service News*, Vol. 12, Dec. 1985, pp. 3.

⁹Grossman, D. T., "F-15 Nose Landing Gear Shimmy: Taxi Test and Correlative Analyses," SAE Paper 801239, 1980.

¹⁰Pazmany, L., *Landing Gear Design for Light Aircraft*, Vol. 1, Pazmany Aircraft Corp., San Diego, CA, 1986.

10

DETAIL DESIGN

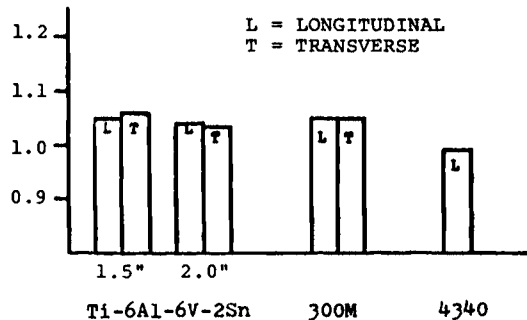
This chapter discusses some of the aspects involved in the detail design of the landing gear. More than other areas, these aspects are apt to become outdated with time. For instance, new materials are always becoming available, better plain bearing materials may be developed, and proximity switches are gaining wider acceptance.

10.1 MATERIALS

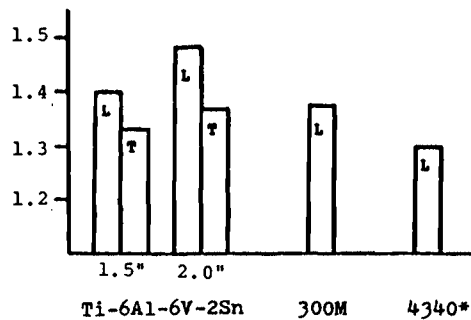
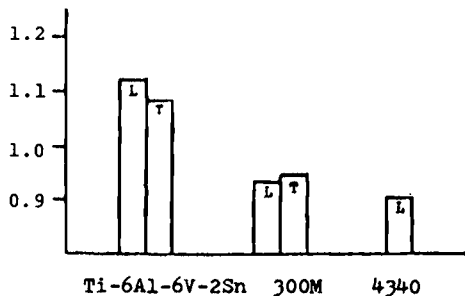
The following are useful guidelines in material selection:

- 1) Where steel forgings are specified, use only vacuum arc remelt parts.
- 2) The preferred method of cold-strengthening steel parts, hardened to tensile strengths of 200,000 psi and above, is to temper the parts while in a straightening fixture.
- 3) Magnetic particle inspection should be performed on all finished steel parts treated in excess of 200,000 psi tensile strength.
- 4) Bushings should be limited to nonferrous materials for the principle static and dynamic joints.
- 5) All joints should be bushed to facilitate rework.
- 6) A considerable number of problems have been experienced where bushings have been made from Teflon and phenolic materials. These should not be used without verification of wear life expectancy and/or rework procedures available for refurbishment of the bearing. Consideration should be given to the need for and the placement of adequate grooves for lubricating the joint.
- 7) All surfaces, except holes under $\frac{3}{4}$ in. diameter, of structural forgings made from alloys susceptible to stress corrosion that, after final machining, exhibit an exposed transverse grain, should be shot-peened or placed in compression by other means.
- 8) Areas of components considered to be critical in fatigue should have a surface roughness in the finished product not exceeding 63 rhr, as defined by ASTM B 46.1* or should be shot-peened with a surface roughness prior to shot-peening of not more than 125 rhr. Unmachined aluminum die forgings should be approximately 250 rhr, except on surfaces where the flash has been removed.
- 9) Efforts should be made to reduce stress corrosion, such as using relief heat treatments (except on aluminum alloys), trying to optimize grain

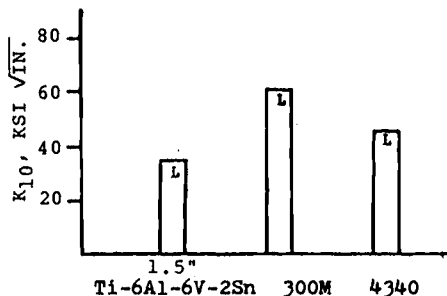
*See Chapter 15 for list of specifications.



a) Typical tensile strength/density ratio.

b) Typical notched/unnotched tensile strength ($K_t = 3, * K_t = 2.9$).

c) Typical compressive strength/density ratio.



d) Typical fracture toughness properties.

Fig. 10.1 Comparison of physical properties of Ti-6Al-6V-2Sn, 300M, and 4340.

flow orientation, using “wet-installed” inserts and pins, and extensive surface cold working.

10) Avoid cross-drilling of joint pins. Drilling operations result in material surface damage and stress risers that are difficult to control.

Steel

The most common landing gear steels are 4130, 4340, 4330V, and 300M. Where stiffness for minimum cost is important (e.g., switch brackets), 4130 is used. For maximum strength/weight ratios 4340 and 300M are used, the former primarily in the 260–280 ksi range and the latter in the 280–300 ksi range. In the last few years, 300M has been used with great success for such items as bogies, pistons, braces, and links. It has about the same fatigue properties as 4340, excellent ductility at very high strength; also, because the material can be interrupted quenched, distortion due to heat treat is greatly reduced. The maximum section size appropriate to heat-treated 300M (280 ksi) is approximately twice the size at which 4340 can attain 260 ksi. Although air-melt material has been widely used, vacuum-melt material should be used in all high-heat-treat applications. Figure 10.1 compares 300M and 4340 with titanium.

Aluminum

Reviewing the commonly used materials, 7079-T6 should not be used in the extruded, forged, or plate form. Until a few years ago, 7075-T6 was widely used because of its higher strength; however, it is very subject to stress corrosion and has been replaced by 7075-T73. This is virtually immune to stress corrosion, but its properties are 12–15% lower than 7075-T6. Then, 7175-T736 was developed—it has the strength of 7075-T6 and the stress-corrosion immunity of 7075-T73. Other materials that are often used are 7049-T73 and 7050-T736. Table 10.1 summarizes the characteristics of these alloys.

Titanium

Alloy Ti-6Al-6V-2Sn can be used effectively where tube buckling or stiffness is significant. Increased wall thickness can be provided using this alloy, without increasing weight, and it does not require corrosion protection. The minimum design ultimate strength in the solution heat treat and age (STA) condition is 170 ksi (150 ksi in the annealed condition). The

Table 10.1 Properties of Several Aluminum Alloys

| Property | 7175-T736 | 7049-T73 | 7050-T736 |
|----------------|-----------|----------|-----------|
| F_{uw} , ksi | 76 | 71 | 72 |
| F_{cy} , ksi | 66 | 61 | 59 |
| Elongation, % | 7 | 7 | 7 |

advantages of this material are a high strength/weight ratio, high un-notched fatigue strength/density, and elongation. However, the cost of the material is relatively high.

Magnesium

Magnesium used to be used for some aircraft wheels, but it is now generally regarded as an unacceptable material for landing gear usage. The causes for this rejection are the fire hazard and its susceptibility to corrosion.

Aluminum Bronze

This is a widely used and extremely satisfactory material for upper and lower shock strut bearings.

Beryllium

Beryllium was discussed in Chapter 7 as a brake heat sink material. It is widely used, however, as a bushing material. It has a higher bearing stress than aluminum bronze, but care must be taken in the design to insure that sharp steel edges do not impinge upon beryllium-copper flange corners. Such an impingement has caused the flanges to crack.

Composites

At the time of this writing, composite materials such as graphite-epoxy and boron-epoxy have not been used to any appreciable extent in production landing gears. However, usage of these materials is spreading rapidly. They offer weight savings (as high as 40% in one case), but their cost is relatively high. Table 10.2 illustrates the weight-saving possibilities. References 1-5 are typical publications on this subject.

From work that has been done in this area, the following are some of the conclusions reached:

- 1) It is possible to make aircraft wheels from composite materials.
- 2) Boron-epoxy was used for the A-37B main landing gear parts, including the outer cylinder, piston, side braces, and torque arms. Weight savings were 2-40% depending upon the component. Tests showed that filament-wound composites were reliable and sustained the required loads. They also showed that further work was required in these areas: fabrication

Table 10.2 Weight Savings Possible with Composite Materials, lb

| | | |
|-------------------------------|--------|--------|
| Total structure | 40,341 | 85,636 |
| Current landing gear | 5,309 | 10,822 |
| Landing gear using composites | 4,460 | 9,090 |

of thick-walled parts, development of suitable liners and coatings for hydraulic cylinders, and analysis and design of attachments and joints.

3) One study showed that a titanium brace cost \$1200 each, based on 200 aircraft, whereas the composite equivalent cost at least \$5000 each.

4) In most cases, the composite part requires more volume than the equivalent metallic part; in such cases, the replacement of a given metallic part may be difficult due to interference problems. For example, a shock strut cylinder made from composites would have a greater outside diameter than a metallic version. This could result in inadequate clearance with adjacent wheels. Therefore, it must be concluded that form, fit, and function constraints may impact the satisfactory replacement of metallic parts with composite parts and that, if composite materials are contemplated for a particular gear, that gear should be designed to accommodate them from the beginning. The resulting design will be lighter, but it will probably be more expensive and will require more stowage volume.

10.2 LUGS AND PINS

Careful design of lugs is essential in order to avoid stress concentrations that lead to fatigue failure. Figure 10.2 depicts a typical well-designed pin joint. In establishing preliminary sizes, make the primary lug thickness no more than half the pin diameter. Using this, the pin diameter D is given by

$$D = \sqrt{2P/F_{br}}$$

This rule-of-thumb method results in a pin that is inherently stiff in bending and is tubular (giving minimum weight). The values for F_{br} shown in Table 10.3 may be used.

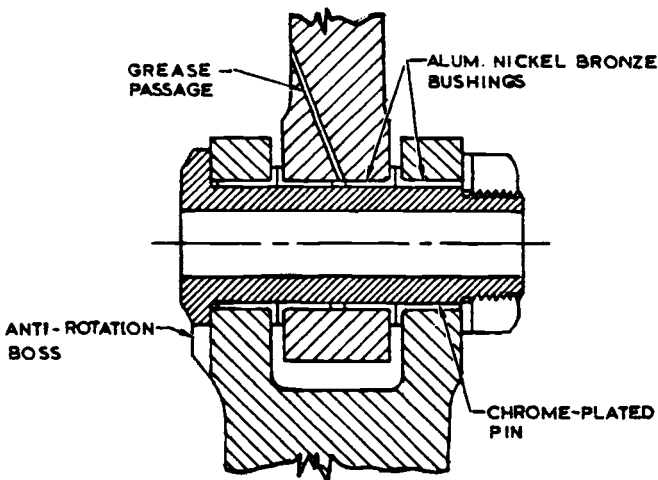


Fig. 10.2 Pin joint.

Table 10.3 Values of F_{br}

| Bushing material | Maximum static capacity, ksi |
|----------------------------------|------------------------------|
| 4130 steel (180 ksi) | |
| ultimate tensile strength | 115 |
| 17-4 steel (AMS 5643) | 90 |
| Beryllium copper (MIL-QQ-C-530) | 90 |
| Al-Ni-bronze (AMS 4640 and 4880) | 60 |
| Aluminum bronze (MIL-QQ-C-465) | 60 |

In designing landing gear joints, the following guidelines should be used:

1) Fit the bushings in all joints to prevent contact of mating structural parts and to greatly simplify correction of deficiencies at the joint.

2) Use bushing material different from the pin or structure material to prevent galling. One good combination is an aluminum-bronze bushing and a chrome-plated steel pin.

3) Surveys indicate that aluminum-nickel bronze and stainless steel (17-4PH) are proving to be very successful bushings in airline usage.

4) Bushings should be installed by shrinkage rather than a press fit, since the latter may remove some of the corrosion protection.

5) All joints should be lubricated, using either grease or self-lubricated bushings. This improves pin removal and fights corrosion.

6) Ensure that corrosion-causing cavities are eliminated. For instance, do not install shouldered bushings in each side of a hole unless a lubricant is injected into the space between them (as shown in Fig. 10.2).

7) Avoid shims and spacers as much as possible. They get lost and are a potential cause of trouble due to being inadvertently forgotten by the ground crew.

8) Allow sufficient material (0.06 in. on the radius), if possible, around the joint to allow for rework of the pin hole and to accept a larger bushing if necessary.

9) The lug hole and faces must be properly protected against corrosion and wear. Cadmium plate and dry film lubrication are inadequate for this.

10) Chromium plate all pins to a minimum of 0.002 in. thickness. Consider corrosion-resistant pin material.

11) Ensure that the grease passage is located such that a fatigue stress riser is not introduced.

12) Do not lubricate more than one point from one grease fitting.

13) Always use protruding Zerk-type grease fittings. The flush types are hard to find on landing gears covered with dirt.

14) Provide generous fillet radii and ensure that all transitions are smooth. Avoid any sharp corners.

Joint Strength

All applied loads should be factored by the following fitting factors:

$$1.0 \times \text{limit load}$$

$$1.15 \times \text{ultimate load}$$

Lug Strength—Axial Load

The lug ultimate strength in shear and bearing is

$$P_{bru} = K_{br} A_{br} F_{tux}$$

where

K_{br} = factor in Fig. 10.3

A_{br} = lug projected bearing area

F_{tux} = lug transverse ultimate tensile strength

= 280 ksi for 300M (280–300 ksi)

= 200 ksi for 4340 steel (200–220 ksi)

= 260 ksi for 4130 steel (260–280 ksi)

= 180 ksi for 4130 steel (180–200 ksi)

= 64 ksi for 7075-T73 die forging

= 71 ksi for 7049-T73 die forging

= 140 ksi for Ti-6Al-6V-2Sn annealed forging

The lug ultimate tension is

$$P_{tu} = K_t A_T F_{tu}$$

where

K_t = factor given in Fig. 10.4

A_T = minimum net tension area

F_{tu} = ultimate tensile strength (same as F_{tux} listed above)

The lug yield is

$$P_y = C \frac{F_{tyx}}{F_{tux}} \cdot P_{u_{\min}}$$

where

C = factor given in Fig. 10.5

$P_{u_{\min}}$ = the smaller of P_{bru} and P_{tu}

F_{tyx} = lug transverse yield tensile strength

= 230 ksi for 300M (280–300 ksi)

= 163 ksi for 4130 steel (180–200 ksi)

= 55 ksi for 7075-T73

= 61 ksi for 7049-T73

= 130 ksi for Ti-6Al-6V-2Sn

Curve A is a cutoff to be used for all aluminum alloy hand-forged billet when the long transverse grain direction has the general direction C in the sketch. Curve B is a cutoff to be used for the aluminum alloy plate, bar, and hand-forged billet when the short transverse grain direction has the general direction C in the sketch, and for die forgings when the lug contains the parting plane in a direction approximately normal to the direction C.

NOTE: In addition to the limitations provided by curves A and B, in no event shall a K_{br} greater than 2.00 be used for lugs made from 0.5 in. thick or thicker aluminum alloy plate, bar, or hand-forged billet.

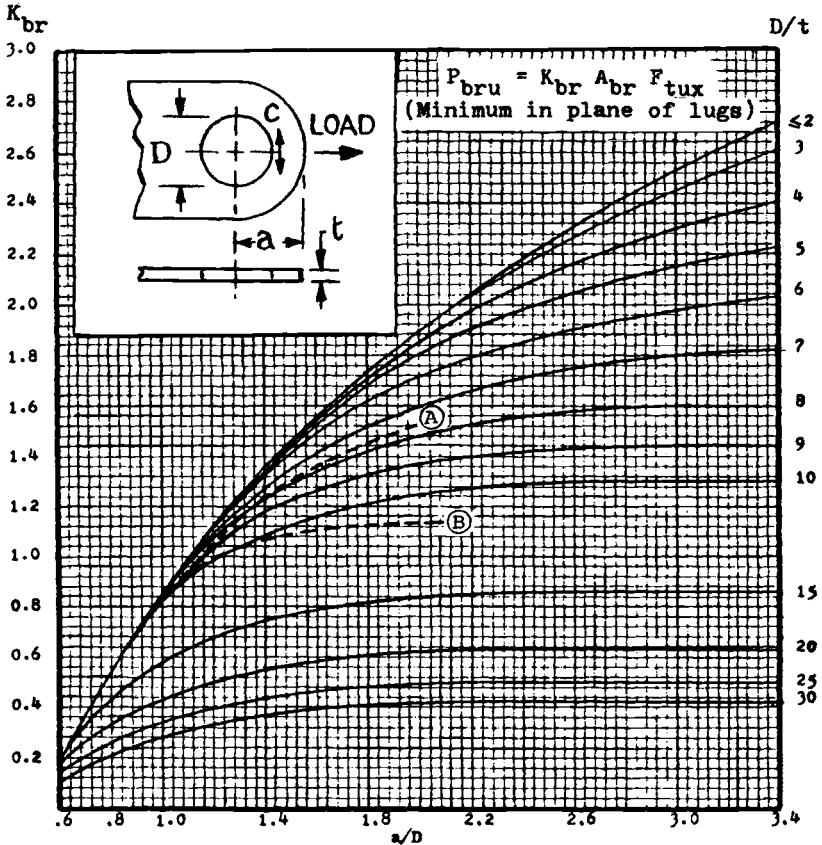
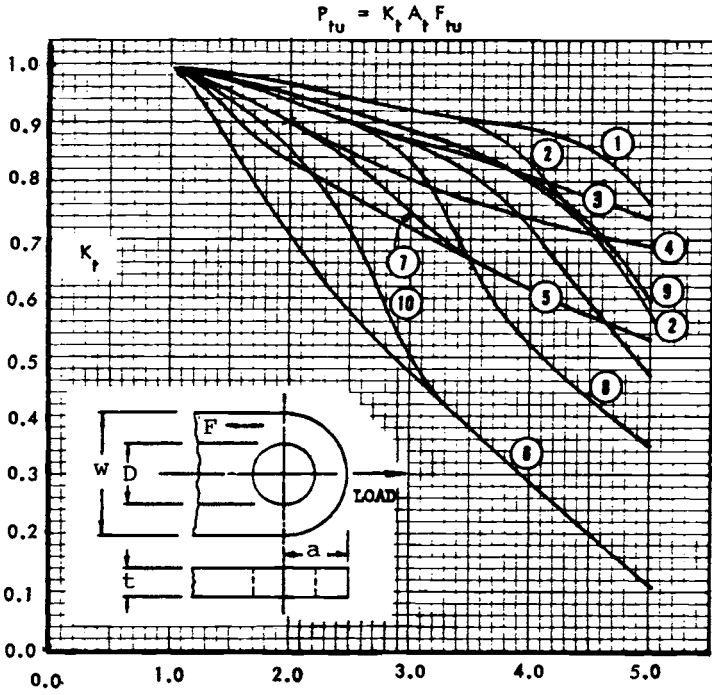


Fig. 10.3 K_{br} values: shear-bearing efficiency factors of lugs made from aluminum alloys and alloy steel with $F_{tu} \leq 160$ ksi.



L, T, and N indicate grain in direction *F* in sketch.
L = longitudinal, *T* = long transverse, *N* = short transverse

- | | |
|---|--|
| <p>1) { 4130 & 8630 steel 2014-T6 & 7075-T6 plate ≤ 0.5 in. (<i>L, T</i>) 7075-T6 bar and extrusion (<i>L</i>) 2014-T6 hand-forged billet ≤ 144 in.² (<i>L</i>) 2014-T6 & 7075-T6 die forging (<i>L</i>)</p> | <p>5) { 195T6, 220T4, & 356T6 aluminum alloy casting 7075-T6 hand-forged billet > 16 in.² (<i>T</i>) 2014-T6 hand-forged billet > 36 in.² (<i>T</i>)</p> |
| <p>2) { 2014-T6 & 7075-T6 plate > 0.5 in., ≤ 1.0 in. 7075-T6 extrusion (<i>T, N</i>) 7075-T6 hand-forged billet ≤ 36 in.² (<i>L</i>) 2014-T6 hand-forged billet ≤ 144 in.² (<i>L</i>) 2014-T6 hand-forged billet ≤ 36 in.² (<i>T</i>) 2014-T6 & 7075-T6 die forgings (<i>T</i>)</p> | <p>6) { Aluminum alloy and plate, bar, hand-forged billet and die forging (<i>N</i>) (Note: for die forging, <i>N</i> direction exists only at the parting plane) 7075-T6 bar (<i>T</i>)</p> |
| <p>3) { 2024-T6 plate (<i>L, T</i>) 2024-T4 & 2024-T42 extrusion (<i>L, T, N</i>)</p> | <p>7) 18-8 stainless steel, annealed</p> |
| <p>4) { 2024-T4 plate (<i>L, T</i>) 2024-T3 plate (<i>L, T</i>) 2014-T6 & 7075-T6 plate > 1.0 in. (<i>L, T</i>) 2024-T4 bar (<i>L, T</i>) 7075-T6 hand-forged billet > 36 in.² (<i>L</i>) 7075-T6 hand-forged billet ≤ 16 in.² (<i>T</i>)</p> | <p>8) { 18-8 stainless steel, full hard (Note: for 1/4, 1/2, and 3/4 hard, interpolate between curves 7 and 8)</p> |
| | <p>9) Steel $F_{tu} = 260$ ksi (<i>L</i>)</p> |
| | <p>10) Steel $F_{tu} = 260$ ksi (<i>T</i>)</p> |

Fig. 10.4 *K_t* values.

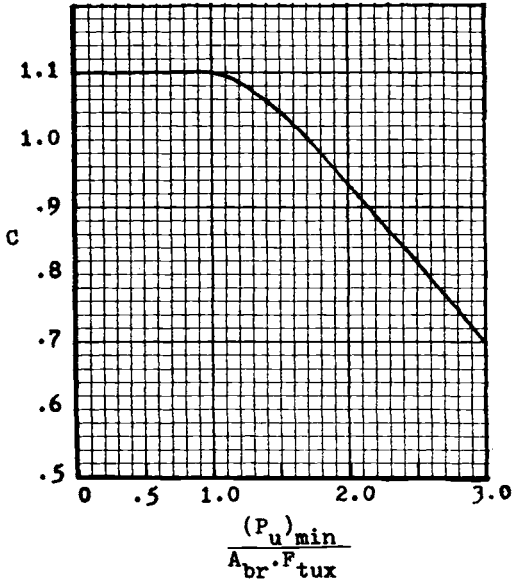


Fig. 10.5 Yield factor for lugs.

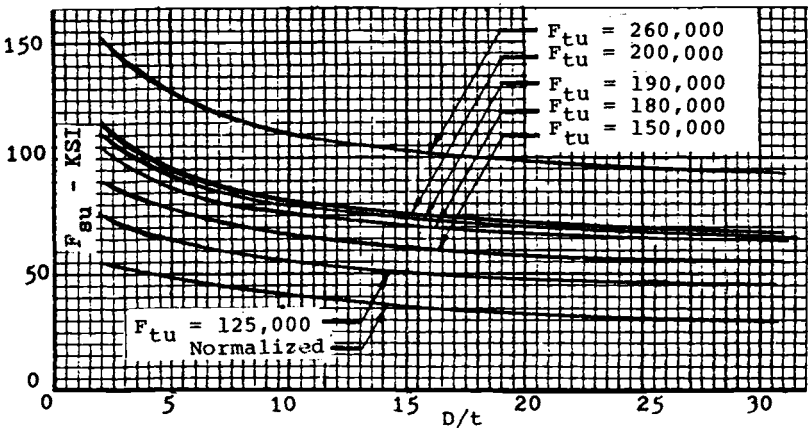


Fig. 10.6 Allowable ultimate transverse shear stress in round steel tubes (no bending).

Pin Strength Shear in Pin, No Bending

Assuming that the pin is tubular,

$$f_s = S/A$$

where f_s is the shear stress in the section, S the shear load, and A the cross-sectional area.

Having determined the stress, Fig. 10.6 is then used to determine the permissible stress.

Ultimate Bending in Pin

Referring to Fig. 10.7, the maximum bending moment = $Pb/2 = m$. Calculate the bending stress in the pin due to m , assuming my/I distribution. Compare this with the bending modulus of rupture stresses for solid ($D/t = 2.0$) round steel bars and pins shown in Table 10.4. If the pin is hollow, use Fig. 10.8 to determine the permissible stress.

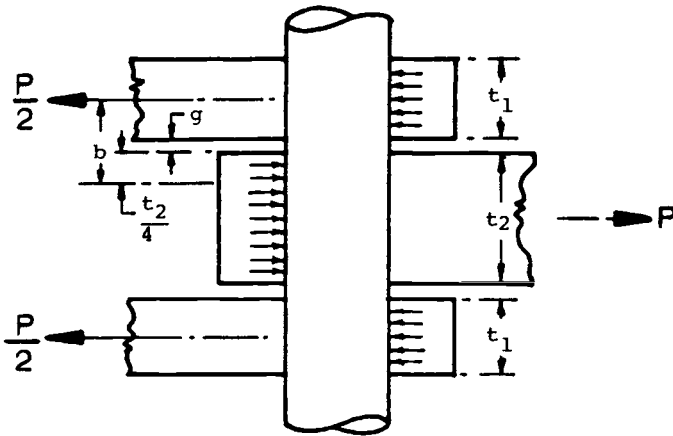


Fig. 10.7 Pin in bending.

Table 10.4 Bending Modulus of Rupture Stresses for Steel Bars and Pins

| Heat treatment, ksi | F_b , ksi | Heat treatment, ksi | F_b , ksi |
|------------------------|----------------|------------------------|----------------|
| 90 | 146 | 180 | 300 |
| 95 | 155 | 200 | 331 |
| 125 | 206 | 260 | 420 |
| 150 | 250 | | |

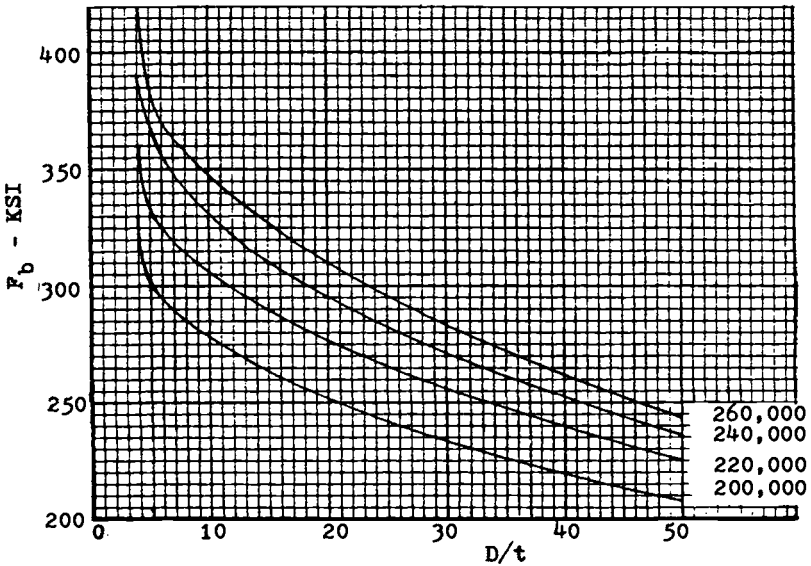


Fig. 10.8 Allowable bending stress in round steel tubes.

This analysis is conservative in that no allowance is made for peaking; the stress engineer may want to make such an allowance in certain circumstances. It recognizes the fact that the load in the lug is not uniform; instead, it peaks toward the outside faces. This reduces the effective moment arm b , an allowable reduction given in most company stress manuals.

Lug Strength—Transverse Load

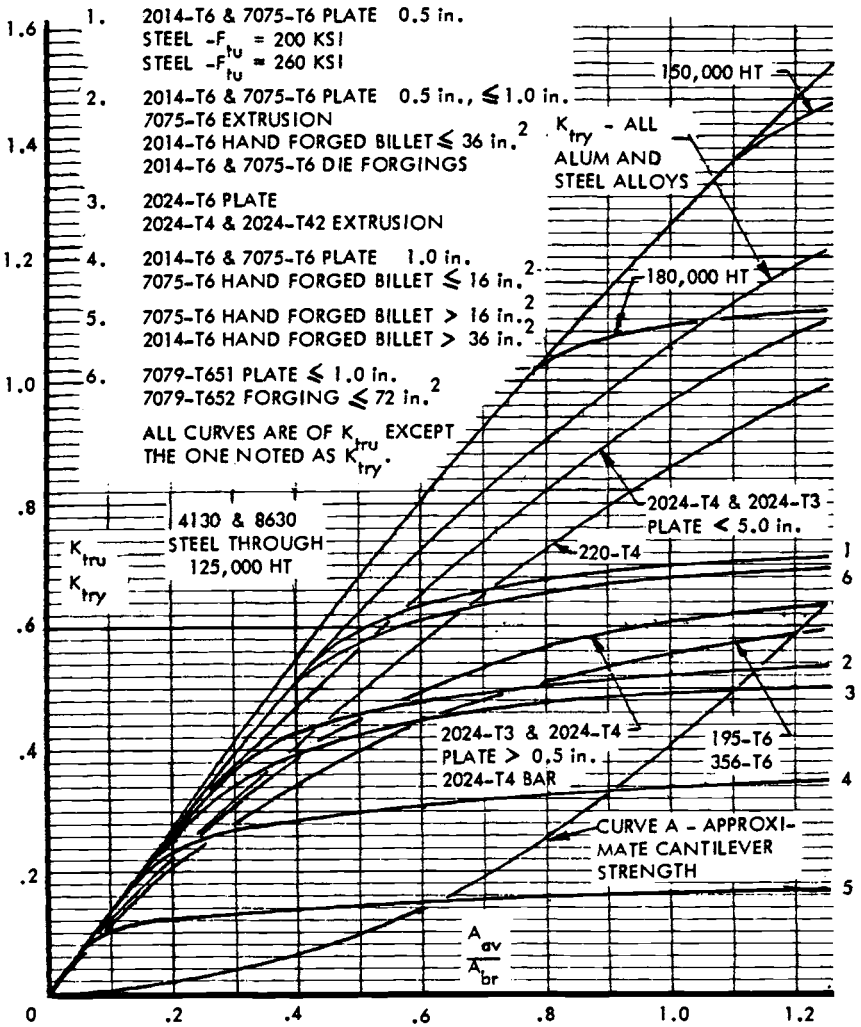
The ultimate strength is

$$P_{tru} = K_{tru} \cdot A_{br} \cdot F_{tux}$$

where K_{tru} is the value given in Fig. 10.9 and F_{tux} the value given previously. Referring to Fig. 10.10,

$$A_{av} = \frac{6}{\frac{3}{A_1} + \frac{1}{A_2} + \frac{1}{A_3} + \frac{1}{A_4}}$$

where A_1 , A_2 , and A_4 are measured as shown in Fig. 10.10 and A_3 is the least area on any radial section around the hole.



NOTE: THESE CURVES DO NOT APPLY TO ALUM. ALLOY LUGS HAVING THE SHORT CROSS GRAIN DIRECTION IN THE PLANE OF THE LUG.

Fig. 10.9 Lug efficiency factors for transverse load.

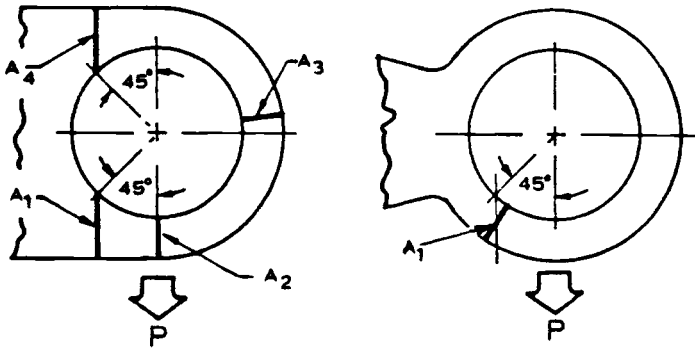
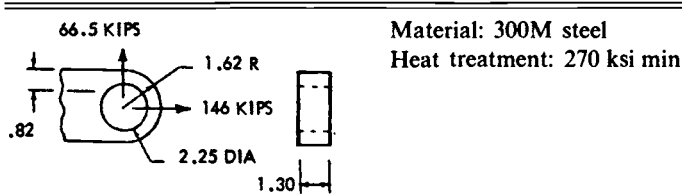


Fig. 10.10 Transverse load on lug.

Table 10.5 Example of Lug Analysis



Axial

$$\begin{aligned}
 A/d &= 1.62/2.25 = 0.82 & K_{br} &= 0.35 \\
 D/t &= 2.25/1.3 = 1.73 & K_t &= 0.92 \\
 W/D &= 3.24/2.25 = 1.44 \\
 A_{br} &= 2.25 \times 1.30 = 2.93 \text{ in.}^2 \\
 A_t &= (3.24 - 2.25)1.3 = 1.29 \text{ in.}^2 \\
 P_{bru} &= 0.35 \times 2.93 \times 270 = 277 \times 10^3 \text{ lbf} \\
 P_{tu} &= 0.92 \times 1.29 \times 270 = 321 \times 10^3 \text{ lbf}
 \end{aligned}$$

Transverse

$$\begin{aligned}
 A_1 &= A_4 = 0.82 \times 1.30 = 1.066 \text{ in.}^2 \\
 A_2 &= A_3 = 0.495 \times 1.30 = 0.644 \text{ in.}^2 \\
 A_{av} &= 6/(4/1.066 + 2/0.65) = 0.878 \text{ in.}^2 \\
 A_{av}/A_{br} &= 0.30 \\
 K_{iru} &= 0.35 \\
 P_{iru} &= 0.35 \times 2.93 \times 270 = 277 \times 10^3 \text{ lbf} \\
 R_a &= 146/277 = 0.527 R_{ir} = 66.5/277 = 0.240 \\
 MS &= \frac{1}{1.15 * [(0.527)^{1.6} + (0.240)^{1.6}]^{0.625}} - 1 = 0.40 MS
 \end{aligned}$$

*Fitting factor.

Lug Strength Oblique Load

Resolve the oblique load into axial and transverse components. In each of these directions, compute P_{bru} , P_{tu} , P_{tru} , and P_y . Calculate the margins of safety as follows:

$$MS = \frac{1}{(Ra^{1.6} + R_{tr}^{1.6})^{0.625}} - 1$$

where

$$Ra = \frac{\text{axial component of applied ultimate load}}{\text{smaller of } P_{bru} \text{ and } P_{tu}}$$

$$R_{tr} = \frac{\text{transverse component of applied ultimate load}}{P_{tru}}$$

An example of a typical calculation is given in Table 10.5.

10.3 BUSHINGS

To illustrate the importance of material and finish selection, consider a typical field problem: the original design utilized 4140 steel bushings and cadmium-plated pins with subsequent application of dry film lubrication. These were difficult to overhaul. The first corrective step was to change the pin finish—they were chrome plated. This was still not good enough, even with lubrication. The fretting and corrosion “froze” the parts together. The problem was finally solved by changing the bushings to aluminum-nickel bronze. There has been no more freezing or corrosion and the parts are functioning properly.

Although some of the following is a repetition of what was said earlier in this chapter, the following guidelines are applicable to bushing design:

- 1) Hard chrome plate all pins or use corrosion-resistant material.
- 2) Do not install shouldered bushings from each side of a hole unless grease is injected into the cavity where the two bushings meet.
- 3) Do not use non-corrosion-resistant steel bushings.
- 4) If beryllium-copper bushings are used, open the inside diameter slightly near the outer edge. This prevents the pin bending deflection from applying a load to the bushing flange. Such loads have caused the flanges to break off.
- 5) If possible, allow the bolts to rotate somewhat inside the bushing. This helps prevent corrosion.

The static capacity for various bushing materials was given in Sec. 10.2. Concerning load-life values, steel bushings are satisfactory for a limited number of cycles, but aluminum-nickel bronze or aluminum bronze bushings are far better if appreciable motion is present. USAF document AFSC DH2-1, DN 6B4 gives more details on this.

TFE-lined bushings should not be loaded to more than 60,000 psi. Bushings of this type are MS 21240 and MS 21241. If they are loaded dynamically, the load should not be more than 25,000 psi.

As noted earlier, bushings should be installed by shrinking, since this does not remove any of the corrosion protection. This type of fit is accomplished by cooling or heating parts so that the resulting contraction or expansion permits assembly without metal-to-metal interference. A dry ice and methanol bath is capable of chilling parts to -120°F , but liquid nitrogen is the preferred coolant and can provide -320°F .

10.4 LUBRICATION

All joints, static and dynamic, should be lubricated. This helps prevent corrosion and helps in joint disassembly during overhaul. Do not mix external (Zerk-type) lube fittings and flush-type fittings; preferably, use the external type on landing gears. Do not lubricate more than one set of bushings from one lubrication fitting and use grease grooves in the bushing to ensure a satisfactory distribution of the grease.

There seems to be no set pattern for lubrication intervals, but 500–700 h intervals are fairly typical, although one airline greases critical joints at every check, i.e., about every 24 h. During washing of the aircraft, the joints should be protected from cleaning compounds and solvents and wiped clean afterward, after which the gear should be lubricated.

10.5 FINISHES

Machined Finish

The degree of permissible surface roughness on landing gear machined parts is expressed in terms of microinches (millionths of an inch) of waviness from a mean line. In landing gear application, the following may be used as a guide:

1) $125\ \mu\text{in}$.—the normal value specified, which costs 40% more than $250\ \mu\text{in}$. It can be accomplished by boring, turning, fly-cutting, face-milling, and broaching and is the minimum obtainable by standard cutting tools. It is used for most landing gear parts having static bearing surfaces, such as holes in parts that accept bushings. It is also used as the finish for piston outside surfaces prior to chrome plating.

2) $63\ \mu\text{in}$.—costs 100% more than $250\ \mu\text{in}$. It can be obtained by grinding, reaming, and boring. It is used for very close tolerance fits. Examples are the axle outside diameter, the cylinder outside diameter where the steering collar revolves, and cam faces. This finish is also applied to most bushings.

3) $32\ \mu\text{in}$.—costs 2.6 times as much as $250\ \mu\text{in}$. and is obtained by grinding. Typical usages are the inside diameter of the cylinder where the lower bearing is housed and chrome-plated pins.

4) $16\ \mu\text{in}$.—costs four times as much as $250\ \mu\text{in}$. It is used for heavily loaded bearings and shafts. Typical usages are the outside of the piston after chrome plating and the inside cylinder diameter on a self-locking actuator where very close tolerances and good fit are required. It is also used on the inside diameter of some very highly loaded bushings such as that at the bogie beam pivot.

Protective Finish

The following summarizes some of the finishes of concern to the landing gear designer:

1) Non-corrosion-resistant alloy steel. The surface should be cadmium-titanium plated or chrome plated on wearing surfaces that are heat treated to 220 ksi and above. On wearing surfaces heat treated below 220 ksi, the surface should be nickel plated and chrome plated. The organic finish is one coat of MIL-C-8514 wash primer, one coat of MIL-P-23377 epoxy primer, two coats of Society for Testing and Materials (STM) 37-307 polyurethane white, with no paint on the functioning or wearing surfaces.

2) Nonclad 2000 and 7000 series aluminum alloy and all aluminum alloy castings. The surface should be sulfuric acid anodized. The organic finish is the same as that quoted above.

3) Clad aluminum alloy and nonclad aluminum alloys other than the above. The surface should be color conversion treated. The organic finish is the same as above.

4) Titanium and titanium alloys. The surface should be cleaned. No organic finish is required, but if paint is required for appearance, use the same finish as above.

5) Fiberglass (covers, shields, etc.). No surface finish is required. If paint is required for appearance, finish with one coat of STM 37-307 white polyurethane.

10.6 SEALS

The seals referred to here are those of major concern to the landing gear designer—that is, shock strut seals. Their main purpose, of course, is to prevent oil leakage. To do this, they may have to contend with out-of-round deflections (e.g., a shock strut cylinder when side loads are applied during a turn), improper installation (rolling), material deterioration and contamination, as well as degraded performance in cold weather.

To overcome these problems, various design features should be incorporated: machine to close tolerances, choose seals that are satisfactory at the temperature expected (or specified), choose seals that have satisfactory performance in stopping leaks when adjacent parts deflect, ensure that seal installation is not conducive to rolling, and, where appropriate, use a scraper ring to minimize seal contamination.

Seal selection for a particular application should be done in consultation with specialists such as Dowty, Greene, Tweed and Company, and Shamban Aerospace Products. Seal designs and materials are constantly being improved; thus, advantage should be taken of the opportunity to gain from user experience.

It is now becoming fairly common practice to install spare seals in a special cavity at the lower end of the shock strut cylinder. This ensures that a means is always available to replace faulty seals with a minimum of delay. Figure 10.11 shows a typical design that incorporates spare seals.

Figure 10.12 is included to show how a typical modern seal functions—in this case, a Greene, Tweed (G-T) seal. There are several variations of this design, all of which are intended to prevent the seal from rolling.

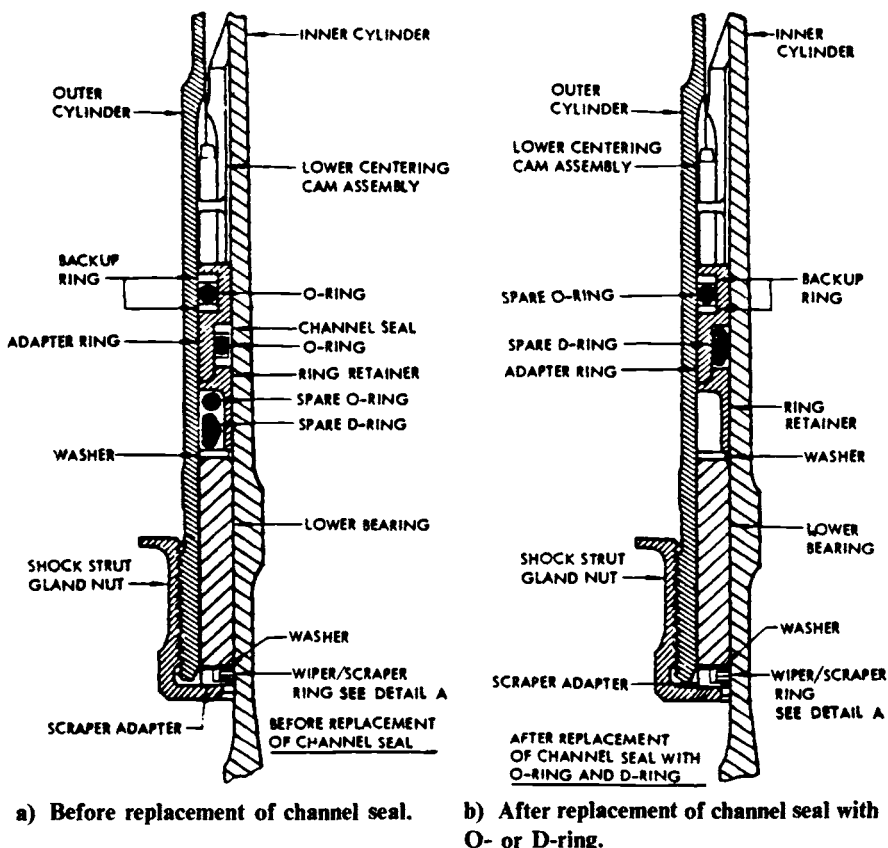


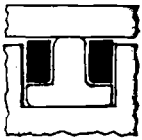
Fig. 10.11 Lower bearing detail.

Scraper rings are used at the lower end of the shock strut cylinder to prevent contaminants from penetrating into the cylinder. Currently, MS 33675 scraper glands are used, accommodating either a MS 28776 bronze scraper or a TFE scraper. Gland details are given in AS 4052. Current scrapers use a split ring that allows contaminants to pass through the gap. It is likely that a nonsplit design will become available to overcome this deficiency.

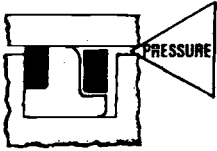
10.7 JACK PADS AND TOW FITTINGS

Jacking loads and requirements are given in MIL-A-8862 and MIL-STD-809(IA), respectively. Provisions must be made to jack up each gear separately for removal of any wheel. Standard jacking pad dimensions, reproduced from AFSC DH2-6 DN 4B2, are shown in Fig. 10.13.

Towing requirements are specified in MIL-STD-805(IA) and MIL-A-8862. The fittings should be arranged so that loads can be applied or reacted in either a forward or aft direction.

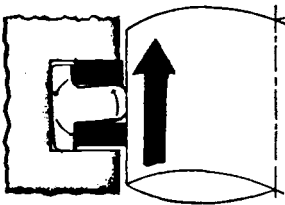
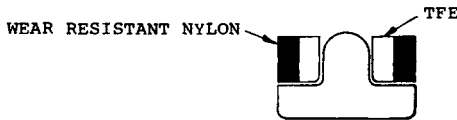
**ZERO PRESSURE**

G-T sealing is installed under radial compression . . . provides a positive seal at zero or low pressure. Backup, nonextrusion rings—normally one on each side—ride free of G-T ring flanges and rod or cylinder wall. These clearances keep seal's friction to minimum at low pressure.

**PRESSURE APPLIED**

Resilient G-T sealing ring reacts as viscous fluid . . . attempts to flow "downstream." Downstream flange is expanded by the extra material added to it and presses nonextrusion ring into positive contact with the surface being sealed—where it prevents extrusion of the softer sealing element. This hydrostatic loading causes a radial expansion of the nonextrusion backup in a piston seal; it creates radial contraction, in a rod seal. Skive cut in nonextrusion ring permits the radial movement.

It is possible, when necessary, to "stage" two or more nonextrusion rings on each side of the seal in order to accommodate even larger clearances, abnormally high pressures, or unusual temperature conditions. The backup rings next to the seal ring are made of a softer material that will not scrape and wear the seal (e.g., TFE); the outer, downstream rings are high-strength material giving the extra stiffness needed to bridge the extrusion gap. Many variations are possible to meet individual situations.



Seal rests, in its groove, on a flat, stable base. Nonextrusion rings "lock" the sealing element in position so it cannot roll around its circumferential axis.

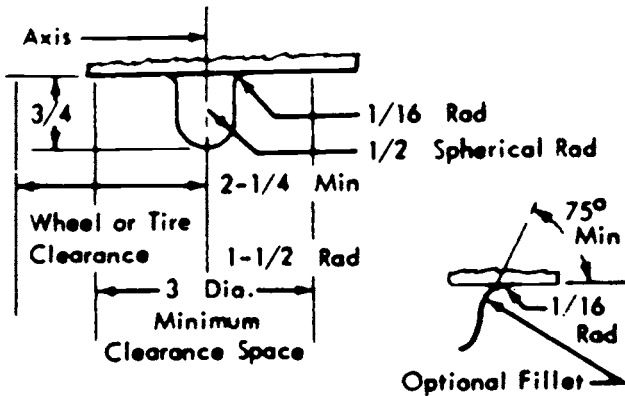
Fig. 10.12 G-T seal operation (source: Greene, Tweed & Co.).

Towing attachments can be either the hollow-axle type or the lug-and-ring type. The appropriate dimensions for both of these attachments are given in AFSC DH2-1 DN 3A4 and reproduced in Table 10.6.

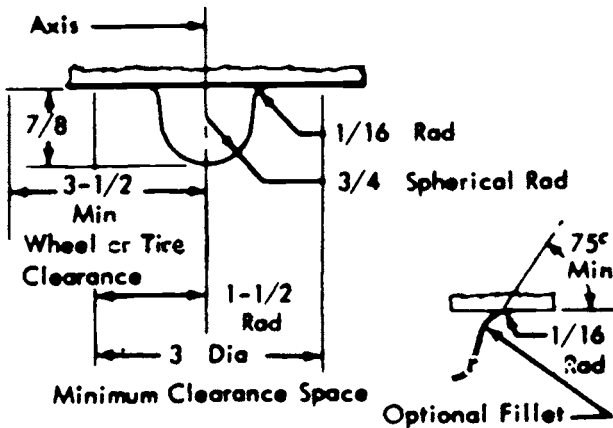
10.8 LOCKS

There are two types of landing gear locks: downlocks and uplocks. These locks can be either internal (inside an actuator) or external and they may be attached to the airframe or to the gear linkage. In the latter case, the linkage itself may provide the lock through appropriate kinematics or overcenter movement. The following guides should be used in designing a lock:

- 1) Keep it simple. A complex lock may be a marvel of ingenuity, but



a) Type III axle jack pads for reactions less than 4536 kg (10,000 lb).



b) Type IV axle jack pads for reactions of 4,536–68,040 kg (10,000–150,000 lb).

Fig. 10.13 Jacking pad dimensions (source: AFSC DH2-6 DN 432).

manufacturing tolerances and errors in assembly/installation/rigging may result in poor reliability.

2) Recognize possible structural/functional deformation and make allowances for it. If the lock grabs the end of the piston, for instance, recognize that internal shock strut friction may cause the full landing gear extension to be less than anticipated and that with a long gear its bending deflection, due to weight, may cause the piston end to droop.

3) If coil springs are used, use compression rather than tension springs.

4) Minimize rigging, because, if it can be misrigged, it will be sooner or later.

Table 10.6 Axle and Lug Towing Attachments

| Axle towing attachments | | |
|-------------------------|--|---|
| Aircraft weight, lb | Axle, inside diameter, in. | Max depth of hollow axle, in. |
| 0-195,000 | $0.75 + 1/64, -0$ | 1 |
| 195,000-495,000 | $1.25 + 1/32, -0$ | 1.5 |
| Towing lug dimensions | | |
| Aircraft weight, lb | Min area of clear opening in lug or ring, in. ² | Min width of clear opening in lug or ring (minor axis of opening) |
| 0-30,000 | 2.00 | Circular hole |
| Over 30,000 | 3.14 | 1.375 in. |

Source: AFSC DH2-1 DN 3A4.

5) Include a straightforward emergency release device in the uplocks to ensure that the lock can be released if the primary release system fails.

6) Avoid having the lock mechanism, other than a primary hook or plunger, subjected to ground loads.

7) Make a careful check of clearances and tolerance buildups to ensure that no more than two faces abut against each other simultaneously.

Always remember that, of all the landing gear parts, it is most important that the locks work properly. For instance, if the uplock jams and prevents the gear from lowering, the aircraft may be destroyed. It is also important that the indication system works properly—telling the pilot that the gear is, indeed, in a safely downlocked condition.

Downlocks

Downlock designs may be categorized as follows:

1) Internal lock in a telescopic brace or actuator, as on the JetStar, Britannia, Concorde, and V-22.

2) Spring-loaded plunger engaging detent in the top of the shock strut, as on the Harrier and A-5.

3) Spring-loaded catch engaging a fixed-gear structure, as on the B.Ae. 748.

4) Articulating radius rods or braces, having a lock at the elbow as on the DC-8, C-141, and C-5.

Figure 10.14 shows the V-22 internal-locking actuator/drag strut (type 1 above) and Fig. 10.15 illustrates a variant of the type 2 latch as it applies to the A-5. In the latter, the mechanism is incorporated in the main gear vertical fitting. It consists of a spring-loaded pin that locks the gear in the

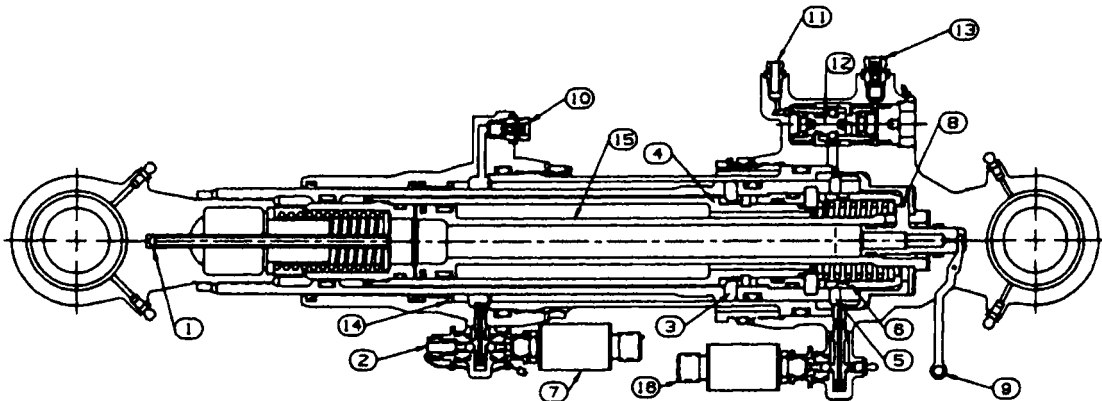


Fig. 10.14 Drag strut actuator (designed and manufactured by Dowty Decoto Inc.) with internal lock on the V-22 main landing gear (source: Ref. 6, reprinted with permission).

- | | |
|--|--|
| <ul style="list-style-type: none"> 1) Ground lock provision 2) Safe downlock visual indication warning for ground crew 3) Downlock segments to provide downlock function ultimate loads extended and locked (120,000 lb compression, 86,000 lb tension) 4) Downlock lock piston 5) Uplock segments to provide uplock function 6) Uplock lock piston 7) Safe downlock electrical indication 8) Uplock unlock piston 9) Manual uplock release-cockpit activated to provide landing gear free fall extension | <ul style="list-style-type: none"> 10) Normal hydraulic retract port (5000 psi) fitting incorporates integral flow control device 11) Emergency nitrogen extend port 12) Shuttle valve 13) Normal hydraulic extend port (5000 psi) fitting incorporates integral flow control device 14) End of stroke snubbing to control landing gear bottoming loads 15) Stand pipe to minimize fluid swept volume 16) Safe uplock electrical indication |
|--|--|

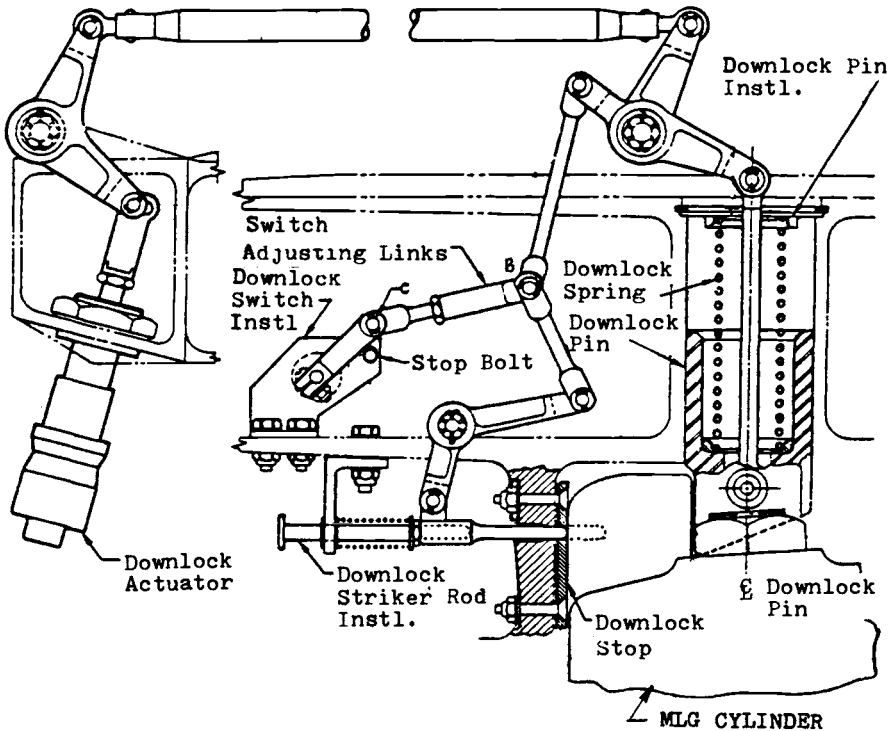


Fig. 10.15 Downlock on A-5 main gear (source: Rockwell International).

down position, a hydraulic actuator that retracts the pin, and a sequencing switch with associated mechanisms. During retraction, the actuator contracts, thus retracting the spring-loaded downlock pin. This movement deactuates the downlock switch. When the downlock pin has been retracted far enough for the strut end to pass, the gear actuator starts to retract the gear.

The type 3 latch is permanently attached to fixed airframe structure. The latch and its support are compact and rugged and its location is known precisely. Its internal deflections are minimal and it can be well protected against environmental hazards. Its correct functioning does not depend on the overcenter latching of long flexible rods on the braces. An illustration of this type lock is shown in Fig. 10.16.

The lock shown in Fig. 10.16 automatically and mechanically locks the gear in the down position and is released hydraulically by an actuator. While the landing gear is being extended, a pin attached to the gear approaches this fixed lock. The pin enters the side plate jaws, contacts the hook, and is subsequently captured by the hook. The sear is loaded by a spring inside the downlock actuator, which causes that unit to be held in the extended position. To unlock the lock, hydraulic pressure is applied to the actuator. This pivots the sear from the hook, after which the hook can

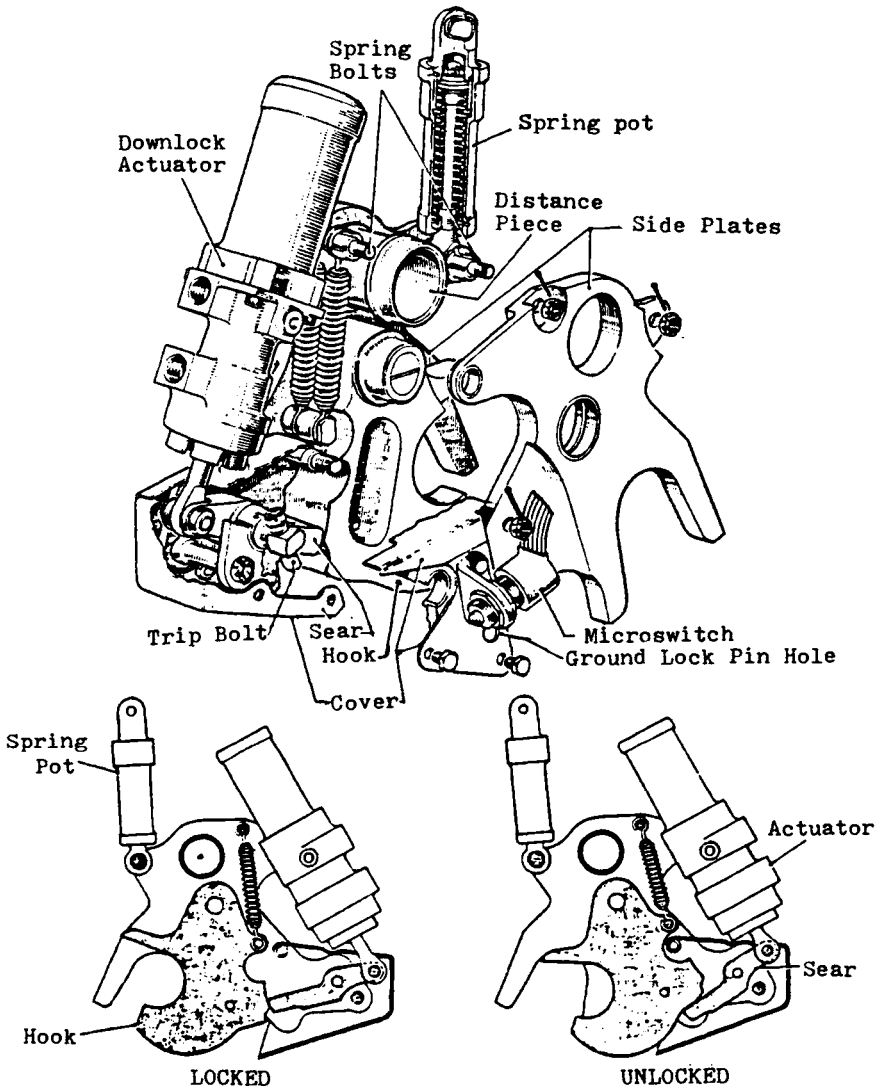


Fig. 10.16 Downlock on B.Ae. 748 main gear (source: British Aerospace Corp.).

be deflected into the open position by the retraction forces on the landing gear pin.

There are many variations of the type 4 lock. The DC-8 main gear uses a conventional locking support at the side brace knee, as depicted in Fig. 10.17. To retract the gear, the downlock bungee cylinders push the actuator levers of the downlock links, breaking the links overcenter. As the bungee cylinders extend, they fold these links to "break" the side braces at the knee.

Similarly, during extension, the side braces rotate around the torque tube and unfold. The bungee cylinders and springs pull on the downlock levers, unfolding the links; when the fully down position is reached, the downlock links are actuated overcenter to lock the gear down.

Figures 10.18 and 10.19 show two other methods of achieving a lock at

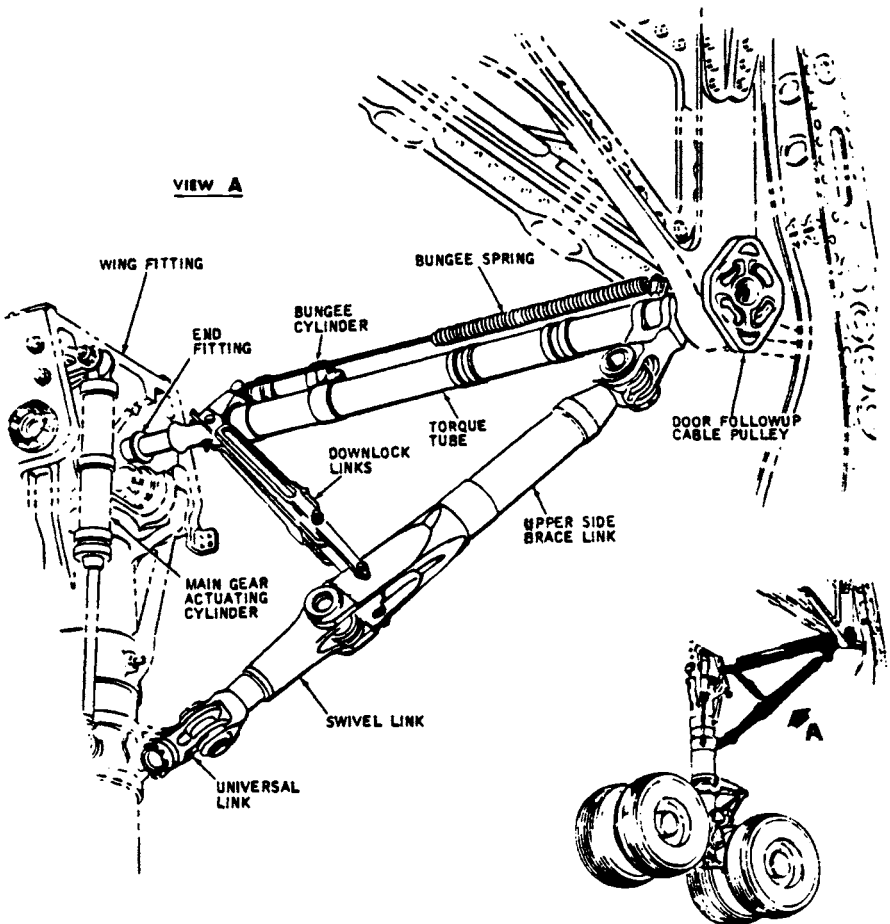


Fig. 10.17 Downlock on DC-8 main gear (source: Douglas Aerospace Corp.).

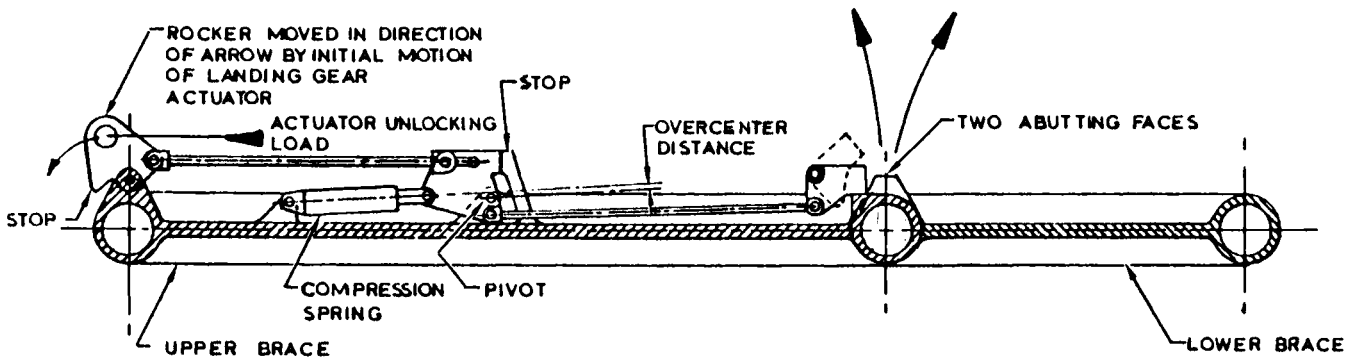


Fig. 10.18 Downlock in knee joint with overcenter link.

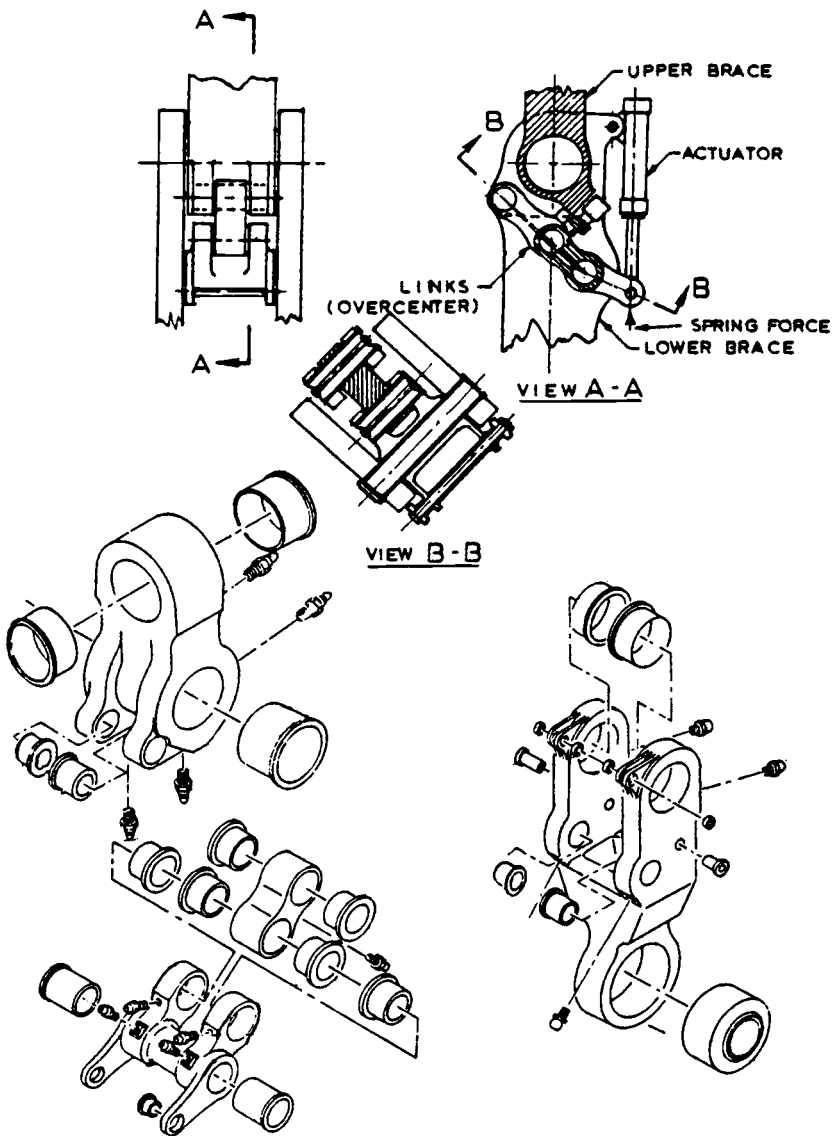


Fig. 10.19 Overcenter toggle link lock.

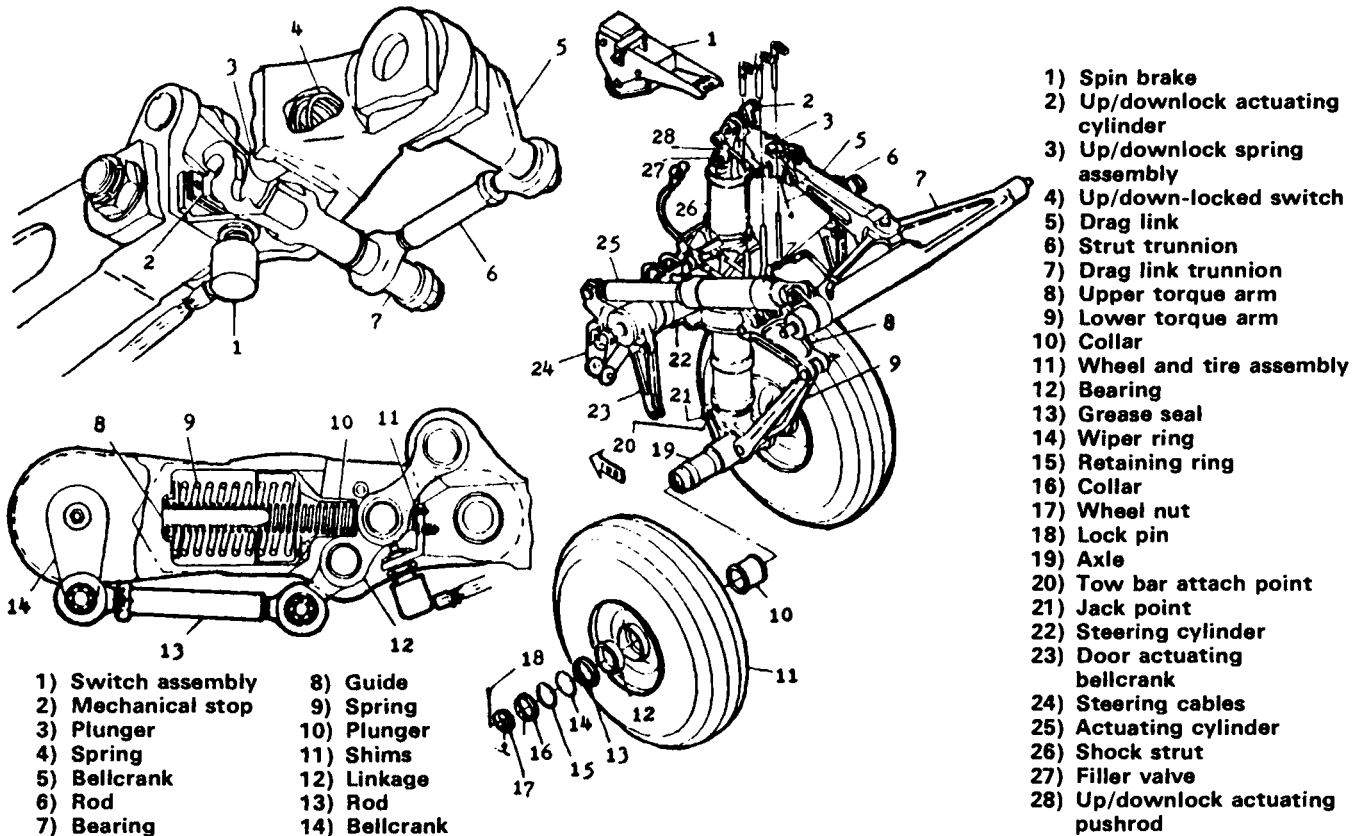


Fig. 10.20 Uplock-downlock on C-141 (source: Lockheed-Georgia Co.).

a brace knee joint. Both are based on overcenter actions of the link/spring combination. Figure 10.20 depicts the combined uplock/downlock used on the C-141 nose gear.

Uplocks

An emergency release system must always be provided in an uplock. Some experts think that hook latches should not be used for uplocks because they are noisy, making passengers uneasy. On the other hand, they are probably the simplest type and can easily be designed to be foolproof. The simplest design, with a guide added for increased reliability, is shown in Fig. 10.21. The hook could have been merely pivoted from the structure, but this would have required more careful rigging and more precise knowledge of gear deflections than the design shown. The hook is spring-loaded to the closed position and, as the gear-mounted pin or roller

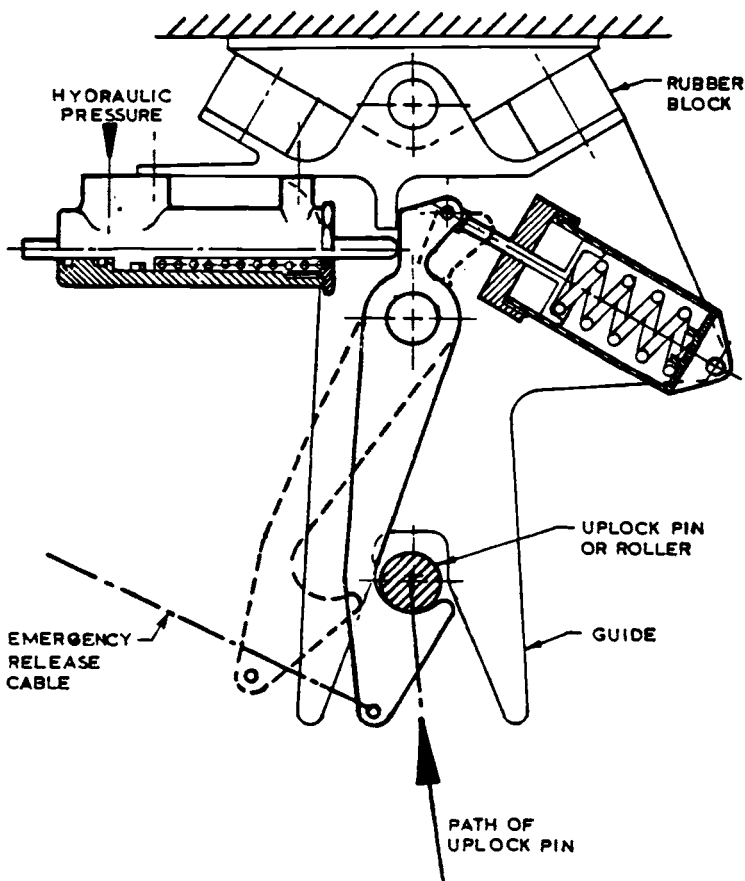


Fig. 10.21 First-order uplock.

approaches the hook, it contacts the ramped face of the hook, pushing the hook over until the pin or roller can ride over the edge of the hook and be captured by it. A hydraulic actuator is used to release the hook and an emergency release cable is provided. The entire hook/actuator/spring assembly is attached to a guide that is suspended from the airframe structure. The guide is centralized by rubber blocks or springs and its two jaws generally line up the hook so that it can pick up the pin or roller without any fine rigging adjustments.

One of the faults of this (first-order) hook is that considerable force is required to push it from under the roller; a way to overcome this is to use a second-order lock such as that depicted in Fig. 10.22. The hook is held both open and closed by secondary latches and, if the guide plates are used, it needs little or no rigging.

Figure 10.23 illustrates a lock in which the hook portions rotate about two centers (effectively a hook on each center). The hooks rotate to capture the uplock pin between them. As the uplock pin D contacts the ramped

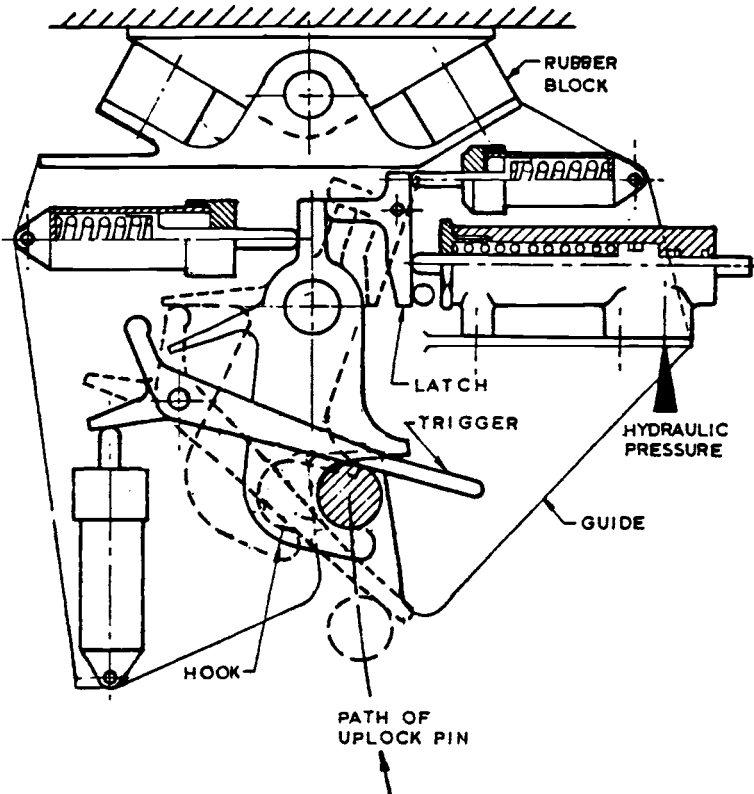


Fig. 10.22 Second-order uplock.

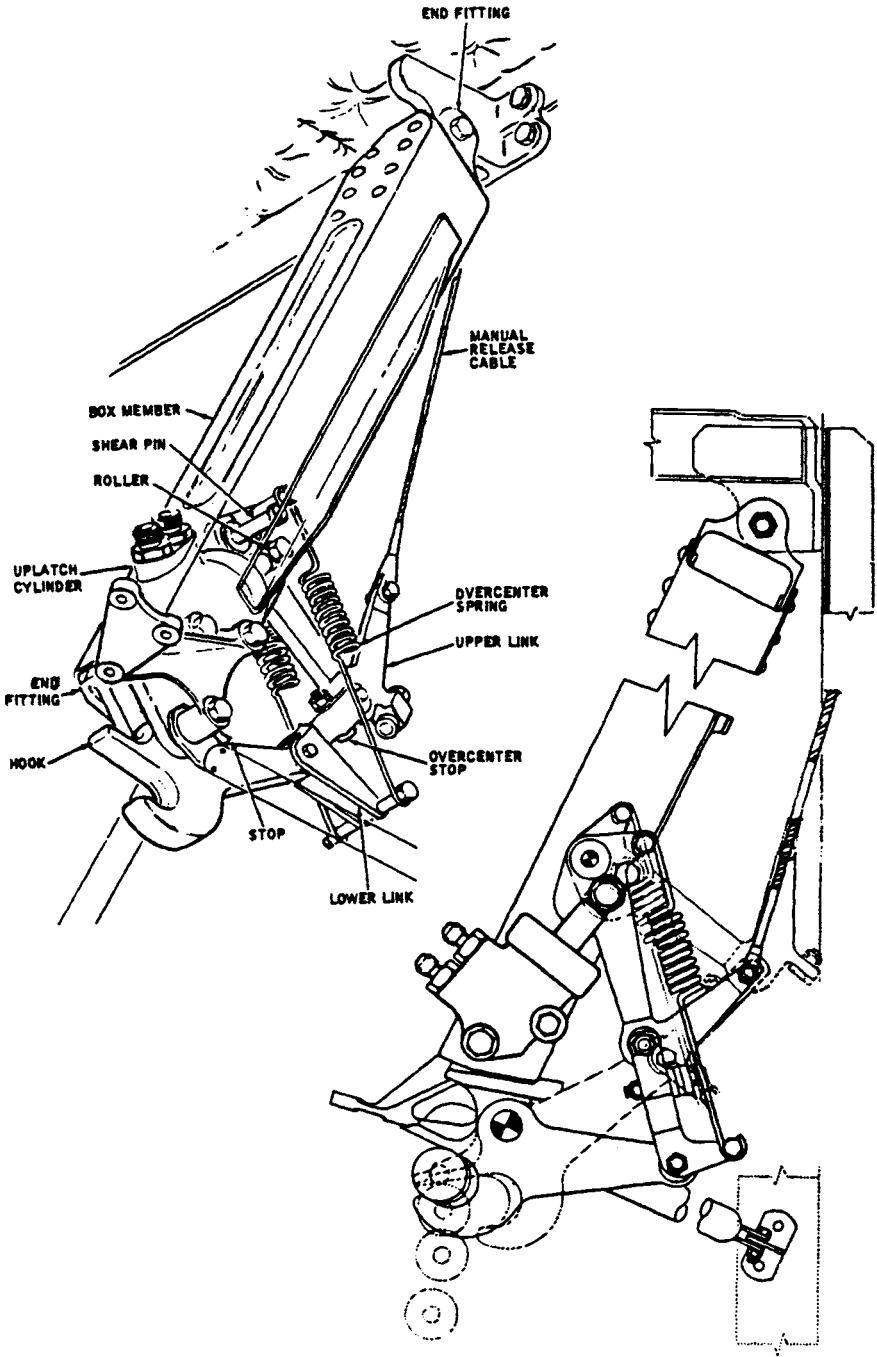


Fig. 10.24 Uplock on DC-8 nose gear.

References

¹Price, A. L., "Filament Composite Wheel Development for Military Aircraft," U.S. Air Force Flight Dynamics Laboratory, Rept. AFFDL-TR-71-144, Oct. 1971.

²"Filament Composite Material Landing Gear Program, Volume," AFFDL-TR-77-20, Vol. 1, Aug. 1972.

³Jensen, L. C. and Pritt, H. L., "Final Report Graphite Composite Landing Gear Components," AFFDL-TR-77-20, Vols. 1 and 2, June 1977.

⁴Bieker, M. J. and Fricker, W. W., "Graphite Composite Landing Gear Components—Upper Drag Brace Hardware for F-14 Aircraft," AFFDL-TR-77-88, Sept. 1977.

⁵Wilson, V. E., "New Concepts in Composite Material Landing Gear for Military Aircraft," AFFDL-TR-78-2, Vols. I and II, Feb. 1978.

⁶Darlington, D. R. F., "Landing Gear—A Complete Systems Approach," *Vertiflite*, (published by the American Helicopter Society), March/April 1987, p. 32.

11 WEIGHT

Landing gear weight prediction is primarily affected by: design landing weight, hardness of landing surface, landing speed, brake requirements, sink speed, and load-deflection characteristics.

It is apparent that an aircraft's first-flight date, or state-of-the-art (SOTA) date, has an impact upon the prediction—no doubt because of the gradual development of materials having higher strength-to-weight ratios. It is noteworthy that, despite the continuing increases in landing speeds and aircraft size, the designer has managed to generally reduce the landing gear weight percentage.

All weight prediction methods are based initially upon statistical data in which actual landing gear weights are reviewed and attempts made to generate equations that fit the data. Consequently, Table 11.1 is presented to allow the reader to observe raw data and, if necessary, to draw conclusions from it.

11.1 WEIGHT ESTIMATION: METHOD 1

Examination of the data reveals that landing gears can be categorized by cantilevered shock strut length, rough field capability, and flotation capability. As other features, such as kneeling, are added to the gear, appropriate allowances must be made. These factors are summarized as follows:

$$\begin{aligned} \text{Strut length } K_{SL} &= 0.85 \text{ (short gears)} \\ &1.00 \text{ (average gears)} \\ &1.32 \text{ (long gears)} \end{aligned}$$

$$\text{Rough-field capability } K_{RF} = 0.15$$

$$\text{High-flotation capability } K_{FL} = 0.11$$

Thus, an aircraft having a short gear, rough-field capability, and high-flotation capability would have a total factor K_{LG} as

$$K_{LG} = 0.85 + 0.15 + 0.11 = 1.11$$

By plotting data from the aircraft listed in Table 11.1, Fig. 11.1 is obtained. The weight equation for the mean line is

$$\text{Landing gear weight} = 0.046K_{LG} \cdot W_L$$

where W_L is the aircraft design landing weight.

Table 11.1 Weight data

| Aircraft | Landing gear weight W_{LG} , lb | Design gross weight W_G , lb | Landing weight used W_L , lb | W_{LG} % of W_G | W_{LG} % of W_L | K_{SL} | Other K Factor ^a | K_{LG} |
|----------------|--------------------------------------|-----------------------------------|-----------------------------------|---------------------------|---------------------------|----------|--|----------|
| Boeing 707-321 | 11,216 | 312,000 | 207,000 | 3.6 | 5.4 | 1.00 | | 1.00 |
| Boeing 727-100 | 6,229 | 161,000 | 137,500 | 3.9 | 4.5 | 1.00 | | 1.00 |
| Boeing 747 | 31,702 | 708,000 | 564,000 | 4.5 | 5.6 | 1.00 | | 1.00 |
| C-5A | 38,153 | 728,000 | 635,850 | 5.2 | 6.0 | 0.85 | 0.15RF 0.11FL 0.19POS 0.04PRE | 1.34 |
| C-46 | 3,087 | 45,000 | 45,000 | 6.9 | 6.9 | 1.32 | | 1.32 |
| C-54 | 4,124 | 50,000 | 50,000 | 8.2 | 8.2 | 1.32 | | 1.32 |
| C-119G | 4,207 | 64,000 | 64,000 | 6.6 | 6.6 | 1.32 | | 1.32 |
| C-124A | 11,888 | 175,000 | 160,000 | 6.8 | 7.4 | 1.32 | | 1.32 |
| C-123B | 2,334 | 54,000 | 51,350 | 4.3 | 4.5 | 0.85 | 0.15RF | 1.00 |
| C-130A | 4,390 | 108,000 | 96,000 | 4.1 | 4.6 | 0.85 | 0.15RF | 1.00 |
| C-130E | 5,077 | 155,000 | 130,000 | 3.3 | 3.9 | 0.85 | 0.15RF | 1.00 |
| C-130H | 5,147 | 155,000 | 130,000 | 3.3 | 4.0 | 0.85 | 0.15RF | 1.00 |
| C-133A | 10,635 | 275,000 | 245,000 | 3.9 | 4.4 | 0.85 | 0.15RF | 1.00 |
| C-135A | 10,444 | 270,000 | 200,000 | 3.9 | 5.2 | 1.00 | | 1.00 |
| C-135B | 10,543 | 274,000 | 200,000 | 3.8 | 5.3 | 1.00 | | 1.00 |
| C-141A | 10,820 | 316,000 | 257,500 | 3.4 | 4.2 | 0.85 | | 0.85 |
| CL-44D-4 | 7,356 | 205,000 | 165,000 | 3.6 | 4.4 | 1.00 | | 1.00 |
| CL-84 | 369 | 10,600 | 10,600 | 3.5 | 3.5 | 0.85 | | 0.85 |
| Constellation | 4,771 | 107,000 | 89,500 | 4.5 | 5.3 | 1.32 | | 1.32 |
| CV 240 | 1,644 | 41,790 | 39,800 | 3.9 | 4.1 | 1.00 | | 1.00 |
| CV 440 | 2,325 | 49,100 | 47,650 | 4.7 | 4.9 | 1.00 | | 1.00 |
| DC-3 | 1,392 | 25,200 | 24,400 | 5.5 | 5.7 | 1.32 | | 1.32 |
| DC-7A | 4,298 | 123,500 | 102,500 | 4.0 | 4.8 | 1.00 | | 1.00 |
| DC-8-61 | 11,692 | 320,000 | 240,000 | 3.7 | 4.9 | 1.00 | | 1.00 |
| DC-9-30 | 4,200 | 108,000 | 95,900 | 3.9 | 4.4 | 1.00 | | 1.00 |
| DHC-4 | 1,084 | 24,000 | 24,000 | 4.5 | 4.5 | 1.00 | | 1.00 |
| DHC-5 | 1,828 | 41,000 | 39,100 | 4.5 | 4.7 | 0.85 | 0.85RF | 1.00 |
| F-104C | 819 | 16,945 | 16,000 | 4.8 | 5.1 | 1.00 | | 1.00 |
| F-15A | 1,305 | 41,947 | 35,000 | 3.1 | 3.7 | 1.00 | | 1.00 |
| F-16 | 913 | 28,569 | 19,500 | 3.2 | 4.7 | 1.00 | | 1.00 |
| Gulfstream | 1,237 | 35,100 | 33,600 | 3.5 | 3.7 | 0.85 | | 0.85 |
| JetStar 1 | 1,081 | 40,921 | 30,000 | 2.6 | 3.6 | 0.85 | | 0.85 |
| L-1011 | 19,923 | 411,000 | 395,000 | 4.9 | 5.0 | 1.00 | | 1.00 |
| Martin 202 | 1,784 | 39,900 | 38,000 | 4.5 | 4.7 | 1.00 | | 1.00 |
| Martin 404 | 1,914 | 45,000 | 43,000 | 4.3 | 4.4 | 1.00 | | 1.00 |
| P2V-7 | 3,782 | 67,500 | 59,000 | 6.6 | 6.4 | 1.32 | | 1.32 |
| XV-5A | 482 | 9,200 | 9,200 | 5.2 | 5.2 | 1.00 | 0.19POS | 1.19 |
| XC-142A | 1,266 | 37,474 | 37,474 | 3.4 | 3.4 | 0.85 | | 0.85 |
| XV-4B | 389 | 12,000 | 12,000 | 3.2 | 3.2 | 0.85 | | 0.85 |

^aFL = high flotation, POS = kneeling, PRE = crosswind positioning, RF = rough field.

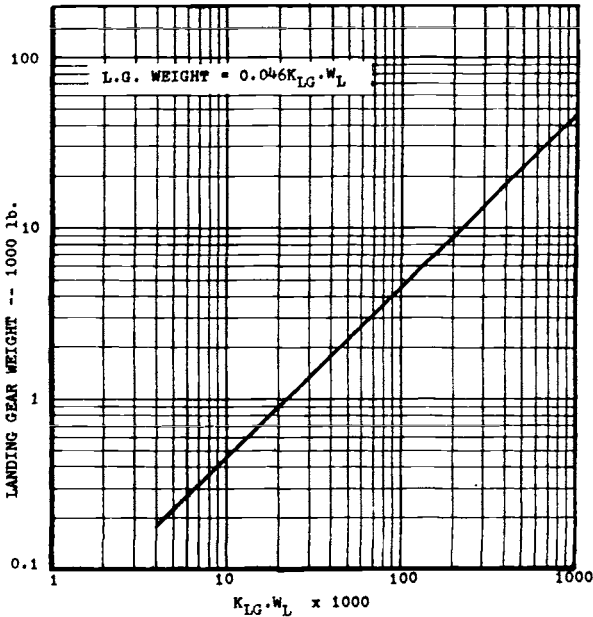


Fig. 11.1 Landing gear weight: method 1.

11.2 WEIGHT ESTIMATION: METHOD 2

This method postulates that landing gear weight is given by

$$W_g = K_G \cdot K_{C_R} (W_L/1000)^n$$

where K_G is the scale factor, K_{C_R} the chronological factor, and n the scale exponent.

To determine the appropriate values for these variables, 12 low-wing transports were examined. They all had similar SOTA years and all were designed for hard surface runways. This examination showed that $n = 1.17$ and $K_G = 20.45$ within 5%.

Summarizing,

$$n = 1.17$$

$$K_G = 20.45$$

Thus,

$$W_G = 20.45 K_{C_R} \left(\frac{W_L}{1000} \right)^{1.17}$$

The value of K_{C_R} varies with the SOTA year and with the runway hardness used in determining the landing gear flotation requirements.

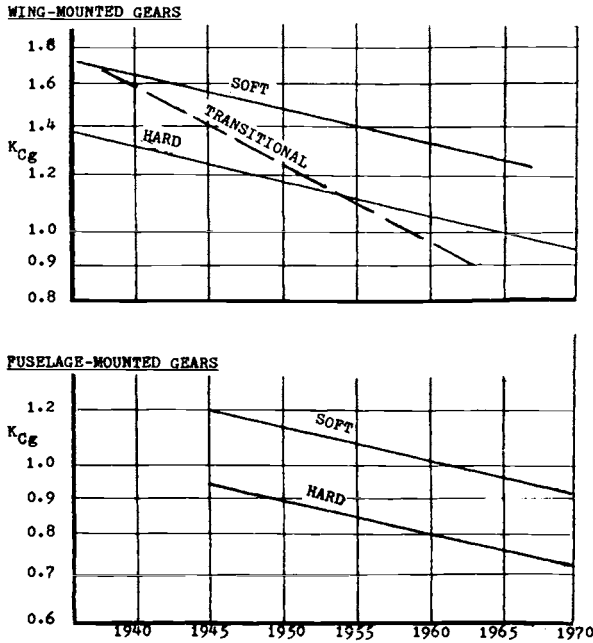


Fig. 11.2 Landing gear weight chronology.

Table 11.2 Values of K_{Cr}

| SOTA Year | Wing mounted | | Fuselage mounted | |
|--------------|--------------|-------|------------------|-------|
| | Soft | Hard | Soft | Hard |
| 1940 | 1.65 | 1.310 | 1.260 | 1.000 |
| 1945 | 1.562 | 1.240 | 1.193 | 0.947 |
| 1950 | 1.479 | 1.174 | 1.129 | 0.896 |
| 1955 | 1.400 | 1.112 | 1.069 | 0.849 |
| 1960 | 1.326 | 1.052 | 1.012 | 0.803 |
| 1965 | 1.255 | 0.997 | 0.959 | 0.761 |
| 1970 | 1.188 | 0.943 | 0.907 | 0.720 |
| 1975 | 1.125 | 0.893 | 0.859 | 0.682 |
| 1980 | 1.065 | 0.846 | 0.813 | 0.646 |
| 1985 | 1.009 | 0.801 | 0.770 | 0.626 |
| 1990 | 0.954 | 0.758 | 0.729 | 0.593 |
| 1995 | 0.904 | 0.718 | 0.690 | 0.562 |

To evaluate these parameters, Fig. 11.2 is used. The term "soft" refers to gears designed for gravel or sod surfaces. "Hard" refers to gears designed for high-strength paved runways. "Transitional" represents gears designed during the period when runways were gradually being replaced by paved runways. From this figure, the following items are noted:

1) Chronological improvement rate is 1.09% per year on wing-mounted gears and 1.25% on fuselage-mounted gears.

2) High-flotation gears are 26% heavier than gears designed for hard surfaces.

3) Fuselage-mounted gears, for a given year, are 24% lighter than wing-mounted gears.

Examination of these data indicates that the K_{Cg} values listed in Table 11.2 should be used.

11.3 METHOD COMPARISON

To compare the results using the two methods, consider a Boeing 707-321 with the following specifications

$$W_L = 207,000 \text{ lb}$$

$$\text{Strut length factor } K_{SL} = 1.00 \text{ (average gear)}$$

$$\text{Rough field } K_{RF} = 0$$

$$\text{High flotation } K_{FL} = 0$$

$$\text{Therefore, } K_{LG} = 1.0$$

$$\text{SOTA year} = 1962$$

$$K_{Cg} = 1.030$$

By method 1,

$$\begin{aligned} W_G &= 0.046 K_{LG} \cdot W_L \\ &= 9522 \text{ lb} \end{aligned}$$

By method 2,

$$\begin{aligned} \text{Actual } W_G &= 20.45 K_{Cg} \left(\frac{W_L}{1000} \right)^{1.17} \\ &= 10,806 \text{ lb} \end{aligned}$$

$$\text{Actual } W_G = 11,216 \text{ lb}$$

Conclusion: method 2 is closer in this particular case and the error is 3.7%.

Table 11.3 Typical Component Breakdown, %

| Breakdown | Business Jets | | Transports | | | |
|-------------|---------------|------------|---------------|----------------|---------------|-----------------|
| | JetStar | Gulfstream | Small B737 | Medium B727 | Large B707 | Jumbo L-1011 |
| Main gear | 80 | 81 | 88 | 85 | 92 | 89 |
| Roll. stock | 44 | 30 | 34 | 34 | 35 | 32 |
| Wheels | 11 | 8 | 7 | 7 | 8 | 6 |
| Tires | 12 | 11 | 11 | 10 | 11 | 10 |
| Brakes | 21 | 11 | 16 | 15 | 16 | 16 |
| Misc. | | | | 2 | | |
| Structure | 26 | 35 | 43 | 42 | 46 | 50 |
| Sh. strut | 24 | 28 | 22 | 21 | 27 | 32 |
| Fittings | 2 | 4 | 15 | 15 | 14 | 12 |
| Braces | | 3 | 5 | 5 | 4 | 5 |
| Misc. | | | 1 | 1 | 1 | 1 |
| Controls | 10 | 16 | 11 | 9 | 11 | 7 |
| Nose gear | 20 | 18 | 12 | 15 | 8 | 11 |
| Roll. stock | 4 | 3 | 2 | 3 | 2 | 2 |
| Wheels | 2 | 1 | 1 | 1 | 1 | 1 |
| Tires | 2 | 2 | 1 | 2 | 1 | 1 |
| Structure | 14 | 10 | 5 | 7 | 3 | 7 |
| Sh. strut | 13 | 8 | 4 | 4 | 2 | 4 |
| Fittings | 1 | 1 | 1 | 2 | Neg | 1 |
| Braces | | 1 | | 1 | 1 | 1 |
| Misc. | | | | | | 1 |
| Controls | 2 | 5 | 5 | 5 | 3 | 2 |

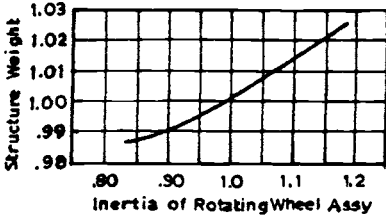
Example: the JetStar main landing gear is 80% of the total landing gear weight. That 80% is made up of 44% rolling stock, 26% structure, and 10% controls. The 44% rolling stock includes 11% wheels, 12% tires, and 21% brakes.

11.4 PRELIMINARY COMPONENT WEIGHT ESTIMATE

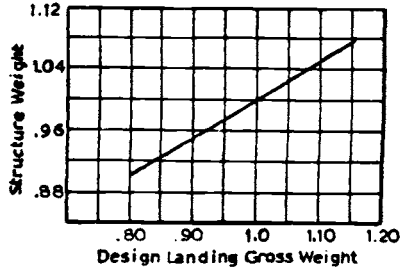
The preceding methods can be used in the preliminary design stage, when the landing gear is not well defined and loading conditions have not been analyzed. As design progresses, it is often desirable and necessary to apply more sophistication to the analysis. The weights of individual components are often estimated at this point and from these preliminary figures some tradeoff analyses can be made. Table 11.3 is presented to enable rough approximations to be made in this regard.

11.5 ANALYTICAL WEIGHT ESTIMATE

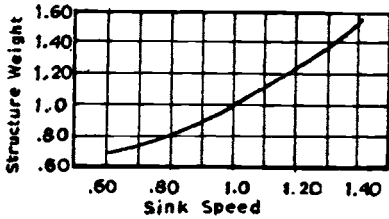
Following the initial preliminary design estimates and while the gear is still in its early design stage, more careful analyses should be made in which the loads and the geometry are recognized. This permits tradeoff analyses in which the following effects on gear weight can be determined: varying shock strut characteristics, varying geometry, varying sink speed, varying



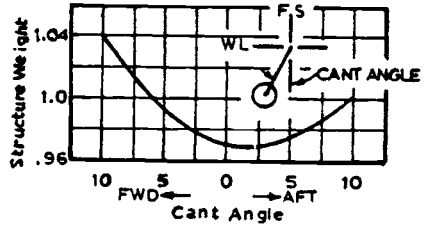
a) Structure weight vs inertia of rotating mass.



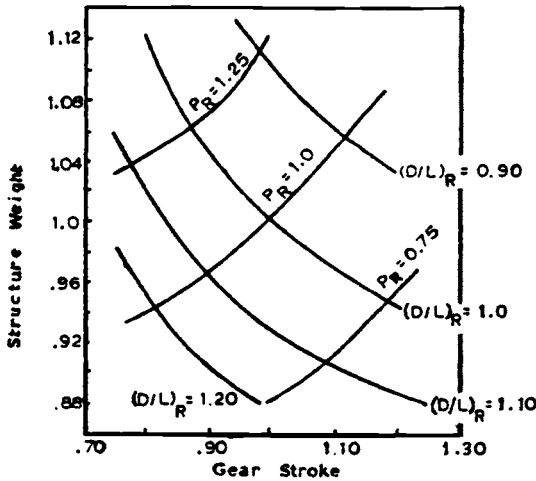
b) Structure weight vs sink speed.



c) Structure weight vs design landing gross weight.



d) Structure weight vs cant angle.



e) Structure weight vs gear stroke: P_R = internal dynamic pressure ratio, $(D/L)_R$ = piston o.d./length ratio.

Fig. 11.3 Typical parametric weight variations.

rolling stock, varying design landing weight, varying cant angle, varying material properties, and varying loading conditions.

A method for conducting this type of study is given in Ref. 1. It uses a computer program and has five basic steps: 1) definition of gear geometry, 2) calculation of applied external loads, 3) resolution of external loads into loads for each structural member, 4) estimation of member cross-sectional areas, and 5) calculation of final real weight of the gear. Figure 11.3 shows typical parametric variations that can be studied by this method.

References

¹Kraus, P. R., "An Analytical Approach to Landing Gear Weight Estimation," Society of Allied Weight Engineers, Chula Vista, CA, Paper 829, May 1970.

Bibliography

Shanley, F. R., *Weight-Strength Analysis of Aircraft Structures*," Dover Publications, New York, 1960.

12 AIRFIELD CONSIDERATIONS

A complete discussion of airfield considerations, as they concern the landing gear designer, would require a volume of its own. Several of the referenced reports, on specific portions of these considerations, are close to 1 in. thick. This chapter must, therefore, be considered a brief summary of the subject, showing only the current methods and generally guiding the reader to various reports for further details.

Although the landing gear designer is not expected to be able to design runways, he is often required to have a working knowledge of their construction and ability to support an aircraft, including the determination of the life of that surface when subjected to aircraft operations. This subject was recognized as far back as the late 1930's, but it steadily increased in importance so that by the 1960's the designer had to contend with specific requirements concerning flotation and airfield roughness.

12.1 BACKGROUND

Two factors influenced the realization that airfield considerations were becoming important: increasing aircraft weight and increased use of unpaved fields (particularly by the military). As depicted in Fig. 12.1, single-wheel loads have increased over the years. Tire pressure have also increased; for instance, the DC-3 main gear tires were inflated to 50 psi, the DC-7 tires were inflated to 127 psi, and the DC-10 tires to 185 psi. Since tire pressure and tire load are two primary factors influencing pavement stresses, it is obvious that surface strength/landing gear characteristics must be evaluated. The DC-3 operated on grass fields, but the DC-10 needs a heavy concrete runway.

From the military standpoint, current doctrine emphasizes the use of unpaved surfaces close to the "front line" and being unpaved it will have considerably more roughness than the more conventional concrete or asphalt runways. If the aircraft cannot tolerate the lower strength surface and higher roughness, it must reduce payload, fuel, or the number of operations on that field—all of which degrade its operational effectiveness.

All of the associated studies, such as gear drag, sinkage, and turning on bare soil, are by-products of the primary study—the ability of a given surface to support the aircraft for a specific number of operations. Analysis methods were devised separately in Canada, Great Britain, and the United States. These methods were considerably improved in the 1960's and

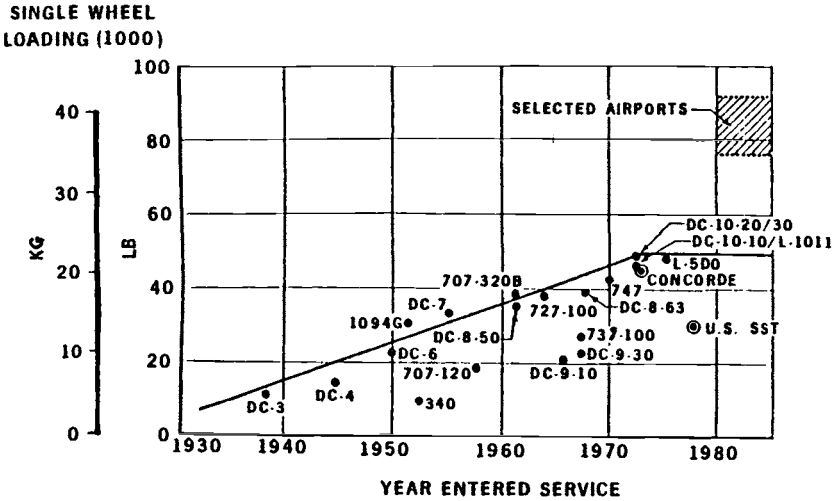


Fig. 12.1 Flotation trend.

1970's, so that by the mid-1980's some international standards were developed.

12.2 DEFINITIONS AND PARAMETERS

Airfield index: a measure of soil strength. It is measured by a cone penetrometer. The force recorded by this instrument while penetrating the surface is an index of the shearing resistance of the soil and is called the airfield index in that plane. Airfield index is defined as the average of a number of penetrometer readings in a given plane.¹ Airfield index (AI) is an alternative to California bearing ratio (CBR). AI can be measured more rapidly and most test data are presented in terms of AI. To quote MIL-L-87139, "AI and CBR correlation varies from soil to soil. This is because CBR is a measure of confined bearing strength of soil, whereas AI is a measure of bearing strength plus soil cohesion." For this reason, Fig. 12.2, which correlates AI and CBR, should be used with caution.

Assembly load: the load on the landing gear assembly used in calculating ground flotation.

Axle base: the distance between the centerlines of the axles (forward and aft) of a main gear bogie.

Contact area: the area of the tire surface in contact with the airfield surface. The area may be calculated by the method given in ASD-TR-68-34.² In some cases it is defined as tire load divided by tire inflation pressure; in other cases, the manufacturer's measured area may be used.

Contact pressure: this is equal to the single-wheel load divided by the contact area and represents the average pressure imposed on the airfield surface.

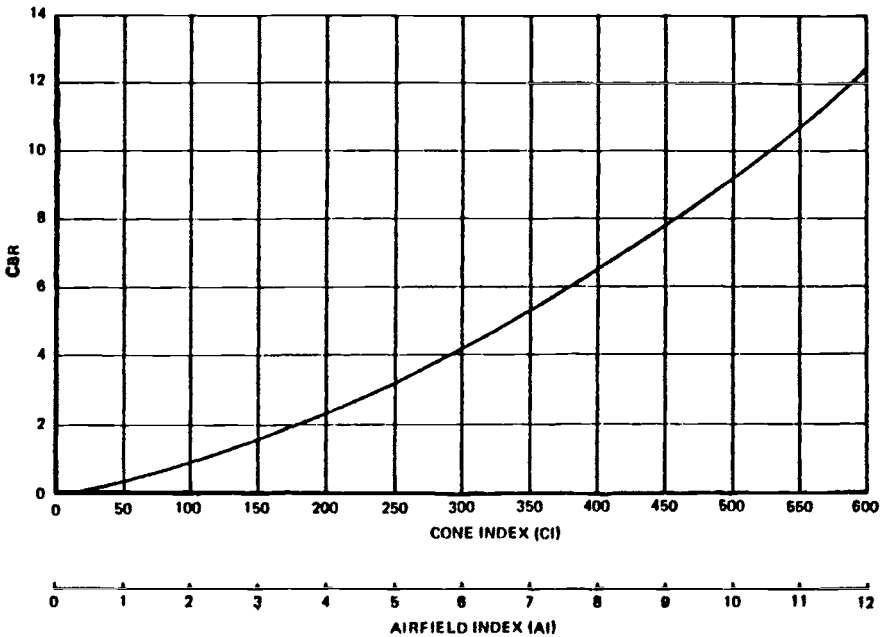


Fig. 12.2 Correlation of CBR, CI, and AI indexes of fine-grained soil.

Coverage (or load repetition factor): sufficient passes of tires in adjacent tire paths to cover a given width of surface one time.

Cone index (CI): an index of soil strength obtained with the cone penetrometer. It is the unit load required to maintain movement of the cone-shaped probe normal to the soil surface. It is measured in pounds per square inch and is directly related to airfield index as shown in Fig. 12.2.

Equivalent single-wheel load (ESWL): the calculated load that, if applied to a single tire, would produce the same effect on the airfield as does a multiple-wheel assembly.

Flotation: a measure of an aircraft's ability to operate on an airfield surface of defined strength. These surfaces may be paved or unpaved. The aircraft characteristics that influence flotation are wheel load, tire contact area, and tire footprint spacing.

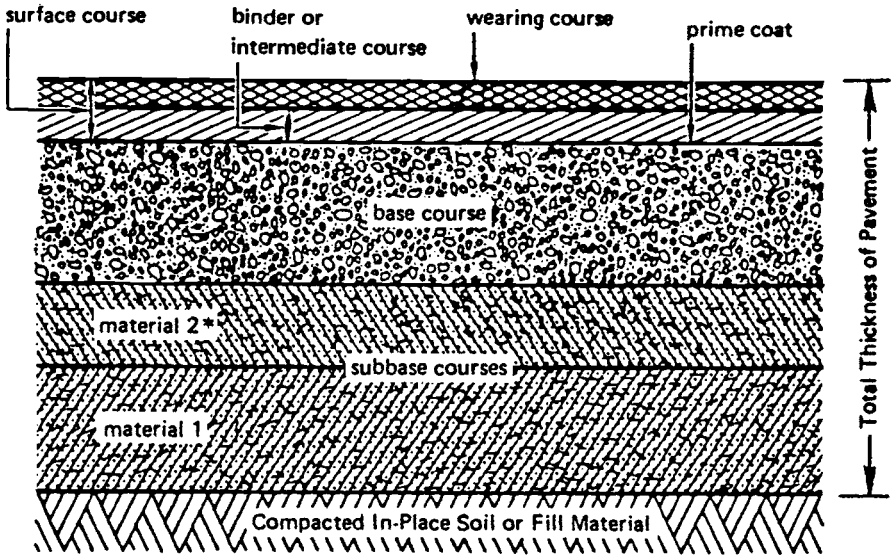
Footprint: the imprint left by the tire in contact with the ground. It is assumed to be elliptical in most cases and to have the following dimensions:

$$\text{Length} = 1.457\sqrt{A}$$

$$\text{Width} = 0.875\sqrt{A}$$

where A is the contact area.

K factor: the modulus of elasticity of the soil; also the coefficient of subgrade reaction and subsoil modulus.



*Material 2 is of a higher quality than material 1.

| | |
|---------------------------|---|
| PAVEMENT | Combination of subbase, base, and surface constructed on subgrade. |
| SURFACE COURSE | A hot mixed bituminous concrete designed as a structural member with weather and abrasion resisting properties. May consist of wearing and intermediate courses. |
| PRIME COAT | Application of a low-viscosity liquid bitumen to the surface of the base course. The prime penetrates into the base and helps bind it to the overlying bituminous course. |
| SEAL COAT | A thin bituminous surface treatment containing aggregate used to waterproof and improve the texture of the surface course. |
| COMPACTED SUBGRADE | Upper part of the subgrade, which is compacted to a density greater than the soil below. |
| TACK COAT | A light application of liquid or emulsified bitumen on an existing paved surface to provide a bond with the superimposed bituminous course. |
| SUBGRADE | Natural in-place soil or fill material. |

Fig. 12.3 Typical flexible pavement (source: Ref. 3, reprinted with permission).
 © 1985 Society of Automotive Engineers, Inc.

Pavement: generally characterized as being rigid or flexible. The former is concrete made with Portland cement. An exception to this are those under the jurisdiction of the Port of New York and New Jersey in which lime, cement, and fly ash are mixed with sand; they have their own method of analysis. Rigid pavement thickness is considered to be the thickness of the concrete (commonly 8–14 in.). Three types of loading are considered: interior, edge, and corner. Interior loading is applied away from the edges and most of the earlier strength calculations used this as the basis for design. For heavy aircraft, the edge conditions are often critical, so this is generally used nowadays. In the United States, corner loading is rarely considered.

Asphalt is the material commonly used for flexible pavements as the surfacing layer and its thickness is considered to be the total of all the materials involved, as depicted in Fig. 12.3.

Subgrade and CBR: the following definition is taken from Ref. 3. Subgrade strength is usually measured in terms of the modulus of subgrade (or soil) reaction k or CBR (California bearing ratio) for flexible pavements. The modulus is the applied pressure on the ground divided by the soil deflection of a rigid plate—thus, k is measured in pounds per cubic inch and typical values are 50–500. As noted previously, it is a parameter used in the evaluation of rigid pavement in which typical values are 200–300. CBR is essentially the ratio of the bearing strength of a given soil sample to that of crushed limestone gravel; it is measured as a percentage of the limestone figure, so that CBR 10 is 10% of the strength of crushed aggregate. CBR 4 is the lowest strength upon which heavy airfield construction equipment can operate effectively. Typical CBR values of 10–20 can be expected on commercial airfield subgrades and CBR 6–9 is the range commonly referred to as a soft field when an unpaved field is being considered. The procedures for measuring k and CBR are given in MIL-STD-621A* and an approximate relationship between the two is shown in Fig. 12.4.

Traffic lane: observations of many landings show that the center portion of the runway will encounter 75% of the landings. Statistics indicate that the traffic lane extends 40 in. on each side of each gear's footprint pattern.

Tread distance: the lateral distance between the centerlines of two adjacent tires.

Wheelbase: the longitudinal distance between the centerlines of the nose gear axle and the main gear axle or bogie pivot.

12.3 AIRFIELD SURFACE TYPES

Rigid Pavement

The general description of rigid pavements is given above. Pavement design is based on Westergaard's theories,^{4,5} which use radius of relative stiffness as a primary parameter in determining the equivalent single wheel

*See Chapter 15 for a list of specifications.

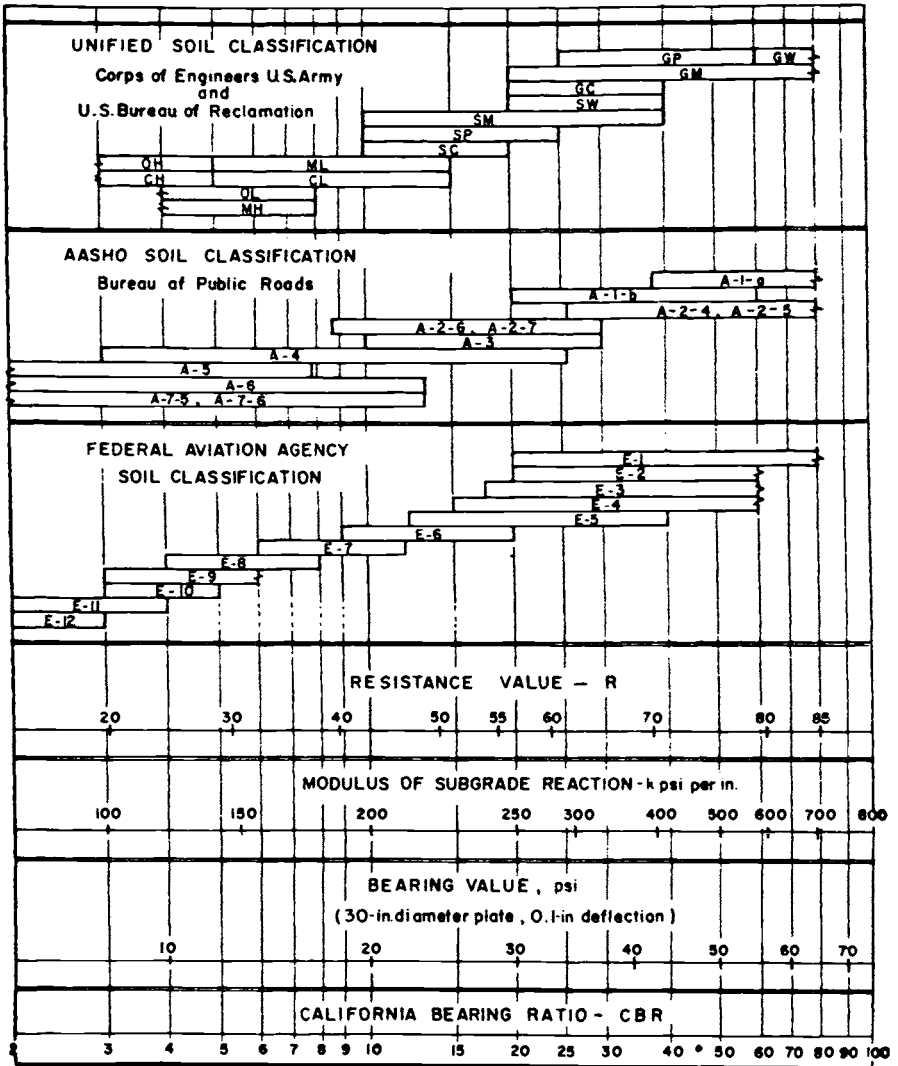


Fig. 12.4 Approximate interrelationship of soil classifications and bearing values (source: Ref. 3, reprinted with permission). © 1985, Society of Automotive Engineers, Inc.

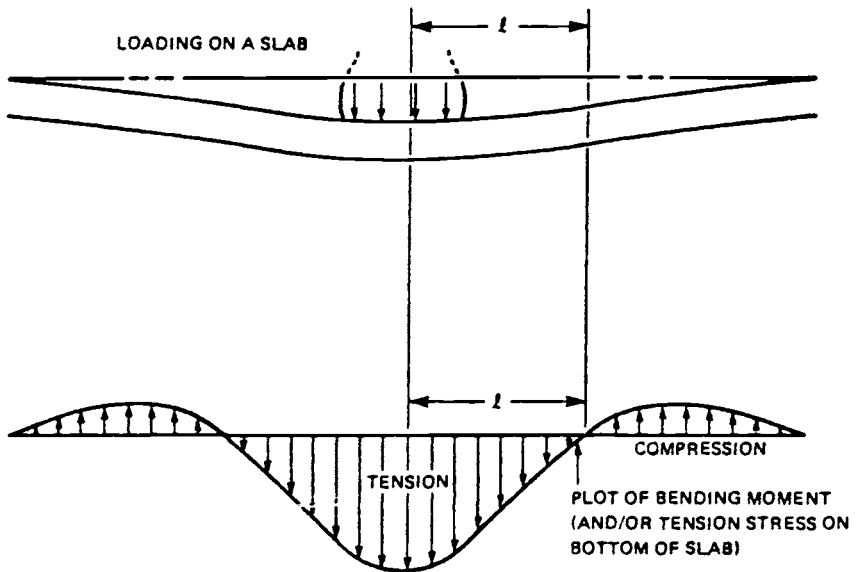


Fig. 12.5 Physical meaning of radius of relative stiffness l .

load (ESWL). Its physical meaning is illustrated in Fig. 12.5. l is a function of the concrete modulus of elasticity, concrete thickness, Poisson's ratio, and the modulus of subgrade reaction, as

$$l = \sqrt[4]{\frac{Eh^3}{12(1-\mu^2)k}}$$

where

E = Young's modulus for concrete, psi

h = slab thickness, in.

μ = Poisson's ratio of concrete

k = subgrade modulus, lb/in.³

Typical values for the above are: $E = 4,000,000$ psi, $\mu = 0.15$, and $k = 300$ lb/in.³

Flexible Pavement

As noted previously, Fig. 12.3 illustrates a section through flexible pavement. Unlike rigid pavement, it uses multiple layers of compacted materials beneath the surface course and total thickness is characterized as being between 8 and 60 in.

Unpaved Airfields

The general category of unpaved field includes bare soil, grass surfaces, mat-covered surfaces, and surfaces that use a membrane between the natural surface and a landing mat. Details of membrane usage are given in Refs. 6 and 7.

12.4 FLOTATION

Flotation is not an exact science. The parameters upon which it is based vary considerably, particularly in the case of unpaved fields, where flotation calculations are based upon heterogeneous materials such as soil—a material that is not generally elastic and yet is not truly plastic either. It is important to recognize this fact. There is a tendency on the part of operations analysts to use flotation values in determining the precise number of landings that can be made at a given location before airfield failure. The ensuing analysis is not realistic. For example, the determination of bare soil field strength cannot recognize all of the soft areas; also, flotation analyses do not recognize the destructive effects of aircraft bounce as it traverses roughness. The definition of failure itself is somewhat arbitrary and many aircraft can make far more landings than predicted before excessive rutting occurs. In summary, flotation analyses are excellent for comparing different aircraft and for obtaining approximate capabilities of an aircraft to operate on a specified surface.

There are currently 16 methods being used for calculating flotation; AIR 1780 discusses most of them. This is partly attributable to the fact that these methods were developed in different countries and by different government agencies. The International Civil Aviation Organization (ICAO) tried to resolve some of them when it published its design manual on pavements, DOC 9157-AN/901. ICAO recommends universal adoption of the load classification number (LCN) method, which originated in Great Britain. The British went on to develop the load classification group (LCG) method, which was also adopted and promoted by ICAO. Subsequently, ICAO has used an industry working group to develop the method known as aircraft classification group—pavement classification number (ACN-PCN). This method does not calculate flotation, but is a simple and useful way of reporting an aircraft's capability to use a given runway and to compare the relative capabilities of various aircraft.

Methods for calculating flotation on bare soil have been extensively pursued in the United States. The method² developed by the USAF in 1968 is still used and is described later in this chapter.

12.5 FLOTATION ON PAVED AIRFIELDS

Rigid and flexible pavements are usually evaluated by the Portland Cement Association (PCA), FAA, United States Tri-Service, LCN, or LCG methods. Until 1983, the results of these calculations were reported in the format appropriate to that particular method; for instance, the PCA method resulted in a chart such as that shown in Fig. 12.6. However, since

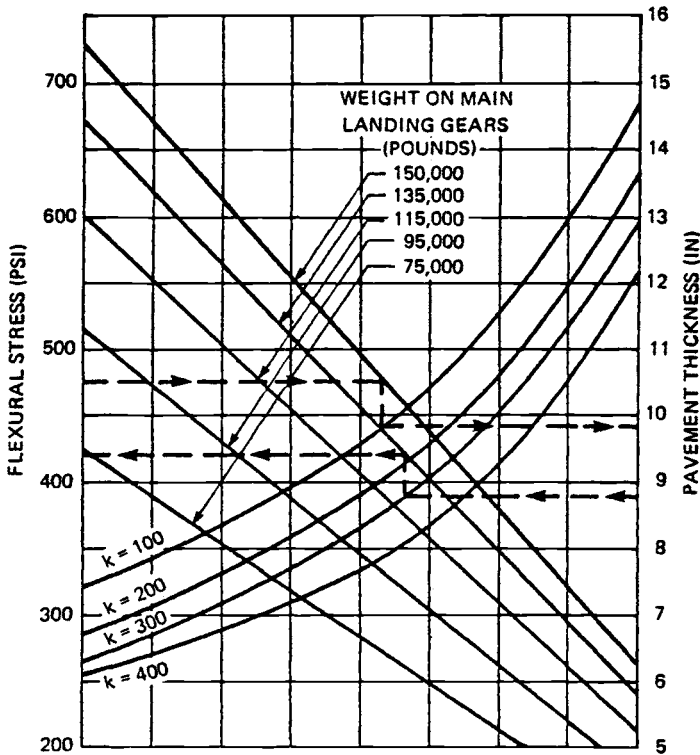


Fig. 12.6 Rigid pavement design chart for L-100, PCA method.

the advent of ACN-PCN, all methods now use a common basis for reporting. This will be discussed later.

Portland Cement Association (PCA) Method

The basis for this method is given in PCA's manual on designing concrete pavement.⁸ The method has now been computerized, but to obtain an understanding of it the original method should be reviewed. The procedure is as follows:

1) Using the influence chart (Fig. 12.7), draw the imprint of the tire(s) on transparent paper to a scale that depends on the scale of the chart (note ℓ at the top of the chart).

2) Place the drawing on the chart in a position that depends on location of load with respect to the point for which values are desired. Figure 12.7 shows a four-wheel bogie superimposed on the chart. Note: the gear may have to be moved to various positions over the chart to establish the most severe intensity of loading. The footprint width in this case is defined as $0.6L$; length L is obtained from footprint area = $0.5227L^2$.

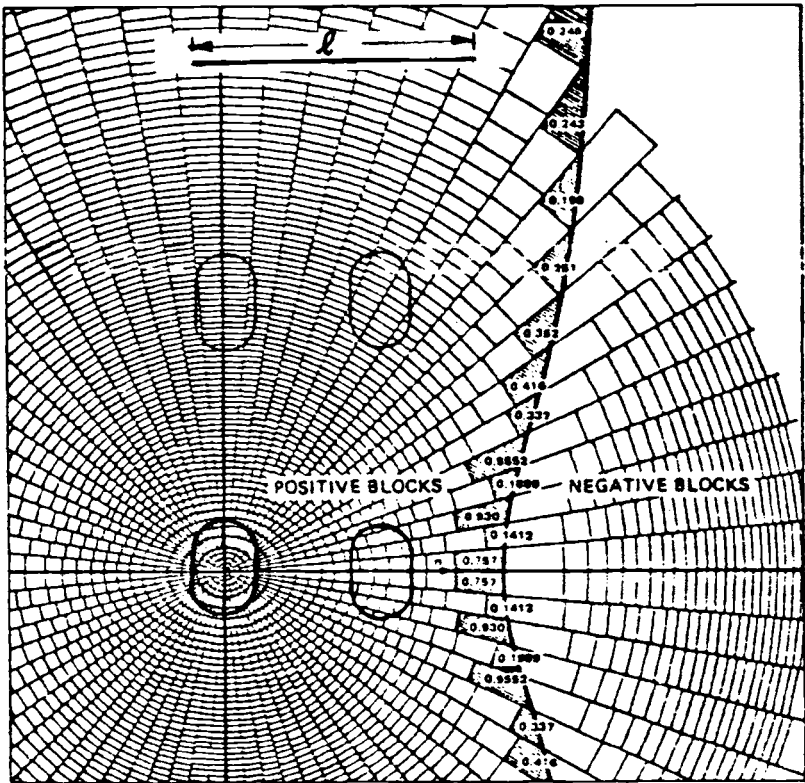


Fig. 12.7 Influence chart for interior-loaded slab.

3) Count the blocks on the chart covered by the diagram, recognizing both positive and negative blocks.

The bending moment in the concrete can then be determined by a formula that relates the number of blocks, pavement rigidity, subgrade rigidity, and loading intensity. From this moment, the stress can be found by dividing the moment by the section modulus. The definition for l was given earlier and Table 12.1 shows its values for some typical conditions.

This tedious process has now been replaced by a PCA computer program, PDILB.⁹ The Aerospace Industries Association (AIA) has published National Aerospace Standard (NAS) 3601, the rigid pavement section of which specifies the PDILB program as the method to be used. The program is also available as microcomputer software.⁹

Full-size design charts for many aircraft are available from PCA. These show the pavement thicknesses required at various weights and with various tire pressures.

Unless otherwise stated, use the 90 day flexural strength of concrete, which is approximately equal to 110% of the 28 day strength. Assume that the 90 day strength is 700 psi, which, with a 1.75 factor, permits a working

Table 12.1 LCN for Rigid Pavements: Values of Radius of Relative Stiffness ℓ

| Thickness of pavement H , in. | ℓ values for $E = 5 \times 10^6$ | | | | | | | | | |
|---|---------------------------------------|-----------|-----------|-----------|-----------|-----------|-----------|-----------|-----------|------------|
| | $k = 50$ | $k = 100$ | $k = 150$ | $k = 200$ | $k = 250$ | $k = 300$ | $k = 350$ | $k = 400$ | $k = 500$ | $k = 1000$ |
| 6 | 36.84 | 30.98 | 27.99 | 26.04 | 24.63 | 23.54 | 22.64 | 21.91 | 20.71 | 17.42 |
| 6.5 | 39.11 | 32.89 | 29.72 | 27.66 | 26.16 | 25.00 | 24.04 | 23.26 | 21.99 | 18.50 |
| 7 | 41.35 | 34.78 | 31.42 | 29.23 | 27.65 | 26.42 | 25.42 | 24.58 | 23.25 | 19.55 |
| 7.5 | 43.55 | 36.62 | 33.08 | 30.79 | 29.12 | 27.83 | 26.77 | 25.89 | 24.49 | 20.59 |
| 8 | 45.71 | 38.43 | 34.73 | 32.32 | 30.57 | 29.20 | 28.10 | 27.17 | 25.70 | 21.61 |
| 8.5 | 47.83 | 40.22 | 36.34 | 33.82 | 31.98 | 30.57 | 29.40 | 28.44 | 26.90 | 22.62 |
| 9 | 49.93 | 41.99 | 37.94 | 35.30 | 33.39 | 31.90 | 30.69 | 29.69 | 28.07 | 23.61 |
| 9.5 | 51.99 | 43.72 | 39.50 | 36.76 | 34.78 | 33.22 | 31.96 | 30.92 | 29.24 | 24.59 |
| 10 | 54.03 | 45.43 | 41.06 | 38.21 | 36.13 | 34.52 | 33.22 | 32.13 | 30.39 | 25.55 |
| 10.5 | 56.05 | 47.13 | 42.59 | 39.63 | 37.48 | 35.81 | 34.46 | 33.33 | 31.52 | 26.50 |
| 11 | 58.04 | 48.81 | 44.10 | 41.04 | 38.82 | 37.08 | 35.68 | 34.51 | 32.64 | 27.44 |
| 11.5 | 60.00 | 50.46 | 45.59 | 42.43 | 40.13 | 38.34 | 36.89 | 35.67 | 33.74 | 28.36 |
| 12 | 61.95 | 52.10 | 47.07 | 43.81 | 41.43 | 39.59 | 38.09 | 36.84 | 34.84 | 29.29 |
| 12.5 | 63.87 | 53.71 | 48.53 | 45.17 | 42.72 | 40.81 | 39.27 | 37.98 | 35.92 | 30.19 |
| 13 | 65.79 | 55.32 | 49.98 | 46.51 | 44.00 | 42.03 | 40.44 | 39.11 | 37.00 | 31.12 |
| 13.5 | 67.67 | 56.91 | 51.42 | 47.86 | 45.25 | 43.23 | 41.61 | 40.24 | 38.05 | 31.99 |
| 14 | 69.54 | 58.48 | 52.85 | 49.18 | 46.50 | 44.43 | 42.76 | 41.35 | 39.11 | 32.88 |
| 14.5 | 71.40 | 60.04 | 54.25 | 50.49 | 47.75 | 45.62 | 43.89 | 42.45 | 40.15 | 33.75 |
| 15 | 73.24 | 61.59 | 55.65 | 51.79 | 48.98 | 46.80 | 45.02 | 43.55 | 41.18 | 34.62 |
| 15.5 | 75.06 | 63.12 | 57.03 | 53.08 | 50.19 | 47.96 | 46.14 | 44.83 | 42.21 | 35.49 |
| 16 | 76.87 | 64.64 | 58.41 | 54.36 | 51.41 | 49.11 | 47.26 | 45.71 | 43.22 | 36.34 |

$$\text{Note: } \ell = \sqrt[4]{\frac{EK^3}{12(1-\mu^2)K}}, \mu = 0.15$$

| For values of E of | multiply value of ℓ given above by |
|----------------------|--|
| 4×10^6 | 0.95 |
| 3×10^6 | 0.88 |
| 2×10^6 | 0.80 |

stress of 400 psi—the value used on the left side of a chart such as that shown in Fig. 12.8. It can also be assumed that $E = 4 \times 10^6$ and $\mu = 0.15$. As a general guide, it is often assumed that the center of the runway is subjected to moving loads and that its thickness need therefore be only 80% of that at the runway ends.

Federal Aviation Administration (FAA) Method

Details of the FAA method are given in Ref. 10. It uses the Westergaard analysis, based on an edge-loaded slab. Parameters involved are: 90 day flexural strength, subgrade modulus k , aircraft weight, and annual departures.

The Advisory Circular includes a series of graphs, such as Figs. 12.9–12.11, to permit simple evaluation of a runway's capability to support an

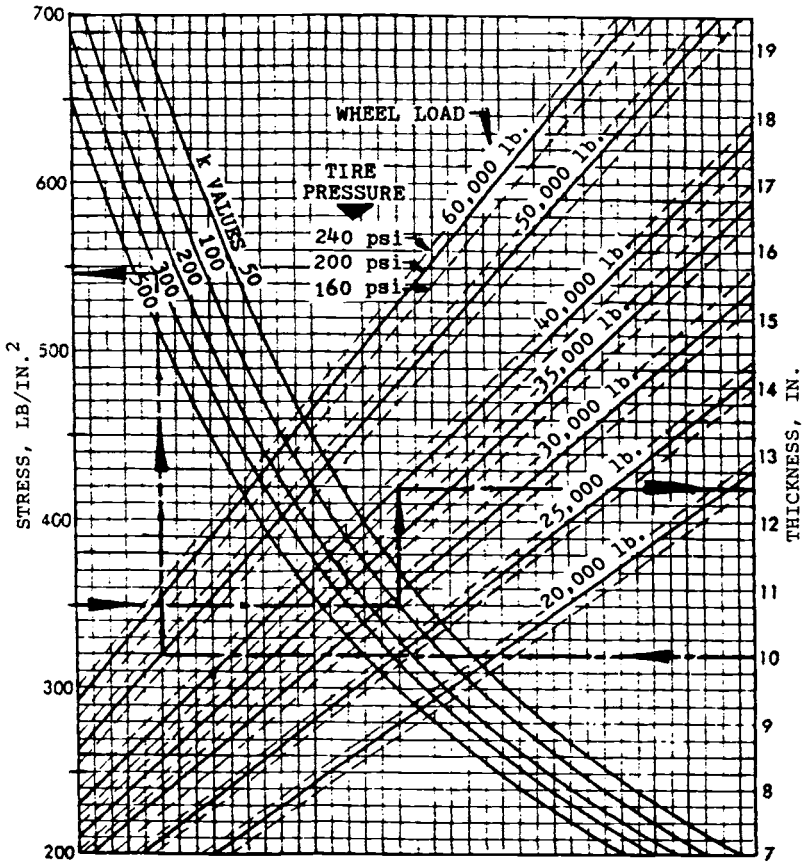


Fig. 12.8 Typical design chart for an aircraft operating on rigid pavement.

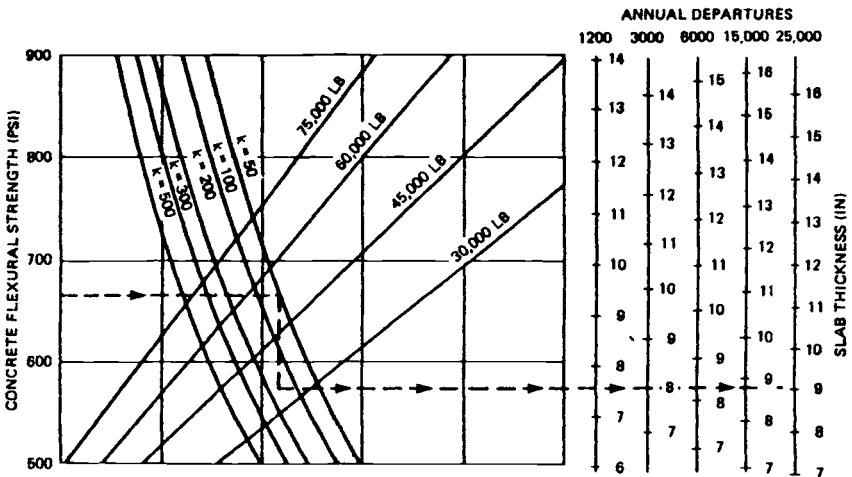


Fig. 12.9 FAA rigid-pavement design curves: single-wheel gear.

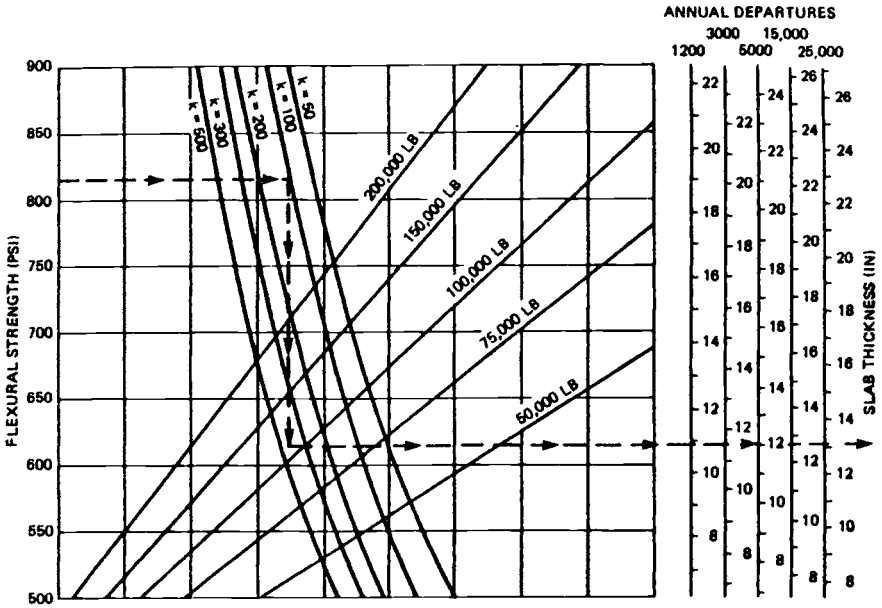


Fig. 12.10 FAA rigid-pavement design curves: dual-wheel gear.

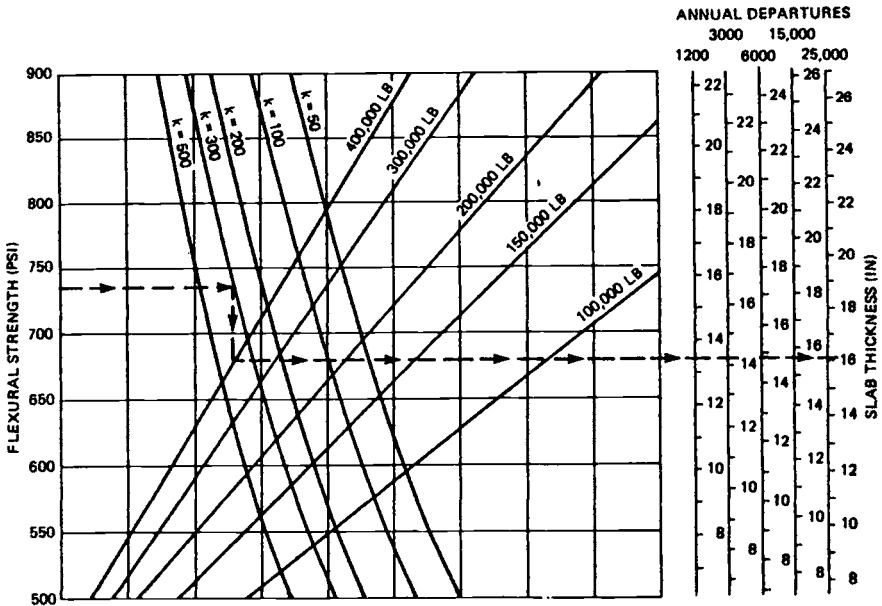


Fig. 12.11 FAA rigid-pavement design curves: dual-tandem gear.

aircraft, based on its gear configuration, tire contact area, aircraft weight, and annual departures. These graphs assume that tire pressure and wheel spacing increase with gross weight. For noncritical areas, the pavement thicknesses can be 10–30% less than those shown on the charts.

United States Tri-Service Methods

The U.S. Departments of the Navy, Army, and Air Force have jointly published documents¹¹ to specify their pavement design criteria. Rigid pavements are covered in Refs. 12–14. For flexible pavements, all three services use the U.S. Army Corps of Engineers CBR method described in Ref. 15.

The rigid pavement analyses use the Westergaard equations, but differ in detail such as edge loading vs interior loading of slabs.

Load Classification Number (LCN)

As noted previously, ICAO promoted the LCN method for international usage. It is widely used today, although ICAO considers it to be superseded by the LCG method. The latter method is quite simple:

1) Determine the ESWL from the charts provided. (They are based on Westergaard's theory based on corner loading.)

2) Apply that load (ESWL) to a standard graph that shows the LCN as a function of ESWL, tire pressure, and tire contact area.

The following describes the usage of the LCN method:

1) Unless otherwise required, assume 90% of gross weight on the main gear of a conventional gear arrangement.

2) Calculate the single-wheel load (SWL) with single-wheel gears as

$$SWL = \frac{0.9 \times \text{gross weight}}{2}$$

or equivalent single-wheel load (ESWL) with multiple-wheel gears as

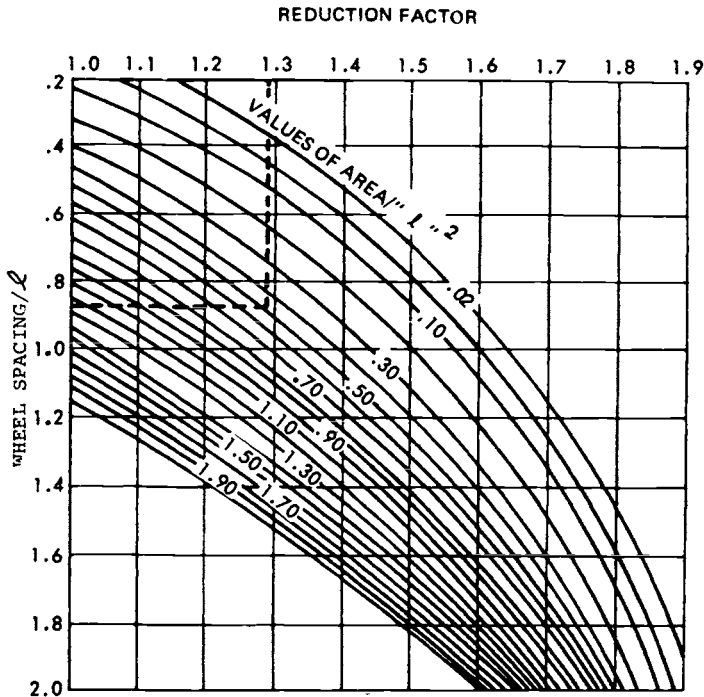
$$ESWL = \frac{\text{Total load on one landing gear assembly}}{\text{reduction factor}}$$

a) For dual or tandem wheels: read the reduction factor from Fig. 12.12. Use the known value of ℓ (radius of relative stiffness) or calculate for two or three possible values such as 30, 40, or 50 in.

b) For four-wheel bogies: read the reduction factor from Fig. 12.13. Again, use the known value for ℓ or calculate for two or three possible values.

3) Read LCN value from Fig. 12.14 at the intersection of ESWL and tire pressure values.

Note: Fig. 12.12 shows the reduction factors for dual-wheel landing gears



ℓ = radius of relative stiffness

Area = total contact area of all wheels of one assembly

Equivalent single-wheel load = total load on one assembly divided by reduction factor

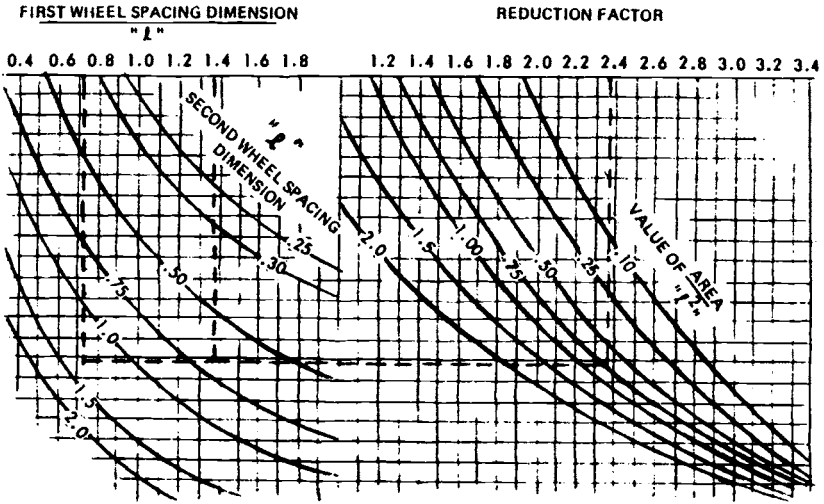
Fig. 12.12 Determination of reduction factor and equivalent single-wheel load for dual-wheel undercarriages on rigid pavement.

as an example. For other gear types, consult ICAO DOC 9157-AN/901 for these factors.

The wheel spacing dimensions used in these calculations are shown in Fig. 12.15.

The LCN methodology quoted above refers to operations on rigid pavements, but calculations for flexible pavements are similar. The only difference is in the calculation of ESWL; for this, reference should be made to the ICAO DOC 9157.

The aircraft LCN values obtained by this method are then compared with the runway LCN (usually obtained by plate bearing tests). The values obtained are for unlimited operation. Where limited operation is required, use the method discussed in Sec. 12.7.



Area = total contact area of all wheels of one assembly
 Equivalent single-wheel load = total load on one assembly divided by reduction factor

Fig. 12.13 Reduction factor and ESWL on dual-tandem undercarriages on rigid pavements.

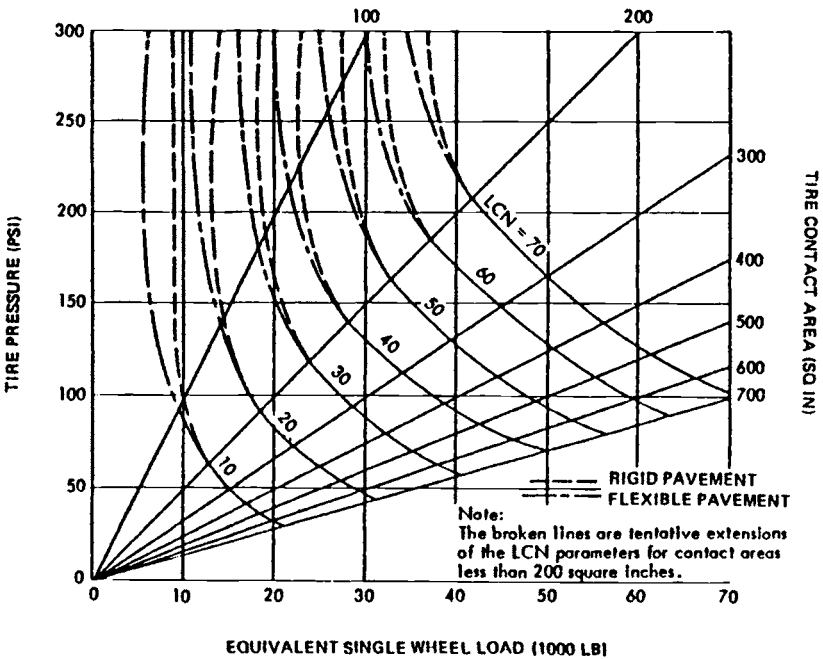


Fig. 12.14 Load classification number chart.

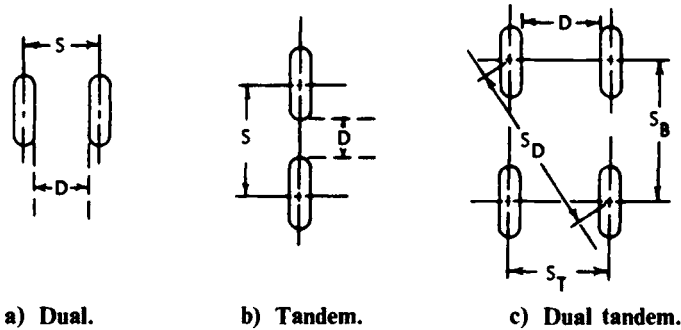


Fig. 12.15 Wheel spacing.

Load Classification Group (LCG) Method

The LCG method evaluates the aircraft LCN and then places that aircraft in a certain group. It is generally considered to be a refinement of the LCN method. However, there is one major difference: the LCN method includes the following relationship:

$$\frac{W_1}{W_2} = \left(\frac{A_1}{A_2} \right)^{0.44}$$

where W_1 and W_2 are the failure loads for contact areas A_1 and A_2 . Subsequent studies indicated that the 0.44 power should be 0.27, which is the value used in calculating the LCN for the LCG method. This change reduces the importance of tire pressure, with the result that the new LCN values are generally lower than the "old" values. Annex 14 of ICAO standard on aerodromes discusses this method in some detail and validates the above relationship.

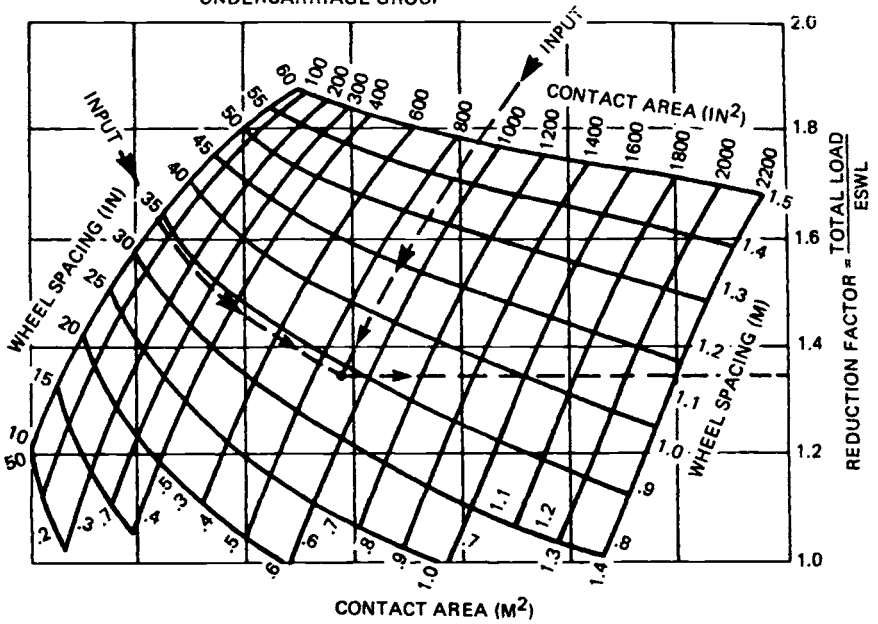
Another difference with the LCN method is that the LCG values are based on a pavement $\ell = 40$ in. $k = 400$ lb/in.³, $\mu = 0.15$, and $E = 5 \times 10^6$ psi, whereas these values had to be known, calculated, or assumed for the LCN evaluation.

The curves for assessing ESWL and LCN for use in the LCG system are shown in Figs. 12.16–12.18. Figure 12.18 also shows the groups into which the LCN values are designated. These groups are listed in Table 12.2. Thus, if an aircraft is said to have an LCN of 25, it can operate without limits on any airfield having an LCG of I–V.

Table 12.2 LCG Groups of LCN Values

| LCG | LCN | LCG | LCN |
|-----|---------|-----|--------------|
| I | 101–120 | V | 16–30 |
| II | 76–100 | VI | 11–15 |
| III | 51–75 | VII | 10 and below |
| IV | 31–50 | | |

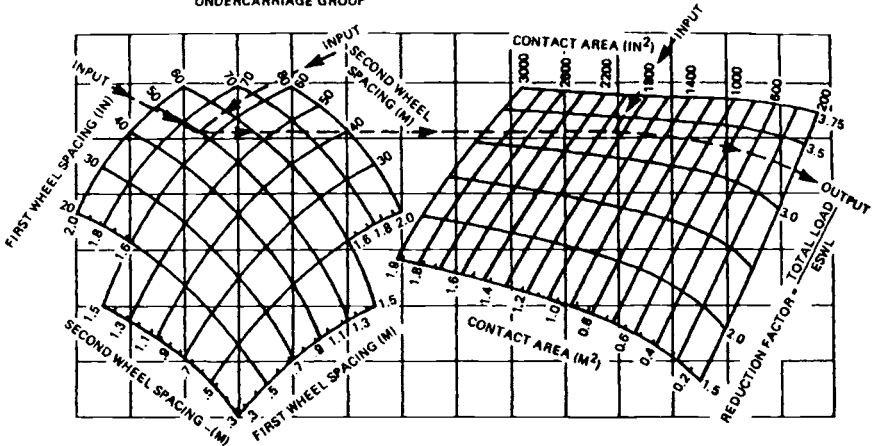
CONTACT AREA = AREA OF ALL WHEELS IN ONE UNDERCARRIAGE GROUP



EXAMPLE: DUAL WHEEL AIRCRAFT, WHEEL SPACING 34 IN (0.864 M)
 C/C, CONTACT AREA OF DUAL WHEELS 900 IN² (0.581 M²)
 REDUCTION FACTOR = 1.352

Fig. 12.16 Equivalent single-wheel load assessment curves: rigid pavements, dual-wheel undercarriages, LCN-LCG.

CONTACT AREA = AREA OF ALL WHEELS IN ONE UNDERCARRIAGE GROUP



EXAMPLE: DUAL TANDEM WHEEL AIRCRAFT WHEEL
 SPACING 84 IN x (1.828 M x 1.245 M)
 C/C, CONTACT AREA OF DUAL TANDEM
 WHEEL 1900 IN² (1.228 M²)
 REDUCTION FACTOR = 3.3

Fig. 12.17 ESWL determination: rigid pavements, dual-tandem undercarriages, LCN-LCG.

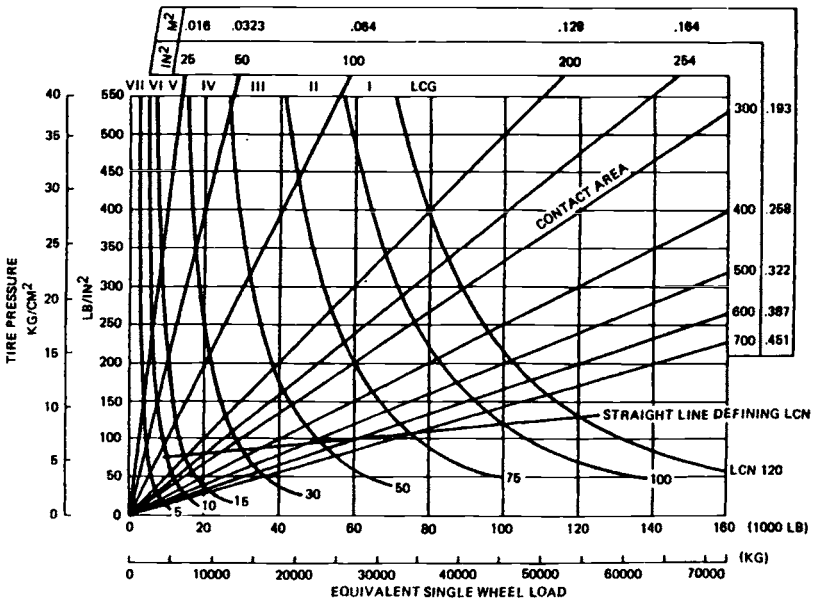


Fig. 12.18 Load classification number and groups.

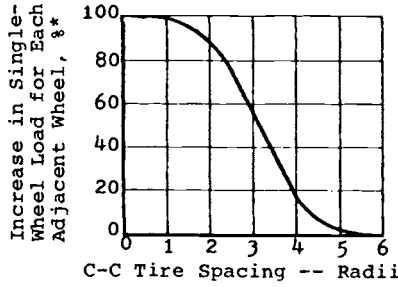
12.6 FLOTATION ON UNPAVED AIRFIELDS

The current method used for calculating flotation on unpaved surfaces is given in Ref. 2. Tire pressure is one of the most important factors and, in some countries, it used to be (and possibly still is) the only factor used in determining whether or not an aircraft can operate from a given field.

Both nose gear and main gear flotations are evaluated and the results combined to show the total aircraft flotation, which recognizes the interaction between nose and main gear effects. The steps involved are as follows:

- 1) Calculate the contact area.
- 2) Calculate the tire contact pressure.
- 3) Using Fig. 12.19, calculate ESWL by multiplying the single-wheel load by the multiplication factor, which depends upon the closest tire spacing in a given assembly. Tire spacing is in terms of R , where R is the radius of the circle that is the equivalent in area to the contact area. R is defined as $R = 0.564\sqrt{A}$, where A is the contact area.
- 4) Determine coverages. Using Fig. 12.20, find the California bearing ratio (CBR) for one coverage. Then, coverages are obtained from the following relationship:

$$C = \left(\frac{\text{CBR of field being evaluated}}{\text{CBR for 1 coverage}} \right)^6$$



*Increase in load on a single wheel of a multiple-wheel gear to account for effects of adjacent wheels of the multiple-wheel gear in arriving at an equivalent single-wheel load.

Fig. 12.19 Multiplication factor for ESWL (source: Ref. 2).

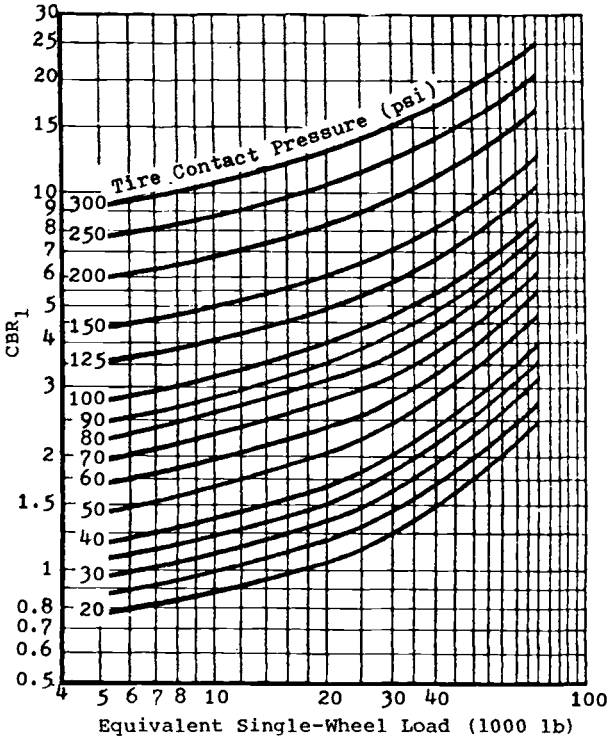


Fig. 12.20 CBR for one coverage (source: Ref. 2).

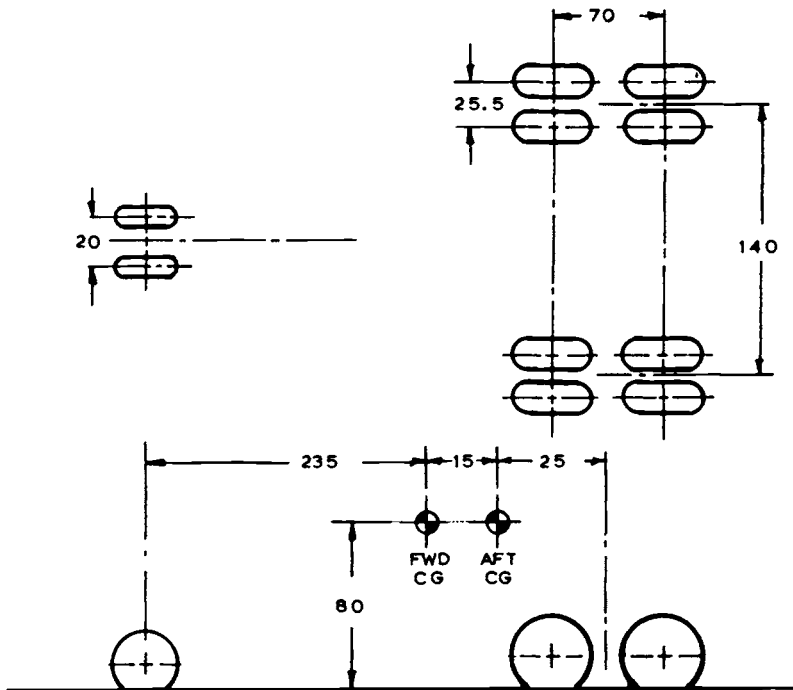


Fig. 12.21 Landing gear arrangement for bare soil flotation calculation.

- 5) Calculate passes per coverage, using

$$\frac{P}{C} = \frac{80 + W + T}{0.75nW}$$

where

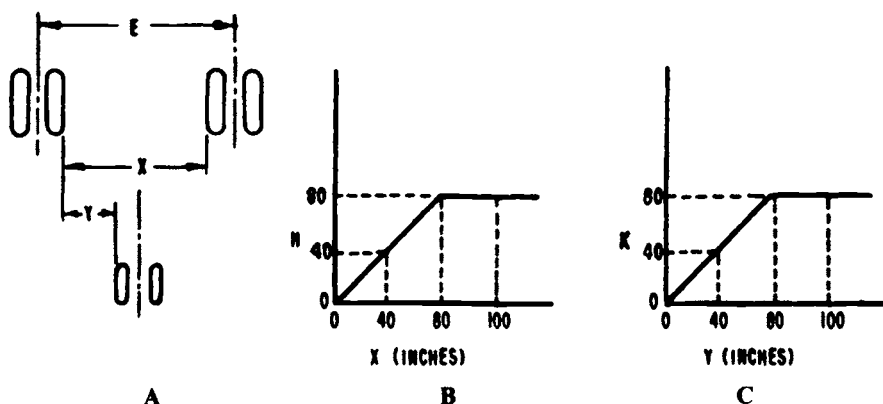
- W = width of footprint = $0.874\sqrt{A}$, in.
 A = footprint area, in.²
 T = distance between adjacent tire, in.
 n = number of tires in the assembly

- 6) Determine passes, where $P = P/C \times C$.
 7) Do this for both the nose and main gears.
 8) Combine these as shown in the example, Figs. 12.21–12.23, and Table 12.3. The passes refer to the number of movements of the aircraft that can be made past one point on the surface; i.e., one landing or one takeoff equals one pass.

| FLOTATION - BARE SOIL | | AIRCRAFT |
|------------------------------|---|--|
| | | DATE |
| ITEM | MAIN LANDING GEAR | NOSE LANDING GEAR |
| TIRE SIZE | 12.50-16 | 9.50-16 |
| SINGLE WHEEL LOAD | 11,364 | 11,789 |
| CONTACT AREA (A) | $d = \frac{b(D_0 - D_f)}{200}$ $d = \text{radial defl. (ins)}$ $D_0 = \text{tire O.D. (ins)}$ $D_f = \text{flange dia (ins)}$ $b = \text{tire defl. (\%)}$ $d = \frac{35(38.5 - 18.5)}{200} = 3.5 \text{ ins.}$ $A = 2.36 d \sqrt{(D_0 - d)(W_T - d)}$ $W_T = \text{tire section width} = 12.75 \text{ ins}$ $A = 8.27 \sqrt{(38.5 - 3.5)(12.75 - 3.5)}$ $= 148.6 \text{ sq. ins}$ Radius of equivalent circle (R) = $564 \sqrt{A}$ $= 6.98$ Footprint width (w) = $.874 \sqrt{A} = 10.65$ | $d = \frac{b(D_0 - D_f)}{200}$ $d = \text{radial defl. (ins)}$ $D_0 = \text{tire O.D. (ins)}$ $D_f = \text{flange dia (ins)}$ $b = \text{tire defl. (\%)}$ $d = \frac{35(33.4 - 18)}{200} = 2.7 \text{ ins}$ $A = 2.36 d \sqrt{(D_0 - d)(W_T - d)}$ $W_T = \text{tire section width} = 9.7 \text{ ins}$ $A = 6.38 \sqrt{(33.4 - 2.7)(9.7 - 2.7)}$ $= 93.4 \text{ sq. ins}$ $R = 5.45$ $w = 8.46$ |
| TIRE CONTACT PRESSURE (PSI) | $TCP = \frac{SWL}{A} = \frac{11,364}{148.6}$ $= 76.5$ | $TCP = \frac{SWL}{A} = \frac{11,789}{93.4}$ $= 126.2$ |
| EQUIVALENT SINGLE WHEEL LOAD | SPACING = 25.5 FACTOR = 1.27 $E SWL = \text{FACTOR} \times SWL = 14,934$ | SPACING = 20.0 FACTOR = 1.29 $E SWL = 15,208$ |
| COVERAGES (C) | $CBR_1 = 2.7$ $C = \left(\frac{\text{CBR OF FIELD CONSIDERED}}{\text{CBR FOR 1 COVERAGE}} \right)^6$ $C = \left(\frac{6}{2.7} \right)^6 = (2.22)^6 = 120$ | $CBR_1 = 4.5$ $C = \left(\frac{\text{CBR}}{\text{CBR}_1} \right)^6$ $C = \left(\frac{6}{4.5} \right)^6 = (1.33)^6 = 5.6$ |
| PASSES PER COVERAGE | $\frac{P}{C} = \frac{80 \cdot w \cdot T}{.75 N w} = \frac{80 \cdot 10.65 \cdot 25.5}{.75(4)(10.65)}$ $= 3.62$ | $\frac{P}{C} = \frac{80 \cdot 8.45 \cdot 20}{.75(2)(8.45)}$ $= 8.56$ |
| PASSES | $P_M = \frac{P}{C} \times C$ $= 3.62 \times 120 = 434$ | $P_N = \frac{P}{C} \times C$ $= 8.56 \times 5.6 = 47.9$ |

Fig. 12.22 Example of bare soil flotation calculation.

Table 12.3 Example of Calculation of Total Airplane Passes



- 1) Determine dimensions

$$X = E - W_M - B$$

$$Y = 0.5(E - W_M - W_N - B - D)$$

- 2) Use Sketch B to determine H and Sketch C for K .

- 3) Compute:

$$AP_M = \frac{80P_M P_N}{80P_N + (80 - H)P_N + (80 - K)P_M}$$

$$AP_N = \frac{80P_M P_N}{80P_M + (80 - H)P_N + (80 - K)P_N}$$

where:

P_M = allowable passes for main gear

P_N = allowable passes for nose gear

- 4) The allowable number of aircraft passes AP is then equal to the smaller value, AP_M or AP_N .

Using the dimensions shown in Fig. 12.21 and the flotation figures calculated in Fig. 12.22 results in

$$X = 140 - 10.65 - 25.5 = 104.0$$

$$H = 80$$

$$Y = (140 - 10.65 - 8.45 - 25.5 - 20)/2 = 37.7$$

$$K = 37.7$$

$$AP_M = 76$$

$$AP_N = 45$$

Therefore, the maximum allowable passes for this aircraft is 45.

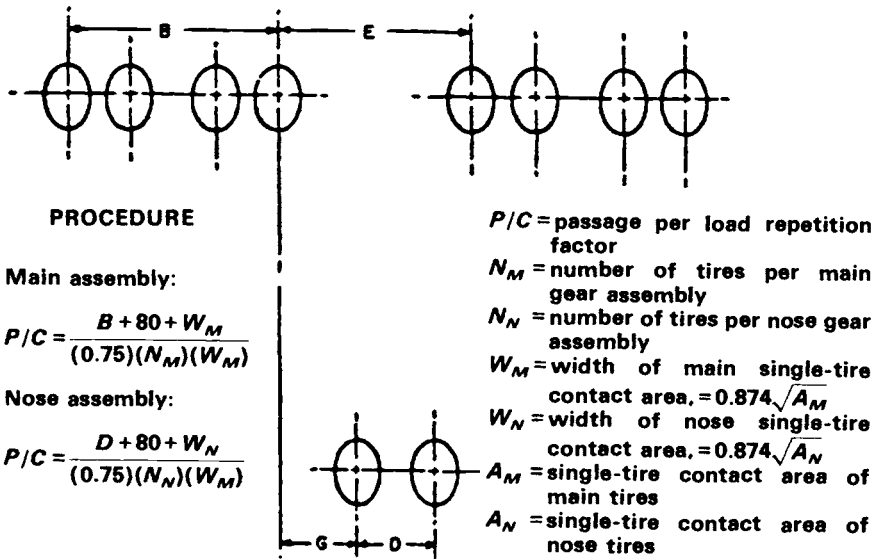


Fig. 12.23 Passes per coverage.

12.7 LIMITED OPERATION

On unpaved surfaces, limited operation is already recognized in the calculations. They define the number of operations possible on a given surface at a given aircraft weight. However, the calculations for paved surfaces assume unlimited operation; but, it is sometimes necessary to determine whether an aircraft that is too heavy for unlimited operation can, in fact, make a smaller number of landings on that surface.

Reference 15 provides details of the U.S. method for limited usage of flexible pavement. It uses the principle that

$$t = \alpha T$$

where t is the thickness for a specified number of operations, α the load repetitions factor, and T the standard (unlimited) thickness for the aircraft on that pavement.

The term α is dependent upon the number of coverages and the number of wheels in the gear assembly. Figure 12.24 shows the values for α . For instance, on a two-wheel assembly such as the Boeing 727, it shows that, if only 10 coverages are required, the thickness need be only about 50% of that required for 5000 coverages.

The LCN system also recognizes limited usage, as indicated in Table 12.4. It also recognizes the difference between channelized (e.g., taxiways) and nonchannelized traffic (e.g., runways).

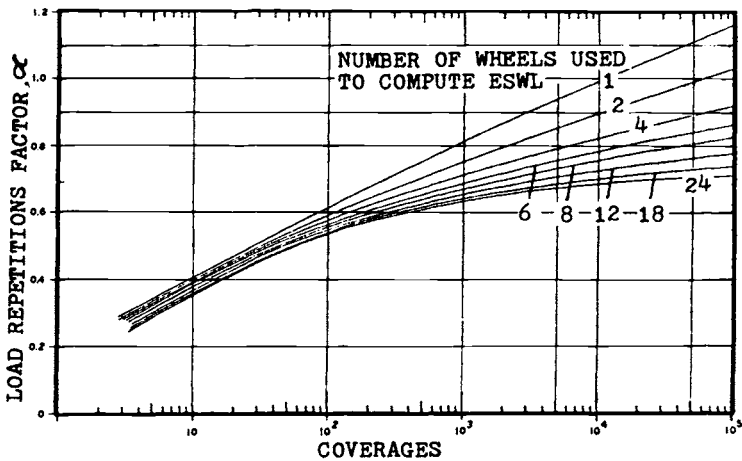


Fig. 12.24 Load repetitions factor vs coverages.

Table 12.4 Limited Usage

| a) LCN for limited payment use | | |
|--|--------------|--|
| Ratio of $\frac{\text{aircraft LCN}}{\text{pavement LCN}}$ | Movements | Remarks |
| Up to 1.1 | Unlimited | |
| From 1.10 to 1.25 | 3000 | Entails acceptance of some minor failures. |
| From 1.25 to 1.50 | 300 | Some cracking may occur in concrete and possibly local failure in flexible surfaces. |
| From 1.5 to 2.0 | Very limited | Permission given only after examination of pavement and test data. |
| Greater than 2.0 | Emergency | |

| Gear configuration | Pass-to-coverage ratio ^a | |
|-----------------------------------|-------------------------------------|----------------|
| | Channelized | Nonchannelized |
| Large aircraft, e.g., C-5 and 747 | 2.00 | 2.75 |
| Dual tandem gear | 2.25 | 4.00 |
| Dual gears | 5.00 | 10.00 |
| Single-wheel gears | 10.00 | 20.00 |

^aIn their usage, a pass is a takeoff and a landing.

12.8 AIRCRAFT CLASSIFICATION NUMBER— PAVEMENT CLASSIFICATION NUMBER (ACN-PCN)

As noted previously, ACN-PCN is not a method for calculating flotation. It is, instead, a convenient and simple way of categorizing and reporting flotation. It is also an excellent method of comparing the flotation of different aircraft. Recognizing the lack of precise mathematical values in surface definition and the inability to truly predict the effect of small variations in tire pressure, the ACN-PCN system wisely uses broad categories such as “high” and “low” pavement strengths and tire pressures. The system also enables any runway to be evaluated by observing the aircraft that have used the runway without causing surface damage. However, it is always preferable to evaluate the surface by regular methods.

In calculating ACN, there are subroutines available for the rigid and flexible pavement computer programs given in Appendix 3 to ICAO Annex 14. To do it manually, use the existing pavement requirements charts to obtain the thickness required at the aircraft weight being considered; then use ICAO conversion charts to translate this “reference thickness” to the derived single wheel load (DSWL) and ACN. The ACN is the DSWL (in kilograms) divided by 500.

On rigid pavements, the thicknesses are determined for subgrade K values of 75, 150, 300, and 500 psi and a concrete working stress of 400 psi. On flexible pavements, the thicknesses are determined for subgrade CBR

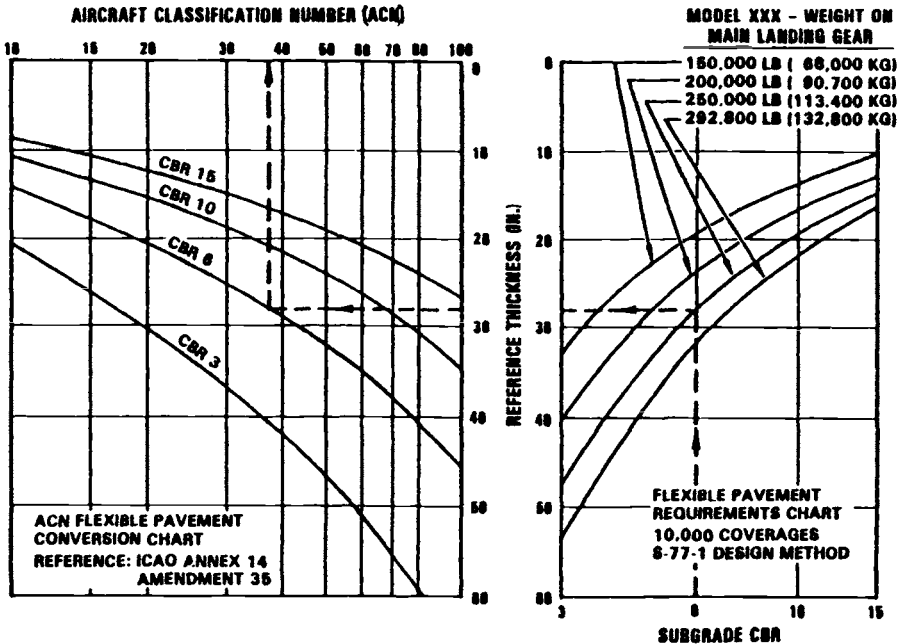


Fig. 12.25 Development of ACN on flexible pavement.

Table 12.5 Typical ACN Values

| Aircraft type | Aircraft mass, kg | Aircraft weight, lb | Load each main gear, % | Tire pressure, psi | Rigid subgrades | | | | Flexible subgrades, % | | | |
|----------------------|---------------------|---------------------|------------------------|--------------------|-----------------|-----------------|--------------|--------------------|-----------------------|--------------|----------|----------------|
| | | | | | High (150 MPa) | Medium (80 MPa) | Low (40 MPa) | Ultra Low (20 MPa) | High (15%) | Medium (10%) | Low (6%) | Ultra low (3%) |
| B-727-100 | 73,028 ^a | 161,000 | 45.7 | 158 | 40 | 43 | 46 | 48 | 37 | 38 | 44 | 49 |
| | 41,322 | 91,000 | 45.7 | 158 | 20 | 22 | 23 | 25 | 19 | 19 | 21 | 25 |
| B-727-200 (standard) | 78,471 | 173,000 | 46.4 | 167 | 46 | 48 | 51 | 53 | 41 | 43 | 49 | 54 |
| | 44,293 | 97,650 | 46.4 | 167 | 23 | 25 | 26 | 27 | 21 | 22 | 24 | 28 |
| B-727-200 (advanced) | 84,005 | 185,200 | 47.8 | 150 | 50 | 53 | 56 | 59 | 46 | 48 | 55 | 60 |
| | 44,298 | 97,661 | 47.8 | 150 | 23 | 25 | 26 | 28 | 21 | 22 | 24 | 29 |
| B-737-100 | 45,722 | 100,800 | 46.3 | 148 | 24 | 26 | 28 | 29 | 22 | 23 | 26 | 30 |
| | 25,941 | 67,190 | 46.3 | 148 | 12 | 13 | 14 | 15 | 12 | 12 | 13 | 15 |
| B-737-200 | 50,340 | 111,000 | 46.35 | 148 | 27 | 29 | 31 | 32 | 25 | 26 | 29 | 33 |
| | 27,005 | 59,535 | 46.35 | 148 | 13 | 14 | 15 | 16 | 12 | 12 | 14 | 16 |
| B-747-100 | 334,752 | 738,000 | 23.125 | 225 | 44 | 51 | 60 | 69 | 46 | 50 | 60 | 81 |
| | 162,704 | 358,700 | 23.125 | 225 | 18 | 20 | 23 | 26 | 19 | 20 | 22 | 28 |
| B-747-200 B.C.F. | 373,307 | 823,000 | 23.075 | 210 | 49 | 58 | 68 | 78 | 52 | 58 | 71 | 93 |
| | 168,873 | 372,300 | 23.075 | 210 | 18 | 20 | 23 | 27 | 20 | 21 | 23 | 30 |
| Concorde | 185,060 | 408,000 | 48.0 | 183 | 61 | 71 | 82 | 91 | 65 | 72 | 81 | 98 |
| | 78,698 | 173,500 | 48.0 | 183 | 21 | 22 | 25 | 29 | 21 | 22 | 26 | 32 |

Source: ICAO Annex 14.

^aFirst row for each aircraft pertains to maximum takeoff gross weight and second row to maximum operators empty weight.

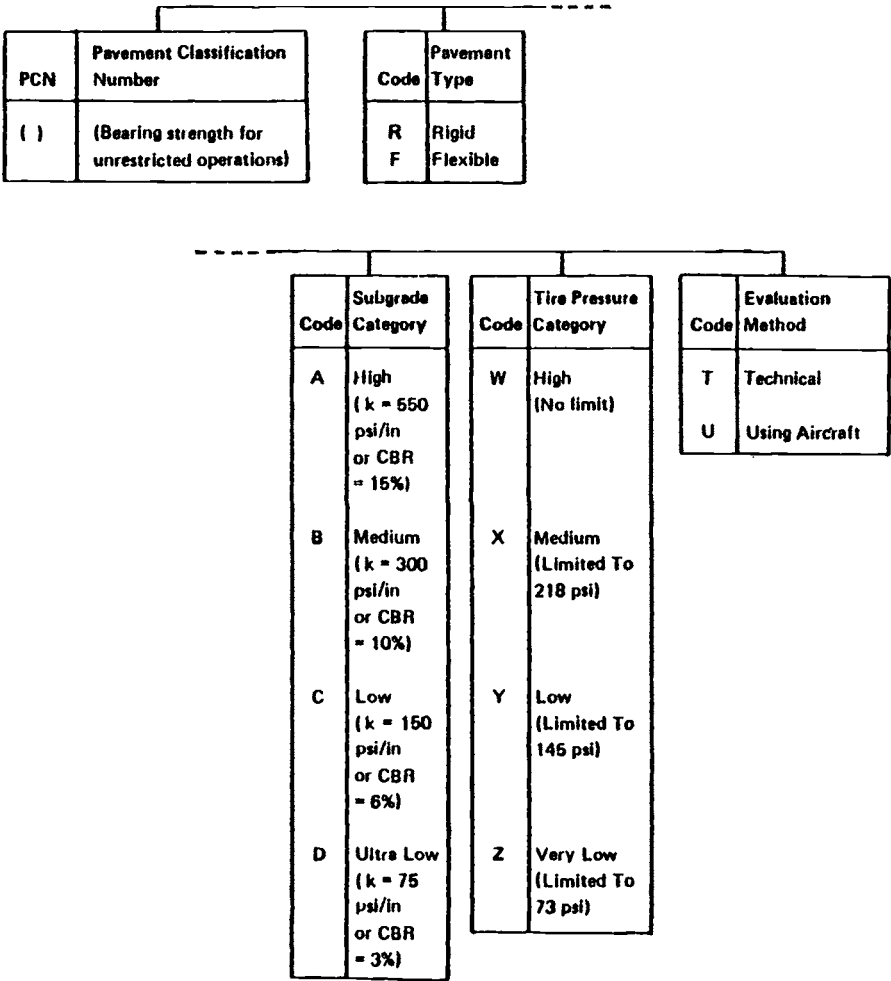


Fig. 12.26 Pavement classification number: category definitions.

values of 3, 6, 10, and 15 for 20,000 coverages. An example is shown in Fig. 12.25. If ACN's are required for weights or tire pressures below those used in the standard ACN evaluation, ICAO provides a chart to show appropriate correction factors.

ICAO Annex 14 shows ACN values for current aircraft, some of which are reproduced in Table 12.5. PCN values may be obtained by any method considered appropriate by the regulatory authority. As noted previously, if complete analyses are not available, then, if it is known that a certain aircraft at a certain weight represents the limit for that pavement (unlimited operation), calculations can be made to show the ACN, which in turn becomes the PCN. Figure 12.26 shows the basis for categorizing PCN. A

Table 12.6 PCN Evaluation Examples

| Technical evaluation | | | | | | | | | | | | | | | | | |
|---|-------------------|--|-------------------|---------|---------|------------|---------|---------|---------|--|--|---------------|-------------------|---------|---------|------|---------|
| <div style="border: 1px solid black; padding: 5px; margin-bottom: 5px;">PCC Concrete Slab 12" Thick (Ref.)</div> <div style="border: 1px solid black; padding: 5px;">Subgrade K 300</div> | PCN 46 RBXT | <div style="border: 1px solid black; padding: 5px; margin-bottom: 5px;">Asphalt Total Thickness 25" (Ref.)</div> <div style="border: 1px solid black; padding: 5px;">Subgrade CBR 10</div> | PCN 50 FBXT | | | | | | | | | | | | | | |
| <p>Assumption: PCA interior design criteria allowable working stress 399 psi.</p> <p style="text-align: center;">DC-10-30 authority 490,000 lb</p> | | <p>Assumption: U.S. Corps of Engineers S-77-1 criteria, passes = 10,000.</p> <p style="text-align: center;">DC-10-30 authority 480,000 lb</p> | | | | | | | | | | | | | | | |
| Using aircraft evaluation | | | | | | | | | | | | | | | | | |
| <p>Concrete pavement. Assume medium subgrade. Current maximum weight limit of aircraft.</p> <table style="width: 100%; border-collapse: collapse;"> <thead> <tr> <th style="text-align: left;">Aircraft type</th> <th style="text-align: left;">Maximum limit, lb</th> </tr> </thead> <tbody> <tr> <td>DC-8-63</td> <td>300,000</td> </tr> <tr> <td>L-1011-500</td> <td>430,000</td> </tr> <tr> <td>747-100</td> <td>700,000</td> </tr> </tbody> </table> <p>Plot these values on comparison chart of medium subgrade and adjust horizontal lines to match closest points and read PCN.</p> <p>Alternate: Read each aircraft chart for ACN at designated weight and find mean value of ACN. This will be reported on PCN.</p> <p style="text-align: center;">PCN = 50 RBXU</p> <p style="text-align: center;">DC-10-30 authority 510,000 lb</p> | | Aircraft type | Maximum limit, lb | DC-8-63 | 300,000 | L-1011-500 | 430,000 | 747-100 | 700,000 | <p>Flexible pavement. Unknown subgrade. Current maximum weight limit of aircraft. Assume medium subgrade.</p> <table style="width: 100%; border-collapse: collapse;"> <thead> <tr> <th style="text-align: left;">Aircraft type</th> <th style="text-align: left;">Maximum limit, lb</th> </tr> </thead> <tbody> <tr> <td>727-200</td> <td>130,000</td> </tr> <tr> <td>707-</td> <td>235,000</td> </tr> </tbody> </table> <p>Read ACN for 727 at 130,000 lb = 30. Read ACN for 707 at 235,500 lb = 34. Use 32 as mean value for PCN report.</p> <p style="text-align: center;">PCN = 32 FXBU</p> <p style="text-align: center;">DC-10-30 authority 350,000 lb</p> | | Aircraft type | Maximum limit, lb | 727-200 | 130,000 | 707- | 235,000 |
| Aircraft type | Maximum limit, lb | | | | | | | | | | | | | | | | |
| DC-8-63 | 300,000 | | | | | | | | | | | | | | | | |
| L-1011-500 | 430,000 | | | | | | | | | | | | | | | | |
| 747-100 | 700,000 | | | | | | | | | | | | | | | | |
| Aircraft type | Maximum limit, lb | | | | | | | | | | | | | | | | |
| 727-200 | 130,000 | | | | | | | | | | | | | | | | |
| 707- | 235,000 | | | | | | | | | | | | | | | | |

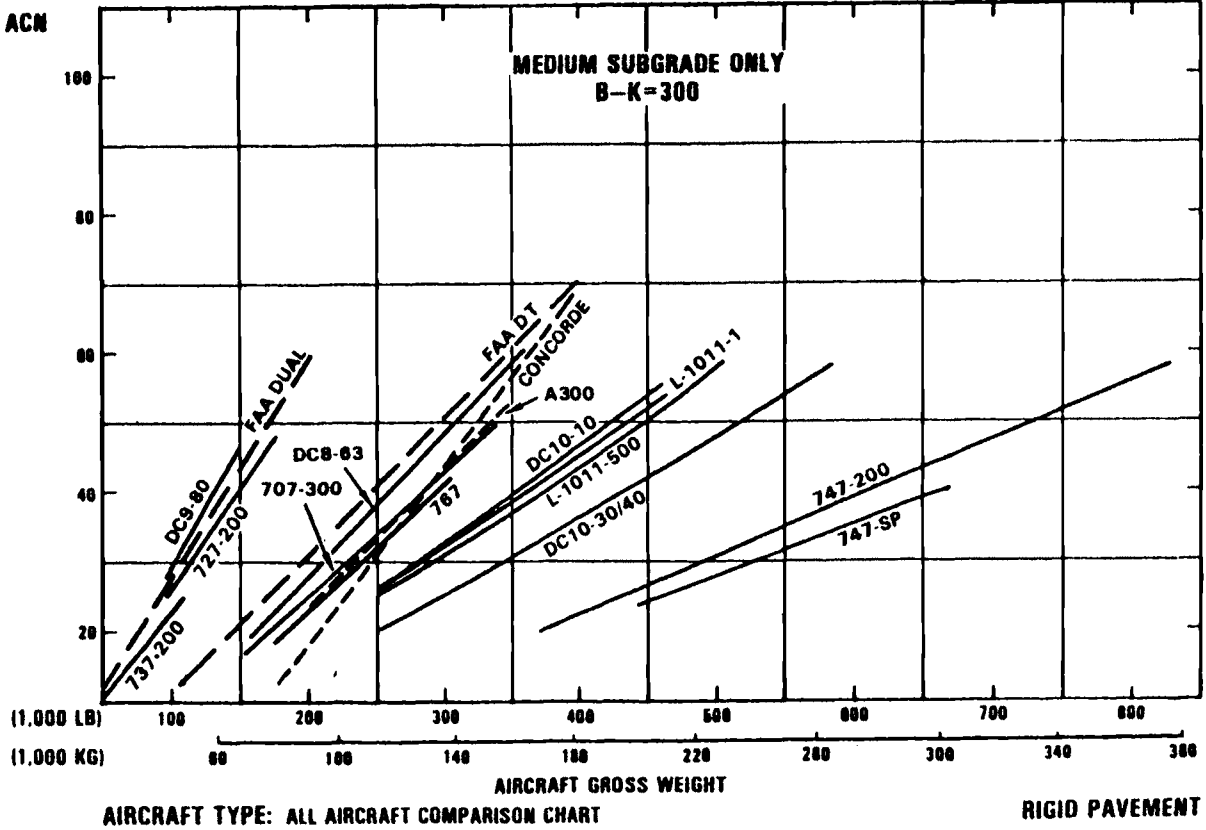


Fig. 12.27 Aircraft classification number comparisons.

value noted as 80 RBWT, for instance, represents a pavement with a PCN of 80 on a rigid surface, with a medium-strength subgrade, that can withstand high tire pressure and has been evaluated by technical analysis rather than using a limiting aircraft.

Table 12.6 shows examples of PCN calculations from a technical evaluation and a using aircraft evaluation. Figure 12.27 shows ACN values plotted vs aircraft weight for a number of aircraft on a rigid pavement with a medium subgrade.

12.9 ROUGHNESS

Airfield roughness affects both the landing gear and the airframe. But, this subject was not fully addressed until the 1960's when roughness was specified in terms of step bumps and $1 - \cos$ waves. There are two reasons why roughness is receiving increased attention:

1) Aircraft are becoming larger and therefore more flexible. Even on paved runways, aircraft fatigue life is now diminished somewhat due to roughness.

2) Military doctrine envisages operation from bomb damaged or unpaved airfields, with associated roughness in each case.

At one time, it was assumed that if the tire section height was large enough to "swallow" a bump, then that bump could be accommodated. This simplistic approach is considered in determining aircraft response and loads when encountering step bumps. But usually the capability to operate on roughness is more subtle and complex. For instance, the USAF specifies roughness in terms of a discrete bump height, bump amplitude vs wave length ($1 - \cos$), or power spectral density.

Runway profiles have been measured around the world and the data reduced to power spectral densities. From these, it is possible to analyze the resultant effects on the airframe.

Natural roughness is viewed as a mix of many heights and wavelengths, rather than a single or multiple $1 - \cos$ wave. This is an instance where the power spectral density becomes valuable. It is difficult to offer a simple definition of power spectral density, but one is provided in Ref. 16. It is measured in terms of square inches per radian per foot. Figure 12.28 shows the power spectral density levels for different airfield types. This figure is taken from MIL-A-8862A and must be used in determining ground loads.

Power spectral density data represent an average of the roughness over the runway length. As discussed in Ref. 17, it fails to distinguish between roughness due to, say, a few high-amplitude bumps and that due to many low-amplitude bumps of the same wavelength. Reference 18 states: "from the analysis of roughness data it was found that although spectral density bears a relation to runway profile and can be used to define a runway roughness, it does not provide an indication of the juxtaposition of bumps causing maximum response." For these reasons, it is usual to calculate the effects of the power spectra, $1 - \cos$ waves defined in Fig. 12.29 and discrete roughness to ensure that the landing gear and airframe are compatible with all of these. Recently, analyses have also focused on the ability to operate

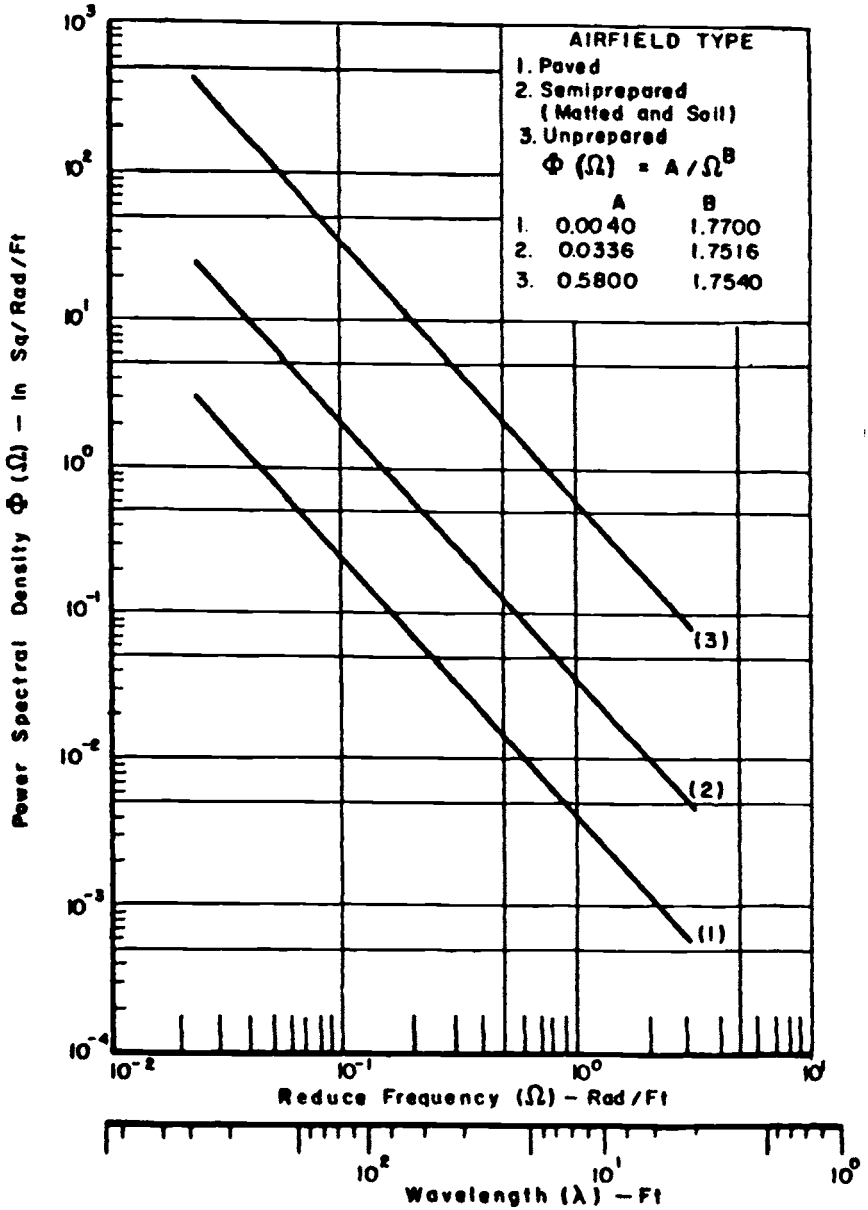
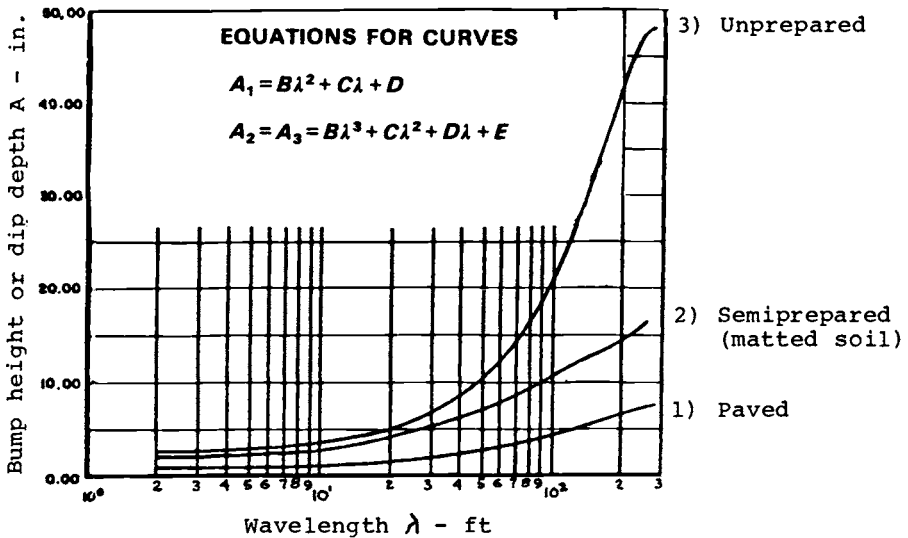


Fig. 12.28 Power spectral density levels for paved, semiprepared, and unprepared airfields (source: MIL-A-8862A).



Coefficients for airfield types 1, 2 and 3:

| | <i>B</i> | <i>C</i> | <i>D</i> | <i>E</i> |
|----|----------------------------|----------------------------|---------------------------|------------------------|
| 1) | -6.072637×10^{-5} | 4.157925×10^{-2} | 9.577638×10^{-1} | — |
| 2) | 0.958798×10^{-6} | -0.545150×10^{-3} | 0.133752×10^0 | 0.176436×10^1 |
| 3) | 0.325526×10^{-5} | 1.102307×10^{-3} | 0.107913×10^0 | 0.253442×10^1 |

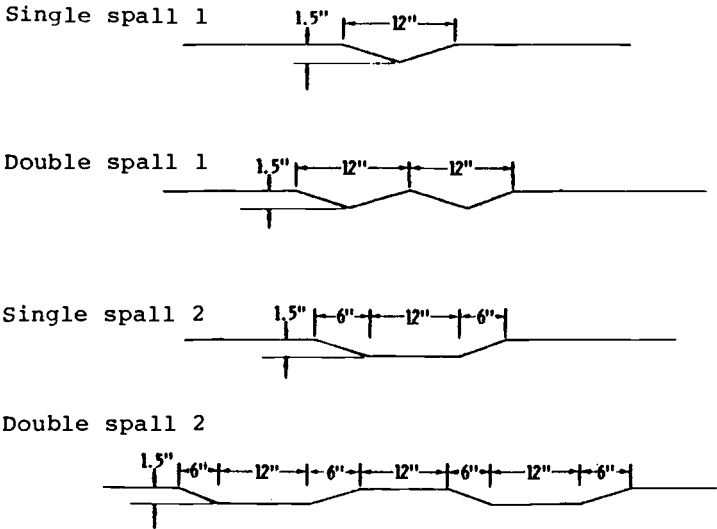
Fig. 12.29 Discrete 1 - cos bump heights or cos - 1 dip depths for paved, semi-prepared, and unprepared airfields (source: MIL-A-8862A).

over bomb-damaged and repaired runways. For analysis purposes, the definitions of the associated roughness are shown in Fig. 12.30.

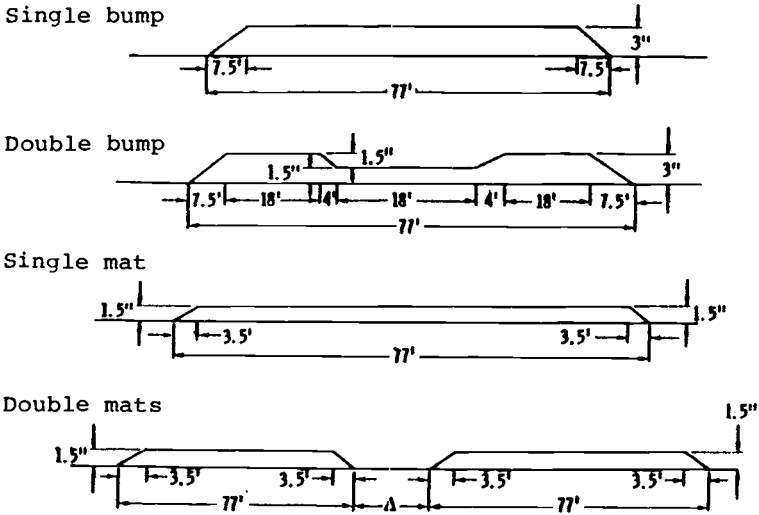
The analysis of operation over roughness involves a number of complex computer programs, the results of which may resemble the data shown in Fig. 12.31, where the braking coefficient and forward speeds were used as inputs to the measured field profile. It is also possible to have long 1 cos undulations with much smaller roughness superimposed upon it.

Reference 19 describes airfield roughness effects in the design of Douglas's entry in the C-5 competition, i.e., an aircraft having multiple main gear struts and many wheels. This concept had six shock struts and four wheels per strut. Reference 19 details the method used to analyze the roughness effects and discusses the complications caused by that type of gear traversing waves that may be at, say, 30 deg to the runway centerline. In this case, one of the 24 tires encounters the bump first and subsequently one of the shock absorbers is affected. While this strut is fully compressed, other struts and tires may be partially affected or not affected. Figure 12.32 shows a typical result of this analysis.

Various methods have been devised to relieve the peak loads from encountering bumps. Large-size tires and trailing-arm gears have obvious



a) Battle-damaged runways.



b) Bomb-damaged repaired runways.

Fig. 12.30 Typical damaged/repared runway roughness.

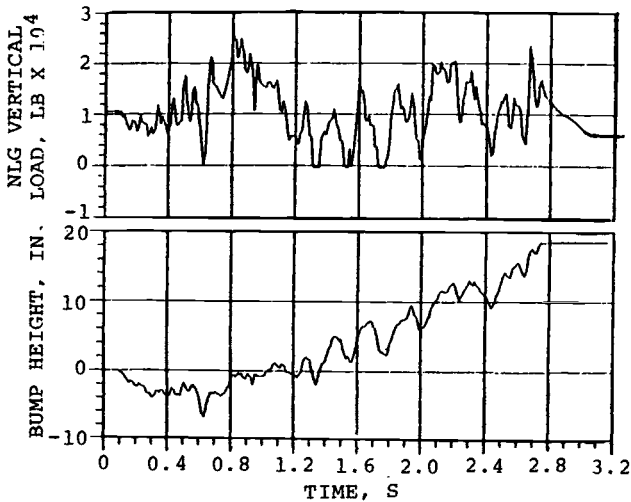


Fig. 12.31 Typical analysis of roughness data.

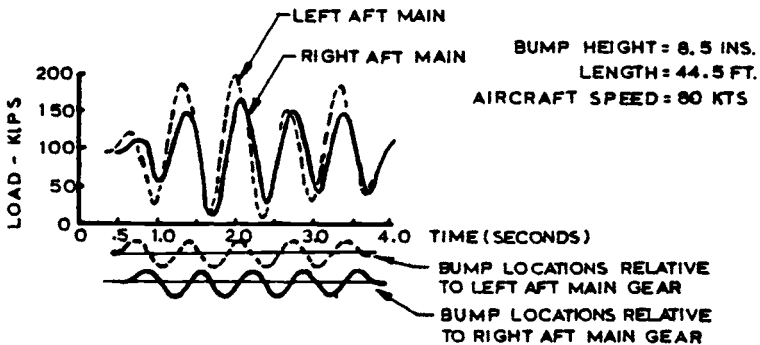


Fig. 12.32 Main landing gear vertical load time history for taxi over multiple 1 cos bumps at 30 deg angle (source: Ref. 19, reprinted with permission).

advantages. The double-acting strut is another method and is discussed in Chapter 5. It is used on the C-5. A spring-loaded piston valve is used on the OV-10 and is described in detail in Ref. 20. Another concept uses an acceleration-sensitive pressure relief valve and is described in Ref. 17.

References

¹"Aircraft Operations on Unsurfaced Soil, Soil Measurement and Analysis, Project Rough Road Alpha," Waterways Experiment Station, U.S. Army Corps of Engineers, Vicksburg, MS, Rept. TR3-624, June 1963.

²Gray, D. H. and Williams, D. E., "Evaluation of Aircraft Landing Gear Ground Flotation Characteristics for Operation from Unsurfaced Fields," Aeronautical

Systems Division, U.S. Air Force Systems Command, Rept. ASD-TR-68-34, Sept. 1968.

³Currey, N. S., "Aircraft Flotation Analysis—Current Methods and Perspective," SAE Paper 851936, Oct. 1985.

⁴Westergaard, H. M., "Stresses in Concrete Pavement Computed by Theoretical Analysis," *Public Roads*, Vol. 7, No. 2, April 1926.

⁵Westergaard, H. M., "New Formulas for Stresses in Concrete Pavements of Airfields," *Transactions of American Society of Civil Engineers*, Vol. 73, May 1947, pp. 687-701.

⁶"Planning and Design of Roads, Airbases, and Heliports in the Theatre of Operations," U.S. Dept. of the Army, Rept. TM5-330 (AFM 86-3, Vol. II), Sept. 1968.

⁷"Paving and Surfacing Operations," U.S. Dept. of the Army, Rept. TM-337, Feb. 1966.

⁸"Design of Concrete Pavement," Portland Cement Association, Chicago, 1955.

⁹Packard, R. G., "Computer Program for Concrete Airport Pavement Design (Program PDILB)," Portland Cement Association, Chicago, 1968. (Microcomputer software program, "Airport," Code MC 006X.)

¹⁰"Airport Paving," Federal Aviation Administration, Washington DC, Advisory Circular AC 150/5320-6C, Aug. 30, 1979.

¹¹"Flexible Pavement Design for Airfields," U.S. Dept. of the Navy, the Army and the Air Force, Navy DM-21.3, Army TM 5-825.2, and Air Force AFM 88-6, Chap. 2, Aug. 1978.

¹²"Rigid Pavements for Airfields other than Army," U.S. Dept. of the Air Force, AFM 88-6, Chap. 3 (TM5-824-3), Dec. 7, 1970.

¹³"Army Airfield and Helicopter Rigid and Overlay Pavement Design," U.S. Dept. of the Army, TM5-823-3, Oct. 1968.

¹⁴"Airfield Pavements," Naval Facilities Engineering Command, Alexandria, VA, NAVFAC DM-21, June 1973.

¹⁵Tereira, A. T., "Procedures for Development of CBR Design Curves," Waterways Experiment Station, U.S. Army Corps of Engineers, Vicksburg, MS, Info. Rept. S-77-1, June 1977.

¹⁶Taylor, James, *Manual on Aircraft Loads*, Pergamon, Oxford, UK, 1965.

¹⁷Ebers, R. S., "Landing Loads from Rough Terrain Environment," LTV Aerospace Corp.

¹⁸Walls, J. H., Houbolt, J. C., and Press, H., "Some Measurements and Power Spectra of Runway Roughness," NACA TN 3305, Nov. 1954.

¹⁹Reyder, D. M. and Mosby, L. B., "Ground Loads for Aircraft with Multiple Wheels and Multiple Landing Gear, and with Requirements for Semi-improved Airfield Operations," *Canadian Aeronautics and Space Institute Journal*, Nov. 1966.

²⁰Cook, C. E., Lane, A. G., and Smiley, T. T., "Rough Terrain Demonstration of the OV-10A," AIAA Paper 69-316, March 1969.

Bibliography

Flotation on flexible pavements:

Ahlin, R. G., "Developments in Pavement Design in the U.S.A.—Flexible Pavements," Paper presented at Third International Conference on the Structural Design of Asphalt Pavements, London, Sept. 1972.

Operation on bare soil:

Womack, L. M., "Tests with a C-130E Aircraft on Unsurfaced Soils," Waterways Experiment Station, U.S. Army Corps of Engineers, Vicksburg, MS, Feb. 1965.

Kraft, D. C., Hoppenjans, J. R., and Edelen, W. F., "Design Procedure for Establishing Aircraft Capability to Operate on Soil Surfaces," U.S. Air Force Flight Dynamics Laboratory, Rept. AFFDL-TR-72-129, Dec. 1972.

Williams, W. W., Williams, G. K., and Garrard, W. C. J., "Soft and Rough Field Landing Gears," SAE Paper 650844, Oct. 1965.

Loads due to roughness:

Kirk, C. L. and Perry, P. J., "Analysis of Taxiing Induced Vibrations in Aircraft by the Power Spectral Density Method," *Journal of the Royal Aeronautical Society*, Vol. 75, March 1971.

Firebraugh, J. M., "Estimation of Taxi Load Exceedances Using Power Spectral Methods," *Journal of Aircraft*, Vol. 5, Sept.-Oct. 1968.

Skidding:

Horne, W. B., "Skidding Accidents on Runways and Highways can be Reduced," *Astronautics and Aeronautics*, Vol. 5, Aug. 1967.

General discussion:

Newman, D. R., "Aircraft Design as Determined by Airport Facilities and the Environment," *Journal of the Royal Aeronautical Society*, Vol. 73, June 1969.

13

UNORTHODOX LANDING GEARS

In addition to the conventional wheel-type landing gears, many unorthodox types have been developed with the objective of improving a particular characteristic. Probably the most sought-after characteristic is to make the aircraft independent of runways. Hereil presents an excellent overview of such developments prior to 1955 in Ref. 1.

Runway independence is still a military priority, since neither general warfare nor low-intensity conflicts necessarily occur in close proximity to paved runways. This is particularly important on transport aircraft that must carry troops and supplies as close as possible to the battlefield. Evidence of USAF interest in runway independence is manifest in its 1986 contract award for the study of a cargo aircraft ground mobility system. This system will be capable of being “strapped on” current aircraft, enabling them to take off from extremely soft surfaces such as marshes, to land over tree stumps, and to taxi over ditches.

13.1 OVERALL REVIEW

Past unorthodox designs generally encompass skids, skis, tracks, and air cushions. The Wright Brothers were the first to use skids; they used them for landing, while the aircraft used a roller and trolley system for takeoff—a system that was emulated by the French S.E.5000 Baroudeur in more recent years. Skids have also been used for many years in an attempt to reduce aircraft weight. Germany was particularly active in their use during World War II. Their Arado 234 and Me 163 are typical examples of aircraft using skids.

Skis are used to permit aircraft operation on snow. Aircraft as large as the C-130 (155,000 lb) now use them to support activities in the Arctic, Antarctic, Alaska, and Greenland. Figure 13.1 shows an LC-130 providing logistic support to “Operation Deep Freeze” in the Antarctic—an exploration and research project that has been underway since 1960. Figure 1.11 showed more details of this aircraft. Ski installations are also quite common on relatively small aircraft operating in areas such as northern Canada; the DHC Beaver and Otter are regularly equipped with this type landing gear.

Various types of tracks have been developed to replace tires, wheels, and brakes; the system developed for the Convair B-36 (Fig. 1.9) is a typical example. In the 1948–1949 period, Boeing and Fairchild built tracked

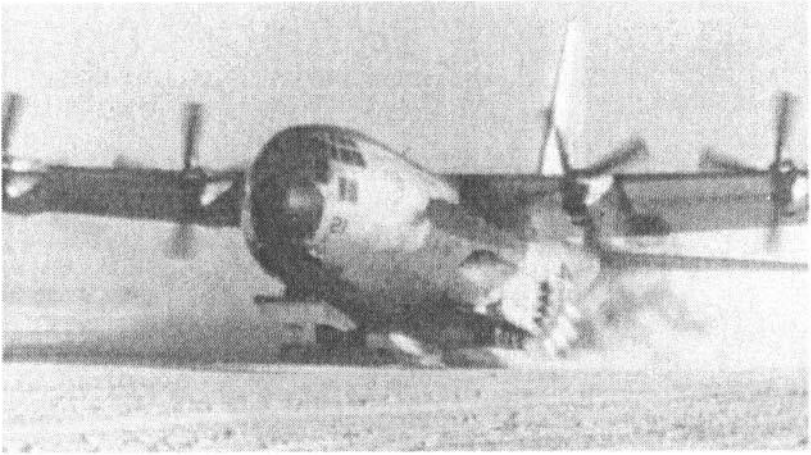


Fig. 13.1 Ski-equipped LC-130 aircraft.

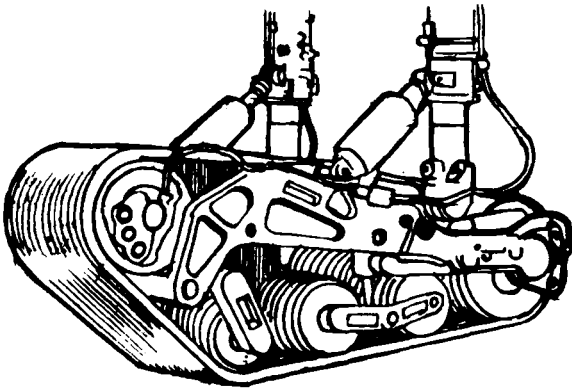


Fig. 13.2 Track gear on Fairchild C-82.

landing gears for their B-50 and C-82 (Fig. 13.2) aircraft, using designs prepared in the latter part of World War II by Britain's George Dowty who had designed such a gear for the Westland Lysander in 1940. The objective was to design a gear that would permit operation on soft and rough surfaces.

A completely different approach to tracked landing gears was developed by the Italian engineer, Count Bonmartini. In 1950, he installed one of his gears on a Piper Cub. He used a belt-like pneumatic tire to surround a number of articulated wheels, similar to a tank. Figure 13.3 illustrates one version of this system; other versions have different numbers of wheels. It is a relatively simple approach, but the weight penalty is severe.

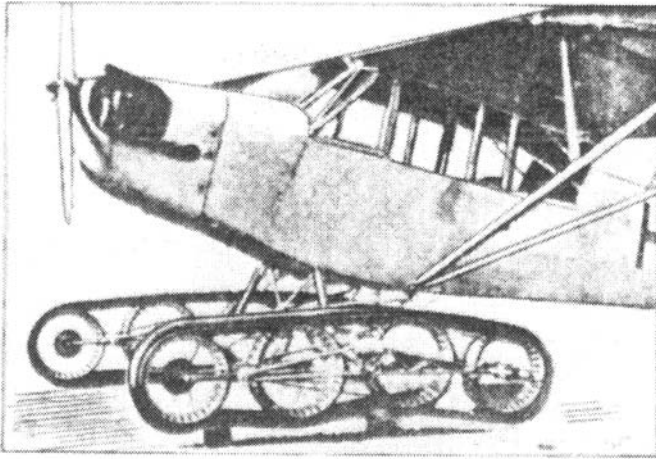


Fig. 13.3 Bonmartini gear.

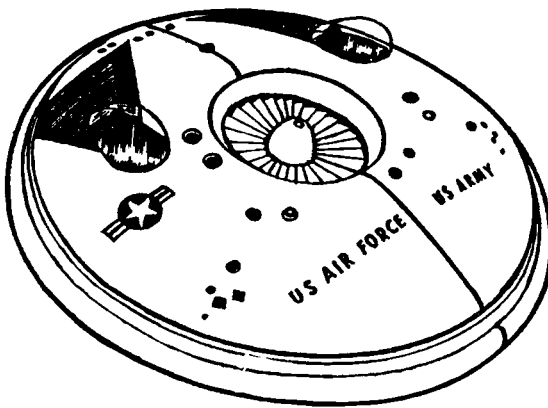
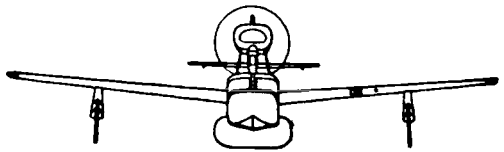


Fig. 13.4 Avrocar project.

The air-cushion landing system (ACLS) is the latest method for operating on austere airfields and is an extension of systems used on air-cushion vehicles. The system was developed by Bell Aerospace and the USAF Flight Dynamics Laboratory. The preceding air-cushion vehicles were known as ground effects takeoff and landing (GETOL) aircraft; Avro-Canada's Avrocar (Fig. 13.4) was one of the most interesting of the type. Powered by small turbojet engines installed inside the center of the vehicle, ducts distributed air to the entire periphery. A series of vanes on this periphery deflected the airflow appropriately to provide forces in whatever direction was desired.

The Bell-modified Lake LA-4 was the first aircraft to be fitted with ACLS. It was a relatively small aircraft, as noted in Table 13.1, and its success encouraged Bell and the USAF to proceed with a system for a

Table 13.1 Bell LA-4 ACLS Test Aircraft

**Dimensions****Aircraft**

| | |
|----------------|---------------------|
| Wing span | 38 ft |
| Overall length | 24.9 ft |
| Wing area | 170 ft ² |

Air cushion

| | |
|--------|--------------------|
| Length | 16 ft |
| Width | 3.8 ft |
| Area | 45 ft ² |

Loadings

| | |
|----------------------|--------|
| Wing loading | 15 psf |
| Air-cushion pressure | 55 psf |

Weight

| | |
|-----------------|---------|
| Gross operating | 2500 lb |
| ACLS | 258 lb |

Power Plants

Propulsion engine: Lycoming O 360 01A, 180 bhp rating

Air-cushion engine: modified McCulloch 4318F (driving two-stage axial fan), 90 bhp rating

Performance

| | | | |
|--------------|---------|-------------|--------|
| Cruise speed | 125 mph | Takeoff run | 650 ft |
| Stall speed | 54 mph | Landing run | 475 ft |

heavier aircraft, the de Havilland Aircraft of Canada CC-115 Buffalo. Since that time, proposals have been made for its use on various transport aircraft, but none have been pursued.

13.2 SKIDS

The general concept of using skids involves a trolley or roller device for takeoff and skids for landing, in which the takeoff device stays on the ground.^{2,3} Some aircraft, however, take off with their skids contacting the ground, using a high thrust/weight ratio and a fairly low-friction surface. Skids are usually lighter than an equivalent wheeled gear; they require less maintenance, are more reliable, and should be less expensive due to the absence of brakes and skid control systems. Their large contact area should also provide superior performance on a soft surface; the skids on the Baroudeur, for instance, apply a ground pressure of 14 psi. This aircraft also incorporates a device to increase the braking force by rotating the skids slightly so that, in plan view, the skids are angled outward from the aircraft centerline. These skids are made from magnesium alloy castings with steel shoes. A layer of plastic is placed between these layers for thermal insulation. The primary disadvantage of the skid is that the aircraft

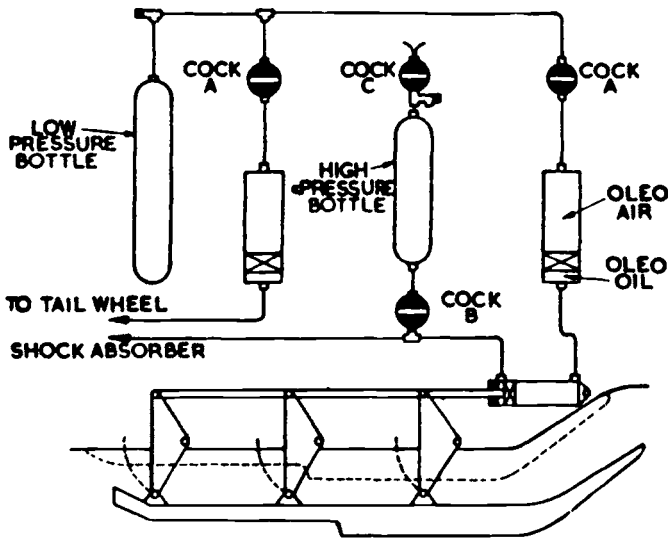


Fig. 13.5 Me 163 skid.

lacks maneuverability on the ground. To overcome this problem, some skids also have a small retractable wheel—but, obviously, this detracts from the skid's low-weight, low-cost, easy-maintenance advantages.

Conway³ quotes some weights for the Me 163. Its total landing gear weight was 217.5 lb, which represented only 2.4% of the aircraft's takeoff weight and 4.7% of landing weight—close to one-half of the values usually associated with wheeled gears. He also diagrammed the skid support mechanism, reproduced here as Fig. 13.5.

Reference 3 also provides some useful guidelines in designing a modern skid, although it seems that composite materials, which have become available since Conway wrote his book, could be used effectively for the skid. His design utilizes a skid angled nose-up by about 15 deg so that its tail contacts the ground first. Its nose is turned upward to ride over 4 in. obstacles and the skid is attached to an oleo-pneumatic strut that also incorporates devices to keep the nose up.

13.3 SKIS

Skis are commonly used for landing on snow and as such they present some problems that are different from skids.⁴⁻⁶ The ski-to-snow friction coefficient is low (about 0.03); consequently, there is very little force to prevent the aircraft from drifting in a crosswind landing. To enable the aircraft to operate also from no-snow surfaces, the ski-equipped aircraft are often equipped with wheels that can be extended as required below the ski or, conversely, the ski is designed to be moved up and down with respect to the wheels. The LC-130 is an example of the latter technique. In

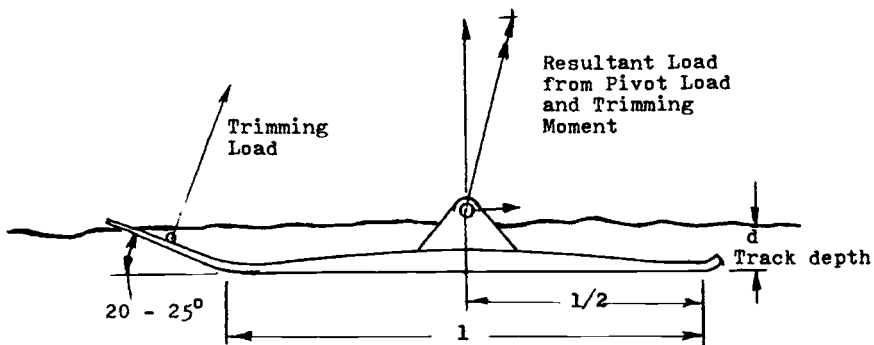


Fig. 13.6 Ski dimensions (source: Ref. 6).

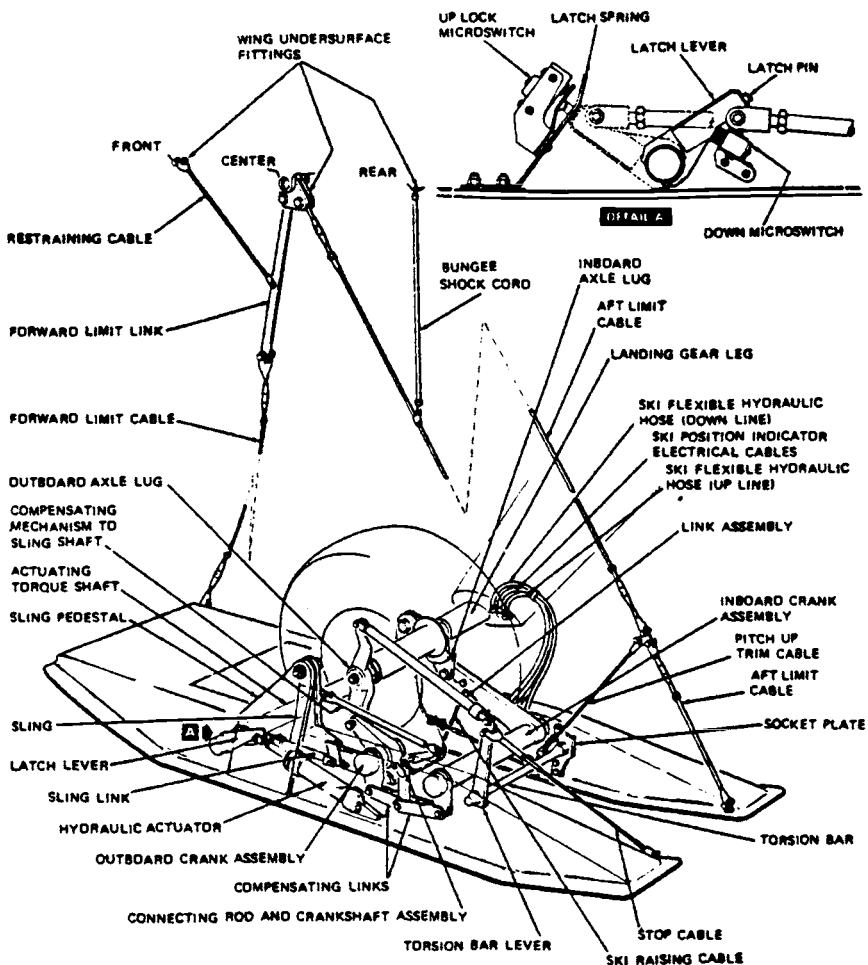


Fig. 13.7 Main wheel ski of DHC 6 Twin Otter (source: de Havilland Aircraft of Canada).

some cases, the wheels merely project below the ski so that when landing on snow the wheels sink until the ski supports the aircraft.

Skis are usually designed so that they attach to the axles. According to Ref. 7, the ski should have a length/width ratio of 6, a contact pressure of 3.5 psi, and the load axis from the axle to the ski should pass through, or close to, the center of the ski. The ski's lower surface should be covered with a material that improves the coefficient of sliding friction and reduces wear rate. Some of these recommendations are summarized in Fig. 13.6. Figure 13.7 is included to show a typical ski—in this case, the one used on the DHC-6 Twin Otter main gear.

13.4 TRACKS

The fact that tracked landing gears have never gone beyond the experimental stage indicates that the wheeled gear is still preferable. Their objective of being able to use soft, unlevelled surfaces by using large contact areas was more or less met, but their problems were never overcome. In later years, wheeled gears, such as that on the C-5 transport, also permitted operation on such surfaces by using many tires, large-diameter tires, and double-acting shock absorbers.

The track concept involves wrapping a belt round a number of track gears or rollers. Static pressures on the Fairchild and B-50 gears were 14 and 50 psi, respectively, and their problems were as follows:

- 1) In crosswind landings, the belt tended to slide off the rollers.
- 2) The gear required a high degree of maintenance.
- 3) Wheel bearing rotational speeds were extremely high, which caused failures.
- 4) High rolling resistance was encountered during takeoff.
- 5) Braking loads caused adhesion problems between the belt and rollers, as well as excessive loads that were transferred to the structure.
- 6) Retraction was abnormally difficult.
- 7) A high weight penalty was unavoidable. On the Fairchild C-82, the track gear was 650 lb heavier than the wheeled gear, a penalty of 1.8% gross weight. On the B-50, the penalty was 4500 lb and 2.7% of gross weight; on the B-36 gear, it was 1.9% of gross weight.

13.5 AIR-CUSHION LANDING SYSTEM (ACLS)

The theory of the ACLS is thoroughly detailed in Ref. 11. The subject is too complex to be detailed in this book, so an overview is given with many references for further reading on the subject. Reference 11 provides all of the mathematics involved and Fig. 13.8 shows a cross section through the trunk. This trunk forms a "doughnut-like" configuration beneath the aircraft similar to that illustrated in Fig. 13.9. Air is supplied to the trunk by a turbojet engine (for example) and exits the trunk through a series of angled holes on its lower surface. The air discharged from the trunk creates an air cushion beneath the aircraft. A layer of air acts as a lubricant between the trunk and the ground.

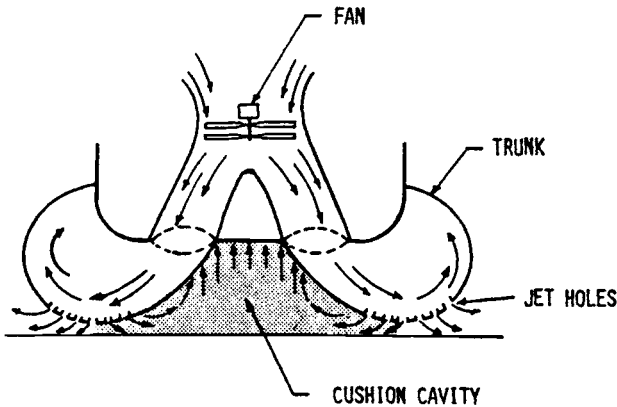


Fig. 13.8 Section through ACLS trunk.

For braking, skid pads and pillows have been employed. These are usually made from tire tread-like material and are “pushed” against the ground when the pilot applies brake pressure.

During a flight, the trunk is deflated and pulled in to the side of the aircraft. There are two basic types of trunk material: elastic and inelastic. The former pulls in to the fuselage automatically, while the latter must use cables (for instance) to pull it in and in its retracted form it has a concertina-like configuration.

ACLS Advantages and Disadvantages

The advantages of ACLS are: 1) operation from very soft and rough surfaces, including ice, snow, and marsh; 2) landing in a slewed attitude in a crosswind; 3) built-in kneeling capability; and 4) using an externally-applied force, the aircraft can be moved easily to a desired location.

Its disadvantages are: 1) need for continuous power; 2) need for separate support when aircraft is parked; 3) poor steering capability and directional control; 4) considerable dust clouds generated; 5) braking less responsive than wheel brakes; 6) high wear rate on the trunk (particularly on paved surfaces); and 7) bag creep and sag.

To illustrate the ACLS capability, the Lake LA-4 which was converted by Bell and first flown on Aug. 4, 1967, operated in 15–24 in. of high grass, over ploughed ground, over tree stumps as high as 14 in., over 3 ft wide ditches, on soft muddy ground, and over both sand and water.¹²

According to Bell Aerospace, the ACLS is lighter than an equivalent wheeled gear. Bell has developed the data shown in Fig. 13.10. Conventional gears weight about 5% of aircraft gross weight, but Bell predicts that the ACLS could be developed with less than 3% gross weight. An overall discussion of ACLS and its feasibility is presented in Ref. 13.

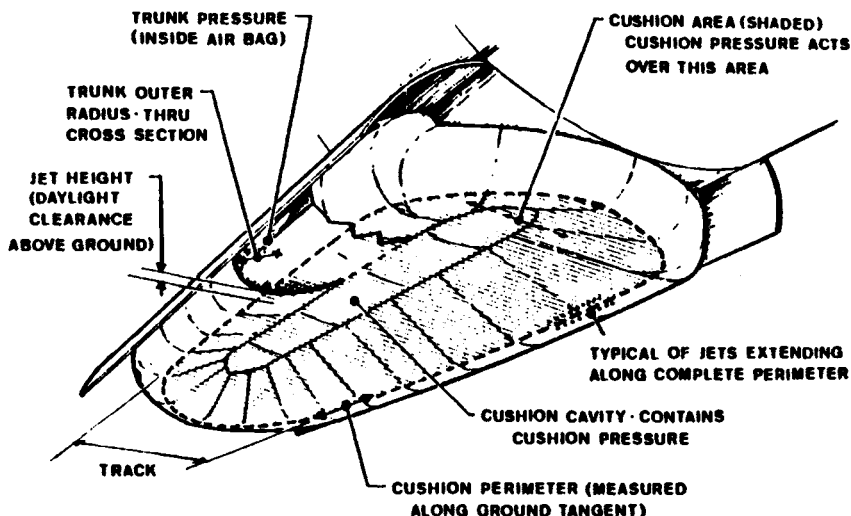


Fig. 13.9 Air cushion landing gear.

ACLS Applied to the Buffalo and Jindivik

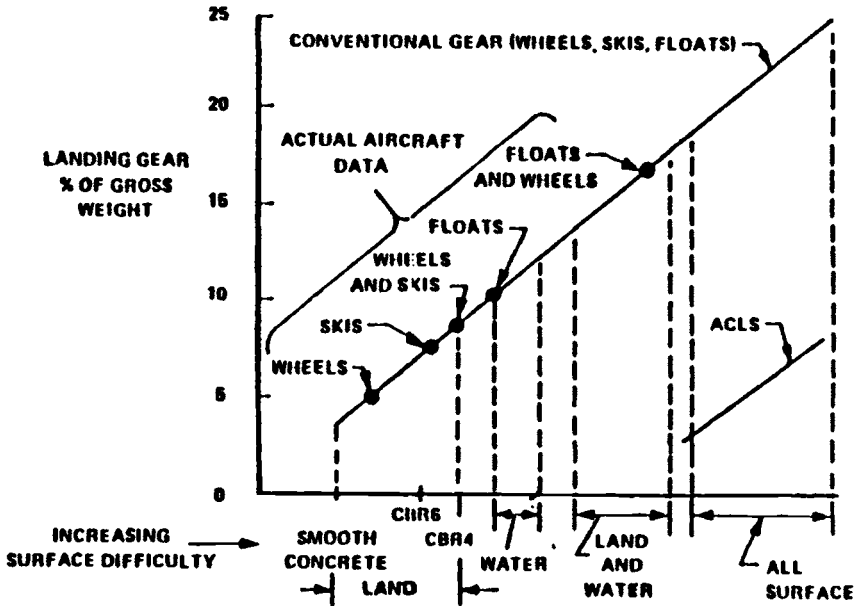
The ACLS has been installed on modified versions of the de Havilland Aircraft of Canada CC-115 Buffalo (XC-8A) and the Australian Government Aircraft Factories Jindivik. The former was a 41,000 lb transport and the latter was a small remote-piloted vehicle.

The Buffalo project¹⁴ was a joint Canadian/United States effort with Bell as the prime contractor. Its first flight was on March 31, 1975. Hamilton Standard modified the propellers to give the pilot direct control of the blade angle ("Beta control"), so that directional control capability would be improved.

The Buffalo's ACLS trunk was inflated by a pair of two-stage axial-fan compressors, each of which was driven by an ST-70 gas turbine mounted in the wing "armpit." Either of these engines could inflate and maintain the trunk pressure. The trunk had approximately 6800 holes on its lower surface and the trunk's footprint area was about 240 ft². With the aircraft weighing 41,000 lb, this is equivalent to 171 psf (1.2 psi) contact pressure.

The aircraft's roll stability was poor at speeds below 60 knots due to the narrow "tread" of the cushion and the loss of aerodynamic control effectiveness at these speeds. As a result of this, the Buffalo was equipped with outrigger pontoons. Six rubber pads were used for braking, each one having a surface area of about 340 in.², but the responsiveness was disappointing with an excessive time lag between brakes on and off. Other problems on the XC-8A were trunk flutter when operating on paved surfaces, low bag life (three bags used in 84 h), and foreign object damage in the engines.

The Jindivik program is discussed in Ref. 15. It was a joint United States/Australian program, with the Australians providing the vehicle and the testing conducted at the USAF Flight Dynamics Laboratory, NASA Langley, and NASA Lewis.



| WHEEL GEAR | | ACLS | |
|--------------|----------------|-------------------|----------------|
| WHEELS | 418.3 | TRUNK SHEET | 975.0 |
| TIRES | 586.0 | BLADDER | 85.0 |
| TUBES | 87.5 | PILLOWS | 60.0 |
| BRAKES | 396.0 | BRAKE SKIDS | 230.0 |
| AIR | 13.5 | AIR | 10.0 |
| | <u>1,501.3</u> | | <u>1,360.0</u> |
| SHOCK STRUTS | 1,675.4 | AUXILIARY ENGINES | 956.5 |
| TRUSSES AND | 714.6 | INSTALLED | |
| LOCKS | | FAN INSTALL | 988.0 |
| | <u>2,390.0</u> | FUEL SYSTEM AND | 340.0 |
| | | FUEL | |
| | | | <u>2,284.5</u> |
| OPERATING | 805.6 | TRUNK ATTITUDE | 563.0 |
| MECHANISM | | AND CONTROLS | |
| AND CONTROLS | | | <u>4,107</u> |
| | <u>4,697.</u> | | |

Fig. 13.10 ACLS weight data (source: Textron Marine Systems).

ACLS Design Data

If an elastic trunk material is used, it can be expected to extend to about 250% of its normal size as a design point. A typical load/stretch curve is given in Fig. 13.11. Typical drag values are shown in Fig. 13.12.

Trunk material selection depends on many factors. There is a large choice of materials, including 17 cloth-like fabrics of various weave, natural rubber, Spandex, Butyl, neoprene, polyurethane, Teflon, hypalon, Viton, Kevlar, and silicone rubber. Earl¹⁷ suggests that, essentially, the material must provide controlled shape when inflated, strength, high tear resistance, ability to sustain damage without catastrophic failure, air containment, and

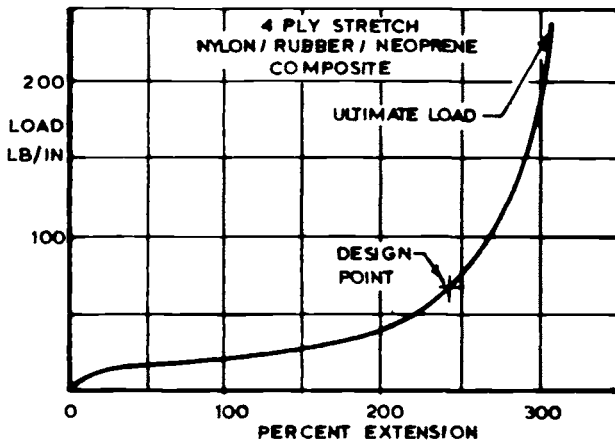


Fig. 13.11 ACLS trunk material stretch data (source: Ref. 16).

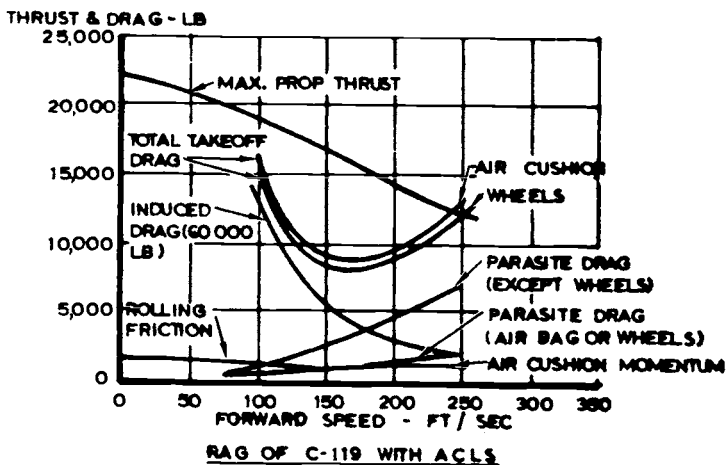


Fig. 13.12 Drag of C-119 with ACLS (source: Ref. 16).

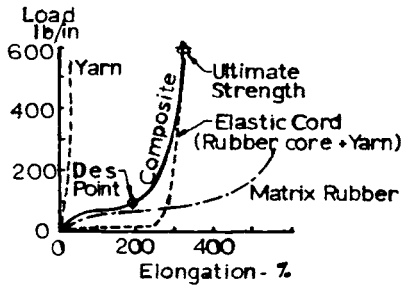


Fig. 13.13 Characteristics of composite trunk materials.

retraction elasticity. To obtain these characteristics, fabric is used to control the shape and to provide strength, while a rubber is used for retraction. The characteristics of such a composite are depicted in Fig. 13.13. In the LA-4 and Buffalo programs, nylon and natural rubber were chosen, but if Kevlar had been available at that time it would probably have been used instead of nylon because of its superior strength. Both materials have high strength-to-weight ratios, however, and adhere well to rubber.

On the XC-8A Buffalo program, the material had bidirectional stretch to avoid wrinkles, gathers, or bulges when retracted. Its characteristics are shown in Fig. 13.14. That material was very well suited to damage containment; in one case, a 8 ft² hole caused the total trunk depth to decrease by only 9%.

It was noted previously that braking is accomplished by pads or expanded pillows being pushed against the ground. Conventional brakes develop an average friction coefficient of about 0.35 during a landing ground roll on dry concrete; this can be compared with candidate ACLS brake pad materials illustrated in Fig. 13.15. Their wear rates are compared in Fig. 13.16. Temperature buildup must be checked to make sure that it does not exceed the allowable value for the adjacent trunk material. A typical contact pressure for the brake pads would be 14 psi.

Design Equations

Referring again to Ref. 16, power requirements can be estimated by extrapolating the performance of the ACLS models that have been tested. For the purpose of this estimate, the ACLS is assumed to behave as a plenum chamber. This is a conservative assumption, since the peripheral jet system is generally more effective than the plenum system. Flow from the plenum is predicted by applying the continuity relationship to the exit plane of the plenum. The exit is illustrated in Fig. 13.17.

Plenum flow is given by the following equation:

$$Q = V \cdot d \cdot S \cdot C_D \quad (13.1)$$

where

- Q = plenum flow
 V = air velocity, ft/s
 d = clearance height, ft
 S = periphery of plenum, ft
 C_D = discharge coefficient

In addition,

$$\frac{P_c}{\rho} + \frac{V_c^2}{2g_0} = \frac{P}{\rho} + \frac{V^2}{2g_0} \quad (13.2)$$

where

- g_0 = acceleration due to gravity, 32.2 ft/s²
 V = velocity from plenum, ft/s
 P = pressures outside plenum, lb/ft² abs
 ρ = air density
 P_c = plenum (cushion) pressure
 V_c = air velocity in plenum

The velocity in the plenum V_c can be assumed to be negligible. Therefore, Eqs. (13.1) and (13.2) give an equation for the flow in the plenum as

$$Q = \left(\frac{2g_0 \cdot P_c}{\rho} \right)^{1/2} d \cdot S \cdot C_D \quad (13.3)$$

where P_c is in pounds per square foot gage.

The air horsepower delivered to the plenum is

$$\text{hp} = P_c Q / 550 \quad (13.4)$$

where hp is the air horsepower.

Substituting Eqs. (13.3) and (13.4), and rearranging, gives

$$\frac{\text{hp}}{(P_c)^{3/2} \cdot S} = \frac{d C_D}{550} \left(\frac{2g_0}{\rho} \right)^{1/2} \quad (13.5)$$

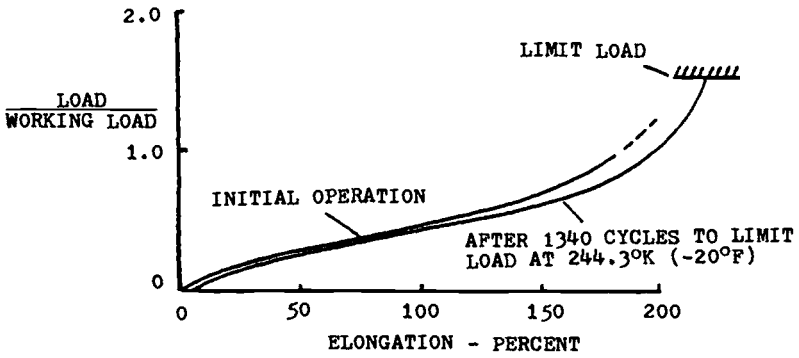
The pressure in the air cushion is totally determined by the aircraft weight and fuselage cushion area as

$$P_c = W/A \quad (13.6)$$

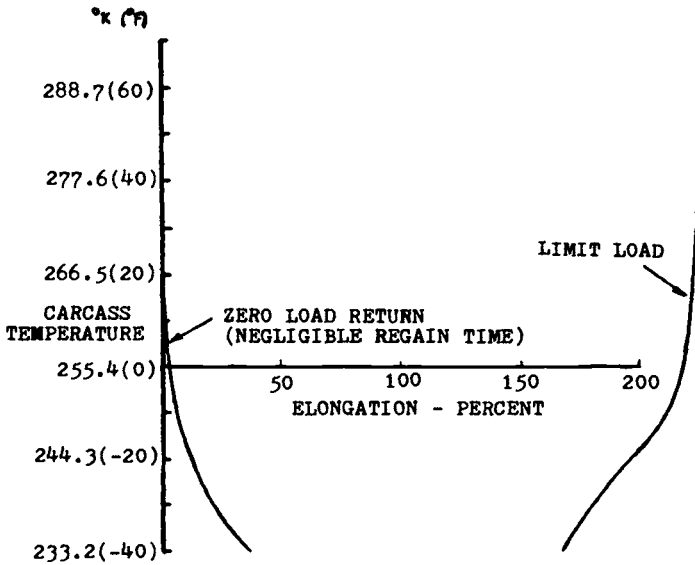
where W is the aircraft weight and A the fuselage cushion area.

Substituting Eq. (13.6) in Eq. (13.5) gives

$$\frac{\text{hp}(A)^{3/2}}{S \cdot (W)^{3/2}} = \frac{d C_D}{550} \left(\frac{2g_0}{\rho} \right)^{1/2} \quad (13.7)$$



a) Effect of low-temperature cycling on trunk material elasticity at 294.3°K (70°F).



b) Low-temperature set and stiffening characteristics.

Fig. 13.14 XC-8A trunk material.

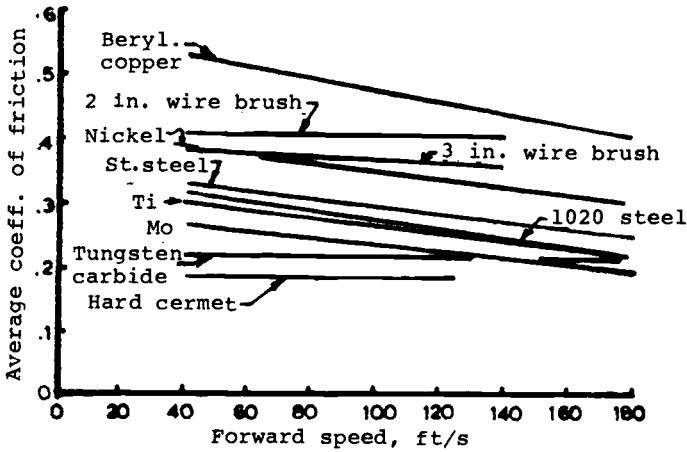


Fig. 13.15 Friction coefficients of skid brake materials.

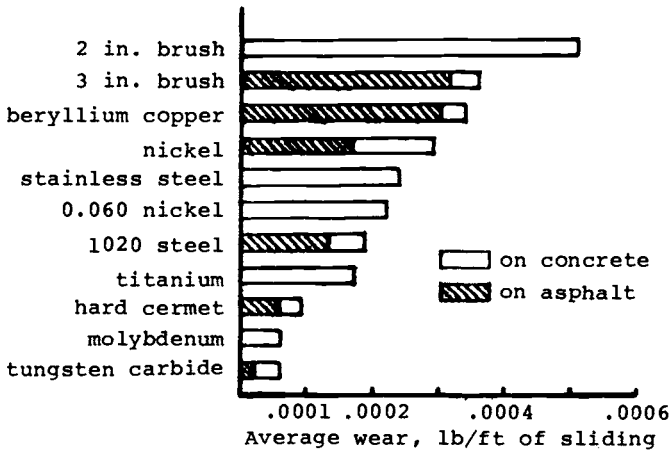


Fig. 13.16 Wear rates of skid brake materials.

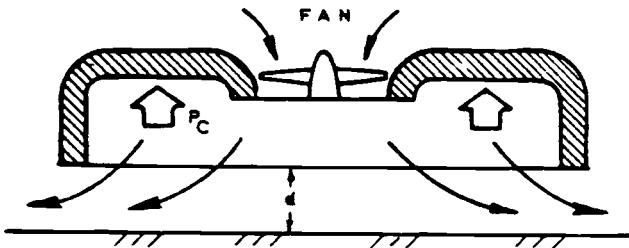


Fig. 13.17 Plenum-type air cushion vehicle.

Equation (13.7) is now used as a basis for extrapolating the power requirements. It shows that, to minimize the power consumption for a given weight, it is desirable to maximize the fuselage area and minimize the periphery, jet height, and discharge coefficient.

Finally, as Digges¹⁶ points out, the ACLS provides a penalty in takeoff distance on hard-surface runways due to the drain in engine power unless supplementary ACLS power is provided. However, on soft runways, this power drain is more than compensated for by the elimination of wheel sinkage and rutting. This feature offers a significant weight saving as well as improvements in flotation and rough-field performance.

References

¹Hereil, G., "Making Aeroplanes Independent of Runways," *Journal of the Royal Aeronautical Society*, Vol. 59, June 1955, pp. 381-414.

²"Aircraft with Skids," *R.A.F. Review*, Nov. 1952, Aug. 1953.

³Conway, H. G., *Landing Gear Design*, Chapman & Hall, London, 1958, p. 323.

⁴"Aluminum Aircraft Skids," *Modern Metals*, May 1947.

⁵Bursh, A. A., "Skis Broaden Aircraft Utility," *Aero Digest*, Sept. 1947.

⁶Klein, G. J., "The Snow Characteristics of Aircraft Skis," National Research Council (Canada), Rept. NRC MM 57, April 1946.

⁷Klein, G. J., "Aircraft Ski Research in Canada," National Research Council (Canada), Rept. NRC MM225, Aug. 1950.

⁸Guderian, G., "Track Undercarriages for Aircraft," *Interavia*, No. 8, 1954.

⁹McSurely, A., "New C82 Installation Developed by Fairchild and Firestone," *Aviation Week*, July 5, 1948, p. 21.

¹⁰Schoenen, H., "The Caterpillar Takes to the Air," *Aero Digest*, Jan. 1950.

¹¹Digges, K. H., "Theory of an Air Cushion Landing System for Aircraft," Air Force Flight Dynamics Laboratory, Rept. AFFDL-TR-71-50, June 1971.

¹²Stauffer, J. R., "Water Operations and Overland Braking Test Report of an Air Cushion Landing System (LA-4)," Bell Aerospace Div., Textron, May 1970.

¹³Earl, T. D., "Air Cushion Landing Gear Feasibility Study," U.S. Air Force Flight Dynamics Laboratory, Rept. AFFDL-TR-67-32, 1967.

¹⁴Coles, A. V., "Air Cushion Landing System CC-115 Aircraft," U.S. Air Force Flight Dynamics Laboratory, Rept. AFFDL-TR-72-4, May 1972.

¹⁵Vaughan, J. C. III, "Air Cushion Take-Off and Landing Systems for Aircraft," *Canadian Aeronautics and Space Journal*, Vol. 21, June 1975, pp. 205-209.

¹⁶Digges, K. H., "Air Cushion Landing System Requirements," U.S. Air Force Flight Dynamics Laboratory, May 1970.

¹⁷Earl, T. D., "Elastically Retracting ACLS Trunks," *Canadian Aeronautics and Space Journal*, Vol. 21, May 1975, pp. 169-173.

Bibliography

Earl, T. D., "Air Cushion Landing Gear for Aircraft," U.S. Air Force Flight Dynamics Laboratory, Rept. AFFDL-TR-68-124, Jan. 1969.

Gardner, L. H., Pizzichemi, C. J., and Milns, P., "STOL Tactical Aircraft Investigation, Vol. VI: Air Cushion Landing System Study," U.S. Air Force Flight Dynamics Laboratory, Rept. AFFDL-TR-73-19, May 1973.

Han, L. S., "Air Cushion Pressure during STIFF-Operation for Air Cushion Landing System," U.S. Air Force Flight Dynamics Laboratory, Rept. AFFDL-TR-71-4, May 1971.

Stauffer, C. L., "Ground/Flight Test Report of Air Cushion Landing Gear (LA-4)," U.S. Air Force Flight Dynamics Laboratory, Rept. AFFDL-TR-69-23, Sept. 1969.

Wyen, G. R., "An Experimental Evaluation of the Isentropic Airflow Assumption for an Aircraft Air Cushion Landing System," U.S. Air Force Flight Dynamics Laboratory, Rept. AFWAL-TR-82-3097, 1982.

14

DESIGN DATA

This chapter provides a summary of data that may be useful to the landing gear designer. It includes tables of information on various aircraft to permit comparative flotation evaluation, tables showing landing gear characteristics and tires used, illustrations of typical landing gears, and detail design data. The tables are self-explanatory and no discussion is therefore provided.

Table 14.1 Commercial Aircraft Characteristics for Flotation Analysis

| Airplane designation | Max gross weight, × 1000 lb | Main landing gear | | | |
|----------------------|-----------------------------|-------------------|------------|-------------------------|-------------------|
| | | Wheels per strut | Tire size | Inflation pressure, psi | Type ^a |
| DC-3 | 28.0 | 1 | 170.0 × 16 | 50 | S |
| DC-4 | 82.5 | 2 | 15.5 × 20 | 82 | T |
| DC-6B | 107.0 | 2 | 15.5 × 20 | 107 | T |
| DC-7C | 143.0 | 2 | 17 × 20 | 127 | T |
| DC-8-63F | 358.0 | 4 | 44 × 16 | 200 | TT |
| DC-9-41 | 115.0 | 2 | 41 × 15 | 165 | T |
| DC-10 | 533.0 | 4 | 50 × 20-20 | 185 | — ^b |
| L-100-30 | 155.0 | 2 | 56 × 20 | 105 | ST |
| L-1011 | 409.0 | 4 | 50 × 20 | 175 | TT |
| L-188 | 116.0 | 2 | 13.5 × 16 | 135 | T |
| L-1049 | 140.0 | 2 | 17.0 × 20 | 130 | T |
| B-707-320C | 336.0 | 4 | 46 × 16 | 180 | TT |
| B-720B | 235.0 | 4 | 40 × 14 | 145 | TT |
| B-727-200 | 173.0 | 2 | 49 × 17 | 168 | T |
| B737-200 | 111.0 | 2 | 40 × 14 | 145 | T |
| B-747B | 775.0 | 4 | 46 × 16 | 210 | DTT |
| Convair 440 | 50.0 | 2 | 34 × 9.9 | 75 | T |
| 880 | 185.0 | 4 | 39 × 13 | 150 | TT |
| 990 | 253.0 | 4 | 41 × 15 | 170 | TT |
| A300B4-200 | 365.7 | 4 | 49 × 17 | 180 | TT |
| F-27-40 | 43.5 | 2 | 33.4 × 9.7 | 80 | T |
| C-160 | 112.4 | 2 | 15.0 × 16 | 55 | TT |

^aS = single wheel, T = twin wheel, TT = twin-tandem wheel, ST = single-tandem wheel, DTT = double twin tandem.

^bTT each side plus T midfuselage.

Table 14.2 Military Transport Aircraft Characteristics for Flotation Analysis

| Airplane designation | Max gross weight × 1000 lb | Main landing gear | | | |
|----------------------|-------------------------------|-------------------|-----------|-------------------------|-------------------|
| | | Wheels per strut | Tire size | Inflation pressure, psi | Type ^a |
| C-5A | 769.0 | 6 | 49 × 17.0 | 155 | — ^b |
| C-7A | 28.5 | 2 | 11.0–12.0 | 40 | T |
| C-8A | 38.0 | 2 | 15.0–12 | 45 | T |
| C-9A | 108.0 | 2 | 40 × 14 | 155 | T |
| C-47D | 33.0 | 1 | 17.0–16 | 56 | S |
| C-54G | 82.5 | 2 | 15.5–20 | 82 | T |
| C-97G | 187.0 | 2 | 55.0–16 | 175 | T |
| C-118A | 112.0 | 2 | 15.5–20 | 120 | T |
| C-119G | 72.7 | 2 | 15.5–20 | 80 | T |
| C-121G | 145.0 | 2 | 17.2–20 | 145 | T |
| C-123K | 60.0 | 2 | 17.0–20 | 81 | T |
| C-124C | 216.4 | 2 | 25.0–28 | 65 | T |
| C-130A | 124.2 | 2 | 56 × 20.0 | 65 | ST |
| C-130B | 135.0 | 2 | 56 × 20.0 | 75 | ST |
| C-130E | 175.0 | 2 | 56 × 20.0 | 95 | ST |
| C-130H | 175.0 | 2 | 56 × 20.0 | 96 | ST |
| C-131E | 60.5 | 2 | 12.5–16 | 70 | T |
| C-133B | 300.0 | 4 | 20.0–20 | 95 | TT |
| C-135A | 277.5 | 4 | 49 × 17 | 170 | TT |
| C-140A | 42.0 | 2 | 26 × 6.6 | 205 | T |
| C-141B | 316.1 | 4 | 44 × 16 | 180 | TT |
| KC-10A | 590.0 | 4 | 52 × 20.5 | 200 | — ^c |
| C-2A | 54.9 | 1 | 36 × 11 | 185 | S |
| C-45G | 9.6 | 1 | 11.0 × 12 | 35 | S |
| C-46F | 55.0 | 1 | 19.0 × 23 | 70 | S |

^aSee Table 14.1.

^bTwo twin-delta bogies in tandem each side.

^cTwin tandem each side plus twin midfuselage.

Table 14.3 Fighter and Bomber Aircraft Characteristics for Flotation Analysis

| Airplane designation | Max gross weight, $\times 1000$ lb | Main landing gear | | | |
|----------------------|------------------------------------|-------------------|------------------|-------------------------|-------------------|
| | | Wheels per strut | Tire size | Inflation pressure, psi | Type ^a |
| Fighters | | | | | |
| A-7D | 42.0 | 1 | 28 \times 9.0 | 280 | S |
| A-37B | 12.0 | 1 | 7.0-8 | 110 | S |
| F-4E | 61.7 | 1 | 30 \times 11.5 | 265 | S |
| F-5F | 25.2 | 1 | 24 \times 8 | 210 | S |
| F-14A | 74.3 | 1 | 37 \times 11 | 245 | S |
| F16B | 35.4 | 1 | 25.5 \times 8 | | S |
| F-86A | 24.3 | 1 | 29 \times 7.7 | 170 | S |
| F-89J | 47.7 | 1 | 46 \times 9.0 | 226 | S |
| F-100C | 35.7 | 1 | 30 \times 8.8 | 220 | S |
| F-101H | 51.0 | 1 | 32 \times 8.8 | 220 | S |
| F-102A | 31.3 | 1 | 30 \times 8.8 | 220 | S |
| F-104G | 29.0 | 1 | 25 \times 6.75 | 208 | S |
| F-105F | 54.6 | 1 | 36 \times 11.0 | 200 | S |
| F-106B | 39.6 | 1 | 30 \times 8.8 | 220 | S |
| F-111A | 98.9 | 1 | 47 \times 18.0 | 150 | S |
| Bombers | | | | | |
| B-52H | 488.0 | 4 | 56 \times 16 | 250 | — ^b |
| B-1 | 389.8 | 4 | 44.5 \times 16 | 200 | TT |

^aS = single wheel, TT = twin-tandem wheel.

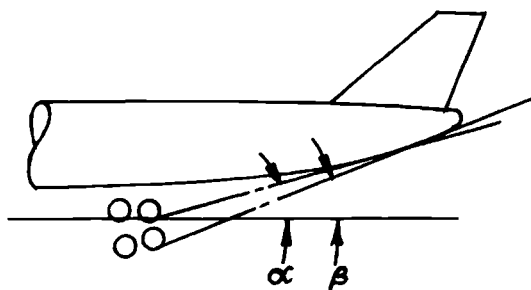
^bTwo sets of dual twin wheels on the fuselage and an outrigger gear near each wing tip.

Table 14.4 Aircraft Flotation Comparison of Concrete Pavement Thickness Requirements*

| Airplane type | | Gross weight, lb | Concrete thickness, in. |
|---------------|------------|------------------|-------------------------|
| Military | Commercial | | |
| C-47 | DC-3 | 31,000 | 5.7 |
| C-54 | DC-4 | 107,000 | 9.4 |
| C-118 | DC-6 | 97,000 | 8.7 |
| C-121 | Connie | 110,000 | 10.8 |
| C-124 | | 216,400 | 11.6 |
| C-130 | L-100 | 155,000 | 9.8 |
| C-135, E3 | 707 | 297,000 | 11.3 |
| C-141 | | 316,000 | 12.3 |
| C-5 | | 769,000 | 10.0 |
| | | 500,000 | 7.2 |
| | DC-8 | 335,000 | 12.4 |
| C-9 | DC-9 | 115,000 | 10.2 |
| | DC-10 | 410,000 | 11.9 |
| E-4 | 747 | 775,000 | 12.8 |
| | L-1011 | 410,000 | 11.9 |

*Concrete flexural stress = 400 psi, subsoil K factor = 300 psi, Poisson's ratio = 0.15.

Table 14.5 Tail-Down Angles

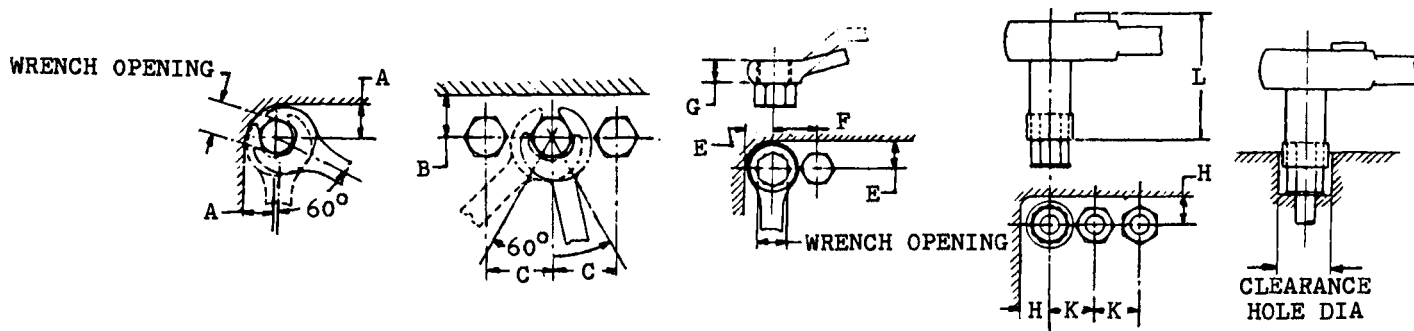


α = angle with landing gear at static position

β = angle with landing gear in extended position

| Aircraft | α | β |
|--------------------|----------|---------|
| Boeing 727-200 | 7 | 10.1 |
| C-130H | 8.5 | 13.5 |
| C-5A | 10 | 11.75 |
| Lockheed Electra | 10 | 13 |
| DHC Twin Otter | | 12 |
| Boeing 707-320C | 10.2 | 12.2 |
| Aero Commander 685 | 11 | 13 |
| Lockheed L-1011 | 11.5 | 13.6 |
| Piper Super Cub | 12 | 13 |
| Mercure | 12 | 14 |
| Concorde | | 14.9 |
| F-104G | 13 | 14.9 |
| Piper Aztec | | 15 |
| Boeing 737-200 | 12 | 15.8 |
| Piper Turbo Navajo | | 16 |
| Beech B99 | 15 | 16 |
| Lockheed JetStar | 14.3 | 17.5 |

Table 14.6 Wrench Clearances, in.



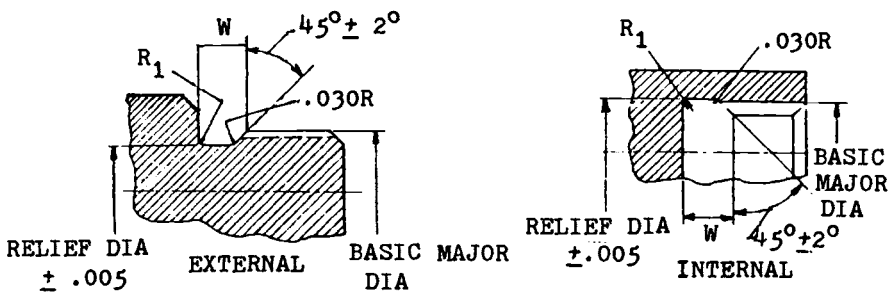
| Bolt diam | Wrench opening (distance across flats) | Open end wrench | | | Box wrench | | | Socket wrench | | | Clearance hole diam, min ^a |
|-----------|--|-----------------|-------|-------|------------|-------|-------|---------------|-------|-------|---------------------------------------|
| | | A min | B min | C min | E min | F min | G min | H min | K min | L min | |
| No. 4 | 0.250 | 0.28 | 0.27 | 0.53 | 0.27 | 0.41 | 0.25 | 0.23 (0.29) | 0.37 | 1.44 | 0.438 (0.562) |
| No. 6 | 0.312 | 0.38 | 0.28 | 0.66 | 0.30 | 0.48 | 0.28 | 0.27 (0.29) | 0.44 | 1.44 | 0.531 (0.562) |
| No. 8 | 0.344 | 0.42 | 0.34 | 0.75 | 0.30 | 0.50 | 0.28 | 0.29 | 0.48 | 1.44 | 0.562 |
| No. 10 | 0.375 | 0.42 | 0.36 | 0.78 | 0.34 | 0.56 | 0.34 | 0.31 | 0.53 | 1.44 | 0.593 |
| 1/4 | 0.438 | 0.47 | 0.42 | 0.89 | 0.40 | 0.66 | 0.36 | 0.37 (0.47) | 0.63 | 2.00 | 0.718 (0.938) |
| 5/16 | 0.500 | 0.52 | 0.47 | 1.00 | 0.45 | 0.74 | 0.38 | 0.40 (0.47) | 0.69 | 2.00 | 0.781 (0.938) |

| | | | | | | | | | | | |
|------|-------|------|------|------|------|------|------|-------------|------|------|---------------|
| 3/8 | 0.562 | 0.59 | 0.52 | 1.13 | 0.51 | 0.84 | 0.41 | 0.44 (0.50) | 0.77 | 2.00 | 0.875 (0.969) |
| 7/16 | 0.625 | 0.64 | 0.55 | 1.23 | 0.56 | 0.92 | 0.47 | 0.47 (0.53) | 0.83 | 2.00 | 0.938 (1.062) |
| | 0.690 | 0.77 | 0.66 | 1.47 | 0.59 | 0.99 | 0.53 | 0.52 (0.56) | 0.92 | 2.00 | 1.031 (1.125) |
| 1/2 | 0.750 | 0.77 | 0.67 | 1.51 | 0.66 | 1.10 | 0.55 | 0.56 (0.59) | 1.00 | 2.00 | 1.125 (1.118) |
| | 0.812 | 0.91 | 0.72 | 1.66 | 0.69 | 1.16 | 0.59 | 0.60 (0.63) | 1.05 | 2.00 | 1.187 (1.250) |
| 9/16 | 0.875 | 0.97 | 0.80 | 1.81 | 0.75 | 1.26 | 0.59 | 0.63 (0.67) | 1.14 | 2.87 | 1.250 (1.312) |
| 5/8 | 0.938 | 0.97 | 0.81 | 1.85 | 0.78 | 1.32 | 0.66 | 0.68 (0.73) | 1.23 | 2.87 | 1.375 (1.438) |
| | 1.000 | 1.05 | 0.88 | 2.00 | 0.81 | 1.39 | 0.72 | 0.73 | 1.31 | 2.87 | 1.438 |
| 3/4 | 1.062 | 1.09 | 0.97 | 2.10 | 0.83 | 1.44 | 0.72 | 0.77 | 1.39 | 2.96 | 1.562 |
| | 1.125 | 1.14 | 1.00 | 2.21 | 0.95 | 1.60 | 0.78 | 0.80 | 1.45 | 3.06 | 1.625 |
| 7/8 | 1.250 | 1.27 | 1.08 | 2.44 | 0.99 | 1.69 | 0.88 | 0.94 | 1.66 | 3.12 | 1.875 |
| | 1.312 | 1.39 | 1.17 | 2.63 | 1.08 | 1.84 | 0.91 | 0.99 | 1.74 | 3.75 | 2.000 |
| 1 | 1.438 | 1.47 | 1.25 | 2.80 | 1.22 | 2.05 | 1.00 | 1.06 | 1.89 | 3.88 | 2.125 |
| | 1.500 | 1.47 | 1.27 | 2.84 | 1.26 | 2.13 | 1.00 | 1.10 | 1.97 | 3.88 | 2.188 |

^aIt should be noted that the upper or drive end of the socket is, in some cases, of greater diameter than the lower or nut end. The larger clearances and counterbores required to accommodate these greater diameters are

shown in brackets in the columns for H and for the counterbore diameter. These values are to be used with deep counterbores or adjacent high shoulders whose depth or height is appreciably greater than that of the nut.

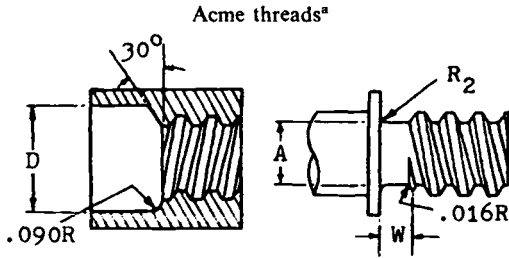
Table 14.7 Standard Thread Reliefs, in.



| Thread diam | T.P.I. | W Width of undercut | R ₁ | Relief diameter | |
|---|--------|------------------------|----------------|-----------------|-------|
| | | | | Ext. | Int. |
| Unified and American National Coarse Thread | | | | | |
| No. 4 | 40 | 0.075 | 0.010 | 0.073 | 0.124 |
| No. 6 | 32 | 0.094 | 0.010 | 0.091 | 0.151 |
| No. 8 | 32 | 0.094 | 0.010 | 0.116 | 0.178 |
| No. 10 | 24 | 0.110 | 0.010 | 0.129 | 0.205 |
| 1/4 | 20 | 0.125 | 0.03 | 0.177 | 0.267 |
| 5/16 | 18 | 0.125 | 0.03 | 0.233 | 0.331 |
| 3/8 | 16 | 0.141 | 0.03 | 0.285 | 0.395 |
| 7/16 | 14 | 0.156 | 0.03 | 0.336 | 0.458 |
| 1/2 | 13 | 0.172 | 0.03 | 0.391 | 0.523 |
| 9/16 | 12 | 0.188 | 0.03 | 0.444 | 0.586 |
| 5/8 | 11 | 0.203 | 0.03 | 0.497 | 0.650 |
| 3/4 | 10 | 0.203 | 0.03 | 0.609 | 0.777 |
| 7/8 | 9 | 0.234 | 0.06 | 0.719 | 0.899 |
| 1 | 8 | 0.250 | 0.06 | 0.826 | 1.032 |
| Unified and American National Fine Thread | | | | | |
| No. 10 | 32 | 0.094 | 0.010 | 0.143 | 0.203 |
| 1/4 | 28 | 0.094 | 0.03 | 0.196 | 0.265 |
| 5/16 | 24 | 0.110 | 0.03 | 0.251 | 0.328 |
| 3/8 | 24 | 0.110 | 0.03 | 0.313 | 0.391 |
| 7/16 | 20 | 0.125 | 0.03 | 0.364 | 0.455 |
| 1/2 | 20 | 0.125 | 0.03 | 0.426 | 0.518 |
| 9/16 | 18 | 0.125 | 0.03 | 0.481 | 0.581 |
| 5/8 | 18 | 0.125 | 0.03 | 0.544 | 0.644 |
| 3/4 | 16 | 0.141 | 0.03 | 0.659 | 0.771 |
| 7/8 | 14 | 0.156 | 0.06 | 0.772 | 0.897 |
| 1 | 12 | 0.156 | 0.06 | 0.881 | 1.025 |
| 1-1/8 | 12 | 0.188 | 0.06 | 1.006 | 1.150 |
| 1-1/4 | 12 | 0.188 | 0.06 | 1.131 | 1.273 |
| 1-3/8 | 12 | 0.188 | 0.06 | 1.260 | 1.400 |
| 1-1/2 | 12 | 0.188 | 0.06 | 1.380 | 1.525 |
| — | 8 | 0.250 | 0.06 | | |

(Table continued on next page.)

Table 14.7 (cont.) Standard Thread Reliefs, in.

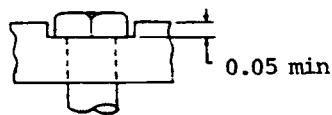


| Thread | Internal | | External | |
|---------|-----------------------|-----------------------|-----------------------|-----------------|
| | $D^{+0.010}_{-0.000}$ | $A^{+0.000}_{-0.010}$ | $W^{+0.015}_{-0.000}$ | $R_2 \pm 0.010$ |
| 3/8-12 | 0.421 | 0.258 | 0.203 | 0.031 |
| 7/16 | 0.484 | 0.320 | 0.203 | 0.031 |
| 1/2-10 | 0.562 | 0.354 | 0.250 | 0.063 |
| 5/8-8 | 0.687 | 0.452 | 0.312 | 0.063 |
| 3/4-6 | 0.812 | 0.532 | 0.421 | 0.094 |
| 7/8-6 | 0.937 | 0.656 | 0.421 | 0.094 |
| 1-5 | 1.062 | 0.745 | 0.500 | 0.094 |
| 1-1/8-5 | 1.187 | 0.870 | 0.500 | 0.094 |
| 1-1/4-5 | 1.312 | 0.994 | 0.500 | 0.094 |
| 1-3/8-4 | 1.437 | 1.066 | 0.625 | 0.125 |
| 1-1/2-4 | 1.562 | 1.191 | 0.625 | 0.125 |
| 1-3/4-4 | 1.812 | 1.440 | 0.625 | 0.125 |

^aThese thread reliefs should be specified for Acme threads, Class 2G.

Table 14.8 Slots and Machining Tolerances for Bolt Heads

Slots



Bolts may be prevented from turning, e.g., where access to the head is difficult or impossible, by machining a slot in the fitting slightly wider than the bolt head. The width is as follows:

| Bolt size | Width of slot, in. ± 0.005 | Bolt size | Width of slot, in. ± 0.005 |
|-----------|-----------------------------------|-----------|-----------------------------------|
| No. 10 | 0.395 | 9/16 | 0.895 |
| 1/4 | 0.458 | 5/8 | 0.958 |
| 5/16 | 0.520 | 3/4 | 1.083 |
| 3/8 | 0.583 | 7/8 | 1.270 |
| 7/16 | 0.710 | 1 | 1.458 |
| 1/2 | 0.770 | | |

Note: If any other bolts are used, the slot width should be taken as the width across flats: $+0.020 \pm 0.005$. The radius at the corners of the slot should be specified as 0.010.

Machining tolerances

| Process | | Tolerance, in. | |
|-----------|------------------------------|----------------|--------|
| | | Plus | Minus |
| Milling | Surface and slot | 0.005 | 0.005 |
| | Straddle (up to 2 in. width) | 0.006 | 0.000 |
| | Straddle (over 2 in. width) | 0.010 | 0.000 |
| | End | 0.005 | 0.005 |
| | Contour | 0.010 | 0.010 |
| Turning | Up to 1 in. diameter | 0.002 | 0.001 |
| | Up to 4 in. diameter | 0.004 | 0.002 |
| Boring | Up to 2 in. diameter | 0.002 | 0.001 |
| | Up to 4 in. diameter | 0.003 | 0.002 |
| Grinding | Cylindrical (internal) | 0.001 | 0.000 |
| | Cylindrical (external) | 0.000 | 0.001 |
| | Cylindrical (centerless) | 0.000 | 0.001 |
| | Surface (per face) | 0.0005 | 0.0005 |
| Broaching | Under 2 in. diameter | 0.001 | 0.001 |
| | 2-3 in. diameter | 0.0015 | 0.0015 |
| | 3-4 in. diameter | 0.002 | 0.002 |

Table 14.9 Tire Usage: Business, Personal, Utility, and Commuter Aircraft

| Manufacturer | Model | Popular Name | MAIN GEAR | | AUXILIARY GEAR | |
|----------------------|---------|-----------------|---------------|------------|----------------|------------|
| | | | Tire Size | Ply Rating | Tire Size | Ply Rating |
| Alon | F-1A | Aircoupe | 6.00-6 | 4 TT | 6.00-6 | 4 TT |
| | 415 | Ercoupe | 5.00-5 | 4 TT | 5.00-5 | 4 TT |
| Ayres | S2RT15 | Turbo Thrush | 29 x 11.00-10 | 10 | 12 1/2 x 4 1/2 | |
| | S2R | Thrush | 8.50-10 | 10 | 12 1/2 x 4 1/2 | |
| Beech Aircraft Corp. | BE 18 | Twin Beech | 11.00-12 | 8 | 14.50 SC | 8 TL |
| | BE 18H | Twin Beech | 8.50-10 | 8 TL | 8.50-10 | 8 TL |
| | BE 19 | Musketeer Sport | 6.00-6 | 4 TT | 6.00-6 | 4 TT |
| | BE 23 | Musketeer | 6.00-6 | 4 TT | 6.00-6 | 4 TT |
| | BE 23C | Sundowner | 6.00-6 | 4 TT | 6.00-6 | 4 TT |
| | BE 24 | Musketeer | 6.00-6 | 4 TT | 15 x 6.00-6 | 4 TT |
| | BE 24-R | Super Sierra | 6.00-6 | 4 TT | 5.00-5 | 4 TT |
| | BE 33 | Bonanza | 7.00-6 | 6 TT | 5.00-5 | 4 TT |
| | BE 33A | Bonanza | 7.00-6 | 6 TT | 5.00-5 | 4 TT |
| | BE 35 | Bonanza | 7.00-6 | 6 TT | 5.00-5 | 4 TT |
| | BE 35B | Bonanza | 7.00-6 | 6 TT | 5.00-5 | 4 TT |
| | BE 36 | Bonanza | 7.00-6 | 6 TT | 5.00-5 | 4 TT |
| | BE 50 | Twin Bonanza | 8.50-10 | 6 TT | 6.50-10 | 6 TT |
| | BE B55 | Baron | 6.50-8 | 8 TT | 5.00-5 | 6 TT |
| | BE C55 | Baron | 6.50-8 | 8 TT | 5.00-5 | 6 TT |
| | BE E55 | Baron | 6.50-8 | 8 TT | 5.00-5 | 6 TT |
| | BE 56TC | Baron | 6.50-8 | 8 TT | 5.00-5 | 6 TT |
| | BE 58 | Baron | 19.5 x 6.75-8 | 10 TL | 15 x 6.00-6 | 4 TT |
| | BE-60 | Duke | 19.5 x 6.75-8 | 10 TL | 15 x 6.00-6 | 4 TT |
| | BE-65 | Queen Air | 8.50 x 10 | 8 TL | 6.50-10 | 6 TL |
| | BE-70 | Queen Air | 8.50 x 10 | 8 TL | 6.50-10 | 6 TL |
| | BE-76 | Duchess | 6.00-6 | 6 TT | 5.00-5 | 6 TT |
| | BE-77 | Skipper | 15 x 6.00-6 | 4 TT | 5.00-5 | 6 TT |
| | BE-80 | Queen Air | 8.50-10 | 8 TL | 6.50-10 | 6 TL |
| | BE-88 | Queen Air | 8.50-10 | 8 TL | 6.50-10 | 6 TL |
| | BE-90 | King Air | 8.50-10 | 8 TL | 6.50-10 | 6 TL |
| | BE-95 | Travelair | 7.00-6 | 6 TT | 5.00-5 | 6 TT |
| | BF-99 | Airliner | 18 x 5.5 | 8 TL | 6.50-10 | 6 TL |

(Table continued on next page.)

Table 14.9 (cont.) Tire Usage: Business, Personal, Utility, and Commuter Aircraft

| Manufacturer | Model | Popular Name | MAIN GEAR | | AUXILIARY GEAR | |
|-------------------------------|-------------------|-------------------|----------------|--------------|----------------|----------------|
| | | | Tire Size | Ply Rating | Tire Size | Ply Rating |
| Beech Aircraft Corp. (cont'd) | BE-100 | King Air | 18 x 5.5 | 8 TL | 6.50-10 | 6 TL |
| | BE-200 | Super King Air | 18 x 5.5 | 8 TL | 22 x 6.75-10 | 8 TL |
| | BE-200 (optional) | Super King Air | 22 x 6.75-10 | 8 TL | 22 x 6.75-10 | 8 TL |
| | BE-2000 | Starship I | 19.5 x 6.75-10 | 10 TL | 19.5 x 6.75-8 | 10 TL |
| | BE-300 | Super King Air | 22 x 6.75-10 | 8 TL | 19.5 x 6.75-8 | 10 TL |
| | BE F90 | King Air | 18 x 5.5 | 8 TL | 22 x 6.75-10 | 8 TL |
| | BE 1900 | Airliner | 22 x 6.75-10 | 8 TL | 19.5 x 6.75-8 | 10 TT |
| | Bellanca | 260A | Bellanca | 6.00-6 | 6 TL | 6.00-6 |
| 17-30A | | Viking | 6.00-6 | 6 TL | 6.00-6 | 4 TT |
| 17-31A | | Viking | 6.00-6 | 6 | 15 x 6.00-6 | 6 TT |
| 17-31ATC | | Super Viking | 6.00-6 | 6 TL | 15 x 6.00-6 | 6 TT |
| 7ECA | | Turbo Viking | 6.00-6 | 6 TL | 15 x 6.00-6 | 6 TT |
| 7GCAA | | Citabria | 6.00-6 | 4 | 5.00-5 | 4 TT |
| 7CBC | | Citabria | 6.00-6 | 4 | 5.00-5 | 4 TT |
| 7KCAB | | Citabria | 7.00-6 | 4 TT | 5.00-5 | 4 TT |
| 8KCAB | | Decathlon | 6.00-6 | 4 TT | 5.00-5 | 4 TT |
| 8GCBC | | Scout | 8.50-6 | 4/6 | 5.00-5 | 4 TT |
| British Aerospace | | HS-125 | | 23 x 7.00-12 | 10 TL | 18 x 4.25-10DC |
| | 3103 | Jetstream 31 | 28 x 9.00-12 | | 6.00-6 | |
| | 748 | Intercity | 32 x 10.75-14 | 12 | 8.50-10 | 10 |
| Canadair | CL-600/601 | Challenger | 26 x 6.6 | 14 TL | 18 x 4.4 | 12 TLDC |
| | CL-215 | | 15.00 x 16 | 16 TT | 6.50 x 10 | 10 TT |
| Casa | 212 | Commuter | 11.00 x 12 | 10 TT | 24 x 7.7 | 8 TT |
| Cessna | 120, 140 | | 6.00-6 | 4 TT | | |
| | 150, 152 | Commuter, Aerobat | 6.00-6 | 4 TT | 5.00-5 | 4 TT |
| | 170 | | 6.00-6 | 4 TT | 5.00-5 | 4 TT |
| | 172 | Skyhawk | 6.00-6 | 4 TT | 5.00-5 | 4 TT |
| | R172 | Hawk XP | 6.00-6 | 4 TT | 5.00-5 | 4 TT |
| | 172 Q | Cutlass | 6.00-6 | 6 TT | 5.00-5 | 4 TT |
| | 172 RG | Cutlass RG | 15.00 x 6.00-6 | 6 TT | 5.00-5 | 4 TT |
| | 175 | Skylark | 6.00-6 | 4 TT | 5.00-5 | 4 TT |

| | | | | | | |
|------------------------|---------------|---------------------------------|--------------|----------|--------------|---------|
| Cessna (cont'd) | 177 | Cardinal | 6.00-6 | 6 TT | 5.00-5 | 4 TT |
| | 177 RG | Cardinal RG | 15 x 6.00-6 | 6 TT | 5.00-5 | 4 TT |
| | 180 | Skywagon | 6.00-6 | 6 TT | 8.00" | 6 TT |
| | 182, T182 | Skylane | 6.00-6 | 6 TT | 5.00-5 | 6 TT |
| | 182RG, T182RG | Skylane RG | 15 x 6.00-6 | 6 TT | 5.00-5 | 4 TT |
| | 185 | Skywagon | 6.00-6 | 6 TT | 10.00" | 8 TT |
| | 188 | AG Wagon | 22 x 8.00-8 | 6 TT | 8.00" | 6 TT |
| | 188 | AG Wagon (optional) | 8.50-10 | 6 TT | 10.00" | 8 TT |
| | 205 | | 6.00-6 | 6 TT | 5.00-5 | 6 TT |
| | 206 | Station Air | 6.00-6 | 6 TT | 5.00-5 | 6 TT |
| | 206, 207 | Optional | 8.00-6 | 6 TT | 6.00-6 | 4 TT |
| | 207 | Skywagon | 6.00-6 | 8 TT | 6.00-6 | 8 TT |
| | 210 | Centurion | 6.00-6 | 8 TT | 5.00-5 | 6 TT |
| | T210, P210 | Turbo, Pressurized Centurion | 6.00-6 | 8 TT | 5.00-5 | 10 TT |
| | T303 | Crusader | 6.00-6 | 8 TT | 6.00-6 | 6 TT |
| | T303 | Optional | 6.50-8 | 8 TT | 6.00-6 | 6 TT |
| | 310, T310 | | 6.50-8 | 6 TT | 6.00-6 | 4 TT |
| | 320, 340 | | 6.50-10 | 6 TT | 6.00-6 | 4 TT |
| | 336 | | 6.00-6 | 6 TT | 15 x 6.00-6 | 6 TT |
| | 337 | Super Skymaster | 18 x 5.5 | 8 TT | 15 x 6.00-6 | 6 TT |
| | 401, 402 | | 6.50-10 | 8 TT | 6.00-6 | 6 TT |
| | 404 | Titan | 22 x 7.75-10 | 10 TL | 6.00-6 | 6 TT |
| | 411 | | 6.50-10 | 8 TT | 6.00-6 | 6 TT |
| | 414 | Chancellor | 6.50-10 | 8 TT | 6.00-6 | 6 TT |
| | 421 | Golden Eagle | 6.50-10 | 8 TT | 6.00-6 | 6 TT |
| | 425 | Conquest I | 6.50 x 10 | 10 TT | 6.00-6 | 6 TT |
| | 441 | Conquest II | 22 x 7.75-10 | 10 TL | 6.00-6 | 6 TT |
| 500 | Citation I | 22 x 8.00-10 | 10 TL | 18 x 4.4 | 10 TLDC | |
| 550 | Citation II | 22 x 8.00-10 | 10 TL | 18 x 4.4 | 10 TLDC | |
| 650 | Citation III | 22 x 5.75-12 | 8 TL | 18 x 4.4 | 10 TLDC | |
| Dassault | 10, 100 | Falcon | 22 x 5.75-12 | 8 TL | 18 x 5.75-8 | 8 TLDC |
| | 20, 200 | Falcon | 26 x 6.6 | 10 TL | 14.5 x 5.5-6 | 14 TLDC |
| | 50 | Falcon | 26 x 6.6 | 14 TL | 14.5 x 5.5-6 | 14 TLDC |
| de Havilland | DHC-6 | Twin Otter | 11 00-12 | 8 TT | 8.90-12.50 | 6 TT |
| | DHC-6 | Twin Otter (Floatation) | 15.00-12 | 10 TT | 8.90-12.50 | 6 TT |
| | DHC-7 | Dash 7 | 30 x 9.00-15 | 10 TT | 6.50-10 | 10 TT |

(Table continued on next page.)

Table 14.9 (cont.) Tire Usage: Business, Personal, Utility, and Commuter Aircraft

| Manufacturer | Model | Popular Name | MAIN GEAR | | AUXILIARY GEAR | | |
|--------------------------|-----------------------|-------------------------|--------------------------------|------------|-------------------------------|-----------------|------|
| | | | Tire Size | Ply Rating | Tire Size | Ply Rating | |
| de Havilland (cont'd) | DHC-7 | Dash 7 (Floatation) | 33 x 10.75-15 | 12 TT | 24 x 7.7 | 10 TT | |
| | DHC-8 | Dash 8 | 26.5 x 8.0-13 | 12 TT | 18 x 5.5 | 10 TT | |
| | DHC-8 | Dash 8 (Floatation) | 31 x 9.75-13 | 10 TT | 22 x 7.75-10 | 10 TT | |
| Dornier | DO-228-100 | 228-100 | 11.00-12 | 10 | 24-7.7 | 8 | |
| | DO-228-200 | 228-200 | 11.00-12 | 10 | 24-7.7 | 8 | |
| Embraer | EMB-110 EMB-120 | Bandeirante Brasilia | 6.70 x 210-12 24-7.25 | 10 TT | 6.50-8 18 x 5.5 | 8 TT | |
| Fairchild Aircraft Corp. | SA226 | Metro/Merlin | 19.5 x 6.75-8 | 10 TL | 18 x 4.4 18 x 4.4 optional | 6 TL 10 TLSC | |
| Fairchild-Hiller | F-27 (J) | | 9.50 x 16 | 12 TL | 8.50-10 | 10 TL | |
| | F-28 | | 39 x 13 | 14 TL | 24 x 7.7 | 10 TL | |
| Fokker | F-27 | Friendship | 34 x 10.75-16 | 10 TT | 9.25-12 | 8 TT | |
| | F-27 (Floatation) | Friendship | 37 x 11.75-16 | 10 TT | 9.25-12 | 8 TTDC | |
| | F-28 | Fellowship | 39 x 13 | 14/16 TT | 24 x 7.7 | 10 TTDC | |
| | F-28 (Floatation) | Fellowship | 40 x 14 | 16 TT | 24.5 x 8.5-10 | 10 TTDC | |
| | F-28 MK2000/5000/6000 | Fellowship | 40 x 14 | 16 TT | 24.5 x 8.5-10 | 10 TTDC | |
| Gates Lear Jet | LR-23 | Learjet | 18 x 5.5 | 10 TL | 18 x 4.4 | 10 TLDC | |
| | LR-24 | Learjet | 18 x 5.5 | 10 TL | 18 x 4.4 | 10 TLDC | |
| | LR-25 | Learjet | 18 x 5.5 | 10 TL | 18 x 4.4 | 10 TLDC | |
| | LR-35/36 | Learjet | 17.5 x 5.75-8 | 12 TL | 18 x 4.4 | 10 TLDC | |
| | LR-55 | Learjet | 17.5 x 5.75-8 | 12 TL | 18 x 4.4 | 10 TLDC | |
| Gulfstream Aerospace | AE-680 T | Turbo Commander | 8.50-10 | 10 TL | 16.4-4 | 4 TL | |
| | AE-680 V | | 8.50-10 | 8 TL | 6.00-6 | 6 TL | |
| | AE-680 W | | 8.50-10 | 8 TL | 6.00-6 | 6 TL | |
| | AE-681 | | 8.50-10 | 8 TL | 6.00-6 | 6 TL | |
| | AE-685 | | 8.50-10 | 8 TL | 6.00-6 | 6 TL | |
| | AE-690, 690 A, 690 B | | 8.50-10 | 8 TL | 6.00-6 | 6 TL | |
| | AE-690C | | 8.50-10 | 10 TL | 15 x 6.00-6 | 6 TT | |
| | AE-720 | | 8.50-10 | 8 TL | 6.00-6 | 6 TL | |
| | AE-1121 | | Jet Commander Commodore Jet | 24 x 7.7 | 16 TL | 16 x 4.4 | 4 TL |
| | 1121 | | | 24 x 7.7 | 16 TL | 16 x 4.4 | 4 TL |

| | | | | | | |
|--|-------------------------|---------------------|-----------------|----------|--------------|---------|
| Gulfstream Aerospace (cont'd) | 112 | | 6.00-6 | 6 TT | 5.00-5 | 4 TT |
| | 112TC | | 7.00-6 | 6 TT | 5.00-5 | 6 TT |
| | 114 | | 7.00-6 | 6 TT | 5.00-5 | 6 TT |
| | G-159 | Gulfstream I | 7.50-14 | 12 TL | 6.50-8 | 6 TL |
| | G-158 | AG-CAT | 8.50-10 | 6 TT | 10.00 | 8 TT |
| | 164 | Gulfstream II | 34 x 9.25-16 | 16 TL | 21 x 7.25-10 | 8 TLSC |
| | | Gulfstream III | 34 x 9.25-16 | 18 TL | 21 x 7.25-10 | 10 TLSC |
| | AA-1B | Trainer | 6.00-6 | 4 TT | 5.00-5 | 4 TT |
| | AA-5 | Tiger | 6.00-6 | 4 TT | 5.00-5 | 4 TT |
| | AA-5B | Tiger | 6.00-6 | 6 TT | 5.00-5 | 4 TT |
| | AA-5A | Cheeta | 6.00-6 | 4 TT | 5.00-5 | 4 TT |
| | GA-7 | Cougar | 6.00-6 | 6 TT | 5.00-5 | 4 TT |
| | AE 200 | Commander | 7.00-6 | 6 TT | 6.00-6 | 4 TT |
| | AE-500, B. U. S | Commander | 8.50-10 | 8 TL | 6.00-6 | 6 TL |
| | AE-560, 560A | Commander | 8.50-10 | 6 TL | 6.00-6 | 6 TL |
| | AE-560E, F | Commander | 8.50-10 | 8 TL | 6.00-6 | 6 TL |
| | AE-680, 680E | Commander | 8.50-10 | 8 TL | 6.00-6 | 6 TL |
| | AE-680F | Commander | 8.50-10 | 8 TL | 6.00-6 | 6 TL |
| | AE-608FP | Commander | 8.50-10 | 8 TL | 6.00-6 | 6 TL |
| | AE-680FL | Grand Commander | 8.50-10 | 8 TL | 6.00-6 | 6 TL |
| | AE-680FLP | Grand Commander P | 8.50-10 | 8 TL | 6.00-6 | 6 TL |
| Hawker-Siddeley | HS-125 up to 800 Series | | 23 x 7.00-12 | 10 TL | 18.4.25-10 | 6 TLSC |
| | HS 748 | AVRO | 32 x 10.75-14 | 12 TT | 8.50 x 10 | 10 TT |
| | 1C | Trident | 34 x 9.50-18 | 14 TT | 29 x 8.00-15 | 12 TT |
| | 1E/2E/3B | Trident | 36 x 10.00-18 | 16 TT | 29 x 8.00-15 | 12 TT |
| Helio | H-250 | Courier | 8.00-6 | 4 TT | 10.00 | 8 TT |
| | H-250 | Courier II | 8.00-6 | 4 TT | 10.00 | 8 TT |
| | H-250 | Courier (XWD) | 6.50-8 | 6 TT | 10.00 | 8 TT |
| | H-295 | Super Courier | 8.00-6 | 6 TT | 10.00 | 8 TT |
| | H-295 | Super Courier (XWD) | 6.50-8 | 6 TT | 10.00 | 8 TT |
| | H-550 A | Stallion | 7.50-10 | 8 TT | 5.00-5 | 4 TT |
| | H 634 | Twin Stallion | 7.50-10 | 8 TT | 5.00-5 | 4 TT |
| Israel Aircraft Industries | 1121 | Jet Commander | 24 x 7.7 | 16/18 TL | 16 x 4.4 | 4 TL |
| | 1123 | Jet Commander | 24 x 7.7 | 14 TL | 16 x 4.4 | 4 TL |
| | 1124 | Westwind | B24 x 9.50-10.5 | 18 TL | 16 x 4.4 | 4 TL |
| | 1125 | Astra | 23 x 7.00-12 | 10 TL | 16 x 4.4 | 6 TL |

(Table continued on next page.)

Table 14.9 (cont.) Tire Usage: Business, Personal, Utility, and Commuter Aircraft

| Manufacturer | Model | Popular Name | MAIN GEAR | | AUXILIARY GEAR | |
|---------------------------|------------------|---------------------------|--------------------|---------------|--------------------|-----------------|
| | | | Tire Size | Ply Rating | Tire Size | Ply Rating |
| Lake | LA-4 | Buccaneer | 6.00-6 | 4 TT | 5.00-4 | 4 TT |
| | LA-4 | Amphibian | 6.00-6 | 4 TT | 5.00-4 | 4 TT |
| | LA-4-200 | Amphibian | 6.00-6 | 4 TT | 5.00-4 | 4 TT |
| Lockheed | LG-1329 | JetStar | 26 x 6.6 | 14 TL | 18 x 4.4 | 10 TLSC |
| | SA 60 | JetStar II Azacarte-60 | 26 x 6.6 6.50-8 | 14 TL 4 TT | 18 x 4.4 6.00-6 | 12 TLSC 4 TT |
| Mitsubishi | MU-2 | Solitaire | 8.50-10 | 8 TT | 5.00-5 | 6 TT |
| | MU-2 | Marquis | 8.50-10 | 8 TT | 5.00-5 | 6 TT |
| | MU-300 | Diamond I | 24 x 7.7 | 12 TL | 18 x 4.4 | 10 TLDC |
| Mooney | MO-20 | Ranger | 6.00-6 | 6 TT | 5.00-5 | 4 TT |
| | MO-21C | Super | 6.00-6 | 6 TT | 5.00-5 | 4 TT |
| | MO-22 | Mustang | 6.00-6 | 6 TT | 15 x 6.00-6 | 4 TT |
| | MO-20E | Chaparral | 6.00-6 | 6 TT | 5.00-5 | 4 TT |
| | MO-20F | Executive | 6.00-6 | 6 TT | 5.00-5 | 6 TT |
| | MO-20J | 201 | 6.00-6 | 6 TT | 5.00-5 | 6 TT |
| | MO-20K | Turbo 231 | 6.00-6 | 6 TT | 5.00-5 | 6 TT |
| Nord | 262 | Airliner | 39 x 13 | 14 TL | 9.00-6 | 10 TL |
| Partenavia | P68C | | 6.00-6 | 6 TT | 5.00-5 | 6 TT |
| Pilatus Britten-Norman | BN 2A | Islander | 7.00-6 | 8 8 TL | 7.00-6 | 8 8 TL |
| | BN 2B-20/2T | | 16 x 7.7 | | 16 x 7.7 | |
| | PC-7 | | 6.50-8 | | 6.00-6 | |
| | PC-9 | | 20 x 4.4 | | 16 x 4.4 | |
| Piper | PA18-135 | Super Cub | 8.00-4 | 4 TT | 6 x 2.00 | Solid |
| | PA18-150 | Super Cub | 6.00-6 | 4 TT | 6 x 2.00 | Solid |
| | PA23,-160-235 | Apache | 7.00-6 | 6 TT | 6.00-6 | 4 TT |
| | PA23-250 | Aztec | 7.00-6 | 8 TT | 6.00-6 | 4 TT |
| | PA24-180 | Commanche | 6.00-6 | 4 TT | 6.00-6 | 4 TT |
| | PA24-250,260,400 | Commanche | 6.00-6 | 6 TT | 6.00-6 | 4 TT |
| | PA25-150 | Pawnee | 7.00-6 | 4 TT | 8 x 3.00-4 | 4 TT |
| | PA25-236, 260 | Pawnee | 8.00-6 | 4 TT | 8 x 3.00-4 | 4 TT |

| | | | | | | |
|---------------------------------------|------------------|--------------------|---------------|-------|---------------|---------|
| Piper (cont'd) | PA28R | Arrow | 6.00-6 | 6 TT | 5.00-5 | 4 TT |
| | PA28-140 | Cherokee | 6.00-6 | 4 TT | 6.00-6 | 4 TT |
| | PA28-150 | Cherokee | 6.00-6 | 4 TT | 6.00-6 | 4 TT |
| | PA28-151, 161 | Warrior | 6.00-6 | 4 TT | 5.00-5 | 4 TT |
| | PA28-160 | Cherokee | 6.00-6 | 4 TT | 6.00-6 | 4 TT |
| | PA28-180 | Cherokee | 6.00-6 | 4 TT | 6.00-6 | 4 TT |
| | PA28-181 | Archer | 6.00-6 | 4 TT | 5.00-5 | 4 TT |
| | PA28-235 | Cherokee | 6.00-6 | 4 TT | 6.00-6 | 4 TT |
| | PA30 | Twin Commanche | 6.00-6 | 6 TT | 6.00-6 | 6 TT |
| | PA31 | Navajo | 6.50-10 | 8 TT | 6.00-6 | 6 TT |
| | PA31-350 | Chieftan | 6.50-10 | 8 TT | 6.00-6 | 6 TT |
| | PA31P | Pressurized Navajo | 6.50-10 | 8 TT | 6.00-6 | 8 TT |
| | PA31T | Cheyenne | 6.50-10 | 8 TT | 18 x 4.4 | 6 TT |
| | PA31T-500 | Cheyenne 1A | 6.50-10 | 10 TT | 18 x 4.4 | 6 TT |
| | PA32 | 6-300 | 6.00-6 | 6 TT | 6.00-6 | 6 TT |
| | PA32 RT300 | Lance | 6.00-6 | 8 TT | 6.00-6 | 4 TT |
| | PA31P-350 | Mojave | 6.50-10 | 8 TT | 17.5 x 6.25-6 | 10 TT |
| | PA36 | Brave | 8.50-10 | 6 TT | 10 x 3.5-4 | |
| | PA38 | Tomahawk | 6.00-6 | 4 TT | 5.00-5 | 4 TT |
| | PA42 | Cheyenne IIIA | 6.50-10 | 12 TL | 17.5x6.25-6 | 10 TT |
| | PA44-180 | Seminole | 6.00-6 | 6 TT | 6.00-6 | 6 TT |
| Saab Fairchild | SF340 | Airliner | 24 x 7.7 | 12 TL | 6.00-6 | 8TL |
| Sabreliner | NA-40/60 | Sabreliner | 26 x 6.6 | 14 TL | 18 x 4.4 | 10 TLSC |
| | NA-40/60 | Sabreliner | 26 x 6.75-14 | 14 TL | 18 x 4.4 | 10 TLSC |
| | NA-60A/65 | Sabreliner | 26 x 6.75-14 | 16 TL | 18 x 4.4 | 10 TLSC |
| | NA-75/75A | Sabreliner | 22 x 5.75-12 | 10 TL | 18 x 4.4 | 10 TLSC |
| Short Brothers | SD3-30 | 330 | 34 x 10.75-16 | 12 TT | 9.00 x 6 | 10 TT |
| | SD3-60 | 360 | 34 x 10.75-16 | 12 TT | 9.00-6 | 10 TT |
| Ted Smith Aircraft (Piper) | 600/601B (PA60) | Aerostar | 6.50-8 | 8 TL | 6.00-6 | 6 TL |
| | 601P (PA60-601P) | Aerostar | 6.50-8 | 8 TL | 6.00-6 | 6 TL |
| | 602P (PA60-602P) | Aerostar | 6.50-8 | 8 TL | 6.00-6 | 6 TL |
| | 700P (PA60-700P) | Aerostar | 6.50-8 | 8 TL | 6.00-6 | 6 TL |

All tires are tubeless unless otherwise specified. Code: TT = tube type, TL = tubeless, CH = deflection chine, LS = low speed.

Note: The application information presented here for general aviation aircraft tires is based on the most current information available and is intended for use as a general reference only. Any inquiries regarding specific model aircraft should be directed to the applicable airframe manufacturer. All B. F. Goodrich commercial aircraft tires are manufactured in accordance with TSO-C62C and/or applicable air-frame manufacturer specifications. The applications provided in these tables are based on information supplied by airframe manufacturers and represents the results of certification testing for individual aircraft of the types listed in the table. Your requirements may vary depending on the actual configuration of your aircraft, particularly if modifications have been made since tire certification. You must verify the proper tire applications in its existing configuration prior to placing your order with B. F. Goodrich. Additionally, inclusion with manual does not necessarily indicate BFG fire availability for all aircraft listed.

FAILURE TO MAKE THIS VERIFICATION AND TO INSTALL UNAPPROVED TIRES ON AN AIRCRAFT MAY RESULT IN TIRE FAILURE CAUSING PROPERTY DAMAGE, SERIOUS INJURY, OR LOSS OF LIFE. Source: B. F. Goodrich Co.

Table 14.10 Tire Usage: Commercial Transport

| Manufacturer | Model | Series | Speed | MLG | | NLG | |
|--------------|---------------|----------------------|-------|-----------------|-------|-----------------|-------|
| | | | | Size | PR | Size | PR |
| Airbus | A300 B2 | 137 tonne | 210 | 46 x 16 | 24 | 40 x 14 | 20 |
| | A300 B2 | 142 tonne | 210 | 46 x 16 | 26 | 40 x 14 | 20 |
| | A300 B4 | 145 tonne | 235 | 46 x 16 | 28 | 40 x 14 | 22/24 |
| | A300 B4 | 150 tonne | 225 | 46 x 16 | 28 | 40 x 14 | 22/24 |
| | A300 B4 | 157.5 tonne | 225 | 46 x 16 | 28 | 40 x 14 | 22/24 |
| | A300 B4 | 157.5 tonne | 225 | 49 x 17 | 30 | 40 x 14 | 22/24 |
| | A300 B4 | 165 tonne | 225 | 49 x 17 | 30 | 40 x 14 | 22/24 |
| | A300 B4 | 165 tonne | 225 | 49 x 19-20 | 32 | 40 x 14 | 22/24 |
| | A300-600 | 165 tonne | 225 | 49 x 17 | 30/32 | 40 x 14 | 22/24 |
| | A300-600 | 165 tonne | 225 | 49 x 19-20 | 32 | 40 x 14 | 22/24 |
| | A310-200 | 139.5/142.5 tonne | 225 | 46 x 16 | 28/30 | 40 x 14 | 22/24 |
| | A310-200 | 139.5/142.5 tonne | 225 | 49 x 17 | 26/28 | 40 x 14 | 22/24 |
| | A310-300 | 150.9 tonne | 225 | 46 x 16 | 28/30 | 40 x 14 | 22/24 |
| | A310-300 | 150.9 tonne | 225 | 49 x 17 | 28/30 | 40 x 14 | 22/24 |
| Aerospatiale | Caravelle | 46 tonne | 180 | 35 x 9.00-17 | 14 | 26 x 7.75-13 CH | 10 |
| | Caravelle | 48, 50, 52, 56 tonne | 210 | 35 x 9.00-17 | 16 | 26 x 7.75-13 CH | 10 |
| | Caravelle | 58 tonne | 210 | 35 x 9.00-17 | 18 | 26 x 7.75-13 CH | 10 |
| | Concorde | Pre-production | 279 | 47 x 15.75-22 | 26 | 31 x 19.75-14 | 20 |
| | Concorde | Production | NA | 1195 x 400-22 | NA | 785 x 275-14 | NA |
| | Nord | 262 | LS | 12.50 x 16 | 12 | 6.00-6 | 8 |
| BAe | BAC-111 | 200 | 210 | 40 x 12 | 16 | 24 x 7.25-12 CH | 10 |
| | BAC-111 | 400 | 210 | 40 x 12 | 18 | 24 x 7.25-12 CH | 10 |
| | BAC-111 | 475 | 210 | 40 x 12 | 16/18 | 24 x 7.25-12 CH | 12 |
| | BAC-111 | 500/510 | 210 | 40 x 12 | 20 | 24 x 7.25-12 CH | 10 |
| | 146 | | 190 | 39 x 13 | 18/22 | 24 x 7.7 | 14 |
| | 146 | | 190 | 42 x 15 | 16/18 | 8.50 x 10 | 12 |
| | Trident | 1C | 210 | 34 x 9.50-18 | 14 | 29 x 8.00-15 | 12 |
| | Trident | 1E, 2E, 3B | 210 | 36 x 10.00-18 | 16 | 29 x 8.00-15 | 12 |
| | Vanguard | | LS | 17.00-20 | 22 | 33 x 9.75-16 | 10 |
| | VC-10 | | 210 | 50 x 18 | 24 | 39 x 13 | 16 |
| | VC-10 (Super) | | 225 | 50 x 18 | 26 | 39 x 13 | 16 |
| | Viscount | | LS | 36 x 10.75-16.5 | 16 | 24 x 7.25-12 | 10 |
| | | | | TT or TL | | | |

| | | | | | | | |
|--------|------------|-----------------|-------------|---------------|-------|------------------|-------|
| Boeing | 707 | 120 | 210 | 46 x 16 | 24 | 39 x 13 | 14 |
| | 707 | 320B | 210 | 46 x 16 | 26/28 | 39 x 13 | 16 |
| | 707 | 320C | 210/225 | 46 x 16 | 28 | 39 x 13 | 16 |
| | 720 | | 210 | 40 x 14 | 24 | 34 x 9.9 | 12 |
| | 720B | | 210 | 40 x 14 | 24 | 39 x 13 | 14 |
| | 727 | 100/QC | 210 | 49 x 17 | 26/28 | 32 x 11.50-15 CH | 12 |
| | 727 | 100/QC | 210 | 50 x 20.0-20 | 26/30 | 32 x 11.50-15 CH | 12 |
| | 727 | 200/C | 210/225 | 49 x 17 | 28/30 | 32 x 11.50-15 CH | 12 |
| | 727 | 200/C | 210 | 50 x 21.00-20 | 28/30 | 32 x 11.50-15 CH | 12 |
| | 737 | 100 | 210 | 40 x 14 | 24 | 24 x 7.7 | 14/16 |
| | 737 | 200 | 210/225 | 40 x 14 | 24 | 24 x 7.7 | 16 |
| | 737 | 200 | 210 | C40 x 18-17 | 24 | C24.5 x 8.5-12 | 14 |
| | 737 | 200 | 210 | C40 x 14-21 | 24 | 24 x 7.7 | 16 |
| | 737 | 200 (Flotation) | 210 | 42 x 15 | 24 | 24 x 7.7 | 16 |
| | 737 | 200 | 210/225 | 40 x 14 | 28 | 24 x 7.7 | 16 |
| | 737 | 200 | 210/255 | H40 x 14.5-19 | 24 | 24 x 7.7 | 16 |
| | 737 | 300 | 225 | H40 x 14.5-19 | 24 | 27 x 7.75-15 | 10 |
| | 737 | 300 | 225 | 42 x 16-19 | 22 | 27 x 7.75-15 | 10 |
| | 747-SP | 613 kt | 210/225 | 46 x 16 | 28/30 | 49 x 17 | 28/30 |
| | 747-SP | 663 kt - 673 kt | 210/225 | 46 x 16 | 28/30 | 49 x 17 | 30 |
| | 747-SP | 696 kt - 705 kt | 210/225 | 46 x 16 | 28/30 | 49 x 17 | 30/32 |
| | 747-SR | 523 kt - 613 kt | 210/225 | 49 x 17 | 28/30 | 49 x 17 | 28/30 |
| | 747-100 | 713 kt | 210/225 | 46 x 16 | 28/30 | 46 x 16 | 28/30 |
| | 747-100 | 738 kt | 210/225 | 46 x 16 | 30/32 | 46 x 16 | 30/32 |
| | 747-100 | 753 kt | 210/225 | 46 x 16 | 30/32 | 46 x 16 | 30/32 |
| | 747-200 | 778 kt | 225/235 | 49 x 17 | 30/32 | 49 x 17 | 30/32 |
| | 747-200 | 788 kt | 225/235 | 49 x 17 | 30/32 | 49 x 17 | 30/32 |
| | 747-200 | 803 kt - 808 kt | 225 | 49 x 17 | 30/32 | 49 x 17 | 30/32 |
| | 747-200 | 823 kt | 225/235 | 49 x 17 | 30/32 | 49 x 17 | 30/32 |
| | 747-200 | 823 kt | 225/235/245 | 49 x 19.0-20 | 32 | 49 x 19.0-20 | 32 |
| | 747-200B | 836 kt | 235/245 | 49 x 19.0-20 | 32 | 49 x 19.0-20 | 32 |
| | 747-200C/F | 836 kt | 235/245 | 49 x 19.0-20 | 34 | 49 x 19.0-20 | 34 |
| | 747-300 | 836 kt | 235 | 49 x 19.0-20 | 32 | 49 x 19.0-20 | 32 |
| | 757 | | 210/225 | H40 x 14.5-19 | 22/24 | H32 x 13-12 | 20 |
| | 767 | | 225 | H45 x 17-20 | 26 | H37 x 14-15 | 20/22 |
| | 767 | | 225 | H46 x 18-20 | 26/28 | H37 x 14-15 | 20/22 |

(Table continued on next page.)

Table 14.10 (cont.) Tire Usage: Commercial Transport

| Manufacturer | Model | Series | Speed | MLG | | NLG | |
|--------------|-----------|--------------------|-----------------|---------------|--------------|------------------|-------|
| | | | | Size | PR | Size | PR |
| Convair | 240 | | LS | 34 x 9.9TT | 12 | 26 x 6TT | 10 |
| | 340, 440 | | LS | 12.50-16TT/TL | 12 | 7.50 x 14 TT/TL | 8 |
| | 540 | | LS | 12.50-16TT/TL | 12 | 7.50 x 14TT/TL | 8 |
| | 580/600 | | LS | 12.50-16TT/TL | 14 | 7.50 x 14 TT/TL | 8 |
| | 580/600 | | LS | 39 x 13 | 14 | 7.50 x 14TT/TL | 8 |
| | 880 | | 210 | 39 x 13 | 20 | 29 x 7.7 | 12 |
| | 880M | | 210 | 39 x 13 | 22 | 29 x 7.7 | 12 |
| | 990 | | 210/225 | 41 x 15.0-18 | 22/24 | 29 x 7.7 | 16 |
| Douglas | DC-3 | | LS | 17.00-16TT/TL | 10 | 9.00-6TT | 10 |
| | DC-4 | | LS | 15.50-20TT | 14/16 | 44" TT | 12 |
| | DC-6B & 7 | | LS | 15.50-20 TT | 20 | 44" TT | 14 |
| | DC-7C | | LS | 17.00-20 | 20/22/24 | 15.00-16 | 14 |
| | DC-8 | | 210 | 44 x 16 | 26 | 34 x 11 | 18 |
| | DC-8 | HV/50F | 225 | 44 x 16 | 28 | 34 x 11 | 20/22 |
| | DC-8 | 61 | 225 | 44 x 16 | 30 | 34 x 11 | 22 |
| | DC-8 | 62 | 225 | 44 x 16 | 30/32 | 34 x 11 | 22 |
| | DC-8 | 62H | 225 | 44.5 x 16.5 | 30 | 34 x 11 | 22 |
| | DC-8 | 63 | 225 | 44 x 16 | 32 | 34 x 11 | 22 |
| | DC-8 | 63 | 225 | 44.5 x 16.5 | 30 | 34 x 11 | 22 |
| | DC-9 | 10 (11-12-14-15) | 210/225 | 40 x 14 | 20 | 26 x 6.6 CH | 8 |
| | DC-9 | 30 (31) | 210/225 | 40 x 14 | 22 | 26 x 6.6 CH | 8/10 |
| | DC-9 | 30 (32) | 225 | 40 x 14 | 24 | 26 x 6.6 CH | 10 |
| | DC-9 | 30 (33-41) | 225 | 40 x 14 | 22/24 | 26 x 6.6 CH | 10 |
| | DC-9 | (Flotation) | 210 | 42 x 15 | 22 | 26 x 6.6 CH | 10 |
| | DC-9 | 50 | 225 | 41 x 15.0-18 | 22/24 | 26 x 6.6 CH | 10 |
| MD-80 | (DC-9-80) | 225 | H44.5 x 16.5-20 | 24/26 | 26 x 6.6 | 12 | |
| DC-10 | 10 | 225 | 50 x 20.00-20 | 32/34 | 37 x 14-14 | 24 | |
| DC-10 | 30/40 | 235 | 52 x 20.5-23 | 28/30 | 40 x 15.5-16 | 26/28 | |
| Fokker | F-28 | | 210 | 39 x 13 | 14/16 | 24 x 7.7 CH | 10 |
| | F-28 | (Flotation) | 210 | 40 x 14 | 16 | 24.5 x 8.5-10 CH | 10 |
| | F-28 | MK2000, 5000, 6000 | 210 | 40 x 14 | 16 | 24.5 x 8.5-10 CH | 10 |

| | | | | | | | |
|-----------------|---------------|----------|-----|---------------|-------|-----------------|-------|
| Lockheed | L-188 | | LS | 13.50-16 | 24 | 7.50-14 | 10 |
| | L-188 | | 210 | 40 x 14 | 24 | 28 x 7.7 | 10/14 |
| | C-130, L-382 | | 210 | 56 x 20.00-20 | 24 | 12.50 x 16TT/TL | 12 |
| | Constellation | | LS | 17.00-20TT/TL | 24 | 34 x 9.9 | 10 |
| | L-1011 | | 225 | 50 x 20.00-20 | 32 | 36 x 11 | 20 |
| | L-1011 | | 225 | 50 x 20.00-20 | 34 | 36 x 11 | 22 |
| | L-1011 | | 225 | 52 x 20.5-20 | 34/36 | 37 x 13-16 | 26 |
| Nihon | YS-11 | | 210 | 39 x 13 | 14 | 24 x 7.7 | 10 |
| | YS-11 | 400, 600 | LS | 12.5 - 16 | 12 | 24 x 7.7 | 10 |

Source: B. F. Goodrich Co.

All tires are tubeless unless otherwise specified. Code: TT = tube type, TL = tubeless, CH = deflection chine, LS = low speed.

Note: All B. F. Goodrich commercial aircraft tires are manufactured in accordance with TSO-C62C and/or applicable airframe manufacturer specifications. The applications provided in these tables are based on information supplied by airframe manufacturers and represent the results of certification testing for individual aircraft of the types listed in the table. Your requirements may vary depending on the actual configuration of your aircraft, particularly if modifications have been made since tire certification. You must verify the proper tire applications in its existing configuration prior to placing your order with B. F. Goodrich.

FAILURE TO MAKE THIS VERIFICATION AND TO INSTALL UNAPPROVED TIRES ON AN AIRCRAFT MAY RESULT IN TIRE FAILURE CAUSING PROPERTY DAMAGE, SERIOUS INJURY, OR LOSS OF LIFE.

Table 14.11 Tire Usage: Military Aircraft

| Manufacturer | DOD Designation | Popular Name | Speed MPH | MAIN GEAR | | AUXILIARY GEAR | | |
|-------------------------------|-----------------|-----------------|-----------|---------------|------------|----------------|------------|------|
| | | | | Tire Size | Ply Rating | Tire Size | Ply Rating | |
| Beech | T34B | Mentor | LS | 6.50-8 | 6 TT | 5.00-5 | 6 TT | |
| | U8F | Seminole | LS | 8.50-10 | 8 TT | 6.50-10 | 6 TT | |
| | T42A | Cochise | LS | 6.50-8 | 6 TL | 5.00-5 | 6 TL | |
| | VC6A | King Air | LS | 8.50-10 | 8TL | 6.50-10 | 6 TL, TT | |
| Boeing | B47E | Stratojet | 250 | 56 x 16 | 36 TL | 26 x 6.6 | 14 TT | |
| | B52F, G, H | Stratofortress | 250 | 56 x 16 | 38 TL | 32 x 8.8 | 12 TT | |
| | C97D | Stratofreighter | 250 | 56 x 16 | 32 TT | 36" SC | 12 TT | |
| | C135B | Stratolifter | 200 | 49 x 17 | 26 TL | 38 x 11 | 14 TL | |
| | VC137C | | 200 | 46 x 16 | 28 TL | 39 x 13 | 16 TL | |
| | E3A | 707 | 210 | 46 x 16 | 28 TL | 39 x 16 | 16 TL | |
| | E4A | 747 | 225 | 49 x 17 | 30 TL | 49 x 17 | 30 TL | |
| | T43A | 737 | 210 | 40 x 14 | 24 TL | 24 x 7.7 | 14 TL | |
| | YC14 | STOL | 190 | B40 x 18.0-16 | 20 TL | B40 x 18.0-16 | 20 TL | |
| | Cessna | O-1E | Bird Dog | LS | 8.00-6 | 6 TL | 8 x 3.0-4 | 4 TT |
| | | T37B | | 160 | 20 x 4.4 | 10 TL | 16 x 4.4 | 6 TT |
| A37 | | | LS | 7.00-8 | 12 TL | 6.00-6 | 6 TT | |
| T41A | | Skyhawk | LS | 6.00-6 | 4 TL | 5.00-5 | 4 TL | |
| U3B | | | LS | 6.50-10 | 6 TT | 6.00-6 | 6 TT | |
| U17A | | Skywagon | LS | 6.00-6 | 6 TT | 10" SC | 8 TT | |
| O2A, B | | | LS | 6.00-6 | 8 TL | 15 x 6.00-6 | 4 TT | |
| de Havilland | | CV-2B | Caribou | LS | 11.00-12 | 8 TL | 7.50-10 | 6 TL |
| | CV-7A | Buffalo | LS | 15.00-12 | 10TL | 8.90-12.50 | 6 TL | |
| | U-1A | Otter | LS | 11.00-12 | 6 TT | 6.00-6 | 6 TT | |
| | U-6A | Beaver | LS | 8.50-10 | 6 TT | 5.50-4 | 6 TT | |
| Fairchild-Hiller | C-119J | Flying Boxcar | 160 | 15.50-20 | 14 TT | 9.50-16 | 10 TT | |
| | C-123B | Provider | 160 | 17.00-20 | 22 TT, TL | 11.00-12 | 8 TT | |
| | C-123J | Provider | 160 | 17.00-20 | 22 TT, TL | 9.50-16 | 10 TT | |
| Fairchild (Republic Division) | F-84F | Thunder Streak | 225 | 30 x 6.6 | 14 TT | 20 x 4.4 | 12 TL, TT | |
| | F-105 | Thunder Chief | 250 | 36 x 11 | 24 TL | 24 x 7.7 | 14 TL | |
| | A-10A | Thunder Bolt II | 200 | 36 x 11 | 22 TL | 24 x 7.7 | 14 TL | |

| | | | | | | | |
|-------------------------|-------------------|-----------------|------------|---------------|--------------|-------------|--------|
| General Dynamics | B-58A | Hustler | 268 | 22 x 7.7-12 | 16 TL | 22 x 7.7-12 | 16 TL |
| | F102A | Delta Dagger | 250 | 30 x 8.8 | 22 TT | 24 x 5.5 | 12 TT |
| | F106A | Delta Dart | 250 | 30 x 8.8 | 22 TL | 18 x 4.4 | 12 TT |
| | C131A | Samaritan | 160 | 34 x 9.9 | 14 TL | 26 x 6.6 | 14 TL |
| | C131B, C, D, E, F | Samaritan | 160 | 12.50-16 | 12 TT | 7.50-14 | 8 TT |
| | RB-57F | | 200 | 44 x 13 | 26 TT | 24 x 5.5 | 12 TT |
| | T29D | | 160 | 34 x 9.9 | 14 TT | 26 x 6.6 | 14 TL |
| | F-16A, B | Fighting Falcon | 230 | 25.5 x 8.0-14 | 18 TL | 18 x 5.5 | 14 TL |
| | F-16C, D | Fighting Falcon | 250 | 25.5 x 8.0-14 | 20 TL | 18 x 5.7-8 | 18 TL |
| | F111A | | 225 | 47 x 18-18 | 30 TL | 22 x 6.6-10 | 16 TL |
| | FB111A | | 250 | 47 x 18-18 | 36 TL | 22 x 6.6-10 | 20 TL |
| FB-111B | | 250 | 47 x 18-18 | 36 TL | 21 x 7.25-10 | 20 TL | |
| Grumman | A6A | Intruder | 160 | 36 x 11 | 24 TL | 20 x 5.5 | 12 TL |
| | E16B | Intruder | 160 | 36 x 11 | 24 TL | 20 x 5.5 | 16 TL |
| | F11A | Tiger | 200 | 26 x 6.6 | 16 TL | 18 x 5.5 | 8 TL |
| | OV-1C | Mohawk | LS | 8.50-10 | 12 TL | 6.50-8 | 6 TL |
| | S-2D | Tracker | 160 | 34 x 9.9 | 14 TT | 18 x 5.5 | 12 TT |
| | F-14A | Tomcat | 219 | 37 x 11.50-16 | 28 TL | 22 x 6.6-10 | 20 TL |
| | E-1B | Tracer | 160 | 34 x 9.9 | 14 TT | 18 x 5.5 | 12 TT |
| | E-2A | Hawkeye | 160 | 36 x 11 | 24 TL | 20 x 5.5 | 12 TL |
| | C-1A | Trader | 160 | 34 x 9.9 | 14 TT | 18 x 5.5 | 12 TT |
| | C-2A | Greyhound | 160 | 36 x 11 | 24 TL | 20 x 5.5 | 12 TL |
| | HU-16E | Albatross | 160 | 40 x 12 | 14 TT | 26 x 6 | 10 TT |
| | Helio | U10A | Courier | LS | 6.50-8 | 6 TT | 10" SC |
| Vought | A7A, B, E | Corsair II | 172 | 28 x 9.0-12 | 22 TL | 22 x 5.5 | 12 TL |
| | A7D | Corsair II | 200 | 28 x 9.0-14 | 22 TL | 22 x 5.5 | 10 TL |
| | F8H, J | Crusader | 200 | 26 x 6.6 | 16 TL | 20 x 5.5 | 14 TL |
| | XC142A | | LS | 11.00-12 | 8 TL | 8.50-10 | 10 TL |
| Lockheed | F104A, B | Starfighter | 275 | 25 x 6.75 | 18 TL | 18 x 5.5 | 14 TT |
| | F104C, D, J, DJ | Starfighter | 275 | 25 x 6.75 | 18 TL | 18 x 5.5 | 14 TT |
| | F104G | Starfighter | 275 | 25 x 6.75 | 18 TL | 18 x 5.5 | 14 TT |
| | F104G | Starfighter | 275 | 26 x 8.0-14 | 16 TL | 18 x 5.5 | 14 TL |
| | SR71 | Blackbird | 275 | 27.5 x 7.5-16 | 22 TL | 25 x 6.75 | 16 TL |
| | P2H | Neptune | 160 | 56" SC | 20 TL | 34 x 9.9 | 14 TL |
| | P3A | Orion | 200 | 40 x 14 | 26 TL | 28 x 7.7 | 14 TL |
| | P3B, C | Orion | 200 | 40 x 14 | 28 TL | 28 x 7.7 | 14 TL |

(Table continued on next page.)

Table 14.11 (cont.) Tire Usage: Military Aircraft

| Manufacturer | DOD Designation | Popular Name | Speed MPH | MAIN GEAR | | AUXILIARY GEAR | |
|-------------------|-----------------------|---------------------|-----------|-----------------|--------------|-----------------|------------|
| | | | | Tire Size | Ply Rating | Tire Size | Ply Rating |
| Lockheed (cont'd) | C121G | Super Constellation | 160 | 17.00-20 | 22 TL | 33" SC | 10 TT |
| | C130A, B, D, E | Hercules | 200 | 20.00-20 | 22 TT | 12.50-16 | 12 TT |
| | S3A | Viking | 248 | 30 x 11.5-14.5 | 24 TL | 22 x 6.75-10 | 18 TL |
| | C130H | Hercules | 200 | 20.00-20 | 26 TL | 12.50-16 | 12 TT |
| | C140A | Jetstar | 200 | 26 x 6.6 | 14 TL | 18 x 4.4 CH | 10 TL |
| | C141 | Starlifter | 200 | 44 x 16 | 28 TL | 36 x 11 | 22 TL |
| | T33 | Shooting Star | 200 | 26 x 6.6 | 14 TL | 22 x 7.25-11.50 | 8 TL |
| | C5A, B | Galaxy | 200 | 49 x 17 | 26 TL | 49 x 17 | 26 TL |
| | AH56A | Cheyenne | 160 | 29 x 11.00-10 | 10 TL | 5.00-4 | 8 TL |
| | McDonnell Douglas Co. | P5B | Marlin | 160 | 15.50-20 | 14 TT | 10.00-7 |
| A1 | | Skyraider | 160 | 32 x 8.8 | 16 TT | 12 1/2 x 4 1/2 | 14 TT |
| A3 | | Skywarnor | 200 | 44 x 13 | 26 TL | 32 x 8.8 | 18 TT |
| A4 | | Skyhawk | 200 | 24 x 5.5 | 16 TT | 18 x 5.5 | 12 TL |
| AV-8B | | Harrier | 160 | 26 x 7.75-13 | 10 TL | 26 x 8.75-11 | 16 TL |
| | | | | Outrigger | 13.5 x 6.0-4 | 14 TL | |
| B-26 | | Counter Invader | 160 | 15.50-20 | 14 TT | 36" SC | 12 TT |
| B66 | | Destroyer | 225 | 49 x 17 | 26 TL | 36 x 11 | 22 TT |
| F6A | | Skyray | 200 | 26 x 6.6 | 16 TL | 22 x 5.5 | 12 TT |
| C47 | | Skytrain | 160 | 17.00-16 | 12 TT | 9.00-6 | 10 TT |
| C54 | | Skymaster | 160 | 15.50-20 | 14 TT | 44" SC | 12 TL |
| C9A | | Nightingale | 160 | 40 x 14 | 24 TL | 26.4-6-CH | 10 TL |
| C117 | | | 160 | 17.00-16 | 12 TT | 9.00-6 | 10 TT |
| VC118 | | Liftmaster | 160 | 15.50-20 | 20 TL | 44" SC | 12 TL |
| C124 | | Globemaster | 160 | 25.00-28 | 30 TT | 15.50-20 | 14 TL |
| C133 | | Cargomaster | 200 | 20.00-20 | 22 TT | 15.00-16 | 10 TL |
| F-101A, C | | Voodoo | 275 | 32 x 8.8 | 24 TL | 18 x 5.5 | 14 TL |
| F-101B | | Voodoo | 275 | 31 x 11.50-16 | 22 TL | 18 x 5.5 | 14 TL |
| F4B | | Phantom II | 248 | 30 x 8.0 | 26 TL | 18 x 5.7-8 | 14 TL |
| F4C, D, E | | Phantom II | 248 | 30 x 11.50-14.5 | 24/26 TL | 18 x 5.5 | 14 TL |
| F4J | | Phantom II | 248 | 30 x 11.50-14.5 | 26 TL | 18 x 5.7-8 | 14 TL |
| F-15A, B, C, D | | Eagle | 260 | 34.5 x 9.75-18 | 26 TL | 22 x 6.6-10 | 18 TL |
| F-18A | | Hornet | 248 | 30 x 11.5-14.5 | 24/26 TL | 22 x 6.6-10 | 20 TL |

| | | | | | | | |
|----------------------|---------|-----------------|----------------|-----------------|----------|-----------------|-------|
| Rockwell Int. | B-1B | | 225 | B46 x 16.0-23.5 | 30 TL | 35 x 11.5-16 | 22 TL |
| | F86 | Sabre | 200 | 26 x 6.6 | 14 TL | 22 x 7.25-11.50 | 8 TL |
| | F100 | Super Sabre | 250 | 30 x 8.8 | 22 TL | 18 x 4.4 | 12 TL |
| | RA5C | Vigilante | 200 | 36 x 11. | 28 TL | 26 x 6.6 | 16 TL |
| | OV10A | Bronco | 160 | 29 x 11.00-10 | 10 TL | 7.50-10 | 12 TL |
| | U4A | Aero Commander | 160 | 8.50-10 | 6 TT | 6.00-16 | 6 TT |
| | T-2B | Buckeye | 160 | 24 x 5.5 | 12 TL | 20 x 4.4 | 10 TL |
| | T-28D | Trojan | 160 | 24 x 7.7 | 10 TT | 24 x 7.7 | 10 TL |
| | T-39 | Sabreliner | 200 | 26 x 6.6 | 14 TL | 18 x 4.4 | 6 TL |
| | X-15 | | — | Skids | | 18 x 4.4 | 12 TL |
| | XB70A | Valkyrie | 225 | 40 x 17.50-18 | 40 TL | 14 x 4.5-8 | 8 TL |
| Shuttle | | 263 | 44.5 x 16.0-21 | 34 TL | 32 x 8.8 | 20 TL | |
| Northrop | F5 A, B | Freedom Fighter | 250 | 22 x 8.5-11 | 16 TL | 18 x 6.5-8 | 12 TL |
| | F5E | Tiger II | 265 | 24 x 8.0-13 | 18 TL | 18 x 6.5-8 | 12 TL |
| | T38A | Talon | 225 | 20 x 4.4 | 12 TL | 18 x 4.4 | 6 TL |
| | F-20 | Tiger Shark | 265 | 24 x 8.0-13 | 18 TL | 18 x 6.5-8 | 12 TL |
| Piper | U7A | | LS | 8.00-4 | 4 TT | TAILSKID | |
| | U11A | Aztec | LS | 7.00-6 | 8 TT | 6.00-6 | 4 TT |

Source: B. F. Goodrich Co.

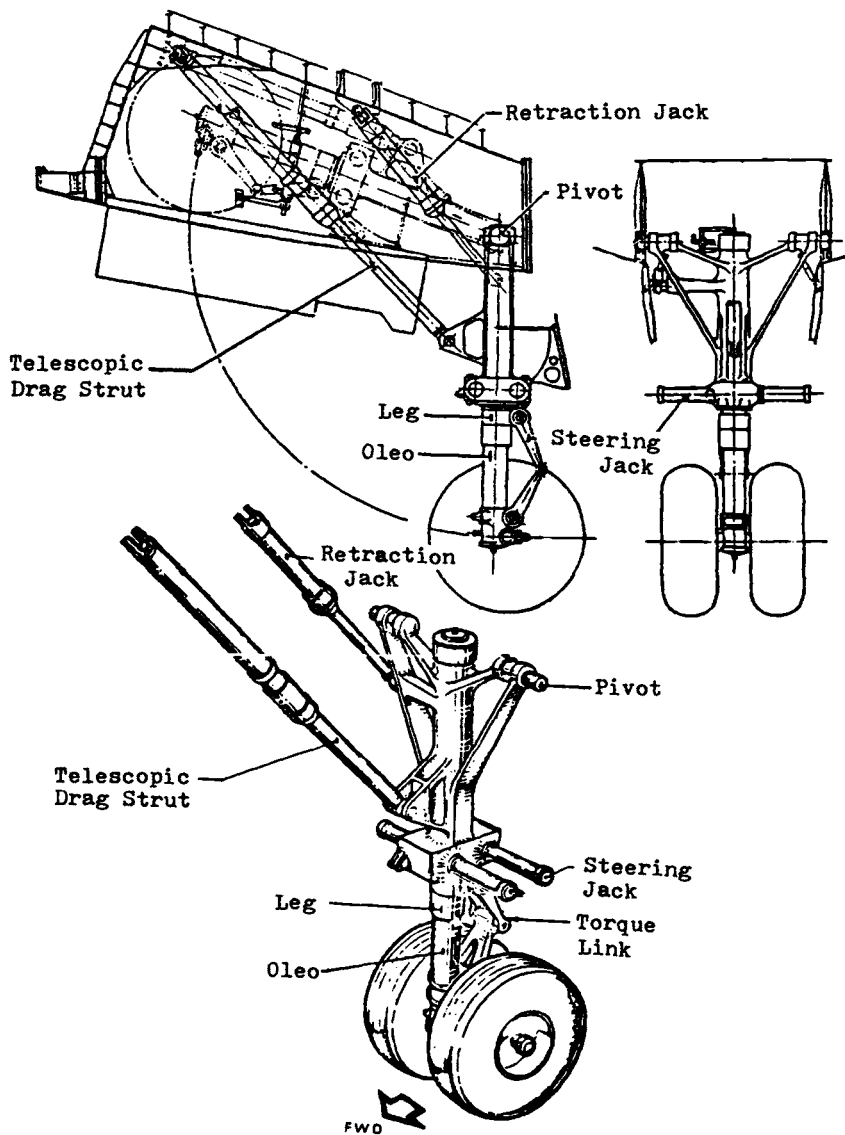


Fig. 14.1 A-300B nose landing gear (source: Aerospatiale).

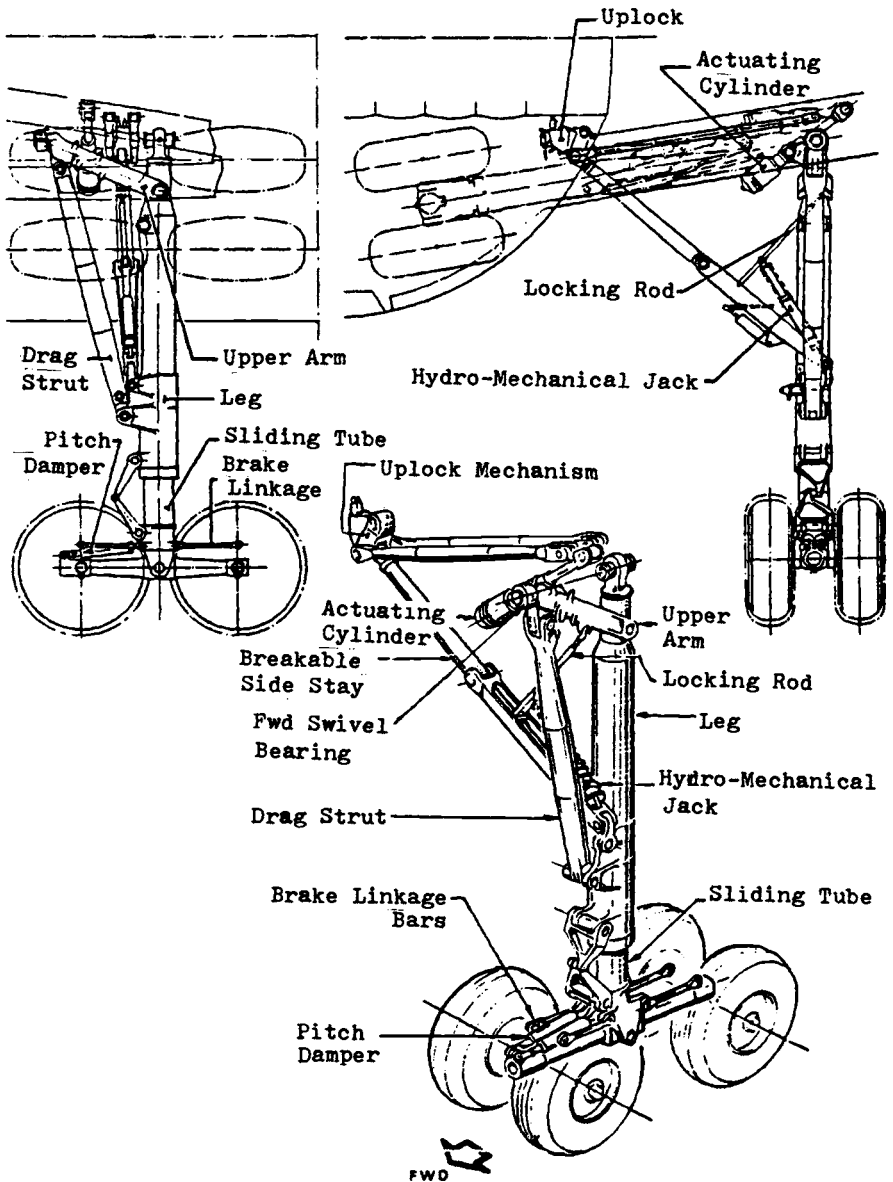


Fig. 14.2 A-300B main landing gear (source: Aerospatiale).

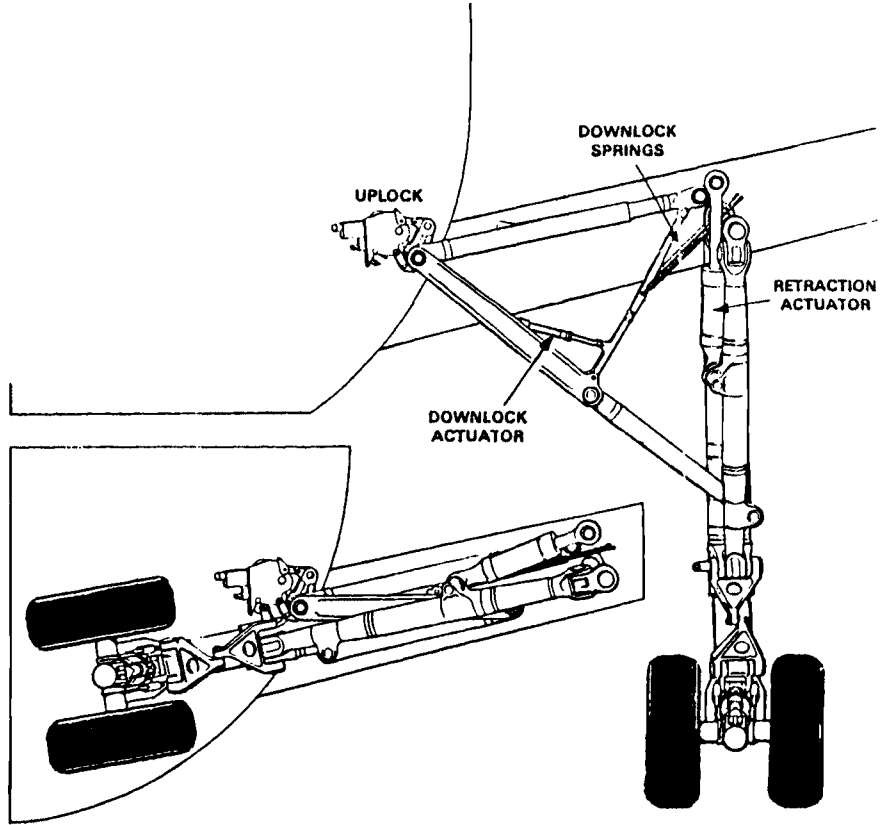
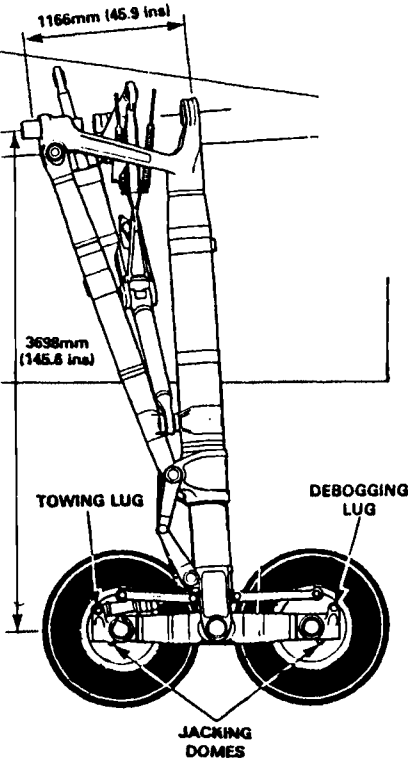


Fig. 14.3 A-310 main landing gear (source: Dowty Rotol Ltd.).

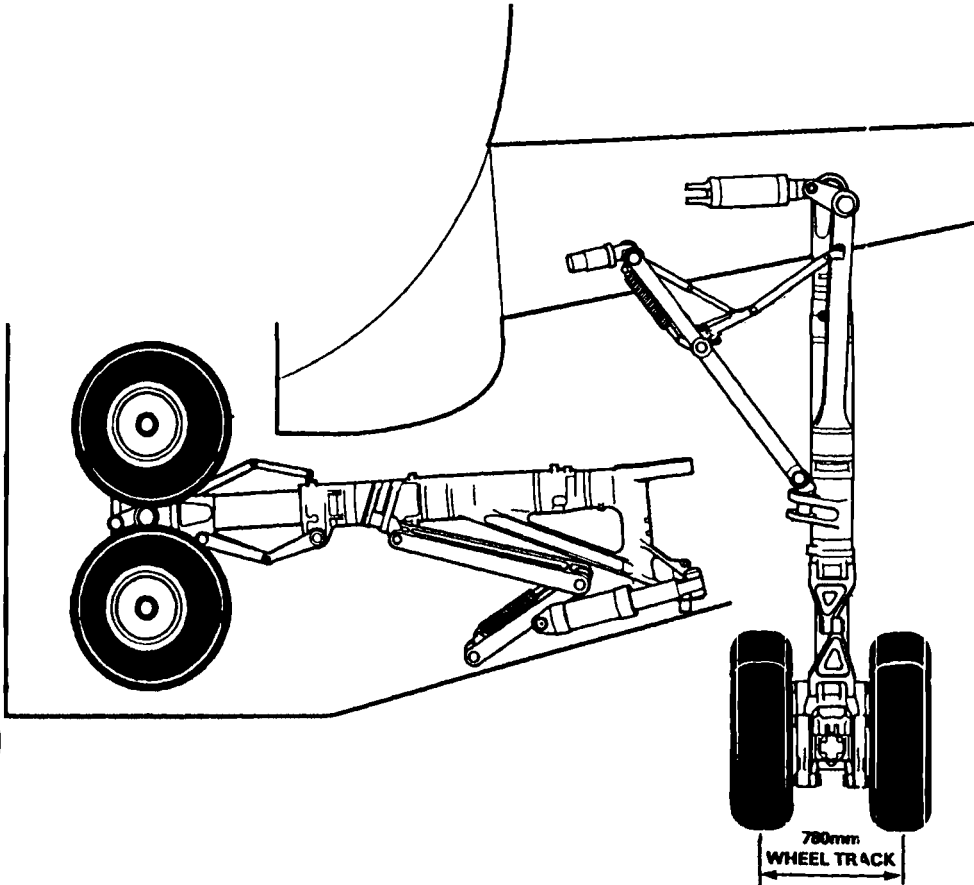
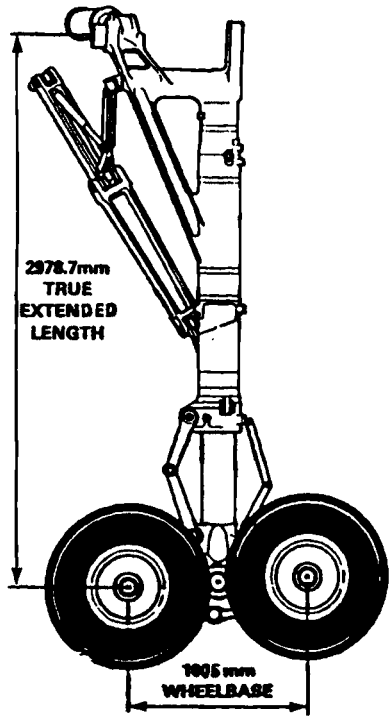


Fig. 14.4 A-320 main landing gear (source: Dowty Rotol Ltd.).

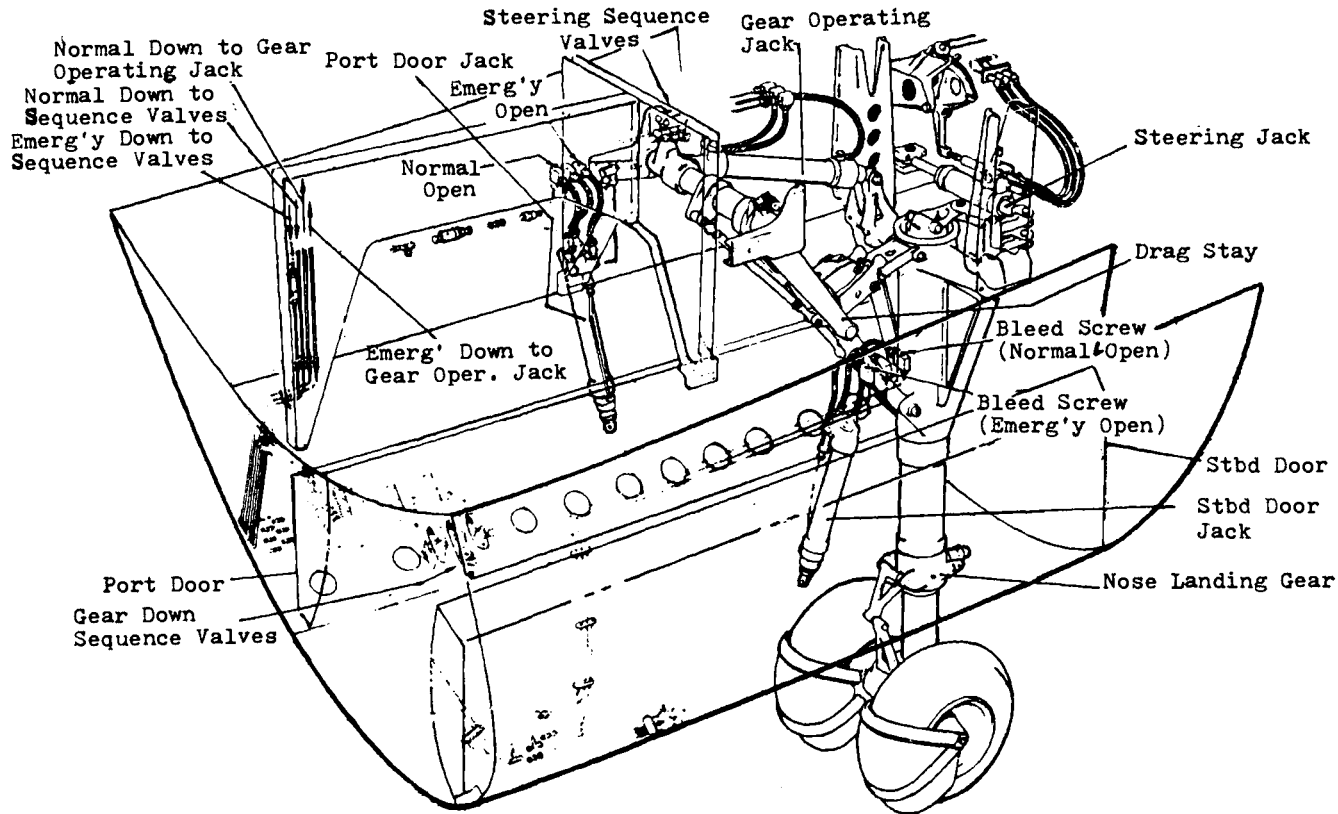


Fig. 14.5 B.Ae. Nimrod nose gear installation (source: British Aerospace Corp.).

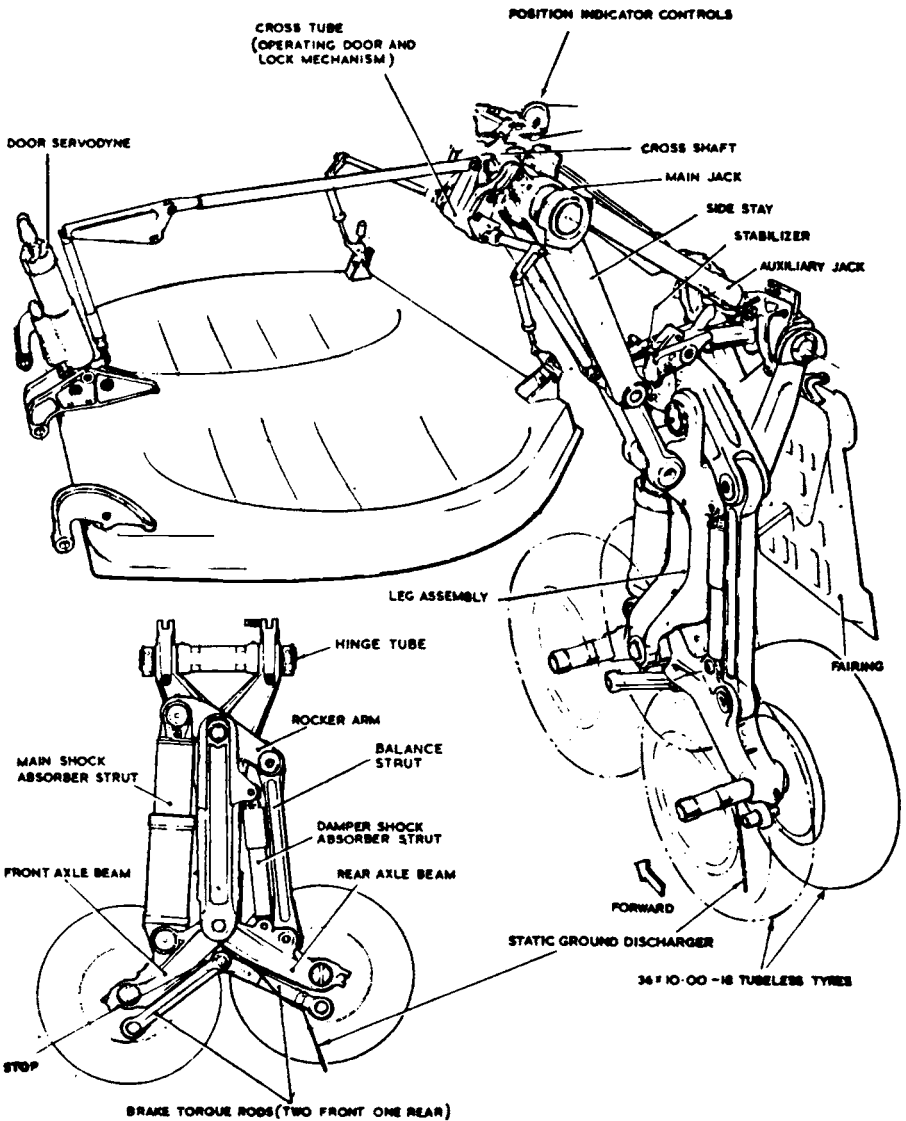


Fig. 14.6 B.Ae. Nimrod main gear (source: British Aerospace Corp.).

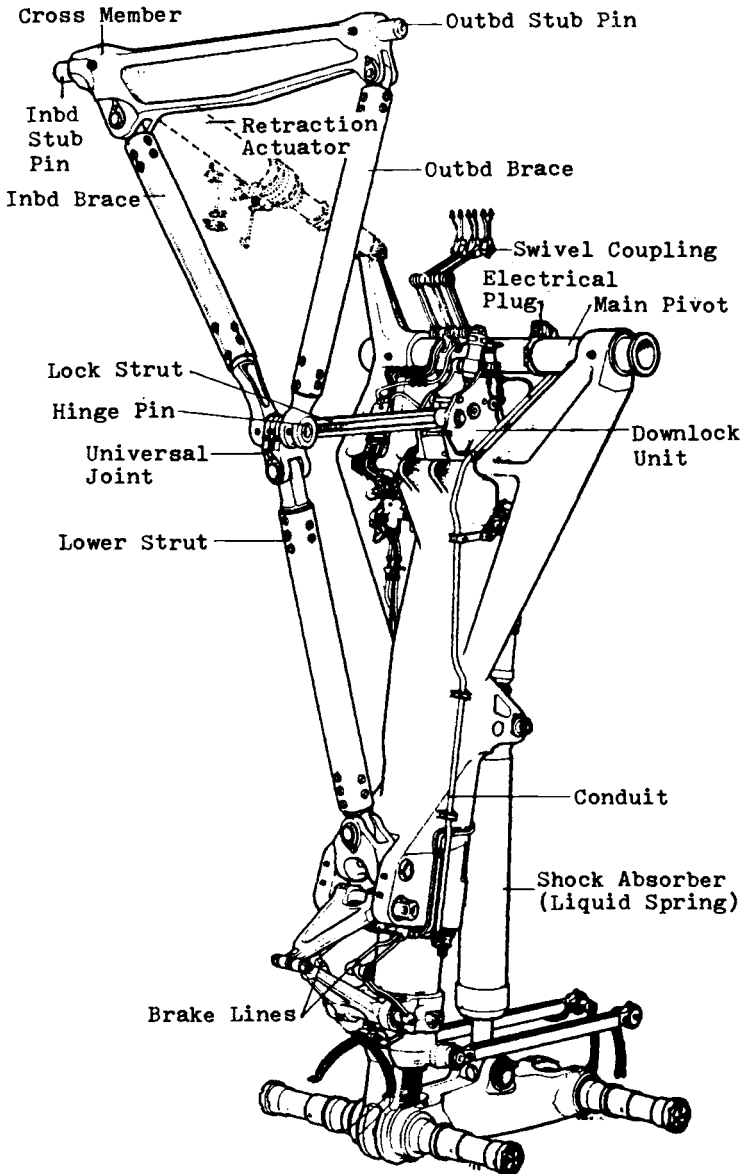


Fig. 14.7 B.Ae. Vulcan main landing gear (source: Dowty Rotol Ltd.).

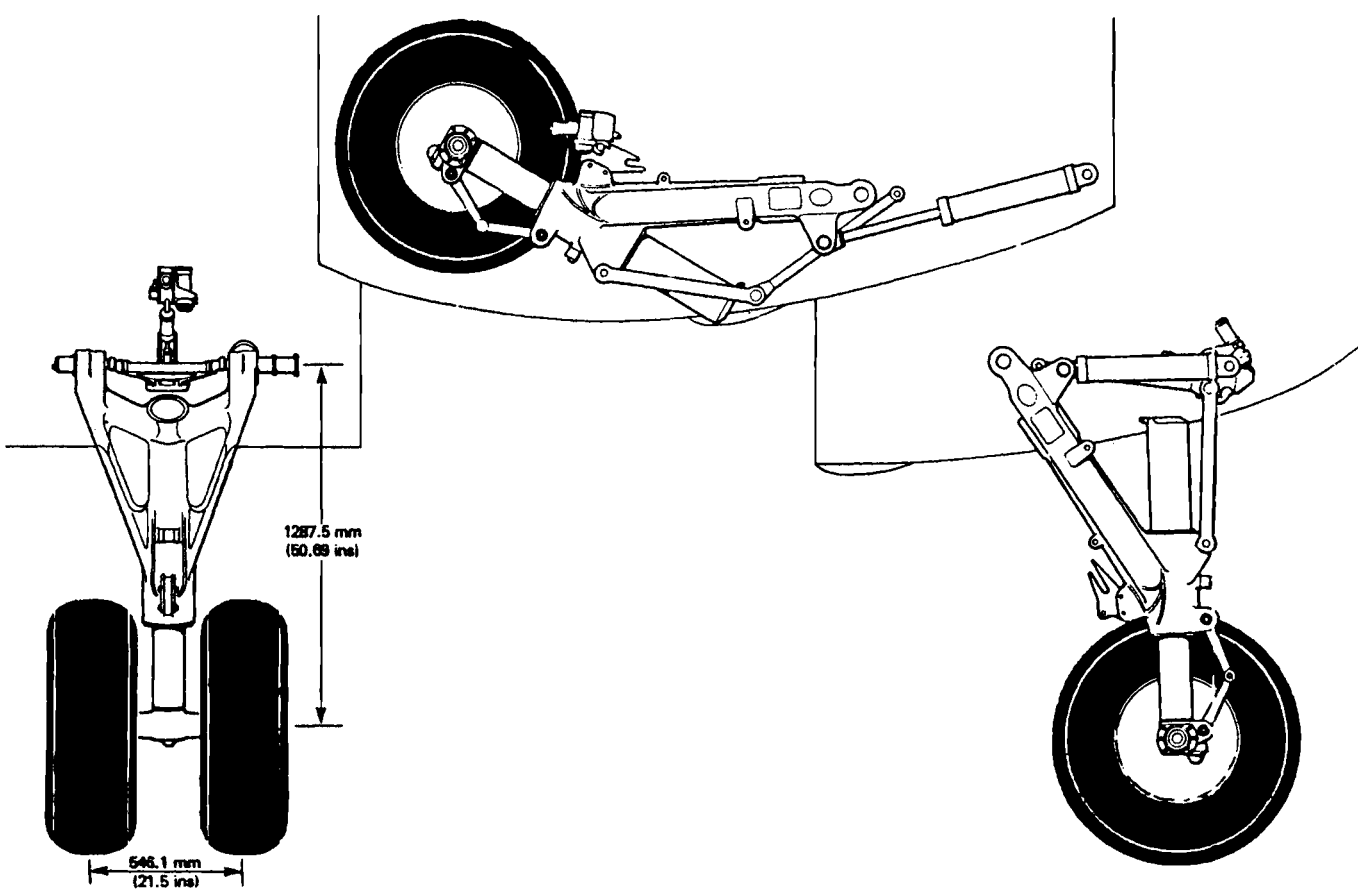


Fig. 14.8 B.Ae. ATP main landing gear (source: Dowty Rotol Ltd.).

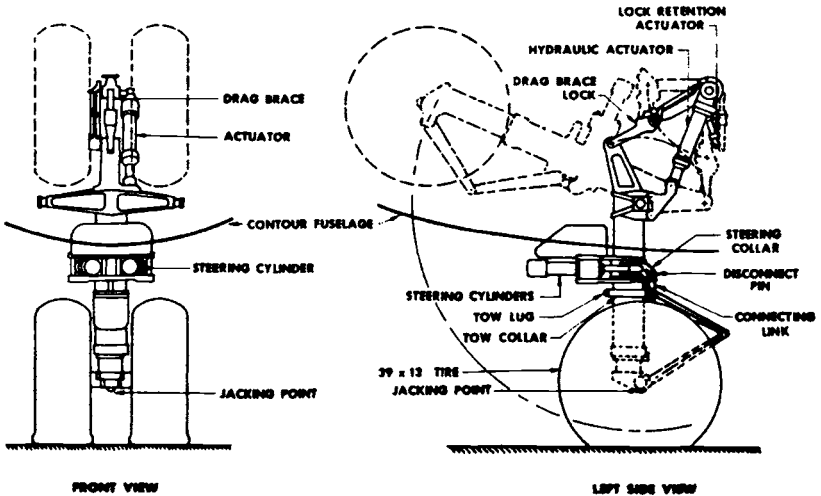
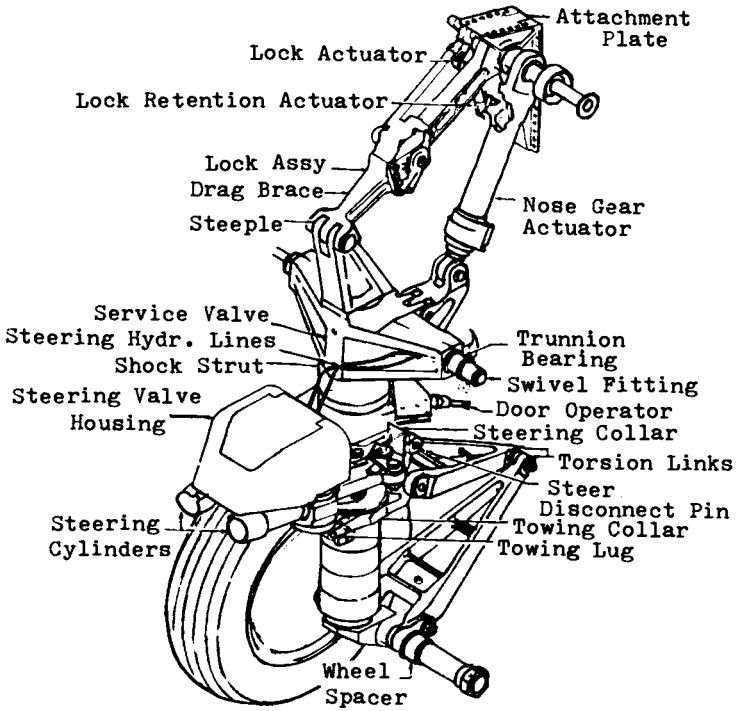


Fig. 14.9 Boeing 707 nose landing gear.

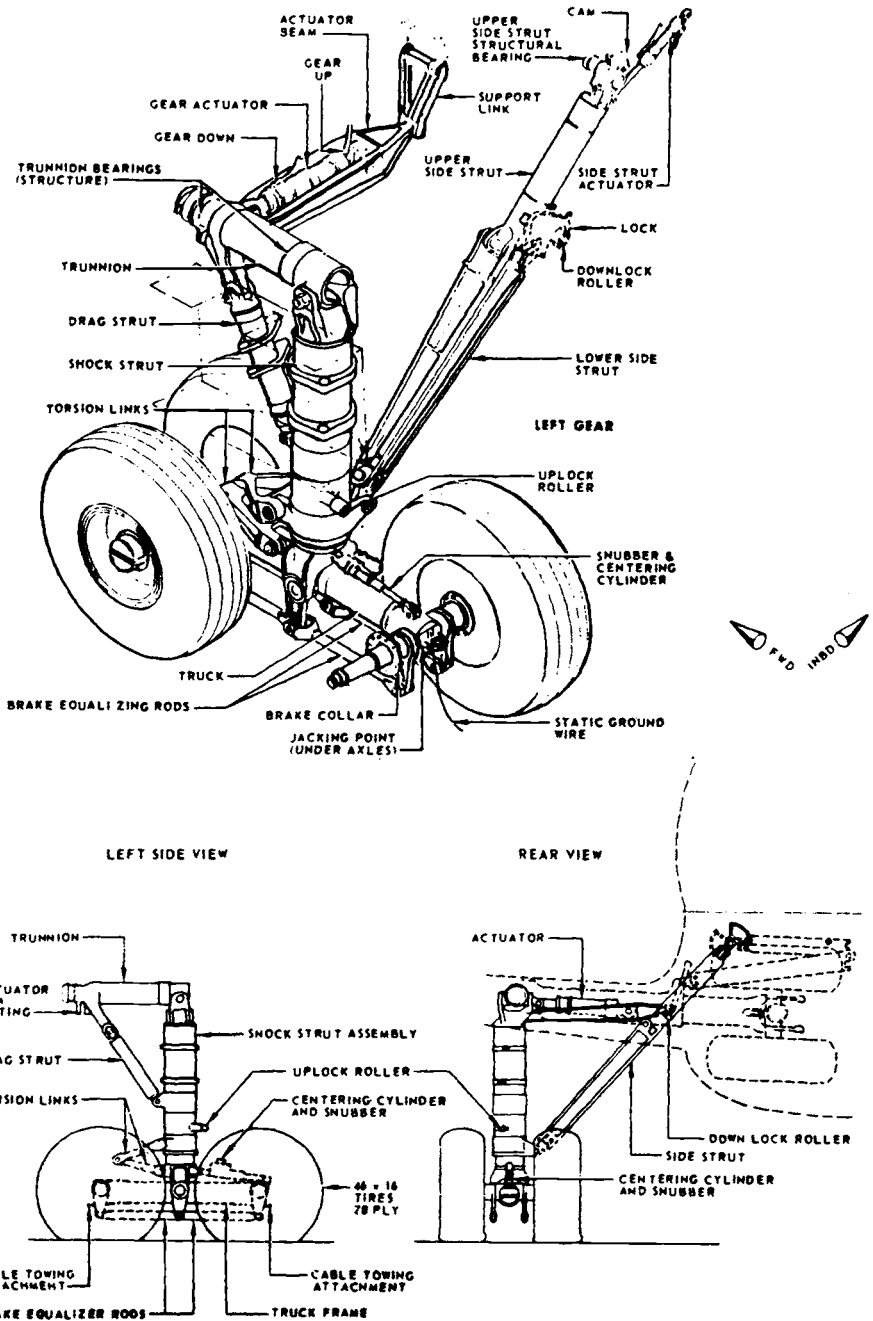


Fig. 14.10 Boeing 707 main landing gear.

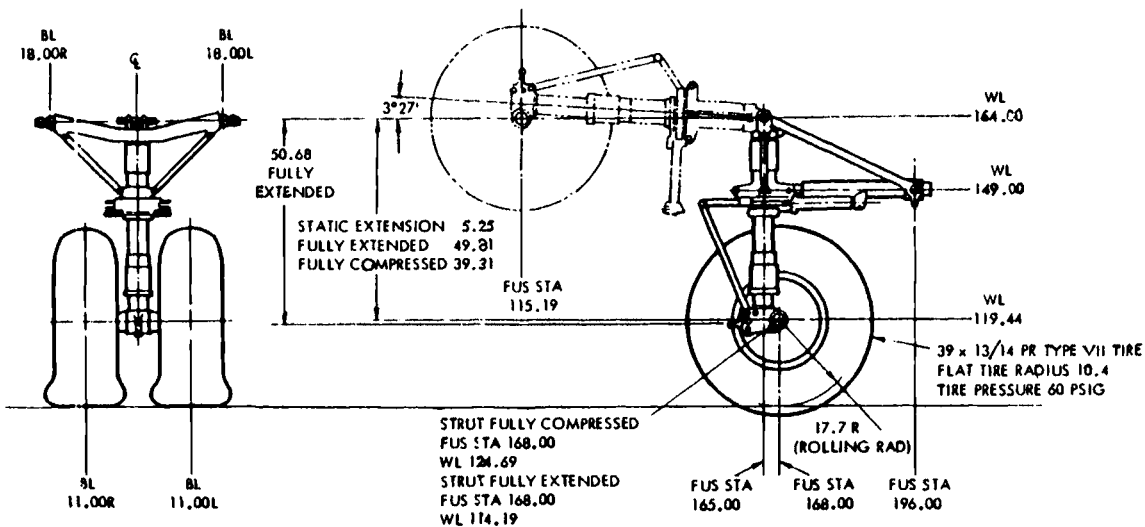


Fig. 14.11 C-130E nose gear geometry (source: Lockheed).

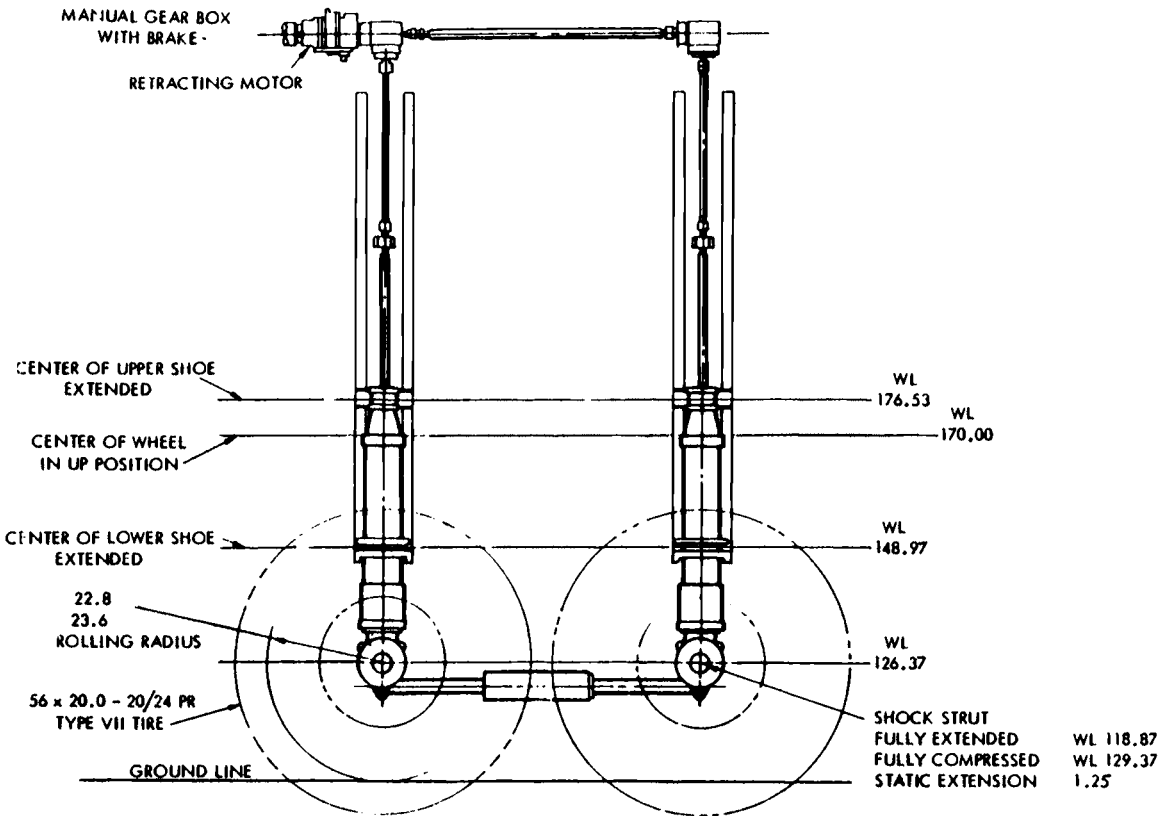


Fig. 14.12 C-130E main gear geometry (source: Lockheed).

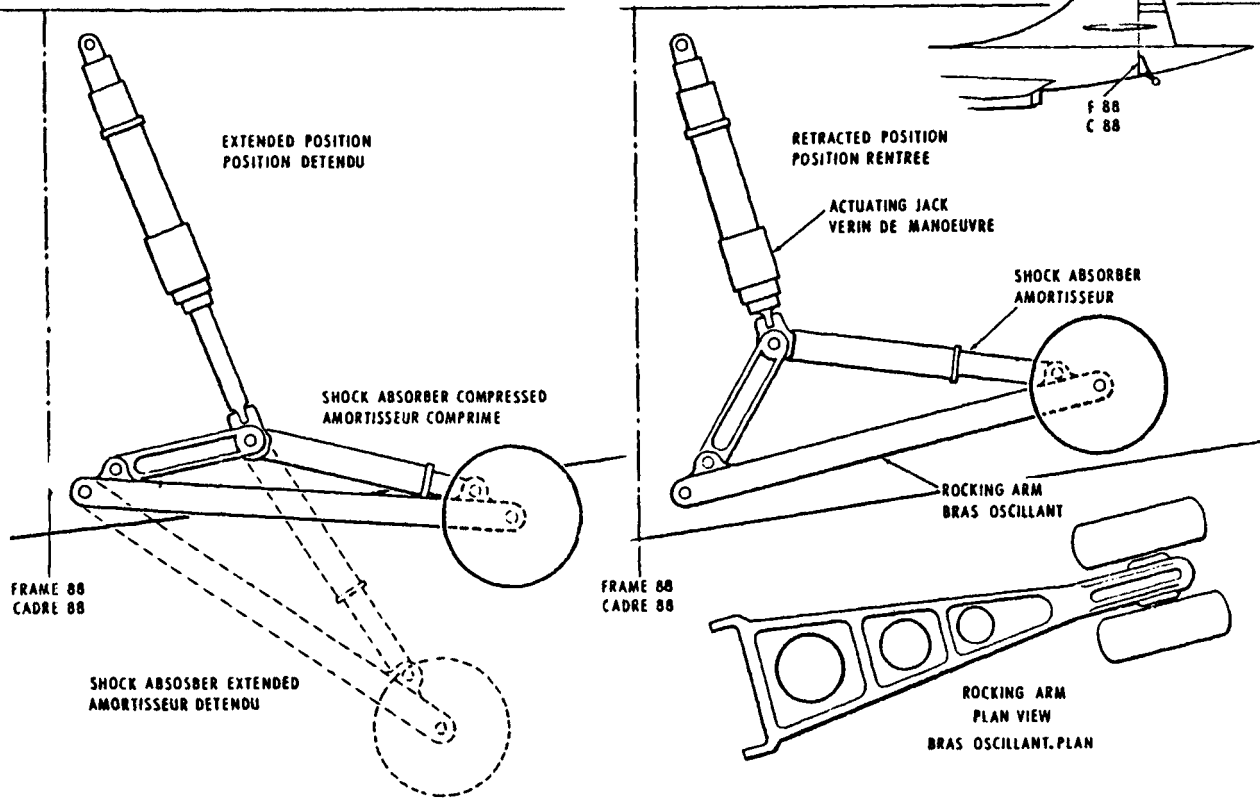


Fig. 14.13 Concorde tail bumper (source: British Aircraft Corp., Aerospatiale).

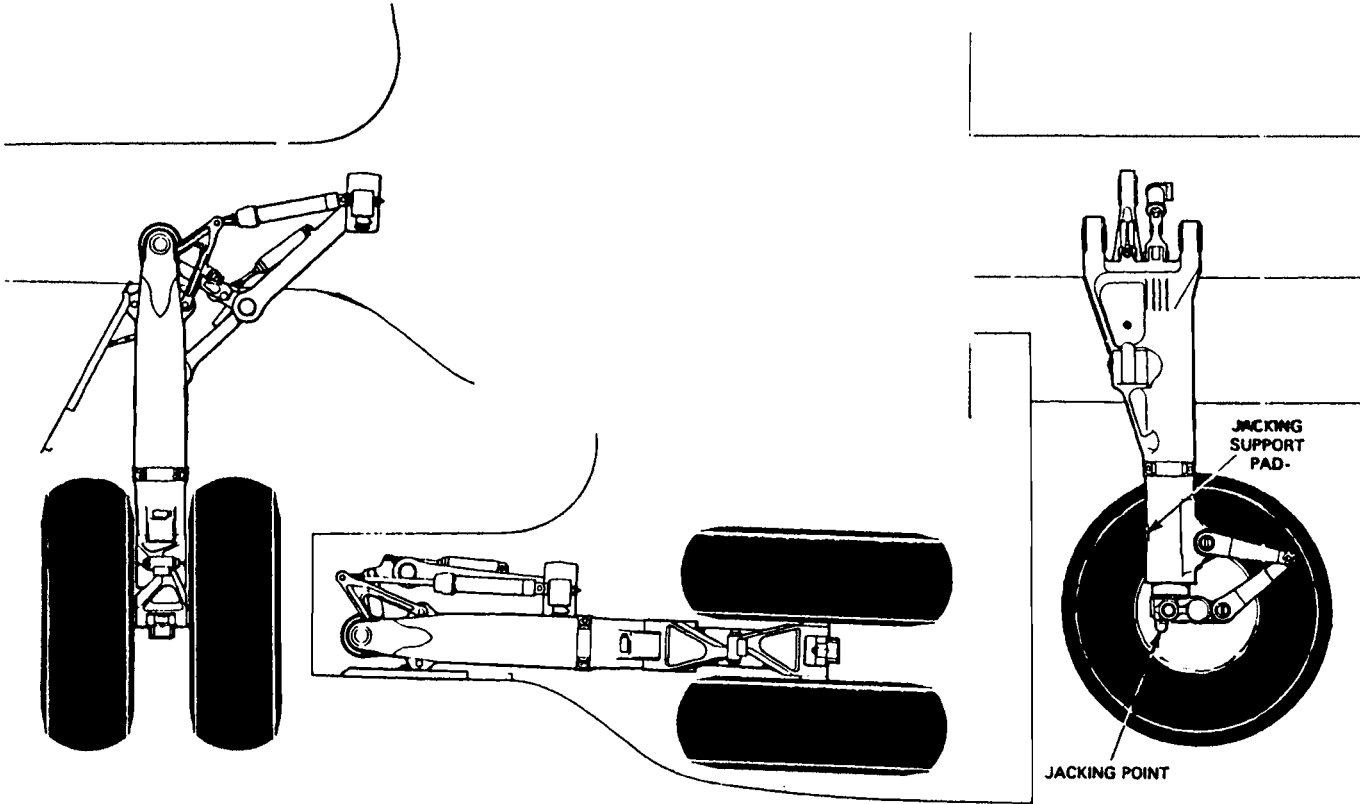


Fig. 14.14 Fokker 100 main landing gear (source: Dowty Rotol Ltd.).

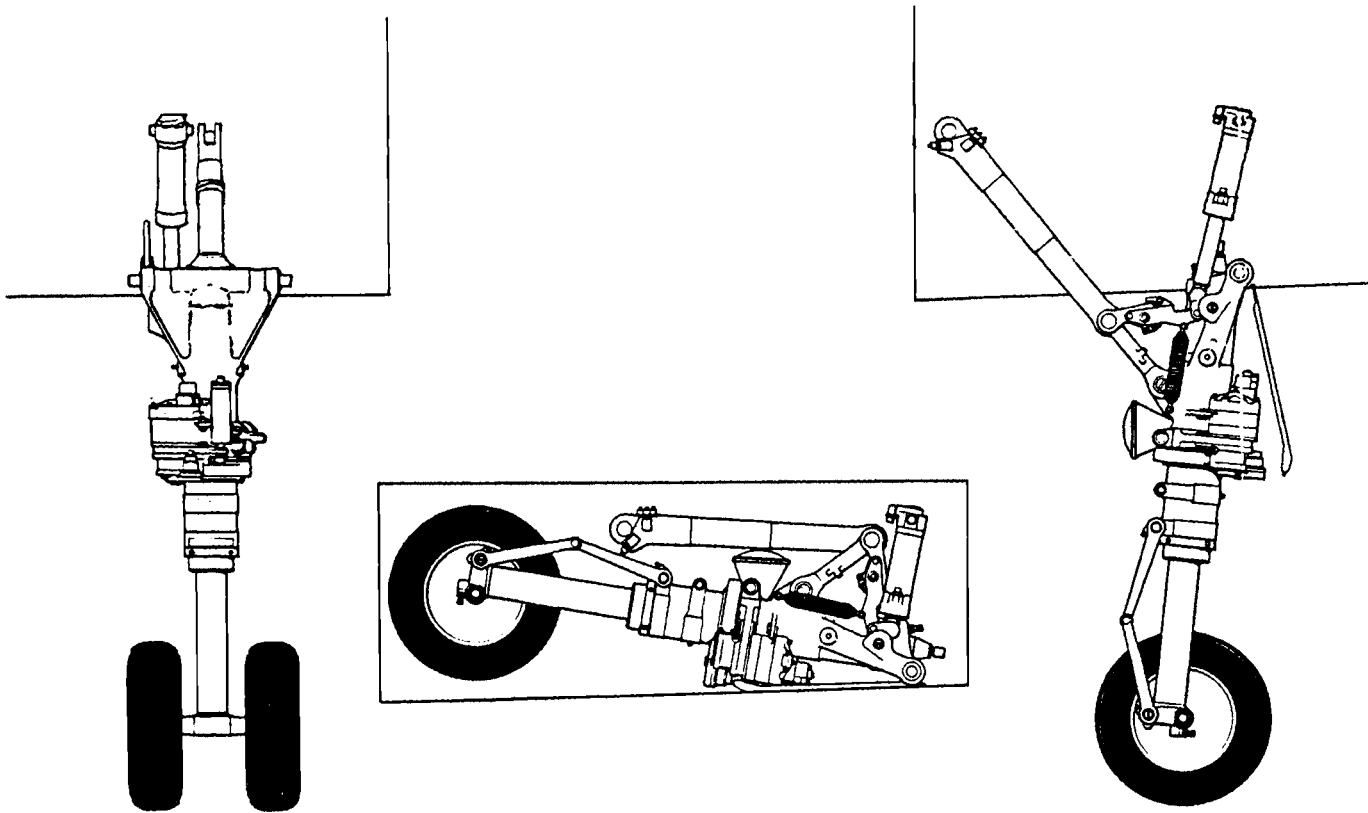


Fig. 14.15 Tornado nose landing gear (source: Dowty Rotol Ltd.).

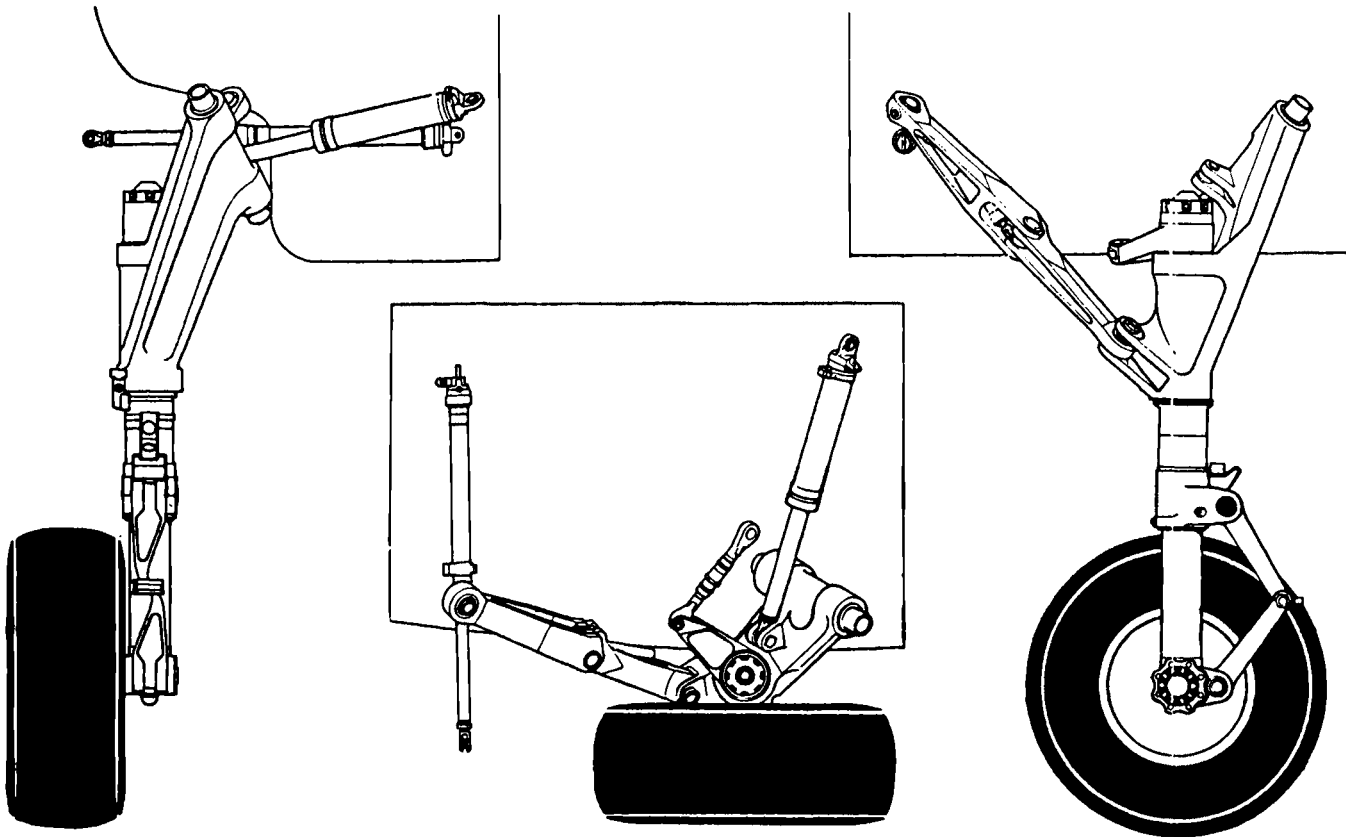


Fig. 14.16 Tornado main landing gear (source: Dowty Rotol Ltd.).

15 SPECIFICATIONS

This chapter lists the industry and government specifications cited in the previous chapters.

INDUSTRY SPECIFICATIONS

(Note: Some titles have been paraphrased for simplicity. (*Society of Automotive Engineers* (400 Commonwealth Dr., Warrendale, PA 15096). The following aerospace information reports, recommended practices, and standards (AIR, ARP, AS) have been developed by the SAE A-5 Aerospace Landing Gear Systems Committee:

| | |
|-----------|--|
| AIR 764B | Skid Control System Vibration Survey |
| AIR 804 | Brake Release Response Time Required for Automatic Skid Control |
| AIR 811 | Disposition of Wheels which Have Been Overheated |
| AIR 1064A | Brake Dynamics |
| AIR 1380 | Measurement of Static Mechanical Stiffness Properties of Aircraft Tires |
| AIR 1489 | Aerospace Landing Gear Systems Terminology |
| AIR 1494 | Verification of Landing Gear Design Strength |
| AIR 1594 | Plain Bearing Selection for Landing Gear Applications |
| AIR 1739 | Information on Antiskid Systems |
| AIR 1752 | Aircraft Nose Wheel Steering/Centering Systems |
| AIR 1780 | Aircraft Flotation Analysis |
| AIR 1800 | Aircraft Tail Bumpers |
| AIR 1810 | Design, Development and Test Criteria—Solid State Proximity Switches/Systems for Landing Gear Applications |
| AIR 1934 | Use of Carbon Heat Sink Brakes on Aircraft |
| ARP 597B | Wheels and Brakes, Supplementary Criteria for Design Endurance, Civil Transport Aircraft |
| ARP 698 | Process of Lubricating and Torquing Threaded Assemblies, Recommendations for Civil Aircraft Applications |
| ARP 764B | Skid Control System Vibration Survey |
| ARP 813A | Maintainability Recommendations for Aircraft Wheels and Brakes |
| ARP 862 | Skid Control Performance Evaluation |
| ARP 1070A | Design of Skid Control and Associated Aircraft Equipment for Total System Compatibility |
| ARP 1107 | Tail Bumpers for Piloted Aircraft |

| | |
|----------|--|
| ARP 1311 | Landing Gear—Aircraft |
| ARP 1322 | Overpressurization Release Devices |
| ARP 1493 | Wheel and Brake Design and Test Requirements for Military Aircraft |
| ARP 1538 | Arresting Hook Installation, Land-Based Aircraft |
| ARP 1595 | Aircraft Nose Wheel Steering Systems |
| ARP 1619 | Replacement and Modified Brakes and Wheels |
| ARP 1786 | Wheel Roll on Rim Criteria for Aircraft Applications |
| ARP 1821 | Aircraft Flotation Analysis Methods |
| ARP 1907 | Automatic Braking Systems |
| AS 483A | Skid Control Equipment |
| AS 586 | Wheel and Brake (Sand and Permanent Mold) Castings—Minimum Requirements for Aircraft Application |
| AS 665 | Tapered Axle Collar Dimensions |
| AS 666B | Cavity Design and O-Ring Selection for Static Seal Use in Aircraft Tubeless Tire Wheels |
| AS 707A | Thermal Sensitive Pressure Release Device for Tubeless Aircraft Wheels |
| AS 1145A | Aircraft Brake Temperature Monitoring System |
| AS 1188 | Aircraft Tire Inflation-Deflation Equipment |

SAE also publishes the Aerospace Material Specifications. The following are cited in this book:

| | |
|----------|--|
| AMS 4640 | Rods, Bars, and Forgings—Aluminum Bronze |
| AMS 4880 | Castings, Centrifugal—Aluminum Bronze |
| AMS 5643 | Bars, Forgings, Mech. Tubing, and Rings |

American Society for Testing and Materials (1916 Race St., Philadelphia, PA 19103):

| | |
|-------------|--|
| ASTM B 46.1 | Now replaced by E54—Chemical analysis of special brasses and bronzes |
|-------------|--|

Aerospace Industries Association of America (1725 De Sales St., N.W., Washington, DC 20036) issues National Aerospace Standards.

| | |
|----------|--|
| NAS 3601 | Data Format of Transport Aircraft Characteristics for Airport Planning |
|----------|--|

MILITARY SPECIFICATIONS

An overall specification is provided in MIL-L-87139. A list of the primary detail specifications, with paraphrased titles, follows. The specifications are available from ASD/EDYEEES, Wright-Patterson AFB, Ohio 45433, and other U.S. Government agencies as appropriate.

| | |
|------------|---|
| MIL-A-8629 | Drop Tests (see also MIL-T-6053) |
| MIL-A-8860 | Airplane Strength—General Specification |

| | |
|--------------|--|
| MIL-A-8862 | Landing and Ground Handling Loads |
| MIL-A-8863 | Airplane Strength and Ground Loads for Navy Aircraft |
| MIL-A-8865 | Airplane Strength and Miscellaneous Loads |
| MIL-A-8866 | Strength and Rigidity Reliability Requirements (Fatigue) |
| MIL-A-8867 | Strength and Rigidity, Ground Tests |
| MIL-A-8868 | Airplane Strength Data and Reports |
| MIL-A-18717 | Arresting Hooks |
| MIL-A-83136 | Arresting Hook Installations (USAF) |
| MIL-B-8075 | Anti-Skid |
| MIL-B-8584 | Brakes—Control Systems |
| MIL-C-5041 | Tire Casings |
| MIL-C-5503 | Hydraulic Actuating Cylinders, General Requirements |
| MIL-C-8514 | Wash Primer |
| MIL-D-9056 | Drag Chute |
| MIL-G-21164 | Grease, Molybdenum Disulfide |
| MIL-H-5440 | Hydraulic Components |
| MIL-H-5606 | Hydraulic Fluid |
| MIL-H-8775 | Hydraulic System Components |
| MIL-L-8552 | Shock Absorbers—AFSC and USN |
| MIL-L-87139 | Landing Gear Systems |
| MIL-P-5514 | Packings—Shock Strut; also O-Rings and Glands |
| MIL-P-5516 | Packing—Shock Strut |
| MIL-P-5518 | Pneumatic Components |
| MIL-P-8585 | Primer—Wheel Wells |
| MIL-P-23377 | Primer—Epoxy |
| MIL-S-8552 | Strut, Aircraft Shock Absorber (Air-Oil Type) |
| MIL-S-8698 | Structural Design Requirements, Helicopters |
| MIL-S-8812 | Steering Systems |
| MIL-T-5041 | Tires, Pneumatic, Aircraft |
| MIL-T-6053 | Drop Tests (see also MIL-A-8629) |
| MIL-T-83136 | Tie Down Requirements |
| MIL-W-5013 | Brakes and Wheels |
| MIL-STD-10 | Surface Roughness, Waviness, and Lay |
| MIL-STD-203 | Controls and Displays in Flight Station |
| MIL-STD-568 | Corrosion Prevention and Control |
| MIL-STD-621A | Test Method for Pavement Subgrade, Subbase, and Base-Course Material |
| MIL-STD-809 | Adapter, Aircraft Jacking Point |
| MIL-STD-878 | Tires and Rims—Dimensions and Clearances |
| MS 21240 | Bushing, TFE-lined |
| MS 21241 | Bushing, TFE-lined |
| MS 28776 | Scraper, Hydraulic Piston Rod |
| MS 28889 | Valve, Air High-Pressure Charging |
| MS 33675 | Ring, Wiper, Installation and Gland Design |
| AND 10071 | Boss and Installation—Air Connection |
| TSO-C26b | Technical Standard Order, Wheels, and Wheel/Brake Assemblies |
| STM 37-307 | Polyurethane White Point |

U.S. Air Force Systems Command

DH2-1 Design Handbook

DH2-1 DN 34A

DH2-6 DN 4B2

U.S. Navy

Specification SD-24 General Specification for Design and Consideration of Aircraft Weapon Systems

CIVIL SPECIFICATIONS*Federal Aviation Agency* (800 Independence Ave., S.W., Washington, DC 20591):

FAR Part 23 Federal Aviation Regulations, Airworthiness Standards: Normal, Utility, and Aerobatic Aircraft

FAR Part 25 Federal Aviation Regulations, Airworthiness Standards: Transport Category Airplanes

25.723-727 Shock Absorption Tests, Limit Drop Tests, Reserve Energy Absorption Drop Tests

British Civil Aviation Authority (Air Registration Board, Brabizon House, Redhill, Surrey, England) issues the British Civil Airworthiness Requirements (BCAR):

BCAR Chapter D3-5 Ground Loads

BCAR Chapter D4-5 Landing Gear Design

International Civil Aviation Organization (1000 Sherbrooke St. West, Suite 400, Montreal, Quebec, Canada H3A 2R2) issues internationally recognized standards:

DOC 9157-AN/901, Pt. 3 Aerodrome Design Manual, Pavements

Annex 14, Amendment 37 International Standard and Recommended Practices, Aerodromes

FEDERAL SPECIFICATIONS

QQ-C-320 Chromium Plating (Electro-deposited)

QQ-N-290 Nickel Plating (Electro-deposited)

QQ-C-465 Copper Aluminum Alloys, Aluminum Bronze

Index

- A-5, 245, 247
A-6, 220
A-7, 47, 64, 182, 220, 325
A-10, 47, 64
A-37, 325
A-300, 39, 179, 205, 323, 348, 349
A-310, 350
A-320, 351
AV-8B, 220
Abbreviations, 43, 98,
ACLS *See* Air-cushion landing system
ACLS materials, 315
ACN-PCN, 274, 292–297
Actuators, 175, 176, 198, 201, 203,
205–207, 209, 211, 216, 246, 254
Advanced brake control system (ABCS),
171
Aero Commander, 39, 96, 327
AIA, flotation, 276
Air-cushion landing system (ACLS), 10,
305, 307, 311–320
Airfield considerations, 267–304
Airfield index, 268
Airfield roughness—*see* Roughness, airfield
Airfield surface types, 271
Air/oil mixing, 81
Airspeed limits, 22, 47
Angle, tail-down, 18, 327
Angle, touchdown, 18
Angle, turnover, 37, 38
Antiskid—*see* Skid control
Arado, 305
Arresting landings, 41, 67
Assembly load, 268
ATR-42, 123
Autobrakes, 165, 167
Avrocar, 307
Axle base, 268
- B-1, 168, 220, 325
B-36, 9, 305, 311
B-47, 40
B-50, 9, 306, 311
B-52, 47, 64, 325
B-57, 47
B-58, 7
B-66, 47, 64
BAC 111, 159, 181, 182
B.Ae. ATP, 355
B.Ae. Harrier, 177, 245
B.Ae. Nimrod, 27, 352, 353
B.Ae. 146, 181, 183
B.Ae. 748, 116, 150, 155, 207, 245, 248
B.Ae. Vulcan, 182, 186, 354
Bare soil flotation, 285–290
Baroudeur, 305, 308
BCAR, 11, 43, 50, 53, 54, 55, 60, 61,
65–67
Bearings, 111, 114
Beech B99, 39, 96, 327
U-21A, 39, 96
Bell Aerospace, 10, 307
Bendix, 161
Beryllium. *See* Materials
Bleriot, 1
Boeing B-47, 38
247-D, 4
707, 5, 30, 39, 96, 220, 260, 263, 323,
326, 327, 356, 357
720, 30, 96, 158, 323
727, 7, 30, 39, 40, 96, 125, 158, 203,
209–213, 218, 220, 260, 264, 290,
293, 323, 327
737, 7, 30, 39, 96, 220, 264, 293, 323
747, 5, 7, 30, 39, 161, 220, 260, 291,
293, 323, 326
757, 15, 148, 165, 168, 220
767, 15, 165, 168, 220
Y1B-9, 4
Bonanza, 39
Bonmartini, 8, 306, 307
Brakes, cooling, 155
control, 169, 170
design, 140, 150–151, 313, 316
emergency system, 168
energy, 20, 140–146
heat, 65, 150, 153–161
material, 20, 145–146, 148, 319
requirements, 53, 65, 137
sizing, 137, 147
squeal and chatter, 151
test, 23
weight, 144, 145
Breguet 941, 39
Bristol, 3
Britannia, 245
British Civil Airworthiness Requirements,
See BCAR
Bungees, 1, 2, 84
Bushings, 239
- C-2A, 7, 30, 324
C-5A, 5, 6, 8, 13–15, 19, 30, 31, 37, 64,
148, 181, 220, 245, 260, 291, 324, 326,
327
C-7A, 30, 324
C-8A, 30, 324
C-9A, 30, 324, 326
C-10A, 30
C-17, 37
C-45, 30, 324

- C-46, 30, 260, 324
- C-47, 30, 324, 326
- C-54, 30, 260, 324, 326
- C-82, 306, 311
- C-97, 30, 324
- C-118, 30, 324, 326
- C-119, 30, 260, 315, 324
- C-121, 30, 324, 326
- C-123, 30, 64, 260, 324
- C-124, 30, 260, 324, 326
- C-130, 7, 9, 10, 30, 31, 37, 64, 79, 81, 82, 96, 220, 221, 260, 305, 309, 324, 326, 327, 358, 359
- C-131, 30, 324
- C-133, 13, 30, 260, 324
- C-135, 64, 260, 324, 326
- C-140, 30, 324 (see also Lockheed JetStar)
- C-141, 30, 37, 39, 96, 181, 203–205, 245, 252, 253, 260, 324, 326
- CL-44, 260
- CV 240, 260
- CV 440, 260
- California bearing ratio, *See* CBR
- Castering gears, 222
- Castings, 22
- CBR, 268, 269, 285, 286
- Centering cam, 198, 200, 209
- Center of gravity, 18, 26, 27
- Cessna, 7, 80
- Characteristics of landing gears, 323
- Clearances, 22, 40, 51, 52
- Cleveland Pneumatic Co., 22
- Cockpit requirements, 64, 203
- Cody, 1
- Comet, de Havilland, 27, 159, 181, 184
- Compression, 97, 100, 102, 113
- Concept, first, 13, 25
- Concorde, 39, 148, 149, 160, 245, 293, 360
- Concrete, 276, 292, 326
- Cone index, 269
- Contact area and pressure, 269, 285
- Contracting shock struts, 118
- Convaire:
 - 440, 30, 323
 - 880, 30, 323
 - 990, 30, 323
- Conway, H. G., 81, 147, 177, 309
- Cooling, brake, 155
- Cornering force, 132
- Corotating wheels 202, 207
- Corrosion, *see* Protection
- Cost, 17, 18, 20, 23
- Coverages, 269, 285
- Critical design review, 20
- Crush load, 128
- Curtiss, 1, 4, 6
- DC-1, 4
- DC-2, 4
- DC-3, 5, 30, 260, 267, 323, 326
- DC-4, 30, 323, 326
- DC-6, 30, 323, 326
- DC-7, 30, 260, 267, 323
- DC-8, 30, 211, 214, 215, 216, 219, 245, 249, 255, 256, 260, 323, 326
- DC-9, 30, 39, 40, 96, 220, 260, 323, 326
- DC-10, 30, 96, 161, 180, 267, 323, 326
- Dead length, 175, 176
- Definitions, flotation, 268
- Deflection, water/gravel, 19
- De Havilland:
 - Comet, 27, 159, 181, 184
 - Dove, 85
 - Mosquito, 70, 72, 73, 85
 - Trident, 7, 159
- Delagrang, 1
- DHC:
 - Buffalo, 38, 39, 260, 308, 313, 316
 - Caribou, 179, 260
 - Dash-7, 38, 220
 - Dash-8, 38
 - Twin Otter, 69, 71, 80, 310, 311, 327
- Doors, 66,
- Double-acting shock struts, 102
- Dowty, Canada, 103, 246
 - George, 306
 - Liquid spring, 74, 75, 88
 - Rotol, 22
 - Seal, 90
 - Sprung wheel, 76
 - Steering system, 205
- Drag, ACLS, 325
- Drop tests, 22, 47, 49, 50, 77, 119
- Dunlop, 139, 153, 159
- E-4, 326
- Earl, T. D., 315
- Electrical system, 20, 22
- Ellehammer, 1
- Emergency system, 65, 168, 197–198
- Energy absorption, 34, 35
- Energy, brake, 20, 140–147
- Equivalent single-wheel load (ESWL) 269, 280, 282, 284, 286
- F-4, 39, 47, 64, 96, 171, 206, 220, 325
- F-5, 47, 64, 202, 220, 325
- F-14, 147, 161, 220, 325
- F-15, 47, 161, 220, 260
- F-16, 47, 64, 168, 171, 202, 260, 325
- F-18, 220
- F-27, 30, 323 (Fokker)
- F-86, 325
- F-89, 325

- F-100, 47, 64, 325
- F-101, 325,
- F-102, 325
- F-104, 39, 96, 260, 325
- F-105, 47, 325
- F-106, 47, 325
- F-111, 47, 64, 168, 171, 325
- FF-1, 4
- FAA flotation method, 277
- FAA requirements, 11, 43, 55, 65, 67
- Fairchild, 9
- Fairey Swordfish, 4
- Farman, 1
- Finishes, 240
- Firestone, 85
- Flexible pavement, 273
- Flight test, 23
- Flotation, 17, 18, 22, 269–296
- FMEA, 23
- Fokker, 181, 183, 361
- Footprint, 217, 269
- Ford Trimotor, 3
- Forgings, 22
- Free Fall, 28
- Fregat, 39
- Friction, 131, 217, 309
- Fusible plugs, 53, 153, 159

- Gee Bee, 4
- Gloster Gladiator, 4
- Goodrich, B. F., 146, 155
- Goodyear, 161, 164
- Growth, aircraft, 32
- Growth, cylinder, 113
- Grumman FF-1, 4
- Gulfstream, 208, 209, 260, 264

- Hand-wheel steering, 203, 209, 217
- Hydraulics, 20, 22, 166–167, 170, 201, 205–209, 211, 216, 217, 246
- Hydro-Aire, 161, 162, 164, 165, 166
- Hydroplaning, 134

- International Civil Aviation Organizations, (ICAO), 274, 280, 281, 283, 294
- Internal locks, 175, 245, 246

- Jacking, 19, 23, 142
- JetStar, *See* Lockheed
- Jindivik, 313
- Junkers 87 Stuka, 4
- Junkers JV 88, 69

- KC-10, 324
- K factor (flotation), 269
- Kinematics, 19
- Kinematic analysis, 188
 - concepts, 23, 36, 176
 - detail, 187
 - guidelines, 175
- Kinetic energy, 54, 146, 147
- Kneeling, 16, 19

- LA-4, 10, 307, 308, 312, 316
- Layout, initial, 25, 46, 48
- Leaf spring, 85
- Levered suspension, 79
- Limited operation (flotation), 290
- Liquid spring, 74, 75, 80, 88
- Load, braking, 29, 31
 - crush, 128
 - factor, 34, 78–79
 - gear, 27, 28, 29, 31, 77
 - rating, 32, 126
 - speed-time, 128, 129
- Load Classification Group (LCG), 274, 280–285
- Load Classification Number (LCN), 274, 280–285, 290
- Loaded radius, 33
- Location, landing gear, 18, 20, 25, 37
- Lockheed:
 - Altair, 4
 - C-5. *See* C-5
 - C-130. *See* C-130
 - C-141. *See* C-141
 - Constellation, 260,
 - Electra, 39, 96, 327
 - JetStar, 96, 175, 176, 177, 203, 207, 221, 260, 264, 327
 - L-100, 30, 39, 168, 171, 275, 323, 326
 - L-188, 30, 323
 - L-1011, 7, 30, 39, 96, 161, 220, 260, 264, 323, 326, 327
 - L-1049, 30, 323
 - S-3A, 7
 - Sr-71, 7
 - Winnie Mae, 4
- Locks, 62, 182, 243–257
- Locks, internal, 175, 245, 246
- Lubrication, 225, 230, 240
- Lugs and pins, 225, 229

- Maintainability, 22, 66
- Martin:
 - 202, 260
 - 404, 260
- Materials, 20, 145, 146, 148, 149, 151, 225, 239, 315, 316, 319
- McCurdy, 1
- Me, 163, 305, 309
- Mean aerodynamic chord (MAC), 25
- Menasco, 22
- Mercure, 39

- Messier-Hispano-Bugatti, 22
- Metering pin, 22, 119
- Michelin, 125
- Military specifications, 366
- Mock-ups, 22
- Multiplication factor, 285–286

- Navy requirements, 41, 48, 49, 50, 52, 53, 60, 62, 64, 65, 78, 79, 128, 206, 368
- Nimrod (B.Ae.), *see* B.Ae.
- NORATLAS, 30

- Oleo-pneumatic shock absorber, 75, 76, 80, 94 (*see also* shock absorber)
- Operating times, 22, 63, 64
- Operating conditions, 44
- Orifice design, 119
- OV-10A, *see* Rockwell

- P2V, 260
- Passes, 287
- Pavement, 271
- Pazmany, L., 222
- PCA flotation method, 274–275
- Piper:
 - Aztec, 96, 327
 - Cherokee, 90
 - Comanche, 39, 96
 - Cub, 80, 306
 - Super Cub, 39, 327
 - Turbo Navajo, 39, 96, 327
- Piston valves, 117
- Pitch/roll clearance, 40
- Placard speeds, 22
- Pneumatic trail, 132
- Pods, 40
- Polytropic compression, 102
- Portland Cement Association method. *See* PCA flotation method
- Power spectral density, 297, 298
- Preliminary design, 15
- Preliminary design review (PDR), 20
- Protection, 65, 230

- Qualification test, 22

- Radius of gyration, 127
- Radius of relative stiffness, 271, 273
- Reliability, 22
- Requirements, 43
- Retraction,
 - forward, 28
 - general, 178–187
 - requirements, 62
- RFP, 13, 18
- Rigid pavement, 271, 275
- Rockwell OV-10A, 117
- Roe, A. V., 1

- Rolling radius, 127
- Roughness, airfield, 6, 10, 18, 20, 22, 80, 109, 117, 126, 297, 312
- Rubber, shock absorber, 70, 84
- Runway loading, 31, 33

- S-3A, 7, 148
- SAE documents, 10, 365
- SE5, 1, 2
- SR-71, 7
- Seals, 90, 241
- Shimmy, 22, 23, 201, 202, 217
- Shock absorber, contracting, 118
 - design, 20, 34, 35, 47, 69, 94, 110
 - double-acting, 102–110
 - efficiency, 22, 49, 70, 75, 77, 119
- Shock absorber, length, 78
 - requirements, 47
 - stroke, 35, 78, 79, 83
 - types, 2, 69
- Short, 1
- Side forces, 132
- Sink speed, 35, 49, 78, 83
- Sizing, shock absorber, 96
- Skid control, 60, 161
- Skids, 10, 305, 308
- Skis, 10, 305, 309
- Slip angles, 132
- Soil classification, 272
- Sopwith Camel, 1, 2
- Spatted landing gears, 5
- Specifications, 365
- Specific Operational Requirements, 25
- Speeds, *See* Airspeed limits
- Steel, *See* Materials
- Steering, angle, 22, 198, 201, 203, 206, 209, 211, 216, 217
 - disconnect, 198, 201, 203, 209
 - mechanism, 198, 199, 207, 210–215
 - requirements, 60, 197, 198
 - torque, 201, 202
- Strength requirement, 66
- Stress concentration, 22, 151, 153
- Stress corrosion, 225
- Subgrade, 271
- Surface roughness on landing gear, 225, 240, 259

- T-37, 47, 64
- T-38, 47, 64, 202
- T-39, 47
- Tail bumper, 27, 67
- Tail-down angle, 18, 327
- Tail tipping, 27
- Taylor Devices, 93, 94
- Temperature, brake, 147, 149, 161
- Temperature effects, tires, 128
- Terminology, 44

- Test, 23
- Threads, 330
- Time to retract, 22, 63, 64
- Tire, aspect ratio, 124
 - clearances, 51, 52
 - construction, 123
 - deflation in flight, 20
 - deflection, 80, 127
 - dimensions, 50, 127
 - footprint, 125
 - friction, 131
 - fuse plugs, 53, 153, 159
 - growth, 51
 - pressure, 50, 51
 - radial, 123-125
 - radius of gyration, 127
 - requirements, 50, 125
 - rolling radius, 127
 - rolling resistance, 125, 130
 - selection, 20, 31, 32, 126
 - temperature effects, 128, 159
 - usage, 30, 333-347
- Tolerances, 332
- Tornado, 205, 362, 363
- Torque link geometry, 176
- Towing, 23, 27, 242
- Tract gears, 8, 9, 305, 311
- Trade studies, 20,
- Traffic lane, 271
- Trail, 132, 217, 220, 223
- Tread distance, 271
- TU-144, 8, 9
- Turnover angle, 37, 38
- Turn radius, 199
- Types of landing gears, 7, 80
- Unpaved surfaces, 274, 285-290, 298
- U.S. Army/USAF flotation, 280
- USAF Layout requirements, 46
- U. S. Navy flotation, 280
- U. S. Navy layout requirements, 48
- V-22, 103, 245, 246
- VC-10, 159
- Vibration, 23
- Voisin, 1
- Volumes, shock absorber, 92, 98, 100, 104, 112
- Vought-Sikorsky "Kingfisher", 4
- Vulcan, 192, 186, 354
- Weight, 125, 144, 145, 147, 149, 228-266, 311, 312, 314
- Westergaard, 271, 277, 280
- Westland "Lysander," 306
- Wheelbase, 271
- Wheel design, 151
 - dimensions, 152
 - internally sprung, 75, 76
 - requirements, 52
- Winnie Mae, 4
- Wrench clearances, 328
- XC-142A, 260
- XC-8A, 313, 316
- XV-4B, 260
- XV-5A, 260